Proceedings of the

U.S.-Southeast Asia Symposium on Engineering for Natural Hazards Protection

Manila, 1977

Edited by A. H-S. Ang

Department of Civil Engineering
College of Engineering
University of Illinois at Urbana-Champaign
1978

Foreword

The US-Southeast Asia Symposium on Engineering for Natural Hazards Protection was held at the Philippine International Convention Center in Manila, Philippines on 26-30 September 1977, sponsored jointly by the Philippine National Science Development Board, the University of the Philippines System, and the U.S. National Science Foundation.

The Symposium consisted of a technical conference and a research workshop. The present volume contains all the technical papers contributed and presented at the Conference part of the Symposium.

It is through the joint support of the above sponsors that made the Symposium in Manila possible. The U.S. contribution to the Symposium was supported by the Division of International Programs of the National Science Foundation under Grant INT 77-15418 to the Department of Civil Engineering, University of Illinois at Urbana-Champaign, which included the funding for the publication of the present volume of proceedings. The Volume represents the collective technical contributions of the authors to the subject of the Symposium; their individual efforts and written contributions are gratefully acknowledged.

It is a great pleasure to acknowledge the organizational leaderships of Dr. E. G. Tabujara of the University of the Philippines and Mr. R. P. Venturina of the National Science Development Board; the successful convening of the Symposium in Manila was, in large measure, due to their efforts.

The assistance of Mr. Lynn Barry of the U. of I. Engineering Publications during the publication of the Volume is greatly appreciated.

A. H-S. Ang
Urbana, Illinois

CONTENTS

RISK AND SAFETY ANALYSIS IN DESIGN FOR NATURAL HAZARDS PROTECTION

by

A. H-S. Ang and Y.K.Wen
University of Illinois at Urbana-Champaign

Synopsis

An approach to the risk-based analysis of safety of structures and facilities against the extreme forces of natural hazards is described. The components of the basic methodology are outlined, and applications to wind and earthquake are emphasized. References to more comprehensive works are provided. The implications for design to insure a desired level of protection (in terms of probability) against natural hazards are indicated.

Introduction

In the design and planning of a structure or facility for resistance against the extreme forces of natural hazards, such as earthquakes and storm winds, the level of protection or safety required for its design is undoubtedly the most important technical problem underlying the planning process. Indeed, resolving the question of "how safe is safe enough?" is central to proper engineering.

In this regard, it is important to recognize that safety, specially for protection against natural hazards, cannot be assured with absoluteness. Realistically, safety may be assured only within the context of some acceptable risk. Either explicitly or implicitly, some risk is unavoidable; few (if any) economies can afford to do otherwise. In short, within limited resources, there is a limit to safety--this is particularly apropos in the case of natural hazards protection.

Within this risk-based concept of structural safety, a quantitative framework for developing safety criteria for design can be developed. The basic risk methodology is summarized herein, and the applications of the approach to natural hazards protection are discussed and developed, with emphasis on wind and earthquake resistant designs.

Methodology for Risk and Safety Assessments

The adequacy of a structure or facility to withstand the maximum environment to which it may be subjected over its useful life is of principal concern in planning its design. Like most natural phenomena, the occurrence of an extreme environmental hazard, such as hurricane or earthquake at a particular site, is difficult to predict; an extreme even may occur at random in time as well as in space. Moreover, the intensity

(i.e. destruction potential) may vary greatly from one event to another. In this light, the maximum environment that may be expected over the life of a structure or facility at a particular location would be difficult to predict with any certainty. It is realistically possible only to determine the potential intensity in terms of probability; specifically, for example, the annual probability of exceedance. Accordingly, the "design environment" may be prescribed with an associated exceedance probability.

During the occurrence of a given natural hazard, such as a hurricane or earthquake, the disturbance is a function of time; again the characteristics of this function may be highly variable from one event to another and thus may be described as a random process. Moreover, in analyzing the response of a given system to a given random process disturbance (requiring dynamic response analysis), the methods of random vibration are appropriate.

The adequacy of a structure or facility against the expected lifetime maximum environment, of course, will depend also on the limiting response capacity of the structure. The determination of this capacity will invariably also contain uncertainty; consequently, the adequacy or safety of a structure against a particular lifetime hazard may only be measured in terms of its probability of failure.

In summary, the determination of the safety of a given or proposed system, therefore, requires the following: (i) definition or specification of the maximum environment that a facility may be subjected to over its intended useful life; (ii) analysis of the response of the system under the estimated lifetime environment; and (iii) determination of the limiting response capacity of the system. Each of these items may be elaborated as follows:

Determination of Lifetime Maximum Environment

The determination of the lifetime maximum environment requires an analysis of the potential hazards expected in the particular locality or site. This may be accomplished by first determining the probability distribution of the short-term (e.g. one year) maximum environment at the site, from which the long-term (i.e. lifetime) maximum environment may be extrapolated through extreme-value statistical theory.

The procedure for determining the short-term (e.g. one year) distribution will depend on the specific hazard under consideration, as will be discussed subsequently for the cases of wind and earthquake. In any case, having determined the distribution of the annual maximum environment, say $F_A(a)$, the annual exceedance probability of the intensity level a is,

$$P(A > a) = 1 - F_A(a) \qquad (1)$$

Graphically, such hazard probabilities may be portrayed qualitatively as shown in Fig. 1.

Then, the distribution of the life-time (say, n years) maximum environment becomes

$$\Phi_{A_n}(a) = [F_A(a)]^n \tag{2}$$

For sufficiently large n, Eq. 2 will approach some asymptotic form of distribution (Gumbel, 1958). Although the rate of convergence (in distribution) will depend on the short-term distribution $F_A(a)$, it is reasonable to assume, in the case of structures and large systems, that the life (in years, n) is sufficiently long to permit the use of the appropriate asymptotic form of the extremal distribution for the lifetime maximum. On this basis, only the key parameters of the extremal distribution need to be determined for a given site; in particular, these are the modal value, u, and the dispersion parameter, α.

The modal value, u, is defined as,

$$F_A(u) = 1 - \frac{1}{n} \tag{3}$$

Hence, u is the annual maximum with the return-period of n years; whereas, α is (see Gumbel, 1958)

$$\alpha = n \cdot f_A(u) \tag{4}$$

Since $1-F_A(a)$ is invariably determined numerically, the necessary derivative,

$$f_A(u) = \left.\frac{dF_A(a)}{da}\right|_{a=u} \tag{5}$$

may be evaluated approximately as,

$$f_A(u) \simeq \frac{F_A(u-\frac{\Delta a}{2}) - F_A(u+\frac{\Delta a}{2})}{\Delta a} \tag{6}$$

from which the parameter α may be evaluated through Eq. 4.

In short, therefore, the main problem in the definition of the lifetime environment is in the determination of the distribution or exceedance probabilities of the short-term (annual) maximum environment. Having established this, the parameters of the lifetime maximum environment can be evaluated from information on the short-term environment as indicated in Eqs. 3 and 4, whereas the distribution form for the lifetime maximum would be the appropriate asymptotic extremal distribution.

Response to Life-time Maximum Environment

Knowledge of the lifetime environment itself, of course, is not sufficient; relative to the consideration of structural safety, the real damage potential of the environment must include the "maximum" response of the structure or system in question. The response of a structure to the

anticipated lifetime maximum environment may be analyzed assuming that it does not significantly deteriorate over its life. The disturbance during a natural hazard event is invariably a fluctuating forcing function over the duration of the event. The response of a system to such a dynamic forcing function may be analyzed by the methods of random vibrations. Such analyses will depend on the definition of failure and associated characteristics of the system. Failure may be defined as the occurrence of the first yielding; in which case, the response may be limited to linear system analysis. However, if failure is defined as some state approaching ultimate collapse of the structure or any of its parts, then the nonlinear-inelastic behavior of the system must be considered.

In any case, the response to the lifetime maximum environment may be denoted as,

$$R_{max} = R(a,\tilde{q})$$

where, $\tilde{q}$ = the parameters of the structure or system, and a = the lifetime maximum environment. R_{max} will remain a random variable, with probability distribution $F_R(r)$.

The methods of random vibration analysis, suitable for the above purposes, will be reviewed subsequently below.

Limiting Response Capacity

For a given structure or system, there is a response level beyond which the structure may fail; this is the limiting capacity of the structure. For a linear system, this may be the limiting displacement (or velocity, or acceleration) beyond which some damage will occur in the structure. However, failure may be defined as a state approaching collapse, in which case the capacity could be related to its energy-absorbing capacity. In any case, the limiting capacity must be defined in terms consistent with the calculated response r. The corresponding probability distribution then may be represented as

$$F_C = F_C(r)$$

Assessment of Risk and Safety

In view of the fact that both the lifetime extreme environment, as well as the capacity of a system may be described only to the extent of the respective probabilities, the assessment of safety may be evaluated in the context of risk and probability of failure. Specifically, the lifetime probability of failure is of interest:

$$p_F(T) = \int_0^\infty F_C(r) \cdot f_R(r)dr \qquad (7)$$

or

$$p_F(T) = \int_0^\infty [1-F_R(r)] \cdot f_C(r)dr \qquad (7a)$$

where $F_R(r)$ or $f_R(r)$, and $F_C(r)$ or $f_C(r)$, are the probability distributions discussed above.

The significance of Eq. 7 or 7a can be seen in Fig. 2. It may be observed from Fig. 2 that $p_F(T)$ is a function of the relative positions between $f_C(r)$ and $f_R(r)$, and the dispersions in these distributions.

The probability of failure is a consequence of the lack of perfect information -- i.e. of uncertainty, as measured by the dispersion of $f_R(r)$ and $f_C(r)$. Uncertainty may be associated with the inherent randomness of the underlying natural phenomenon, as discussed above, or could be due to imperfections in the prediction of the real state of nature. In either case, it leads to the lack of absolute assurance for safety, and hence the need for assurance in terms of probability. For this reason, the probability distributions in Eq. 7 or 7a must reflect all the sources of uncertainty; in particular, the uncertainties associated with model imperfections should be included in the respective probability distributions (Ang, 1973).

Wind Hazard Analysis

Extreme winds are generally caused by severe storms, which vary in size, intensity, and occurrence frequency, and could range from extensive extra-tropical storms, scattered thunderstorms, hurricanes, to very local tornadoes. Extremely high winds (e.g. over 150 mph) may be produced only by hurricanes and tornadoes which occur much less frequently than the other storms; e.g. with a frequency of around 10^{-1} ~ 10^{-2} per year per site for hurricanes, and 10^{-2} ~ 10^{-3} for tornadoes in the United States. Therefore, unless the local wind climate is well-behaved (i.e. dominated by one storm system), the extreme winds are likely to be a mixed population of low intensity-high frequency and high intensity-low frequency storm systems. Local wind data of the high-intensity storms are usually limited or non-existent. Therefore, purely data-based statistical prediction may lead to significant error in the extreme wind hazard and selection of the design wind speed, especially in the range of small exceedance probability (or long return-period). The inadequacy of using a single Fisher-Tippett extreme-value distribution for locations of mixed wind climate has only recently been recognized. An alternative approach by which the hazard may be evaluated more realistically is to develop a risk model for each storm, taking into consideration the occurrence frequency and physical properties of the storm, and then combining the results to arrive at the overall hazard. A method for such wind hazard analysis is outlined in the following.

Extratropical Storm

Because of its high frequency and large area of influence, good records generally exist for wind due to extratropical storms. The annual maximum wind can be adequately described by a Fisher-Tippett Type I extremal distribution,

$$P(V_e < v) = \exp\{-\exp[-\alpha(v - u)]\} \qquad (8)$$

in which the mode u and dispersion parameter α are determined from wind da

Thunderstorms

In regions where thunderstorms occur frequently, high winds may be produced in the gust front of the thunderstorm downdraft. Although the frequency of such wind may be less than those due to extratropical storms, the availability of area or regional thunderstorm data may allow one to predict the extreme wind probability by combining the intensity and occurrence statistics as follows (Gomes and Vickery, 1976);

$$P(V_{th} < v) = \sum_{n=0}^{\infty} P(V'_{th} < v)^n P(n) \approx [P(V'_{th} < v)]^{\bar{n}} \qquad (9)$$

in which V_{th} = the annual maximum gust wind due to thunderstorm. $P(V'_{th} < v)$ = probability distribution of area or regional maximum thunderstorm gusts. $P(n)$ = probability mass function of thunderstorm frequency per year at the site. $\bar{n} = E(n)$ = mean number of thunderstorms at the site. In Gomes and Vickery (1976), $P(V_{th} < v)$ is modeled by a Fisher-Tippett Type I distribution and $P(n)$ by a discrete Weibull distribution with parameters determined from thunderstorm data. Therefore, Eq. (9) may be rewritten as

$$P(V_{th} < v) = \exp\{-\exp[-\alpha(v - u - \frac{1}{\alpha} \ln \bar{n})]\} \qquad (9a)$$

in which u = mode, α = dispersion parameter of thunderstorm gusts.

Tornado

Although tornado is a world-wide phenomenon, severe ones occur mostly in the United States and Australia, with the majority (80%) in the U.S. In spite of its high occurrence frequency (over 600 per year in the U.S.), it is an extremely localized phenomenon, with an average coverage area of about one square mile. Therefore, wind speed data for tornado at a site is virtually nonexistent. In the U.S., wind speed estimates rely mostly on damage survey and photogrammetric methods. Motivated by the stringent safety requirements of nuclear power plant structures, analytical models for tornado risk analysis, based on area or regional tornado occurrence data, intensity, and wind field statistics, have been developed (e.g. Wen and Ang, 1975; Wen, 1976; Garson, et al, 1975). Such analyses generally give the exceedance probability of wind speed v over a time period t as

$$P(V_T > v) = 1 - \exp[-\nu R(v)t] \qquad (10)$$

in which ν = mean number of tornado occurrence per unit area per year; $R(v)$ = tornado speed-area function, having a unit of area, a function through which the variability of tornado intensity, size and wind field are included. $R(v)$ is obtained based on tornado statistics and available three-dimensional wind field model for the tornado vortex boundary layer.

$$R(v) = 2 \int_v^\infty \int_o^\infty \int_o^{nr_{max}} \frac{1}{g\, r_{max}} f_{r_{max}, V_{max}} (r_{max}, v/g) \cdot \qquad (11)$$

$$\cdot dD\, dr_{max}\, dv \cdot E[r_{max}, L]$$

in which V_{max} = maximum tangential wind; r_{max} = radius of V_{max}; D = distance of a site to the path of the tornado center; L = tornado path length; f = joint probability density function; and g = three-dimensional tornado wind field function = g (z,D,r_{max}), where z is the height above ground.

An alternative method of assessing the risk of tornado wind speed (see Abbey, 1976) is to evaluate the annual probability of damage from violent tornado (F-4 and F-5 on the Fujita intensity scale) directly from local tornado statistics. This approach has the advantage of including the regional and intensity variation along the tornado path; however, it must rely completely on direct tornado damage statistics which may be limited.

Hurricanes, Typhoons, Cyclones

The Fisher-Tippett Type II extremal distribution has been suggested (e.g. Thom, 1968) for describing the wind speed of hurricanes in the United States; thus,

$$P(V_h < v) = \exp\{-(\frac{v}{\sigma})^{-\gamma}\} \qquad (12)$$

in which σ and γ are the scale and shape parameter. However, since the occurrence of hurricanes is relatively rare and available wind data are usually limited to less than 20 years of record, the parameters σ and γ are sensitive to the number of hurricanes observed over the record period (Simiu and Filliben, 1976). For example, at Darwin, Australia, cyclone Tracy of 1975 produced gusts of twice the maximum speed recorded in the previous ten years; therefore, in this case a single cyclone would alter the distribution parameters significantly. An alternative procedure is to use phenomenological models (Russel, 1971) in which the important hurricane parameters are treated as random variables and the distribution of the maximum wind obtained by Monte-Carlo calculations. The storm parameters could include occurrence frequency, wind field, forward speed, central pressure differential and radius of maximum speed, in which the probability distributions of these variables are based on regional hurricane statistics.

It may be pointed out that the foregoing tornado model can be applied to hurricane winds with some modifications. Since hurricanes are known to "fill" (decay) once it penetrates a coast line, an important factor is the distance y from the site to the coastline. The exceedance probability can then be given by

$$P_t(V_h > v) = 1 - \exp[-\nu R(v, y)t] \qquad (13)$$

in which ν = mean number of hurricane crossing per mile of coastline per year, and

$$R(v,y) = \int\int\int\int g(y,\theta,\ell,V_{max},s)\, f_{\theta,\ell,V_{max},s}\; d\theta\, d\ell\, dV_{max} ds \quad (14)$$

in which g = hurricane wind field function after landfall, θ = heading angle of hurricane, ℓ = depth of inland penetration, V_{max} = maximum tangential wind, S = forward speed of hurricane, f = joint probability density function of these variables, which may be determined from hurricane statistics.

Combination of Extreme Winds

At locations with mixed wind climate, the overall probability of annual maximum wind can be derived by combining the foregoing distribution functions; thus,

$$P(V < v) \approx P(V_e < v)\, P(V_{th} < v)\, P(V_h < v)\, P(V_T < v) \quad (15)$$

in which the independence among the different storm winds has been assumed. Ordinarily, at a given location, there may only be one or two prevailing storm winds; e.g. hurricanes and thunderstorms may dominate along coastal areas, whereas extratropical storms and tornadoes may dominate for inland areas. As an example, a case where all storm winds contribute significantly is shown in Fig. 3, where each storm wind may dominate the distribution for a certain range of wind speed; e.g. extratropical storms for V < 50 mph, tornadoes for V > 150 mph, and thunderstorm and hurricanes for the range in between. In this case, local wind data may not exist for wind beyond return-periods of 50 years (V > 60 mph); however, through the above method of modeling, the risk of very high wind speeds may be estimated with some confidence.

Seismic Hazard Analysis

In the case of earthquakes, the hazard that may be expected at a site will depend on the size of earthquakes in the region surrounding the site, as well as on the distances to the potential zones of ruptures in the region. The seismic hazard of interest to engineering is the maximum ground motion intensity that can be expected at a site over the life of a structure. Invariably, this has to be determined through regional information or recorded earthquake data for the region in question.

The maximum intensity of ground motions that may be expected over the life of a structure, or facility, will obviously depend on the seismicity and tectonic geology of the regions surrounding the site of the structure. In particular, it will depend on the distances to existing faults, the expected frequency of significant earthquakes in the region, as well as the relative frequencies of earthquakes of different magnitudes that are potentially possible in the region. As these regional and seismic parameters are difficult to specify exactly, the expected lifetime maximum ground motion is also difficult to determine precisely. Determination of the lifetime maximum ground motion at a given site is realistically possibl only in terms of probability; specifically the annual probability of exceedance.

The necessary exceedance probabilities for a given site may be obtained through seismic risk analysis; different models may be used for this purpose. The model of Der Kiureghian and Ang (1977) is proposed and described herein. This model is consistent with the tectonic theory of earthquakes, which assumes that an earthquake is the release of stored energy in the earth's crust through a series of intermittent ruptures along zones of weakness in the crust, known as faults. In particular, the Der Kiureghian-Ang model includes the effects of the length of the rupture zone, and the maximum ground motion at a site is determined by its shortest distance to the rupture of an earthquake. With this model, the region surrounding a site may be modeled by one or more of three different types of potential earthquake source origins, depending on the available knowledge of the seismo-tectonic characteristics of the region, as follows:

Type 1 source -- known faults; in this case, the location and direction of the fault line(s) are known, and the rupture will originate somewhere on the fault and subsequent ruptures will be along the fault.

Type 2 source -- fault orientation known; in this case, when an earthquake occurs the exact location of the rupture is unknown, but the orientation of the rupture is along the fault orientation.

Type 3 source -- unknown faults; both the orientation and location of the rupture are completely unknown, and the fault ruptures may propagate in any direction starting from the focus of the earthquake.

When an earthquake occurs somewhere in the region surrounding a site, the motion that will be recorded or felt at the site will depend specifically on the following:

a. The magnitude of the earthquake, m.

b. The length of the fault rupture which is related to the magnitude; e.g. by the relation $s = e^{am-b}$.

c. The intensity-magnitude-distance relation, or attenuation equation, that determines the ground motion at the site as a function of magnitude m and distance r to the fault rupture; i.e. $y = f(m,r)$.

Moreover, as far as the maximum lifetime ground motion that may be expected at the site is concerned, it will also depend on the frequency or average occurrence rate of significant earthquakes ($m \geq m_o$) in the region. Since the magnitude of an earthquake is not predictable, it may be described as a random variable. Following Richter's law of magnitude, the appropriate probability distribution is the truncated exponential distribution.

$$F_M(m) = k\left[1-e^{-\beta(m-m_o)}\right]; \qquad m_o \leq m \leq m_u \tag{16}$$

where, $k = 1-e^{-\beta(m_u-m_o)}$.

On the basis of the above, and the assumption that the occurrence of significant earthquakes (i.e. with magnitude $m \geq m_o$) constitutes a Poisson process, the probability of the annual ground motion exceeding y is

$$P(Y > y) = \sum_{i=1}^{n} \nu_i P(Y > y|E_i) \tag{17}$$

where:

E_i = the occurrence of an earthquake with magnitude $m \geq m_o$ in source i;

ν_i = mean occurrence rate of earthquakes with $m \geq m_o$ in source i;

n = number of different sources in the region.

Since the magnitude of the event E_i is random, and may be described with the probability density function $f_M^i(m)$, the conditional probability in Eq. 17 becomes

$$P(Y > y|E_i) = \int_{m_o}^{m_u} P(Y > y|E_{i,m}) \, f_M(m) \, dm \tag{18}$$

in which,

$E_{i,m} = E_i$ with magnitude between m and m + dm.

m_u = maximum possible magnitude in source i.

The main problem in the calculation of the annual exceedance probability, therefore, is the evaluation of $P(Y > y|E_{i,m})$. This will depend on the type of potential source, i.e. whether it is type 1, 2, or 3. The details of calculating the appropriate annual exceedance probability for each of the three source types are described in Der Kiureghian and Ang (1977).

The result of a seismic risk analysis, as outlined above, may be presented in terms of the annual exceedance probability curve for all ground motion intensities of interest as illustrated in Fig. 4 for a site in Diablo Canyon (Ang and Newmark, 1977). For this particular site, the modal value of the lifetime maximum acceleration (in 100 years), from Fig. 4, is 0.175 g.

Response of Structures to Natural Hazard Environment

Most of the loadings associated with natural hazards are dynamic and random. The response of a structure, or system, to such a loading environment is also random; hence, the statistics of the maximum response are of interest and needed in the assessment of structural safety.

The required response statistics may be determined through repeated Monte Carlo calculations; results obtained by Monte Carlo simulations, however, are difficult to generalize; moreover, because large samples of repeated solutions are required, the method could be costly if used routinely, especially for the maximum response of multi-degree-of-freedom

systems. Recent analytical methods for determining the maximum response statistics are summarized in the following.

Linear Systems

If only the linear response is under consideration, e.g. in the study of unserviceability, and the excitations can be modeled as stationary Gaussian processes, closed-form solution for the response statistics of both single and multiple degree of freedom systems can be obtained by the random vibration method. Such is the case in the analysis of the response of structures to wind (excluding tornadic wind which is generally transient and may produce extremely nonlinear structural behavior). Under such conditions, the maximum response over a duration, t_o, can be described approximately by a Fisher-Tippett Type I extreme-value distribution with a mean and standard deviation given by (see Davenport, 1964)

$$E(Y_{max}) = \bar{Y} + \left(\sqrt{2\ln \nu t_o} + \frac{.5772}{\sqrt{2\ln \nu t_o}}\right) \sigma_y \tag{19}$$

$$\sigma_{Y_{max}} = \frac{\pi}{\sqrt{6}} \frac{\sigma_y}{\sqrt{2\ln \nu t_o}} \tag{20}$$

in which $\bar{Y}$ = the mean response; σ_y = the root-mean-square (r.m.s.) response; ν = apparent frequency = $\frac{1}{2\pi} \sigma_{\dot{Y}}/\sigma_Y$; and $\sigma_{\dot{Y}}$ = the r.m.s. value of $\dot{Y}$. σ_Y and $\sigma_{\dot{Y}}$ can be obtained by a power spectral density analysis of the response. The foregoing is essentially the theoretical basis of the gust-response factor method adopted by many building codes for the estimation of the dynamic wind effect.

For nonstationary excitations, such as earthquake ground motions, the analytical solution of the random response is generally more involved. Methods (e.g. Lin, 1964; Corotis and Vanmarcke, 1975) have been developed for the solution of the time-dependent moments of the response; however, thus far, simple and closed-form solution of the maximum response statistics can be obtained only when an equivalent stationary response approximation is invoked.

Nonlinear Systems

In the study of structural safety, the response statistics in the nonlinear range are of greater interest since most structures behave nonlinearly prior to collapse. Analytical studies of random vibration of nonlinear systems have been much more limited thus far. Exact solution exists only under very restrictive conditions (e.g. Caughey, 1964). Among the approximate analytical methods, the method of equivalent linearization (Caughey, 1963) has been most widely used. The accuracy of this method is surprisingly good for nonhysteretic systems even with large nonlinearity. However, for hysteretic systems with large nonlinearity, such as elasto-pla or nearly elastoplastic systems, the equivalent linearization method underestimates the r.m.s. response by as much as 60%. This is apparently

due to the fact that for hysteretic systems, the current equivalent linearization method relies on a narrow-band assumption and the average over one cycle of oscillation, which overestimates the energy dissipation capacity of the system. Other methods for hysteretic systems have been based on the principle of balance of power (Lutes and Takemiya, 1974), or the discretization of the response variable using either a finite difference scheme (Paez and Yao, 1976; Vanmarcke and Veneziano, 1973) or a Galerkin method (Wen, 1976). Thus far, applications have been limited to single-degree-of-freedom systems.

The limitations of the equivalent linearization method for hysteretic systems has recently been relaxed (Wen, 1978). A large class of hysteretic restoring forces, i.e. softening or hardening systems with different hystereses, can be modeled by a nonlinear differential equation,

$$\dot{z} = -\gamma|\dot{x}|z - \beta\dot{x}|z| + A\dot{x}, \tag{21}$$

in which z = restoring force; x = displacement; and the equation of motion of the system can be linearized in closed-form as a third-order oscillator. With this improved linearization technique, no narrow-band assumption or averaging over one cycle of oscillation, is needed. In Fig. 5, the restoring forces represented by Eq. 21 for periodic displacement and several combinations of the system parameter γ and β ($A = 1.0$) are shown. A comparison of the results for a nearly elasto-plastic SDF system with Monte-Carlo solutions is shown in Fig. 6. In Fig. 6, Y = yielding displacement, ζ = viscous damping ratio, D/Y = nondimensional excitation intensity. This comparison indicates that the accuracy of the technique is excellent at all response levels. This method can be readily extended to multi-degree-of-freedom systems. The covariance matrix of the response variables can be obtained by solving $3N$ (N = degrees of freedom) linear algebraic equations iteratively for the stationary solution, and by integrating ordinary differential equations numerically for nonstationary solution. Details of this method will be reported elsewhere.

Recently, semi-empirical methods have also been developed for MDF hysteretic systems. The advantage of this method is that the computational effort is relatively insignificant compared with other methods. A method was proposed for elasto-plastic systems (Gazetas and Vanmarcke, 1976), in which the random vibration theory is used but some of the inelastic response parameters require time-history analyses.

Implications for Design

As observed earlier in Eq. 7, the level of safety of a structure against the potential forces of natural hazards may be given in terms of its lifetime probability of failure $p_F(T)$. Also, this will depend on the severity of the lifetime maximum environment; hence, in designing to insu a desired level of protection, the realistic definition of the lifetime maximum environment is important -- an underestimation of the lifetime environment could lead to an unsafe design, whereas an overestimation of the environment may be unnecessarily wasteful.

The level of safety is also a function of the factor of safety, which is a measure of the relative positions of $f_C(r)$ and $f_R(r)$ in Fig. 2. In determining the appropriate safety factor necessary to insure a desired level of safety requires a careful analysis of all sources of uncertainty. This has been a subject of recent interest in the development of reliability-based design (e.g. Ang, 1973), and related applications to earthquake resistant design (Portillo, 1977) and wind resistant design (Rojiani, 1978).

It may be emphasized that for design pruposes, it is the maximum hazard expected over the life of a structure that is relevant; hence, the proper and realistic definition of the maximum environment over this duration, or of its probability distribution, is clearly important. However, specification of the "design" environment or loading, of itself, is not sufficient to insure safety; such an assurance (in terms of an acceptable failure probability) requires the specification of an appropriate factor of safety to be used with the "design" loading.

References

Abbey, R. F., "Risk Probabilities Associated with Tornado Wind Speeds," Proceedings of Symposium on Tornadoes, Assessment of Knowledge and Implications for Man, Lubbock, Texas, June 1976.

Ang, A. H-S., and Newmark, N. M., "A Probabilistic Seismic Safety Assessment of the Diablo Canyon Nuclear Power Plant," Rept. to U.S. Nuclear Regulatory Commission, Nov. 1977.

Ang, A. H-S., "Structural Risk Analysis and Probability-Based Design," Jour. Str. Div., ASCE, Vol. 99, No. ST9, Sept. 1973, pp. 1891-1910.

Caughey, T. K., "On the Response of a Class of Nonlinear Oscillators to Stochastic Excitation," Proc. Colloquium Internationale du Centre National de la Recherche Sientifique, No. 148, Marseille, France, Sept. 1964.

Caughey, T. K., "Equivalent Linearization Techniques" Journal of Acoustic Society of America, Vol. 35, No. 11, 1963.

Corotis, R. B., and Vanmarcke, E. H., "Time-Dependent Spectral Content of System Response," Journal of Engrg. Mech. Div., ASCE, Vol. 101, No. EM5, Oct. 1975, pp. 623-637.

Davenport A. G., "The Distribution of Largest Values of a Random Function with Application to Gust Loading," Proc. Institute of Civil Engineers, London, Vol. 28, 1964.

Der Kiureghian, A., and Ang, A. H-S., "A Fault Rupture Model for Seismic Risk Analysis," Bull. of Seismological Soc. of Am., Vol. 67, No. 4, Aug. 1977, pp. 1173-1194.

Garson, R. C., Catalan, J. M., and Cornell, C. A., "Tornado Design Winds Based on Risk," Jour. Structural Division, ASCE, Vol. 101, No. ST9, Sept. 1975, pp. 1883-1897.

Gazetas G., and Vanmarcke, E. H., "Approximate Random Vibration Analysis of Elasto-plastic Multi-Degree-of-Freedom Structures." Proc. of Int. Symp. on Earthquake Engineering, Vol. 2, St. Louis, Missouri, Aug. 1976.

Gomes, L., and Vickery, B. J., "On Thunderstorm Wind Gusts in Australia", Civil Eng. Trans., Inst. of Eng. Aust., CE18, 2, 1976.

Gumbel, E. J., Statistics of Extremes, Columbia Univ. Press, New York, 1958.

Lin, Y. K., "On Nonstationary Shotnoise", Journal of Acoust. Soc. Am., Vol. 36, 1964, pp. 82-84.

Lutes, L. D. and Takemiya, H., "Random Vibration of Yielding Oscillator" Journal of Engrg. Mech. Div., ASCE, Vol. 100, No. EM2, April 1974, pp. 343-358.

Paez, T. L., and Yao, T. P., "Probabilistic Analysis of Elasto-plastic Structures," Journal of Engrg. Mech. Div., ASCE, Vol. 102, No. EM1, Feb. 1976, pp. 105-120.

Portillo, M., "Evaluation of Safety of Reinforced Concrete Buildings to Earthquakes" Ph.D. Thesis, Dept. of Civil Engineering, University of Illinois at Urbana-Champaign, July 1976.

Rojiani, K. B., "Evaluation of Reliability of Steel Buildings to Wind Loadings" Ph.D. Thesis, Dept. of Civil Engineering, University of Illinois at Urbana-Champaign, Jan. 1978.

Russell, L. R., "Hurricane Effects," Jour. of Waterways and Harbor Div., ASCE, Vol. 97, No. WW1, Feb. 1971, pp. 139-154.

Simiu, E., and Filliben, J. J., "Probability Distribution of Extreme Wind Speeds," Jour. Structural Div., ASCE, Vol. 102, No. ST9, Sept. 1976, pp. 1861-1877.

Thom, H.C.S., "New Distributions of Extreme Winds in the United States," Jour. Structural Division, ASCE, Vol. 94, No. ST7, July 1968, pp. 1787-1801.

Vanmarcke, E. H., and Veneziano, D., "Probabilistic Seismic Response of Simple Inelastic System," paper No. 362, 5th World Conference on Earthqua Engineering, Rome, 1973.

Wen, Y. K., and Ang, A. H-S., "Tornado Risk and Wind Effect on Structures Proc. 4th Int. Conf. on Wind Effect on Buildings and Structures, London, England, Sept. 1975, pp. 63-73.

Wen, Y. K., "Note on Analytical Modeling in Assessment of Tornado Risks," Proc. of Symposium on Tornadoes, Assessment of Knowledge and Implications for Man, Lubbock, Texas, June 1976.

Wen, Y. K., "Method for Random Vibration of Hysteretic Systems," Journal of Engrg. Mech. Div., Vol. 102, No. EM2, April 1976, pp. 249-263.

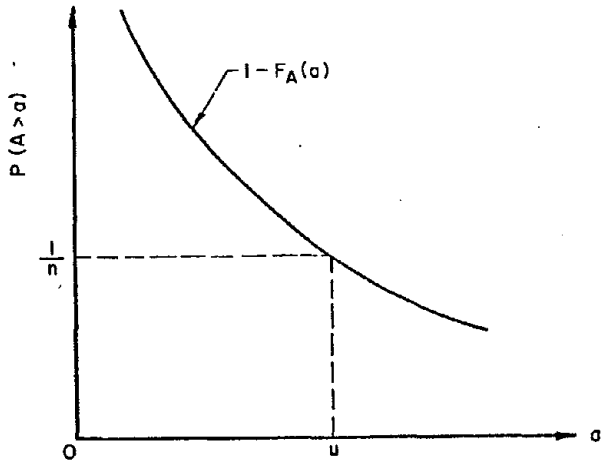

Fig. 1. Exceedance Probability Curve

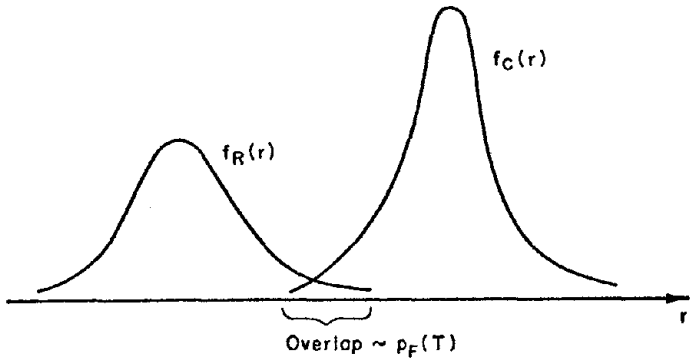

Fig. 2. Probability of Failure

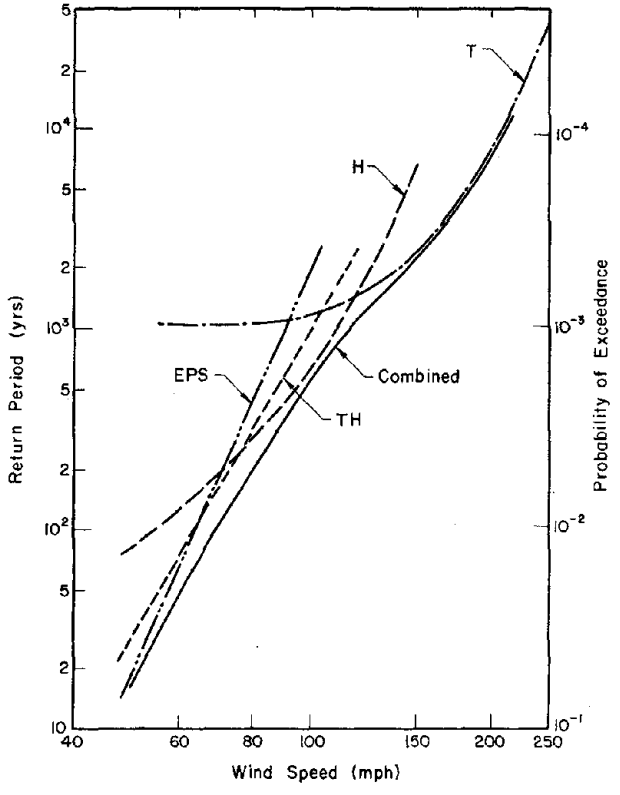

Fig. 3. Exceedance Probability Curve for Mixed Wind System

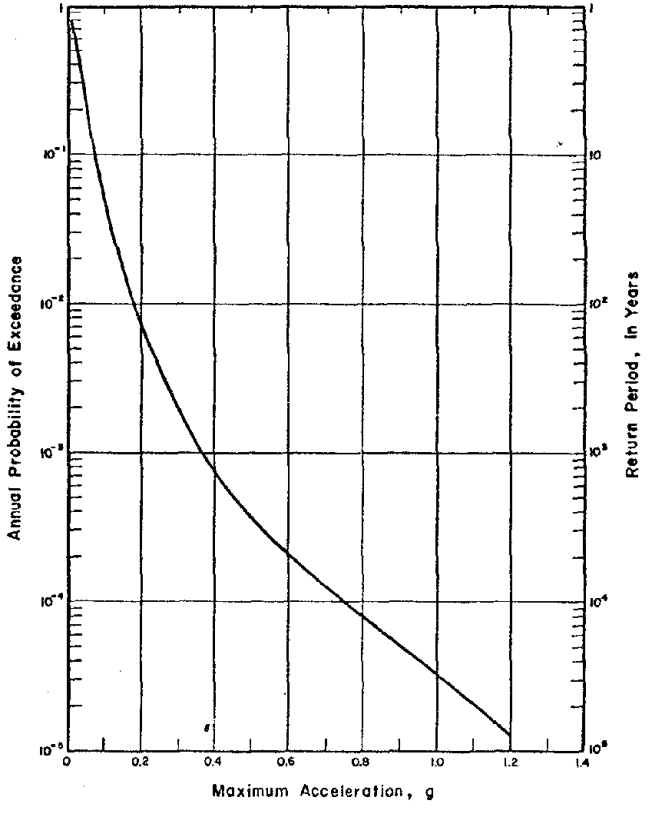

Fig. 4. Exceedance Probability Curve for Earthquake Ground Acceleration (After Ang and Newmark, 1977)

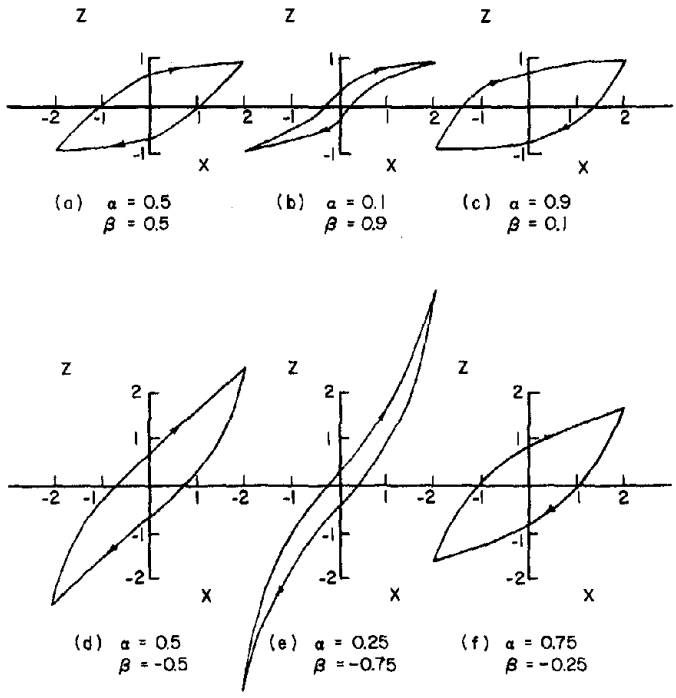

Fig. 5 Shapes of Hysteretic Restoring Force

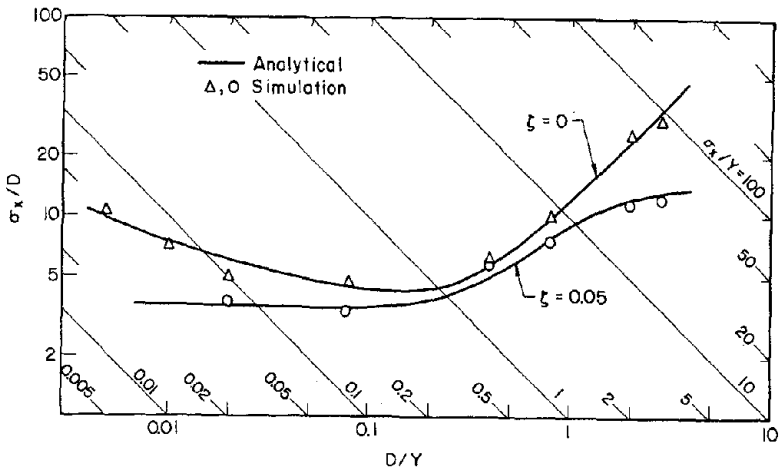

Fig. 6 Comparison of Solutions for Hysteretic Systems

RISK AND DECISION IN ENGINEERING FOR NATURAL HAZARDS PROTECTION

Erik H. Vanmarcke

Massachusetts Institute of Technology

Synopsis

The paper presents a framework of decision analysis within which many of the critical engineering decisions about natural hazards protection can be usefully viewed. The rational resolution of problems of design, surveillance, and rehabilitation of structures in the face of natural hazards requires an understanding of the delicate interplay of technical, economic, and social issues. The proposed approach attempts to put these issues into focus by organizing factual information about risks, costs and losses, both monetary and non-monetary. The paper introduces a quantitative measure of the effectiveness of measures to mitigate hazards, and develops a procedure for evaluating the probable benefits of a hazard mitigation program.

Introduction

Engineering decision-making in the face of natural hazards involves a fundamental trade-off between costly higher levels of protection and higher risks of future economic, social and environmental losses. Much of what we do as professionals is designed to combat and minimize uncertainty: exploration and testing, application of improved analytical procedures, gathering of data about loading and environmental conditions, and so on. But no amount of effort can ever completely eliminate doubts about the predicted performance of structures and foundations. Even after extensive laboratory and field investigation, there always remains some uncertainty about true field conditions, about appropriate design loads and environmental conditions, and about material properties. Therefore, the engineer must invariably make decisions about exploration, analysis, design, construction, and surveillance, under uncertainty.

To date, the profession has quite successfully, essentially by trial and error, developed procedures which do not require explicit, quantitative treatment of risk and uncertainty. For example, the factor of safety format declares a design acceptable if the computed factor of safety exceeds a prescribed value, for example 1.5. But existing factors of safety obviously do not imply absolute safety. They imply a small and presumably acceptable risk of failure during the service life of the structure. Similarly, deformations are computed using a variety of deterministic procedures, ranging from crude and frequently conservative back-of-the-envelope calculations to elaborate nonlinear finite eleme routines for which input parameters must be obtained from extensive field laboratory testing.

In the interest of safety, to compensate for uncertainties, engineers dently make conservative assumptions about the applied load, about the eff the load, about the available resistance, and frequently about all of thes ever, as the uncertainties remain largely unquantified, the degree of cons tism achieved may greatly vary from project to project, and depends on suc tors as the engineer's attitude towards risk and his confidence in the res

a particular set of analyses. Moreover, the confidence is not necessarily justified. A recent study on embankment performance prediction (Hynes and Vanmarcke, 1975) suggests that engineers tend to be overconfident in predictions they themselves make. Failure to make sufficient allowance for real uncertainty jeopardizes safety, while over-reaction to uncertainty leads to "wasteful over-conservatism and less satisfactory solutions than if reasonable risks were accepted" (Peck, 1977).

While most major constructed facilities such as dams, bridges, buildings and highways do properly perform their intended function, and, in the process, generate great benefits for society, they also pose potential hazards to the public, to life and property, and to the environment. The public, government, clients and owners have become increasingly aware of these hazards. In recent years, with people's attention drawn more to finite resources, there is an increasing demand for designers and builders of these facilities to justify the decisions they make and the levels of risk these decisions imply.

Among the natural hazards of concern to civil engineers are extreme wind, earthquake, wave, and snow loads on structures, extreme rainfall or snowmelt causing flooding, and various geological hazards, e.g., limestone solution activity, expansive soil, and landslides.

At issue is not whether or not there is a risk of "failure" of a new or existing structure or foundation. Zero risk is but a lawyer's dream. Unless exorbitant sums of money are spent on data gathering and on inspired interpretation of these data, one must assume that there is some degree of risk. Some of the key questions are then: "how much risk is there?"; "how can risk be controlled, reduced, perhaps avoided, and at what cost and effort?"; and "what level of risk is acceptable, appropriate, or perhaps optimal?"

Engineering Decision Situations

Decisions Involving A Single Project

Engineers must make many kinds of decisions in the face of natural hazards. In the course of a single project, an engineer may be involved in all of the following decision situations:

Site Selection: choose location of the facility, when natural load probabilities are site dependent, or when foundation conditions pose hazards: e.g., solution activity, expansive soils, or erratic soft clay strata.

Exploration and Testing: choose amount and type of exploration and testing, spacing of borings and sample locations.

Design: choose shallow foundation or deep foundation, choose structura out and component dimensions.

Site Improvement: choose whether or not to compact, preload, grout or move questionable materials.

Construction: choose method of construction, rate of construction, met of excavation support.

Surveillance: choose type and scope of surveillance effort (e.g., whe how often to measure deformations, pore pressures, stresses, accelera

All these decision situations have the following features in common: in each case, the engineer must make a choice among alternatives that imply different levels of cost and risk; in each case, the engineer must weigh the cost of each alternative against its effectiveness in reducing risks or better defining risks. Usually, the least expensive alternative (or "solution") implies the greatest risk, while the solution involving least risk costs most. This trade-off between risk and cost is an essential feature of decision-making in engineering.

The decision situations presented above are all interrelated and, to some extent, hierarchical. For example, a hazardous condition (e.g., limestone solution activity) about which one speculates at first, becomes better defined as a project progresses through exploration and construction, and it may be kept in check by a surveillance program during operations.

Decisions Involving Many Existing Structures.

A challenging decision situation faces an engineer, or a group of technical people, charged with the responsibility for the safety of a large number of dams, bridges, or "lifeline" components within some jurisdictional area. Typically (as in the case of dams), there is a mix of existing structures of various sizes, ages, and types of construction, some privately owned, others publicly. Failure of one of the structures may have catastrophic consequences far exceeding the repair or rebuilding cost. The premise of the hazard mitigation program must be that all structures are at risk, and the objective of the program is to minimize future losses due to failure.

This kind of situation poses new and challenging problems for engineers in charge of hazard protection programs. Often operating under severe financial constraints and with limited manpower, they are called upon to affirm the safety of very many structures for which limited technical inspection criteria are available. They also encounter the problem of effectively communicating with the non-technical people who provide funds for the safety programs, i.e., of demonstrating to them the benefits of such programs.

Objectives of Decision Analysis

To respond satisfactorily to the challenges of decision-making under risk, it is useful to have an explicit procedure for combining factual information about costs and risks involved in natural hazards protection; in particular: the potential economic losses in the event of a (catastrophic) failure, the risk (or the probability of failure) attributable to various natural hazards, with or without added protection, and the cost of providing protection. Other important aspects of the problem often cannot be quantified in dollar terms, e.g., human suffering and environmental damage attendant upon a failure event. The de analysis procedure presented in the following section provides a framework organizing all this information and develops specific procedures for (i) q fying risks and benefits in the face of multiple hazards for a single stru (ii) quantifying the (aggregate) benefits of (possible alternative) safety grams, and (iii) dealing with the problem of allocating limited program fu the inspection of many structures with different risks and hazard potentia

Elements in the Decision Analysis for Natural Hazards Protection

Event of Concern and Hazard Potential

A general framework for analyzing decisions about natural hazards protection is shown in Fig. 1. First, one must consider all events of concern and their associated consequences. For example, in dam design and surveillance, the event of greatest concern is a catastrophic failure which results in a sudden discharge of the reservoir contents. The major consequences are loss of human life and property damage in the downstream area. In many other decision situations, the engineer is primarily concerned with lower levels of "failure" which limit the function or serviceability of the structure and which can be repaired, but which do not pose a direct threat to human life. The hazard potential refers to the sum of the potential losses resulting from "failure." Generally, it is a sum of a component which can be expressed in monetary terms and a component which cannot. The quantity C_m will be used to denote the monetary component of the hazard potential; another component may be the life loss potential C_ℓ (measured in number of human lives). These components need not (and many would argue, cannot) be combined into a purely monetary equivalent.

Status Quo or Reference Alternative

In analyzing the benefits of measures aimed at reducing risks, it is very useful to express costs as well as risks in relative or marginal terms, referenced to an existing structure or to an available preliminary design. In other words, one of the alternatives is allowed to serve as a reference or status quo solution. In decisions about repair, inspection, or additional exploration, the reference action may be to "do nothing." In design decisions, the reference solution may be the design obtained on the basis of "common practice." The idea is that if the reference action is taken, no added cost is incurred ($\Delta c = 0$) and some particular (frequently unknown) level of risk (p) is incurred. The risk p denotes the probability of "failure" within a specified period of time (for example, one year or the intended life of the structure). The event "failure" must be defined through its consequences or hazard potential. Specifically, since the quantity C_m is used to denote the monetary component of the hazard potential, the product $C_m p$ equals the probable monetary loss due to failure.

Risk and Relative Risks

In this paper, the term "risk" is interchangeable with "probability of failure." It must be defined in reference to a specific set of consequences (hazard potential) and to a specific time period. Annual risk refers, of course, to the probability of failure during one year. For example, a study of available historical information on dam failures on a national and international basis suggests that an average value for the annual risk of failure of a dam (for al types of dams) is of the order of 10^{-4}, or one in ten thousand per year.(*)

(*) Feld (1965) estimates that 1% of modern dams fail catastrophically durin their "active life" (perhaps 50 to 100 years). Based on data assembled by Middlebrooks (1953), Meyerhof (1970) estimates the frequency of an earth em ment sliding (not necessarily resulting in a catastrophic failure) during t first few service years (5 years?) at 0.5%. Carlier (1974) states that the rent world-wide frequency of catastrophic failure among an estimated 10,000 over 45 feet high is one every 15 months (at a cost of 50 human lives, on t average).

Importantly, the (annual) risk can always be expressed as a sum of contributions due to various causative hazards, e.g., hydrological, seismic and geological hazards. For example, in the case of a dam, catastrophic failure may be caused by overtopping during a flood, internal erosion, ground motion during earthquakes, etc. Specific strategies for protection are often designed to limit the risk posed by a specific hazard. Spillway capacity is upgraded to counter the threat posed by floods, piezometers are installed to monitor seepage, etc. It is therefore useful to express the risk p as a summation of probabilities each of which refers to a specific cause of failure.(*)

$$p = \sum_j p_j \qquad (1)$$

where p_j = risk due to hazard j. Another useful interpretation of Eq. 1 is that the subscript j refers to a specific mode of failure or level of failure. For example, in analyzing landslide risks, failure events may be categorized according to type (rockfall, slide, flow), velocity, or volume of sliding material. It is also advantageous in many cases to allow the (components of the) hazard potential to depend on j; specifically, the probable monetary loss due to failure can then be expressed as follows: $C_m p = \sum_j C_{m,j}\, p_j$, where C_m = average monetary loss due to failure, and $C_{m,j}$ = monetary loss due to failure in mode j. This particu- model is further analyzed in a later section (see Eqs. 7-11). Whichever the precise interpretation of the subscript j, the ratios p_j/p in Eq. 1 are relative risks which sum to one.

In the case of an existing dam, relative risks will be about the same for all dams of the same type (e.g., earth dam, with or without spillway, etc.), within the same age range and with similar foundation conditions. Dam location may become a significant factor if the jurisdictional area involved is large: for example, if it covers several different seismic zones. Based on a study of the causes of past dam failures, the report of an ICOLD (Int. Comm. on Large Dams) Committee (1976) gives the following relative risks for all types of dams:

Foundation problems	40%
Inadequate spillway	23%
Poor construction	12%
Uneven settlement	10%
High pore pressures	5%
Acts of war	3%
Inept operation	2%
Earthquakes	1%
Miscellaneous	4%
Total:	100%

Foundation problems and inadequate spillway capacity are the leading cause dam failure. A breakdown of these results according to the type of dam (g arch, buttress, and earthfill or rockfill), and according to age, is also able (see 1974 ICOLD report on "Lessons from Dam Incidents").

The main point is that in a typical dam safety program, perhaps no mo about a dozen sets of relative risks will have to be estimated. Each rela

(*) Eq. 1 assumes that all contributing hazards or modes of failure are re ted in the summation, and that the individual mode failure events cannot o simultaneously.

risk value is expressed as a percentage of failures likely to be caused by a particular hazard, and can be estimated from information about the causes of past failures supplemented by professional judgment and mathematical probability analysis.

Effectiveness of Added Protection

The most important step in a decision analysis is to analyze all alternatives that differ from the reference alternative. These are measures or strategies for providing different levels of protection against "failure": changes in design, site improvements, repair measures, surveillance programs, reservoir lowering, etc. For each alternative, the engineer must evaluate the incremental cost Δc and the effectiveness in reducing the risk (associated with the reference alternative). While differences in initial costs are relatively easy to deal with, engineers have little or no experience with quantitative evaluation of the benefits of added protection. These benefits take the form of a reduction in the probability of failure, and hence in the probable losses (economic and social) resulting from failure.

Suppose one is attempting to evaluate the merits of a specific action intended to provide added protection against failure due to natural hazards. The probability of failure with and without the added protection are denoted by p' and p, respectively. Define

$$p' = p(1-r) \tag{2}$$

where the quantity r = the effectiveness of the added protection; it measures the fraction of the risk eliminated by the added protection. The value $r=0$ indicates a totally ineffective measure, since it implies $p' = p$, i.e., there is no change in the risk. The value $r=1$ indicates full (or 100%) effectiveness, implying $p'=0$, i.e., the risk is eliminated. A measure which is 90% effective ($r=0.9$) reduces the risk by a factor of 10, while 99% effectiveness implies a risk reduction by a factor of 100, etc. A negative value of r means that the measure under consideration is expected to increase the risk of failure.

The probability p' may also be expressed as a sum of contributions due to the individual contributing hazards or causes of failure, in a manner similar to Eq. 1:

$$p' = \sum_j p'_j = \sum_j p_j(1-r_j) \tag{3}$$

where p'_j = the risk due to hazard j following implementation of the protective measure under consideration, and r_j = the effectivensss of the protective measure in reducing the risk due to hazard j. Note that the relationship $p'_j = p_j(1-r_j)$ is entirely analogous to Eq. 2. Indeed, r_j may be interpreted in the same way as r. The quantity r_j is the effectiveness in reference to a cific causative hazard, whereas r is the "overall" effectiveness; r_j measur the fractional risk reduction in mode j. Combining Eqs. 1 and 3 yields the lowing simple but important relationship between the values r and r_j , and relative risks (p_j/p):

$$r = \sum_j \left(\frac{p_j}{p}\right) r_j$$

This equation expresses the overall effectiveness r as a weighted combinati the r_j values. The weighting factors (which sum to one) are the relative r p_j/p.

Specific design, repair, or monitoring measures are often quite effective in reducing the risk in a "target" mode of failure (perhaps by an order of magnitude, so that $r_j \simeq 0.9$), but they may be ineffective (or counter-effective) relative to other hazards. As an example, consider the case in which an engineer must decide whether or not to raise the crest of an existing earth dam. There are two competing hazards: overtopping caused by a flood (the risk of which will be reduced by raising the crest) and foundation instability (the risk of which will be increased). Assuming that the risks associated with other causes of failure will not be affected by this design change (i.e., $r_3 = 0$, $r_4 = 0$, etc.), the overall effectiveness will depend only on the relative risks (p_1/p) and (p_2/p) and on the effectiveness indices r_1 and r_2, in accordance with Eq. 4. A negative value of r would assure a decision against raising the crest of the dam, regardless of how much it might cost.

Evaluation of the Benefits of Hazard Protection

Recall that C_m denotes the component of the hazard potential which can be expressed in monetary terms. The average monetary losses with and without added protection are $C_m p'$ and $C_m p$, respectively. The difference between these losses is the average economic benefit resulting from the action under consideration:

$$b_m = C_m p - C_m p' = C_m p r \quad . \tag{5}$$

Provided r is not negative, b_m will range between zero and the maximum value $C_m p$, depending upon the effectiveness of the protection provided.

Higher levels of effectiveness can usually be achieved only at higher cost. This is illustrated in Figure 2. Various strategies for added protection are characterized by their cost Δc and their hazard reduction effectiveness r. The effectiveness can be expressed in monetary terms by computing the expected monetary benefit, $b_m = C_m p r$. Direct comparison of Δc and b_m may be helpful, but other non-monetary components of the benefits (e.g., in the reduction of the hazard to human life) may also have to be considered in arriving at a decision regarding the appropriate level of effort to reduce the risk of failure.

The methodology just presented can also be used to evaluate a social component of the benefits of providing protection, measured in expected number of lives saved per year. It suffices to substitute the economic component of the hazard potential, C_m, by the life loss potential, C_ℓ (measured in number of lives). The risk p and the effectiveness r frequently remain the same. Completely separate treatment of the different components of the hazard potential is sometimes desirable, however. For example, installation of a warning system at a dam site may be aimed solely at preventing life loss (by providing timely warning of an impending failure). In this case, the effectiveness in reducing life loss m close to 100%, while the effectiveness in reducing property loss is nil.

Cost of Providing Protection

The final element in the decision analysis is the cost of providing a protection. A moderate risk reduction may be attainable at little cost, w a virtually complete elimination of the risk might be prohibitively expens A permanent improvement or repair action can be evaluated in much the same as a continuing (year-round) safety program, namely in terms of a reduced risk and of an equivalent annual cost (like a mortgage payment) computed f the fixed repair cost using an appropriate discount rate. (See Whitman et 1975.)

Combining the Elements in the Decision Analysis

To evaluate alternatives in a decision situation, the effectiveness (r) and the incremental cost (Δc) of each alternative, and the hazard potential, must all be considered. A useful format for assembling this information is presented in Fig. 3, which lists the various contributing hazards, their associated relative risks, and, for each alternative considered, the hazard reduction effectiveness indices r_j. This information can now be pieced together to evaluate the "overall" effectivenss and the expected benefits for each alternative.

The decision analysis procedure thus provides a framework for organizing all the information relevant in a decision situation, and for arriving at balanced hazard protection solutions in which no single contributing hazard or cost component unduly dominates the hazard mitigation effort. It also facilitates communication about risk and the cost of risk reduction among the parties involved in decisions about natural hazards protection, i.e., engineers, owners, contractors, regulatory bodies, and the public.

Optimizing Hazard Protection Programs Involving a System of Existing Structures

The results developed in the preceding sections can also be used to deal with a case that is of considerable practical interest, i.e., where decisions must be made about inspection and rehabilitation of many existing structures, e.g., dams or bridges, subject to multiple sources of hazard. The subscripts i and j will be used to refer to a specific structure in the system and a hazard, respectively. For example, p_{ij} is the (annual) risk of failure of structure i due to hazard j, and r_{ij} measures the effectiveness of a safety program in reducing the failure risk of structure i due to hazard j. The total expected annual economic benefits of a safety program are obtained by summing the benefits associated with each structure in the system:

$$\sum_i b_{m,i} = \sum_i C_{m,i}\, p_i\, r_i = \sum_i C_{m,i}\, p_i \sum_j \left(\frac{p_{ij}}{p_i}\right) r_{ij} \qquad (6)$$

where p_{ij}/p_i = the relative risk of failure of structure i due to hazard j, $p_i = \sum_j p_{ij}$ = the total annual risk of failure of structure i, and $C_{m,i}$ = the monetary component of the hazard potential of structure i. (The probable annual number of lives saved can be evaluated using an expression similar in form to Eq. 6, but with $C_{m,i}$ substituted by $C_{\ell,i}$).

As mentioned before, in the case of dams, it appears that the average risk of failure of a typical dam is of the order of 1 in 10,000 per year. It is fore reasonable to adopt this common value $p_i = p \simeq 10^{-4}$ in Eq. 6. (Of cour based on judgement and/or careful examination of available dam failure reco the engineer may wish to refine this estimate by allowing it to depend on t type, age, and design criteria of the dam). For each category of dams for a set of relative risks is developed, one should attempt to construct a tab (as shown in Figure 3) which depicts the effectiveness measures r_{ij} for eve alternative monitoring (or repair) strategy considered for that dam categor call that the r_{ij} values will typically lie between 0 and 1; they indicate fractional amounts by which the decision-maker expects the annual risks to duced following the implementation of the inspection scheme. Most r_{ij} valu

will be close to zero (implying the procedure has little impact on the risk) or close to one (implying a risk reduction by an order of magnitude or more). They must be determined based on a combination of professional judgment, theoretical probability analysis and, to the extent possible, examination of actual failure records.

Eq. 6 also provides a format for studying, in quantitative terms, the interdependence among structures in a system. For example, the flood hazard at a particular dam site may depend on measures taken at upstream dam sites, and may in turn influence the safety of downstream dams. Protection provided against overtopping of one dam has a beneficial effect on all downstream dams.

Given a fixed annual budget for a safety inspection program covering many structures of different types and sizes, a reasonable objective in designing the program, i.e., choosing the mix of protective actions to be taken, is to maximize the total expected benefits. Unless economic issues strongly dominate, one is led into the domain of multiobjective analysis (see for example, Major, 1973, Lind, 1976, and Whitman et al., 1975), which attempts to consider all components of the hazard potential simultaneously.

Extension of Results: Multiplicity of Limit States

A generalization of the aforementioned analyses is possible. It will be of interest when one must deal with different limit states (i.e., different degrees of failure) and levels of consequences, or when protective measures under consideration affect not only the failure probabilities, but also the consequences in the event of failure (i.e., the hazard potential). For a discussion of limit states, associated costs, and indirect consequences in relation to the seismic hazard to structures, see Rosenblueth (1973).

All results will now be expressed in terms of expected losses instead of probabilities, and effectiveness will be measured in terms of fractional reduction of expected losses. The equations below parallel those presented in Eqs. 1 through 5. The monetary component of the hazard potential is dealt with herein, but other components could be analyzed in the same way.

First, the expected monetary loss without added protection is expressed as a sum of contributions:

$$C_m p = \sum_j C_{m,j}\, p_j \qquad (7)$$

Note that different failure modes now have different (monetary) consequences $C_{m,j}$ If $C_{m,j} = C_m$, Eq. 7 reduces to Eq. 1. If added protection is provided, the total expected monetary losses become

$$C'_m p' = \sum_j C'_{m,j}\, p'_j = \sum_j C_{m,j}\, p_j\, (1-r'_j)$$

where r'_j = effectiveness in reducing expected losses attributable to failure mode j. The overall effectiveness r is defined by

$$C'_m p' = C_m p\, (1-r)$$

Combining Eqs. 7, 8, and 9 yields

$$r = \sum_j \left(\frac{C_{m,j}\, p_j}{C_m p} \right) r_j \qquad (10)$$

which is analogous to Eq. 4. The ratio $(C_{m,j}\, p_j)/(C_m p)$ denotes the fraction of the expected monetary losses attributable to failure in mode j. Finally, the average economic benefit of added protection is

$$b_m = C_m' p' - C_m p = C_m p r \qquad (11)$$

which is identical (in form) with Eq. 5. Note, however, that the overall effect now expresses a fraction of the product $C_m p$, not of p alone; and it is also differently related to the effectiveness indices r_j. The tabular portrayal in Fig. 3 can very easily be modified by replacing (p_j/p) by $(C_{m,j} p_j / C_m p)$.

Concluding Comments

The paper has presented a methodology to deal quantitatively with risk and decision in engineering for natural hazards protection, when there is a multiplicity of hazards, levels of failure (limit states), and components of hazard potential. It appears that the key quantities in the proposed analysis (fractional expected losses and effectiveness indices) are relatively easy to assess based on engineering judgment, data about the causes and consequences of past failures, and mathematical probability analysis.

Many decisions in engineering for natural hazards can be usefully examined in a decision analysis framework just presented. The approach attempts to put technical and socio-economic issues into proper focus by organizing factual information about risks, costs and losses, both monetary and non-monetary. It is particularly helpful in clarifying the role and the potential use of risk evaluation in engineering practice. Specifically, the tools of risk and decision analysis will help engineers by:

(a) providing a format for summarizing and transmitting information about past failures, about the relative frequency of various causes of failure, and about the effectiveness of different methods for preventing (or reducing the likelihood of) failure.

(b) providing a framework for achieving balanced designs in which no single contributing hazard or cost component unduly dominates the hazard mitigation effort.

(c) clarifying issues of liability in engineering. Which party (engineer, owner, contractor, public) is exposed to what type of risk during which phase of a project? Explicit recognition of where the risks lie, how large they are, and how they can be controlled, may also lead to better contracting through agreed-upon assignment of risks in contracts.

(d) facilitating communication about risk and the cost of risk reduction among the parties involved in decisions about natural hazards protection, including owners, regulatory agencies, and the public.

(e) quantifying the benefits of, and justifying expenditures for, measures which are primarily aimed at risk reduction, such as improved design and analysis procedures, more exploration and/or testing, or a surveillance effort during construction or operation.

Finally, it may be of interest to raise some other issues in the area of natural hazards mitigation which have not been covered herein, but which could profitably be viewed in the framework provided. These are: (i) the benefits of land use control policies which may help to reduce the hazard potential, (ii) the trade-off between governmental expenditures for post-diaster aid vs. safetv inspection and rehabilitation, and (iii) the choice between providing for h levels of protection at the design stage and spending more on instrumenta surveillance during construction and operation.

References

1. Carlier, M., "French Laws and Regulations Regarding Dam Supervision and Inspection," Proceedings Engineering Foundation Conference on Inspection Maintenance and Rehabilitation of Old Dams, Asilomar, Calif., Sept. 1973, published by ASCE, 1974, p. 198.

2. Feld, J., "The Factor of Safety in Soil and Rock Mechanics," Proc. Sixth International Conference on Soil Mechanics and Foundation Engineering, Montreal, 1965.

3. Hynes, M.E. and Vanmarcke, E.H., "Reliability of Embankment Performance Prediction," Proc. ASCE Engineering Mechanics Division Specialty Conference, U. of Waterloo, Canada, May 1976. Also M.I.T. Research Report R75-42, October 1975.

4. ICOLD Committee on Failures and Accidents to Large Dams, "Lessons from Dam Incidents," 1974.

5. ICOLD Committee on Risks to Third Parties from Large Dams, Report issued March 1976, Mexico D.F., 1976.

6. Lind, N.C., "Consequences of Failure (Including Human Reaction)," Proceedings of the Sixth World Conf. on Earthquake Engineering, New Delhi, India, Jan. 1977.

7. Major, D.C., "Multiobjective Redesign of the Big Walnut Project," in Systems Planning and Design, R. de Neufville and D. Marks, Eds., Prentice Hall, 1974.

8. Middlebrooks, T.A., "Earth-Dam Practice in the United States," Transactions ASCE, 1953.

9. Peck, R.B., "Pitfalls of Overconservatism in Geotechnical Engineering," Civil Engineering, ASCE, February 1977, pp. 62-66.

10. Rosenblueth, E., "Analysis of Risk," Invited Paper, Proceedings 5th World Conference on Earthquake Engineering, Rome, Italy, 1973.

11. Vanmarcke, E.H., "Decision Analysis in Dam Safety Monitoring," Proceedings Engrg. Foundation Conference on Safety of Small Dams, Henniker, New Hampshire, Published by ASCE, 1974, pp. 127-148.

12. Vanmarcke, E.H., Cornell C.A., Whitman, R.V. and Reed, J.W., "Methodology for Optimum Seismic Design," Proceedings 5th World Conference on Earthquake Engineering, Rome, Italy, 1973.

13. Whitman, R.V., Biggs, J.M., Brennan, J.E., Cornell, C.A., de Neufville, and Vanmarcke, E.H., "Seismic Design Decision Analysis," Journal of the Structural Division, ASCE, Vol. 101, May 1974, pp. 1067-1084.

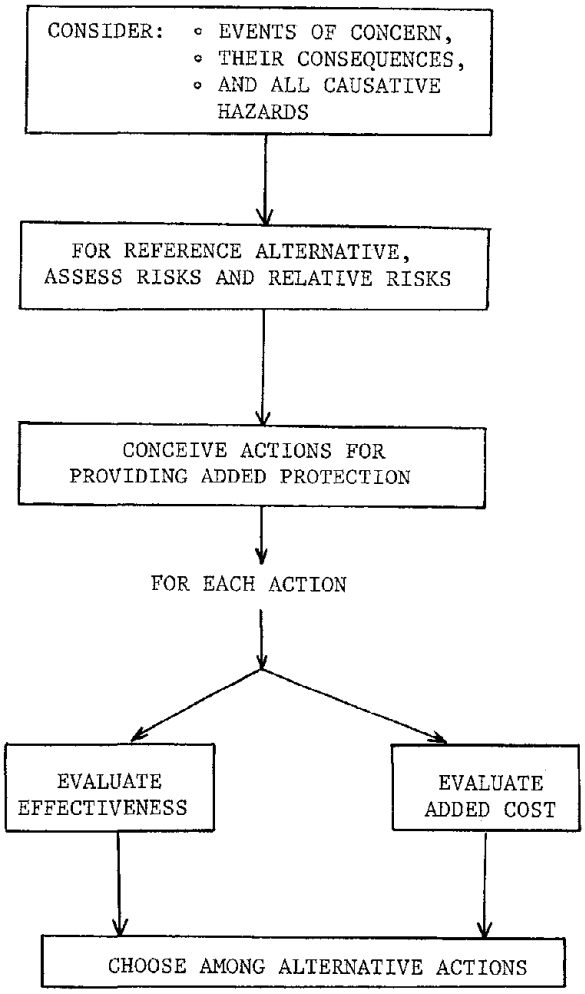

Figure 1 - General Framework of Decision Analysis For Natural Hazards Protection

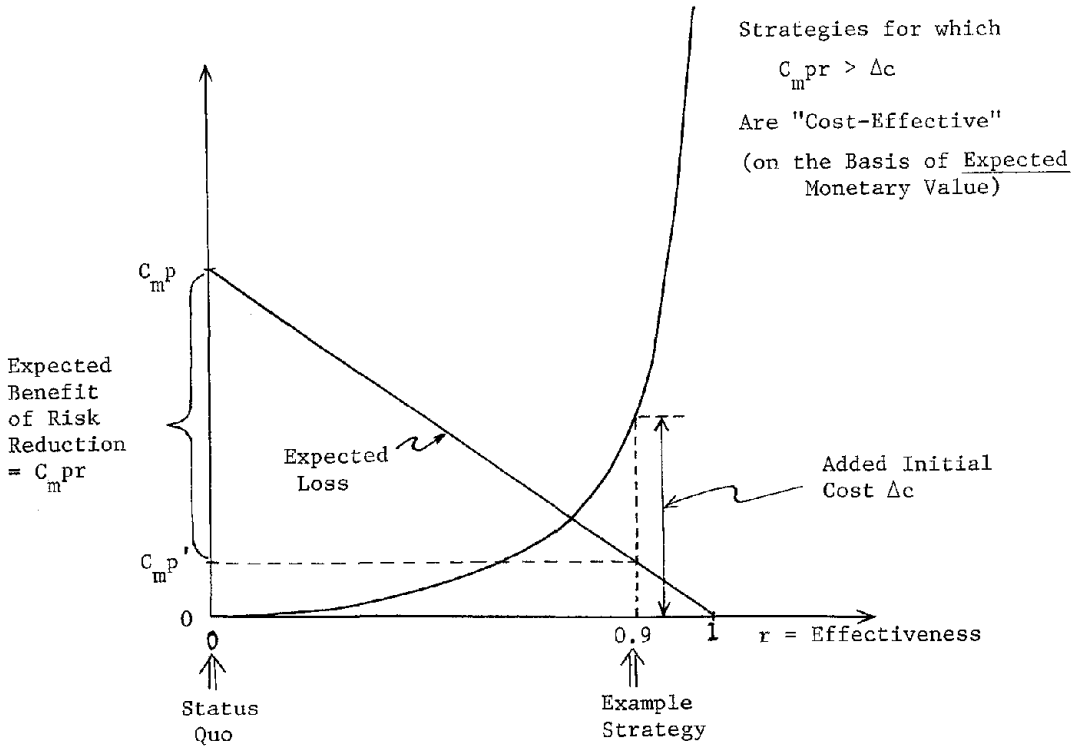

Figure 2 - Portrayal of the Effectiveness, Added Cost, and Expected Benefits of Alternative Strategies for Providing Added Protection. All Strategies are Compared to a Status Quo or Reference Action.

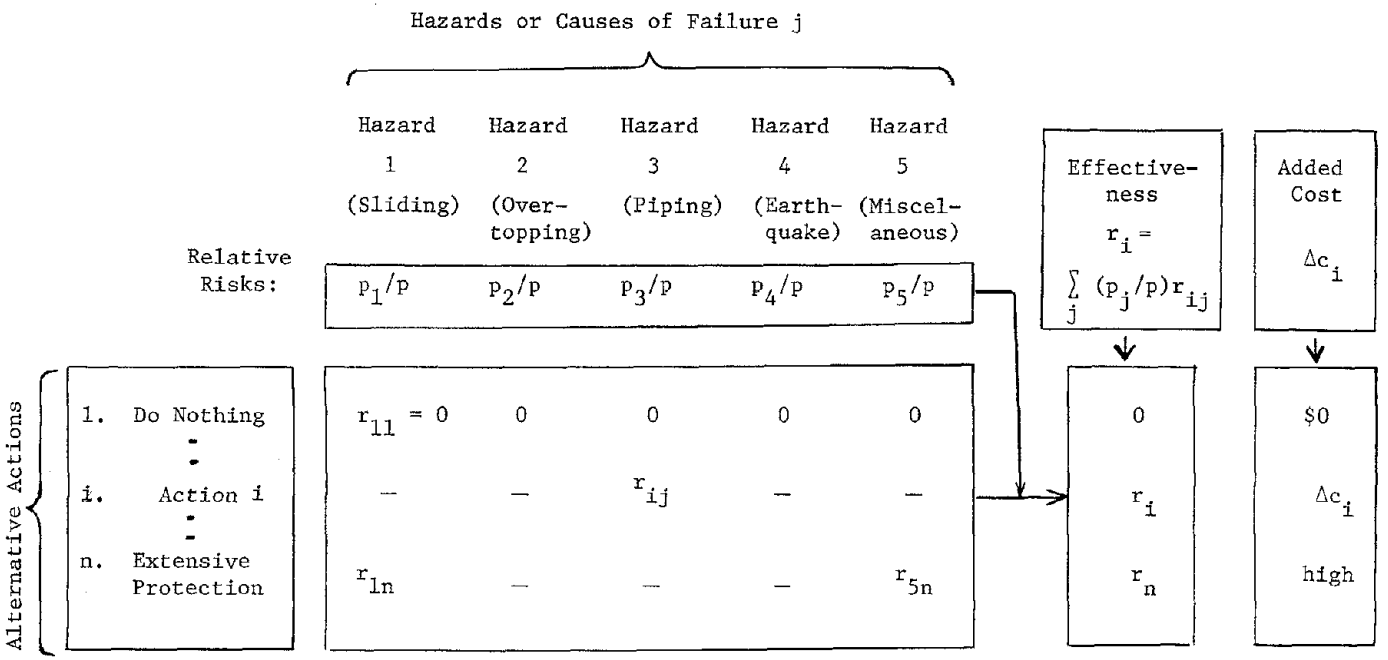

Figure 3 - Example of an "Effectiveness Matrix" Showing Causes of Failure, Their Relative Risks, and the (Risk Reduction) Effectiveness of Alternative Actions for Natural Hazards Protection.

EARTHQUAKE RISK ANALYSIS FOR METRO MANILA

Fr. Sergio S. Su, S.J.
Manila Observatory

Abstract

Gumbel's extreme value theory is applied to the estimation of probabilities of occurrence and return periods of large earthquake intensities in Metro Manila. The probability model of Epstein and Lomnitz is used. Methods of calculation follow those of E & L, as well as of Shakal and Willis. Two sets of data are analyzed, namely, from 1861 to 1940, and from 1952 to 1976. Results of regression analysis show very good agreement between the two sets, even though their time intervals differ considerably. This work for Metro Manila is a pilot project for a much larger undertaking, that is, the seismic zoning of the entire Philippines.

EARTHQUAKE RISK ANALYSIS FOR METRO MANILA

Fr. Sergio S. Su, S.J.
Manila Observatory

Theory and Method

In Gumbel's theory (1954), the "Type 1" distribution of the largest values is:

$$G(y) = \exp(-\alpha e^{-\beta y}) = Pr(Y \leq y) \qquad (1)$$

This is the probability that an observed Y is less than a chosen y, or the probability that y is a maximum in a given period, e. g. a year. Only two assumptions are required: namely, that the parent population of the observations have some form of exponential distribution; and that the observed extremes are independent. Making their separation interval equal to a year seems to assure this independence.

Epstein and Lomnitz (1966) arrive at the same distribution (1) by a different model, based on two other assumptions: namely, that the annual number of earthquakes follow a Poisson distribution; and that the earthquake magnitude is a random variable following a cumulative exponential distribution. Their return period for a given magnitude y is

$$T_y = 1/N_y = -1/\ln G(y)$$

Shakal and Willis (1972), on the other hand, following Gumbel' original derivation, give the return period:

$$T_y = 1/(1-G(y))$$

In practice, (2) and (3) agree very closely for T_y greater tha

yrs. Conceptually, (3) gives the return period in the "extreme" population while (2) gives the return period in the parent population. (3) gives the average interval between two annual maxima of value y, while (2) gives the interval between events of value y, regardless of their relationship to the year. In this paper (2) is used because, for lower values of y, it seems to give more reasonable values of T_y.

For purposes of calculation, (1) is put in logarithmic form:

$$\ln (-\ln G) = \ln \alpha - \beta y \qquad (4)$$

Substituting intensity (Modified Mercalli), I_{mm}, for y:

$$I_{mm} = (\ln \alpha)/\beta - 1/\beta \ln (-\ln G) \qquad (5)$$

Which gives the regression line, with intercept $(\ln \alpha)/\beta$, and slope $-1/\beta$. $(\ln \alpha)/\beta$ is called the modal annual maximum, or the most probable or most frequently observed annual maximum.

The observed annual maxima I_j are arranged in increasing order. To each I_j is associated a G(y) or $G(I_j) = j/(n+1)$. The points I_j are plotted against ln (- ln G).

From the regression line (least square fit), values of $N_y = -\ln G$ are obtained for given values of I. $T_y = 1/N_y$. 95 % Confidence Intervals for the T_y's are obtained by standard statistical procedure.

Data

Two sets of earthquake intensity data are used. Intensit: for the first set, covering a period of 80 years, from 1861 to : are directly taken from the Philippine Weather Bureau Bulletins the given years. Rossi-Forel intensity, I_{rf}, is converted to M fied Mercalli intensity, I_{mm}. Intensities for the second set,

ing a period of 25 years, from 1952 to 1976, are derived from the magnitude data of USGS, making use of Intensity-Attenuation Curves for the Philippines (Fig. 1). These curves are derived from the isoseismal maps of 40 Philippine earthquakes compiled by Fr. M. Saderra Maso, S.J. (1895).

Regression analysis results are shown in Fig. 2 and Fig. 3. It may be noted in these figures that there are two regression lines for each set of data. This is due to the fact that allowance is given for two possible values for each of the very large intensities. This is indicated in the figures by the arrows connecting the two possible values. This practice is dictated by the fact that two different catalogues of destructive Philippine earthquakes in two separate issues of the Philippine Weather Bureau Bulletins give variant values for some very large earthquakes. Note for example in Table 1, that there are two possible values for the intensity of the 1658 earthquake.

Return periods for various intensities, as listed in Table 2, show very good agreement between one regression line of the 1861-1940 interval and another regression line of the 1952-1976 interval.

Relationship between I_{mm} and horizontal peak ground acceleration is usually given by the Gutenberg-Richter formula (1956):

$$\log a_h = 0.333\ I_{mm} - 0.5$$

where a_h is given either in cm/sec^2 or in % g.
Murphy and O'Brien (1977) give a summary of other correlation tions derived by other authors.

For microzoning of Metro Manila, other data, such as so amplification factors for different parts of the city, should superimposed on the results of this study.

This study is a pilot project for a proposed larger undertaking, the seismic zoning for the whole Philippines.

REFERENCES

Epstein, B. and C. Lomnitz (1966). "A Model for the Occurrence of Large Earthquakes", Nature v. 211, 954-956.

Gumbel, E. J. (1954). "Statistical Theory of Extreme Values and Some Practical Applications", National Bureau of Standards, Appl. Math. Series 33, U.S. Gov't. Printing Office, 51 pp.

Gutenberg, B. and C. F. Richter (1956). "Earthquake Magnitude, Intensity, Energy and Acceleration", Bull. Seism. Soc. Am. v. 46, 105.

Maso, M. S., SJ (1895). "La Seismologia en Filipinas", Observatorio de Manila, 122 pp.

Murphy, J. R. and L. J. O'Brien (1977). "The Correlation of Peak Ground Acceleration Amplitude with Seismic Intensity and other Physical Parameters", Bull. Seism. Soc. Am. v. 67, 877-915.

Shakal, A. F. and D. E. Willis (1972). "Estimated Earthquake Probabilities in the North Circum-Pacific Area", Bull. Seism. Soc. Am. v. 62, 1397-1410.

Table 1

Destructive Earthquakes Felt in Manila

Year	I_{rf}	I_{mm}	Interval in yrs.
1601	9	8.5	
			44
1645	10	9.5	
			13
1658	9 (10?)	8.5 (9.5?)	
			41
1699	9	8.5	
			72
1771	9	8.5	
			59
1830	9	8.5	
			22
1852	9	8.5	
			11
1863	10	9.5	
			17
1880	9	8.5	
			57
1937	9	8.5	
			31
1968	9 (8.5?)	8.5 (8.0?)	

Average interval for $I_{mm} \geq 8.5$ is 36.7 yrs.

σ (S. D.) = 20.2 yrs.

Average interval for $I_{mm} = 8.5$ is 45.9 yrs.

σ = 16.7 yrs.

Table 2

I_{mm}	1861 - 1940 Return Period	1952 - 1976 Return Period
10.0	130.03 ± 18.83*	134.18 ± 39.74*
9.5	83.98 ± 11.02	85.61 ± 22.91
9.0	54.25 ± 6.39	54.61 ± 13.07
8.5	35.04 ± 3.67	34.84 ± 7.36
8.0	22.63 ± 2.07	22.23 ± 4.09
7.5	14.62 ± 1.16	14.18 ± 2.23
7.0	9.44 ± 0.63	9.05 ± 1.19
6.5	6.10 ± 0.34	5.77 ± 0.62
6.0	3.94 ± 0.19	3.68 ± 0.33

* 95 % Confidence Interval

1861 - 1940:

$$I = 4.43171 - 1.14392 \ln(- \ln G)$$

1952 - 1976:

$$I = 4.54939 - 1.11256 \ln(- \ln G)$$

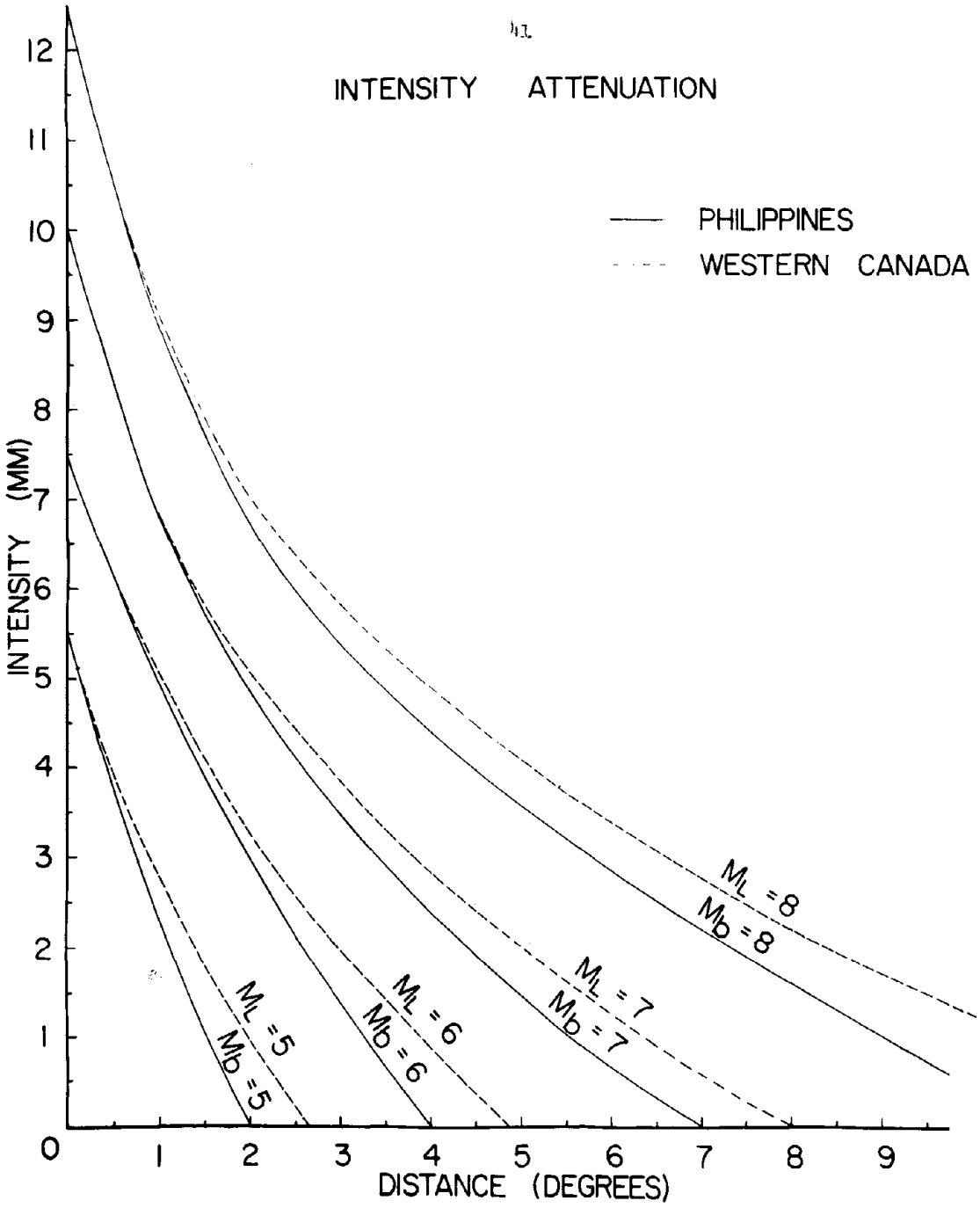
INTENSITY ATTENUATION
PHILIPPINES
WESTERN CANADA
INTENSITY (MM)
DISTANCE (DEGREES)
ML =8
Mb =8
ML =7
Mb =7
ML =6
Mb =6
ML =5
Mb =5

FIGURE 1

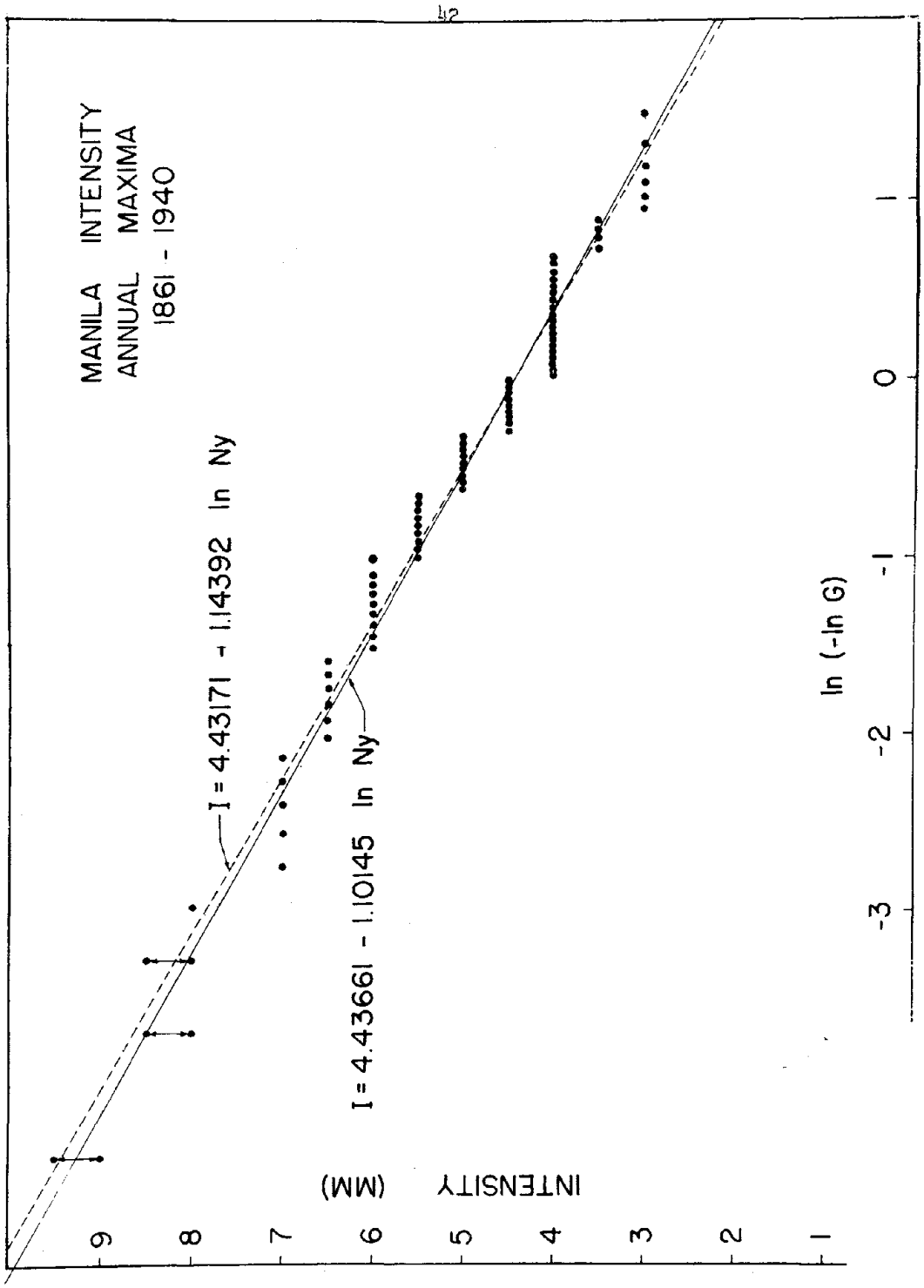
MANILA INTENSITY
ANNUAL MAXIMA
1861 - 1940
I = 4.43171 - 1.14392 ln Ny
I = 4.43661 - 1.10145 ln Ny
INTENSITY (MM)
ln (-ln G)
9
8
7
6
5
4
3
2
1
-3
-2
-1
0
1

FIGURE 2

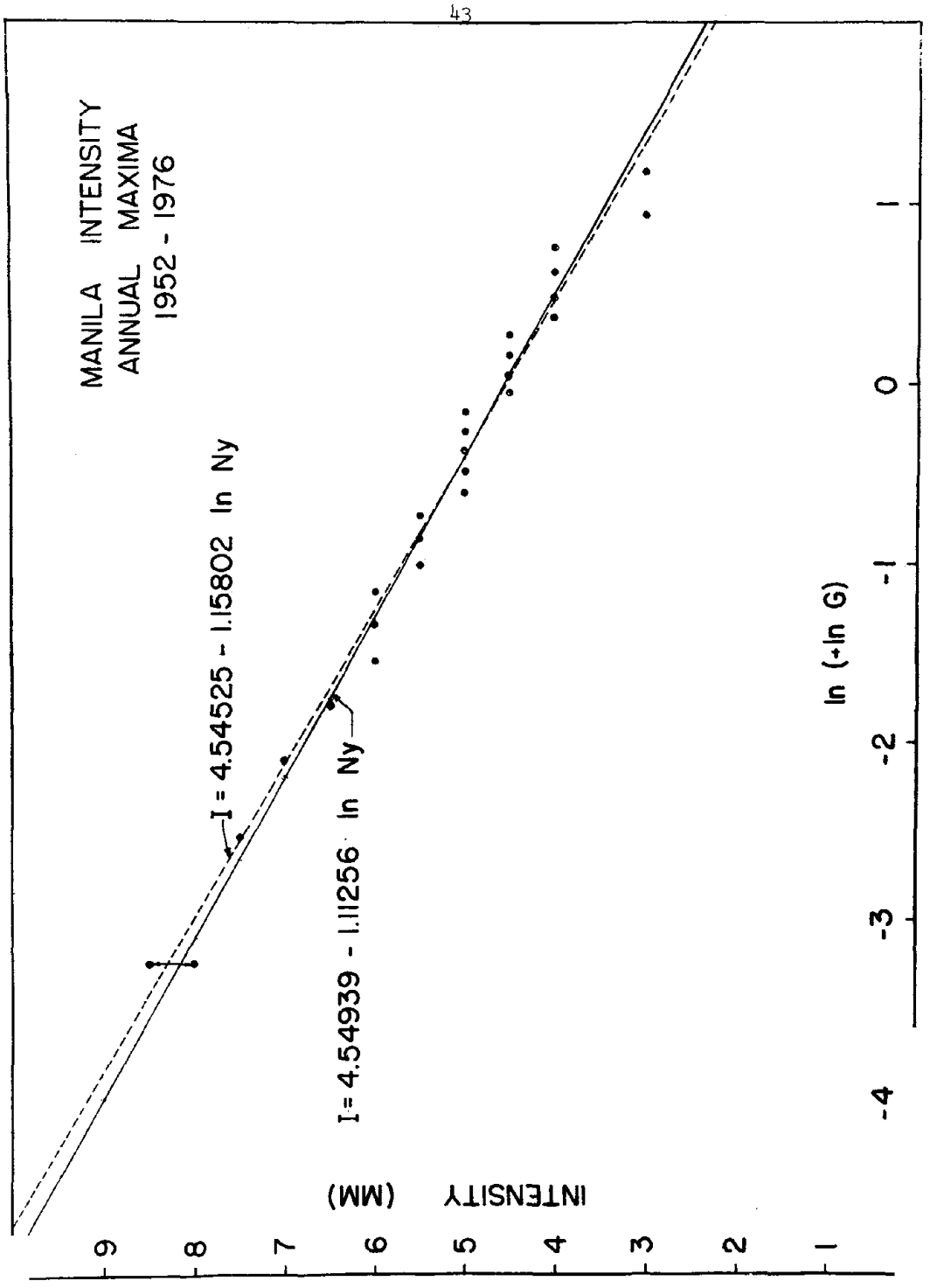
MANILA INTENSITY
ANNUAL MAXIMA
1952 - 1976
I = 4.54525 - 1.15802 ln Ny
I = 4.54939 - 1.11256 ln Ny
INTENSITY (MM)
ln (-ln G)
9
8
7
6
5
4
3
2
1
-4
-3
-2
-1
0
1

FIGURE 3

RISK ANALYSIS OF UNDERGROUND LIFELINE NETWORK SYSTEMS

by

M. Shinozuka*
S. Takada**
and
H. Kawakami***

Department of Civil Engineering and Engineering Mechanics
Columbia University

*Professor of Civil Engineering, Columbia University

**Research Associate, Department of Civil Engineering and Engineering Mechanics, Columbia University

***Senior Research Assistant, Department of Civil Engineering and Engineering Mechanics, Columbia University

Synopsis

A methodology of risk analysis for underground lifeline systems is developed and applied to the water transmission system in the City of Tokyo. The topological or the network characteristics of the system are analyzed for the evaluation of its possible unserviceability. The unserviceability basically results from failures of the water pipelines under the earthquake acceleration and depends on the local ground conditions, the intensity of the earthquake and the resisting capacity of the pipe structure. The local ground conditions, the intensity and the occurrence of earthquakes are treated as random quantities with characteristics unique to the Tokyo area. The probability of unserviceability of the system subjected to an earthquake of a specific intensity is evaluated for the system.

Introduction

In one of the first papers dealing with network systems, Panousis (1974) modeled a lifeline system as a network of interconnected links and evalua the probability of the network to function properly after an earthquake o random size and location. Taleb-Agha (1975) then extended Panousis' work that the probability can be evaluated for networks of much larger size un the assumption that the resisting strength of each link is an independent variable. However, there still remain many problems unresolved before th risk analysis for underground lifeline systems can be considered even rea ably well established. Particularly notable are (a) the effect of variab of local ground conditions which will result in the variability of consid able magnitude form location to location in the ground amplification fact and (b) the estimation of the resisting capacity of the local pipe struct

as well as that of the network system as a whole. As to the item (a) above, Shinozuka and Kawakami (June 1977 and August 1977) made use of the random process theory in describing such spatial variability of the soil property, evaluated the intensity of the free field strains resulting from the variability and demonstrated the existence of significant correlation between such strain intensity and the frequency of the damage in the water transmission and distribution pipeline system in the Tokyo Metropolitan Area due to the 1923 Kanto Earthquake as provided by Kubo and Katayama (1977). As to the item (b) Panousis (1974) and Taleb-Agha (1975) used the maximum force that a link can withstand without failure as its resisting capacity. In the case of an underground pipeline system, however, experimental as well as theoretical studies indicate that the strain or the relative displacement within the system will serve as the most appropriate measure of the resisting capacity.

The purpose of the present study is to develop a methodology of seismic risk analysis for underground lifeline systems reflecting the special technical features described above and demonstrate a use of such methodology in the risk analysis of the water transmission network system in the City of Tokyo for which the data on underground soil conditions are available. It is also the purpose of the present study to indicate, in the course of such a demonstration, the difficulties in the analysis to be resolved by further studies and to delineate those items on which additional information is vitally needed to make the risk analysis more realistic.

This paper represents a shortened version of a report by Shinozuka, Takada, and Kawakami (1977) to which the readers are referred for details.

Topological Transformation of Networks

The underground lifeline systems to be considered here function as network systems for which not only the structural reliability but also the system serviceability must be examined from the viewpoint of risk analysis. Two basic networks, series system and parallel system, play an essential role in the risk analysis. The probability of failure of the system P_F can be evaluated as

$$P_F = 1 - \prod_{i=1}^{n} (1 - P_{fi}) \tag{1}$$

for the series system and

$$P_F = \prod_{i=1}^{n} P_{fi} \tag{2}$$

for the parallel system where P_{fi} denotes the probability of failure of the i-th link in the system consisting of a total of n links. The implications of Eqs. 1 and 2 are rather obvious: Eq. 1 indicates that the series system wil fail if any one of the n links fails while Eq. 2 implies that the parallel sy will fail if all of the n links fail. It is important to note, however, th Eqs. 1 and 2 are valid only when the failure of one link is independent of the failures of other links of the system.

The actual lifeline network systems are obviously much more complicate These complicated network systems however can be reorganized analytically f an easier evaluation of the probability by means of the tie-set or the cut-analysis, where a tie-set consists of a set of links forming a single path

(series system) connecting between an input node and output node while a cut-set consists of links whose removal from the network results in a malfunction of the system. For example, Fig. 1 shows a network of series systems in parallel (SSP) where each series system is a tie-set network.

In general, an SSP system consist of NT component tie-sets (series system); TS_1, TS_2,... TS_k,..., TS_{NT} with the k-th tie-set, TS_k, consisting of NL_k links; L_{1k}, L_{2k},..., $L_{NL_k,k}$. Taleb-Agha (1975) formulated the method of evaluating the probability of failure of such an SSP system. In particular, the probability P_s (any p/NT) that any p of the NT tie-sets in the SSP system would survive was given by

$$P_s(\text{any } p/NT) = \sum_{i=1}^{NT} K_{pi} \sum_{j=1}^{NC_i} T_{ji} \tag{3}$$

where

$$NC_i = \binom{NT}{i}; \quad K_{pi} = K_{(p-1)(i-1)} - K_{p(i-1)} \; ; \; 1 < p \leq i \; ;$$

$$K_{pi} = 0; \; p > i; \quad K_{1i} = (-1)^{i-1}$$

For an SSP system where tie-sets are all mutually independent without sharing any link between any pair of component tie-sets, the quantity T_{ji} in Eq. 3 is given by

$$T_{ji} = \prod_{k \epsilon I_j^i} P_s(TS_k) \tag{4}$$

with

$$P_s(TS_k) = \prod_{m=1}^{NL_k} P_s(L_{mk}) \tag{5}$$

where $P_s(TS_k)$ and $P_s(L_{mk})$ indicate respectively the probability of survival of the k-th tie-set and that of the m-th link in the k-th tie-set. Since I_j^i is a set of positive integers defining the tie-sets of the combination of NT tie-sets taken i tie-sets at a time, T_{ji} is the probability that all the tie-sets of that combination will survive.

However, for an SSP system consisting of dependent tie-sets with the same link or links appearing more than one tie-set, the probability T_{ji} is given by

$$T_{ji} = \prod_{L_n \epsilon US_j^i} P_s(L_n) \tag{6}$$

with

$$US_j^i = \bigcup_{k \epsilon I_j^i} TS_k \tag{7}$$

where U denoted the union as usual, and L_n identifies the n-th link in the set of all links in the entire system which consists of $\sum_{k=1}^{NT} NL_k$ links. The derivation of the probability T_{ji} in Eqs. 4 and 6 is based on the assumption that the resisting capacity of each link is not a random variab but the strain produced by an earthquake is.

Fig. 2 shows a modified version of the water transmission system in the City of Tokyo consisting of twenty-three (23) links of arc-welded stee

pipes of diameter 1500 mm or more. In Fig. 2, eleven (11) solid circles 1 through 11 indicate junctions of transmission pipelines, three (3) solid squares A, B, and C water supply stations and the arrows the direction of the water flow.

We now consider that the probability of failure of such a system is synonymous to the probability of unserviceability, and attempt to evaluate the probability at a certain output node, say at node 9, as an example: Thus, the probability that water will not reach node 9 from any of the three supply stations is considered as the probability of failure in this example. Under these circumstances, the original network shown in Fig. 2 is transformed into an SSP network as shown in Fig. 3. In constructung Fig. 3, the routes which go through the same nodal points more than once have been excluded. Hence, any node appears in a tie-set of the SSP network at most once.

Annual Risk of Earthquake Occurrence

The locations and magnitudes of the past nineteen earthquakes that occurred in the region within a 300 km radius around Tokyo City during a ninety-six (96) year period between 1872 and 1968 with a magnitude M of 7.0 or more are examined, and the expected annual rate of earthquake with magnitude larger than or equal to M is evaluated as a function of M.

A number of empirical formulas have been proposed for the attenuation law describing the relationship between epicentral intensity and the site intensity in terms of some measure of ground motion. For example, Seed (1968) proposed the attenuation law for the base rock material in terms of the relationship between the peak acceleration α (in g) and the epicentral distance R (in km) as shown in Fig. 4. This is based on the formula provided by Esteva and Rosenblueth (1963) where the relationship is given between the magnitude M and the epicentral distance R. The conversion of the magnitude M into the peak acceleration can be made by approximation, for example, by

$$\alpha = ae^{bM}R^{-c} \tag{8}$$

where a = 110, b = 0.8 and c = 1.6. Eq. 8 permits us to convert the expected rate of earthquake with magnitude larger than or equal to M into the expected rate of earthquake with peak acceleration larger than or equal to α (in percent g) as a function of α in the region of 300 km radius. Combining the expected rate information just derived with the attenuation law given in Fig. 4, we can estimate the annual expected rate of "earthquake intensity" larger than or equal to α at the base rock of Tokyo City. The open circles in Fig.5 show the result of such estimation plotted on the sa diagram as established for the espected rate for a Boston site by Whitman et al (1974) for comparison. In view of the scatter these open circles exhibit, it appears necessary to construct, although subjectively, upper and lower bounds. The shaded area between these bounds then "generally" indicates the base rock annual earthquake risk for the City of Tokyo. For example, the acceleration to be felt at the base rock of Tokyo City area with 50 year return period is approximately 30 gals.

Estimation of Free Field Strains

The behavior of buried pipes under the action of an earthquake is highly complicated and its general quantitative analysis is of overwhelming difficulty. The consensus of the researchers on the behavior of underground straight pipes, however, may be summarized as follows: (a) Pipes generally move with the surrounding soil. The pipe displacements are, however, less than those of the surrounding soil. (b) Natural frequencies of pipes are too high to cause the state of resonance under an earthquake acceleration. (c) The pipe strains are highly sensitive to the phase differences in the waves propagating through the soil along the pipe axis. (d) Axial strains usually dominate in the pipes of smaller diameter while bending strains become important in larger pipes. In view of these observations, the state of the free field strains in the ground surface layer where underground lifeline pipes are buried is first analyzed and examined as a significant measure that would indicate the state of the pipe strains under earthquake acceleration.

The state of the free field strains in the surface layer can be highly complex since an earthquake generally gives rise to seismic waves with different directions of propagation and particle motion involving Rayleigh, Love as well as P- and S- waves. In the current study, however, we consider the wave propagation analysis of the first order approximation not only acceptable for its tractability but also desirable to strike a balance with other aspects of the study (e.g., estimation of annual earthquake risk at a site) in terms of the quality and quantity of available information.

On the basis of these observations, we consider a displacement wave of the following form propagating through the surface layer

$$\delta = f\{\xi - c(\omega)\cdot t\} \tag{9}$$

where δ = particle displacement, ξ = a measure of distance, and $c(\omega)$ = wave velocity as a function of frequency ω. From Eq. 9, it follows that

$$\frac{\partial \delta}{\partial \xi} = - \frac{1}{c(\omega)} \frac{\partial \delta}{\partial t} \tag{10}$$

This equation provides a relationship between the particle or ground velocity, $\partial\delta/\partial t$, and the quantity $\partial\delta/\partial\xi$ which in the present study is considered as a measure of normal or shear strain. Indeed, making use of Eq. 10 in this sense, we obtain the following expression for the strain spectrum $\varepsilon(\omega)$ in terms of the velocity spectrum $S_V(\omega)$ both on the ground surface:

$$\varepsilon(\omega) = S_V(\omega)/c(\omega) \tag{11}$$

The strain associated with pipe bending will be disregarded since it is usually much less than the axial strain considered above.

In the range of the frequency of our current interest, however, $4Hf$, the shear wave velocity associated with the lowest predominant frequency f and the wave length $4H$ is used for $c(\omega)$ in approximation, where H indicate the thickness of the surface layer. It has turned out that the values of $4Hf$ are in a majority of cases between c_1 (= lowest shear wave velocity o the surface sub-layers) and c_2 (shear wave velocity of the base rock).

The velocity spectrum $S_V(\omega)$ on the ground surface depends on the soil conditions of the surface layer and the base rock and also on the nature of the seismic wave arriving at the site propagating through the base rock. For the purpose of the present study, we assume that the velocity spectrum $S_o(\omega)$ at the interface between the surface layer and the base rock can be provided in a specific form common to the entire Tokyo area and further assume that $S_V(\omega)$ can be obtained by multiplying $S_o(\omega)$ by the amplification factor that depends on the local soil conditions.

The soil conditions of the Tokyo Metropolitan area are provided by Kawasumi, Sato and Shima (1974) at nodal points of a grid of meridians (Y) and parallels (X) at 1 km intervals (see Fig. 2). A part of the grid is shown in Fig. 6 with typical nodal points 1,2,3 and 4. At each nodal location, the soil conditions of the surface layer consisting of a number of sub-layers are identified in terms of the shear wave veolocity (VEL), the density (DENS), the thickness of sub-layers (THICK) and damping factor in terms of Q values as shown in Tables 1a for node 1 and 1b for node 4. In Table 1, the first column identifies the sub-layers counting downward from the top while the last row represents the soil conditions of the base rock. Figure 6 also shows the response curves at nodes 1 and 4 which plot the amplification factor m as a function of the frequency under the one-dimensional shear beam assumption, taking into account the varying soil conditions of the sub-layers. For a first approximation, the amplification factor m_i associated with the lowest predominant frequency f_i of node i is used to evaluate $S_V(\omega)$ at the same node as

$$S_V(\omega) = m_i S_o(\omega) \tag{12}$$

Similar curves are constructed for all the nodes of the grid. These curves are constructed, however, using different values of the base rock shear velocity c_2 for different nodal locations. This is not quite consistent with our underlying assumption tacitly made earlier that the base rock consists of a homogeneous material with a unique shear velocity. In the present study, however, such consistency is traded for the analytical practicality, although we recover some of it by using in Eq. 12 the amplification factor m defined as a function of c_2/c_1:

$$m = 1.68 + 1.375\ (c_2/c_1) \tag{13}$$

Equation 13 is proposed by Kawasumi, Sato and Shima (1974) on the basis of empirical data.

To summarize, the procedure of evaluating the free field strain at a node consists of: (a) Find c_1, c_2, H and the lowest predominant frequency f at the node, (b) find the peak acceleration α associated with specified return period from Fig. 5, (c) evaluate the amplification factor m by means of Eq (d) calculate S_V as

$$S_V = m\alpha/(2\pi f) \tag{1}$$

and finally (e) compute the free field strain spectrum as

$$\varepsilon = S_V/(4Hf) \tag{1}$$

Note that the strain spectrum is now independent of ω because of a number assumptions made in the procedure for simplicity and conservativeness. T strain spectrum is then evaluated at all of the nodes of the mesh. In th

evaluation of the probability of failure of the pipeline buried within an area of 1 km^2, the mean value ε_o and the standard deviation σ_ε of the values of the strain spectrum evaluated at the four corner nodes of the square play a significant role. They are defined as:

$$\varepsilon_o = \sum_{i=1}^{4} \varepsilon_i/4 \ , \qquad \sigma_\varepsilon^2 = \{ \sum_{i=1}^{4} (\varepsilon_i - \varepsilon_o)^2/3 \} \tag{16}$$

Probability of Unserviceability

If λ denotes the probability of damage per unit pipe length under an earthquake and if the binomial assumption is made as to the spatial distribution of occurrence of such damage along the pipe, then the probability of damage of a pipe of length ℓ can be written, with $\Delta\ell$ denoting the length element, as

$$P_f(\ell) = 1 - (1 - \lambda\Delta\ell)^{\ell/\Delta\ell} \tag{17}$$

Considering only the axial strain in what follows, we assume for straight pipes that the axial pipe strain can be estimated by multiplying the corresponding free field strain by a factor β which depends on the bondage and slippage conditions between pipes and the surrounding soil. Usually it is considered reasonably conservative to take the value of 1.0 for this factor. Recent studies generally indicate that the effect of curvature of curved pipes or the effect of stress or strain concentration at joints may also be introduced into the analysis thorugh such a multiplying factor. These studies appear to suggest a factor of 1.0 to a maximum of 3.0 for such purposes.

With the mean value ε_o and the standard deviation σ_ε for an area element of 1 km^2 as computed in Eq. 16, we assume that the free field strain ε at any point within the area element has a Gaussian distribution with mean ε_o and standard deviation σ_ε and evaluate the probability that the failure strain ε_f, representing the resisting capacity of the pipe, will be exceeded by the pipe strain $\beta\varepsilon$ as

$$\lambda' = P(\beta\varepsilon \geq \varepsilon_f) = 1 - \Phi\{(\varepsilon_f - \beta\varepsilon_o)/(\beta\sigma_\varepsilon)\} \tag{18}$$

where $\Phi\{\cdot\}$ indicates the standardized Gaussian distribution function. Although λ' does not, rigorously speaking, represent the probability that the buried pipe of certain length will fail under an earthquake, it is used to represent a relative degree of probability with which a pipe of unit length in the area element will fail. Hence, the conclusion of the current analysis would indicate, for example, approximate relative probabilities of unserviceability of different links and different tie-sets. The degree of approximation achieved by this simplified method of failure probability estimation even in the relative sense remains to be examined in a future study. We feel however, that the method does provide reasonable relative values for such probabilities.

Under the assumption introduced above and using Eq. 17, we can write

$$P_f(\ell) = 1 - (1 - \lambda')^{\ell/1} \tag{19}$$

which will be used throughout in the numerical computation.

Finally, it is assumed in the following numerical example that the damage or failure of at least one link in any tie-set implies the failure of that tie-set and that the serviceability of the system (water reaches node 9 by way of any tie-set from any source) requires survival of at least one tie-set in the SSP network.

Numerical Example and Discussion

The method presented above is applied to evaluate the unserviceability probability of the (modified) water transmission system in the City of Tokyo. The shear velocity c_2 of the base rock is assumed to be 600 m/sec while the acceleration spectrum at the interface between the surface layer and the base rock is 30 gal representing the expected peak acceleration with the return period of 50 years. This acceleration value is converted into a corresponding strain value at a node of the grid by means of Eqs. 14 and 15 after being multiplied by the amplification factor m (Eq. 13). Having evaluated the strain values at all the nodes of the grid we use Eq. 16 to compute the mean strain ε_0 and the standard deviation σ_ε of the free field strain ε.

In the present study, no curved pipes, T-shaped pipes or joints are considered, and hence $\beta = 1.0$ is taken throughout for simplicity. The probability λ' is then evaluated with the failure strain $\varepsilon_f=0.002$ and $\beta=1.0$ for each area element by Eq. 18 and modified to $P_f(\ell)$ by Eq. 19 to represent the probability of failure of that part of the pipeline (of length ℓ) within the area element. The use of Eq. 1 will then enable us to evaluate the failure probability of a link. For example, referring to Fig. 2 and looking at the link 6→9, we see that it traverses five (5) area elements a,b,c,d, and e. Write 6→9(a), 6→9(b),..., 6→9(e) for the portions of the link in the area elements a,b,...,e and also write P_{fa}, P_{fb},..., P_{fe} for the corresponding probabilities of failure. We then use P_{fa}, etc. in place of P_{f1}, etc. in Eq. 1 to obtain the probability of failure P_F of the link, which, in the notation of Eq. 5, is L_{mk} or in that of Eq. 6, L_n.

Because some of the links appear in more than one tie-set in the SSP network, we use Eq. 3 together with Eqs. 6 and 7. Also, in view of the assumption made earlier on what constitutes the system unserviceability, the value of p in Eq. 3 is taken to be unity.

The result of the computation is given in Fig. 7 which shows the probabilities of failure of the fourteen (14) tie-sets of the SSP network and of the transmission system itself as a function of the failure strain ε_f. We can see from Fig. 7 that the tie-sets from water supply station A are always destroyed, the one from C is frequently destroyed and in all probabi ties the water will be supplied to node 9 from station B. A closer examinati Fig. 7 further reveals that the tie-set VI (B-4-1-2-6-9) shows the smalles probability of failure for $0.001 < \varepsilon_f < 0.0025$ while the tie-set IX (B-4-7-8- shows the smallest probability for $\varepsilon_f > 0.0025$, each contributing the most among the tie-sets to the serviceability of the system in the respective regions of ε_f just mentioned. The contribution from other tie-sets is not negligible, however. We recognize this from the fact that, when for example $\varepsilon_f = 0.003$, the probability of failure of the system is 0.00023, 1/32 of th failure probability 0.0074 of the most serviceable tie-set IX (B-4-7-8-9).

With respect to the analysis we have just seen, the following comments appear to be in order:

(a) The seismic analysis performed here should be improved by more elaborate statistical analysis on the earthquake occurrence data as well as on the attenuation law.

(b) The method used for the evaluation of the free field strain obviously has some room for improvement even though our interest is in the order of magnitude estimation of the free strain. The method assumes that the strains resulting from the surface layer waves through homogeneous surface layer are the most significant. The spatial variability of the surface layer may, however, have a considerable effect on the magnitude of the strains. The ground amplification factor displays a large scatter which must be taken into consideration in the future analysis. The assumption of constant spectral acceleration or velocity at the interface between the base rock and the surface layer needs to reexamined. The response curves do not necessarily exhibit sharp peaks and therefore physical significance of the predominant frequency may also have to be reexamined.

(c) Conversion of the free field strain into the pipe strain is probably the most difficult step in the proposed procedure of risk analysis. More experimental and analytical studies are definitely needed in this respect for a better assessment of the pipe strains.

(d) In the present study, the probability of pipe failure per unit length is evaluated in a gross approximation. The validity and accuracy of the approximation should be examined more carefully.

(e) The topological analysis performed is for one of the simplest serviceability conditions. The different degrees of serviceability with different consequences must be considered in the future study. This is one of the steps which must be taken in order to extend the current analysis into that of the design decision where the cost-benefit considerations play a dominant role.

(f) Another one of these steps is to evaluate the probabilities of unserviceability at other levels of earthquake intensity. These probabilities must then be combined with the probabilities of such levels of earthquake intensity to describe the overall unserviceability of the system in the seismic environment of the Tokyo area.

Conclusion

As a prelude to a more elaborate risk analysis and eventually to the design decision analysis for the underground lifeline system in seismic environments, a methodology of risk analysis has been developed and applied to a water transmission system in the City of Tokyo. The analysis has provided us with a trend in which the transmission system would behave under an earthquake condition and at the same time with the insight into the complexity of the analysis in terms of necessary data base, computer programming effort, computer time requirement, theoretical sophistication required, etc. Limitations and assumptions involved in the analysis have been delineated and examined, and potential methods of improvement of the approach have been suggested whereever possible.

Acknowledgement

This work was supported by the National Science Foundation under Grant No. ENV-76-09838 (Prime Contractor, Weidlinger Associates; Subcontractor, Columbia University). The authors are grateful to Dr. S.C. Liu of the National Science Foundation for his encouragement and support. They are also grateful to Mr. J. Wright of Weidlinger Associates for his valuable suggestions and discussions during the course of this investigation.

References

Esteva, L. and Rosenblueth, E., "Espectros de Temblores A Distancias Moderadas y Grandes", Proc., Chilean Conf. on Seismology and Earthquake Engineering, Vol. 1, University of Chile, July 1963.

Kawasumi, H., Sato, Y., and Shima, E., "Investigation on the Ground Response and the Distribution of Seismic Intensity for the 23 Districts in the City of Tokyo", Report to the Tokyo Metropolitan Disaster Prevention Congress, 1974 (in Japanese).

Kubo, K., and Katayama, T., "Survey on Underground Pipe Damages due to Earthquake", Report to Tokyo Metropolitan Disaster Prevention Congress, 1977 (in Japanese).

Panoussis, George, 1974, "Seismic Reliability of Lifeline Networks", Seismic Design Decision Analysis - Report No. 15, MIT, Dept. of Civil Eng. Res. Rep. R74-57.

Seed, H.B., Idriss, I.M. and Kiefer, F.W., "Characteristics of Rock Motion During Earthquakes", Rep. No. 68-5, EERC, UC Berkeley, Sept. 1968.

Shinozuka, M., and Kawakami, H., "Underground Pipe Damages and Ground Characteristics", Proc. of TCLEE Specialty Conference at UCLA, August 30-31, 1977, pp. 293-307.

Shinozuka, M., and Kawakami, H., "Free Field Strains and Ground Characteristics", Technical Report No. CU-2, under NSF Grant No. ENV-76-09838, August 1977.

Shinozuka, M., Takada, S., and Kawakami, H., "Risk Analysis of Underground Lifeline Network Systems", Technical Report No. CU-3, under NSF Grant No. ENV-76-09838, in print.

Taleb-Agha, G., "Seismic Risk Analysis of Networks", Seismic Design Decision Analysis - Report No. 22, MIT, Dept. of Civil Engineering Researc Report R75-43, Nov. 1975.

Taleb-Agha, G., "Seismic Risk Analysis of Lifeline Networks" Seismic Desig Decision Analysis - Report No. 24, MIT, Dept. of Civil Eng. Res. Rep. R75-49, Dec. 1975.

Whitman, R. V, et al, "Methodology and Pilot Application", Seismic Design Decision Analysis, Report No. 10, Department of Civil Engineering, MIT, July 1974.

Table 1

Soil Conditions at nodes 1 and 4

(a) X = 7, Y = 18

No.	VEL	DENS	THICK	Q
1	100	1.5	2.7	20
2	100	1.5	3.0	20
3	200	1.5	4.0	20
4	300	1.9	1.0	20
5	200	1.5	9.0	20
6	400	2.0	——	20

Units: VEL, m/sec,
DENS, gram/cm^3
THICK, m

(b) X = 7, Y = 19

No.	VEL	DENS	THICK	Q
1	100	1.5	1.4	20
2	170	1.8	1.8	20
3	100	1.5	3.3	20
4	200	1.5	4.3	20
5	300	1.9	5.6	20
6	200	1.5	7.8	20
7	300	1.9	2.3	20
8	400	2.0	4.0	20
9	250	1.8	——	20

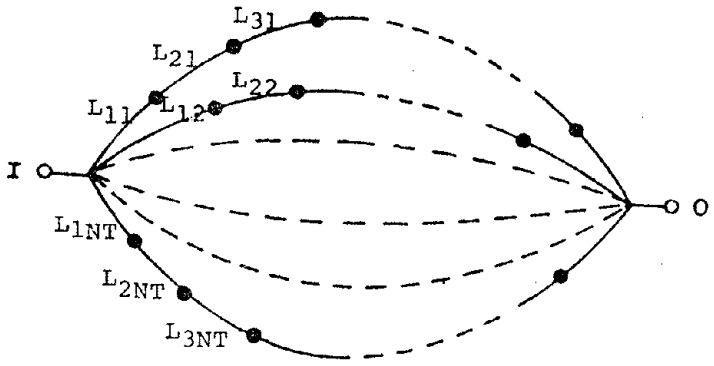

Fig.1 An SSP Network.

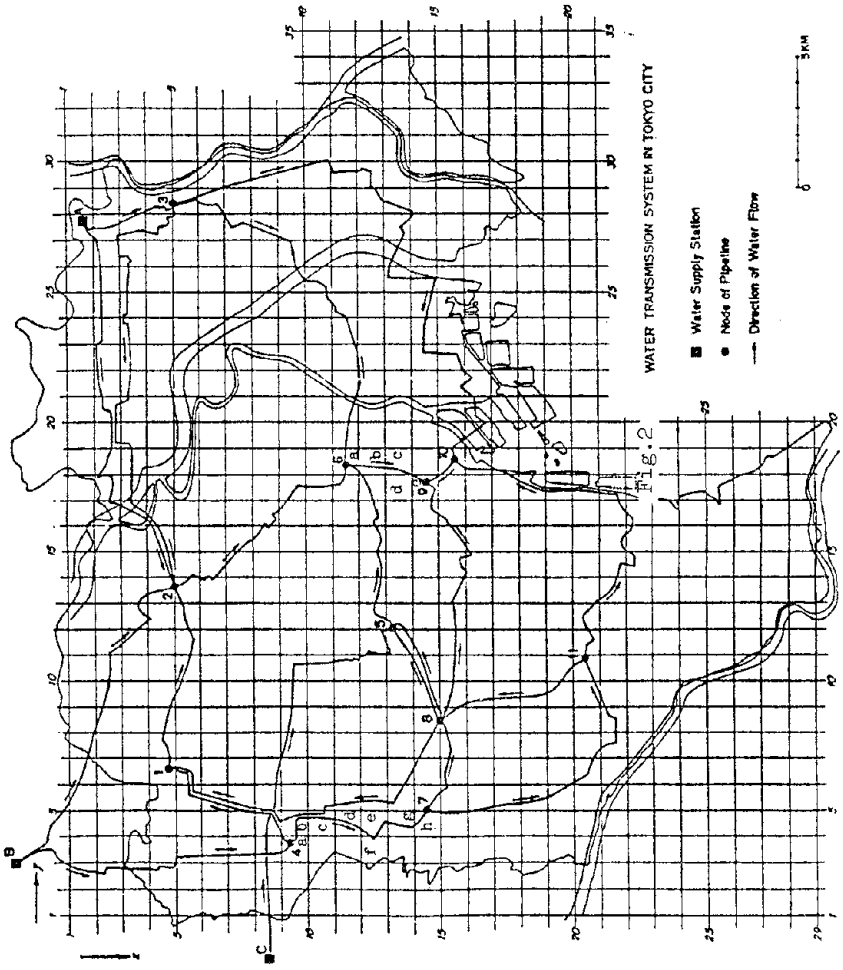
WATER TRANSMISSION SYSTEM IN TOKYO CITY
Water Supply Station
Node of Pipeline
Direction of Water Flow
5KM

Fig.2

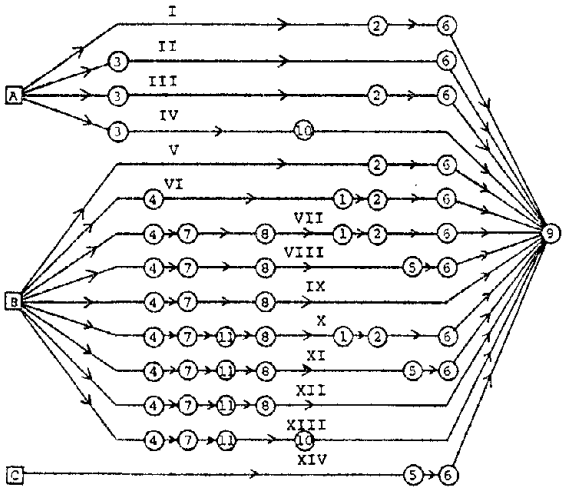

Fig.3 Equivalent SSP Network.

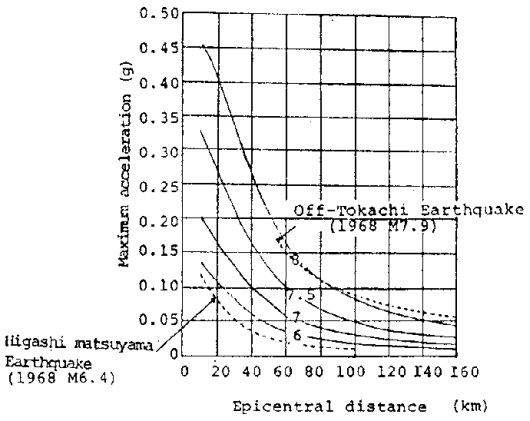

Fig.4 Relationship among acceleration, magnitude, and epicentral distance by Seed.

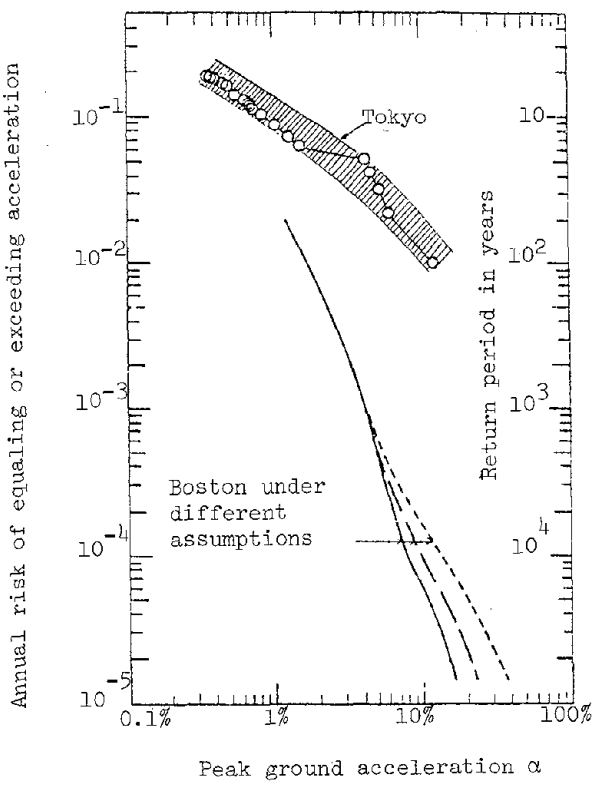

Fig.5 Estimated seismic risk at a Tokyo site on base rock.

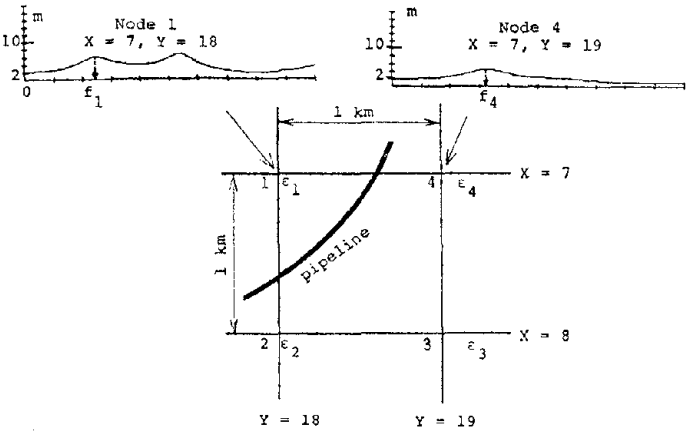

Fig.6 Response curves at corner nodes of 1 km square.

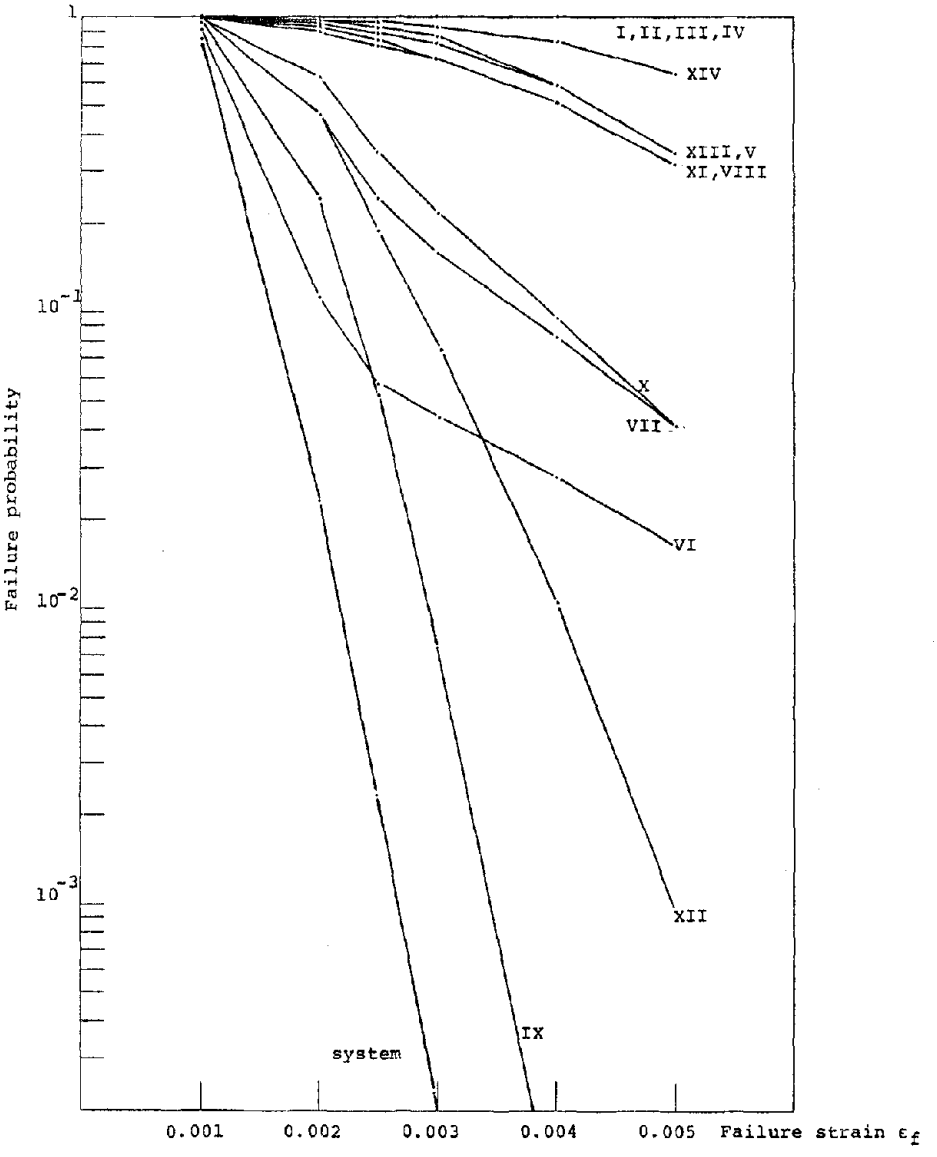

Fig.7 Relationship between failure probability (of tie-sets and system) and failure strain.

STATISTICAL NATURE OF EARTHQUAKE GROUND MOTIONS AND STRUCTURAL RESPONSE

by

Joseph Penzien
University of California, Berkeley

Synopsis

The variable characteristics of strong earthquake ground motions are discussed to provide a basis for the selection of motions for design purposes considering local soil conditions. Emphasis is placed on the selection of motions having statistical characteristics similar to past recorded motions. The variable nature of structural response is presented with the objective of assessing expected damage levels and possible losses.

Introduction

In recent years, the availability of high speed digital computers has dramatically changed methods and procedures used by practicing engineers in designing certain important structures such as nuclear power plants and high rise buildings. Basic knowledge gained from analytical and experimental research and from field investigations can now be applied effectively in developing new and improved seismic resistant designs.

While this change has obviously been beneficial to all concerned, it has raised many questions causing confusion in both the research community and the practicing profession. The author of this paper is of the opinion that many of the problems can be brought into better focus, if the statistical nature of earthquake ground motions and structural response is recognized during the design process. At least much of the confusion can be diminished by formally introducing concepts of probability.

It is therefore the main purpose of this paper to create an awareness of the variable characteristics of earthquake ground motions and structural response so that more realistic assessments of expected damage levels and possible losses will be made.

Variable Characteristics of Ground Motions

The ground motions produced by strong earthquakes are highly irregular with respect to both time and direction. Motions of this type are recorded by accelerographs in terms of three orthogonal components of acceleration, i.e. the vertical and two horizontal directions. Figure 1 presents a single component of acceleration as recorded for each of three U.S. earthquakes, namely, the Western Wa earthquake of April 13, 1949, the Kern County earthquake of July 21, 1952, Parkfield, California earthquake of June 27, 1966. Also presented are the responding components of velocity and displacement which were derived analy directly from their respective accelerograms. It is important to note that three components of ground motion have quite different characteristics. Th differences are readily seen in terms of frequency content, levels of intens shapes of envelope functions, individual pulse shapes, and durations.

Differences in characteristics can also be observed in Fig. 2 which sh relative velocity response spectrum curves for damping values of 0, 2, 5, 1 20 percent of critical for each of the three components of motion describe

This figure also shows by dashed line the Fourier amplitude spectrum for each of the three components of motion. Note that the shapes of the corresponding spectra for the three components of motion are very different. For example, the spectra for the Western Washington earthquake are sharply peaked at a period of about 0.9 seconds with two other lower peaks at about 1.1 and 1.3 seconds. The spectra for the Kern County earthquake are quite different in form showing high peaks at about 0.8 and 1.7 seconds. In contrast with the spectra for these two earthquakes, the spectra for the Parkfield, California earthquake have no pronounced peaks but are rather flat in form over a wide range of periods. Wide differences are also noted in the ordinates for corresponding spectra of the three earthquakes over the entire range of periods represented.

If one should inspect the recorded motions and corresponding response and Fourier spectra for many other earthquakes, significant differences of the type described above would be observed between any two arbitrarily selected components. Thus, it is clear that the form of future ground motions and their characteristics as represented by response and Fourier spectra can be predicted only on a statistical basis.

Selection of Ground Motions for Design

Recorded Accelerograms

While earthquake ground motion at a point actually has six components, Rosenblueth (1973), 3 translational and 3 rotational, it is usually sufficient to consider only the three translational components for design purposes. A very simple approach to defining these three components would be to assume that certain recorded ground motions of a past earthquake are representative of the future site ground motions to be defined. The three accelerograms recorded during the Taft, California, earthquake of 1952 as shown in Fig. 3 are often normalized to the desired intensity level and used for this purpose. One can, of course, question this simple approach as two recorded accelerograms, even for the same site location, often have quite dissimilar characteristics.

Synthetic Accelerograms

Another approach to defining the three translational components of motion for design purposes is to generate synthetic accelerograms which are derived from a set of prescribed response spectrum curves, Tsai (1972) and U.S. Atomic Energy Commission (1973). Two sets of smooth response spectrum curves (normalized to 1g peak acceleration) now commonly used for this purpose are shown in Fig. 4, Newmark, Blume, and Kapur (1973). These smooth curves, which were obtained by a statistical analysis of response spectrum curves for many past recorded accelerograms, represent the mean-plus-one standard deviation level. Two synthetic accelerograms derived from the smooth design response spectrum curves of Fig. 4 are shown Fig. 5. The actual response spectrum curves for the synthetic accelerogra Fig. 5 representing horizontal motion are shown by the solid curves in Fig. they can be compared with the prescribed design spectrum curves. The diff between corresponding actual and prescribed spectrum curves are due to num inaccuracies introduced when generating the synthetic accelerogram. This m of generating ground motions for design purposes can also be questioned for same reason mentioned earlier for the method that simply uses past recorded accelerograms, i.e. the actual characteristics of the future motions produc single earthquake may be significantly different from those of the synthet accelerograms. This method does however have a certain statistical basis, lends support to the method, since the prescribed smooth spectrum curves s represent the mean-plus-one standard deviation level. Therefore, if this

indeed represented and if the intensity of motion based on peak acceleration could be established in probabilistic form for the site, the probability of occurrence for each spectral value in Fig. 4 supposedly could be estimated. There are however certain factors which lead one to question the validity of the spectral values in Fig. 4 as representing the mean-plus-one standard deviation response level, e.g. the effects of local soil conditions on the shapes of response spectra are not considered.

Random Processes

A third approach to defining the three translational components of motion for design purposes is to use the random process defined by

$$\begin{aligned} a_x(t) &= \zeta(t)\ b_x(t) \\ a_y(t) &= \zeta(t)\ b_y(t) \\ a_z(t) &= \zeta(t)\ b_z(t) \end{aligned} \qquad (1)$$

, Penzien and Watabe (1974), where $\zeta(t)$ is a prescribed deterministic intensity function which converts stationary random processes $b_x(t)$, $b_y(t)$, and $b_z(t)$ to nonstationary processes $a_x(t)$, $a_y(t)$, and $a_z(t)$, respectively. This approach has the distinct advantage that a complete ensemble (or family) of possible accelerograms can be generated for each component of motion. The corresponding response spectrum curves can then be generated from which mean spectral values and their variances can be obtained. If the effects of local soil conditions are significant and they can be defined, then such effects should be encorporated into the generation of stationary processes $b_x(t)$, $b_y(t)$, and $b_z(t)$. It should be pointed out that random process a(t) as given by Eq. (1), while having been used very often by researchers, has its own deficiencies in truly representing future ground motions. However, since the number of recorded strong motion accelerograms is rapidly increasing in the world, more sophisticated methods of statistical analysis will undoubtedly be used to better define nonstationary processes $a_x(t)$, $a_y(t)$, and $a_z(t)$. In the meantime, it is the present authors opinion that a simple stochastic model, such as that defined by Eq. (1), can be used effectively to reflect the statistical nature of strong earthquake ground motion.

Effects of Local Soil Conditions

As indicated above, the effects of local soil conditions on the characteristics of free field surface ground motions should be introduced into any method used for defining design earthquake ground motions, provided that they are significant and that they can be quantified in a realistic way. If there is sufficient statistical evidence to warrant it, one should define different smooth design response curves for different soil conditions; thus reflecting the influence of these tions on the generated synthetic accelerograms. Likewise, one should use d filter parameters in the stochastic model to reflect this same influence on ensemble of accelerograms obtained.

Deterministic analyses have been used to attempt to quantify the influ soil conditions on the free surface ground motions. Most of these studies used the one-dimensional shear beam model shown in Fig. 7, Schnabel and Lys (1972). This shear beam is usually modelled linearly but with the elastic viscous damping properties adjusted to reflect mean stiffnesses and total e absorption (hysteretic + viscous), respectively, consistent with the shear levels developed. The horizontal acceleration $a_b(t)$ representing bedrock m is applied at the base of the shear beam and the resulting horizontal surfa

acceleration $a_d(t)$ is determined from a time-history dynamic analysis. If the soil extends uniformly over a large horizontal distance and if the bedrock is indeed moving in one horizontal direction as a rigid body, one can expect reasonable results from this model. However, significant departures from these ideal conditions are often present; therefore, the shear beam model can be seriously questioned. For example, out-of-phase components of horizontal and vertical motions at point c over those present at point b have an influence on the horizontal surface motions at d. If these out-of-phase components are significant in a distance bc of the same order of magnitude or less than the depth of the soil layer, then the rigid horizontal bedrock motion assumption is no longer valid. It would be most helpful in studying this problem if cross correlations of the components of motions at points b and c were known as a function of the distance bc separating them.

It should be recognized that considerable differences in points of view exist among those who attempt to quantify the influence of local soil conditions on the characteristics of free surface ground motions. Even those adopting similar deterministic analytical procedures obtain a wide range of predicted response spectral values for similar site conditions and seismic intensity. Figure 8 is intended to depict this range of values in a qualitative sense only. Considering the fact that large variations in the response of nonlinear systems can occur with small changes in model parameters or in excitation characteristics, this wide range of spectral values can be expected.

The above described variations in results obtained by deterministic methods suggest that perhaps a direct statistical analysis should be used to determine the influence of local soil conditions on the characteristics of surface ground motions. One such study carried out in this manner has been published by Seed (1974). Figure 9 showing the average value of the ratio of response spectral acceleration to maximum ground acceleration plotted against period for four different site conditions has been taken directly from his report. The number of accelerograms used to obtain average values for each site condition is shown in the figure. Figure 10 showing the 84 percentile ratio values (represent average plus one standard deviation for normal distribution) plotted against period for each site condition was also taken directly from Seed's report. Using the mean values in Fig. 9, subtracting from the 84 percentile values in Fig. 10 to estimate the corresponding standard deviations, and assuming both Gumbel Type I (G) and the normal (N) type probability distributions, one obtains results as shown in Figs. 11 and 12 for a period of 1.0 seconds and for rock and deep cohesionless soils, respectively. It is important to note that while there is indeed a correlation of spectral response with site conditions, the coefficients of variation of spectral values in each case are quite large. Therefore, in defining ground motions for design purposes, such variabilities should be reflected in the ground motion modelling.

Variable Characteristics of Structural Response

Probability Distribution of Maximum Response for Fixed Intensity of Ground

Obviously since the characteristics of ground motion are highly varia
can expect the maximum values of structural response to also be highly var
even if we ignore uncontrollable variations in the structure's material an
geometric properties. To illustrate this point, let us examine the result
reported by Penzien and Liu (1969) for a damped single degree of freedom s
using three model types (1) linear, (2) elasto-plastic, and (3) stiffness-
degrading. Subjecting these models, with the elastic period of vibration
2.7 seconds, to stationary filtered (Kanai filter; $\xi = 0.6$, $\omega_g = 15.6$ rad/
white noise excitation of fixed intensity ($S_o = 0.0516$ ft^2/sec^3), the prob

distribution function for maximum relative displacement can be approximated in each case by a straight line on Gumbel (Extreme Type I) plots as shown in Fig. 13. Curves 1, 2, and 3 represent elastic, elasto-plastic, and stiffness-degrading models, respectively, when the viscous damping ratio is set at 2 percent. Curves 4, 5, and 6 are the corresponding curves when the viscous damping ratio is set at 10 percent. Relative displacement can be expressed in terms of ductility factor for the non-linear models and the probability distribution can, for all cases, be expressed in terms of return period measured in number of earthquakes. The significant features of the distributions in Fig. 13 are the following: (1) The most probable maximum displacements at 0.33 on the probability distribution scale are considerably greater for those models having 2 percent of critical damping than for their corresponding models having 10 percent of critical damping; however, these values vary little from one model to another. (2) The standard deviations of maximum displacement are considerably larger for the elasto-plastic and stiffness-degrading models than for their corresponding linear models and are appreciably larger for the elasto-plastic models than for their corresponding stiffness-degrading models. (3) Increasing the viscous-damping ratio increases the standard deviations of extreme value response for each model type. What is more significant to note in this discussion is that maximum response of nonlinear systems have very large variations. These variations are caused by differences allowed in the phase angles of the harmonics present in the ground motion excitations. They are not caused by variations in intensity of ground motion. It has been shown that the variability of response for multi-degree of freedom systems is similar to that shown above for single degree of freedom systems.

Probability Distribution of Maximum Response for Variable Intensity of Ground Motion

If the maximum intensity of excitation to be experienced by the single degree of freedom system is also treated as a random variable, one can expect probability distributions of maximum relative displacement as shown in Fig. 14. Curves 1, and 2 are based on the maximum intensity of excitation having an Extreme Type II probability distribution while curves 3, and 4 are based on a similar distribution but with the tail of the distribution cut off to reflect a finite upper bound to the maximum intensity. The probability distribution of maximum relative displacement for a fixed intensity of excitation is assumed to be Extreme Type I with a coefficient of variation equal to 0.4 for curves 2 and 4 but is taken as a unit step function, with the step occurring at the mean value of the Extreme Type I distribution, for curves 1, and 3. The latter step function distribution corresponds to a coefficient of variation equal to zero. Since for low risk structures, we are interested in that value of maximum response corresponding to some prescribed value near one on the probability distribution scale, a final distribution corresponding to curve 4 which recognizes both intensity of excitation and maximum response as random variables should be used. For a nonlinear system, a coefficient of variation equal to 0.4 is easily possible as shown in Fig. 1 therefore, the distribution given by curve 4 is quite representative of wh could expect in a qualitative sense.

Assessment of Possible Losses

Having established maximum levels of dynamic response for the mathema model in probabilistic form, the results must be interpreted in terms of p performance and possible loss.

As pointed out by Sawyer (1964), failure of a structure under increas generally occurs in successively more-severe stages under successively les probable levels of load. To illustrate this point, he published the relat

given in Fig. 15 which shows failure-stage vs. load (pseudo-static type increasing monotonically) for a typical statically indeterminate reinforced concrete building and states, "The first failure stage is that caused by minor tensile cracking which almost always occurs and which causes very small loss. With higher load reinforcement yields at one, then more progressively longer regions, leading to wide cracking, objectionable deflections, loss of user-confidence, and need for repairs. With further increases in load, spalling and crushing occur, deflections become excessive, and the building is soon evacuated. The final failure stages are the collapse of portions of the frame, followed by the limit stage of collapse of the entire frame." While this relationship is highly variable and depends very much on structural type and structural detailing, it does illustrate very well the basic concept which should be used in assessing performance and possible losses to be expected during the life of a structure, Tichy (1964). Due to the variability of loss for a given load (or the variability of load for a given loss), the relationship shown in Fig. 15 should be considered as representing mean values of the random variables involved. The full distribution, as represented by Fig. 16, can in some cases involve large variances.

For seismic excitation, loss relationships similar to those shown in Figs. 15 and 16 can be estimated where the load and load probability scales are changed to intensity of ground motion and intensity probability, respectively. Such relationships should include possible losses to architectural components such as the interior finish, exterior facing and windows and to mechanical equipment such as elevators. Since these losses are directly associated with inter-story drifts, expected yielding in the main structural system should be limited appropriately.

To make a final realistic assessment of the safety of a structural system as designed, one must recognize all of the uncontrollable variabilities related to such factors as ground motion intensity, ground motion characteristics, structural properties, and mathematical modelling. Since these variabilities are large, the only meaningful assessment is one involving concepts of probability. Therefore, one should attempt to establish the probability distribution function for maximum damage level (or loss) during the expected life of the structure. If the structure is designed to provide very low risk of damage or failure, e.g. nuclear power plant Category I structure, it must be designed with the intent of remaining elastic throughout its life span. The probability distribution function for maximum damage level can then be expected to be similar to that shown in Fig. 17, Type A structure. On the other hand, if the acceptable risk level is considerably lowered so that appreciable inelastic deformations are permitted under maximum credible earthquake conditions, the probability distribution function for the maximum damage level might very well have the appearance of that shown in Fig. 18, Type B structure.

It is important to recognize the large variance associated damage level in the latter case, Fig. 18; particularly, when concerned with the safety of a large number of buildings. The probability that one structure out of a populati will experience a maximum damage level equal to or greater than D is [1 - This indicates that the individual damages of buildings of similar design struction located equal distances from an earthquake epicenter can range f damage to heavy damage or collapse. Observations following damaging earth confirm the validity of this statement.

The above assessment of the safety of a structural system as designed that available knowledge has been applied effectively. Unfortunately, too this is not the case as evidenced by many structural failures where the ca be traced to errors in design or construction or to a lack of quality cont Every effort should, of course, be made to eliminate these causes.

Concluding Remarks

An attempt has been made in this paper to create a better awareness of the uncertainties involved in predicting structural response and to encourage the use of probabilistic methods in assessing seismic risk. All probability distributions presented are intended to reflect realistic statistical trends but should not be assumed accurate in a quantitative sense. Hopefully, the general discussion presented will be helpful in bringing certain problems involved in seismic design into better focus.

Acknowledgment

This paper is based primarily on the contents of a keynote address given by the author at the Second Canadian Conference on Earthquake Engineering, McMasters University, Hamilton, Ontario, Canada, June 4-5, 1975, which has been published in the Proceedings of that Conference.

References

[1] California Institute of Technology, Earthquake Engineering Research Laboratory, "Strong Motion Earthquake Accelerograms".

[2] Newmark, N. M., Blume, J. A., and Kapur, K. K., "Design Response Spectra for Nuclear Power Plants," Proceeding ASCE Annual Meeting, San Francisco, Ca., April 1973.

[3] Penzien, J., and Watabe, M., "Simulation of 3-Dimensional Earthquake Ground Motions," Bulletin of the International Institute of Seismology and Earthquake Engineering, Vol. (1974).

[4] Rosenblueth, E., "The Six Components of Earthquakes," Proceedings of the Australian and New Zealand Conference on the Planning and Design of Tall Buildings, Sydney, Australia, August 14-17, 1973.

[5] Schnabel, P. B., and Lysmer, J., "SHAKE, A Computer Program for Earthquake Response Analysis of Horizontally Layered Sites," Earthquake Engineering Research Center Report No. EERC 72-12, University of California, Berkeley, 1972.

[6] Seed, H. B., Ugas, C., and Lysmer, J., "Site-Dependent Spectra for Earthquake-Resistant Design," 1974.

[7] Tsai, N. C., "Spectrum-Compatible Motions for Design Purposes," Journal of Engineering Mechanics Division, ASCE, Vol. 98, No. EM2, Proceedings Paper 8807, April 1972.

[8] U. S. Atomic Energy Commission, "Design Response Spectra for Seismic I Nuclear Power Plants," Regulatory Guide 1.60, Rev. 1, Directorate of Regulatory Standards, December 1973.

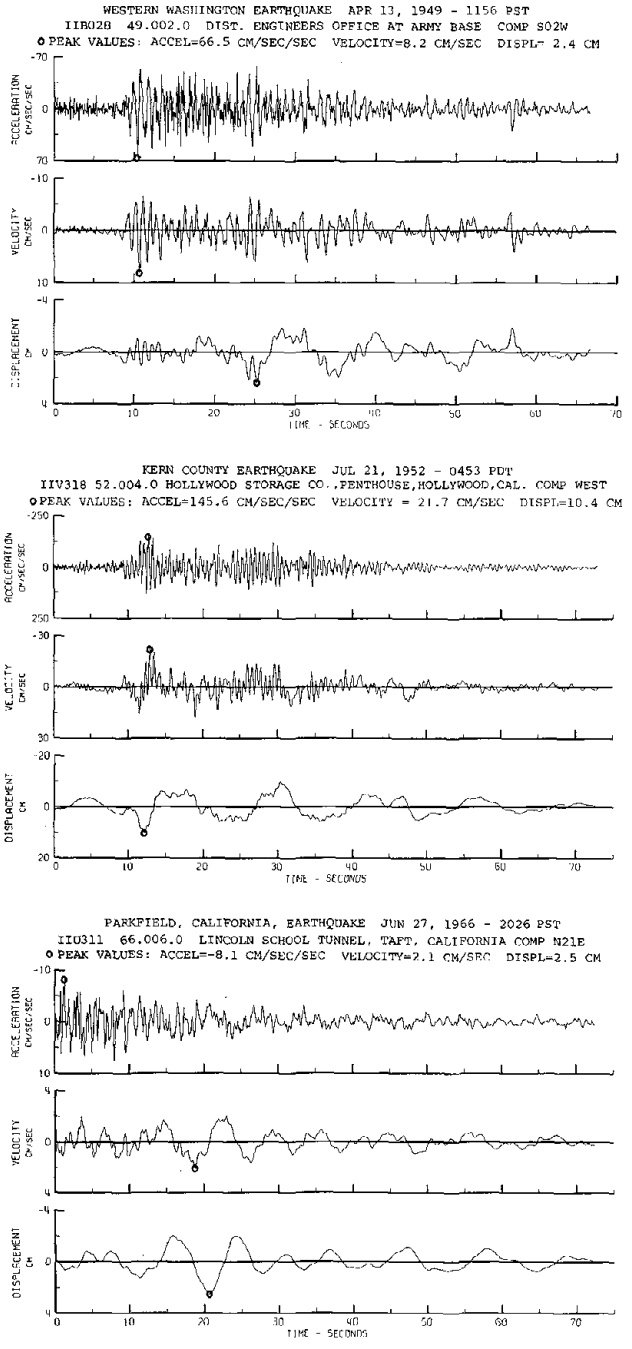

FIG. 1 Ground motions recorded during three different earthquakes - from Ref. 1

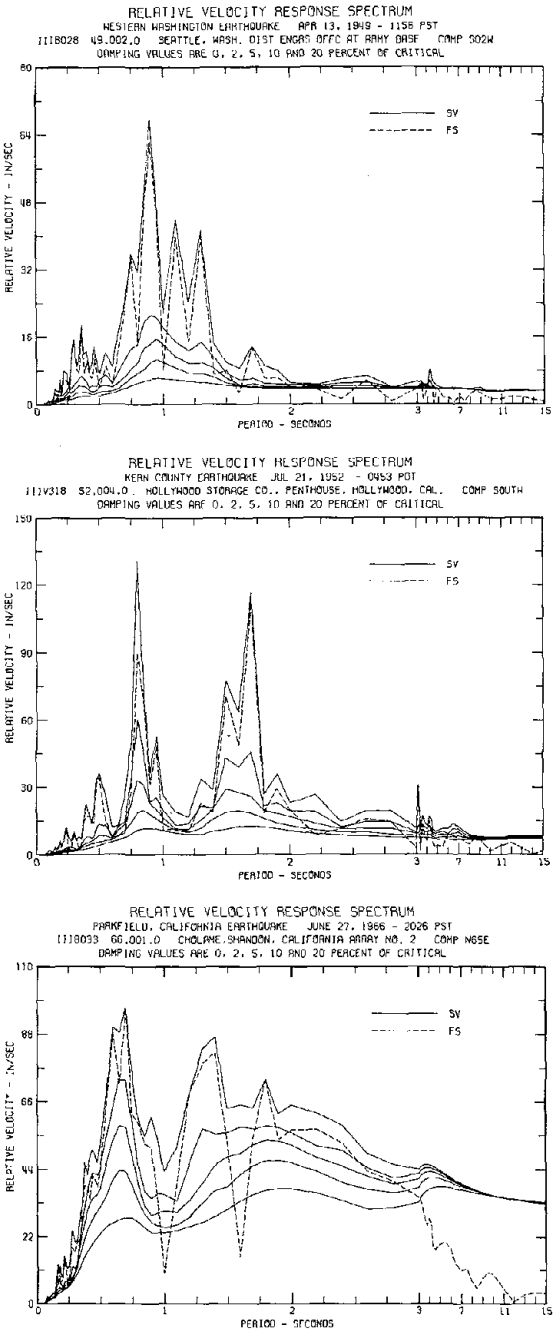

FIG. 2 Response spectra for ground motions in Fig. 1 - from Ref. 1

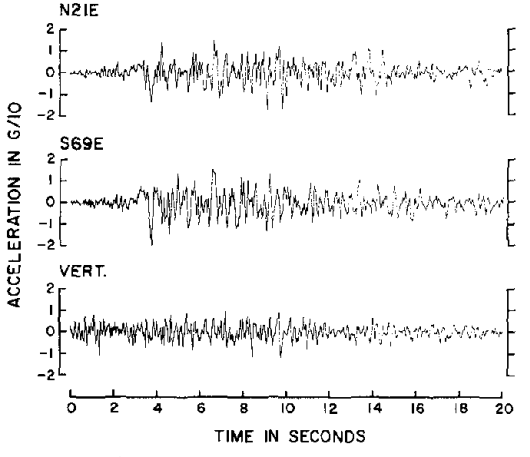

FIG. 3 Accelerograms
Taft, California, earthquake,1952

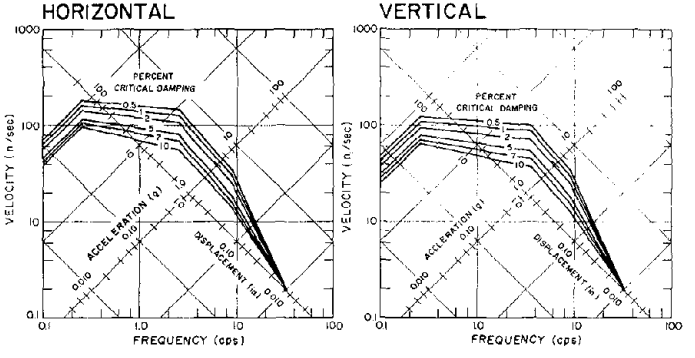

FIG. 4 Smooth design response spectrum curves (mean + 1σ levels) normalized to 1g peak acceleration

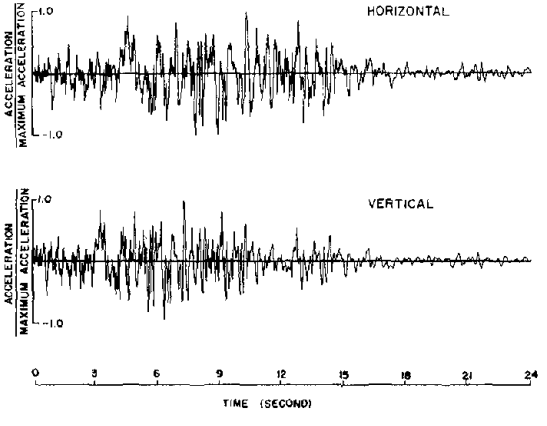

FIG. 5 Synthetic accelerograms representing ponse spectrum curves

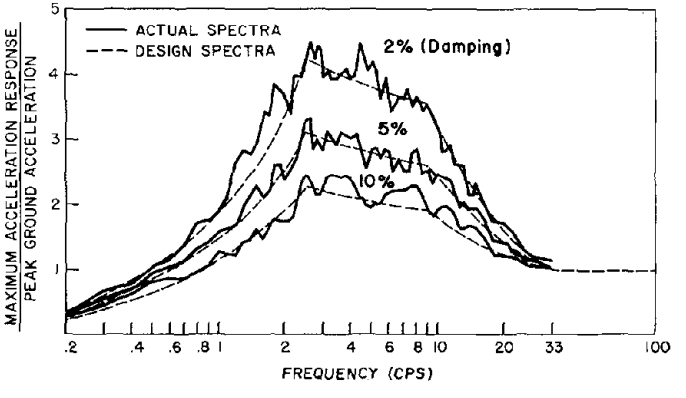

FIG. 6 Actual response spectrum curves of synthetic accelerogram for horizontal motion

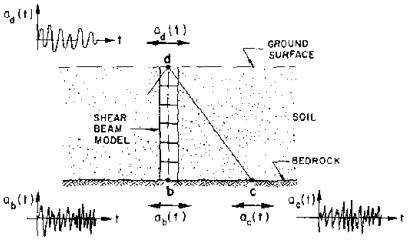

FIG. 7 The shear beam model used for soil response analysis

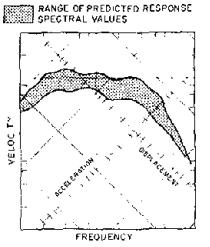

FIG. 8 Range of predicted response spectra for a given site

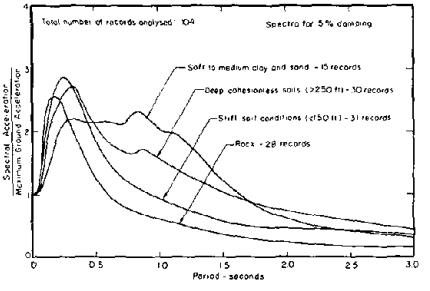

FIG. 9 Average acceleration spectra

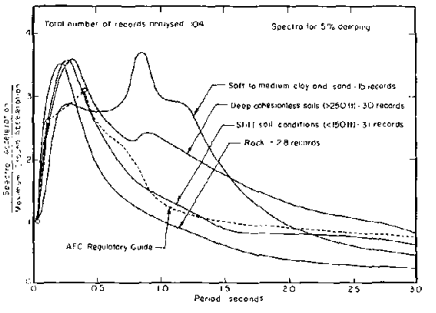

Fig. 10 84 percentile acceleration spectra

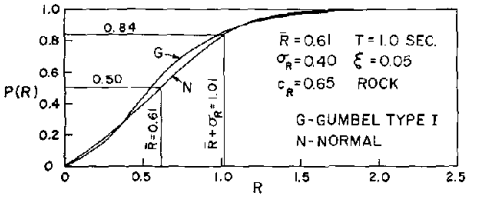

Fig. 11 Probability distribution for spectral response - rock

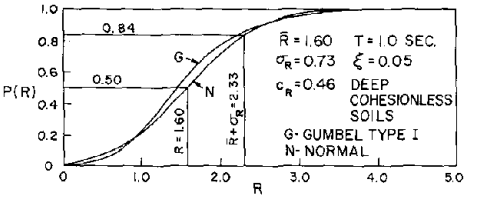

Fig. 12 Probability distribution f spectra response - deep cohesionles soils

$$R \equiv \frac{\text{SPECTRAL ACCELERATION}}{\text{MAXIMUM GROUND ACCELERATION}}$$

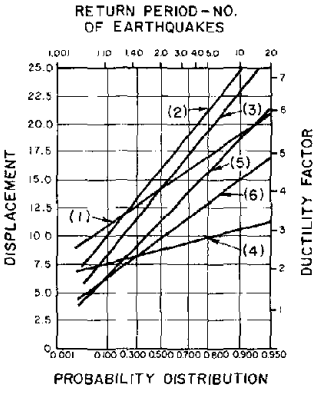

FIG. 13 Probability distribution of maximum response for single degree of freedom systems subjected to ground accelerations of fixed intensity.

	STR. RESPONSE	G.M. INTENSITY
(1)	MEAN VALUE	EXTREME TYPE II
(2)	EXTREME TYPE I (c_v=0.4)	EXTREME TYPE II
(3)	MEAN VALUE	UPPER BOUNDED
(4)	EXTREME TYPE I (c_v=0.4)	UPPER BOUNDED

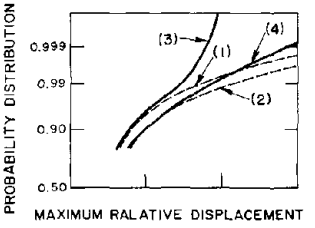

FIG. 14 Probability distribution of maximum response for single degree of freedom systems subjected to ground accelerations of variable intensity

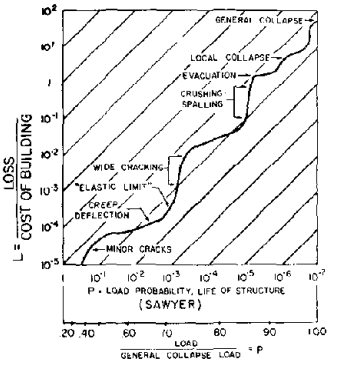

FIG. 15 Assessment of mean losses versus load probabilities during the life of structure

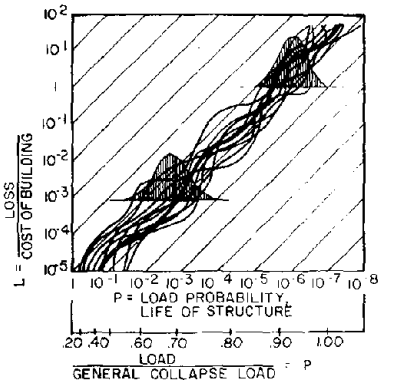

FIG. 16 Distribution of losses versus load probabilities during the life of structure

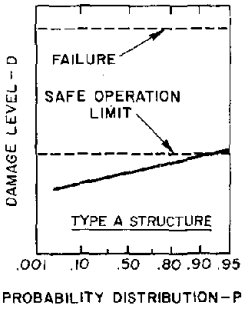

FIG. 17 Probability distribution of maximum damage level during life of structure

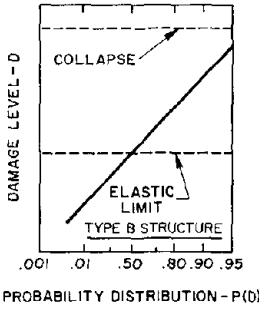

FIG. 18 Probability distributic of maximum damage level during life of structure

Stochastic Process Models of Strong Earthquake Motions for Inelastic Structural Response

by

Hiroyuki Kameda

Associate Professor of Civil Engineering
Kyoto University, Kyoto, Japan

Synopsis

Methods for modeling strong motion accelerograms are discussed. Stochastic process models are developed so that elastoplastic structural response including deformation and total hysteretic energy will agree, in the mean, with corresponding recorded accelerograms. Intensity, frequency content, and duration are incorporated in a consistent manner. Conventional amplitude-modulated stationary processes are reviewed first. On this basis, significance of extension to evolutionary process models is discussed, and preliminary analysis is made.

Introduction

Simulation of strong earthquake motions using random process models is a common tool for modern structrual response analysis and design for seismic loads. Various stochastic models have been proposed for this purpose. In the early stage, stationary processes were used for the model(2,6,7,18). They were extended to models that account for nonstationarity in rms intensity (1,4,9,10,14,17). Such models are called amplitude-modulated stationary processes, or amplitude-modulated processes in short, in this study. Based on accumulation of strong motion accelerograms, time-varying frequency content was recognized and was incorporated in simulation of earthquake motion: the simulation models are evolutionary processes with nonstationary frequency content and rms intensity (5,15,19).

Most of these models have been tested successfully on their usefulness by checking if they provide linear response spectra similar to those for typical recorded accelerograms or their average. However, agreement in linear response spectra deos not directly lead to applicability of the models to inelastic response. Particularly the total hysteretic energy dissipated by structures is more sensitive to the duration of excitation than the maximum deformation as pointed out in the previous study (12). It is also of interest to find the usefulness of the amplitude-modulated model relative to the evolutionary model. It is clear that evolutionary processes can incorporate more of the statistical nature of earthquake motions than amplitude-modulated processes. For engineering purposes, however, amplitude-modulated processes possess advantage for their simplicity as far as they agree with recorded accelerograms relative to their elastic and inelastic structural response.

The study described herein is an extension of the previous study (12): comprehensive analysis is made. The topics dealt with in this paper are:

1. To develop amplitude-modulated process models that can be applied to inelastic structural response through an appropriate evaluation of the duration of

earthquake motion, and to identify limitation, if any, to the applicability of such models.
2. To extend the models to evolutionary processes in the same context as described in 1.
3. Comparison of typical accelerograms recorded in Japan (earthquakes which occurred in the pacific off-shore seismic region along the Japanese island arc; M=7.5, 7.9) and those recorded in the United States (western United States; M=6.4~7.7), Table 1, in view of the simulation models dealt with in this study.

The contents covered in this paper are in preliminary steps toward prediction models that can be used for generating a set of possible future earthquake motions with given location and site conditions. They have been intended to identify ground motions parameters relevant to simulation models useful for engineering purposes.

Formulation of Amplitude-Modulated Process Model

Basic Form

The amplitude-modulated process model for earthquake acceleration $x(t)$ is expressed as

$$x(t) = \sigma_{max} f(t) g(t) \tag{1}$$

in which σ_{max}=maximum rms intensity, $f(t)$=nonstationary envelope function, and $g(t)$=stationary Gaussian process with a zero mean and unit variance. Values of σ_{max} and $f(t)$ for a recorded accelerogram $y(t)$ are obtained by taking the square root of the moving average of the squared acceleration. A bell-shaped cosine window function with equivalent averaging time of 4 sec was used (12). The peak value of the resulting time function is σ_{max}, and normalizing the time function by σ_{max} gives $f(t)$, denoted by $f_y(t)$ to show it corresponds to a recorded accelerogram. Values of σ_{max} are shown in Table 1, and an example of $f_y(t)$ is shown in Fig.1(a).

Modeling of Nonstationarity Using Equivalent Duration

As a measure for modeling the nonstationary envelope function, the equivalent duration of the ground motion is defined by

$$T_n = \int_0^\infty \{f(t)\}^n dt \tag{2}$$

in which n is an arbitrary constant. When the duration of recorded accelerograms is discussed, $f(t)$ in Eq.2 is replaced by $f_y(t)$. The value of T_n decreases with n, as the strongest part of $f(t)$ contributes increasingly to the integral in Eq.2. Fig.2 shows examples of T_n for recorded accelerograms.

Three types of nonstationary envelope function are used for $f(t)$; (a) ponential-type envelope of the form te^{-at}, (b) the envelope proposed by Ami Ang (1), and (c) a simple stationary envelope, Fig.1(b). These functions a expressed as follows.

exponentioal envelope:
$$f(t) = \begin{cases} 0 & ; \quad t \leqq 0 \\ \dfrac{t}{t_0} \exp\left(1 - \dfrac{t}{t_0}\right) & ; \quad t \geqq 0 \end{cases} \quad (3)$$

$$\text{Amin-Ang envelope:} \quad f(t) = \begin{cases} 0 & ; \quad t < 0 \\ (t/t_1)^2 & ; \quad 0 \leqq t \leqq t_1 \\ 1 & ; \quad t_1 \leqq t \leqq t_2 \\ e^{-c(t-t_2)} & ; \quad t \geqq t_2 \end{cases} \tag{3.b}$$

$$\text{stationary envelope:} \quad f(t) = \begin{cases} 1 & ; \quad 0 \leqq t \leqq t_3 \\ 0 & ; \quad t < 0, \ t > t_3 \end{cases} \tag{3.c}$$

The parameters for these functions are adjusted so that $f(t)$ gives the same equivalent duration as $f_y(t)$ for corresponding recorded accelerograms. On this basis, t_0, t_1, t_2, t_3 are determined from the following:

$$t_0 = \frac{n^{n+1} T_n}{e^n \Gamma(n+1)} \tag{4.a}$$

$$\left.\begin{aligned} &t_1 = 1.5\text{sec}, \ t_2 = T_n + \frac{3}{2n+1} - \frac{1}{0.18n} \ (\text{sec}), \quad c = 0.18\text{sec}^{-1}, \\ &\qquad \text{if} \quad T_n \geqq \frac{1.5}{2n+1} + \frac{1}{0.18n} \ (\text{sec}); \\ &t_1 = t_2 = T_n / \left(\frac{1.5}{2n+1} + \frac{1}{0.27n}\right), \quad c = 0.27/t_1 \\ &\qquad \text{if} \quad T_n < \frac{1.5}{2n+1} + \frac{1}{0.18n} \ (\text{sec}) \end{aligned}\right\} \tag{4.b}$$

$$t_3 = T_n \tag{4.c}$$

The models of nonstationarity described above clearly depends on the value of n for determining the equivalent duration T_n. As characterized by the arbitrary constant n, definition of the duration of earthquake motions is somewhat arbitrary, and several definitions have been proposed (3,8,13,20). For engineering purposes, however, it is desirable to define the duration in relation to the structural response. The parameter n in the present analysis has been introduced for such purposes.

The value for n may be determined so that recorded and simulated accelerograms result in similar structural response; i.e., if $x(t)$ and $y(t)$ have same σ_{max} and same frequency content and they generate similar, if not same, structural response, we assert that $x(t)$ and $y(t)$ have a same duration. An optimum value for n is obtained along this line in a later section in relation to inelastic structural response.

Spectral Functions

The following three types of single-peaked functions were examined for modeling the power spectral density function of $g(t)$.

$$\text{Type A:} \quad G_n(\omega) = \frac{\gamma_A}{\omega_g} \frac{1+4\beta_g^2(\omega/\omega_g)^2}{H(\omega)} \tag{5}$$

$$\text{Type B:} \quad G_n(\omega) = \frac{\gamma_B}{\omega_g} \frac{(\omega/\omega_g)^2}{H(\omega)} \tag{5}$$

$$\text{Type C:} \quad G_n(\omega) = \frac{\gamma_C}{\omega_g} \frac{\omega/\omega_g}{H(\omega)} \tag{5}$$

where:

$$\gamma_A = \frac{4\beta_g}{\pi(1+4\beta_g^2)} \quad , \quad \gamma_B = \frac{4\beta_g}{\pi} \quad , \quad H(\omega) = \{1-(\omega/\omega_g)^2\}^2+4\beta_g^2(\omega/\omega_g)^2$$

$$\gamma_C = \begin{cases} \dfrac{8\beta_g\sqrt{1-\beta_g^2}}{\pi} \Big/ \left\{1+\dfrac{2}{\pi}\tan^{-1}\dfrac{1-2\beta_g^2}{2\beta_g\sqrt{1-\beta_g^2}}\right\} ; & 1 > \beta_g > 0 \\ 2; \quad \beta_g = 1 \\ 4\beta_g\sqrt{\beta_g^2-1} \,/\ln\{(\beta_g+\sqrt{\beta_g^2-1})/(\beta_g-\sqrt{\beta_g^2-1})\} ; & \beta_g > 1 \end{cases}$$

The frequency parameter ω_g is represented in terms of the peak frequency f_p (in Hz) by

Type A: $\omega_g = 4\pi\beta_g f_p / \sqrt{\sqrt{1+8\beta_g^2}-1}$ (6.a)

Type B: $\omega_g = 2\pi f_p$ (6.b)

Type C: $\omega_g = 2\pi\sqrt{3/(1-2\beta_g^2+2\sqrt{1-\beta_g^2+\beta_g^4})}\, f_p$ (6.c)

Typical cases of these functions are shown in Fig.3. They have different trends particularly in low frequency regions which have great effects on the response of long period structures. These functions were least-square fitted to the squared Fourier amplitude spectra of recorded accelerograms normalized to have unit areas, and the best-fitting spectral function was selected for each accelerogram. The type of function, and the values of the parameters f_p and β_g are shown in Table 1. These results are used for generating simulated accelerograms in the following section.

Inelastic Structural Response and Simulation Error

The model of earthquake motion described above is tested if it gives appropriate inelastic structural response statistics relative to recorded accelerograms. A major concern here is to search for an optimum value for the equivalent duration parameter n that can be applied to wide ranges of natural frequency of structures and response ductility factor.

Sample functions for the simulation model of earthquake motion were generated for each of the recorded accelerograms listed in Table 1. Seven values of n ranging between 1/4 ~ 8 were used, and a sample function was generated for each value of n. Response of elastoplastic systems with 2% viscous damping to simulated and recorded accelerograms are compared in the following manner. Let V_s and V_r be simulated and recorded deformation spectra, respectively, for a given duct factor μ. Similarly, E_s and E_r denote total hysteretic energy for simulate corresponding recorded accelerograms. Then parameters r_d and r_e defined as may be used as a measure of error in the simulation model.

$$r_d = \ln(V_s/V_r) \quad , \quad r_e = \ln(E_s/E_r) \qquad ($$

It is intended to find a model for which sample means $\bar{r}_d$ and $\bar{r}_e$ assume sma absolute values.

Figs.4 and 5 show dependence of the mean simulation errors on the val Sample means were obtained for the Japanese and the US accelerograms liste

Table 1 separately for comparison. It may be interesting to note that the mean simulation error does not depend very much on the ductility factor μ. This seems to justify appliction of simulation models established for linear responses to inelastic response analysis. Observe, however, that the mean error $\bar{r}_e$ in the hysteretic energy is more sensitive to n than that for the deformation spectra. This requires careful evaluation of the duration of earthquake motions when the models are intended to apply to inelastic response.

The simulation error for the stationary envelope shows the greatest dependence on n, whereas that for the exponential envelope varies less significantly with n. The result for the stationary envelope is affectd greatly by n since the total duration t_3 of the model is equal to the equivalent duration T_n shown in Fig.2. In contrast, when the exponential envelope is used, the value of T_n has smaller effects on t_0 as shown, for example, for the US records in Table 1. This is a consequence of modeling the initial transient phase and the subsiding tail in the exponential envelope. The Amin-Ang envelope has an intermediate nature between the above two envelopes. It is also observed in Figs.4 and 5 that the simulation errors for the Japanese records are more sensitive to n than those for the US records. This results from high dependence of T_n on n for the Japanese records relative to the US records as shown in Fig.2. In this regard, the values for t_0 for the Japanese and the US records in Table 1 may be compared as to its dependence on n.

It should be emphasized that low dependence of the simulation error on n for the exponential envelope does not mean it is the most suitable model among the three. This point is discussed in the following sections.

The sample standard deviations of r_d and r_e denoted by s_{r_d} and s_{r_e}, respectively, generally varies with the natural frequency and does not depend very much on the ductility factor. The values of s_{r_d} with n=2 for the samples used herein vary in the range 0.3 ~ 0.6, and those of s_{r_e}, in the range 0.5 ~ 1.2, regardless of the type of envelope function and the Japanese or the US records.

Acceptable Range of Equivalent Duration Parameter n

Adimitting an allowable range of ±0.5 for the mean simulation errors $\bar{r}_d$ and $\bar{r}_e$, the acceptable ranges of n are established in the same manner as in the previous study (12). The results are shown in Fig.6. Cases with high dependence of $\bar{r}_d$ and $\bar{r}_e$ on n result in narrow acceptable ranges of n for a given natural frequency. In Fig.6, therefore, narrower bands of acceptable n have been obtained for hysteretic energy than for deformation spectra, also for the stationary envelope than for the the Amin-Ang envelope and moreover for the exponential envelope, and for the Japanese records than for the US records.

Remarks on Nonstationary Envelope Functions for Amplitude-Modulated Mod

The nonstationary envelope function and the equivalent duration in the going analysis primarily reflects time-variation of the predominant harmonic components corresponding to medium frequency regions: the f_p values in Table range between 0.6 ~ 5.2 Hz for the Japanese records and 0.4 ~ 3.0 Hz for the US records. For these frequency regions, all cases in Fig.6 provide common a able values of n. n = 1 ~ 2 seems appropriate for this purpose. Particularly observe the case of the exponential envelope for the US records, Fig.6(b). A /alues in the region n = 0.25 ~ 8 are acceptable for f_g = 0.3 ~ 3 Hz . Howeve this particular case fails to possess an acceptable value of n within the lo limit considered herein for the frequency region above 3 Hz . At a low freque of 0.15 Hz , the accetable value of n is also limited to a value of some 8, t

upper limit. A broad band of acceptable n and its applicability limited to an intermediate frequency region characterize this extreme case.

This result is a consequence of nonstationary frequency content of the recorded accelerograms. There is a known trend that low frequency components last longer than higher frequency components. This trend is reflected in the shape of Fourier amplitude spectra: when harmonic components have uniform peak rms intensities, those with longer duration generate larger values of Fourier amplitudes than those with shorter duration. Therefore, using the squared Fourier amplitude for the amplitude-modulated models under the assumption of time-invariant frequency content tends to underestimate the duration and overestimate the peak rms intensity for lower frequency components, and vice versa for higher frequency components. To compensate this, large values must be used for n in low frequency regions, and small values in high frequency regions. This is particularly true when the simulation error for a given type of nonstationary envelope function does not depend largely on the value of n; the exponential envelope function used for the US records is a typical case.

On the basis of the above arguments and within the numerical results examined in this study, one may conclude regarding the usefulness of nonstationary envelope functions relative to inelastic structural response in the following manner. The Japanese records used herein were recorded during typical major earthquakes occurring in the pacific off-shore region along the Japanese island arc. They can be characterized by large values of the equivalent duration T_n and relatively high dependence of T_n on n. The value n=2 may be used for determining the equivalent duration and the nonstationary envelope function. The stationary envelope is applicable for the natural frequency region of f_o = 0.1 ~ 10 Hz, whereas the exponential envelope and the Amin-Ang envelope with a single value of n=2 may be used for f_o = 0.3 ~ 10 Hz. For the US records used herein, typical strong accelerograms recorded in the western United States, the value n=2 may also be used. Either the Amin-Ang envelope or the stationary envelope can be used for the natural frequency region f_o = 0.1 ~ 10 Hz. However, for its wide acceptable range of n, the Amin-Ang envelope has advantage over the stationary envelope in this case. The exponential envelope is not a suitable form for its narrow applicable frequency range.

In order to refine the models dealt with in the foregoing discussion, measures must be taken to account for the duration of harmonic components varying with frequency. To maintain the simplicity of the amplitude-modulated processes by using a single nonstationary envelope function, and to widen the applicability of the model to all kinds of envelope function, the power spectrum obtained with the aid of the squared Fourier amplitude should be adjusted so that the simulation error will vanish approximately for a single value of n for wide natural frequency ranges. This involves another problem of modeling, and may reduce the simplicity of the amplitude-modulated process models, but will be worth developing fc engineering purposes. The technique for generating spectrum-compatible ear motions (16,21) established for linear response spectra may be extended tc lastic responses for this purpose. Studies in this direction are underway.

The evolutionary process is the only physically consistent model that incorporate all properties of the earthquake motion discussed above. It is dealt with in the next chapter.

Extension to Evolutionary Process Model

Basic Form

On the basis of the results on the amplitude-modulated models of earthquake motions, this chapter deals with modeling with evolutionsry processes. Although several models have been proposed using evolutionary processes (5,15) for describing strong earthquake motions, they have not been established for inelastic structural response. In this chapter, evolutionary processes are tested relative to inelastic responses including deformation spectra and hysteretic energy in the same manner as in the previous chapter. The duration of individual frequency components are evaluated in a manner slightly different from the method used for amplitude-modulated process models.

Using an evolutionary process, the earthquake acceleration is represented by

$$x'(t) = \sum_{k=1}^{m} \sqrt{2G_{x'}(t,\omega_k)\Delta\omega}\,\cos(\omega_k t+\phi_k) \tag{8}$$

in which $G_{x'}(t,\omega)$=evolutionary spectrum of $x'(t)$ for time t and frequency ω, $\omega_k=2\pi f_l+(k-1)\Delta\omega$, $\Delta\omega=2\pi(f_u-f_l)/(m-1)$, ϕ_k=independent phase angle distributed radomly over 0~2π. The upper and lower bounds of frequency f_u and f_l, respectively, are taken as f_u=15 Hz , f_l=0.1 Hz for the Japanese records, and f_u=15 Hz , f_l=0.07 Hz for the US records. The number of superposition m is taken as m=251.

If $y(t)$ is the corresponding recorded accelerogram, its evolutionary spectrum $G_y(t,\omega)$ can be obtained by means of a multi-filter technique (9).

Model of Time Variation for Evolutionary Spectra

The following time-varying function is adopted for the model of $G_{x'}(t,\omega)$.

$$G_{x'}(t,\omega) = \begin{cases} 0\ ; & t \leq t_s \\ \dfrac{\alpha_m(t-t_s)}{t_p}\exp\left(1-\dfrac{t-t_s}{t_p}\right)\ ; & t \geq t_s \end{cases} \tag{9}$$

in which the time parameters $t_s=t_s(f)$ and $t_p=t_p(f)$ are functions of the frequency f. $\alpha_m=\alpha_m(f)$ is the peak value of $\sqrt{G_{x'}(t,2\pi f)}$, and is also a function of f. In Eq.9, an exponential function similar to Eq.3.a has been adopted for low dependence of the corresponding simulation error on the equivalent duration parameter n in the previous chapter. Since modeling is made for individual frequency components, the above reason suffices for choosing the time function of the form of Eq.9 for modeling the time variation of $G_{x'}(t,\omega)$.

The parameters t_s, t_p, and α_m are obtained in the following manner. The starting time $t_s(f)$ is defined as the time at which the evolutionary spectrum $G_y(t,2\pi f)$ of the corresponding recorded accelerogram $y(t)$ exceeds ε times its value for the first time: ε=0.1 is used in this study. In determining $t_p(f)$ $\alpha_m(f)$, equate the areas under $\{G_{x'}(t,2\pi f)\}^{n'/2}$ and $\{G_y(t,2\pi f)\}^{n'/2}$, and also their first moments about the time origin; i.e., set

$$\int_0^\infty \{G_{x'}(t,2\pi f)\}^{n'/2}dt = A_0(f),\quad \int_0^\infty t\{G_{x'}(t,2\pi f)\}^{n'/2}dt = A_1(f) \tag{10}$$

where

$$A_0(f) = \int_0^\infty \{G_y(t,2\pi f)\}^{n'/2} dt \ , \quad A_1(f) = \int_0^\infty t\{G_y(t,2\pi f)\}^{n'/2} dt \tag{11}$$

in which n' is an arbitrary constant which has an effect similar to the equivalent duration parameter n. Applying Eq.9 to Eq.10 , and solving for t_p and α_m gives the following expressions:

$$\left.\begin{aligned} t_p(f) &= n' \frac{\Gamma(n'+1)}{\Gamma(n'+2)} \left(\frac{A_1(f)}{A_0(f)} - t_s(f) \right) \\ \alpha_m(f) &= \frac{n'}{e} \left(\frac{\Gamma(n'+2)}{\Gamma^2(n'+1)} \frac{A_0(f)}{A_1(f)/A_0(f) - t_s(f)} \right)^{1/n'} \end{aligned} \right\} \tag{12}$$

If the equivalent duration $T'(f)$ of the harmonic component corresponding to the frequency f is defined in the same manner as Eq.2, the following expression is obtained.

$$T'(f) = \frac{A_0(f)}{\alpha_m^{n'}(f)} = \frac{e^{n'}\Gamma(n'+1)}{n'^{(n'+1)}} t_p(f) \tag{13}$$

Typical examples of recorded and simulated evolutionary spectra are shown in Fig.7. As n' grows large, the simulated spectrum $G_{x'}(t,\omega)$ is fitted more closely to the high peaks of the recorded spectrum $G_y(t,\omega)$. This is the same effect as that of n in the previous chapter. Examples of t_s, t_p and α_m are shown in Fig.8. Modeling of t_s, t_p and α_m along the frequency axis has not yet been established. Statistical analysis including regression on magnitude and distance is uderway. Therefore, the original values for these parameters are used for generating sample functions of the simulated motion in this study.

In Fig.9, recorded and simulated accelerograms are shown. It may be observed that the simulated accelerograms reproduce fairly well the nonstationary frequency content of corresponding recorded accelerograms. Note also that the wave form of simulated accelerograms for the Hachinohe, EW record varies with n', whereas that for the Olympia, NO4W record does not depend greatly on n'. This difference is again a general trend in the Japanese and the US records used herein.

Simulation Error

The simulation error statistics for the evolutionary process model is surveyed. The error criteria are similar to those used in the previous chapter for amplitude-modulated models. In addition to the simulation errors r_d and r_v deformation spectra and hysteretic energy defined by Eq.7, the error in pe acceleration and that in total power (integral of squared accelerogram ove total time duration) with the following expressions are examined.

$$r_a = \ln(a_s/a_r) \ , \quad r_p = \ln(P_s/P_r) \tag{}$$

in which a_s and a_r are the peak accelerations of simulated and recorded ac ograms, respectively, and P_s and P_r are the total powers thereof.

In Table 2, the sample means $\bar{r}_a$, $\bar{r}_p$ and the sample standard deviation s_{r_p} for the Japanese and the US records are shown for n'=1,2,4. Note that simulation errors $\bar{r}_a$ and $\bar{r}_p$ are satisfactorily close to zero for all value

The standard deviation s_{r_a} is about 0.3~0.4 for the Japanese records and 0.16~0.25 for the US records. The simulation error for the total power is even closer to zero, ranging between -0.03~0.08, its standard deviation being also small with the maximum of 0.16.

The simulation error in the inelastic response is shown in Figs.10 and 11. The results do not vary greatly with the value of n' nor with the ductitilty factor μ. Independence from n' is a consequence of the exponential function in Eq.9 for modeling $\sqrt{G_{x'}(t,\omega)}$. These results permit one to use any value between 1 and 4 for n'. To preserve consistency with the amplitude-modulated process models in the previous chapter, the value of n'=2 will be preferrable. On the other hand, for a better simulation of waveforms on the time axis, the use of n'=4 may be recommended particularly for the Japanese records including that in Fig.9(a).

Validity of the evolutionary process models is demonstrated by the mean simulation errors $\bar{r}_d$ and $\bar{r}_e$ in Figs.10 and 11 that are close enough to zero for the whole frequency region dealt with herein. The standard deviation s_{r_d} of the simulation error for deformation spectra is approximately constant with the natural frequency, assuming values of some 0.2~0.5. The standard deviation of the error in hysteretic energy fluctuate more with f_o, the largest value being about 0.9. The values of s_{r_d} and s_{r_e} may become larger than those shown in Figs. 10 and 11 when prediction models for t_s, t_p, and α_m are established through future statistical analysis. However, the usefulness of the evolutionary process model is obvious from the clear independence of the simulation error from f_o.

Conclusions

Major conclusions derived from this study may be summarized as follows.

1. Amplitude-modulated process models of earthquake motion applicable to inelastic structural response can be established by consistent evaluation of peak rms intensity, duration, and frequency content.

2. For this purpose, an equivalent duration of the earthquake motion has been proposed and evaluated in relation to inelastic structural response including deformation and hysteretic energy.

3. The equivalent duration parameter of the value $n = 2$ minimizes simulation error for wide ranges of natural frequency. This value can be used for the groups of typical accelerograms recorded in Japan and the United States examined in this study. Suitable forms of the nonstationary envelope function has been suggested.

4. Evolutionary process models have been developed on the basis of the above results. The equivalent duration parameter n' for individual frequency components have been introduced.

5. Evolutionary process models with $n' = 1 \sim 4$ provides satisfactory ag between inelastic structural responses for simulated and recorded accelero

Since the evolutionary process is capable of incorporating details of accelerograms affecting inelastic structural response, it has advantage ov amplitude-modulated process, provided sufficient information on frequency- paramters t_s, t_p, and α_m is available. However, in the absense of such inf or when over-all response data are required for engineering purposes, the tude-modulated process models are significant tools for simulating earthqu motions.

References

1. Amin, M., and Ang, A. H-S., "Nonstationary Stochastic Model of Earthquake Motions," *Jour. Eng. Mech. Div.*, ASCE, Vol.94, No.EM2, pp.559-583, 1968.
2. Barstein, M. D., "Application of Probability Methods for Design, the Effect of Seismic Forces on Engineering Structures," *Proceedings*, 2nd WCEE, Vol.2, pp. 1467-1481, 1960.
3. Bolt., B. A., "Duration of Strong Ground Motion," *Proceedings*, 5th WCEE, Vol.1, pp.1304-1313, 1973.
4. Goto, H., and Toki, K., "Structural Response to Nonstationary Random Excitation," *Proceedings*, 4th WCEE, Vol.1, pp.130-144,1969.
5. Hoshiya, M., and Ishii, K., "Worst Earthquake Acceleration with Frequency and Amplitude Nonstationarity," *Proceedings*, JSCE, No.242, pp.1-14, 1975.
6. Housner, G. W., "Characteristics of Strong-Motion Earthquakes," *BSSA*, Vol.37, pp.19-31, 1947.
7. Housner, G. W., and Jennings, P. C., "Generation of Artificial Earthquakes," *Jour. Eng. Mech. Div.*, ASCE, Vol.90, No.EM1, pp.113-150, 1964.
8. Housner, G. W., "Intensity of Earthquake Ground Shaking Near the Causative Faults," *Proceedings*, 3rd WCEE, Vol.1, pp.III~94-115,1965.
9. Iyengar, R. N., and Iyengar, K. T. S. R., "Nonstationary Random Process Model for Earthquake Accelerograms," *BSSA*, Vol.59, pp.1163-1188, 1969.
10. Jennings, P. C., Housner, G. W., and Tsai N. C., "Simulated Earthquake Motions for Design Purposes," *Proceedings*, 4th WCEE, Vol.1, pp.145-160, 1969.
11. Kameda, H., Evolutionary Spectra of Seismogram by Multifilter," *Jour. Eng. Mech. Div.*, ASCE, Vol.101, No.EM6, pp.787-801, 1975.
12. Kameda, H. , and Ang, A. H-S., "Simulation of Strong Earthquake Motions for Inelastic Structural Response," 6th WCEE, Preprint Vol.2, pp.149-154, 1977.
13. Kobayashi, Y., "Duration Strong Ground Motion," *Proceedings*, 5th WCEE, Vol.1, pp.1314-1315, 1973.
14. Ruiz, P., and Penzien, J., "Stochastic Seismic Response of Structures," *Jour. Eng. Mech Div.*, ASCE. Vol.97, No.EM2, pp.441-457, 1971.
15. Saragoni, G. R., and Hart, G. C., "Simulation of Artificial Earthquakes," *Int. Jour. Earthquake Eng. and Struc. Dynamics*, Vol.2, pp.249-267, 1974.
16. Scanlan, R. H., Sachs, K., "Earthquake Time Histories and Response Spectra," *Jour. Eng. Mech. Div.*, ASCE, Vol.100, No.EM4, pp.635-655, 1974.
17. Shinozuka, M., and Sato, Y., "On the Numerical Simulation of Nonstationary Random Processes," *Technical Report*, Dept. of Civil Eng. and Eng. Mech., Columbia Univ., No.31, 1966.
18. Tajimi, H., "A Statistical Method of Determining the Maximum Response of a Building Structure during an Earthquake," *Proceedings*, 2nd WCEE, Vol.2, pp.781-797, 1960.
19. Trifunac, M., "A Method for Synthesizing Realistic Strong Ground Motion," *BSSA*, Vol.61, pp.1739-1753, 1971.
20. Trifunac, M., and Brady, A. G., "On the Duration of Strong Earthquake Ground Motion," *BSSA*, Vol.65, pp.581-626, 1975.
21. Tsai, N-C., "Spectrum-Compatible Motions for Design Purposes," *Jour. E Mech. Div.*, ASCE, Vol.98, No.EM2, pp.345-356, 1972.

Abbreviations
- ASCE: American Society of Civil Engineers
- BSSA: Bulletin of the Seismological Society of America
- JSCE: Japan Society of Civil Engineers
- WCEE: World Conference on Earthquake Engineering

Table 1. Recorded Accelerograms and Parameters for Simulation Model

	Record				Intensity		Time parameters, in sec									Spectral function		
	No.	Earthquake Date Magnitude	Site	Comp.	Peak acc. (gal)	σ_{max} (gal)	T_n ($=t_3$)			t_0			t_2			Type in Eq.5	f_p (Hz)	β_g
							n=1	n=2	n=4	n=1	n=2	n=4	n=1	n=2	n=4			
Japan	J1	1968 Tokachi-oki 16-5-1968 M=7.9	Hachinohe	NS	226	78.8	34.1	14.9	5.6	12.5	8.1	4.4	29.5	13.3	5.5	C	0.84	1.10
	J2			EW	183	87.6	24.4	9.7	4.9	9.0	5.3	3.8	19.8	8.1	4.8	C	1.11	0.61
	J3		Miyako	NS	111	49.5	54.2	30.8	13.3	19.9	16.7	10.4	49.6	29.2	13.2	A	5.24	0.08
	J4			EW	95	36.4	64.0	41.5	21.5	23.5	22.5	16.8	59.4	39.9	21.4	A	5.61	0.09
	J5		Aomori	NS	210	69.5	48.9	26.6	11.8	18.0	14.4	9.2	44.3	25.0	11.8	C	0.67	0.39
	J6			EW	173	55.4	62.9	38.8	20.5	23.1	21.0	16.0	58.3	37.2	20.5	C	0.65	0.47
	J7		Muroran	NS	199	64.6	29.2	15.4	7.9	10.7	8.3	6.2	24.6	13.8	7.9	C	2.41	0.34
	J8			EW	133	59.1	28.4	15.9	8.8	10.4	8.6	6.9	23.8	14.3	8.7	C	2.21	0.87
	J9	1968 Hyuga-nada 01-4-1968 M=7.5	Hosojima	NS	203	104.0	14.4	4.3	1.2	5.3	2.3	0.9	9.8	2.7	1.1*	B	1.00	0.11
	J10			EW	236	84.4	20.4	7.7	3.5	7.5	4.2	2.7	15.8	6.1	3.5	B	1.04	0.09
	J11		Kochi	NS	69	28.7	28.2	14.4	8.1	10.4	7.8	6.3	23.6	12.8	8.1	B	0.98	0.08
	J12			EW	96	43.1	21.6	10.9	6.5	7.9	5.9	5.1	17.0	9.3	6.5	B	0.75	0.11
U.S.A.	A1	Imperial Val. 08-5-40 M=6.7	El Centro	S00E	342	114.0	14.2	10.3	4.4	5.2	4.4	3.4	9.6	6.6	4.4	B	1.19	0.80
	A2			S90W	210	74.8	19.3	15.6	8.3	7.1	7.4	6.5	14.7	12.1	8.3	A	1.91	0.42
	A3	Kern County 21-7-52 M=7.7	Taft	N21E	153	52.1	16.8	13.4	7.5	6.2	6.2	5.9	12.2	9.9	7.4	C	1.46	1.08
	A4			S69E	176	58.1	15.4	12.0	6.3	5.6	5.4	4.9	10.8	8.4	6.3	A	2.37	0.45
	A5	Western Wash. 13-4-49 M=7.1	Olympia	N04W	162	64.3	16.3	12.8	6.4	6.0	5.9	5.0	11.7	9.2	6.4	C	1.59	1.13
	A6			N86E	275	69.2	18.9	16.0	9.9	7.0	7.7	7.7	14.3	12.7	9.8	A	3.03	0.43
	A7	San Fernando 09-2-1971 M=6.4	Pacoima Dam	S16E	1148	270.9	9.6	7.9	5.0	3.5	3.7	3.9	5.0	5.3	5.0	C	1.63	1.14
	A8			S74W	1055	266.4	9.4	7.6	4.7	3.5	3.6	3.7	4.8	5.0	4.6	B	2.01	0.61
	A9		Orion Blvd.	N00W	250	87.0	14.7	11.8	7.0	5.4	5.5	5.5	10.1	8.6	7.0	C	0.88	1.08
	A10			S90W	132	52.4	19.0	16.2	10.8	7.0	7.9	8.4	14.4	13.1	10.7	C	0.40	1.89
	A11		Castaic	N21E	309	88.6	9.6	6.6	3.1	3.5	2.8	2.4	5.0	3.5	3.1	B	1.85	0.74
	A12			N69W	265	92.0	12.1	8.7	3.7	4.4	3.8	2.9	7.5	5.3	3.6	B	1.82	0.37

* $t_1=t_2$ and $c = 0.25\ \text{sec}^{-1}$ for this case. For all other cases, $t_1 = 1.5$ sec and $c = 0.18\ \text{sec}^{-1}$

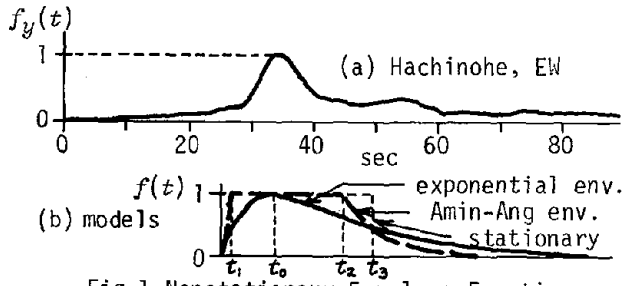

Fig.1 Nonstationary Envelope Function

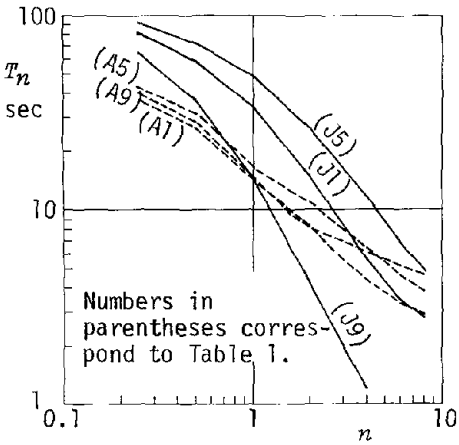

Fig.2 Equivalent Duration

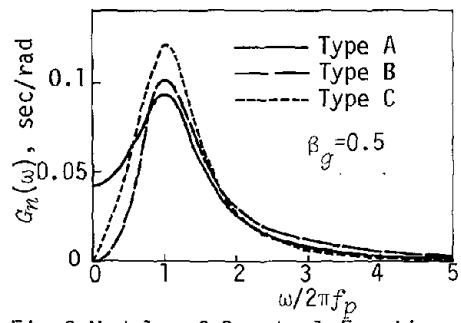

Fig.3 Models of Spectral Function

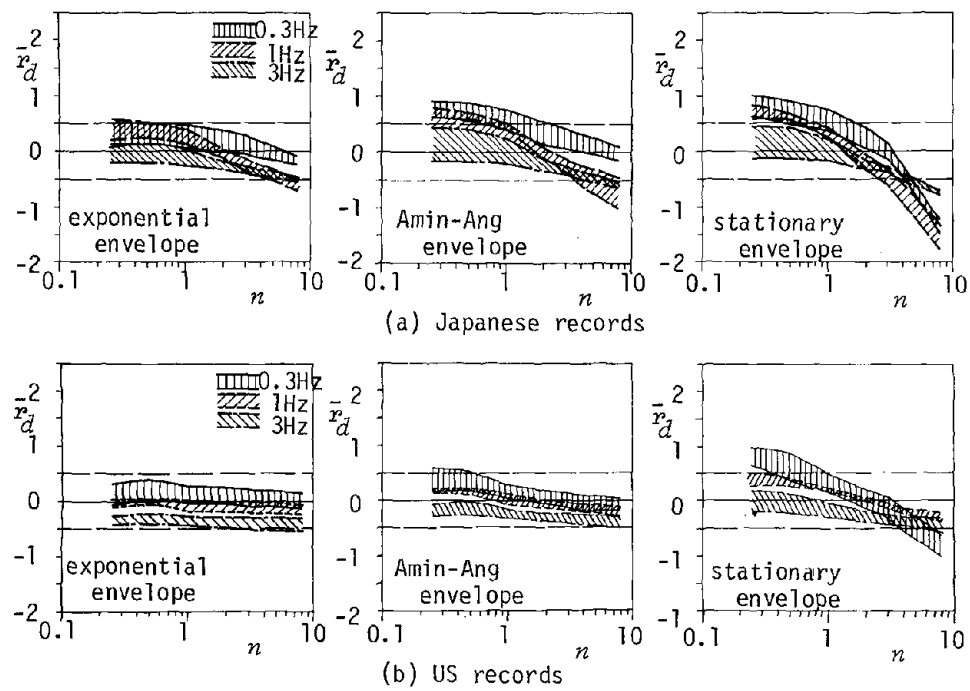

Fig.4 Simulation Error in Deformation Spectra (A-M model; μ=1~6)

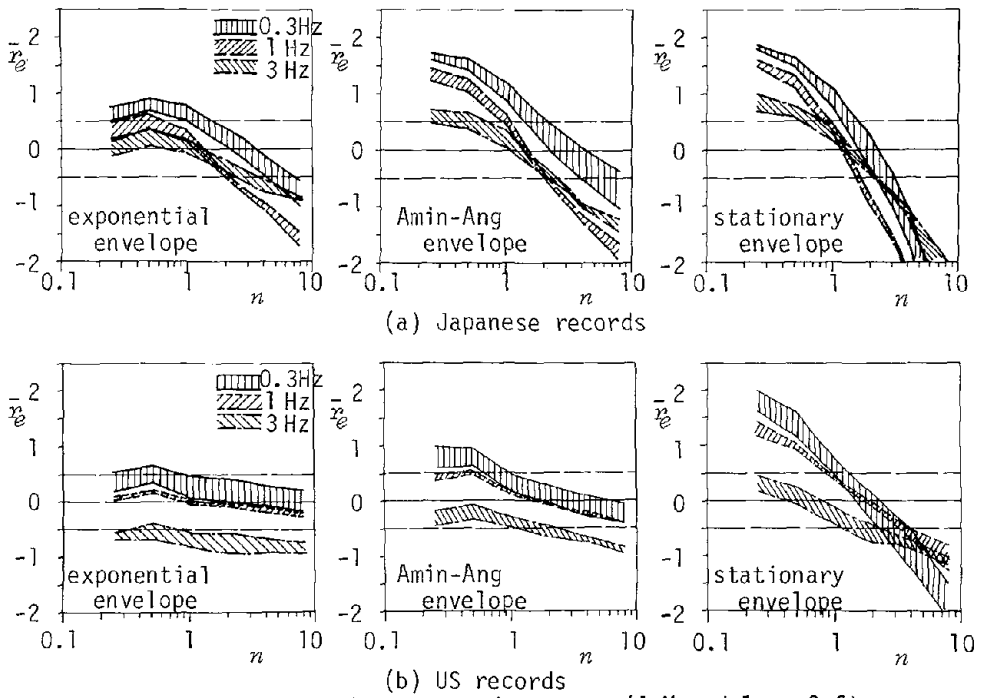

(a) Japanese records

(b) US records

Fig.5 Simulation Error in Hysteretic Energy (A-M model; μ=2~6)

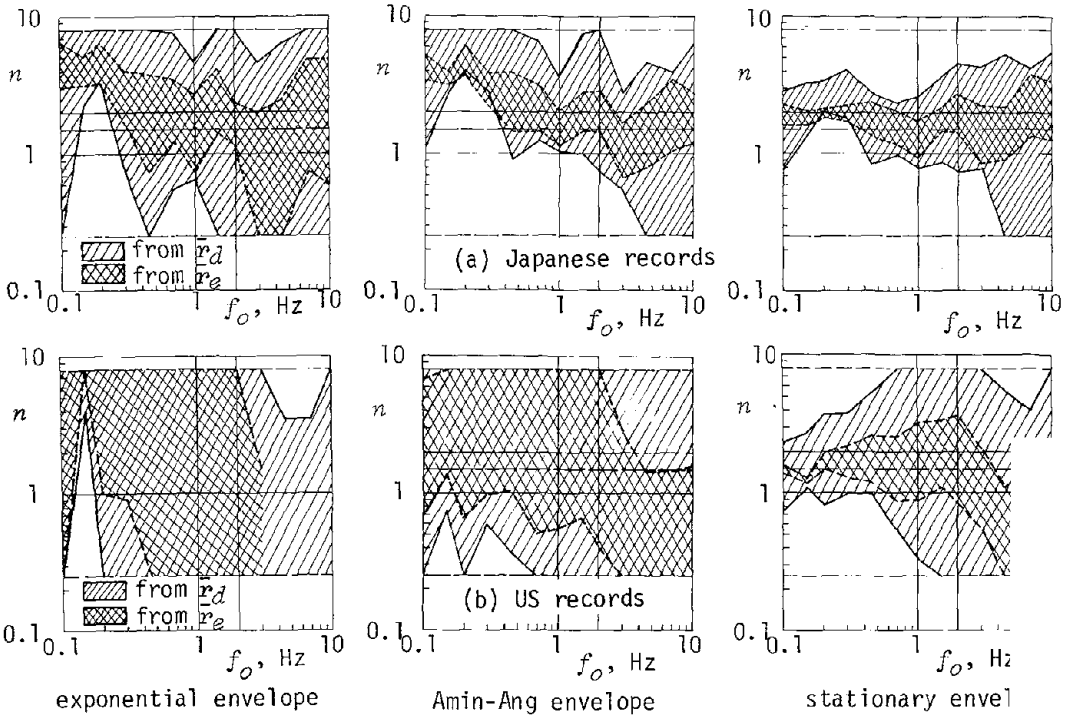

Fig.6 Acceptable Range of n

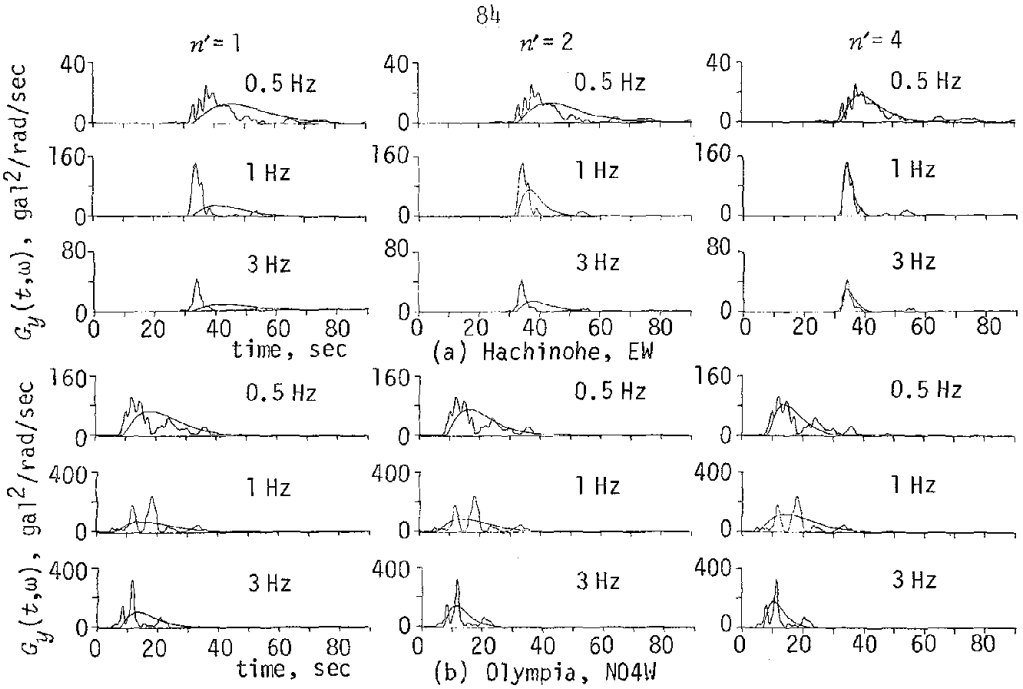

Fig.7 Recorded and Simulated Evolutionary Spectra

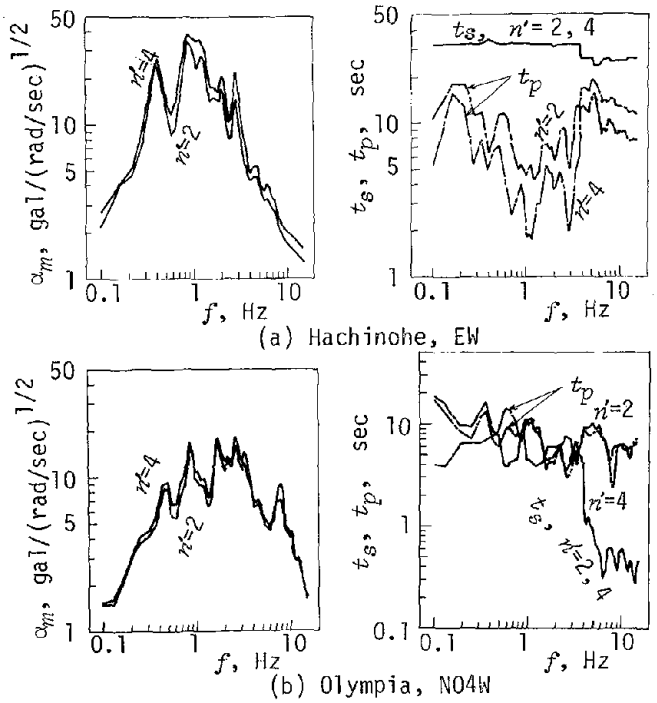

Table 2. Simulation Error in Peak Acceleration and Total Power (Evolutionary Process Model)

			n = 1	n = 2	n = 4
Japan	Peak acc.	$\bar{r}_a$	0.04	0.12	0.17
		s_{r_a}	0.43	0.30	0.34
	Total power	$\bar{r}_p$	0.07	0.05	0.08
		s_{r_p}	0.16	0.05	0.08
U.S.A.	Peak acc.	$\bar{r}_a$	-0.11	-0.02	0.01
		s_{r_a}	0.17	0.1	
	Total power	$\bar{r}_p$	-0.03	0.0	
		s_{r_p}	0.07	0.0	

Fig.8 Parameters for Evolutionary Process Models

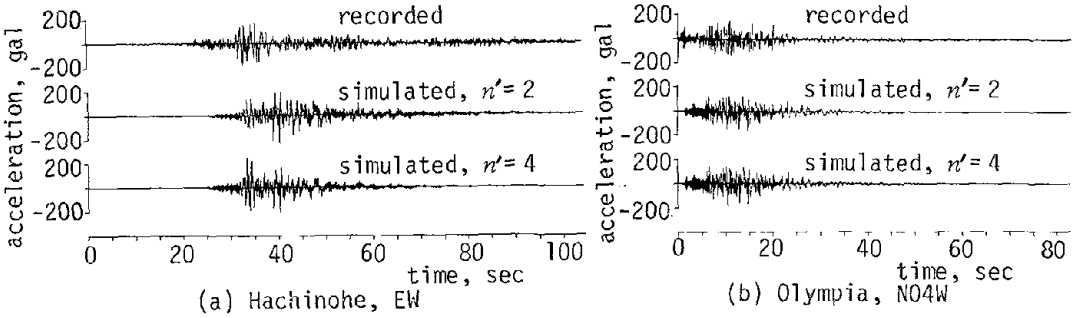

Fig.9 Recorded and Simulated Accelerograms (Evolutionary Process Model)

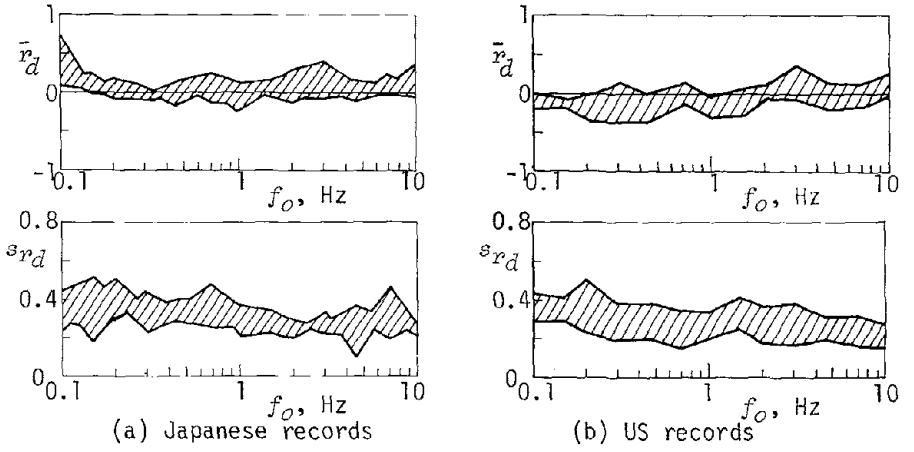

Fig.10 Simulation Error in Deformation Spectra
(Evolutionary Process Model; n'=1~4, μ=1~6)

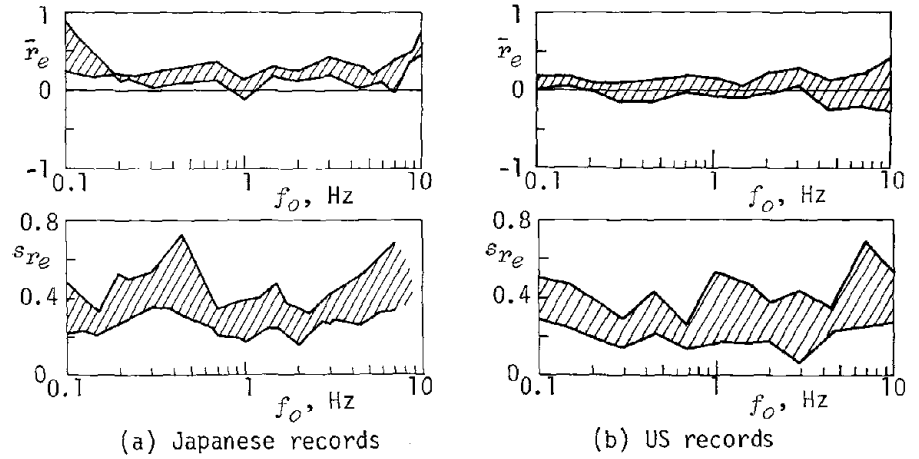

Fig.11 Simulation Error in Hysteretic Engergy
(Evolutionary Process Model; n'=1~4, μ=2~6)

VULNERABILITY ANALYSIS OF NATURAL DISASTER RISKS FOR THE METRO MANILA AREA

NATHANIEL von EINSIEDEL
Program Director
Human Settlements Commission
Makati, Philippines

1. ABSTRACT

In the past, limited attention has been given to the risk of natural disasters in the physical planning process of most disaster-prone developing countries. Coupled with the increasing population of major urban centers, is the subsequent exponential increase in the loss of lives and damage caused by natural disasters in the disaster-prone developing countries. To overcome a major part of this problem, the United Nations Disaster and Relief Organization (UNDRO), has for a considerable period, advocated the formulation and application of a general methodology for vulnerability into the physical and urban planning process. Cognizant of the effects of natural disasters on major urban centers in the Philippines, the Philippine government through the Human Settlements Commission requested the assistance of the UNDRO to undertake and carry out a systematic vulnerability analysis, with the Metro Manila area as the ideal setting, based on the following reasons:

1. in addition to being the prime urban center of the Philippines, Metro Manila is expose to natural hazards (especially earthquakes, floods and typhoons)

2. for integration of the composite risk map into the overall comprehensive plan for Metro Manila

This paper deals with the methodologies and factors connected with the vulnerability analysis, specific to the natural characteristics of Metro Manila which are as follows:

1. fairly flat area, without significant differences from one zone to another as far as typhoon risk is concerned

2. no major risk of landslides, and

3. earthquakes and floods being two major sources of natural disaster

The applicability of this technology to land use planning in MMA wo be discussed in brief.

2. INTRODUCTION

In recent years, inspite of a growing scientific understanding natural disaster risk has increased. This condition is due largely increasing density of population in hazardous areas. In both devel developing countries, there have been pressures to occupy and devel exposed to natural hazards. Limited resources and increased popula growth have forced settlements on the coastal areas, exposed to tro

cyclones and tsunamis, or on marginal lands exposed to drought and erosion.

Another consequence of population growth has been increasingly destructive impact of man on the environment. Practices such as deforestation which destroys vegetal cover has aggravated the process of natural disaster thereby increasing the potentials for destructive flooding and soil loss.

Massive rural-urban migration has also contributed in some cases to an increase in disaster risk. Whereas, in the predominantly rural society, population is dispersed and is therefore less vulnerable to disaster risks in concentrated high intensity urban areas. The trend of rapid urbanization and industrialization has led to the careless and arbitrary development causing damage to the environment. Ironic as it seems, hazards coincide with the rich resources inherent in certain countries; flood plains are often rich agricultural land; rich volcanic soil for agriculture may surround lethal volcanoes; by-products of great active faults are often minerals, springs and magnificent scenery; coastal and river location are often essential for trade and industry.

3. BACKGROUND ON NATURAL DISASTER

A natural disaster is a natural event affecting the human community, from which the community does not have the capacity to recover.[1] A natural disaster can be measured in terms of human sufferings, property loss and social disruption it causes in vulnerable communities. Natural events in themselves do not constitute disasters. The severity on natural disasters primarily depends on two factors:

1. the intensity of the natural event impact, and

2. the vulnerability of the affected human settlement

As settlement patterns can be defined, so too, can the probable natural event occurence. The overlap of the two patterns may be seen to define an area of potential disaster loss.

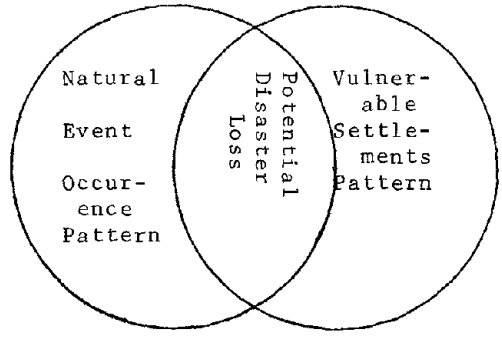

[1] UNESCO/SC/WS/500 Working Group on the Statistical Study of Natural Hazards and their Consequences, Paris, 1972.

Though we cannot define with certainty the time, location and magnitude of natural event occurence, we can at least quantify over uncertainty in the form probabilistic estimates. The same holds true for vulnerability; while we are not able to predict with certainty the performance of constructed facilities subjected to loads imposed by natural events, we can make probabilistic estimates of performance conditional on intensity of impact.

As both event intensity and settlement vulnerability are components of loss potential, the probability of disaster or disaster risk is the product of hazard (event probability) and vulnerability (conditional damage probability);

DISASTER RISK = (HAZARD) X (VULNERABILITY)

The implications of this simplified expression is that the efforts to reduce disaster risk should be directed towards the reduction of hazards (the probability of damaging intensity levels) or the reduction of vulnerability (damage probability).

4. METHODOLOGY

4.1 SEISMIC VULNERABILITY ANALYSIS

An earthquake, even of moderate intensity, releases an enormous amount of energy that triggers a complex chain of events. The 3 categories of chain effects generated by an earthquake can be generally defined as such:

a. the direct effects of the earthquake which are related to its magnitude, fault displacement and ground shaking

b. modifications of ground motions on unstable geological features or structures (ground motions are either amplified or reduced by local geological conditions), and

c. the reaction of man-made structures to earthquake forces (which in fact several specific vulnerability of these structures)

During an earthquake, two kinds of phenomena liable to cause disasters can be defined:

a. ground response as determined by ground acceleration and soil composition in a given place

b. resonance which relates the amplitude of ground v with the natural period of built structures.

The latter is related specially to the height of buildings, the former phenomenon is related to the thickness of sedime determining vulnerability due to resonance, soil analysis ar required down to bedrock level.

4.1.1. Physical factors related to ground response

Geological data are the basis for determining ground response. However, it is not possible to find standard geological maps containing sufficient data, particularly in areas underlain by unconsolidated sedimentary deposits, where large earthquake and loss of lives have occured. Such sedimentary soils are found in flat low-lying areas, often densely populated and highly developed. Using the finding of geotechnical studies, a ground response index can be built up with the following components:

a. a basic component (i) related to subsoil composition and the volume of sedimentary layers

b. other components on the specific characteristics of the area, the presence of faults (f), loose sand layer(s).....

$I = i + f + s + ...$

where I = total ground response index.

The measurement of each of these components is defined as follows:

a. basic ground response component (i)

- this component usually determines primarily the level of ground response in a given place

b. loose sand layers (liquefaction potentials) (s) component

- the existence of loose sand layers susceptible to be liquefied is identified by the component (s) and must be added to (i) defined above

c. faults (f) component

- the displacement risk of faults and related ground-shaking can be expressed with a coefficient (f) which varies from 0 (non-existence of fault) to a maximum value (nf).

This value is added to the preceeding components (i) and (s) of the ground response index.

d. total ground response index (I)
$I = i + s + f + ...$

- the intensity. Components studied above are aggregated in an additive formula, wherein all of these components are not independent. The relative weight of each is a direct function of the local conditions and can be de-

termined only after field survey.

4.1.2. Resonance: (R)

It has been observed that for a number of destructive earthquakes the shaking of the ground surface is related to the thickness of soft sedimentary or alluvial soils. The greater the thickness the greater the displacement and longer the predominant period. From past observations of micro-tremors, it has been found that whenever there is a thick layer of soft mud, a longer period, for instance 0.5, seconds, or more is predominant in the period distribution curve. Where there is a thin layer of soft material covering bedrock or where the superficial layer is not too soft, the predominant period becomes shorter. On bedrock itself, the period of ground movement is one of the most impotant factors influencing the impact of earthquake forces on buildings and civil engineering works.

The higher the building, the longer the natural period. Thus, if a building is located on a thick layer of unconsolidated deposits which have a long predominant period, the whole structure begin to vibrate rythmically with the ground, with the effects of ground shaking being amplified to a high level by the phenomenon of resonance. In this context, the thickness of soft soil is a fairly good index for estimating resonance.

4.1.3 Comprehensive Seismic Vulnerability Index Grid (I/R)

Each zone (Square Hectares, Square Milles, etc.) of the study area can be plotted with the corresponding values of ground response (I) and resonance (R). The range of I and R can be split into a number of classes. In the case of Metro-Manila, the following classes have been defined, based in past earthquakes of intensity 10 on the ROSSI-FOREL Scale;

- 4 classes for ground response I (weak, strong, very strong, violent)
- 3 classes for Resonance R (weak, medium, strong)

On this basis a vulnerability grid could be established and its subsequent relationships.

Resonance (thickness) R	Total Ground Response I		WEAK A	STRONG B	VERY STRONG C	VIOLI D
	WEAK	1	A1	B1	C1	D1
	MEDIUM	2	A2	B2	C2	D2
	STRONG	3	A3	B3	C3	D3

The I and R indices are not entirely independent since the thickness parameter is also introduced into the ground response I. It is therefore probable, that extreme cases usch as the corresponding squares on the lower left and upper right of the grid are in fact hypothetical and do not occur in reality.

4.1.4 Land Use and Building Constraints

As has already been indicated, seismic analysis reveals that earthquake may cause damage to human settlements through ground response and resonance, the first having general effects and the latter on the type of construction. Therefore, other related constraints must be defined both in the fields of land use and building. The following list indicates the major constraints which should be assigned according to the seismic condition of each given zone in an urban planning area:

1 - open space only

2 - no low rise building (0-2) storeys)

3 - no medium-rise building (3-7 storeys)

4 - no high-rise buildings (8 storeys and more)

5 - no public places, such as schools, markets, shopping centers, theaters, offices, etc.

6 - no dangerous industries and storage facilities, which may cause explosions or fire (chemical plants, oil processing plants, gas storage, fuel storage, etc.)

7 - no industries and services vital to the community (electricity, water, treatment hospitals, telecom, etc.)

It is obvious that constraint 1 is most severe and will be applicable to the most dangerous zones. However, it must be stressed that this list does not imply any ranking, since the assignment of a constraint, or a set of constraints will depend on 2 separate index values (or co-ordinates), i.e. ground response intensity and resonance. These constraints are referred to by a number in the vulnerability index grids that follow, as applied on specific zone by a defined unit of area:

R \ I	A WEAK	B STRONG	C VERY STRONG	D VIOLENT
1 - Short			6,7	4,5,6,7
2 - Medium			3,5,6	3,4,5,6,7
3 - Long		4,7	3,4,5,6,7	1

For R/1 ground responses A & B (ground motion) are not deemed strong enough to cause damage. Therefore, no constraints are indicated. For a very strong ground response, C only dangerous industries (constraint 6) and vital industries and services (constraint 7) are vulnerable. For a violent ground response, D, the same constraint must be retained, plus two new constraints (4,5) related to activities liable to jeopardize human lives. For rows 2 and 3, the process of determining constraints is exactly the same, but the resonance factor is of greater significance. Thus, squares A and B on row 2 are not affected by any constraints, whereas all blocks of row 3 have constraints. Constraint 1 (open space only) is introduced in square D3 due to the fact that even low-rise buildings, which have generally light structures, with a low center of gravity, may be affected. As it is the most extreme of the 7 constraints, it excludes all other possibilities.

4.1.5. Interpretation by Columns

Studying the vulnerability index grid vertically, for a given ground response (I), variations of the resonance phenomenon, R, occur as the thickness of loose or unconsolidated soils increase (R/1, R/2, R/3). Thus restrictions are placed on the siting of high-rise buildings on thick, unconsolidated soils.

In vertical columns I/A and I/B, for relatively weak or mild ground responses, the risks are negligible in shallow deposits, but they increase significantly where these deposits become thicker, especially with regard to high-rise, reinforced frame structures.

When examining vertical columns I/C and I/D, the ground response is sufficiently strong increase risks all around, even when ground response is minimal. As the ground thickness increa: the resonance factor increases, and both resonance and intensity

act in concert to magnify disaster risks to such an extent that severe constraints have to be imposed. Thus, in column I/C the constraints increase from 6 to 7 in horizontal row R/1 to 3,4,5,6 & 7 in row R/3.

4.1.6 Synthesis of Seismic Vulnerability

The seismic factors governing land use and building constraints are usually not uniform over a given area. Their relative importance may vary significantly even over minute distances. Thus, the use of micro-zoning grid map appears as the most appropriate solution. On such maps, the size of each square is related to several factors:

- the scale of planning exercise
- the accuracy of field studies
- the future intended use of the maps

For urban planning, a micro-zoning grid of 1 km. x 1 km. square seems to be practical enough, provided the structure of the area (topography) is not too complex. In turn, physical factors related to seismic I and R indices are recorded on each grid.

4. 2 Flood Vulnerability Analysis

The determination of flood risks is in general less complex than in the case of earthquakes. Usually a flood has two direct means of impact:

1. the flood level
2. its velocity

The frequency and intensity of flooding can be easily estimated. Moreover the relative simplicity of the flooding process, compared to the complex chain of events triggered by seismic shaking, allows one to estimate with a fair degree of accuracy the vulnerability of a given location.

4.2.1 Land Use and Building Constraints (flood)

In the preceeding paragraphs on seismic risk, seven land use and building constraints were defined, all of which is applicable to flood vulnerability analysis, with the addition of an 8th constraints, which is as follows:

8 - capital intensive industries or activities comprising heavy investments in extremely costly or sophisticated equipment (modern textile plants, assembly plants, ligh industry, etc.)

4.2.2 Identification of constraints for the Vulnerability Index Grid

a) For frequent floods (high frequency)

FLOOD LEVELS	CONSTRAINTS
low	-
medium	2,5,7
high	2,3,4,5,6,7

b) For infrequent floods (low frequency)

FLOOD LEVELS	CONSTRAINTS
low	-
medium	7,8
high	2,7,8

By integrating these constraints on the following grid, we obtain the total combination of constraints for areas affected by both flood types (frequent and infrequent):

Flood Level (high frequency) \ Flood Level (low frequency)	0m.	0.5m.	2m.	4m.
0m.	-	7,8	2,7,8	
0.20m	-	7,8	2,7,8	
0.50m	2,5,7	2,5,7	2,5,7,8	2,5,7,8
1.0m.	1	1	1	1

4.3 Integration of Land Use and Building Constraints

(Seismic & Flood in a Composite Risk Map Vulnerability Grid Map)

The synthetic map which summarizes all the constraints described in the preceeding paragraphs must be a grid map in which the grid scale and location will be the same for seismic and flood risks. The integration of constraints related to earthquake and flooding is carried out by superimposing all constraints belonging to the same blocks of the grid.

It must be emphasized that these constraints are cumulative. If given a block, for instance, we have the following constraints:

earthquake - (2,3.6)
flood - (2,4,6,7), then

the general constraints related to the total risk will be:

TOTAL - (2,3,4,6,7)

the integration of these two map is what is called the TOTAL VULNERABILITY GRID MAP.

5. THE APPLICATION OF VULNERABILITY ANALYSIS TO URBAN PLANNING PROCESS OF THE METRO-MANILA AREA.

In recent years, land use planning and zoning of communities, towns or cities have been undertaken within a two dimensional structure relative to a specific geographic area. However, at present, land use planners have been clamoring for a more sophisticated techniques in land use planning and zoning by adding a three dimensional perspective or aspect into land use and zoning plans.

With the introduction of sub-soil condition analysis as inputs into land use and zoning plans, the three dimensional aspect is achieved. The total vulnerability index map is one indispensable tool to define land use and building constraints utilizing the investigation of sub-soil condition. These constraints are applicable both to zones which are already built-up (urban center) and to areas planned for new developments (new towns, regional growth centers, etc.).

The synthesis map of constraints is the final result of the vulnerability analysis, and provides the planner with the physical planning tool which forms part of the basic for lan use allocation and building restrictions.

Furthermore, the integration of the synthesis map of constra would form the vital physical attributes inputed into the ge graphic base filed system to facilitate and build up the monitoring and information system for the MMA.

The synthesis map of constraints although undertaken on a 1 km. x 1 km. grids could be easily related to the geographic base files which utilizes the ordinary block through the system of sups blocks to form approximately a 1 sq. km. grid. The integration and synthesis of this physical and socio-economic attributes into the geographic base files is at present being undertaken by the Technology Resource Center to help and guide planners in the formulation of urban design guidelines and criteria for urban renewal and undevelopment projects.

The vulnerability analysis undertaken for the Metro Manila Area is at present being used as inputs in the preparation of its land use and zoning plans. Areas where constraints have been identified such as open spaces only (1), have been identified as areas to be devoted to parks or for natural recreation areas, inorder to optimize the use of prime urban land. In areas susceptible to flooding, limited housing types and designs would be allowed, i.e., 1-storey residential structure on stilts. In areas where constraints due to seismic factors have been identified, again limited residential structures could be allowed following certain requirements in building construction and materials with more flexibility and elasticity.

Aside from the usefulness of vulnerability analysis to the physical planning process, it likewise serves as essential background information for the structural design of new buildings. It directs the attention of the structural designer towards the critical parameters of his design.

Finally, for all intents and purposes, the methodology devised for the vulnerability analysis on natural risk disaster seeks to evolve a certain amount of awareness such that constraints due to seismic and flooding factors could be utilized and harnessed not only for disaster mitigation but also as a vital tool for guiding national development.

A C K N O W L E D G E M E N T S

TO MR. JACQUES DIDON AND MR. MICHEL COUILLAUD, OF THE UNITED NATIONS DISASTER AND RELIEF ORGANIZATION (UNDRO) WHO PREPARED THE REPORT ON THE "METHODOLOGY FOR COMPOSITE VULNERABILITY ANALYSIS ASSOCIATED WITH NATURAL DISASTER RISKS" FOR THE METROPOLITAN MANILA AREA, FEBRUARY 1977.

3.1 TOTAL VULNERABILITY GRID MAP

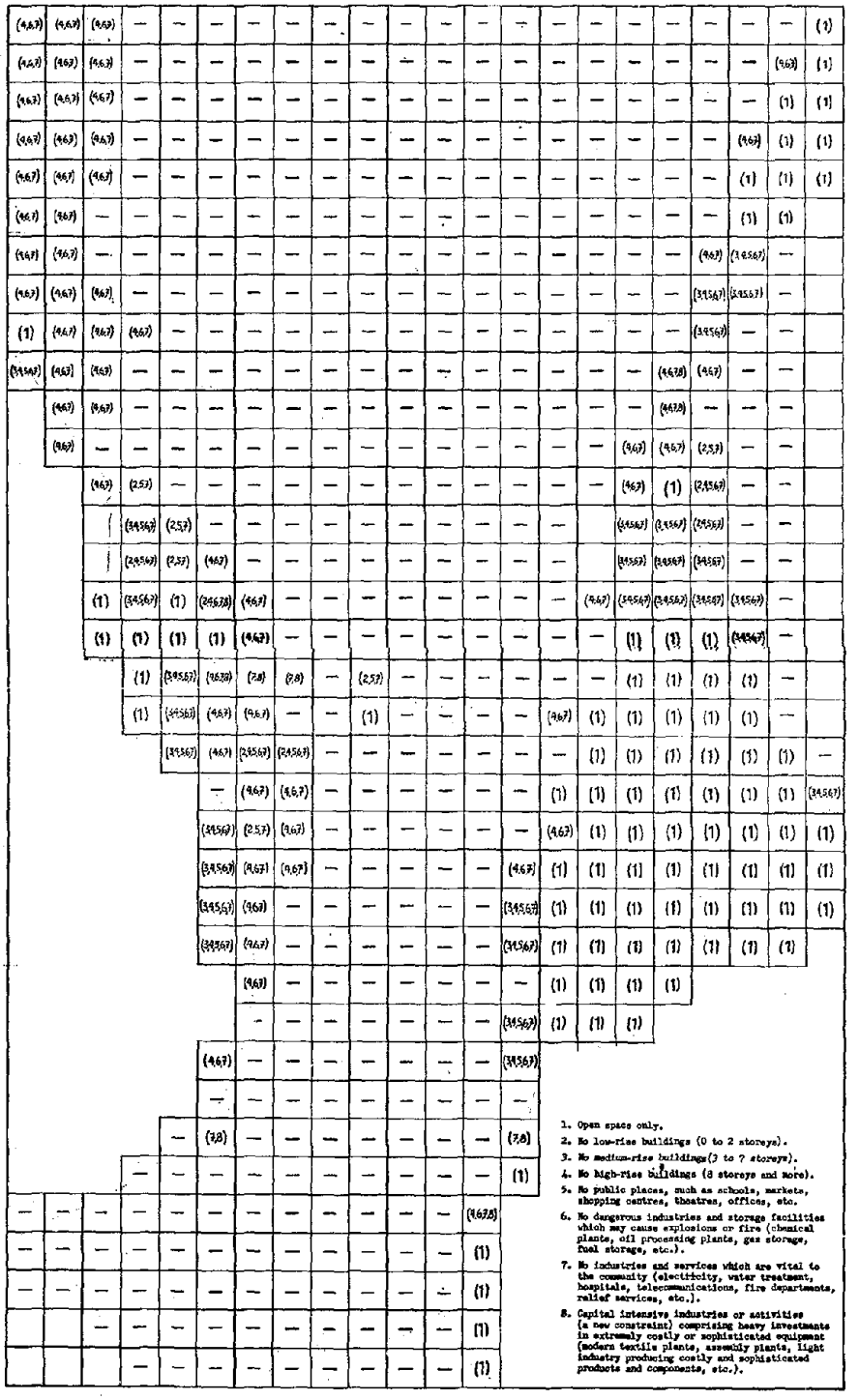

1. Open space only.
2. No low-rise buildings (0 to 2 storeys).
3. No medium-rise buildings(3 to 7 storeys).
4. No high-rise buildings (8 storeys and more).
5. No public places, such as schools, markets, shopping centres, theatres, offices, etc.
6. No dangerous industries and storage facilities which may cause explosions or fire (chemical plants, oil processing plants, gas storage, fuel storage, etc.).
7. No industries and services which are vital to the community (electricity, water treatment, hospitals, telecommunications, fire departments, relief services, etc.).
8. Capital intensive industries or activities (a new constraint) comprising heavy investments in extremely costly or sophisticated equipment (modern textile plants, assembly plants, light industry producing costly and sophisticated products and components, etc.).

SEISMIC RISK ANALYSIS INCLUDING ATTENUATION UNCERTAINTY

by

Armen Der Kiureghian
Assistant Professor of Civil Engineering
University of Southern California
Los Angeles, Ca. 90007,U.S.A.

SYNOPSIS

Methods for seismic risk analysis are discussed. The effects of various uncertainties on seismic risk are compared, and it is shown that attenuation uncertainty is the most significant source of uncertainty. A general formulation for seismic risk analysis, including attenuation uncertainty, is presented. The procedure is applied to an actual site in San Francisco. Computed risks with and without attenuation uncertainty are compared. It is shown that the attenuation uncertainty has a highly significant effect on the calculated seismic risk.

Introduction

The earthquake resistant design of a structure in a seismic region requires an assessment of the peak ground motion intensity, at the site of structure, due to future earthquakes. Since locations, magnitudes, and other characteristics of future earthquakes affecting a region are, in general, random, such an assessment can only be achieved on a probabilistic basis. If it is assumed that for the time period of interest (i.e., the life of structure) major changes in the seismicity of a region do not occur, then, future seismic activity can statistically be evaluated on the basis of the historical data of earthquakes in the region. In particular, if ground motion intensities felt at a given site during past earthquakes are known, then, the required probabilities could be estimated using the techniques of extreme value statistics. Such data for an arbitrary site, however, are seldom available and such a direct analysis is usually not possible. The information that is more generally available is the magnitude and location of past earthquakes, empirical laws defining attenuation of strong shaking with distance, and possibly some knowledge of the types of potential seismic sources in the region of interest. Analytical models are, therefore, required in order to synthesize all such regional information and to derive probabilities associated with various levels of ground motion.

One of the first analytical models for seismic risk analysis was develop by Cornell (1968). In this development the spatial distribution of earthqua was defined through several idealized models. In each case it was implicitl assumed that the entire energy of an earthquake is released at a point--the focus. This assumption, although reasonable for small magnitude earthquakes is not realistic for major earthquakes which may originate as intermittent series of ruptures along long faults. (The rupture length could be as long several hundred kilometers for a major earthquake.) Recognizing this fact, D Kiureghian and Ang (1975, 1977) developed a model in which earthquakes were assumed to originate as "lines" rather than "points". These "lines" were as

sumed to occur randomly along known or unknown faults. They, thus, included the effect of rupture length in the evaluation of seismic risk. This model includes Cornell's model as a special case when the rupture length is assumed to be zero. A number of other models have also been developed which are closely related to the ones discussed above.

A major problem in implementing any seismic risk model is the uncertainty associated with the regional information which forms the basis for the analysis. More specifically, five major sources of uncertainty in seismic risk analysis are identified. These are;1) errors in estimating magnitude recurrence rates, 2) errors in idealizing a seismic region into a number of mathematically tractable source models, 3) uncertainty in specifying the largest possible earthquake in each potential source, 4) scatter of data around the rupture length-earthquake size relationship, and 5) scatter of data around the regional intensity attenuation law.

To investigate the significance of each of these uncertainties, Der Kiureghian (1977) estimated the contribution from each source of uncertainty to the total coefficient of variation of the peak intensity at an actual site. Figure 1 taken from this reference compares the coefficients of variation attributed to the various sources of uncertainty and for a range of time durations of interest. δ_y in this figure denotes the variation in the peak intensity which results from the randomness in number, size, location, and direction of rupture of future earthquakes, and Δ_1 to Δ_5 represent variations in the peak intensity which are caused by the five sources of uncertainty mentioned above. It is observed in this figure that the attenuation uncertainty is highly significant. It is concluded, therefore, that the effect of this uncertainty must directly be included in the evaluation of seismic risk.

It should be pointed out that the significance of attenuation uncertainty on seismic risk has long been recognized. Esteva (1971), Esteva and Villaverde (1974), and Der Kiureghian and Ang (1975, 1977) pointed out this significance and approximately included the effect of this uncertainty in the calculated risk.* More recently, Anderson and Trifunac (1978) have explicitly considered the scatter around the attenuation law in an analysis with a model similar to Cornell (1968).

A general formulation for seismic risk analysis including attenuation uncertainty is presented below. Certain details in the formulation which are specific to the various models and can be found in the respective references are not given here. Instead, more attention is given to demonstrating the effect of attenuation uncertainty on the calculated probabilities.

Formulation of Seismic Risk

Suppose the seismic region surrounding a given site is modeled into n tential sources. Let ν_i denote the mean rate (i.e., mean number per year earthquakes occurring in source i which are of magnitude m_0 or greater, w m_0 represents a lower bound magnitude for earthquakes of concern to engin say, about 4 on Richter scale. If occurrences of earthquakes both in tim space are assumed to be statistically independent and to constitute a sim Poisson process, then, it can be shown that the probability of the T-year

* The nature of this approximation will subsequently be discussed.

treme intensity, Y_T, exceeding a given level y is

$$P(Y_T>y)=1-\exp\left[-T\sum_{i=1}^{n}P(Y>y|E_i)\nu_i\right], \tag{1}$$

and the average return-period associated with the level y is

$$\overline{T}_y=\frac{1}{\sum_{i=1}^{n}P(Y>y|E_i)\nu_i}, \tag{2}$$

where $P(Y>y|E_i)$= the probability that the random intensity at the site, Y, will exceed the level y given the occurrence of an earthquake in source i. Using the theorem of total probability, this term may be calculated as

$$P(Y>y|E_i)=\int_{m_o}^{m_u}P(Y>y|m)f_M(m)dm, \tag{3}$$

where m_u is the magnitude of the largest possible earthquake in source i, $P(Y>y|m)$=probability of Y>y given a magnitude m earthquake in source i, and $f_M(m)$ is the probability density function of magnitudes. Based on Richter's magnitude recurrence law, it is easy to show that

$$f_M(m)=\frac{\beta\exp\left[-\beta(m-m_o)\right]}{1-\exp\left[-\beta(m_u-m_o)\right]}, \tag{4}$$

where β is the regional seismicity parameter and is related to the slope of the magnitude recurrence line (see Der Kiureghian and Ang, 1977).

To evaluate the conditional probability in the integral of Equation 3, an attenuation law relating intensity at the site to the earthquake magnitude and distance is required. Such a relationship can, in general, be specified in a functional form as

$$y=f(m,r), \tag{5}$$

where y may represent any selected measure of intensity, such as a maximum ground motion parameter, the Modified Mercalli intensity, or a response spectral amplitude at a specific frequency; m represents the earthquake magnitude, and r denotes the distance to the source of energy release. Since energy is released along the entire fault break, obviously no single distance is completely appropriate in the above equation. It is argued by Der Kiureghian and Ang (1977) that the intensity at a site is primarily caused by the energy released in the closest portion of the rupture. For this reason, they use the shortest distance to the fault break. On the other hand, Cornell (1968), and most other investigators following his approach, disregard the rupture length and use the epicentral or hypocentral distance for r, this being tantamount to the assumption that the entire energy is released at the focus. This assumption may lead to an underestimation of risk, as demonstrated by Der Kiureghian and Ang (1977).

It should be pointed out that other parameters besides m and r may also enter into the attenuation relationship given in Equation 5. These may include parameters defining subsoil and geologic conditions at the site and in the region, the direction of motion under consideration, and the frequency in the case of spectral analysis (see Trifunac, 1976). These parameters, however, have no effect on the formulation to be presented here.

Attenuation laws of the type given in Equation 5 are usually obtained empirically through regression analysis of recorded data of past earthquakes. Such data always shows significant scatter around calculated mean curves. This uncertainty may be attributed to: 1) the randomness in earthquake generation mechanism, 2)variabilities in the characteristics of wave propagation paths, 3) variabilities in subsoil and geologic conditions at the recording sites, and 4) overall variabilities in the geologic characteristics of various seismic regions. The effects of the first two items obviously vary from one earthquake to another, whereas the effects of the last two items are independent of earthquakes. For a specific site in a region,the latter two uncertainties may be excluded if it is possible to obtain a sufficient number of records in the region which have the same site conditions as the site under consideration.

To include the effects of attenuation uncertainties, a random correction factor is included and the attenuation law is written as

$$y=Zf(m,r). \tag{6}$$

Here Z is a random variable which could, in general, depend on m, r and other parameters that may be involved. In constrast to the deterministic attenuation law of Equation 5, Equation 6 can be regarded as a random attenuation law. The difference between the two is schematically illustrated in Figure 2 for a particular m and r, where it is observed that whereas Equation 5 predicts a specific value of intensity, as indicated by a dot, Equation 6 describes a distribution of possible intensities.

A possible approach for the analysis of attenuation uncertainty is to assume that the values of Z at various occurrences are statistically independent. This assumption is reasonable if the uncertainty in attenuation can primarily be attributed to items 1 and 2 above. (Note that items 3 and 4 are particular to the site and the region, respectively, and are independent of earthquakes. The effects of both items at various occurrences would generally be correlated.) If it is also assumed, for convenience, that Z is independent of distance, then, using the theorem of total probability one can write

$$P(Y>y|m)=\int_0^\infty P(Y>y|m,z)f_{Z|M}(z,m)dz, \tag{7}$$

where

$$P(Y>y|m,z)=\int_0^\infty P(Y>y|m,z,r)f_{R|M}(r,m)dr.$$

In the above $f_{Z|M}(z,m)$ and $f_{R|M}(r,m)$ represent the conditional probabilit sity functions of Z and R, respectively, and $P(Y>y|m,z)$ and $P(Y>y|m,z,r)$ the conditional probabilities of Y>y given m, z and m,z,r, respectively.

The density function $f_{Z|M}(z,m)$ is evaluated through standard statisti techniques applied to the residuals of the regression analysis of attenua data (see, for example, Donovan, 1973). The dependence of Z on magnitud

usually neglected due to lack of sufficient data in various magnitudes bands.

The evaluation of Equation 8 depends on the definition and the geometry of a source. This integral has been evaluated in closed form for a number of idealized source models. As an example, Figure 3 shows three such models defined in Der Kiureghian and Ang (1977). The selection of an idealized model for a source is based on its type and the extent of information available about it. The type 1 source model in Figure 3a is for a well-known active fault; the type 2 source model in Figure 3b is for an active area in which fault ruptures occur in a preferred orientation; and the type 3 source model in Figure 3c is for an area with unknown faults. The detailed description of each source model and the corresponding solutions are given in Der Kiureghian and Ang(1977) and will not be repeated here.*

Once Equation 8 is evaluated for a source, numerical integrations of Equations 7 and 3 yield the required conditional probability for the source. By substitution of these conditional probabilities for each source in Equations 1 and 2, the T-year exceedance probability and the average return-period, respectively, are evaluated.

A second approach for the analysis of attenuation uncertainty is to assume that the values of Z at various occurrences remain the same, i.e., they are perfectly correlated. In addition, it is assumed that Z is independent of magnitude and distance. This procedure was implicitly followed by Esteva (1971), Esteva and Villaverde (1973), and Der Kiureghian and Ang (1975, 1977).

With Z at various occurrences assumed to remain unchanged, using the theorem of total probability the T-year exceedance risk may be obtained as

$$P(Y_T>y)=\int_0^\infty P(Y_T>y|z)f_Z(z)dz, \tag{9}$$

where $f_Z(z)$ is the density functional of Z and $P(Y_T>y|z)$ is the conditional risk for Z=z, i.e, the risk based on the attenuation law y=zf(m,r). This conditional risk is the same as the risk at intensity y/z as evaluated on the basis of the deterministic attenuation law of Equation 5. Letting the subscript d denote the risk based on deterministic attenuation, Equation 9 then becomes

$$P(Y_T>y)=\int_0^\infty P_d(Y_T>\frac{y}{z})f_Z(z)dz. \tag{10}$$

To obtain the risk with deterministic attenuation, one may disregard Equati 7 and the values of z in Equation 8, and substitute from Equation 8 directl into Equation 3.

The above approach is computationally simpler than the approach discuss before since it avoids the double integration of Equations 3 and 7. It is

*To obtain the solutions of Equation 8 from Der Kiureghian and Ang (1977), t attenuation law in that reference should be replaced with y=zf(m,r), where z is the known value of the random variable Z.

however, not realistic since the values of Z at various occurrences would generally have little correlation due to the significance of items 1 and 2 (i.e., the randomness in earthquake mechanism and variabilities in propagation paths) on attenuation uncertainty. This approach, nevertheless, would be realistic if it is used to correct the calculated risk for uncertainties which are independent of earthquake occurrences, such as those due to items 3 and 4 mentioned above.

It should be pointed out that perhaps a better method is a combination of the above two procedures, in which the risk curve as corrected with the first procedure for items 1 and 2 is further corrected with the second procedure for items 3 and 4. There seems to be no analytical difficulty in implementing this method; however, it would require a separation of uncertainties due to the various items which may not be easily obtainable due to the lack of sufficient data.

Discussion of Results

The procedures outlined above have been applied to the seismic risk analysis of a site in San Francisco. The historical data and the details of seismicity idealization are given in Der Kiureghian and Ang (1975). For the analysis of this site, the attenuation equation

$$y=1.10e^{0.5m}(r+25)^{-1.32} \tag{11}$$

given by Donovan (1973) is used, where y is the maximum ground acceleration in g's, m is in the Richter scale, and r is in kilometers. This equation was obtained as the mean curve to a set of 550 records obtained from all regions of the world.

In developing this equation, Donovan (1973) demonstrated that the residuals of the logarithm of the ratio of measured to computed intensities when plotted on a normal probability paper show conformity with the normal distribution. This clearly suggests a log-normal distribution for Z. The mean and standard deviation of ℓnZ, as obtained from this plot, were 0.0 and 0.707, respectively, which gave a mean of 1.28 and a standard deviation of 1.03 for Z.

Using the above distribution for Z, the 50-year exceedance probabilities for this particular site are calculated and are shown in Figure 4. Results of analysis with random attenuation following the first procedure (solid curve) and the second procedure (dashed curve) as well as deterministic attenuation are shown in this figure. By comparison of the curves, the effect of attenuation uncertainty is seen to be rather drastic. This comparison, thus, serves to demonstrate the significance of including the attenuation uncertainty seismic risk analysis. It is also observed that the results obtained for dom attenuation with the two procedures are not too different for the cas under consideration.

The corresponding density functions for the 50-year extreme intensity also evaluated and are shown in Figure 5. It is observed that the effect the additional uncertainty in attenuation is the stretching and shifting the density function towards higher intensities.

It should be pointed out that the data used for derivation of the attenuation equation included records from all regions of the world regardless of regional characteristics or recording site conditions. If, for this region, sufficient data were available such that an appropriate set of records consistent with the conditions at the site could be selected, then, the uncertainties due to site conditions and regional characteristics could be reduced. It is believed that the statistical analysis would then yield a smaller variation for Z than that predicted in Donovan's study. Therefore, it is thought that the risk curves in Figure 4 are conservative estimates appropriate for a site with unknown local and regional characteristics.

Conclusions

Several problems in seismic risk analysis are discussed. It is shown that the uncertainty associated with the attenuation law is the most significant source of uncertainty in seismic risk analysis. A general formulation for seismic risk analysis is presented which includes the spatial and temporal randomness of future earthquakes as well as the attenuation uncertainty.

Results of seismic risk analysis for a site in San Francisco, both including and excluding attenuation uncertainty, are presented. By comparison of the results, it is concluded that the effect of attenuation uncertainty on calculated seismic risk is highly significant. It is recommended, therefore, that this uncertainty be routinely included in seismic risk analysis.

Acknowledgment

The author acknowledges M. D. Trifunac and J. G. Anderson for their critical reviews and constructive comments.

REFERENCES

1. Anderson, J.G. and M.D. Trifunac (1978), "Uniform Risk Functional for Characterization of Strong Earthquake Ground Motion," Bull, Seism. Soc. Am. 68, Feb.

2. Cornell, C.A. (1968), "Engineering Seismic Risk Analysis, "Bull. Seism. Soc. Am. 58, 1583-1606.

3. Der Kiureghian, A. (1977), "Uncertainty Analysis in Seismic Risk Evaluation," in Advances in Civil Engineering through Engineering Mechanics, New York; Amer. Soc. of Civil Eng. 320-323.

4. Der Kiureghian, A. and A. H-S. Ang (1975), "A Line-Source Model for Seismic Risk Analysis," University of Illinois at Urbana-Champaign, Civil Eng. St dies, SRS No. 419.

5. Der Kiureghian, A. and A. H-S. Ang (1977), "A Fault-Rupture Model for Sei mic Risk Analysis," Bull. Seism. Soc. Am. 67, 1173-1194.

6. Donovan, N.C. (1973), "A Statistical Evaluation of Strong Motion Data Including the February 9, 1971 San Fernando Earthquake," Proc. Fifth World Conf. on Earthq. Eng., Rome, Italy.

7. Esteva, L. (1971), "Seismic Risk and Seismic Design Decisions," in Seismic Design for Nuclear Power Plants, M.I.T. Press, Cambridge, Mass.

8. Esteva, L., and R. Villaverde (1973), "Seismic Risk, Design Spectra and Structural Reliability," Proc. Fifth World Conf. on Earthq. Eng., Rome, Italy.

9. Trifunac, M.D. (1976), "Preliminary Empirical Model for Scaling Fourier Amplitude Spectra of Strong Ground Motion in Terms of Earthquake Magnitude, Source to Station Distance, and Recording Site Conditions," Bull Seism. Soc. Am., 66, 1343-1373.

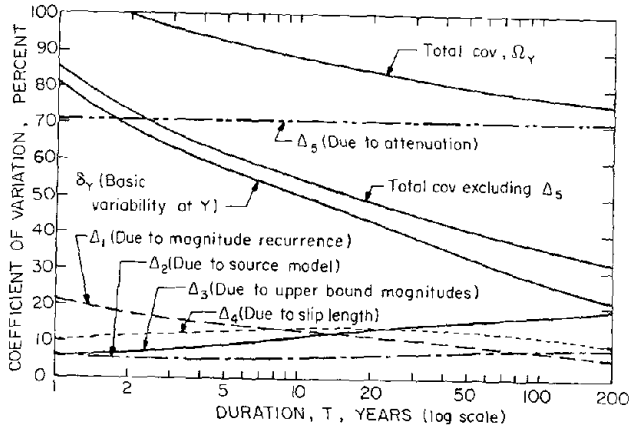

Figure 1. Significance of Uncertainties on Seismic Risk (Der Kiureghian, 1977).

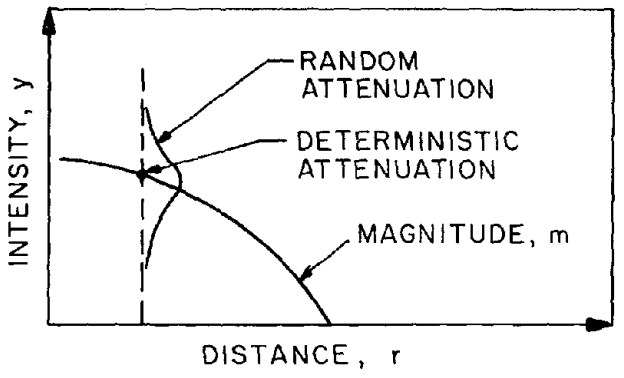

Figure 2. Illustration of Deterministic and Random Attenuation Laws.

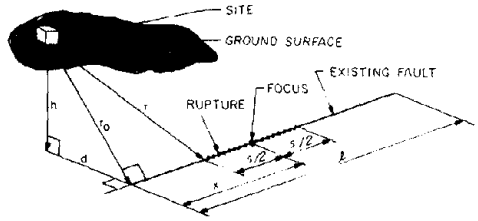

(a) Type 1

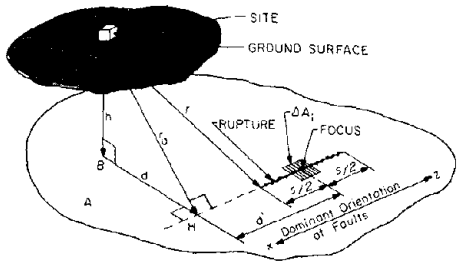

(b) Type 2

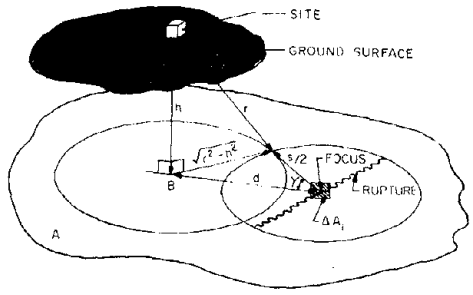

(c) Type 3

Figure 3. Idealized Source Models (Der Kiureghian and Ang, 1977).

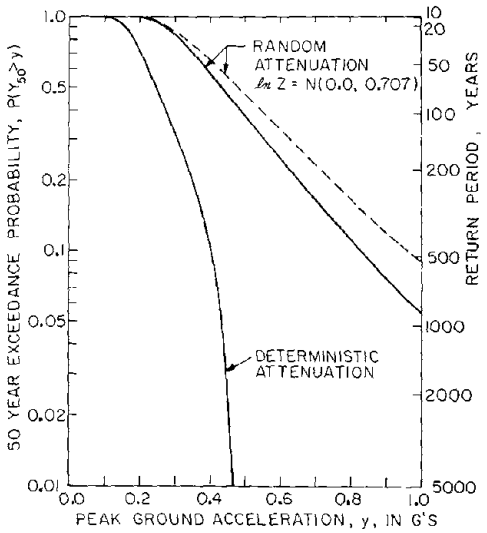

Figure 4. Calculated Seismic Risks Based on Random and Deterministic Attenuation Laws.

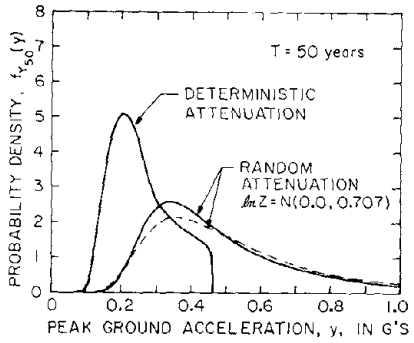

Figure 5. Calculated Density Functions for 50-Year Extreme Intensity.

PROBABILISTIC SOLUTION TO HYSTERETIC SYSTEMS SUBJECTED TO EARTHQUAKES

by

PISIDHI KARASUDHI
Associate Professor
Asian Institute of Technology
Bangkok, Thailand

CHI-CHIN WU
Graduate Student
Asian Institute of Technology
Bangkok, Thailand

HIROKAZU TAKEMIYA
Associate Professor
Okayama University
Okayama-Shi, Japan

Synopsis

Nonlinear terms in the Fokker-Planck equation of bilinear hysteretic systems are replaced by linear terms, each containing a single coefficient which is determined by minimizing a properly weighted mean square difference between two corresponding nonlinear and linear terms. This study is carried out first for single-degree-of freedom systems, then extended to multi-degree-of freedom systems. The statistical seismic response of these systems is obtained involving a complex eigenvalue problem. In addition, a linearization method involving two coefficients for each corresponding pair of nonlinear and linear terms in Fokker-Planck equations is studied.

Introduction

There are three main approaches for the analysis of nonlinear systems under random excitation; i.e., the Fokker-Planck approach, perturbation approach, and equivalent (statistical, stochastic) linearization approach. A brief review of these approaches has been made by Atalik and Utku (1976). All these methods seem well applicable to problems with a singlevalued force-deformation relationship, but not so for hysteretic systems where the nonlinearity involves velocities as well as displacements. For bilinear hysteretic systems, Kaul (1972) has constructed a Fokker-Planck equation and replaced nonlinear terms in this equation by equivalent linear terms, and then transformed the resulting linearized Fokker-Planck equation into a set of matrix differential equations of a Liaponov form. These matrix equations has been solved by the Runge-Kutta numerical method. Assuming stationarity for the response and taking the hysteretic force as the sum of an equivalent viscous damping force and a linear spring force, Takemiya (1976) has solved the problem through a formulation of a set of equivalent linear equations of motion.

In this paper, a linearization technique is developed, involving a single coefficient for each stiffness element which connects two adjacent masses. This coefficient is obtained by minimizing the statistical mean square difference between two corresponding terms in the Fokker-Planck equations of the no system and the equivalent linear model. In addition, a linearization in two coefficients for each stiffness element is also investigated. Resul various methods are compared.

Single-Degree-of-Freedom (SOF) Systems

SOF Bilinear Hysteretic System

An SOF bilinear hysteretic system can be illustrated by a model com a linear spring, a viscous damper and a Coulomb stiffness element as sho Fig. 1 and its force-deformation curve is as shown in Fig. 2. In these f w denotes the stretch of the spring which is connected to the Coulomb sli

x the mass displacement, Y the yielding displacement α strain hardening coefficient, and A the mass displacement amplitude. The equation of motion can be expressed as

$$\ddot{x} + c\dot{x}/m + \alpha kx/m + (1-\alpha)kw/m = f(t) \tag{1}$$

where f(t) is the input excitation taken as a gaussian white noise with a mean of zero, i.e.,

$$E[f(t)] = 0 , \quad E[f(t_1)f(t_2)] = 2\pi S_o \delta(t_1 - t_2) \tag{2a,b}$$

in which S_o is the white noise spectral density, $\delta(\ )$ is the Dirac-delta function, and E[ ] denotes an expectation or an emsemble average.

Assuming further that the excitation is a finite order Markov process, and the vector $X(t) = (x,\dot{x},w)$ is a Markov vector, the following Fokker-Planck equation (Lin, 1967) is obtained

$$\frac{\partial P}{\partial t} = -\frac{\partial}{\partial \dot{x}}[\{-c\dot{x}/m-\alpha kx/m-(1-\alpha)kw/m\}P] - \frac{\partial}{\partial x}(\dot{x}P) - \frac{\partial}{\partial w}[\dot{x}\theta(|w|-Y)P] + \pi S_o \frac{\partial^2 P}{\partial \dot{x}^2} \tag{3}$$

in which $P = P(X,t; X_o,t_o)$ is the probability density function of vector X occurring at time t under the condition that vector X_o has already occurred at time t_o, and

$$\begin{aligned} \theta(z) &= 1 , \quad z < 0 \\ &= 0 , \quad z \geq 0 \end{aligned} \tag{4}$$

Equivalent Linear Model of SOF System

It is difficult to obtain the exact solution of Eq. 3, because of the nonlinear term

$$\dot{x}\theta(|w| - Y) \tag{5}$$

As shown in Fig. 3, an equivalent linear model is introduced by replacing the slider in the Coulomb stiffness element of the original system by equivalent damper with coefficient C_d. The Fokker-Planck equation of this equivalent linear model takes the same form as Eq. 3 excepting that the nonlinear term (Eq. 5) is replaced by

$$\dot{x} \sim \beta w \tag{6}$$

where β is $(1-\alpha)k/C_d$ and can be obtained by minimizing a properly weighted mean square error between these two terms, i.e.

$$\frac{\partial}{\partial \beta} \int_{-Y}^{Y} \int_{-\infty}^{\infty} [\dot{x}\theta(|w|-Y) - \{\dot{x} - \beta w\}]^2 P(\dot{x},w) d\dot{x} dw = 0$$

in which P(x,w) is a marginal probability density function, i.e.

$$P(\dot{x},w) = \begin{cases} P_\ell(\dot{x},w) & |w| < Y-\varepsilon \\ P_w(Y)\delta(|w|-Y)P_\ell(\dot{x}) & Y-\varepsilon \leq |w| < Y \end{cases}$$

where $P_\ell(\dot{x},w)$ and $P_\ell(\dot{x})$ are nearly gaussian normal probability distributions

$P_w(Y) = (E[ww]/Y^2)^{\bar{m}}$, $\bar{m}$ must be at least 2, and ε is an infinitely small value of x_i. The derivation of Eq. 8 has been carried out by Kaul (1972) basing his analysis on purely physical considerations. From Eq. 7, β can be obtained in the form

$$\beta = (\frac{2}{\pi})^{\frac{1}{2}} (\frac{Y^2}{E[ww]}) (\frac{\sqrt{E[\dot{x}\dot{x}]}}{Y}) (\frac{E[ww]}{Y^2})^{\bar{m}} \tag{9}$$

Multi-Degree-of-Freedom (MOF) Systems

In the MOF system with n degree of freedom considered in this study, each pair of adjacent masses are linked by a stiffness element consisting of a linear spring, a viscous damper and a Coulomb stiffness element, as shown in Fig. 4; and the equations of motion are

$$[M]\{\ddot{u}\} + [C]\{\dot{u}\} + \{F(u)\} = -[M]\{1\}\ddot{u}_g \tag{10}$$

in which [M] denotes the diagonal mass matrix of element m_i, [C] damping matrix, $\{F(u)\}$ the bilinear hysteretic restoring forces of the type shown in Fig. 2, $\{u\}$ the displacements of masses relative to the ground, and u_g the absolute acceleration of the ground.

Denoting that x_i the displacement of the mass m_i relative to its preceding mass m_{i-1}, i.e., $x_i = u_i - u_{i-1}$; $\{x\}$ can be related to $\{u\}$ as

$$\{x\} = [I_2]\{u\} \tag{11}$$

In other words, x_i denotes the drift of mass i relative to mass i-1. The restoring force matrix $\{F(u)\}$ may be written in the form

$$\{F(u)\} = [I_2]^T\{\alpha[K_i]\{x\} + (1-\alpha)[K_i]\{w\}\} \tag{12}$$

where $[K_i]$ is a diagonal matrix of elements k_i, and $\{w\}$ denotes the stretches of the springs in the Coulomb stiffness elements. Substituting Eqs. 11 and 12 into Eq. 10 yields

$$\{\ddot{x}\} + [C^w]\{\dot{x}\} + [K^u]\{x\} + [K^w]\{w\} = -\{N\}\ddot{u}_g \tag{13}$$

in which

$$[C^w] = [I_2][M]^{-1}[C][I_2]^{-1} \quad , \quad [K^u] = \alpha[I_2][M]^{-1}[I_2]^T[K_i] \tag{14a,b}$$

$$[K^w] = (1-\alpha)[I_2][M]^{-1}[I_2]^T[K_i] \quad , \quad \{N\} = [I_2]\{1\} \tag{14c,d}$$

Ground Motion Model

Since statistical investigations showed that earthquakes have some p frequency contents rather than a constant one, an earthquake modelled by a white noise through a nonstationary shot noise filter (Amin & Ang, 1968 adopted in this study. The filter involved can be characterized by an eq of SOF system of the form

$$\ddot{u}_o + 2\xi_g\omega_g\dot{u}_o + \omega_g^2 u_o = -\ddot{u}_b$$

in which $\ddot{u}_o$ is the acceleration of the ground level relative to and resul the input acceleration $\ddot{u}_b$; ω_g and ξ_g the indicators of the predominant fr and the damping factor of the function concerned, respectively. The valu and ξ_g can be estimated from certain averages generated from real earthqu

The input acceleration $\ddot{u}_b$ adopted here is a shot noise characterized by

$$E[\ddot{u}_b(t)] = 0 \quad , \quad E[\ddot{u}_b(t)\ddot{u}_b(t+\tau)] = 2\pi S(t)\delta(\tau) \tag{16a,b}$$

where $S(t)$ is a deterministic intensity function. The total ground acceleration is the superposition of $\ddot{u}_o$ and $\ddot{u}_b$, i.e.,

$$\ddot{u}_g = \ddot{u}_o + \ddot{u}_b \tag{17}$$

Equivalent Linear Model

Assuming further that the earthquake excitation is a finite order Markov process, and the vector $X(t) = (\dot{x}_1, \dot{x}_2 \cdots \dot{x}_n, x_1 \cdots x_n, w_1 \cdots w_n, \dot{u}_o, u_o, \dot{u}_b)$ is a Markov vector, the following Fokker-Planck equation (Lin, 1967) is obtained

$$\begin{aligned}\frac{\partial P}{\partial t} = &-\sum_{i=1}^{n}\{\frac{\partial}{\partial x_i}(\dot{x}_i P) + \frac{\partial}{\partial \dot{x}_i}[\sum_{j=1}^{n}(-c_{ij}^{w}\dot{x}_j - k_{ij}^{u}x_j - k_{ij}^{w}w_j + 2\xi_g\omega_g n_i\dot{u}_o + n_i\omega_g^2 u_o)P] \\ &+ \frac{\partial}{\partial w_i}[\dot{x}_i\theta(|w_i|-Y_i)P]\} - \frac{\partial}{\partial u_o}(\dot{u}_o P) + \frac{\partial}{\partial \dot{u}_o}(2\omega_g\xi_g\dot{u}_o + \omega_g^2 u_o)P \\ &+ \pi S(t)[\frac{\partial^2 P}{\partial \dot{u}_b^2} + \frac{\partial^2 P}{\partial \dot{u}_o^2} - 2\frac{\partial^2 P}{\partial \dot{u}_b \partial \dot{u}_o}]\end{aligned} \tag{18}$$

where c_{ij}^{w}, k_{ij}^{u} and k_{ij}^{w} are elements at i-row and j-column of matrices $[C^w]$, $[K^u]$ and $[K^w]$, respectively, and n_i is i-row element of matrix $\{N\}$.

In a similar way as in the SOF system, an equivalent linear model of this MOF system can be constructed by replacing the slider in each Coulomb stiffness element of the original system by an equivalent damper with coefficient C_{di}, as shown in Fig. 5. Accordingly, the Fokker-Planck equation takes the same form as Eq. 18 excepting that the nonlinear term $\dot{x}_i\theta(|w_i|-Y_i)$ is replaced by a linear term $\dot{x}_i - \beta_i w_i$, where $\beta_i = (1-\alpha)k_i/C_{di}$ and can be obtained in the form

$$\beta_i = (\frac{2}{\pi})^{\frac{1}{2}}(\frac{Y_i^2}{E[w_i w_i]})(\frac{\sqrt{E[\dot{x}_i\dot{x}_i]}}{Y_i})(\frac{E[w_i w_i]}{Y_i^2})^{\frac{-}{m}} \quad , \quad i = 1,2,3,\ldots,n \tag{19}$$

Random Response Analysis

The most important characteristics of the response of structures to a random excitation, such as an earthquake, is the second order covariance functions. Kaul (1972) has developed a method to determine these functions from a linearized Fokker-Planck equation. However, it is deemed simpler and more efficient tc solve directly the equations of motion of the equivalent linear model.

Second Order Covariance Functions

The equations of motion of the equivalent linear model, in view of Eqs. and 17, can be put in the form

$$\{\dot{y}\} + [D]\{y\} = \{Q\}\ddot{u}_b$$

where

$$\{y\} = (\{\dot{x}\}\{x\}\{w\}\ \dot{u}_o\ u_o)^T \qquad (

$$\{Q\} = (\{0\}\{0\}\{0\}\ 1\ \ 0)^T \tag{21b}$$

$$[D] = \left[\begin{array}{c|c|c|c|c} [C^W] & [K^U] & [K^W] & 2\omega_g\xi_g\{N\} & -\omega_g^2\{N\} \\ n\times n & n\times n & n\times n & n\times 1 & n\times 1 \\ \hline -[I] & [0] & [0] & \{0\} & \{0\} \\ n\times n & n\times n & n\times n & n\times 1 & n\times 1 \\ \hline -[I] & [0] & [\beta_i] & \{0\} & \{0\} \\ n\times n & n\times n & n\times n & n\times 1 & n\times 1 \\ \hline [0] & [0] & [0] & \begin{matrix}2\omega_g\xi_g & \omega_g^2 \\ -1 & 0\end{matrix} & \\ 2\times n & 2\times n & 2\times n & 2\times 2 & \end{array}\right] \tag{21c}$$

and $[\beta_i]$ is a diagonal matrix with diagonal elements β_i. The solution of Eq. 20 cannot be obtained by the commonly used method of classical normal modes, due to the irregular form of the associated damping matrix. In this study, the method of complex mode transformation of the form

$$\{y\} = [\Phi]\{r\} \tag{22}$$

is adopted, where $[\Phi]$ is the matrix of eigenvectors associated with the complex eigenvalues λ_i of matrix $[D]$. Accordingly, Eq. 20 is transformed into the following

$$\{\dot{r}\} + [\lambda_i]\{r\} = [\Phi]^{-1}\{Q\}\ \ddot{u}_b \tag{23}$$

where $[\lambda_i]$ is a diagonal matrix of elements λ_i. Adding the matrix differential equation obtained by postmultiplying Eq. 23 by $\{r\}^T$ to the one obtained by premultiplying the transpose of Eq. 23 by $\{r\}$, and taking the mathematical expectation for the associated random variables of the resulting matrix differential equation, one can get

$$\frac{d}{dt}[R_r] + [\lambda_i][R_r] + [R_r][\lambda_i] = [\Phi]^{-1}\ E[\{Q\}\{r\}^T\ddot{u}_b] + E[\{r\}\{Q\}^T\ddot{u}_b]([\Phi]^{-1})^T \tag{24}$$

in which $[R_r] = E[\{r\}\{r\}^T]$, and $\frac{d}{dt}[R_r] = E[\{\dot{r}\}\{r\}^T + \{r\}\{\dot{r}\}^T]$. Elements in matrix $[R_r]$ are second order covariance functions of the normal coordinates r. S Eq. 23, yields

$$\{r\} = \int_o^t e^{[\lambda_i](t-\tau)}\ [\Phi]^{-1}\{Q\}\ \ddot{u}_b(\tau)d\tau$$

In view of Eqs. 16 and 25, the expectation functions on the right hand sid Eq. 24 can be obtained in the form

$$E[\{Q\}\{r\}^T\ddot{u}_b] = \pi S(t)[\{Q\}\{Q\}^T]([\Phi]^{-1})^T$$

$$E[\{r\}\{Q\}^T\ddot{u}_b] = \pi S(t)[\Phi]^{-1}[\{Q\}\{Q\}^T]$$

Substituting Eqs. 25 and 26 into Eq. 24 yields

$$\frac{d}{dt}[R_r] + [\lambda_i][R_r] + [R_r][\lambda_i] = 2\pi S(t)[\Phi]^{-1}[\{Q\}\{Q\}^T]([\Phi]^{-1})^T \tag{28}$$

of which the solution is in the form

$$[R_r]_{ij} = \frac{1-e^{-(\lambda_i-\lambda_j)t}}{\lambda_i+\lambda_j}[G]_{ij} \tag{29}$$

in which $[G] = 2\pi S(t)[\Phi]^{-1}\{Q\}\{Q\}^T([\Phi]^{-1})^T$, and $[R_r]_{ij}$ denotes the element at row i and column j of matrix $[R_r]$. After obtaining $[R_r]$, the original second order covariance matrix $[R_x] = E[\{y\}\{y\}^T]$ can be obtained as

$$[R_x] = [\Phi][R_r][\Phi]^T \tag{30}$$

Numerical Solution Scheme

Since the damping submatrix $[\beta_i]$ in [D] changes with time, the only way to solve Eq. 24 is by a time-step-by-step-method with a due care for the starting point. At t = 0, $[R_r]$ and $[\beta_i]$ are null matrices, and $x_i = w_i$. Accordingly, 2n + 2 eigenvalues and $[R_r]$ of the size $(2n+2)\times(2n+2)$ are computed from Eq. 29 assuming a constant S(t) for $t = \Delta t$, the first time step. Then $[R_r]$ is enlarged to its full size of $(3n+2)\times(3n+2)$ by noting that $x_i = w_i$, and $[R_x]$ is computed from Eq. 30. For the next time step, $[\beta_i]$ is evaluated according to Eq. 19 using the current $[R_x]$; and assuming a constant S(t), Eq. 29 can be written in the form

$$[R_r]_{ij,t+\Delta t} = \frac{1}{\lambda_i+\lambda_j}\left\{(1-e^{-(\lambda_i+\lambda_j)\Delta t})[G]_{ij} + e^{-(\lambda_i+\lambda_j)\Delta t}[R_r]_{ij,t}\right\} \tag{31}$$

and $[R_x]_{t+\Delta t}$ can be obtained as $[\Phi][R_r]_{t+\Delta t}[\Phi]^T$. The procedure from now should be obvious. The required accuracy of the results can be achieved by using a small Δt such that the imaginary part of every $[R_x]_{ij}$ is sufficiently close to zero, and the current absolute value of each $[R_x]_{ij}$ is used for next time step.

In this study, the complex eigenvalue problem of [D] is solved by means of an existing computer scientific program. The inverse of $[\Phi]$ is found to be difficult and time consuming. A special partition method (see Wu, 1977 for det has been developed for this inverse.

Equivalent Linear Model with Two Coefficients

There is another existing method (Kaul, 1972), in which the statistical ponse is solved from the linearized Fokker-Planck equation; which is derived replacing the term $\dot{x}_i\theta(|w_i|-Y_i)$ in the nonlinear Fokker-Planck equation, as in Eq. 18, by an equivalent linear combination of $\dot{x}_i$ and w_i involving two co ient a_i and b_i for each stiffness element connecting a pair of adjacent mas nd m_{i-1}. These coefficients are determined by minimizing a properly weigh ean square error between the nonlinear term $\dot{x}_i\theta(|w_i|-Y_i)$ and the equivalent

term $a_i\dot{x}_i + b_i w_i$, i.e.,

$$\frac{\partial}{\partial a_i}\int_{-Y_i}^{Y_i}\int_{-\infty}^{\infty}[\dot{x}_i\theta(|w_i|-Y_i) - (a_i\dot{x}_i + b_i w_i)]^2 P(\dot{x}_i,w_i)d\dot{x}_i dw_i = 0$$

$$\frac{\partial}{\partial b_i}\int_{-Y_i}^{Y_i}\int_{-\infty}^{\infty}[\dot{x}_i\theta(|w_i|-Y_i) - (a_i\dot{x}_i + b_i w_i)]^2 P(\dot{x}_i,w_i)d\dot{x}_i dw_i = 0$$

$$, \quad i = 1,2,3,\ldots,n \qquad (32a,b)$$

in which $P(\dot{x}_i,w_i)$ is as given in Eq. 8. Accordingly, a_i and b_i are obtained in the form

$$a_i = 1 - \frac{h_i\{E[w_i w_i]E[\dot{x}_i\dot{x}_i] - E[\dot{x}_i w_i]\sqrt{2E[\dot{x}_i\dot{x}_i]/\pi}\,Y_i\}}{E[\dot{x}_i\dot{x}_i]E[w_i w_i] - (E[\dot{x}_i w_i])^2} \qquad (33a)$$

$$b_i = \frac{h_i\{E[\dot{x}_i w_i]E[\dot{x}_i\dot{x}_i] - E[\dot{x}_i\dot{x}_i]\sqrt{2E[\dot{x}_i\dot{x}_i]/\pi}\,Y_i\}}{E[\dot{x}_i\dot{x}_i]E[w_i w_i] - (E[\dot{x}_i w_i])^2} \qquad (33b)$$

in which $h_i = (E[w_i w_i]/Y_i^2)^{\bar{m}}$, and $\bar{m}$ is at least 2. The linearized Fokker-Planck equation for this case is

$$\frac{\partial P}{\partial t} = -\sum_{i=1}^{n}\{\frac{\partial}{\partial\dot{x}_i}(\dot{x}_i P) + \frac{\partial}{\partial\dot{x}_i}[\{\sum_{j=1}^{n}(-c_{ij}^{w}\dot{x} - k_{ij}^{u}x_j - k_{ij}^{w}w_j + 2\xi_g\omega_g n_i\dot{u}_o + n_i\omega_g^2 u_o)\}P]$$
$$+ \frac{\partial}{\partial w_i}[(a_i\dot{x}_i + b_i w_i)P]\} - \frac{\partial}{\partial u_o}(\dot{u}_o P) + \frac{\partial}{\partial\dot{u}_o}(2\omega_g\xi_g\dot{u}_o + \omega_g^2 u_o)P$$
$$+ \pi S(t)[\frac{\partial^2 P}{\partial\dot{u}_b^2} + \frac{\partial^2 P}{\partial\dot{u}_o^2} - 2\frac{\partial^2 P}{\partial\dot{u}_b\partial\dot{u}_o}] \qquad (34)$$

Covariance Differential Equation

The covariance matrix $[R_x]$ for the random variables, $\dot{x}_1,\dot{x}_2,\ldots,\dot{x}_n,x_1,x_2,\ldots,x_n,w_1,w_2,\ldots,w_n,\dot{u}_o,u_o,\dot{u}_b$ can be written in the form

$$[R_x] = E[\{y\}\{y\}^T] \qquad (35)$$

in which $\{y\}^T = (\dot{x}_1,\dot{x}_2,\ldots,\dot{x}_n,x_1,x_2,\ldots x_n,w_1,w_2,\ldots,w_n,\dot{u}_o,u_o)$. Multiplying Eq. 34 by all possible products of two random variables and integrate with respect to all variables and $\dot{u}_b$ (Kaul & Penzien, 1972 & 1974), a Liaponov form of matrix differential equation is obtained in the form

$$\frac{d}{dt}[R_x] + [D][R_x] + [R_x][D]^T = [S]$$

in which

$$[D] = \left[\begin{array}{c|c|c|c|c} [C^W] & [K^U] & [K^W] & -2\omega_g\xi_g\{N\} & -\omega_g^2\{N\} \\ n\times n & n\times n & n\times n & n\times 1 & n\times 1 \\ \hline -[I] & [0] & [0] & \{0\} & \{0\} \\ n\times n & n\times n & n\times n & n\times 1 & n\times 1 \\ \hline -[a_i] & [0] & -[b_i] & \{0\} & \{0\} \\ n\times n & n\times n & n\times n & n\times 1 & n\times 1 \\ \hline 0 & 0 & 0 & 2\omega_g\xi_g & \omega_g^2 \\ 2\times n & 2\times n & 2\times n & -1 & 0 \end{array}\right] \tag{37a}$$

$$[S] = \left[\begin{array}{c|cc} [0] & [0] & \\ 3n\times 3n & 3n\times 2 & \\ \hline [0] & 1 & 0 \\ 2\times 3n & 0 & 0 \end{array}\right] 2\pi S(t) \tag{37b}$$

With a transformation of the form of Eq. 30, Eq. 36 is put in the form of Eq. 28 in which $[\Phi]$ is the matrix of eigenvectors associated with the complex eigenvalues λ_i of $[D]$ of Eq. 37a, and $\{Q\}$ is as defined in Eq. 21b. Subsequently, the second order covariance functions for this case can be obtained with the same scheme proposed for the previous case.

SOF Systems

To be compatible with the existing results (Takemiya, 1973 and Wen, 1975), the total ground acceleration $\ddot{u}_g$ for SOF systems studied herein is taken as a gaussian white noise with a zero mean, i.e., f(t) in Eq. 2. The numerical results of standard deviations, $\sigma_{\dot{x}} = \sqrt{E(\dot{x}\dot{x})}$ and $\sigma_x = \sqrt{E(xx)}$, by various methods are presented in Figs. 6 and 7 for $\bar{m} = 3$ and various values of α and other two parameters ξ and N, which are defined as follows

$$\xi = c/(2\omega_n m) \quad , \quad N = \sqrt{2S_o}/(\omega_n^{\frac{3}{2}} Y) \tag{38a,b}$$

where $\omega_n = \sqrt{k/m}$. In fact, ω_n and ξ are the undamped natural frequency and damping degree of the system, respectively.

MOF Systems

A 33 story shear-beam type building modelled into a 5-mass system (Take 1976) is studied. The mass of each level is 14.14, 14.14, 13.13, 12.12, 9.7 ton-sec^2/cm; and the stiffness matrix is

$$[K] = \begin{bmatrix} 828 & -342 & & & 0 \\ -342 & 606 & -264 & & \\ & -264 & 475 & -211 & \\ & & -211 & 337 & -126 \\ & 0 & & -126 & 126 \end{bmatrix} \text{ ton/cm}$$

The yield value for the drift of each level Y_i is 10.02, 12.20, 12.38, 10.52, 8.49 cm. The damping ratio of this system is assumed to be 2 percent of the critical value for every normal mode of vibration. Accordingly, the damping matrix [C] can be determined by the method developed by Wilson and Penzien (1972). The indicators ω_g and ξ_g of the nonstationary shot noise filter and the intensity function S(t) follow Takemiya (1976), i.e., $\omega_g = 4$ rad/sec, $\xi_g = 0.5$, and

$$\begin{aligned} S(t) &= S_o t^2/t_1^2 && 0 \le t \le t_1 \\ &= S_o && t_1 \le t \le t_2 \\ &= S_o e^{-d(t-t_2)} && t_2 \le t \end{aligned} \tag{40}$$

in which $S_o = 112.625$ cm^2/sec^4/rad/sec, $t_1 = 1.5$ sec, $t_2 = 15$ sec, and $d = 0.18$ sec^{-1}. The values of the ductility factor, $\sigma_{x_i}/Y_i = \sqrt{E[x_i x_i]}/Y_i$, of each level of this system by various methods are compared in Fig. 8.

Discussions and Conclusions

From Figs. 6, 7 and 8, it should be noted that various methods agree well for the case that the statistical response does not exceed the yielding level much. For the case that the statistical response is far exceeding the yielding level ($\sigma_x > Y$), the agreement is not as good. However, the latter case does not occur often, since it should be avoided in design. It should also be noted that Takemiya's results differ most from the rest especially for the case that the response is far exceeding the yielding level.

In term of the numerical computation, the results by the single-coefficient method could be computed with bigger time step than by the two-coefficient method, e.g., 0.5 sec by the former versus 0.25 sec by the latter. This type of observation is even more pronounced for the case that the statistical response is far exceeding the yielding level.

The single-coefficient method may be considered as less accurate than the two-coefficient method, since the former is a special case of the latter, but the former seems more attractive due to the following facts: it can be explained by a real physical model, its formulation and numerical computation are much simpler, and for a future investigation, it can be applied more readily to a system with multi-linear stiffness element.

References

Amin, M. and Ang, A.H.-S., "Nonstationary Stochastic Model of Earthquake Journal of Engineering Mechanics Division, ASCE, Vol. 94, No. EM2, Proc. 5906, pp. 559-583, April, 1968.

Atalik, T.S. and Utku, S., "Stochastic Linearization of Multi-Degree-of-F Nonlinear Systems", International Journal of Earthquake Engineering and S tural Dynamics, Vol. 4, pp. 411-420, 1976.

Kaul, M.K., "Stochastic Inelastic Response of Offshore Towers to Strong M Earthquakes", Report of Earthquake Engineering Research Center, Universit California, Berkeley, EERC 72-4 (PB 215 713), 1972.

Kaul, M.K. and Penzien, J., "Stochastic Seismic Analysis of Yielding Offshore Towers", Journal of Engineering Mechanics Division, ASCE, Vol. 100, No. EM5, Proc. Paper 10884, pp. 1025-1038, October, 1974.

Lin, Y.K., "Probabilistic Theory of Structural Dynamics", McGraw-Hill, New York, 1967.

Takemiya, H., "Equivalent Linearization for Randomly Excited Bilinear Hysteretic Oscillator", Proceedings of the Japan Society of Civil Engineers, No. 219, pp. 1-13, November, 1973.

Takemiya, H., "Stochastic Seismic Response Analysis of a Multi-Degree-of-Freedom Hysteretic Structure", Proceedings of the Japan Society of Civil Engineers, No. 245, pp. 17-26, January, 1976.

Wilson, E.L. and Penzien, J., "Evaluation of Orthogonal Damping Matrices", International Journal for Numerical Methods in Engineering, Vol. 4, pp. 5-10, 1972.

Wen, Y.K., "Approximate Method for Nonlinear Random Vibration", Journal of the Engineering Mechanics Division, ASCE, Vol. 101, No. EM4, Proc. Paper 11500, pp. 389-401, August, 1975.

Wu, C.C., "Statistically Equivalent Linear Model for a Hysteretic System under Random Vibration", M.Eng. Thesis, Asian Institute of Technology, Bangkok, Thailand, No. 1030, 1977.

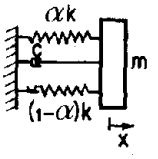

Fig. 1 - SOF Bilinear Hysteretic System

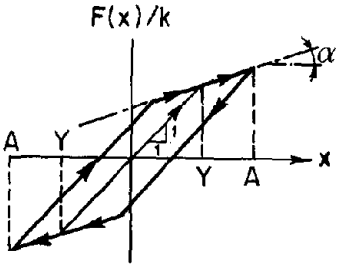

Fig. 2 - Bilinear Hysteretic Force-Displacement Relationship

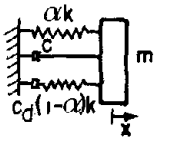

Fig. 3 - SOF Equivalent Linear Model

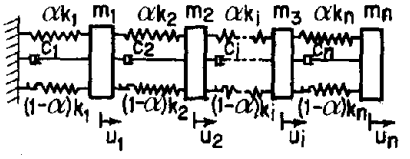

Fig. 4 – MOF Bilinear Hysteretic System

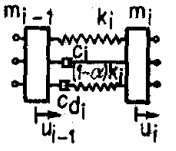

Fig. 5 - MOF Equivalent Linear Model

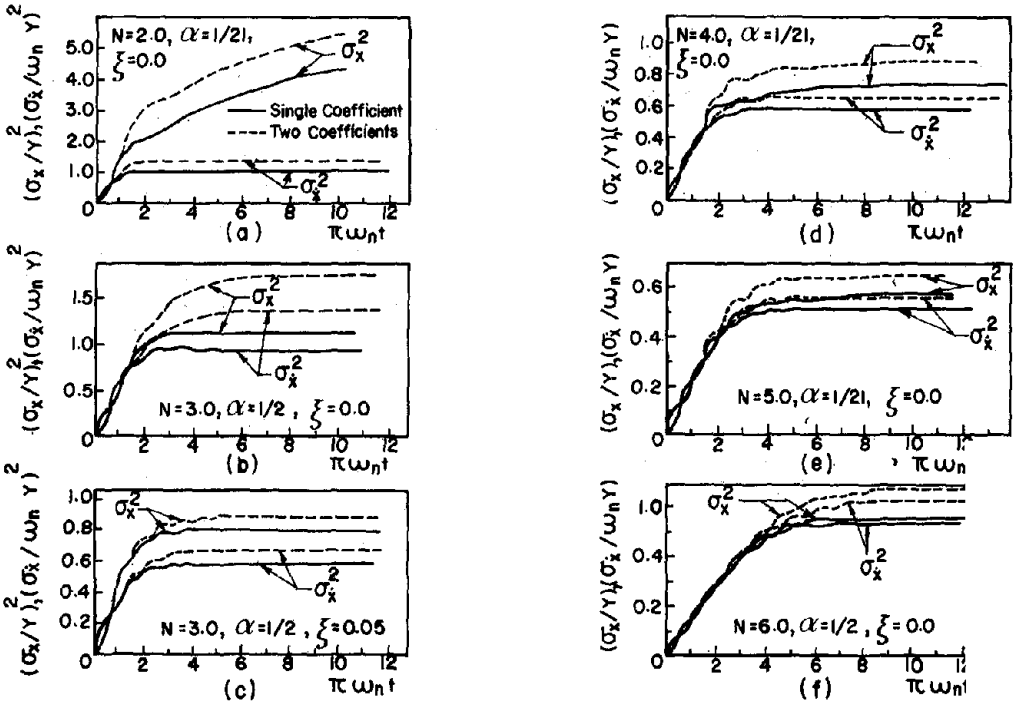

Fig. 6 - Results for SOF System Linearized with Single and Two Coefficients

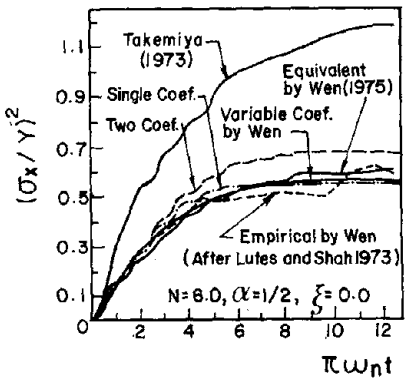

Fig.7 - Comparison of SOF Mean-Square Displacement with Other Solution

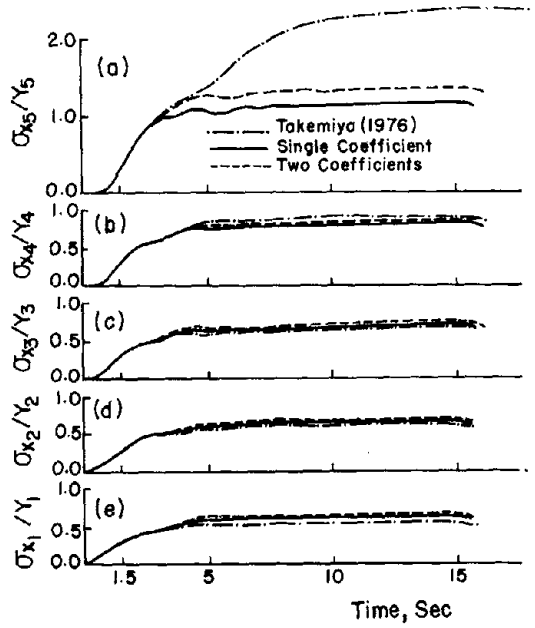

Fig.8 - Statistical Ductility Factors of MOF System with Five Masses by Various Methods

SEISMIC ANALYSIS OF SOIL-BUILDING INTERACTION SYSTEMS

by

PISIDHI KARASUDHI
Associate Professor
Asian Institute of Technology
Bangkok, Thailand

THAMBIRAJAH BALENDRA
Former Graduate Student
Asian Institute of Technology
Bangkok, Thailand

SENG-LIP LEE
Professor and Head
Department of Civil Engineering
University of Singapore
Singapore

Synopsis

An efficient method is presented to analyse a multi-story shear building resting on the surface of an elastic soil medium. Recognizing that the superstructure admits classical normal modes, the problem is reduced to the solution of two coupled integro-differential equations, by which the first few of these modes are found sufficient to produce a good approximation to the exact seismic response of the total system.

Introduction

Most of the investigation dealing with the interaction forces at the soil-structure interface are based on the results obtained for a harmonic excitation of the foundation resting on a homogeneous isotropic, elastic half-space (Parmelee, 1967; Sarrazin, 1970; Sato & Yamaguchi, 1960; Scavuzzo et al, 1971). As these interaction forces are frequency dependent, the seismic response of a soil-building system must be obtained by means of Fourier transform or Laplace transform method (Bielak, 1971; Castelloni, 1970; Liu & Fasel, 1971; Meek & Veletsos, 1972) which is complicated and time consuming. To avoid this difficulty, Parmelee et al (1969) approximated the interaction forces, for the case when Poisson's ratio is zero, by frequency independent differential forms. This is equivalent to approximating the interaction force by a spring and dashpot in parallel. Veletsos & Verbic (1974) obtained more accurately the expressions for the interaction forces in integro-differential forms in the analysis of an elastic half-space subjected to impulsive forces.

In this study, the seismic response of a multi-story building resting on the surface of an elastic soil is investigated. By modal analysis of the superstructure, the governing equations of the structure-foundation system are obta the form of two coupled integro-differential equations relating the trans and rotation of the base of the structure with the ground acceleration. integro-differential equations are solved by a numerical method, and the number of classical normal modes of the superstructure required for compu response of the soil-building system accurately is investigated. The eff shear wave velocity and Poisson's ratio of the soil medium on the interac tems are also made.

Soil-Structure Interaction

For a structure situated on the surface of an elastic soil medium, t be three interaction forces at the soil-structure interface corresponding

three possible modes of motion of the base of the structure, i.e., vertical, horizontal and rotational modes. In normal circumstances, only the last two modes are dominant during seismic response of the structure. These interaction forces can be, represented in two ways: (1) in a differential form; and (2) in integro-differential form.

Differential Form of Interaction Forces

Bycroft (1956) studied the dynamic response of a rigid circular plate on a homogeneous, isotropic elastic half-space subjected to harmonic excitation by assuming that the stress distribution correspond to those under static loading conditions and obtained approximations to the displacements of the rigid plate by taking a weighted average of the resulting displacements at the center and the periphery of the plate. These approximated displacements were related to the amplitudes of the exciting forces by frequency dependent dynamic stiffness and damping coefficients. Parmelee et al (1969) approximated these frequency dependent coefficients for zero Poisson's ratio by average constants in the frequency range $0 \leq pr/V_s \leq 1.5$, where p = the circular frequency of the harmonic exciting force, V_s = the shear wave velocity of the foundation medium and r = the radius of the disk. This is equivalent to approximating each interaction forces by a spring and dashpot in parallel. The spring constants and dashpot coefficients are respectively, for plate translation,

$$K_T = 4.4\ V_s^2 \rho r \quad , \quad D_T = 2.7\ V_s \rho r^2 \tag{1a,b}$$

and, for plate rotation,

$$K_R = 2.3\ V_s^2 \rho r^3 \quad , \quad D_R = 0.31\ V_s \rho r^4 \tag{1c,d}$$

where ρ = the mass density of the half-space which is related to the shear wave velocity V_s by

$$V_s = \sqrt{G/\rho} \tag{1e}$$

in which G = shear modulus of the half-space. For a prescribed horizontal displacement U_b and rotation ϕ, the interaction horizontal force and moment are respectively given by

$$P(t) = K_T U_b(t) + D_T \dot{U}_b(t), \quad Q(t) = K_R \phi(t) + D_R \dot{\phi}(t) \tag{2a,b}$$

where t denotes time and dot ($\cdot$) denotes a time derivative.

Integro-Differential Form of Interaction Forces

Veletsos & Verbic (1974) obtained approximate closed form expressions for responses to harmonic excitations of a massless rigid disk which is supported the surface of an elastic half-space. The procedure used to arrive at these e pressions was as follows. The form of the expressions were taken the same as indicated by the results presented by Meek & Veletsos (1973) for which the sup porting medium was approximated as a semi-infinite, truncated cone deforming i shear only; and the coefficients of the terms in these expressions were adjust so that the results obtained were in a reasonable agreement with the available merical data (Veletsos & Wai, 1971) for the harmonic response of an elastic lf-space in the range of $0 \leq pr/V_s \leq 10$ and for various values of Poisson's tios. Applying an inverse Fourier transform to these approximate expression r harmonic response functions yields the impulse response functions

$$q_x(t) = K_x[\delta(t) + b_o(\frac{r}{V_s})\dot{\delta}(t)] \tag{3a}$$

$$q_\phi(t) = K_\phi[(1-b_1)\delta(t) + b_1 b_2(\frac{r}{V_s})\dot{\delta}(t) + b_3(\frac{r}{V_s})^2\ddot{\delta}(t) + \frac{b_1}{b_2} e^{-V_s t/(b_2 r)}] \tag{3b}$$

where $q_x(t)$ = the force associated with a unit impulsive horizontal displacement at $t = 0$; $q_\phi(t)$ = the moment associated with a unit impulsive rotation at $t = 0$; b_n, $n = 0,1,2,3$ are the numerical constants presented in Table 1; and $\delta(t)$ = the Dirac unit impulsive functions referred to real time t. Furthermore, in Eq. 3, K_x and K_ϕ represent the static stiffnesses of the disk defined approximately as

$$K_x = \frac{8Gr}{(2-\nu)} \quad , \quad K_\phi = \frac{8Gr^3}{3(1-\nu)} \tag{4a,b}$$

For a prescribed horizontal displacement U_b and rotation ϕ, the interaction horizontal force and moment can be respectively written in the form of convolution integrals

$$P(t) = \int_o^t U_b(\xi)q_x(t-\xi)d \quad , \quad Q(t) = \int_o^t \phi(\xi)q_\phi(t-\xi)d \tag{5a,b}$$

Substituting Eq. 3 into Eq. 5 yields the integro-differential relationships between the interaction forces and displacements,

$$P(t) = K_x[U_b(t) + b_o\frac{r}{V_s}\dot{U}_b(t)] \tag{6a}$$

$$Q(t) = K_\phi\Big[(1-b_1)\phi(t) + b_1 b_2\frac{r}{V_s}\dot{\phi}(t) + b_3(\frac{r}{V_s})^2\ddot{\phi}(t) + \frac{b_1}{b_2}\frac{V_s}{r}\int_o^t \phi(\xi)e^{-(V_s/b_2 r)(t-\xi)}d\xi\Big] \tag{6b}$$

It can be shown readily that the integral term in Eq. 6b can be replaced exactly by a term of θ, and Eq. 6 can be rewritten as

$$P(t) = K_x[U_b(t) + b_o\frac{r}{V_s}\dot{U}_b(t)] \tag{7a}$$

$$Q(t) = K_\phi[(1-b_1)\phi(t) + b_1 b_2\frac{r}{V_s}\dot{\phi}(t) + b_3(\frac{r}{V_s})^2\ddot{\phi}(t) + b_1\theta] \tag{7b}$$

where θ and ϕ are related by

$$b_2\frac{r}{V_s}\dot{\theta} + \theta - \phi = 0 \tag{7c}$$

Equations of Motions

The structure-foundation system is represented as shown in Fig. 1, N-story shear building (Rogers, 1959) resting on the surface of an elast space. This system has N+2 degrees of freedom, namely horizontal trans each floor mass, horizontal translation of the base mass and rotation of system in the plane of motion. The equations of motions of this system pectively, for the horizontal translation of the whole system,

$$m_o(\ddot{U}_b + \ddot{U}_g) + \sum_{j=1}^{N} m_j\ddot{U}_j + P(t) = 0$$

for the rotation of the whole system,

$$I_t\ddot{\phi} + \sum_{j=1}^{N} m_j h_j \ddot{U}_j + Q(t) = 0 \tag{8b}$$

and for the horizontal movement of each floor of the superstructure above the base mass,

$$[M]\{\ddot{U}_j\} + [C]\{\dot{V}_j\} + [K]\{V_j\} = 0 \tag{8c}$$

In these equations, V_j = the horizontal displacement of the superstructure at the jth floor relative to the base mass (Fig. 1); U_b = the interaction displacement of the base mass; U_g = the free field displacement; ϕ = the rotation of the base mass; h_j = the height of the jth floor above the base mass; and U_j = the total horizontal displacement of the jth floor with respect to a fixed vertical axis, i.e.,

$$U_j = U_g + U_b + h_j\phi + V_j \tag{9a}$$

Furthermore, m_j = the mass of the jth floor; $I_t = \sum_{j=o}^{N} I_j$, where I_j is the moment of inertia of the jth floor mass about a diameter; P(t), Q(t) = the interaction force and moment, respectively, between the base mass and the soil; [M] = the diagonalized mass matrix of the superstructure,

$$[M] = \begin{bmatrix} m_1 & & & \\ & m_2 & & 0 \\ & & \ddots & \\ 0 & & & m_N \end{bmatrix} \tag{9b}$$

Also [K] = the square matrix of the lateral stiffness of the superstructure if it were supported on a rigid foundation; [C] = the damping matrix of the superstructure assumed to be proportional to the stiffness matrix as defined by

$$[C] = \Omega[K] \tag{9c}$$

where Ω = the constant proportionality factor which is evaluated on the basis of certain percent of critical damping in the fundamental mode of vibration of the structure supported on a rigid foundation.

The equations of motion, Eq. 8, can be reduced into two coupled integro-differential equations by means of modal analysis of the superstructure. Substituting Eq. 9a into Eq. 8c yields

$$[M]\{\ddot{V}_j\} + [C]\{\dot{V}_j\} + [K]\{V_j\} = -(\ddot{U}_g + \ddot{U}_b)[M]\{1\} - \ddot{\phi}[M]\{h_j\}$$

By recognizing the fact that the superstructure admits classical normal mode (Caughey, 1960), V_j can be related to the normal coordinates q_k by

$$\{V_j\} = [\gamma_{jk}]\{q_k\} \tag{(}$$

or

$$\{V_j\} = \{\sum_{k=1}^{N} \gamma_{jk} q_k\} \tag{(}$$

where

$$[\gamma_{jk}] = [\{\gamma^{(1)}\}\{\gamma^{(2)}\} \ldots \{\gamma^{(N)}\}] \tag{12a}$$

in which $\{\gamma^{(k)}\}$ = the eigenvector corresponding to the kth eigenvalue of the following system

$$[K]\{V_j\} - \omega_k^2[M]\{V_j\} = 0 \tag{12b}$$

These eigenvalues, arranged in an ascending order, i.e., $\omega_1^2 < \omega_2^2 < \ldots < \omega_N^2$, and their corresponding eigenvectors can be obtained by means of a standard computer program, e.g., NROOT of IBM. Substituting Eq. 11 into Eq. 10 and premultiplying the result by the transpose of $[\gamma_{jk}]$ lead to

$$\ddot{q}_k + 2\zeta_k\omega_k\dot{q}_k + \omega_k^2 q_k = -(\ddot{U}_g + \ddot{U}_b)\beta_k - \ddot{\phi}\alpha_k \; ; \; k = 1 \text{ to } N \tag{13a}$$

where

$$\alpha_k = \sum_{k=1}^{N} m_j h_j \gamma_{jk} \Big/ \left(\sum_{k=1}^{N} m_j \gamma_{jk}^2\right) \tag{13b}$$

$$\beta_k = \sum_{k=1}^{N} m_j \gamma_{jk} \Big/ \left(\sum_{k=1}^{N} m_j \gamma_{jk}^2\right) \tag{13c}$$

$$\zeta_k = \Omega\omega_k / 2 \tag{13d}$$

The solution to Eq. 13a is given by

$$q_k = -\frac{1}{\omega_k\sqrt{1-\zeta_k^2}} \int_o^t F_k(\xi) J_k(t-\xi)\, d\xi \; ; \quad k = 1 \text{ to } N \tag{14a}$$

where

$$J_k(t) = e^{-\zeta_k\omega_k t} \sin \omega_k\sqrt{1-\zeta_k^2}\, t \tag{14b}$$

and

$$F_k(t) = \beta_k\ddot{U}_g(t) + \beta_k\ddot{U}_b(t) + \alpha_k\ddot{\phi}(t) \tag{14c}$$

It should be noted that the second time derivative of q_k is

$$\ddot{q}_k = \omega_k\int_o^t F_k(\xi)\kappa_k(t-\xi)\, d\xi - F_k(t) \; ; \quad k = 1 \text{ to } N \tag{15a}$$

where

$$\kappa_k(t) = \frac{1}{\sqrt{1-\zeta_k^2}}\, e^{-\zeta_k\omega_k t} \cos(\omega_k\sqrt{1-\zeta_k^2}\, t - \Psi_k)$$

in which

$$\Psi_k = \tan^{-1}\frac{1-2\zeta_k^2}{2\zeta_k\sqrt{1-\zeta_k^2}}$$

In view of Eqs. 9a, 11b, 15a and the following identities,

$$\sum_{j=1}^{N} m_j = \sum_{k=1}^{N} M_k \tag{16}$$

$$\sum_{j=1}^{N} m_j h_j = \sum_{k=1}^{N} Z_k \tag{17}$$

Eqs. 8a and 8b can be written, respectively, in the form

$$m_o(\ddot{U}_b + \ddot{U}_g) + \sum_{k=1}^{N} M_k \omega_k \int_o^t [\ddot{U}_g(\xi) + \ddot{U}_b(\xi)] \kappa_k(t-\xi) d\xi$$
$$+ \sum_{k=1}^{N} Z_k \omega_k \int_o^t \ddot{\phi}(\xi) \kappa_k(t-\xi) d\xi + P(t) = 0 \tag{18a}$$

$$I_t \ddot{\phi} + \sum_{k=1}^{N} Z_k \omega_k \int_o^t [\ddot{U}_b(\xi) + \ddot{U}_g(\xi)] \kappa_k(t-\xi) d\xi$$
$$+ \sum_{k=1}^{N} I_k \omega_k \int_o^t \ddot{\phi}(\xi) \kappa_k(t-\xi) d\xi + Q(t) = 0 \tag{18b}$$

where

$$M_k = \left(\sum_{j=1}^{N} m_j \gamma_{jk}\right)^2 \Big/ \left(\sum_{j=1}^{N} m_j \gamma_{jk}^2\right) \tag{19a}$$

$$Z_k = \left(\sum_{j=1}^{N} m_j \gamma_{jk} h_j\right)\left(\sum_{j=1}^{N} m_j \gamma_{jk}\right) \Big/ \left(\sum_{j=1}^{N} m_j \gamma_{jk}^2\right) \tag{19b}$$

$$I_k = \left(\sum_{j=1}^{N} m_j \gamma_{jk} h_j\right)^2 \Big/ \left(\sum_{j=1}^{N} m_j \gamma_{jk}^2\right) \tag{19c}$$

Thus the governing equations of the total system expressed by Eq. 8 with N + 2 degrees of freedom are reduced to two coupled integro-differential equations in terms of the base displacements U_b and ϕ. This reduction of degrees of freedom allows a considerable saving in computing time.

It has been shown that the seismic response of a system having classical normal modes is primarily due to the first few of these modes (Clough, 1962). Expecting the same phenomenon to exist in structure-foundation systems, which do not posses classical normal modes, the summation with respect to index k in Eq. 18 will be restricted to the first n classical normal modes of the superstructure, where n is much smaller than N, and the response will be obtained by

$$\{V_j\} = \left\{ \sum_{k=1}^{n} \gamma_{jk} q_k \right\} \tag{20}$$

in place of Eq. 11. This leads to a great reduction of computing time. In study, the numerical method proposed by Fleming & Romualdi (1963) and the tr pezoidal rule of numerical integration for the integrals involved are used t solve Eq. 18.

The interaction stiffness in the form of Eq. 6 is adopted in this study Equation 2 is not adopted, since it is restricted only to zero Poisson's rat On the other hand, the use of Eq. 7 in the solution of Eq. 18 will create a advantage, since 3 coupled integro-differential equations will be involved. Takemiya (1977) described one way of using Eq. 7; however, the method still volves the solution of a complex eigenvalued problem.

Numerical Example

A twenty-story steel building is analysed by the proposed method. The square plan of this building is eighty feet wide. The ratio of the base mass to the floor mass of the building is 3.0, and the radius r of the base mass is taken as the radius of a circle having the same area as the plan of the building (Thomson & Kobori, 1963). Each floor has a unit weight of 100 psf and each story height is twelve feet. The total moments of inertia of the columns for the first to the last floors are, in 10^3 in^4; 17.6, 16.8, 16.0, 15.2, 14.0, 13.6, 12.8, 12.0, 11.2, 10.4, 9.6, 8.8, 8.0, 7.2, 6.4, 5.6, 4.8, 4.0, 3.2 and 2.4, respectively. The constant Ω in Eq. 9c is evaluated on the basis of two percent critical damping in the fundamental mode of the superstructure. The density of the soil medium is taken as 120 lb/ft^3.

The response of this building to the N-S component of the El Centro 1940 earthquake is presented in Figs. 2 through 5 for various values of shear wave velocity and Poisson's ratio of the soil medium. Figures 2 and 3 illustrate that the first few normal modes of the superstructure are sufficient to produce an excellent approximation to the exact response of the total system. Figures 4 and 5 show that the effect of Poisson's ratio is significant for low values of shear wave velocity.

Conclusions

The present and previous studies (Parmelee, 1967; Parmelee et al, 1968; Perelman, 1968; Parmelee et al, 1969) have indicated that the most important factor which affects the response of structure-foundation system is the shear wave velocity of the soil medium. In addition, the present study shows that the Poisson's ratio of the soil medium is significant when the shear wave velocity is low.

A soil-building system can be analysed very efficiently by the proposed method due to the following reasons: (1) the problem of a system possessing N+2 degrees of freedom is reduced to the solution of two coupled integro-differential equations without involving a complex eigenvalued problem; and (2) only the first few classical normal modes of the superstructure are needed in the analysis to obtain an excellent approximation to the exact response.

References

Bielak, J., "Earthquake Response of Building-Foundation System", Report EERL 71-04 Earthquake Engineering Research Laboratory, California Institute of Technology, Pasadena, California, U.S.A., 1971.

Bycroft, G.N., "Forced Vibration of A Rigid Circular Plate on A Semi-Infinite Elastic Space and on An Elastic Stratum", Philosophical Transactions, Royal Soc. London, Series A, Vol. 248, No. 948, pp. 327-368, 1956.

Castelloni, A., "Foundation Compliance Effects on Earthquake Response Spec Jour. Soil Mech. Found. Div., A.S.C.E., Vol. 96, No. SM4, pp. 1335-1356, 1

Caughey, T.K., "Classical Normal Modes in Damped Linear Dynamic Systems", Jour. App. Mech., Vol. 27, pp. 1-3, 1960.

Clough, R.W., "Earthquake Analysis by Response Spectrum Superposition", Bu Seism, Soc. Am., Vol. 52, pp. 647-660, 1962.

Fleming, J.F. and Romualdi, J.P., "A General Procedure for Calculating Dynamic Response due to Impulsive Loads", Jour. Frank. Inst., Vol. 275, No. 2, pp. 107-120, 1963.

Liu, S.C. and Fasel, L.W., "Earthquake Interaction by Fast Fourier Transform", Jour. Eng. Mech. Div., A.S.C.E., Vol. 97, No. EM5, pp. 1223-1237, 1971.

Meek, J.W. and Veletsos, A.S., "Dynamic Analysis and Behavior of Structure Foundation System", Structural Research at Rice, Report No. 13, Department of Civil Engineering, Rice University, Houston, Texas, 1972.

Meek, J.W. and Veletsos, A.S., "Simple Models for Foundation in Lateral and Rocking Motion", Proceedings, Fifth World Conference on Earthquake Engineering, Rome, Italy, pp. 2610-2613, 1973.

Parmelee, R.A., "Building-Foundation Interaction Effects", Jour. Eng. Mech. Div., A.S.C.E., Vol. 93, pp. 131-152, 1967.

Parmelee, R.A., Perelman, D.S., Lee, S.L., and Keer, L.M., "Seismic Response of Structure-Foundation System", Jour. Eng. Mech. Div., A.S.C.E., Vol. 94, pp. 1295-1315, 1968.

Parmelee, R.A., Perelman, D.S., and Lee, S.L., "Seismic Response of Multiple-Story Structures on Flexible Foundations", Bull. Seism. Soc. Am., Vol. 59, pp. 1061-1070, 1969.

Perelman, D.S., Parmelee, R.A., and Lee, S.L., "Seismic Response of Single-Story Interaction Systems", Jour. Struct. Div., A.S.C.E., Vol. 94, pp. 2597-2608, 1968.

Rogers, G.L., "Dynamics of Framed Structures", John Wiley & Sons, Inc., New York, 1959.

Sarrazin, M.A., "Soil-Structure Interaction in Earthquake Resistance Design", M.I.T., Department of Civil Engineering, Report R 70-59, 1970.

Sato, Y. and Yamaguchi, R., "Vibration of A Building Upon An Elastic Foundation", Bull. Earthquake Res. Inst., Tokyo University, 38, pp. 369-383, 1960.

Scavuzzo, R.J., Bailey, J.L., and Raftpoulos, D.D., "Lateral Structure Interaction With Seismic Waves", Jour. App. Mech., Vol. 38, pp. 125-134, 1971.

Takemiya, H., "Simplified Model for Building-Foundation Interaction", Jour. Eng. Mech. Div., A.S.C.E., Vol. 103, No. EM2, pp. 345-351, 1977.

Thomson, W. and Kobori, T., "Dynamic Compliance of Rectangular Foundation on Elastic Half-Space", Jour. App. Mech., Vol. 30, pp. 579-584, 1963.

Veletsos, A.S. and Verbic, B., "Basic Response Function for Elastic Foundatic Jour. Eng. Mech. Div., A.S.C.E., Vol. 100, No. EM2, pp. 189-202, 1974.

Veletsos, A.S. and Wei, Y.T., "Lateral and Rocking Vibration of Footings", Jc Soil Mech. Found. Div., A.S.C.E., Vol. 97, No. SM9, pp. 1227-1248, 1971.

Table 1 - Values of b_i

b_i	$\nu = 0$	$\nu = 1/3$	$\nu = 0.45$	$\nu = 0.5$
b_o	0.775	0.650	0.600	0.600
b_1	0.525	0.500	0.450	0.400
b_2	0.800	0.800	0.800	0.800
b_3	0.000	0.000	0.023	0.027

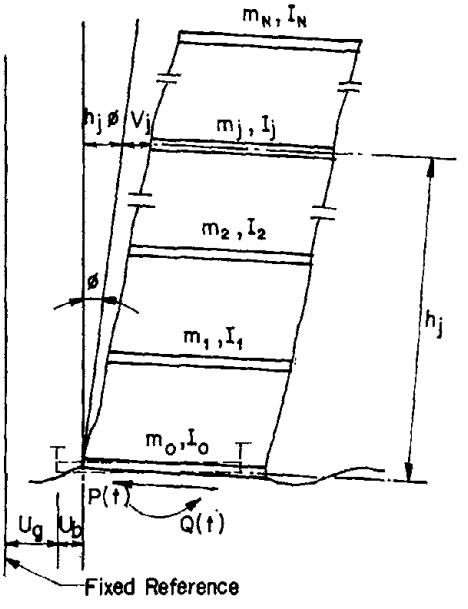

Fig. 1 – Soil – Building Interaction System

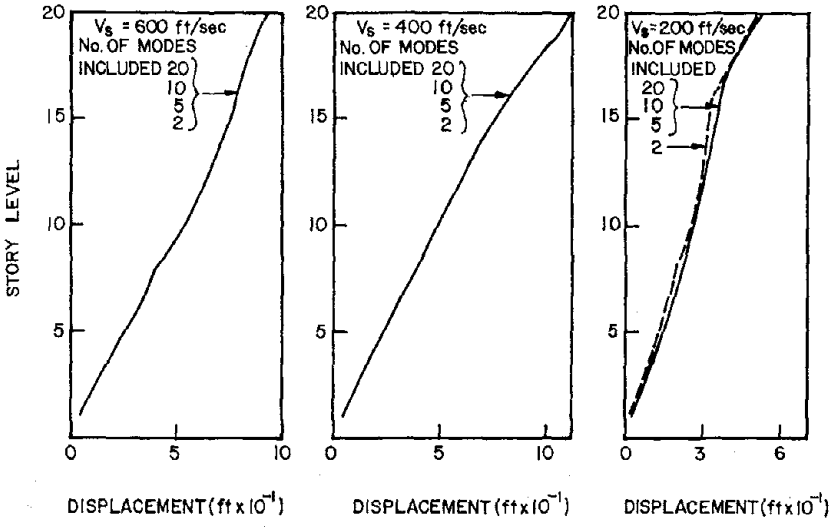

Fig. 2 - Effect of Number of Normal Modes on Maximum Floor Displacement Relative to Building Base

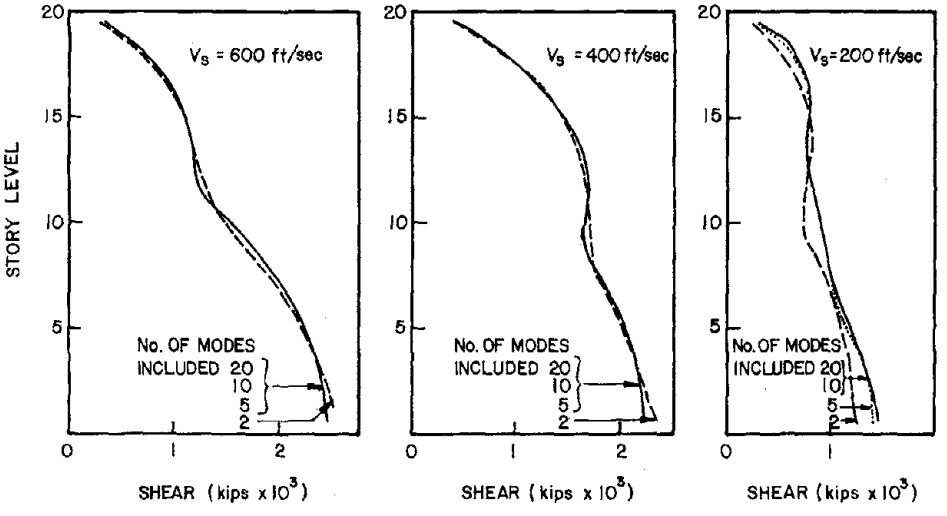

Fig. 3 - Effect of Number of Normal Modes on Maximum Story Shear

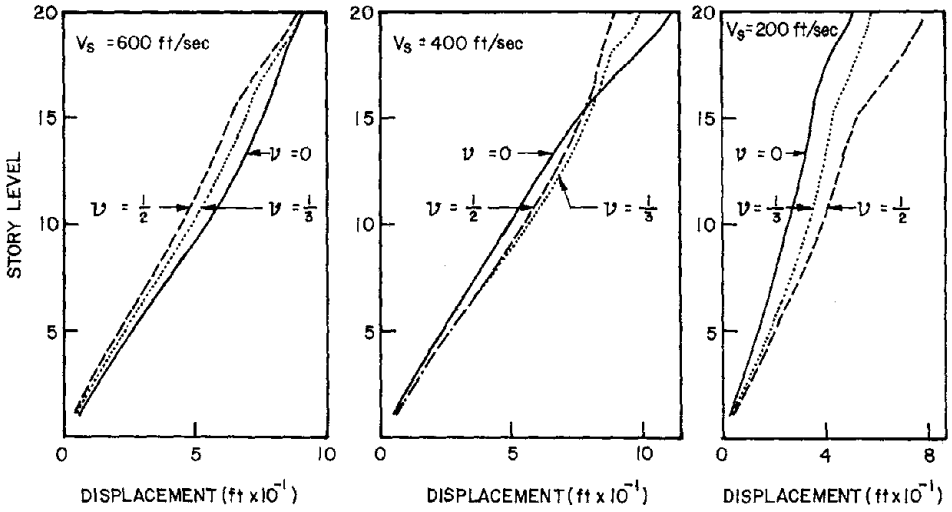

Fig. 4 – Maximum Floor Displacement Relative to Building Base

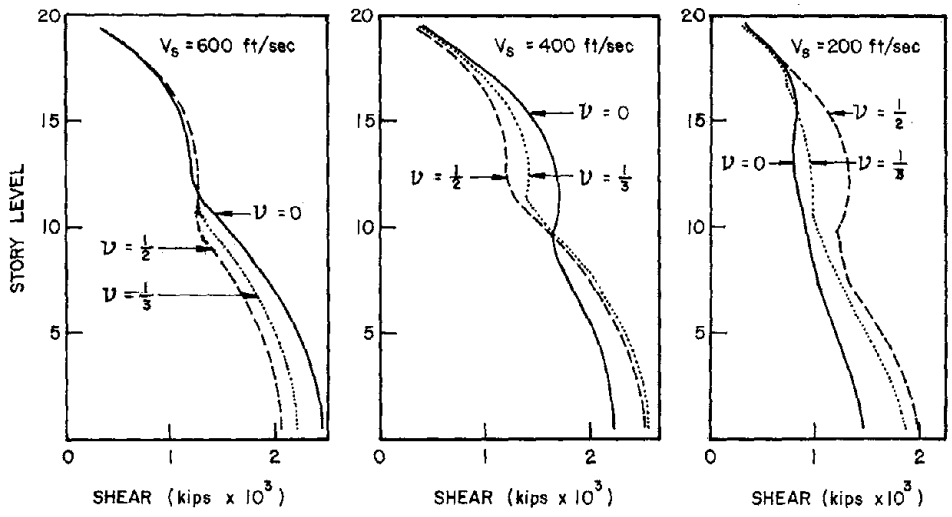

Fig. 5 – Maximum Story Shear

SEISMIC RESPONSE AND RELIABILITY OF MECHANICAL SYSTEMS EFFECTS OF UNCERTAINTY OF GROUND MOTIONS

by

Heki Shibata ,

T. Shigeta and A. Sone

Institute of Industrial Science, University of Tokyo

Abstract

This paper is dealing with the uncertainty of responses of structures to vibratory ground motions and its effect on the anti-earthquake design. Mechanical systems in the title involve equipment, pipings and vessels, which are found in nuclear power stations, petro-chemical plants and other industrial facilities. Failure of some such items may cause very hazardous effect on their environment. Therefore, we must evaluate the uncertainty of a future destructive earthquake to make the margin of the design clear. The uncertainty mainly comes from the mechanism of fault movements, sampling effect of ground motions in a stochastic sense and so on. The authors try to discuss them through their experience in field observations.

§1. Introduction

Seismic response analysis using a large-size computer is very often required for a part of structural design procedure of important facilities, such as nuclear power stations, chemical engineering plants, oil refinaries and also many high-rised buildings. In other words, the safety of these facilities under a destructive earthquake is ensured by the result of the seismic response analysis. If so, how are such response analyses reliable? The answer is " Not so as we think ". We can calculate the dynamic behavior usually on a very complicated structure to given time history data of a certain earthquake, such as El Centro earthquake or Taft earthquake. However, if someone ask us how this structure will behave in a destructive earthquake in some particular area, we really can not answer this question. Because we do not have any information, such as, the time history dara, the duration of the ground motions, of future earthquakes. Data of El Centro earthquake is the record of ground motions at a generating station in El Centro city in the case of Imperial Valley earthquake-1940, and that of Taft earthquake is those at the basement of some building in Taft in the case of Kern County earthquake-1952. As mentioned before, we can calculate the behavior of a structure to given data with a certain accuracy; however, there are many factors to diminish the reliability of estimating the behavior structure to future earthquakes. And if the reliability of response ana is questionable, then structural reliability may decrease greatly.

The authors have been discussing this subject in several occasions 1973, that is, 5WCEE [1973][1], SMiRT-3 [1975][2], ELCALAP [1975][3], US-Ja Joint Seminar [1975][4] and HOPE JSME International Symp. [1977][5]. The tion of data of uncertainty of responses of structures was started in 19 it has been continued through an analog simulation, theoretical analysis random process model, field monitering stations of model structures to t Matsushiro Earthquake Swam in Nagano City, and to local frequent earthqu Chiba field stations of Institute of Industrial Science, University of T

and shaking test of model structures using a 100 ton shaking table. We obtained the almost definite conclusion, that is, the fluctuation of structural response factors is usually very high, the dispersion factor, the ratio of the standard deviation to the mean, is 30 % for a single-degree-of-freedom model, and 50 % for an apendage system on the floor of a supporting structure.

The authors want to summarize the results of the papers mentioned-above, and to point out the significance of response analysis of equipment and piping systems in the anti-earthquake design of industrial facilities such as nuclear power stations and petro-chemical engineering plants.

The following factors are mainly concerned with the accuracies of estimating a response of structures:

1) Magnitude of a future earthquake,
2) Its focus,
3) Its vibration characteristics,
4) Local ground condition of vibration,
5) Existence of torsional ground motion.

The first three items are related to the mechanism of earthquakes which we want to estimate the response to. The last two items come from local ground condition at the site. These matters will be elaborated in the forms discussed in the following chapters. Actually most efforts are usually concentrated in the decision of the magnitude and the possible focal position for the design basis earthquakes. Their choice is often made in a very conservative way, however, in some cases it is not so conservative. Sometimes we use a response spectrum instead of the direct description of the earthquake itself. In this case their conservatism mainly depends on whether we choose the response spectrum for a particular site or that for more general ones.

The authors are trying to show that the choice of the response spectrum is important as well as that of the magnitude and focal distance, and also show that we can not decide them with high accuracy that is usually expected of ordinary mechanical designs.

§2. Fluctuation of Responses

The authors had been trying to find out the practical scheme of evaluating the response of a piping system bridged between two independent buildings. Through that study, the authors obtained the responses to one hundred pseudo-earthquakes from a low-frequency noise generator of the model as in Fig. 1. As the authors refered in the several reports [1973][1], the dispersion factor of the result was very large. And their moving averages are as shown in Fig. 2. The shapes of curves and their dispersion factors are quite independent to the parameters of the system in the case of Fig. 2, for example, the ratio of the eigen period of a supporting building to that of the other. The average response factor fluctuates rapidly where the number of earthquakes is less than ten, and in the regions of over twenty the average seems to be almost settled. The fluctuation in the case above-mentioned is based on the fact that the pseudo-earthquakes belong to a stochastic random process. Including this mechanism, there are several reasons to cause such fluctuations in response analysis. That is:

1) How do the nest of sources of earthquakes distribute?
2) What path do earthquake waves transmit through?
3) How do the responses fluctuate by the sampling effect from the family of earthquakes belong to the same nest?
4) How are the responses affected with initial conditions of a responding system for each earthquake?

As shown by □ dots in Fig. 5 later, sometimes response factors of various points of the plant took the same values to successive earthquakes. There were three successive earthquakes from the same region within an hour in the case of Fig. 5. The responses to these two earthquakes were observed and their values were very similar to each other. However, those to other earthquakes from the same region were not equal to them and much scattered.

The same things [1973][1] happened on earthquakes in El Centro city. Two successive earthquakes were occured in the early morning of Feb. 9, 1956. Their auto-correlation functions are quite similar to each other as shown in Fig. 3. But that of the famous El Centro earthquake (top of Fig. 3) is more white, and lacks components of longer periodic waves comparing to those in 1956.

To observe the responses of a model plant, that is, a three story building equipped with a single-pressure-vessel-and-two-piping system and other equipment models, to Matsushiro Earthquake Swam, it was built in Nagano City, 25 km North from the epicenter region [1970][9], [1971][10]. About sixty records had been recorded over the period from January 1968 to March 1969. Among these sixty records, the authors picked up eleven earthquakes which are judged to be originated from the same nest. The maximum values of the acceleration of these earthquakes from 1.09 gal to 25.0 gal. At first, the auto-correlation functions of those earthquakes were calculated separately after normalizing them, and by averaging them the mean auto-correlation function was obtained. The standard deviation has no tendency to diverge with the time. By transforming it into power spectrum by Wiener-Khinchin method, the estimated mean power spectrum $E\{A_{sN}(\omega)\}$ in Fig. 4 was obtained.

The dotted line shows the standard deviation of power spectra of eleven earthquakes. At the peak f_{s1} the relative dispersion is about one third, and it is the same order to other relative dispersion factors which the authors have been discussed in the previous chapters.

The responses of the model building and equipment were scattered very much. The response factors of the acceleration of the third floor to the basement had been from 1.4 to 6.9. And those of the equipment and pipings were more scattered, for example, out-of-plane motions of a Z-shape piping system responded in the factor from 4.4 to 22.8. As we could foresee it on the results which would be obtained in Chiba several years later from these results, it is no possibility that the expected future earthquake will behave in the same way that of the past strong earthquake which we are using for our design analysis.

§3. Response Observation in Chiba Field Station

In Chiba Field Station 50 km away from Tokyo to the east, the observation of response of a plant model to natural earthquakes has been continuing. The model consists of a monolithic building, a tower type tank, a hanged tank, a saddle supported type elevated tank and two pipings connecting these two t The vibration characteristics of the main items are as shown in Table 2. Sept. 1971 horizontal response and also since Oct. 1973 vertical response observed. The distributions of their vertical responses are shown in Fig. The behavior of vertical responses of some items like pipings and a horiz elevated tank is quite similar to that of responses to horizontal ground m Their statistical data are summarized in Table 3. There are no eminent di between response to horizontal motions and that to vertical motions. Espe the pipings behave very dynamically to both directions, and the mean of re factors to vertical motions is larger than that to horizontal motions. Th relative dispersion factors of flexible systems are around 30 ∿ 40 % and t the elevated horizontal tank is over 50 %. Their tendency and values are

with the theory. Response factor can be said to be governed by the duration of ground motions and their spectrum usually, and these two parameters are related to their magnitudes and focal distances. To check it, earthquakes were classified to near field ones (A, A', AB and T, of which hypocenter distances were from 30 km to 100 km) and others. Responses of the hanged tank are plotted separately to earthquakes in each categoly. In Fig. 6 the responses to near field earthquakes are shown. Here the abscissa is the surface ground acceleration instead of the magnitude, because the hypocenter distances of these earthquake were almost same range. There seems to be a tendency of decreasing of the response factor according to increasing of the ground acceleration. On the other hand, the opposite tendency can be found on the response factors to other groups. Through such manupration we can not reduce their scattering, that means, there is other factors for them.

§4. Abnormally High Response Factor

We usually treat a data scattering problem under an assumption of some distribution like normal distribution or log-normal one. In such cases the maximum value of data is very seldom to exceed an upper bound value, $m + 3\sigma$, however, the authors observed rather often such phenomena as shown some examples in Tables 3 and 4. The distribution of response factors of the hanged tank HT is shown in Fig. 7. A part of histogram where response factor is less than 27 seems to be a normal distribution, and six data between 27 and 36 and also 69 are obviously abnormal. In Table 3, the values show in parentheses are those excluding these seven data. These data are outside of the upper bound value of 3σ.

The reason of occuring such abnormally high response factors can be estimated as a kind of resonance. In a case of Fig. 8, the elevated saddle type tank shows beating response of rather high frequency range in 18 Hz. This value corresponds to one of eigen frequencies of it as shown in Table 2.

The hanged tank has an eigen frequency of 4.73 Hz as a coupled mode to pipings. The frequency of this mode coincides with one of peaks appeared in the result of Fourier analysis of ground motion waves. In Fig. 9 some examples of PSD are shown. Some peaks appear always, for example, near to the frequency of 5.15 Hz. However, in some cases they are much different like Earthq. #867 in Fig. 9 (c). Such difference mainly comes from the focus area of them. "A" "A'" "T" in Table 4 indicate that areas of foci are near to the site and "U" means that is not identified. Some of such peaks appear in response diagram, as an example shown in Fig. 10. The eigen frequency of the hanged tank corresponds to one of these peaks.

The partterns of ground motions which have such PSD diagram are usually classified into two groups as shown "B" and "N" in Table 4. "B" stands for beating sinusoidal waves, and "N" stands for narrow-banded white-noise. The wave form of "N" is waves whose zero-crossing points are very periodic, and on the other hand peak amplitudes are variable and show a Rayleigh distribution.

Behavior of such peaks is also a stochastic phenomenon, however, the modeling technique has not established.

§5. Torsional Ground Motions

The last problem in this paper is a problem of torsional ground motions. Observation has been continued since Feb. 1972 and approximately one hundred data were obtained [1976][7]. There are problems which have been still not so
ıe of those is cross-talk characteristics between torsional ground motions a
ɔrizontal ground accelerations. It depends on a pick-up by a pick-up at pre
ɐ obtained a some relation shown later between torsional and horizontal grou

motions. If it is really true and comprehensive one, then torsional ground motions will have large effects on a certain structure under destructive earthquakes.

§5.1 Pick-up and Local Condition

This pick-up is set on a concrete foundation 1 m × 1 m × 1 m, which is buried on the free-surface ground, approximately five meter thickness Kuwanto Roam layer, with other three components of acceleration pick-ups. This foundation is 2,490 mm from the wall of a two story reinforced concrete building for instruments and recorders. This site is located at the point 1 km far from cliff line along the former sea-shore line.

This moving-coil-type pick-up was developed by Professor Furukawa, Chuo University, to measure torsional vibration of machine tools like vertical axis turning lathe. The pendulum, which consists of coils and supporters, is suspended by very thin and short wires. Magnetic path is approximately D-shape. Its size is 65 mm in diameter and 100 mm in height. Its natural frequency is 1.0 Hz and the critical damping ratio is 0.7. The electro-motive-force from the pick-up is proportional to torsional velocity in the range from 1 Hz to 30 Hz according to the authors' test. The cross-talk term between torsional motion and horizontal acceleration is less than 10 % in general, however, one of them is extremely bad.

Mean sensitivity of six pick-ups, which the authors have, 5×10^{-1} mV/mrad/sec. Here 1 mrad/sec = 1×10^{-3} rad/sec.

§5.2 Results and their Characteristics

The authors obtained about ninety records the period from Feb. 1972 to July 1976. Out of these data, nineteen data, of which the maximum torsional velocities exceed 0.04 mrad/sec, are plotted as shown in Fig. 11. The gradient of the average line in a logarithmic chart is almost 1/2. Therefore, the relation of the maximum horizontal acceleration (NS component) to the maximum torsional velocity is expressed by following equation:

$$\dot{\Omega}_{max}\,(mrad/sec) = 1.893 \times 10^{-3}\,\alpha_{max}^{1.988}\,(gal) \tag{7}$$

The authors made response analyses of some of them. Figs. 12 and 13 are shown the comparison of those to the torsional ground motion and the horizontal ground acceleration of a near-field earthquake. At peaks in the lower frequency range around 5 Hz, both curves are similar to each others, however, in the higher frequency range, the torsional ground motion is more dominant than the horizontal ground acceleration. This is also observed in the result of Fourier analysis as shown in Fig. 14.

In some cases of the near-field earthquakes originated from another of sources, the higher frequency component is less than the peaks of the modes around the frequency 5 Hz, however, the case shown-above, the highe frequency components more than 10 Hz are the most dominant. The peak sha PSD of the torsional ground motion in the range of 5 ∿ 6 Hz is only simil that of NS component of the horizontal ground acceleration.

The authors continue the observation of response of a model to torsi ground motions. Now they have several records. In most cases it was res to horizontal motions, in two cases it was responded to purely torsional

§6. Probability of Failure

The authors have been trying to become clear the relation of the error of estimating response value to the increase of the risk of fracture caused by exceeding earthquake loadings caused by the estimation error.

As mentioned in the previous chapters, the standard deviations of response factor are 30 % and 50 % of the mean in direct response spectrum and floor response spectrum respectively. Here we also assume that the error of estimating the magnitude of design basis earthquake is ±0.3 and it corresponds to the error of range 2σ. And the errors corresponding to 3σ of DRS and FRS give 90 % and 150 % over response respectively. Then [Mean response + Response Fluctuation and Error caused by magnitude estimation] is 240 % and 300 %, where the error of the magnitude ±0.3 gives 150 % error in ground velocity or acceleration. If the stress caused by earthquake loadings is 20 % of the total stress or the arrowable stress, then 18 % and 30 % over stresses may cause at the probability of $1/2\ (5 \times 10^{-2}) \times 1/2\ (3 \times 10^{-4}) = 4 \times 10^{-5}$. The ratio of the stress by an earthquake loading to the total stress is defined as Earthquake Loading Factor, ELF.

The relation of the increase of the probability of failure to over-stress was summarized by Ikeda as a chart in his report [1975][11] from Udoguchi and Tagart's papers. From the chart the authors assume that 20 % over-stress would give the increase of the probability by approximately 10^3. These over loads caused by error of estimation increase the probability of the failure as shown in Table 5, and finally the risk of failure including the error of estimating the magnitude increase by ΔR , that is, 5×10^{-1} and 5×10^{1} when mean direct response spectrum and mean floor response spectrum are used for design respectively. These figures mean that mean DRS is good enough as the design criteria, but FRS should have the allowance of 1σ width to their mean in the case that the stress caused by earthquake loadings that is, ELF is 20 % of the total load.

However, if ELF is 50 %, ΔR becomes 1.1×10^{6} and 4×10^{10}. So when we use DRS for the design of such members, we should add at least the width of 3σ to the mean. And to use FRS, we should expect high uncertainty for the design result. The value of 4×10^{10} is not so exact because the relation of stress to the failure probability which the authors assumed is very rough. The authors should emphasize that the response analysis has extremely low reliableness, and we should cover the structural reliability by giving the over-all ductility of the structure or by limiting the stress by earthquake loadings within a certain range of the allowable stress, even if other stress does not exist. Some theoretical response curve is also useful. The curves obtained by Sato [1965][12] according to the theory of extreme are some examples. These curves are mean floor response spectra, and covering FRS to El Centro and other earthquakes almost in all regions.

§7. Design Method of Appendages

The design procedure of equipment and pipings currently used is a unidirectional one. That is, it starts from the response analysis of a building structure, and we obtain the FRS and estimate the response of equipment, dist bution of earthquake loading stresses on over-all equipment under an assumpti of non-coupling to the building. However, this design method always enforces the response analysis and stress analysis of equipment in each design case.

If we can obtain the Allowable Limit Response Curve, ALRC, on each equip ment, we can check their anti-earthquake design only by comparing both curves without any calculation. This curve can be obtained by both numerical analys nd qualification test.

For the standarization of equipment including vessels, this method will

a very powerful support. Because if we obtain the allowable limit response curve, ALRC, once for a specific type of equipment, afterwards we can eliminate a fairly good amount of awakward jobs to compute the response and stress distribution of the design object. Only the thing we had to do is a comparison of ALRC already prepared to the floor response spectrum, FRS, at the position where it will be installed.

However, to adjust the margin between ALRC and FRS, we need exact knowledges on the fluctuation of FRS which the authors have described through this paper. Especially, the control of earthquake loading factor, ELF, is extremely important.

§8. Concluding Remarks and Acknowledgement

The authors make the following facts clear in accordance with the authors' previous works;

1) The fluctuation of responses of a structure to earthquakes is very large. Their standard deviation is 30 % of the mean of a single-degree-of-freedom system and is 50 % of the mean of a two-degree-of-freedom system.

2) One of main causes of such fluctuation comes from the stochastic nature of the mechanism of generating and transmitting of earthquake waves. And it is very difficult to reduce their dispersion by categolizing the origin of earthquakes, the duration and so on.

3) The error of estimating the magnitude is said to be ± 0.3, and this value corresponds to 40 % error of the ground velocity and acceleration.

4) In the case that both magnitude and response factor run to the extreme, the error might be 140 % of the mean. If the stress caused by earthquake loadings is 20 % of the total load, and if a member is designed as 100 % of the allowable stress, the error mentioned-above cause 28 % over-stress. This over-stress increase the probability of failure of the number by 1.4×10^{4}. If we assume that the probability of occuring such an extreme case would be 4×10^{-5}, the total risk of failure by the extreme case of the future strong earthquake would be almost twice.

5) For the design response curve, no width would be added to the mean direct response spectrum, and 3σ of width should be added to the mean floor response curve, if we can assume that the stress caused by earthquakes is 20 % of the total load or the allowable stress. If it is 50 %, it is very difficult to obtain the reliable design result, so we should pay more attention to keep the system ductility or try to decrease this ratio.

6) Analysis using a single or a few time history data gives only the result which has a possibility to have a big error. So time history analysis is not recommendable for the design analyses except those in non-linear regions, for examples, elasto-plastic, frictional and so on.

7) Although on generating time history data from a given response spectrum, the consideration of phase relation between each component is very important. this technique has not developed well. The idea of the least favorable e quake has the possibility to develop for this purpose.

The authors owe to much the co-authors of the previous papers which refered in this paper. They wishes to express their gratitudes to them f their valuable co-operations and discussions, and also their many thank t members of the sub-committee in the Japan Electric Association for the discussion on the risk assesment.

They also indebted to Miss Ogino for having reviewed and prepared th manuscript and drawings.

§9. Reference

1) Shibata, H. and others: "On Fluctuation of Responses of a Structure", *Proc. of 5th WCEE*, #367 (1973)

2) Shibata, H.: "On Response Analysis for Structural Design and its Reliability", *Proc. of 3rd Structural Mechanics in Reactor Technology*, K4/3*, (1975)

3) Shibata, H.: "Some Comments on the Seismic Loading Condition and the Design Criteria of Nuclear Vessels, Pipings and Other Equipment", *Proc. of Extreme Load Conditions and Limited Analysis Procedures for Structural Reactor Safeguards and Containment Structures*, U5/1, (1975)

4) Shibata, H.: "On the Reliability of Anti-Earthquake Design of Structures", *Reliability Approach in Structural Engineering*, (Maruzen), (1975) p.111.

5) Shibata, H. and others: "On Decline of Reliability of Response Analysis", *Preprint of HOPE International JSME Symposium*, (1977)

6) Shibata, H.: "Some New Problems of Response Analysis for the Design", *Pre-print of JSME Meeting*, No. 760-3, (April 1976) p.135.

7) Shibata, H. and others: "On Some Results of Observation of Torsional Ground Motions and Their Response Analysis", *Bull. of ERS*, (Inst. of Ind. Sci., Univ. of Tokyo), No. 10, (Dec. 1976) p.44.

8) Shimizu, N.: "A Study on Aseismic Design of Mechanical Equipment and Piping System", *Rept. of Inst. of Industrial Sci.*, Univ. of Tokyo, Vol. 22, No. 1, (1972) p.1.

9) Japan Electric Assoc.: "Rept. on Vibration Characteristics of Nuclear Building, Equipment and Piping", (1970)

10) Shibata, H. and others: "Response Analysis of a Piping System in Three Story Building on Shaking Table", *Bull. of ERS*, (Inst. of Ind. Sci., Univ. of Tokyo), No. 5, (1971) p.1.

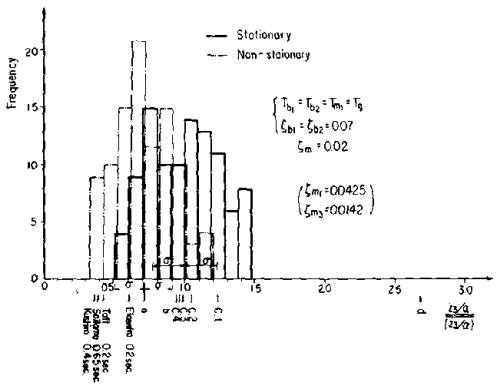

Fig. 1: Histograms of Response Factors of Bridged Piping to 100 Pseudo-Earthquakes

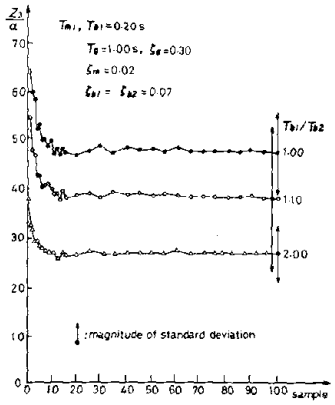

Fig. 2: Moving Average of Response Factors of Bridged Piping to 1 ∿ 100 Pseudo-Earthquakes

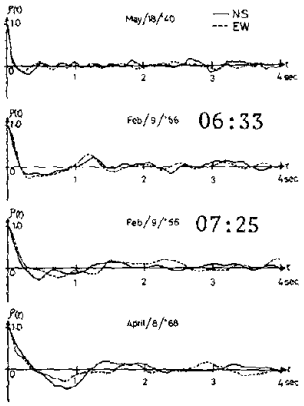

Fig. 3: Auto-correlation Functions of Four Earth-quakes in El Centro City

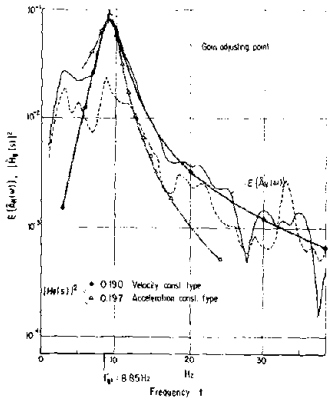

Fig. 4: Mean Power Spectra and Transfer Function of Estimated Model

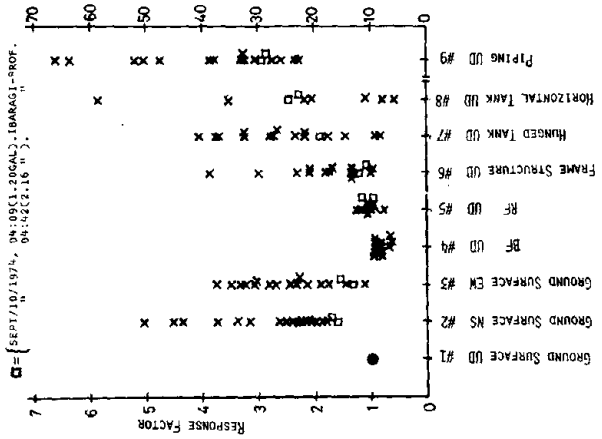

Fig. 5: Distribution of Responses of Model Chem Engineering Plant to Na Earthquakes (Vertical G Motion)

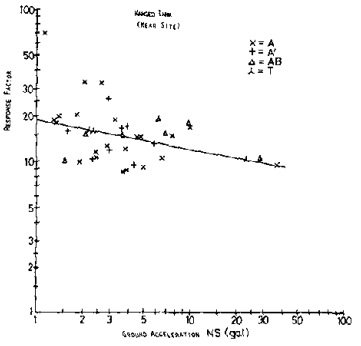

Fig. 6: Response Factor *vs.* Ground Acceleration, Hanged Tank (to Near Field Earthquake)

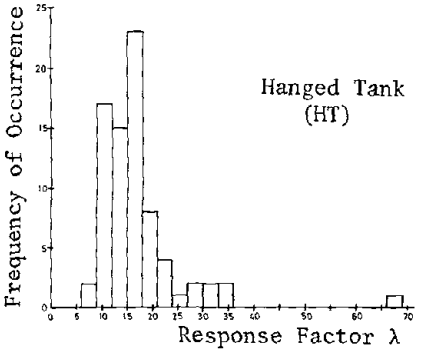

Fig. 7: Distribution of Response Factor

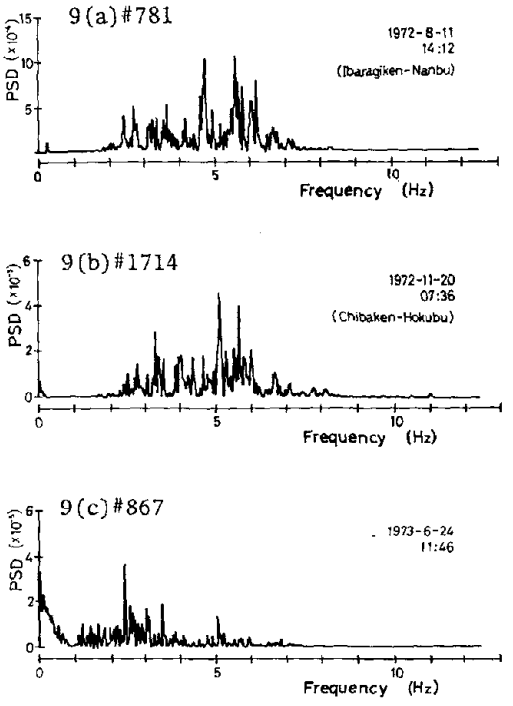

Fig. 9(a)(b)(c): Results of PSD Analysis

Fig. 8: Record of Responses of Chemical Engineering Plant: Abnormal Response of Horizontal Tank

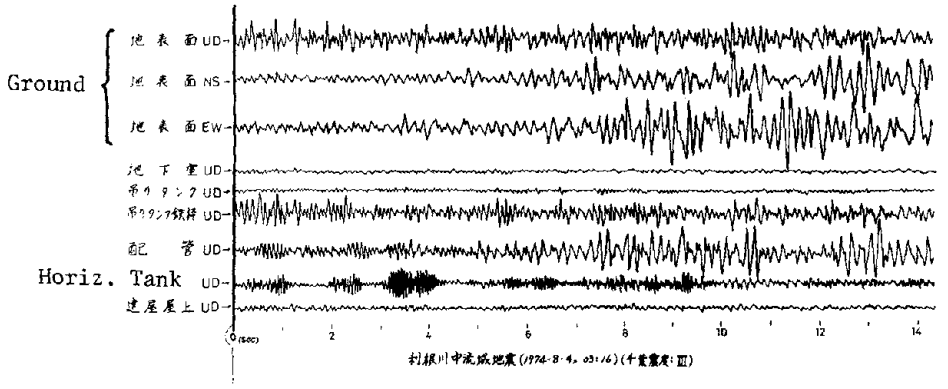

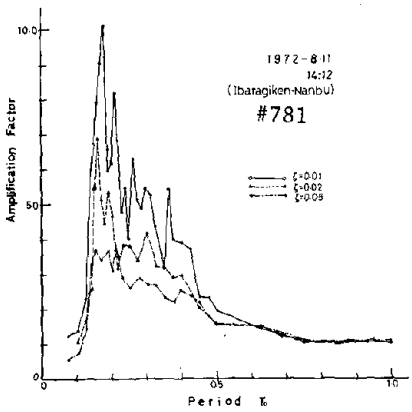

Fig. 10: Result of Response Analysis of Earthquake Shown in Fig. 9(a)

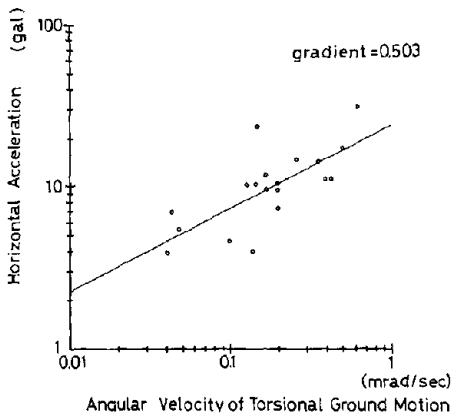

Fig. 11: Relation of the Maximum Horizontal Acceleration to the Maximum Torsional Ground Velocity

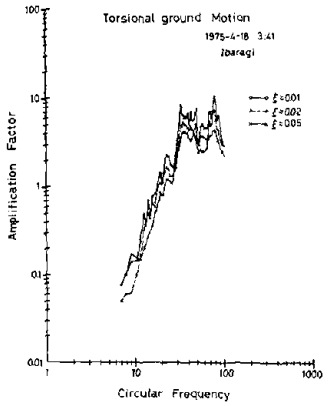

Fig. 12: Acceleration Response Spectrum of Torsional Ground Motion (1975/4/18 03:41)

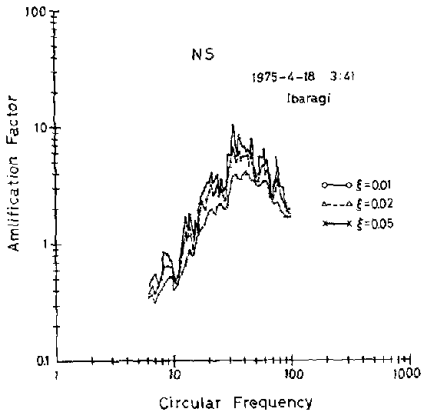

Fig. 13: Acceleration Spectrum of Horizontal Ground Motion (NS) (1975/4/18 03:41)

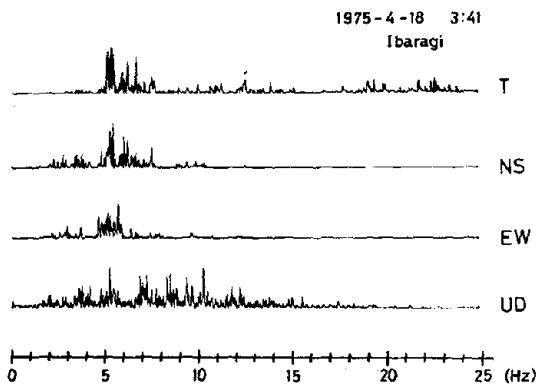

Fig. 14: Fourier Spectra of Torsional and Three Components of Ground Motion (1975/4/18 03:41)

Table 1: Relative Dispersion Factor of a Single-degree-of-freedom System *vs.* Vibration Characteristics

Critical Damping Ratio [%]	Relative Eigen Period of Structure T_b/T_g	Relative Dispersion [%]
7	0.2	12
	1.0	21
	4.0	29
2	0.2	12
	1.0	32
	4.0	44
0.7	0.2	18
	1.0	42
	4.0	50

Table 2: Vibration Characteristics of Main Items

	Eigen Freq. [Hz]	Critical Damping Ratio [%]
Piping UD	5.50	1
Horiz. Tank UD	18.3	1
" NS	6.38	1
" NS	4.72	2
Hanged Tank NS	4.73	3

Table 3: Response Factor

	Hanged Tank (HT)	Pipings (P)	Saddle-type Tank (PT)	Vertical Tank (VT)
Number of Data	77	57	58	58
Mean	16.97 (15.01)	22.86	5.87	1.344
Dispersion Factor	0.492 (0.262)	0.345	0.538	0.248
Upper Bound Value of 3σ	41.0 (26.8)	46.4	15.6	2.34
Maximum Value of Data	69.0	166	14.7	2.98
Eigen Frequency	4.73	7.59 (5.50)	4.72 6.38	----
Damping Ratio (%)	3	2,(1)	2, 1	----

Table 4: Examples of Abnormal Response and Peak Distribution

Earthq. Number	Source Div.	1st. Peak	2nd Peak	3rd Peak	Type of Wave Form	Locations
781	A	5.58	4.70	6.20	B	HT
862	A	2.75	5.15	5.03	B	HT, P, PT
875	A	3.13	3.03	3.25	N	P
1719	A'	5.10	5.78	3.30	B	HT, P
731	I	4.80	6.06	5.03	N	P, PT
1723	U	5.15	5.70	5.03	B	P
867	U	0.06	0.10	2.37	B	P

Table 5: Increase of Possibility of Failure under Over-stress Condition by Earthquake Loadings

Load Factor by Earthq.	Classification of Resp. Spec.	Rel. Disp. of Resp. d	$3d$ [%]
0.2	DRS	0.3	90
	FRS	0.5	150
0.5	DRS	0.3	90
	FRS	0.5	150

Mean + Resp. Fluct. + Error by Mag. Est. [%]	Over-stress [%]	Increase of Possibility of Failure by Over-stress	Increase of Total Risk of Failure
240	28	1.4×10^4	5×10^{-1}
300	40	1.4×10^6	5×10^1
240	70	3×10^6	1.1×10^6
300	100	1.3×10^{15}	4×10^{10}

DRS: direct response spectrum
FRS: floor response spectrum

If the configuration of a structure is fixed by architectural or other requirements, the designer has a restricted choice in the development of the strength and ductility required to insure adequate seismic behavior. It is not always possible to say that some design layouts are better than others for dynamic resistance, although it is fairly clear that different choices of framing can lead to vastly different requirements of strength and ductility. For example, a framed structure is generally less stiff and usually lower in frequency than a shear wall structure with nearly solid walls providing lateral resistance. Hence the design forces may be smaller for the framed structure than for the shear wall structure, although the required ductility may be larger.

The methods of analysis, and also the details of design specifications, have implications on the cost and the performance capability of the design. Refinements in calculational procedures inconsistent with the accuracy of the assumptions made and parameters used may lead to a false sense of security. If the specifications are unduly conservative the design may be forced into a type that is strong but less ductile than is desirable. It is difficult to avoid differences in the degree of conservatism among different types of structures, and in some cases it is undesirable to do so. Some materials by their nature, including their variability or lack of adequate control of properties, may require a greater factor of safety than other materials the properties of which are more accurately determinable and controllable. The margin between incipient failure and complete collapse may differ for different materials and may therefore involve a difference in the factor of safety required in the design. It is desirable, in the development of the basis for a performance criterion, that the designer's approach not be too greatly constrained. For example, it may be unwise to prescribe limits for both strength and ductility in such a way that the balance between the two cannot be adjusted to take account of new material properties or new structural types as they are developed. A trade-off between ductility and strength should be available in the methods that are permitted, so as to achieve economy without the sacrifice of safety. But whether one is interested in achieving strength or ductility, or both, the materials and framing systems have to be employed in an appropriate fashion, and adequate methods of inspection and control of construction are needed to insure that their use is proper.

The most desirable type of design code or specification is one which puts the least restrictions on the initiative, imagination and innovation of the designer. Such a code might involve only criteria for: (1) the loading or environment; and (2) the level of response, the stresses and deformation, or the performance of the structure under the specified loading or environmental conditions. It is highly desirable to have the controlling criteria parameters appear explicitly, rather than implicitly, in the design process; unfortunately such is not the case now in many existing building codes. The lack of rational proce-
dures can lead to misunderstanding of the desired function or behavior a
some cases can lead to poor design. The desired approach need not, and
erably should not, indicate how the designer is to reach his objective,
he can demonstrate -- through documentation of adequacy -- that he has a
a structural capability to resist the specified environmental conditions.
approach is generally the one now used for the design of nuclear reactor
stations. Experience over the past several years in approaching seismic
criteria in this way has indicated a number of problems, but also has bee
sonably successful in avoiding constraints due solely to the specificati
themselves, although there have been constraints based on the environmen
ditions and the stress and deformation levels allowed. The foregoing phi
to the extent possible has been used in the design of nuclear plants in t
States and was used in developing the Applied Technology Council (ATC III
lines described later herein.

SEISMIC DESIGN PHILOSOPHY FOR MAJOR PROJECTS

General Philosophy

For major projects the design criteria and recommendations normally take into account the seismic motions and seismic generated forces that have a reasonable degree of probability of occurrence along the route of a pipeline or at the building or facility site. The basis for the selection of these criteria and recommendations involves consideration of the acceptable risk of exceeding the design levels for the system and various classes of associated structures, equipment and facilities. For the most critical classes, where failure, defined as exceeding the allowable recommended levels, would have a bearing on life and safety of the population or might adversely affect the environment, or where for economic reasons interruption of the service provided is not tolerable, the margins of safety implicit in such criteria often may be greater than those now used in the seismic design of major buildings in highly seismic regions of the United States. For the least critical class, the margins of safety are at least as great as those provided by current building codes such as the Uniform Building Code or the SEAOC code (Ref. 9). In any event the procedures outlined should result in a design having appropriate factors of safety against seismic disturbances when combined with the other applicable operating and environmental conditions.

In accordance with principles developed for use in the design of nuclear reactor power plants, the design criteria generally encompass two levels of earthquake hazard. The lower level is that associated with a return period for the design earthquake of approximately 50 to 100 years and is designated herein as the "Design Probable Earthquake". The higher level is that associated with a longer return period, of the order of about 200 to 300 years or more, and is designated as the "Design Maximum Earthquake". Under some situations it may be expedient to use only one such level, generally the latter. The ATC III approach for buildings is somewhat different as discussed later.

Conceptually one might consider the first earthquake as one through which the nuclear facility or pipeline should be able to operate and continue operation after its occurrence, while the larger earthquake should not produce damage that has not been anticipated in the design. However, to do this in a systematic way usually would involve an unreasonable degree of design effort and moreover often may be based on inaccurate or insufficient seismic data for the region. When this is the case the relationship between the intensities of the two earthquakes normally has been taken arbitrarily as a factor of two.

The earthquake intensity by itself has limited significance in terms of design to resist seismic motions. Of equal importance are the structural parameters governing response, such as stress or strain and deflection, that the designer intends to use for the particular earthquake hazard selected. Normal these criteria are selected to make the Design Maximum Earthquake govern the design. Furthermore the criteria are such that, in the event of the smaller earthquake, the pipeline or nuclear facilities, if properly designed in acco dance with the recommendations, will generally be able to continue operation

As an illustration of the difference in design concepts for aboveground belowground items it is instructive to note the following general points. S tures, including aboveground piping which act like a structure, respond to a arthquake in a way associated with their dynamic parameters. Buried piping he other hand responds to earthquake motions by moving with the ground in s

The amount of inelastic deformation that a structure can undergo without suffering undue damage also affects its response, in terms of the stresses in it and the corresponding deformations and deflections. The allowable values of ductility depend on the material of which the structure is made and on its manner of construction, principally the way in which joints are made. For example welded steel structures of high-quality steel, made with good welding techniques and attention to details possess high ductility. Properly reinforced masonry structures also can be made to possess reasonable levels of ductility. Under certain circumstances the ductility can be impaired by a tendency to fracture in a brittle mode or to undergo local buckling. For these reasons, the ductility levels used in a design must be verified to determine that the materials themselves and their fabrication processes, and especially the details of construction for reinforced concrete, are controlled in such a way that the value of ductility used can actually be achieved while maintaining the requisite strength; it is recommended that the design and details be made capable of developing a ductility factor of at least 1.5 times that used in the design spectrum. Possible ductility levels under ordinary conditions are discussed in Ref. 10. Where the permissible level of structural response does not involve yielding at all, then the ductility factor used is limited to a value of unity.

Response and Design Spectra -- The response spectrum (Refs. 1, 4 and 10) is a plot of the maximum transient response to dynamic motion of a simple dynamic system having viscous damping. An elastic response spectrum has peaks and valleys, but in general has a roughly trapezoidal shape, similar to the curve denoted elastic response of Fig. 1. Spectral amplification factors for horizontal motion, in the elastic range, for damping values ranging from 0.5 to percent of critical as developed in recent studies by Newmark, Hall and Mohraz are shown in Table 2.

To draw the elastic response spectrum for any Design Maximum Earthquake motion for a structure, one takes the values of ground motion for any one of the zones from Table 1, using the "structural design" values, and applies the appropriate amplification factors from Table 2 for the particular percentage of damping to the accelerations, velocities, and displacement, respectively. One obtains in this way a roughly trapezoidal form of response spectrum similar to the elastic response curve in Fig. 1. The intersections of the upper two knees of the elastic response spectrum are determined by the amplified motion lines. The two lower knees, at the higher frequencies, are taken as 8 hertz and 33 hertz, respectively. The value of the spectral acceleration at 33 hertz and beyond is taken as the maximum ground acceleration for the elastic response spectra.

Spectra also may be drawn for the operating earthquake for any zone, where the ground motion values are taken as half of those that correspond to the larger earthquake. In general, the amplification values, because of the different values of damping that might be used for the lower intensity earthquake, will not be the same as for the larger earthquake.

To determine the design spectra for acceleration (or seismic coeffi
the inelastic case one takes the appropriate value of ductility factor f
3 for the seismic design class (defined later herein) and divides the va
elastic displacement and velocity bounds by the value of ductility facto
The values of the controlling elastic acceleration bound (between about
hertz) however, are divided by the quantity $\sqrt{2\mu - 1}$, where μ is the duct
tor. For frequencies higher than 33 hertz, the design acceleration leve
same as the elastic acceleration (Ref. 4). The maximum inelastic displa
obtained by multiplying the acceleration (or yield displacement) spectru
1 by μ.

From the procedure described, it is clear that the intensity of earthquake motion as defined by the applicable response spectrum, must be considered in the light of the way in which that earthquake motion is used in design. In other words, one would prescribe that a lower value of acceleration be used with a procedure that involves the use of working stresses than a procedure that involves yield point (or limit) strengths. One cannot compare the earthquake accelerations prescribed by various codes without taking into account the design criteria used in the codes. The Uniform Building Code of the United States, which generally is based on the SEAOC code, has up to the present time used working stress design criteria, and the seismic coefficients described in the SEAOC code are consistent with those values; the ATC III document (Ref. 6) is based on limit strength concepts. One would have to increase the seismic coefficients prescribed in the code to arrive at values comparable with those developed herein, which are to be used at yield levels.

Classification for Seismic Design

Because of the importance of the amount of deformation or stress that can be permitted in buildings of various types subjected to earthquakes, guidance is necessary in arriving at an appropriate means of selecting the design requirements. For this purpose for major facilities a seismic classification system, encompassing three classes has been recommended for use by Newmark.

Class I includes those items of equipment (including instruments) performing vital functions that must remain nearly elastic, or any items for which the allowable probability of exceeding design levels must be extremely low. Obviously, items that are essential for the safe operation of the facility or pipeline, where damage to the particular unit would cause extensive loss of life or major environmental damage, would be in Class I. Other items might be included in Class I if failure of such items would entail large costs in repair or replacement, or lengthy shutdown of the pipeline.

Class II includes buildings, equipment, and aboveground piping that can deform inelastically to a moderate extent without loss of function. This class also includes any items for which the allowable probability of exceeding design limits can be somewhat larger than in Class I. However, piping or systems which might fail in a brittle mode, or whose failure might tend to propagate over considerable distances, causing extensive damage and/or possibly danger to life in populated regions, perhaps should be put in Class I or in a classification intermediate between Classes I and II.

Class III includes, in general, buildings or equipment that can be permitted to deform significantly, or any items that are not essential for safety; it includes those items for which the allowable probability of exceeding design limits can be moderately high. However, buildings that contain Class I or Class II and which might damage or put out of action those items if the Class III buil should deform excessively, should be moved to a higher class, perhaps interme between Classes II and III.

An example of the damping and ductility factors that might be used in de fining the design spectra for the various seismic design classes is given in 3. These give results that are consistent with the class definitions above, atisfy the criterion that the Design Maximum Earthquake, with its higher int ty, should in general give more stringent requirements than the Design Prob rthquake. Sets of spectra like those in Fig. 1 can be developed for each c d earthquake level in accordance with the principles given earlier.

APPLIED TECHNOLOGY COMMITTEE SEISMIC DESIGN PROVISIONS FOR BUILDING STRUCTURES

Background

Most of the seismic design and analysis requirements presently employed in the U.S. building codes were developed for the Recommended Lateral Force Requirements and Commentary published by the Seismology Committee of the Structural Engineers Association of California in 1959-1960. In the intervening years, improvements and modifications have been made at frequent intervals (Ref. 9). Several years ago it became apparent that a comprehensive review should be made of the seismic provisions to incorporate the latest state-of-the-art in analysis and design.

In this regard an effort was undertaken by The Applied Technology Council (ATC) in late 1974 to develop comprehensive seismic design provisions. The work was performed under a contract with the National Bureau of Standards (NBS), with funding by the National Science Foundation (RANN) and NBS. The project is part of the Cooperative Federal Program in Building Practices for Disaster Mitigation initiated in 1972 under the leadership of NBS. Some eighty-five participants were involved and included representatives of practicing professionals, academicians, researchers, and representatives of code groups and regulatory and governmental agencies. R. L. Sharpe was appointed Project Director and N. M. Newmark as Chairman of the Task Group Coordinating Committee, overseeing the operation of 14 technical committees organized into five task groups. The author served on two of the technical committees, the Committee on Seismic Ground Motions and the Committee on Structural Design Provisions. Drafts of the report have received widespread review and the final report (Ref. 6) is to be issued soon.

The ATC III provisions were developed to establish design and construction criteria for buildings subject to earthquake motions with the purpose of minimizing the hazard to life and to improve the capability of specific essential facilities to function during and after an earthquake. The design earthquake motions specified in the provisions were selected with the expectation that there would be a low probability of their being exceeded during the normal lifetime expectancy of buildings. Buildings, their components, and elements which are designed to resist the specified motions and which are constructed in accordance with the requirements for framing and materials, may suffer damage but should have a low probability of collapse due to seismic-induced ground shaking.

Seismic Risk Maps

One major task involved development of seismic design regionalization maps for the U.S. These were based on an evaluation of historic seismicity, frequency of earthquake occurrence, and geology to the extent possible. The maps r[illegible] the best data available in the 1976 time frame as tempered by experience ment.

In the development of these maps a number of considerations were tak account. Among these was the observation that the relationship between c lateral force and period of a structure should take into account the dist the site from the earthquake source. Studies of seismic data show that t higher frequencies of ground motion attenuate more rapidly with distance lower frequencies and therefore flexible structures at a distance from th quake source may be significantly affected by the earthquake motions wher stiffer structures would feel little effect. This reasoning was one basi

preparation of two separate ground motion parameter regionalization maps. Another consideration was to try to insure that the probability of exceeding the design ground motion would be roughly the same in all parts of the United States, and that maps not be drawn for the most intense motion that might conceivably occur at a specific location; this reasoning follows that described earlier in this paper. For the most part the zoning maps used previously in the United States in design guides and codes have been based upon estimates of the maximum ground shaking during recorded history without any consideration of the frequency of occurrence of earthquakes. Another decision in the development of the maps was to avoid microzonation, and not to denote actual faults on the maps. It was believed that local studies should be reserved for detailed investigation by qualified experts.

Two sets of seismic design regionalization maps for normal building design were drawn, one denoted Effective Peak Acceleration (EPA) and the other Effective Peak Velocity (EPV). In accordance with the previous discussions on response spectra given herein, the EPA is proportional to spectral values for periods in the range of about 0.1 to 0.5 seconds whereas the EPV maps are proportional to spectral values for periods of about 1 second; the latter is intended to reflect the effect of distant earthquakes. The development of the EPA map was facilitated by the work of Algermissen and Perkins of the USGS (Ref. 11) and in many respects is similar to their map.

Categorization of Seismic Performance

For categorization purposes one locates the site on the EPA and EPV maps and from procedures given in the guide determines the seismicity index (values range from 1 to 4, 4 being the highest). Also there are three seismic hazard exposure groups, Group III corresponding to buildings housing essential facilities necessary for post-earthquake recovery, Group II includes buildings housing large numbers of occupants or buildings in which the occupant's movements are restricted, and Group I includes all other buildings. A table relates seismicity index and seismic hazard exposure group and leads to designation of a seismic performance category, of which there are four groups (A through D). Category A includes buildings, whether regular of irregular, which need not be analyzed for seismic forces. Buildings in Category B are to be analyzed as a minimum in accordance with the equivalent lateral force procedure. Buildings in Category C conform to the framing system requirements for Category B and to additional requirements delineated in the guide, including special framing options, requirements for considering interaction and deformation effects, special analysis procedures, design and detailing requirements and materials controls. Seismic Category D is the most stringent and incorporates all of the requirements of Category C and in addition has a number of additional height limitations.

Design Forces and Analysis

The design spectrum is used in the simplified analyses (equivalent late load force procedure) through the use of an equivalent lateral force factor more specialized cases with the modal analysis procedure. The use of the re spectrum concept as well as modal analysis procedures are new concepts for l guides and codes. The site conditions are incorporated through the use of a factor which varies from 1.0 (for firm soil or rock) to 1.5 (for soft soils) simplified procedure was arrived at after considerable study of the various involved and it was felt that the best approach at present for incorporating conditions was through modifications of the response spectra.

In the case of the equivalent lateral force procedure the base shear is ained by the expression $V = C_s W$, where V is the base shear, C_s is the seismi

design coefficient and W is the total effective weight of the building. The quantity C_s is given by the relationship:

$$C_s = \frac{1.2A_vS}{RT^{2/3}}$$

In this relationship, the quantities are defined as follows:

A = Effective Peak Acceleration value based on the EPA and EPV maps.

S = Soil profile factor ranging from 1.0 for rock and stiff soil sites to 1.5 for soft soil sites.

R = Response modification coefficient depending on type of structural system, including vertical and horizontal lateral force distribution systems, and type of materials employed, inherent ductility and damping.

T = Measure of fundamental period of vibration based on framing method and geometry of building.

The value of C_s need not exceed 2.5 A_a/R for rock or stiff soil sites or deep soil sites nor 2.0 A_a/R for soft soil sites where $A_a \geq 0.3$.

As an example of the manner in which the seismic coefficients vary as a function of period, Fig. 2 is taken from Ref. 12 and shows the spectral variation for typical different locations in the United States. These are computed for buildings on rock or firm ground and in general the values would be increased for softer soils; some of the values in Fig. 2 now differ slightly from those given in the latest ATC III draft. It will be noted that the design acceleration spectrum decreases with the two-thirds power of the fundamental period, in contrast to the theoretical value of decrease with period on firm ground and with the period squared on very deformable ground. The reasons for using the rate of decrease specified in the ATC guide are to provide uniformity and simplicity and to take account of the fact that for long periods the cost of the building is less sensitive to seismic hazard reliability. Other reasons relate to the loss likely to occur by such a failure, the higher probable number of significant degrees of freedom in long period structures, and the changes in periods and mode shapes that may arise from nonlinear behavior. For such conditions in general one can afford to design more conservatively.

The distribution of seismic shears over the height of the building for the purpose of computing shears and overturning moments is based on a power function giving a linear distribution for periods less than 0.5 seconds, and a parab distribution for periods greater than 2.5 sec., with a linear interpolatior tween those limits.

Provisions are given for increased seismic forces when the safety of t building is dependent on the survival of a single major force resisting ele Similar provisions are made for increases in seismic factors when large dis uities in story strengths or stiffness occur.

Overturning moments computed from the seismic force distributions may duced under certain conditions, but generally not in the upper ten stories building, and not by more than 20 percent in the building itself, with an

additional 20 percent reduction permitted in determining the foundation forces under the building but with certain restrictions on locations of the resultant base force.

Soil-Structure Interaction

Two different approaches can be used to assess the soil-structure interaction during seismic response. One procedure consists of modifying the stipulated free field design ground motion and evaluating the response of the structure to the modified base motion; the other procedure consists of modifying the dynamic properties of the structure and evaluating the response of the modified structure to the prescribed free field ground motion. The ATC design provisions are based on the latter approach.

The result of incorporating this procedure leads to (1) an increase in the fundamental natural period of the structure and (2) a change (usually an increase) in the effective damping. The increase in period accounts for the compressibility of the foundation soil whereas the change in damping accounts primarily for the effects of energy dissipation in a supporting soil by radiation damping and hysteretic action. Expressions are given in the guide for the reduction in total lateral force or base shear for the structure as a function of parameters of the type noted. Obviously a structure could be designed conservatively without any consideration of soil-structure interaction and the guide is set up such that the use of the relations for soil-structure interaction are optional with the designer.

Other Special Design Provisions

Other general design requirements which are discussed concern combinations of loads, orthogonal effects, the handling of discontinuities in strength (especially vertically), redundant systems, provisons for continuity, details for ties and anchorage for concrete or masonry walls as well as nonstructural systems, the use of diaphragms, vertical seismic motions, delfection and drift limits, torsion, and P-delta effects.

Two types of torsional effects are implicitly recognized in the guide. "Calculated" torsion arising from irregularities in the structural rigidity and masses. Such torsional effects are handled statically by calculating the torsional moment as equal to the story shear times the eccentricity between the center of resistance and apparent center of mass. "Accidental" torsion can arise in symmetrical structures from irregular and multi-directional earthquake ground motion effects. The design provisions require that an "accidental" torsional moment equal to the story shear times an eccentricity equal to at least 5 percent of the building dimension normal to the direction of the earthquake be considered.

P-delta effects arising from the eccentricity of the gravity load abov level being considered, especially when large lateral deformations are enc are considered in the design provisions. For buildings subjected to later the moments and stresses in the members due to the gravity loads are augmer moments equal to the lateral drift times the weight of the elements of the ture above the level under consideration. Stability coefficient guideline given in the ATC III document for establishing situations in which P-delta must be investigated.

The role of redundancy in structural system performance is clearly sir out for attention in the guide. The provisions in the guide prescribe pen when redundancy is not provided in the seismic resisting system. It is st

that good engineering practice calls for incorporating redundancy into the system, as well as that steps be taken to insure that failure of any one or a small number of members will not cause progressive or catastrophic collapse.

Other sections in the ATC III document deal with seismic design of such items as foundations, architectural, mechanical and electrical elements, and the upgrading of existing buildings. Special sections deal with properties of materials (wood, concrete, steel, and masonry) and all four sections are based on general yield or limit strength concepts. Also there is considerable attention given to quality assurance and quality control. It is believed that a large amount of the earthquake damage throughout the world could be reduced significantly through good engineering design and construction and especially with more attention to the quality of materials, quality of construction and continuity.

In conclusion there are many innovative features of the ATC document which most assuredly will affect the development of design codes and standards in the United States in the immediate years to come. The foremost contribution may well be that of explicitly and rationally (rather than implicitly) incorporating in the procedures the factors which control the design and analysis.

RECENT RESEARCH STUDIES ON BUILDING STRUCTURES

In the Civil Engineering Department at the University of Illinois as part of the research program entitled, "Design for Protection Against Natural Hazards", sponsored by the National Science Foundation (RANN), a number of studies are going forward dealing with such topics as the design of low-rise and high-rise structures, response of primary and secondary systems, response spectrum techniques for handling nonlinear behavior, and the interrelationship of wind and earthquake design techniques.

One study (Ref. 7) dealing with the seismic design of low-rise steel buildings has examined in part the earthquake resistant analysis and design procedures for steel low-rise shear buildings, moment frame buildings and X-braced frame buildings. A number of two and three story buildings were studied using time-history analysis, modal analysis and the quasi-static building code approach, including procedures similar to ATC III. The base story was found to be the critical link in the lateral seismic load resisting system for the shear buildings, the moment frame buildings proportioned with weak columns, and the X-braced buildings considered. For the moment frame buildings proportioned with strong columns and weak beams, inelastic response was distributed fairly uniformly throughout the beams of the buildings. From the results of the time-history studies, it appeared that inelastic deformations (of reasonable magnitude) can be estimated from the elastic deformations by means of the design rules that have been developed for single-degree-of-freedom systems, and that the quasi-static building code approach with response spectrum input was the most efficient appropriate method to use at present for low-rise buildings.

Another study (Ref. 8) dealt with procedures for determining (for pre design purposes) design story shears and overturning moments in high-rise ings. Various distributions over the height of a structure were determine function of several parameters which included the type of structure (flexu shear behavior), the height of structure, the vertical configuration (incl setbacks) and the foundation compliance. These variables led in turn to s tures whose fundamental period fell in various ranges of the normal respon spectrum. For each model a modal analysis was performed and responses wer erated, generally by the SRSS technique. Polynomial regression analyses w

performed on the normalized distributions and coefficients were determined to account for the effects of the parameters varied. These coefficients in turn can be used for preliminary design purposes.

These two studies were singled out for attention briefly to indicate the nature of some studies underway. The studies have been useful in providing a check on some of the proposed ATC guideline procedures and it is expected that portions of the studies will find direct application in practice.

Insofar as future research requirements for earthquake resistant design are concerned it is the author's belief that at the moment the primary needs are (a) for additional realistic experimental resistance data for structural members and systems carried into the nonlinear range, (b) for development of simple and rational design and analysis procedures that incorporate nonlinear behavior, and (c) for research into, and development of, appropriate applications of probability concepts to design. A broader base of information and understanding in these areas is needed badly. A final suggestion pertains to investigation of earthquake damage; it would be helpful in such investigations to document (and to study) in detail the performance behavior of structures which are undamaged, as well as those which are damaged, and thereby employ comparative evaluation to develop improved design procedures or to confirm superior performance. Our common goal is to produce research results of significance which can be transferred to practice rapidly, thereby helping reduce damage and casualties arising from severe earthquake excitation as well as other natural and man-made hazards.

REFERENCES

1. N. M. Newmark and W. J. Hall, "A Rational Approach to Seismic Design Standards for Structures," Vol. 2, pp. 2266-2275, Proc., Fifth World Conf. on Earthquake Engin., Int. Assoc. for Earthquake Engin., Rome, 1974. (See also "Procedures and Criteria for Earthquake Resistant Design," Nat. Bur. of Standards Building Science Series 46, Building Practices for Disaster Mitigation, pp. 209-236, Feb. 1973).

2. W. J. Hall and N. M. Newmark, "Seismic Design Criteria for Pipelines and Facilities," in The Current State of Knowledge of Lifeline Earthquake Engineering, Proc. TCLEE Spec. Conf., ASCE, pp. 18-34, Aug. 1977.

3. N. M. Newmark and W. J. Hall, "Seismic Design Spectra for Trans-Alaska Pipeline," Vol. 1, pp. 554-557, Proc., Fifth World Conf. on Earthquake Engin., Int. Assoc. for Earthquake Engin., Rome, 1974.

4. N. M. Newmark and W. J. Hall, "Vibration of Structures Induced by Ground Motion," in Shock and Vibration Handbook, edited by C. M. Harris and C. E. Crede, McGraw-Hill, Inc., 2nd Ed., pp. 29-1 to 29-19, 1976.

5. N. M. Newmark and W. J. Hall, "Seismic Design Criteria for Nuclear Reactor Facilities," Proc. Fourth World Conf. on Earthquake Engin., Int. Assoc., for Earthquake Engin., Santiago, Chile, 13-18 Jan. 1969, Vol. II, Session B-4, pp. 37-50, 1969.

6. "Recommended Comprehensive Seismic Design Provisions for Buildings," ATC III Study, Applied Technology Council, 480 Calif. Ave., Suite 205, Palo Alto, Calif. 94306 (Available late 1977).

7. C. J. Montgomery and W. J. Hall, "Studies on the Seismic Design of Low-Rise Steel Buildings," Civil Engin. Studies, Struct. Res. Series No. 442, Dept. of Civil Engin., Univ. of Illinois, Urbana, Ill., 169 pp., 1977.

8. R. Smilowitz and N. M. Newmark, "Seismic Shears and Overturning Moments in Buildings," Civil Engin. Studies, Struct. Res. Series No. 441, Dept. of Civil Engin., Univ. of Illinois, Urbana, Ill., 137 pp., 1977.

9. Structural Engineers Association of California, "Recommended Lateral Force Requirements and Commentary," 1975; Uniform Building Code, Int. Conf. of Building Officials, Whittier, Calif., 1976.

10. N. M. Newmark and E. Rosenblueth Fundamentals of Earthquake Engineerin Prentice-Hall, Inc., Englewood Cliffs, N. J. 1971.

11. S. T. Algermissen and D. M. Perkins, "A Probabilistic Estimate of Maxim Acceleration in Rock in the Contiguous United States," U.S. Geol. Surve Open File Report, 76-416 (1976).

12. N. C. Donovan, B. A. Bolt and R. V. Whitman, "Development of Expectancy Maps and Risk Analysis," ASCE Reprint 2805, Sept. 1976.

TABLE 1 DESIGN SEISMIC MOTIONS

	Ground Motion			Structural Design		
Magnitude	Accel % g	Veloc in./sec	Displ in.	Accel % g	Veloc in./sec	Displ in.
8.5 and 8	60	29	22	33	16	12
7.5	45	22	16	22	11	8
7.0	30	14	11	15	7	5.5
5.5	12	6	4.5	10	5	4

TABLE 2 SPECTRUM AMPLIFICATION FACTORS FOR HORIZONTAL ELASTIC RESPONSE

	One Sigma (84.1%)			Median (50%)		
Damping, % Critical	A	V	D	A	V	D
0.5	5.10	3.84	3.04	3.68	2.59	2.01
2	3.66	2.92	2.42	2.74	2.03	1.63
3	3.24	2.64	2.24	2.46	1.86	1.52
5	2.71	2.30	2.01	2.12	1.65	1.39
7	2.36	2.08	1.85	1.89	1.51	1.29
10	1.99	1.84	1.69	1.64	1.37	1.20

TABLE 3 EXAMPLE OF DAMPING AND DUCTILITY LEVELS FOR VARIOUS DESIGN CLASSES AND EARTHQUAKES

Earthquake	Class	Damping % Critical	Ductility Factor (μ)
Design Probable	I	2	1.5
	II	3	2
	III	5	3
Design Maximum	I	3	2
	II	5	3
	III	7	5

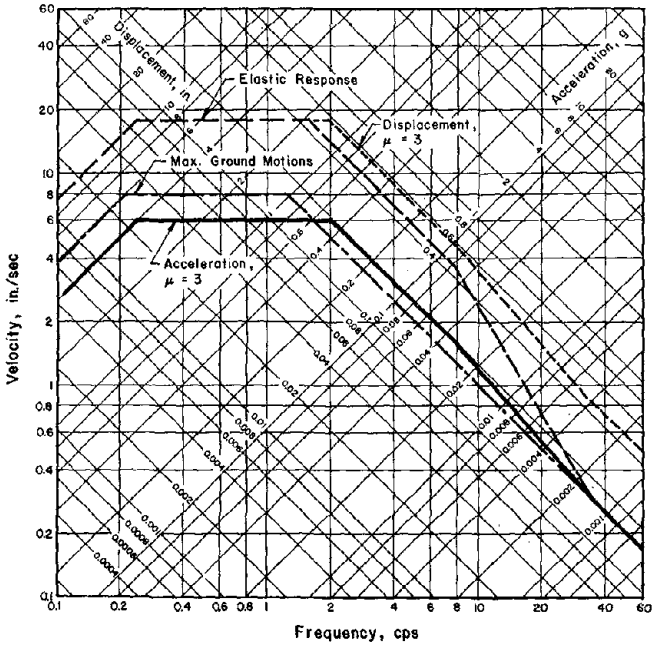

FIG. 1 ELASTIC AND INELASTIC DESIGN SPECTRA

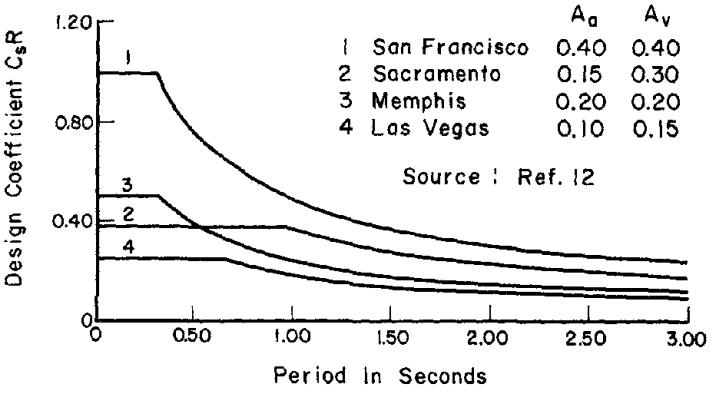

FIG. 2 REPRESENTATIVE - DESIGN COEFFICIENT CURVES

DEVELOPMENT OF EARTHQUAKE RESISTANT DESIGN METHOD EMPLOYING ULTIMATE CAPACITY CONCEPT

by

Hiroyuki Aoyama

Associate Professor
University of Tokyo

Synopsis

The "Earthquake Load", recently proposed in Japan, is introduced and discussed. This is to provide simple and practical means of "post-design" examination of earthquake resistant capability by evaluating the ultimate lateral capacity, and potential nonlinear response displacement through a simplified dynamic analysis and perfectly elasto-plastic model. Use of an effective period is shown to be useful in evaluating nonlinear response displacement associated with reinforced-concrete-type hysteresis. A proposed modification to the "Earthquake Load" incorporating the concepts of effective period and ductility class is introduced as a possible fundamental scheme of limit state earthquake resistant design method.

Introduction

In the long history of earthquake resistant design of reinforced concrete building structures in Japan, the most remarkable developments have been made in the last decade, stimulated by the experience of structural damages caused by the Tokachioki earthquake of 1968. The Architectural Institute of Japan published a book entitled "Earthquake Load and Earthquake Resistance of Building Structures" in January 1977, compiling the results of most recent coordinated activities of many structural committees of the Institute. In this publication a new concept of the "Earthquake Load" was proposed, and it was examined from the point of view of various structural materials. It may be stated that most of the significant achievements in the last decade in Japan were culminated in this recent publication.

Although Japan had experienced many destructive earthquakes before the Tokachioki earthquake of 1968, this earthquake was characteristic in many aspects. Among others, it was the first experience for many reinforced concrete low-rise buildings built in accordance with the modern Japanese design method based on the Building Standard Law and Standards issued from the Architectural Insti of Japan, to undergo severe seismic shaking. In consequence, medium or hea damages occurred to approximately 15 percent of reinforced concrete buildin existing in the affected area.

By the time when Tokachioki earthquake occurred in 1968, methods of dy response analysis had been well developed as design tools for high-rise bui ings. Dynamic response analysis considerably broadened the scope of invest gations into causes of earthquake damages. Unlike Kanto earthquake of 1923 Fukui earthquake of 1948, many research projects were carried out where res analysis was applied in order to examine the dynamic behavior of low-rise

reinforced concrete buildings. Several books were published as the results of these research activities, among which were two volumes resulting from U.S.-Japan Cooperative Science Program (1971 and 1976), two volumes from the Architectural Institute of Japan (1971 and 1975), and one book edited by Umemura (1973).

Summarizing all these efforts since the Tokachioki earthquake, it may be stated that the dynamic response of buildings during earthquakes, including the possibility of failure, could be estimated, provided that a mathematical model was set up which would appropriately represent the nonlinear restoring force characteristics. Also it was found that the lateral strength of the buildings governed most directly the magnitude of response deformation.

As an important by-product of these investigations, it was pointed out that the lateral strength of buildings would vary tremendously even though they had been designed for the same seismic coefficient by the same design procedure. The reason for this fluctuation was analyzed by the author (1977). The practical problem here is that the increase of lateral strength is not dependable. It just does not always happen. Depending on the structural planning and proportioning, some buildings may scarcely have excess strength, yet they may lack in ductility. A more rational design method is needed which would provide more uniform seismic safety.

The Vibration Committee of the Architectural Institute of Japan, which is responsible for the development of design seismic loading, announced two Proposals of "Earthquake Load", in 1973. One of them, called the "First Proposal" was examined by various structural Committees in the Institute. In particular, the Reinforced Concrete Committee studied the proposal of "Earthquake Load" quite intensively, and came out with a proposed modification to the originally proposed "Earthquake Load". This report attempts to summarize the outline of original and modified proposals of the "Earthquake Load (First Proposal)".

Body of the Proposed "Earthquake Load"

In this section, the "Earthquake Load (First Proposal)" as proposed by the Vibration Committee of the Architectural Institute of Japan (1977) will be outlined.

Classification of Buildings

Concept of building classification was introduced in which buildings belonging to different divisions were to be designed for earthquakes by different methods.

Division One is for buildings where structural calculations are not required, such as the one following the already approved standard design.

Division Two is for buildings to be designed in accordance with the current Building Standard Law only, such as low-rise construction restricte by minimum requirements for wall ratio and so on.

Division Three is for general buildings to be designed considering dynamic effect. Proposed Earthquake Load is intended for this division.

Division Four is for special buildings, with complicated system, new material or new construction method, whose design and analysis are to be examined individually by a board of specialists.

Scope of the "Earthquake Load"

Buildings in Division Three whose structural design has been made in accordance with the Building Standard Law or similar ordinances shall be examined for earthquake motions of maximum intensity by the following method. In this sense the "Earthquake Load" is intended, not to provide design seismic load, but to provide means of "post-design" examination. Whatever the design parameters or design procedures are, a building is judged to be satisfactory, if it meets this post-design examination. In this sense the "Earthquake Load" provides the "performance type" design criteria rather than the "specification type".

Velocity Response Value for Examination

Velocity response value for the post-design examination is given by the following formula.

$$V_D = Z\ G\ S\ D\ V_o \qquad (1)$$

where

- V_D : velocity response value for examination.
- Z : coefficient for zoning (1.0 - 0.8).
- G : coefficient for soil classification as specified in Table 1.
- S : spectral value determined by the ratio of natural period in each mode of building T and critical period of ground T_c as in Fig. 1, where T_c is specified in Table 1.
- D : coefficient for damping characteristics of building as specified in Table 2.
- V_o : standard value of velocity spectrum, taken to be 85 cm/sec.

Values of V_D for $Z = D = 1$ is shown in Fig. 2. Figure 3 shows the corresponding acceleration spectra. Although not explicitly stated in the "Earthquake Load", it is inferred that the spectra in Figs. 2 and 3 correspond to earthquake motions with maximum ground acceleration of about 0.3 g.

Natural Periods and Modes of Building

Natural periods and modes are computed taking stiffness of frames and walls into account. If large amount of sway and rocking at the base of building are expected their effect may be accounted for.

Elasto-Plastic Response Displacement and Ductility

Relative displacement and ductility of each story considering elasto-plastic response shall be calculated by the following equations.

$$\delta_r = \mu_r \, \delta_{re} \tag{2}$$

$$\mu_r = \frac{1}{2}\left\{\left(\frac{Q_{rD}}{Q_{ru}}\right)^2 + 1\right\} \qquad (Q_{rD} \geq Q_{ru})$$

$$\mu_r = Q_{rD}/Q_{ru} \qquad (Q_{rD} < Q_{ru}) \tag{3}$$

where

δ_r : elasto-plastic response relative displacement of r-th story
δ_{re} : elastic limit relative displacement of r-th story
μ_r : ductility factor of r-th story
Q_{ru} : ultimate lateral capacity of r-th story
Q_{rD} : elastic response shear force of r-th story

The elastic response shear force Q_{rD} shall be calculated by the following equation.

$$Q_{rD} = \sqrt{\sum_{i=1}^{k}\left(\sum_{j=r}^{n} m_j \, \beta_i \, u_{ji} \, \omega_i \, V_D\right)^2} \tag{4}$$

where

m_j : mass of j-th floor
β_i : participation factor for i-th mode
u_{ji} : natural mode shape (eigen vector) for i-th mode at j-th floor
ω_i : natural circular frequency of i-th mode
k : maximum order of modes to be considered
n : number of stories

Equations (2) and (3) are derived based on the following two assumptions. First, nonlinear response displacement of a single-degree-of-freedom system is related to the linear response as in Fig. 4, originally proposed by Newmark and others. Implicitly assumed here is that the restoring force characteristics of the building can be idealized into perfectly elasto-plastic hysteresis. Second, above relation is applicable to each story in a multi-story building. This postulates that each story yields simultaneously and deforms to approximately same ductility factor, or at least this condition is not violated on a large scale.

Equation (4) is so-called modal superposition by root-sum-square law. Since such complicated buildings as might vibrate in torsional modes are excluded out of the scope, maximum order of modes to be considered, k, may be taken to be 3.

Acceptance Criteria for Earthquake Resistance

Buildings are judged to be acceptable when all the following relations are satisfied.

$$\mu_r \leq \mu_a / I_r \tag{5}$$

$$\delta_r / H_r \leq 1/125 \tag{6}$$

$$\sum_{r=1}^{n} \delta_r / \sum_{r=1}^{n} H_r \leq 1/150 \tag{7}$$

where

μ_a : allowable ductility factor determined for each type of construction
I_r : importance factor as specified in Table 3
H_r : height of r-th story

Equation (5) requires the response ductility of each story to remain within the allowable limit with a safety margin which is dependent on the importance of the story. Allowable ductility factor μ_a of 5 for steel and SRC, 3.5 for RC frame, 2.0 for RC wall were once proposed, but their final decision was left to each Structural Committee.

Equations (6) and (7) require the response deformation in terms of translation angle to remain within the prescribed limit. The limiting values are subject to further discussions.

In case the building fails to satisfy these criteria, structural design must be modified. In general, greater strength will be provided to the structure. However, it is permissible to improve detailing so that greater allowable ductility is available.

Examination for overturning and appendages such as penthouse must also be made. Provisions for these items will be added in the future.

Effective Period for Reinforced Concrete

As the proposed "Earthquake Load" was developed on the basis of perfectly elasto-plastic restoring force characteristics, it is difficult to apply this procedure directly to the reinforced concrete structures whose restoring force characteristics are significantly different from the above-mentioned assumption.

The restoring force characteristics of reinforced concrete structures failing primarily in flexure can be idealized into so-called degrading trilinear (D-Tri) model, shown in Fig. 5. This model was first studied by Fukada (1969). As an example a family of displacement response spectra for various yield strength is shown in Fig. 6. Cracking and yield strength are expressed in terms of seismic coefficient, and the maximum acceleration of i ground motion is normalized to 1.0 g. Yield stiffness ratio α_y is taken to 0.5. As seen here the displacement in the long period range is close to the linear response, but it increases drastically from linear response value in the short period range and for low yield strength.

A study was made by the author and others at the University of Tokyo to develop a simple and effective method to predict the trend of reinforced concrete response as shown in Fig. 6, from the linear response spectrum.

For the single-degree-of-freedom system having yield strength of k_y in terms of seismic coefficient and subjected to earthquake with maximum acceleration coefficient of k_g, nonlinear response displacement can be approximated by

$$\delta = \frac{1}{2}\{(\frac{k_e(T)}{k_y})^2 + 1\}\,\delta_y(T) \tag{8}$$

where

δ : nonlinear response displacement
$k_e(T)$: linear response shear coefficient for period T
k_y : yield shear coefficient
$\delta_y(T)$: yield displacement for period T

and the period T is selected by the following rule.

$$\begin{aligned} T &= T_e \quad \text{if} \quad k_y \geq k_{y1} \\ T &= T_{eq} \quad \text{if} \quad k_{y1} > k_y > k_{y2} \\ T &= T_y \quad \text{if} \quad k_y \leq k_{y2} \end{aligned} \tag{9}$$

where

T_e : period associated with initial (uncracked) stiffness
T_y : period associated with yield stiffness ($T_y = T_e/\sqrt{\alpha_y}$)

and

$$k_{y1} = 0.3\,(1.5 - T_e) \tag{10}$$

$$k_{y2} = 0.3\,(1.5 - T_y) \tag{11}$$

$$T_{eq} = 1.5 - k_y/0.3 \tag{12}$$

The rule of Eq. (9) is illustrated in Fig. 7. As seen here this rule specifies that elastic period T_e be used in Eq. (8) when either elastic period or yield shear coefficient is large enough, but that an equivalent period, longer than the elastic period, be used when both elastic period and yield shear coefficient are small. This equivalent period T_{eq} is determined by Eq. (12) which is upper-bounded by yield period T_y.

For the class II soil, zoning coefficient Z = 1, and for reinforced concrete D = 0.8, we have from Eq. (1)

$$V_D = \begin{cases} 163\,T \text{ cm/sec.} & (T \leq 0.5 \text{ sec.}) \\ 81.6 \text{ cm/sec.} & (T \geq 0.5 \text{ sec.}) \end{cases} \tag{13}$$

Assuming that the maximum ground acceleration associated with the response of Eq. (13) is 0.3 g, we obtain linear and nonlinear response displacement spectra for 1.0 g earthquake as shown in Fig. 8. Yield stiffness ratio α_y of 0.5 was used here. Figure 8 is directly comparable to Fig. 5. When such comparison was made for several earthquake records and for diffe ent parameters as shown in Fig. 9, it was concluded that the above-mention effective period may be used for the evaluation of D-Tri response in the r of ductility factor up to about 5.

"Earthquake Load" Adapted to Reinforced Concrete

Based on the foregoing study, following modification to the "Earthquake Load" was proposed by the Reinforced Concrete Committee of the Architectural Institute of Japan (1977). As the author's views, the modified procedure as described below will constitute the fundamental scheme of future limit state design code to be developed in Japan.

a. Calculate natural periods and participation functions of each mode based on the elastic (uncracked) stiffness.

b. Evaluate the yield stiffness ratio α_y either by calculation or guess work. Recommended is a value of 0.5.

c. Calculate the ultimate lateral capacity of each story, and obtain the yield shear coefficient from the following equation.

$$k_y = \frac{\sum_{i=1}^{n} Q_{ru}\, h_r}{\sum_{i=1}^{n} \left(W_r \sum_{j=1}^{r} h_j\right)} \qquad (14)$$

where

Q_{ru} : ultimate lateral capacity of r-th story
h_r : story height of r-th story
W_r : weight of r-th floor

Equation (14) was derived from the equation of motion in the plastic flow assuming that the mode shape was an inverted triangle.

d. Obtain the effective natural period of the first mode from Eqs. (9), (10), (11) and (12) where T_e is the elastic natural period of the first mode. If it is different from the elastic period, modify all the higher mode periods by the same ratio as that of the first mode.

e. Find the linear response shear force in each story from Eqs. (1) and (4), using the periods modified as above.

f. Find the ductility factor in each story, defined for the yield displacement from the following expressions.

If $k_y \geq k_{y1}$

$$\mu_r = \frac{\alpha_y}{2}\left\{\left(\frac{Q_{rD}}{Q_{ru}}\right)^2 + 1\right\} \qquad (Q_{rD} \geq Q_{ru})$$

$$\mu_r = \alpha_y\, Q_{rD}/Q_{ru} \qquad (Q_{rD} < Q_{ru}) \qquad (15)$$

If $k_{y1} > k_y > k_{y2}$

$$\mu_r = \left(\frac{T_{eq}}{T_1}\right)^2 \frac{\alpha_y}{2} \left\{\left(\frac{Q_{rD}}{Q_{ru}}\right)^2 + 1\right\} \qquad (16)$$

If $k_y \leq k_{y2}$

$$\mu_r = \frac{1}{2} \left\{\left(\frac{Q_{rD}}{Q_{ru}}\right)^2 + 1\right\} \qquad (17)$$

where

μ_r : ductility factor of r-th story defined for yield displacement
α_y : yield stiffness ratio
Q_{rD} : linear response shear force of r-th story
Q_{ru} : ultimate lateral capacity of r-th story
T_1 : elastic natural period of first mode
k_y, k_{y1}, k_{y2}, T_{eq} : refer to Eqs. (14), (10), (11), (12), use T_1 for T_e in Eqs. (10) and (11)

g. Calculate nonlinear response story displacement from the following equation.

$$\delta_r = \mu_r \delta_{ry} \qquad (18)$$

where

δ_r : nonlinear response story displacement of r-th story
δ_{ry} : yield story displacement of r-th story

h. Following acceptance criteria are to be used where the story slope is the principal criteria and the other two are referred to only as auxiliary criteria.

Story slope : $\delta_r / H_r \leq 1/100$ (19)

Total slope : $\sum_{r=1}^{n} \delta_r \Big/ \sum_{r=1}^{n} H_r \leq 1/120$ (20)

Ductility : $\mu_r \leq 3.5$ (21)

i. A new concept of "ductility class" is introduced. According to the calculated story slope, columns and girders belonging to each story are classified into three classes as shown in Table 4, and they must be designed for shear by appropriate methods to ensure deformability associated with each class. The detail of design methods for shear will be developed in future. There will be differences of the following items: evaluati of seismic shear force in the members, shear capacity equation, limiti values of axial compression, web reinforcement, and shear span ratio, criteria for development length, and confinement for bond splitting.

Figure 10 shows the flow diagram of design procedure proposed by the Reinforced Concrete Committee in the modification of the "Earthquake Load" Traditional design follows the left branch directly. The right branch is new addition, which is quite simple and easy for most structural engineers

It is necessary for the Committee to examine various problems in order to develop details of the design procedure, among which are the followings.

a) Define clearly the scope of application of the design flow shown in Fig. 10. In other words define more clearly the Divisions Two, Three and Four.

b) Choose appropriate design seismic coefficient (or load factor to the seismic coefficient in the Building Standard Law) to design most efficiently, avoiding the circulation shown by the dashed arrow in Fig. 10.

c) Select, or develop as needed, ultimate strength equations for flexure and shear in conjunction with the associated deformability, and determine material safety factor or member capacity reduction factor.

d) Provide effective means to calculate ultimate lateral capacity, both for hand and automatic calculations.

e) Determine permissible limits of response deformation and ductility more firmly.

References

Aoyama, H., "A Review of Recent Research in Japan as Related to the Earthquake Resistant Design of Reinforced Concrete Building Structures," to be printed, Proc. Workshop on ERCBC, Berkeley, Calif., 1977.

Architectural Institute of Japan, "Earthquake Load and Earthquake Resistance of Building Structures," 670pp, 1977.

Architectural Institute of Japan, "School Building Planning," 726pp, Dec. 1971.

Architectural Institute of Japan, "Seismic Safety Diagnosis and Strengthening of Reinforced Concrete School Buildings," 106pp, June 1975.

Fukada, Y., "Study on the Restoring Force Characteristics of Reinforced Concrete Buildings (Part 1) -- Response Computation for Degrading Stiffness Trilinear Models," Proc. Kanto Dist. Symp., Arch. Inst. Japan, No. 40, 1969.

Japan Earthquake Engineering Promotion Society, "Proc. U.S.-Japan Seminar on Earthquake Engineering with Emphasis on the Safety of School Buildings," 1971.

Japan Earthquake Engineering Promotion Society, "Proceedings of Review Meeting, U.S.-Japan Cooperative Research in Earthquake Engineering with Emphasis on the Safety of School Buildings," 1976.

Umemura, H. ed., "Dynamic Earthquake-Resistant Design of Reinforced Concrete Buildings," Giho-do Publishing Co., 442pp, Aug. 1973.

Table 1 Value of T_c and G

Soil Classification	T_c (sec)	G
Class I	0.3	1.0
Class II	0.5	1.2
Class III	0.8	1.5
Class IV	1.2	2.0

Table 2 Value of D

Construction Classification	D
Steel	1.0
RC, PC frame	0.8
RC, PC wall	0.8
SRC	0.8

Table 3 Importance Factor

Use of Buildings	I_r		Note
	Lowest story	Uppermost story	
Broadcasting Stations Hospitals	2.0	2.0	Linearly interpolate for intermediate stories
Telephone Exchanges Fire Stations	1.8	1.5	
Government Buildings School Buildings	1.6	1.3	
Others	1.3	1.0	

Table 4 Ductility Class

Calculated Story Slope R	Ductility Class
$1/150 \leq R < 1/100$	I
$1/200 \leq R < 1/150$	II
$R < 1/200$	III

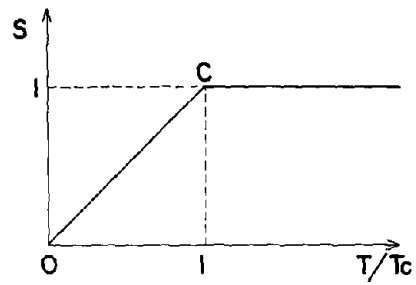

Fig. 1 S vs T/T_c

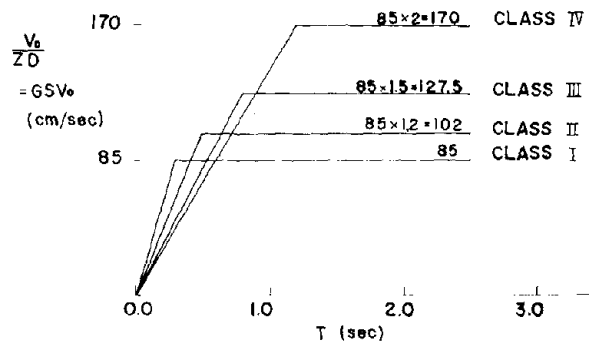

Fig. 2 Velocity Spectra

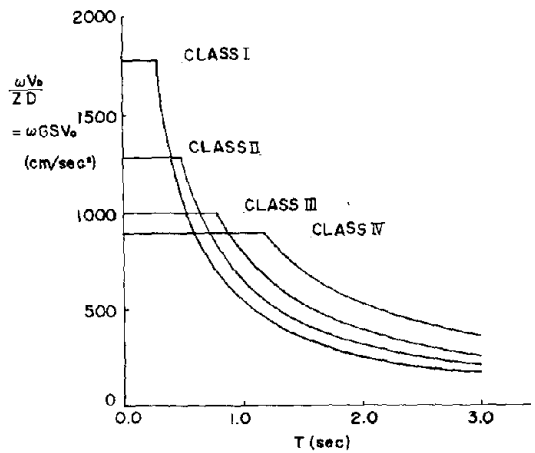

Acceleration Spectra

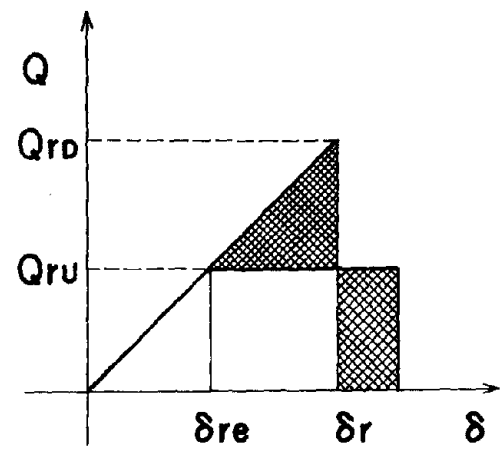

Fig. 4 Linear and Nonlinear Systems

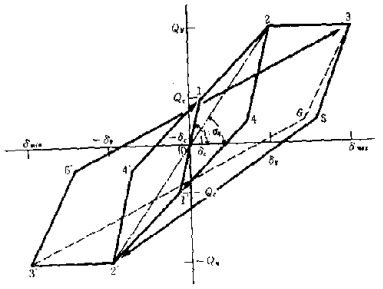

Fig. 5 Degrading Trilinear Model

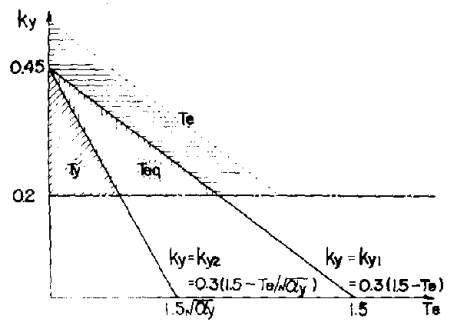

Fig. 7 Rule for D-Tri Response Evaluation

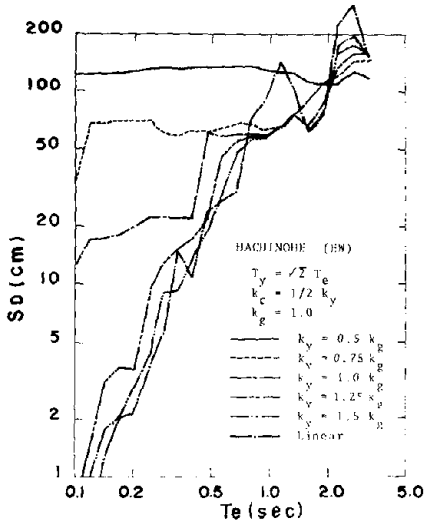

Tri Response to Hachinohe
cord of Tokachioki Earthquake

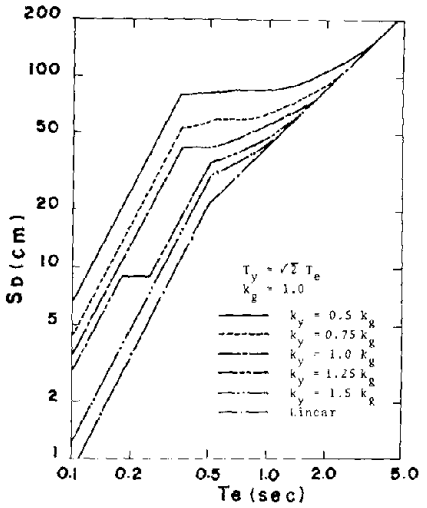

Fig. 8 Estimated D-Tri Response

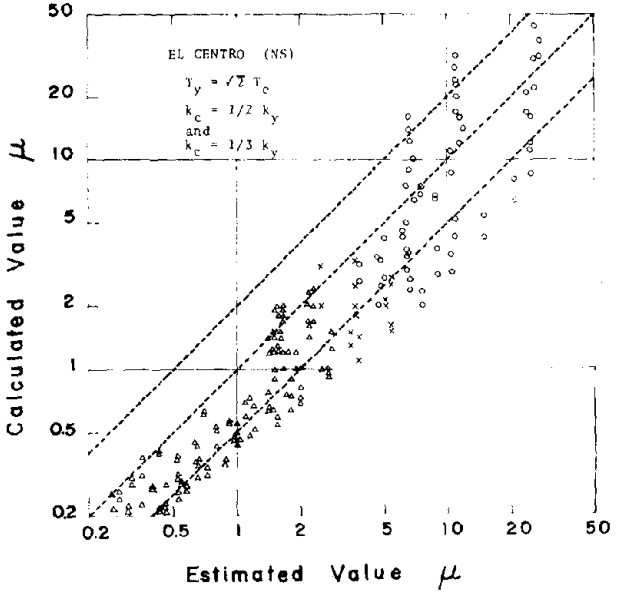

(a) El Centro - 1940

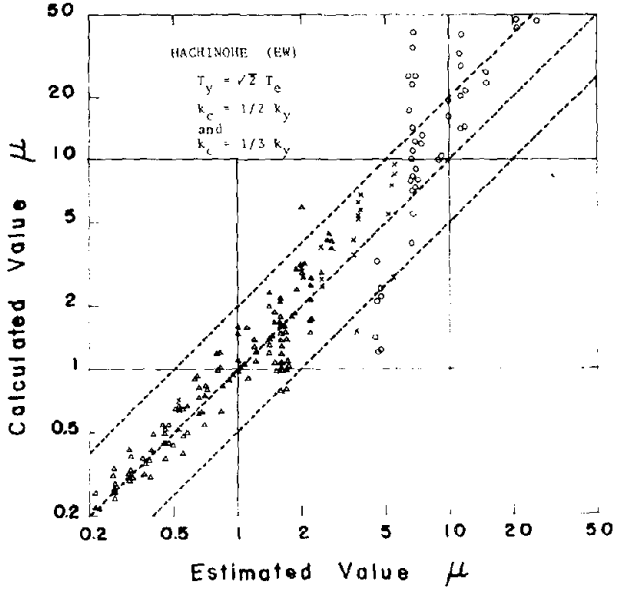

(b) Hachinohe - 1968

Fig. 9 Comparison of Calculated vs Estimated Values

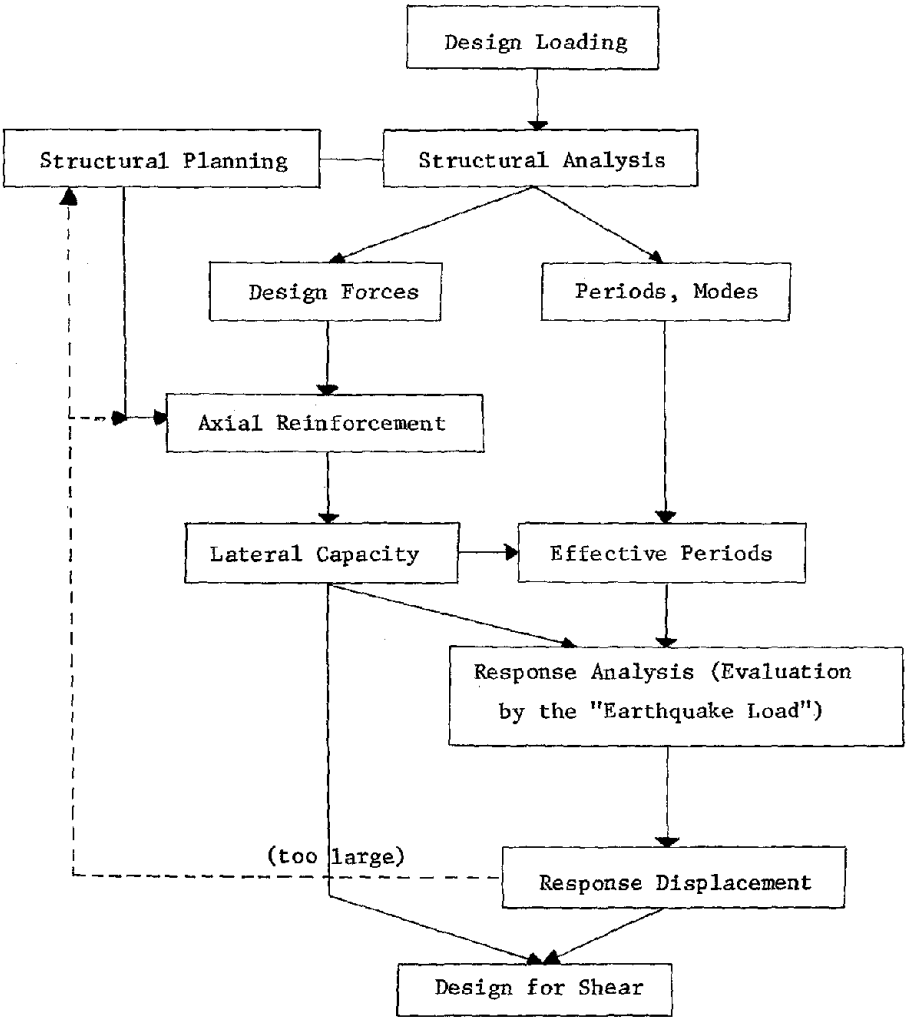

Fig. 10 Flow Chart for Earthquake Resistant Design

SEISMIC DESIGN OF MASONRY STRUCTURES

M.J.N. Priestley

Senior Lecturer, Department of Civil Engineering, University of Canterbury, Christchurch, New Zealand.

SYNOPSIS

The current status of the seismic design of masonry structures is reviewed. It is noted that many codes of practice require elastic design for masonry, but specify seismic lateral load levels which imply significant post-yield ductility. It is recommended that a rational design approach accepting and designing for ductility be adopted. Recent experimental work on cyclic testing of masonry units is reviewed, and limits to available ductility are proposed. Different masonry structural systems including cantilever shear walls, perforated walls, and masonry in-filled frames are discussed and evaluated. The feasibility of base-isolation to reduce seismic forces in masonry structures is briefly discussed.

INTRODUCTION

Despite inroads made by more recent construction materials and methods, masonry construction is still widely used throughout the world, including areas of high seismic risk. In under-developed countries, masonry structures tend to be constructed by traditional methods without regard for lateral inertia forces. Because of the weight and inherent weakness of unreinforced masonry, collapse under seismic loading is common, often with a heavy toll on human life. Even in developed areas where codified seismic design requirements have forced changes in construction form to provide lateral-load resistance, performance of masonry structures under recent earthquakes has frequently been poor.

Common failure modes of reinforced masonry in recent earthquakes noted by Glogau (1974) include:

(a) toe failure of walls due to the combined action of flexural compression and shear,

(b) modification of seismic forces resulting from the stiffening effects of supposedly non-structural partitions and in-fill panels,

(c) diagonal shear failures due to high shear loads and inadequate shear reinforcement,

(d) vertical shear failures in stack-bonded walls.

These common forms of failure are the result of faulty detailing, and demonstrate a lack of understanding of the nature of seismic response of ma structures rather than a fundamental weakness of masonry as a construction material for seismically active regions. Masonry structures of substantial can be designed to perform adequately under major earthquakes provided care design and detailing requirements are followed.

This paper briefly examines the design requirements for adequate seismic response of masonry buildings and discusses the influence of differences between various masonry structural systems on seismic response. The discussion is limited to reinforced masonry. Except where local seismicity is very low, unreinforced masonry should not be considered for construction of other than minor structures, unless calculations indicate that the peak elastic response to the design earthquake accelerations can be safely supported.

MATERIALS

MASONRY UNITS

Reinforced Masonry is a composite of four materials: masonry unit, mortar, grout and reinforcement. The masonry unit may be of many different material types:- shale, clay, slate, stone and concrete. Only clay brick and concrete, the two most common materials for reinforced masonry will be considered in this paper. Both materials have high compression strength (up to 35 MPa (5000 psi) and 70 MPa (10,000 psi) for concrete and clay brick respectively), and low tensile strengths. Where design is based on ductile response, as discussed below, it is recommended that minimum acceptable crushing strengths of 17.5 MPa (2500 psi) and 27.5 MPa (4000 psi) be specified for concrete and clay brick units respectively.

MORTAR

A reasonably high strength mortar is required to ensure adequate crushing strength and general competence of masonry construction. Current New Zealand practice (S.A.N.Z. 1974) requires a minimum mortar crushing strength of 12.5 MPa (1800 psi).

GROUT

Adequate grout strength is necessary to provide bond transfer between reinforcement and masonry, and also has significance to the masonry compression capacity. Although it is difficult to predict grout strength in-the-wall on the basis of crushing tests on grout cylinders formed in steel moulds, it is generally felt that a minimum strength of 17.5 MPa (2500 psi) should be specified.

REINFORCEMENT

Steel of normal or high strength grades may be used to carry the tension forces associated with flexure and shear. However, for flexural reinforcement the yield plateau should be as long as possible to reduce the effects of moment overcapacity, resulting from strain hardening, discussed further below.

COMPRESSION FAILURE OF WALLS AND PRISMS

When a vertical masonry prism consisting of several courses of masonr and mortar is loaded in axial compression, failure is generally initiated vertical splitting of the strong masonry unit rather than by crushing of t weaker mortar. The crushing strength of the prism f'_m is higher than th mortar crushing strength, but lower than the unit material strength. Walls in axial or flexural compression exhibit similar vertical splitting in the crushing zones. As this has a profound effect on the integrity and subseq performance when ductile response is required, an examination of the failu mechanism is warranted.

Hilsdorf (1967) has explained this behaviour as being a consequence of the lower modulus of elasticity and crushing strength of the mortar, and of the rapid increase in the mortar Poisson's ratio as the crushing stress is approached (see Fig. 1a). Restraint of the mortar lateral expansions resulting from these factors by the stiffer masonry unit induces lateral compression in the mortar and lateral tension in the clay brick or concrete unit. Since the mortar is effectively in triaxial compression, the prism crushing strength exceeds that of the unconfined mortar, and failure is initiated when the biaxial tension strength of the unit is exceeded, resulting in vertical cracking initiating close to the mortar bed (Fig. 1c). Failure may occur immediately in an explosive manner due to the sudden reduction in lateral confinement of the mortar, or more commonly, in a gradual fashion as more vertical cracks form.

MASONRY STRUCTURAL SYSTEMS

Four common forms of masonry construction are illustrated in Fig. 2. Reinforced Grouted Masonry (Fig. 2a) and Reinforced Hollow Unit Masonry (Fig. 2b) are both independent systems capable of providing the full vertical and lateral load resistance requirements for multistorey buildings, generally in the form of shear walls, whereas the masonry in Infill-panel (Fig. 2c) and Veneer wall construction (Fig. 2d), is complimentary to the main structural framework.

Reinforced Grouted Masonry (RGM) consists of two skins, or wythes of clay brick or concrete block, normally solid, separated by a cavity in which the vertical and horizontal reinforcement is placed, and which is grouted as the wythes are built. Wythes are normally 50 - 100 mm (2 - 4 in) thick and the grout gap 60 - 100 mm ($2\frac{1}{2}$ - 4 in) wide.

Reinforced Hollow Unit Masonry (RHUM) is constructed from concrete or clay brick units with internal vertical voids or cells, some or all of which will contain vertical reinforcement, and will be grouted. Horizontal reinforcement is placed in courses consisting of special bond - beam units containing depressed webs, as shown in Fig. 2b. Size and design of the units varies considerably and widths from 100 - 300 mm (4 - 12 in) are common.

Masonry infill may be of solid, perforated or reinforceable units, forming panels within reinforced concrete or structural steel frames. A variation of this form of construction common in Latin America consists of peripheral reinforced masonry columns and bond - beam elements with unreinforced masonry infill. Whether or not the panels are isolated from the structural frame, masonry infill has traditionally been neglected in assessing the seismic performance. As discussed later, this is not necessarily a conservative approach.

Masonry veneers, generally unreinforced, are frequently connected to structural backings of timber or reinforced masonry, and are generally requi only to support their own weight, and lateral face-loads from wind and inert forces.

QUALITY OF CONSTRUCTION

The recommendations discussed below are all based on the assumption of competent level of workmanship resulting in a good quality of construction. is the writer's experience that these criteria are less often obtained with masonry than (say) reinforced concrete construction. Mortar droppings in th grout cavities are often not cleaned out, segregation of grout, and inadequa

vibration may result in poor quality construction, and the level of supervision is often less than exacting. In New Zealand there is a deleterious tendency for designers to be prepared to accept a standard of masonry construction lower than that they would require for other materials. This is an unfortunate circumstance which they must change if sound masonry construction is to result.

DESIGN FORCES FOR MASONRY BUILDINGS

ELASTIC FORCE LEVELS

Many design codes require elastic design for masonry structures under seismic loading. It may be assumed that this is largely due to a lack of confidence in the ultimate load characteristics of masonry, but it is also at least partly because masonry codes have not reflected the tendency for change from elastic to ultimate strength design adopted by other material codes. Although elastic design generally results in conservative structures, this is not necessarily the case when seismic loading is considered. As will be seen from the composite response spectra of Fig. 3a (Skinner, 1964), elastic response of masonry structures to earthquakes of El Centro magnitude will be high because of the low natural periods resulting from the stiff structural forms adopted. Assuming 5% equivalent viscous damping, peak elastic response of the order of 0.8 g can be anticipated.

Seismic coefficients included in most loadings codes are based on ductile response, with structure ductility in the vicinity of four. Reference to Fig. 3b shows that elastic design to these load levels will still result in the ultimate capacity being attained, but with a reduction in the required structure ductility. In fact, the 'equal displacement' principle, on which Fig. 3b is based, underestimates the peak lateral displacement of low period structures, so the required structure ductility for a structure designed elastically to code levels of lateral load will exceed Δ_u/Δ'_y, the value predicted by the approach in Fig. 3b.

DUCTILITY OF MASONRY ELEMENTS

Since these arguments indicate that elastic response of masonry buildings can only be obtained if uneconomically high lateral force coefficients are adopted, it is felt that a more satisfactory philosophy is to recognise that inelastic deformations will occur under severe seismic attack, and to design accordingly.

Recent research has shown that carefully designed masonry walls of various different forms of construction possess reasonable ductility in the flexural failure mode. Fig. 4 shows load - deflection curves for a reinforced grouted clay brick masonry wall with moderate maximum shear force, and a reinforced hollow unit concrete masonry wall of higher shear capacity (Priestley and Bridgeman, 1974, Priestley, 1977). For these walls, cycling at displaceme ductility factors less than 4 resulted in reduction in peak loads from the maxima (which exceeded or were close to the theoretical ultimate load pred the basis of measured material properties) to stable values at about 80 - 9 the ultimate capacity, with a narrowing, or pinching of the hysteresis loc Displacement ductility factor is defined here as the ratio of maximum disp to displacement found from extrapolation of the post-cracking elastic load deflection curve to the theoretical ultimate load. The stiffness degradat apparent in Fig. 4 and other similar tests was invariably found to be the of sliding of the entire wall along the base-course. The extent of base-c sliding increased with increasing ductility factors and the hysteresis loc resemble the degrading stiffness model described by Clough (1966).

Similar ductile behaviour has been reported by Meli (1974) for walls constructed from masonry peripheral frames with unreinforced masonry infill, though the reliable level of ductility was somewhat lower than attained in the walls of Fig. 4. Klingner and Bertero (1977) report high displacement ductility factors for reinforced concrete frames with heavily reinforced masonry infill panels.

DESIGN LEVEL OF LATERAL LOAD

The tests reported above indicate that masonry can be designed to perform in a ductile manner under seismic loading, but that the extent of ductility is somewhat lower than could be expected from comparable reinforced concrete elements. The level of design seismic loading for masonry should reflect this point. The New Zealand Loadings Code (S.A.N.Z. 1976) requires incorporation of a masonry materials factor $M = 1.2$ in calculating the required force level. Coupled with other factors reflecting variation of response with natural period, zone, and structural type, this can result in seismic design coefficients as high as 0.288 g. Dynamic analysis of short period structures designed to this level of load using a degrading stiffness hysteresis characteristic resulted in ductilities of less than 4 under El Centro 1940 N-S excitation. In terms of the available ductility discussed in the previous section, this is felt to represent satisfactory behaviour for New Zealand conditions.

DESIGN OF MASONRY SHEAR WALLS

STRUCTURAL FORM

This section considers lateral load design aspects of walls constructed of the RGM and RHUM systems described in Fig. 2a and 2b.

One of the prime considerations of satisfactory masonry design for seismic loads is structural simplicity. For this reason the two cantilever shear wall structures shown in Fig. 5 are considered more suitable for ductile response than the examples of shear walls with large openings in Fig. 6. The structures in Fig. 5 consist of a number of cantilever shear walls linked by flexible floor slabs. Analysis of such structures under lateral load is simple, as each wall can be considered to carry that fraction of the total lateral load in proportion to its relative stiffness. The flexibility of the floor slabs ensures that vertical shear transfer between the cantilever walls is negligible.

When the shear walls contain openings of sufficient size to destroy the basic cantilever action, behaviour is more complex. In Fig. 6a, characterised by deep, stiff spandrels and comparatively slender piers, behaviour is similar to shear frames, with ductility resulting from flexural plastic hinging or shear failure of the piers. For this type of system it is virtually impossible to avoid concentration of plastic hinging in the piers of one storey, generally the with consequential extremely high ductility demand at that level. As with reinforced concrete frames, use of columns or piers as energy dissipating e is highly desirable for structures more than two storeys in height.

Fig. 6b shows a system where spandrels are weaker than the piers, resu in coupled shear wall characteristics. Under seismic loading, very high du is required of the spandrels, and it is probable that under inelastic cycli capacity of the masonry spandrels, which cannot be effectively detailed for ductility, would rapidly degrade to a fraction of the initial value. The coupled shear wall behaviour would degrade to linked shear wall behaviour w increased base bending moment as illustrated in Fig. 6c. Alternatively, fo

given base moment capacity, ductility required from the base plastic hinges will be greater than anticipated, and failure could result. Under these circumstances it is best not to rely on the spandrels as part of the energy dissipating mechanism.

FLEXURAL CAPACITY

The results of a wide range of test programmes show that the flexural strength of masonry shear walls is conservatively predicted by reinforced concrete ultimate strength theory. Despite these results there is a common misconception that it is more 'efficient' to concentrate the reinforcement close to the ends of the wall. Examination of the two alternative steel distributions illustrated in Fig. 7 will show that for the typically low steel percentages, and low axial loads common in masonry buildings designed for seismic loading, the ultimate flexural capacity is insensitive to the steel distributions. For uniformly distributed steel, the small neutral axis depth will ensure tensile yield of virtually all vertical reinforcement, resulting in an ultimate capacity of

$$M_u \simeq A_{st}.f_y.\frac{d}{2} + N_u.\frac{d}{2} \qquad (1)$$

where A_{st} is the total area of vertical steel distributed along the wall, and the other variables are defined in Fig. 7. For reinforcement concentrated near the ends of the wall, the tension force, at $\frac{1}{2}A_{st}.f_y$ is approximately half that for the distributed case, but at roughly twice the lever arm, so the flexural capacity remains unaltered.

In fact, there are good reasons for even distribution of the flexural steel along the wall. Distributed steel will result in a higher masonry compression force, and therefore more efficient compression shear transfer, and provides a clamping force along the wall base joint, which is an area of potential sliding. Concentration of steel close to the wall ends results in high bond stresses on the limited grout area, and due to vertical cracking in the crushing zone, lateral stability provided by the blockwork will often be inadequate to prevent the compression steel from buckling.

Cardenas et al (1973) have shown that the ultimate flexural capacity of a rectangular wall length l_w containing uniform distributed vertical reinforcement of total area A_{st}, and subjected to axial force N_u can be approximated by

$$M_u = 0.5 A_{st}.f_y.l_w \left(1 + \frac{N_u}{A_{st}.f_y}\right)\left(1 - \frac{c}{l_w}\right) \qquad (2)$$

where c is the distance from the neutral axis at ultimate to the extreme compression fibre.

Because of the typically high steel strains at ultimate (see Fig. 7), hardening of some of the tensile steel may commence before the ultimate cr strain of the masonry is reached. The extent of strain hardening will dep largely on the length of the yield plateau of the steel stress-strain curv For f_y = 414 MPa steel (HY60) the length of the yield plateau may be as lo 4 x yield strain, and the steel stress at ultimate flexural capacity may substantially exceed f_y, increasing the ultimate flexural capacity above predicted by eqn. 2. This behaviour is clearly evident in Fig. 4b, where theoretical ultimate load P_u based on measured steel yield stress, is ex by a substantial margin on several cycles.

DEGRADATION OF FLEXURAL CAPACITY UNDER CYCLIC LOADING

Under cyclic loading at high ductilities, the flexural capacity of masonry shear walls degrades as a result of collapse of the toe and heel of the wall (Priestley and Bridgeman, 1974). This behaviour is related to the compression failure mechanism described in Fig. 1. During an initial inelastic cycle, vertical cracks form in the crushing zone. These reduce the stability of the compression zone under the combined action of compression and shear, and the fractured zone may be 'blown-out'. Under reversal of the loading direction, steel at the wall end that was formerly in compression is now subjected to tensile yield with residual strains and wide open cracks remaining on the removal of the load. On the next load reversal, this steel must now be yielded in compression before the cracks can close and compression be transmitted through the masonry. The fractured state of the compression area may now result in insufficient lateral restraint to prevent the compression steel buckling, again resulting in collapse of the compression zone. As noted above, this behaviour is exacerbated by concentrating the flexural steel at the wall ends. To avoid this degradation it is advisable to limit ductility requirements by the specification of higher seismic coefficients for masonry, as mentioned above. An alternative to higher coefficients has been suggested by Priestley and Bridgeman (1974) who showed that collapse of the compression zone could be eliminated if 3 mm ($\frac{1}{8}$ in.) stainless steel confining plates were placed in the mortar beds of potential crushing zones of the wall. These resist the lateral mortar expansions and therefore reduce the biaxial tension stress in the masonry units, inhibiting vertical cracking. The plates are shaped to the outline of the walls for the required length, with an allowance for pointing, and have holes corresponding to the size of the grout cavities. A secondary benefit from the plates is increased lateral restraint against compression bar buckling. Mayes et al (1972) have also reported improved behaviour of masonry piers that incorporated similar confining plates.

SHEAR CAPACITY

Design Shear Force-- Masonry walls failing in shear have very limited ductility. The failure mechanism generally involves the formation of a wide diagonal crack with rapid reduction in lateral load capacity. Consequently it is necessary to provide sufficient shear strength to exceed the flexural strength, using a capacity design approach. Thus the required design shear force V_D will be substantially higher than the code specified base shear V_B, on which the flexural capacity will be based. To provide adequate protection against a shear failure it is necessary that

$$V_D = \frac{\phi_o}{\phi_f} . V_B \qquad (3)$$

where ϕ_f = flexural undercapacity factor (typically 0.7 for masonry)
and ϕ_o = flexural overcapacity factor.

ϕ_o represents the ratio of maximum feasible flexural strength to ideal flexu strength based on nominal material strengths, and includes the effects of ste yield exceeding the specified minimum value, and the likely occurrence of str hardening due to the high steel strains. Commonly accepted values of ϕ_o (P and Paulay, 1975) are ϕ_o = 1.25 for f_y = 275 MPa (40,000 psi) and ϕ_o = 1.4 f_y = 414 MPa (60,000 psi).

Consequently $V_D \doteqdot \frac{1.25}{0.7} V_B = 1.78V_B$ for $f_y = 275$ MPa (4a)

$V_D \doteqdot \frac{1.4}{0.7} V_B = 2.0 V_B$ for $f_y = 414$ MPa (4b)

Shear Reinforcement-- For walls designed for ductile response, the entire shear load should be carried by shear reinforcement. With reversed cyclic loading, flexural cracks may be open for the full wall length until sufficient moment is supplied to yield the compression steel and close the crack at the compression end. Vertical splitting of the compression zone will reduce the compression shear capacity. Shrinkage cracks, poor mortar bond at header joints, and high variability of workmanship common in masonry construction make the shear capacity of masonry unreinforced for shear highly unreliable.

Vertical steel crossing a potential diagonal shear crack (Fig. 8a) has to transfer the shear load by dowel action, and thus is very much less efficient than horizontal steel, which resists the shear force by direct tension. Priestley and Bridgeman (1974) have shown that under optimum conditions the force carried by dowel action will be about 30% of that carried by the same steel deployed horizontally. Since dowel capacity reduces as the crack width increases, horizontal steel properly anchored at the wall ends by bending vertically or hooking round the extreme vertical bars should be used to carry the entire shear force. The total area of shear steel crossing each potential 45° crack should be

$$A_v = \frac{V_D}{\phi_s \cdot f_y} \quad (5)$$

where ϕ_s = shear capacity reduction factor (typically $\phi_s = 0.85$)

Recent research (Priestley and Bridgeman (1974), Priestley (1977)) has indicated that RGM and RHUM walls designed to these criteria can develop ductile flexural failure modes at shear stresses as high as 2.6 MPa (380 psi) based on the gross cross-section area. However, severe degradation due to sliding shear along the base construction joint will generally occur at shear stresses well below those capable of being sustained by masonry shear walls. As noted above the extent of structural degradation from this cause increases with increasing ductility factor, and on the basis of test results (Priestley, 1977) it is conservatively recommended that the ultimate design shear be limited according to the relationship

$$v_u < 1.2 + 0.8(\frac{4}{D} - 1) \text{ MPa but } \not> 2.0 \text{ MPa} \quad (6)$$

$$(175 + 115(\frac{4}{D} - 1) \text{ psi but } \not> 290 \text{ psi}$$

where D = design ductility factor.

Assuming an inverse relationship between D and dependable flexural stren and a code requirement for flexural strength based on a ductility factor o eqn. 6 may be rewritten

$$v_u < 1.2 + 0.8 (R - 1) \text{ MPa but } \not> 2.0 \text{ MPa}$$

$$(175 + 115 (R - 1) \text{ MPa but } \not> 290 \text{ psi.}$$

where R is the ratio of flexural strength provided to flexural strength ed by code. These values are significantly higher than allowed by most cu

masonry design codes (eg. SANZ (1974), ACI (1970)). It is believed that codified masonry shear stresses may have been based on earlier research by Schneider (1959) and Scrivener (1967) into the shear strength of panels which contained insufficient shear steel to carry the full shear load.

MASONRY INFILLED FRAMES

Masonry infill, unless carefully designed, can result in unsatisfactory seismic performance from otherwise well designed frames. There are numerous examples of earthquake damage that can be traced to structural modification of the basic frame behaviour by so-called non-structural masonry partitions and infill panels.

Incorporation of masonry infill results in a decrease in fundamental period and an increase in seismic shears, frequently resulting in shear failure of the frame columns. Brittle failure of unreinforced infill has resulted in shedding of masonry into streets below, or into stairwells, with great hazard to life. If the designer wishes to ignore interaction between frame and infill and rely on normal frame action for seismic resistance, then the infill panel must be structurally separated on the sides and top to allow free deformation of the frame relative to the panel. The separation must be adequate to allow the required interstorey frame drift to develop, and connection between the panel top and frame must be sufficiently flexible to avoid development of significant force in the panel. Even with these precautions, the panel may provide a substantial stiffening effect to the beam supporting the panel, inhibiting the formation of a beam-plastic hinge mechanism and forcing energy dissipation into column members. Newmark and Rosenblueth (1971) review different methods of isolating panels from frame deformations.

The alternative to separation is to recognise the structural action of the infill, and design accordingly for composite frame/panel action. Although initial behaviour at low loads may be analysed using beam theory, at higher loads separation between frame and panel occurs due to differences between flexural deformations of the frame and shear deformation of the panel (see Fig. 9a). After separation occurs, the panel acts as a diagonal strut with an effective width, w, less than that of the full panel. Stafford-Smith and Carter (1969) have developed expressions for the effective width, w , in terms of relative stiffness of frame and panel, the stress-strain curves of the materials, and the load level. For lateral stiffness and natural period calculations, a conservatively high value of

$$w = 0.25\,d \qquad (8)$$

may be adopted. This gives reasonable agreement with Stafford-Smith and Carters results for typical masonry infill properties.

FAILURE MECHANISMS OF MASONRY INFILLED FRAMES

There are several different possible failure modes for masonry infilled frames, including

(1) tension failure of the tension column resulting from applied moment: This will generally only occur with frames of high aspect ratio and high she strength

(2) diagonal tensile cracking of the panel. This does not generally onstitute a failure condition, as higher lateral loads can be supported unt

(3) compression failure of the diagonal strut

(4) sliding shear failure of the masonry along horizontal mortar courses (generally at or close to panel midheight)

(5) flexural or shear failure of the columns.

Typically column failure represents the final stage of a failure sequence, preceded by either a diagonal compression failure or a sliding shear failure.

Sliding Shear-- The sliding shear failure has been described by Fiorato et al (1970) and involves a basic change in structural mechanism from the braced frame shown in Figs. 9a and 9b to the knee-braced frame of Fig. 9c. Support provided by the masonry panel forces column hinges to form at approximately midheight and top or bottom of the columns. If column shear capacity is based on formation of yield moments at top and bottom of the column, as for frame action, the increase in shear force due to the reduced distance between hinges in the knee-braced frame mechanism (Fig. 9c) may result in a shear failure.

Lateral capacity of the knee-braced frame mechanism can be conservatively estimated as

$$V_u = \frac{2}{h_e} (Mu_c + M_{ut}) \qquad (9)$$

ignoring the frictional resistance to sliding shear in the panel, which degrades rapidly on cycling. In eqn. (9) Mu_c and Mu_t are the ultimate moment capacities of the compression and tension columns respectively, including effects of axial forces resulting from gravity loads and overturning moments.

Compression Failure of Diagonal Strut-- Trigo (1968) found that the following modified form of the diagonal compression failure force predicted by Stafford-Smith and Carter gave a conservative agreement with test results

$$R_c = \frac{2}{3} \alpha . t . f'_m \sec \theta \qquad (10)$$

where f'_m = masonry prism strength, t = panel thickness and α defines the contact length between panel and column (Fig. 9a), given by

$$\alpha = \frac{\pi}{2} \sqrt[4]{\frac{4E_f I_f h_m}{E_m t \sin 2\theta}} \qquad (11)$$

where E_f and I_f are the modulus of elasticity and moment of inertia of the frame columns, E_m and h_m are modulus of elasticity and height of infill, and θ is the angle between the diagonal strut and the horizontal. On inelastic cycling the behaviour of the diagonal strut will degrade and behaviour will approximate the knee-braced frame of Fig. 9c.

DUCTILITY OF MASONRY INFILLED FRAMES

Most of the possible failure modes for infilled frames listed above
to the knee-braced frame mechanism, which will generally involve energy dissipation by column hinging in the bottom storey. To provide the requi
total structure ductility, the level of ductility required of the hinging storey' will be very large for frames more than a few storeys high. Cons
the design level of structure ductility must be reduced with increasing n
storey heights, and in accordance with the 'equal-displacement' principle the level of design lateral load increased proportionately. For infilled higher than about 5 storeys this will generally mean design for elastic r

unless well detailed and distributed horizontal and vertical reinforcement is placed in the infill panels, spliced to dowel starters in the frame columns and beams (Klingner and Bertero 1977).

VENEERS

Masonry veneers, properly isolated from the in-plane deformation of the structural backing by flexible connections, need only be designed for the seismic inertia forces of their own mass. However, it must be remembered that excitation of the veneer in multistorey buildings will be provided by the response accelerations of the building, rather than directly by the earthquake ground motion. If the natural frequency of the veneer and backing is close to a natural frequency of the building, resonant excitation can result in high response accelerations. This will particularly be the case for upper floors, where building response accelerations will be a maximum.

Recent dynamic tests in New Zealand (Thorby and Bridgeman, 1977) on unreinforced clay brick masonry veneers connected with approved veneer ties to timber backing (Fig. 2d) have indicated that response accelerations as high as 1.0 x g can be safely sustained, with only minor cracking of the veneer. In cases where high veneer accelerations are predicted, it is advisable to use reinforced veneers to avoid the possibility of masonry shedding into streets below.

SEISMIC BASE ISOLATION OF MASONRY STRUCTURES

It has been noted that masonry structures should be designed for comparatively high seismic lateral loads because of the limited available ductility. To protect against shear failure, a capacity design approach is necessary, resulting in high seismic design shears.

An alternative approach that shows some merit is to provide a degree of structural isolation from earthquake attack by separating the building from its foundations with mechanical energy dissipators, as shown in Fig. 10a. Skinner and McVerry (1975) describe different hysteretic energy dissipators using torsional or flexural yield of notch-ductile steel, or plastic deformation of lead. Fig. 10b shows a typical detail incorporating elastomeric bridge bearings to support the vertical loads, and two vertical steel cantilevers connected by a sliding sleeve providing lateral load resistance. The cantilevers are tapered to spread plasticity.

The yield strength of the energy dissipators is designed to exceed the maximum base shear likely to occur in a major wind storm. Typically a value of 5% of building weight is appropriate. Under seismic attack, energy dissipation is provided by plastic deformation of the devices, and the masonry structur above can be designed for elastic response. Priestley, Crosbie and Carr (19 have shown on the basis of dynamic inelastic analyses that the maximum momen and shears developed in the isolated building depend on the lateral stiffnes of the elastomeric bearings and the influence of higher modes of vibration o supported structure, as well as the yield level of the devices and the earth characteristics. For low period structures substantial reductions in peak moments were obtained for buildings designed to the New Zealand Loadings Cod (SANZ, 1976), but the advantage decreased as period increased, as illustrate Fig. 11, largely due to the increasing significance of higher mode response.

Since elastic response is assured by properly designed base-isolation devices, a capacity design approach for shear is not necessary, and substant savings result. Non-structural damage should be reduced due to lower respo

accelerations and reduced inter-storey drift. After a major earthquake an isolated building should still be able to function normally as damage is confined to the replaceable energy dissipators

CONCLUSIONS

Masonry buildings can, and should be, designed for ductile response to seismic excitation. The alternative of elastic response will generally mean design to uneconomically high levels of lateral load.

Structural masonry elements should be kept simple to ensure energy dissipation occurs in regions that are capable of providing the necessary ductility. Simple vertical load-bearing cantilever shear walls linked to flexible floor slabs are considered preferable to shear walls containing large openings.

Inelastic response of masonry infill construction will generally result in the formation of a soft-storey, with high member ductilities required of lower floor columns. Higher levels of lateral design load are required for this form of construction to reduce required member ductility to an acceptable value.

Significant reduction in design moments and shears, and elimination of structural damage are potential advantages resulting from isolation of low period masonry structures by hysteretic energy dissipators. The devices are less effective for higher period structures.

ACKNOWLEDGEMENTS

Some of the figures in this paper have been submitted to Pentech Press Ltd for incorporation in a chapter on masonry in a book entitled "Design of Earthquake Resistant Structures", Edited by E. Rosenblueth.

REFERENCES

ACI Committee 531, 'Concrete Masonry Structures - Design and Construction', Journal American Concrete Institute, Vol. 67, No. 6, pp 442-460, June 1970.

CARDENAS, A.E. et al, 'Design Provisions for Shear Walls', Jour. A.C.I. Vol. 70, No. 3, pp 221-230, March 1973.

CLOUGH, R.W., 'Effect of Stiffness Degradation on Earthquake Ductility Requirements Univ. of Cal. Struct. Eng. Lab. Report No. 66-16, 66pp. Oct. 1966.

FIORATO, A.E., SOZEN, M.A. and GAMBLE, W.L., 'An Investigation of the Interaction of Reinforced Concrete Frames with Masonry Filler Walls", Struct. Res. Series No. 370. U. of Ill., Nov. 1970.

GLOGAU, O.A., 'Masonry Performance in Earthquakes', Bulletin of the N.Z. for Earthquake Eng., Vol. 7, No. 4, pp 149-166, Dec. 1974.

HILSDORF, H.K., 'Investigation into the Failure Mechanism of Brick Masonr in Axial Compression', Proc. Int. Conf. on Masonry Structural Systems, U. 1967, published as 'Designing, Engineering and Constructing with Masonry Johnson, F.B. Editor, Gulf Pub. Co. Houston 1969.

KLINGNER, R.E. and BERTERO, V.V., 'Infilled Frames in Aseismic Constructi Sixth World Conf. on Earthquake Eng., New Delhi, Jan. 1977.

MAYES, R.L., OMOTE, Y. and CLOUGH, R.W., 'Cyclic Shear Tests on Masonry Piers', Proc. Sixth World Conf. on Earthquake Eng. New Delhi, Jan. 1977.

MELI, R., 'Behaviour of Masonry Walls under Lateral Loads', Proc. Fifth World Conf. on Earthquake Eng., pp 853-862, Rome 1974.

NEWMARK, N.M. and ROSENBLUETH, E., 'Fundamentals of Earthquake Engineering', Prentice-Hall Inc., Englewood Cliffs, N.J. (1971).

PARK, R. and PAULAY, T., 'Reinforced Concrete Structures', John Wiley & Sons, New York, 1975.

PRIESTLEY, M.J.N., 'Seismic Resistance of Reinforced Concrete Masonry Shear Walls with High Steel Percentages', Bull. N.Z. Nat. Soc. for Earthquake Eng. Vol. 10, No. 1, pp 1-16, March 1977.

PRIESTLEY, M.J.N. and BRIDGEMAN, D.O., 'Seismic Resistance of Brick Masonry Walls', Bull. N.Z. Nat. Soc. for Earthquake Eng. Vol. 7, No. 4, pp 167-187, Dec. 1974.

PRIESTLEY, M.J.N., CROSBIE, R.L. and CARR, A.J., 'Seismic Forces for Base Isolated Masonry Structures', Bull. N.Z. Nat. Soc. for Earthquake Eng. Vol. 10, No. 2, June 1977.

STANDARDS ASS. OF NEW ZEALAND (SANZ), 'General Structural Design and Design Loadings for Buildings', NZS 4203:1976.

SANZ, 'Masonry Design and Construction', Draft Code, DZ4210 (1974).

SCHNEIDER, R.R., 'Lateral Load Tests on Reinforced Grouted Masonry Shear Walls', Univ. of Sth. Calif. Eng. Centre Report 70-101, Sept. 1959.

SCRIVENER, J.C., 'Static Racking Tests on Concrete Masonry Walls', Proc. Int.Conf. on Masonry Structural Systems, Uni. of Texas, pp 185-191, 1967.

SKINNER, R.I., 'Earthquake-Generated Forces and Movements in Tall Buildings', N.Z. Dept. of Scientific and Industrial Res. Bull. No. 166, 1964.

SKINNER, R.I. and McVERRY, G.H., 'Base Isolation for Increased Earthquake Resistance of Buildings', Bull. N.Z. Soc. for Earthquake Eng. Vol. 8, No. 2, pp 93-101, June 1975.

STAFFORD-SMITH, B. and CARTER, C., 'A Method of Analysis for Infilled Frames', Proc. I.C.E. Vol. 44, pp 31-48, Sept. 1969.

THORBY, P. and BRIDGEMAN, D.O., 'Behaviour of Seven Brick Masonry Veneer Pa Under Simulated Earthquake Loading', Unpub. report D43, N.Z. PACRA, Aug. 19

TRIGO, J.d'A., 'Estructuras de Paineis sob a Accão de Solicitacoes Horizont Laboratorio Nacional de Engenharia Civil, Lisbon, 1968.

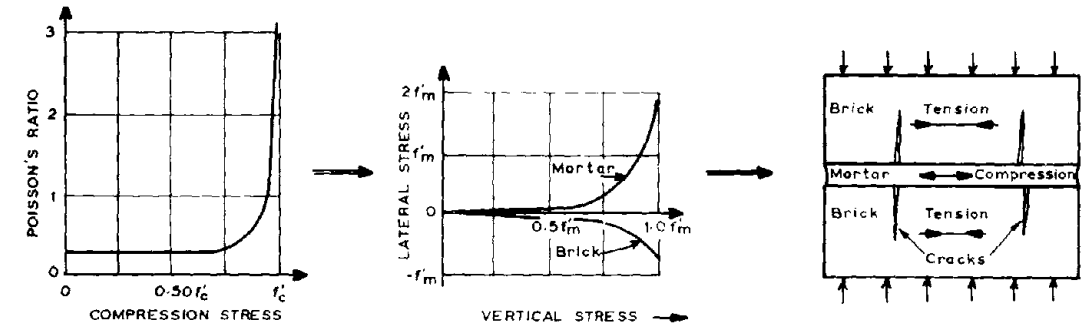

(a) Variation of Mortar Poisson's Ratio with Compression Stress.

(b) Lateral Stress vs. Vertical Stress.

(c) Tension Cracking of Masonry Unit.

FIG. 1 FAILURE MECHANISM FOR MASONRY PRISMS

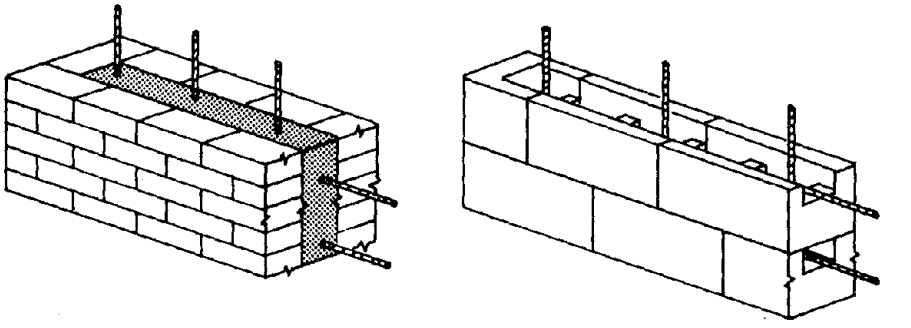

(a) Reinforced Grouted Masonry.(RGM)

(b) Reinforced Hollow Unit Masonry(Rhum) (using open-end bond-beam units.)

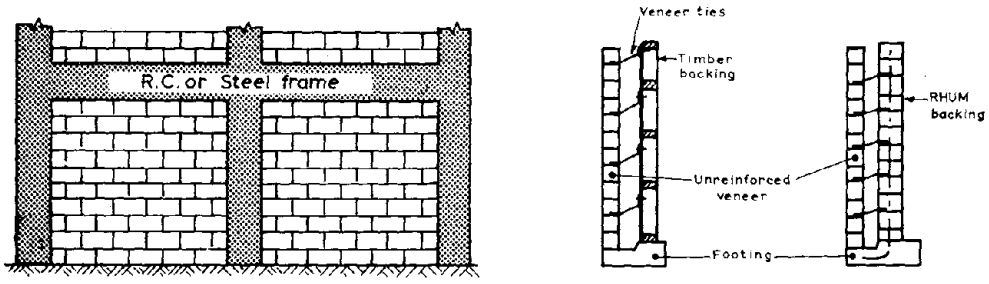

(c) Masonry In-fill Panel Construction

(d) Masonry Veneer Wall Constr

FIG. 2 COMMON FORMS OF MASONRY CONSTRUCTION

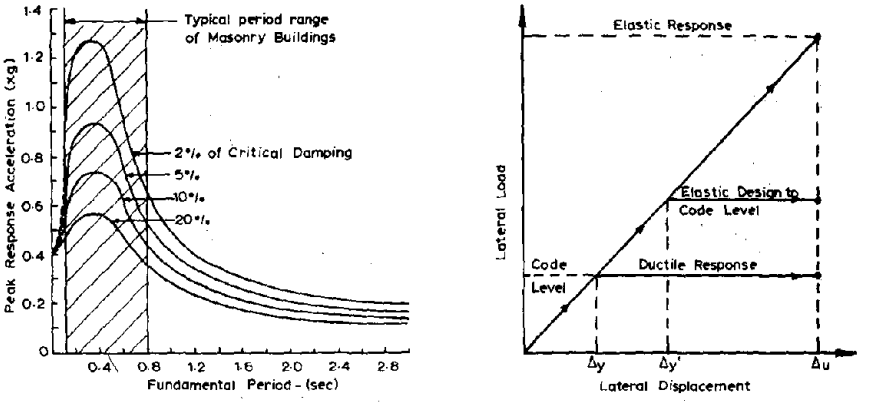

(a) Composite Response Spectra from Eight Accelerograms Scaled to El Centro 1940 N-S (after Skinner)

(b) Peak Lateral Load using "Equal-displacement" Principle.

FIG. 3 LATERAL LOADS FOR SEISMIC DESIGN

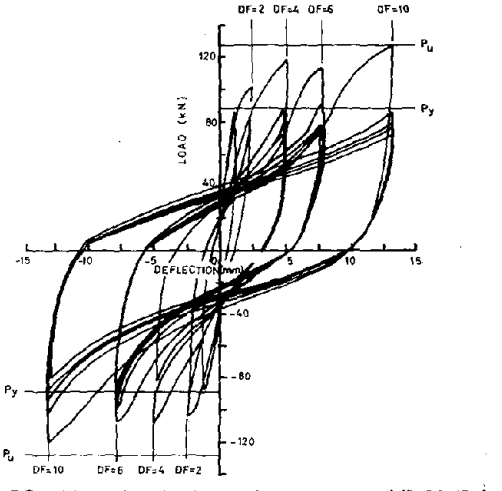

(a) RGM Wall with Confining Plates. Y_u=56psi (0·39MPa)

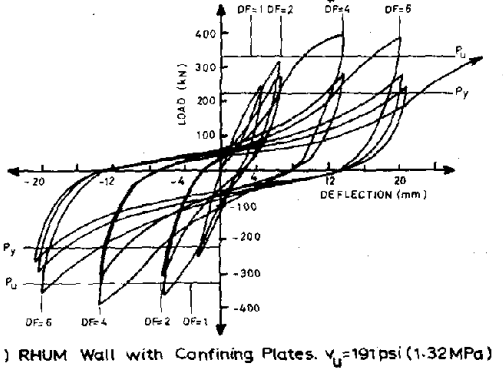

(b) RHUM Wall with Confining Plates. Y_u=191psi (1·32MPa)

FIG. 4 TYPICAL LOAD DISPLACEMENT LOOPS FOR MASONRY WALLS

(P_u = theor. ult. P_y = theor. first yield)

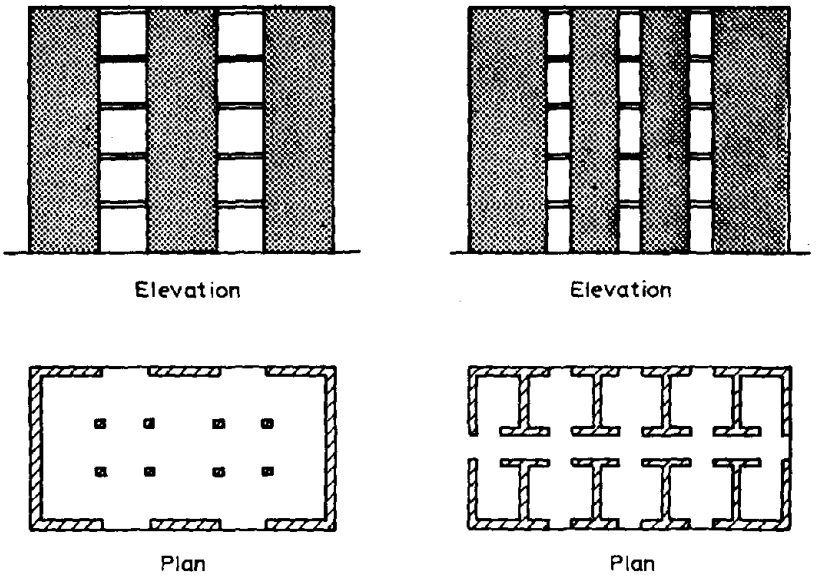

FIG. 5 TYPICAL EXAMPLES OF MASONRY CANTILEVER SHEAR WALLS

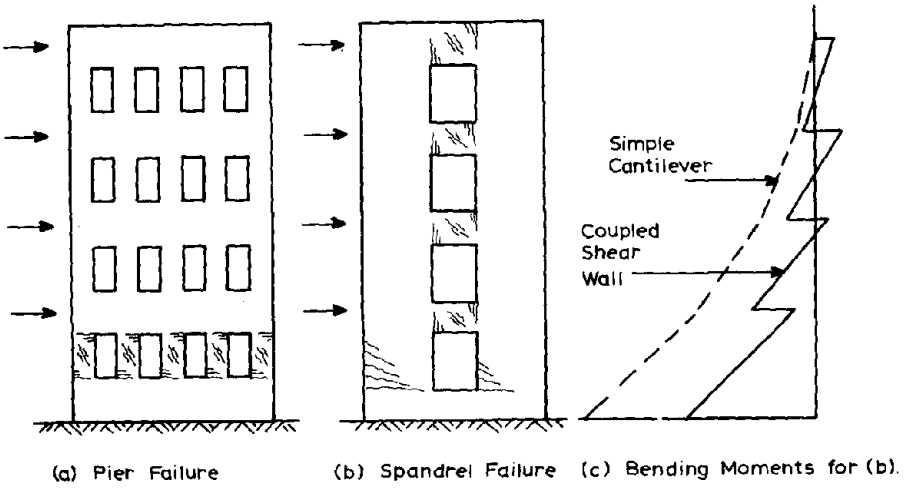

FIG. 6 FAILURE OF SHEAR WALLS WITH OPENINGS

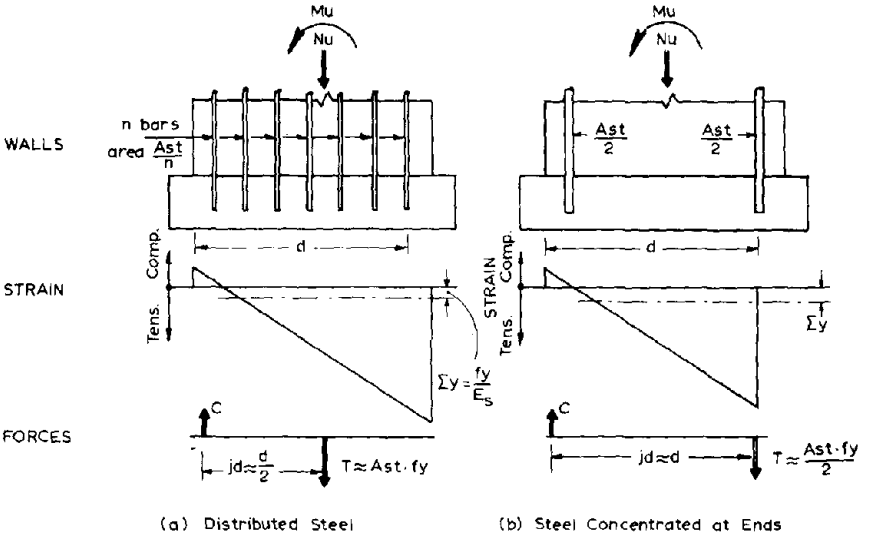

(a) Distributed Steel (b) Steel Concentrated at Ends

FIG. 7 EFFECT OF STEEL DISTRIBUTION ON FLEXURAL CAPACITY

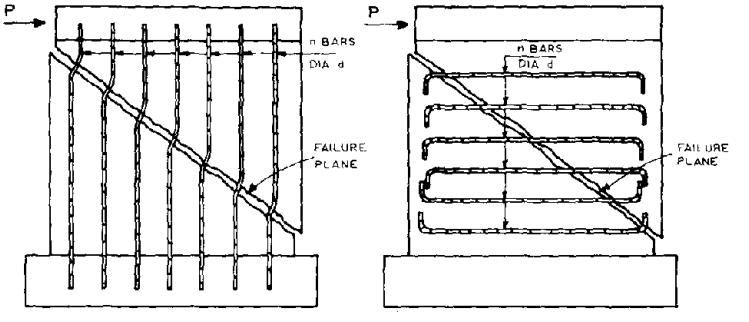

(a) Steel Carries Shear by Dowel Action. P max ≒ 0·24nd.^{2} f_y

(b) Steel Carries Load by Tension. P max ≒ 0·785nd.^{2} f_y

FIG. 8 RELATIVE EFFECTIVENESS OF VERTICAL AND HORIZONTAL SHEAR STEEL

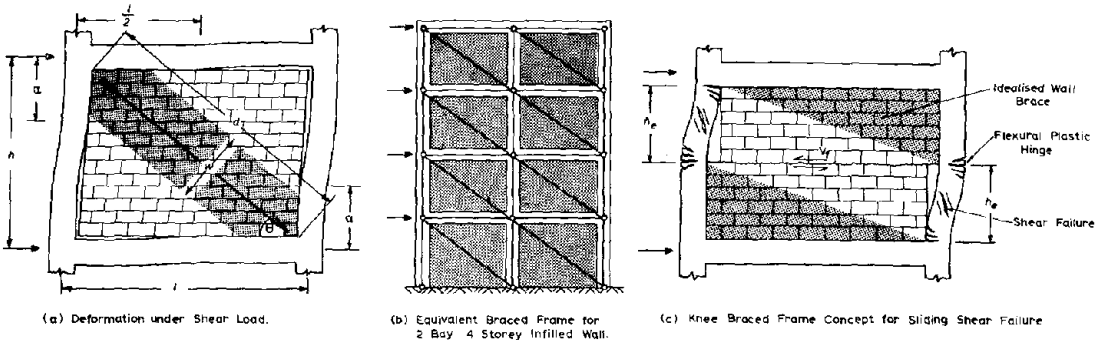

FIG. 9 BEHAVIOUR OF MASONRY INFILLED FRAMES UNDER LATERAL LOAD

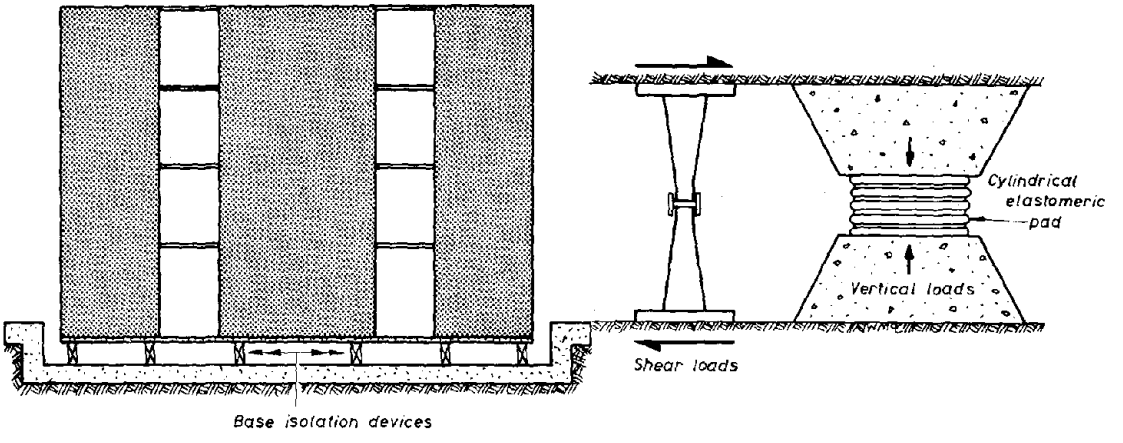

FIG. 10 BASE ISOLATION FOR MASONRY BUILDINGS

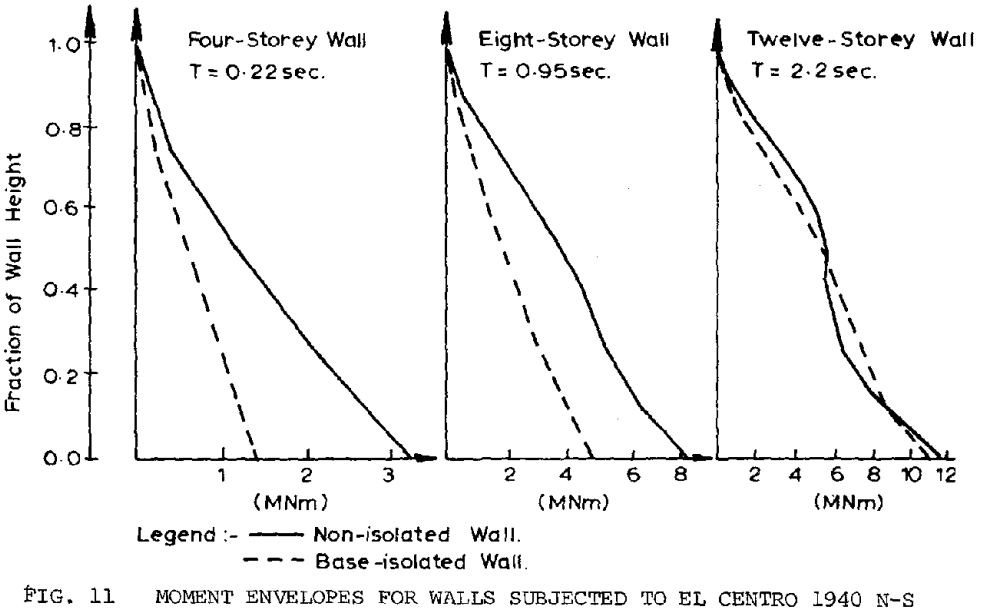

FIG. 11 MOMENT ENVELOPES FOR WALLS SUBJECTED TO EL CENTRO 1940 N-S

PROBLEMS IN WIND ENGINEERING

by

M. P. Gaus
Senior Engineer
Division of Advanced Environmental
Research and Technology
Directorate for Research Applications
National Science Foundation
Washington, D.C., U.S.A.

Synopsis

The importance of natural hazard research in the U.S. is reviewed in terms of annual economic and sudden loss potentials. A need to reduce losses and improve design for wind effects has developed a discipline of Wind Engineering. A comprehensive outline of the elements of a Wind Engineering Program are presented and a few typical NSF supported research projects are discussed. Finally, activities aimed at stimulating and coordinating wind research and at achieving utilization of research results are reviewed.

Introduction

Man and his works are subjected to hazards arising from forces and disturbances occurring in the natural environment. These natural hazards may be dynamic in nature such as earthquakes and wind or may produce their damaging effects over relatively long periods of time, such as the effect of expansive soils. The range of natural hazards which might have to be considered in planning or design of engineered works in the U.S.A. are shown in Fig. 1. Of course not all of these hazards would generally occur simultaneously or may even be present in one part of the country, but there is sufficient interaction between them over the life of many common structures to make an integrated hazard approach desirable for engineering design.

Losses Due to Natural Hazards

It is also interesting to attempt to gain some perspective on the importance of a particular hazard by examining the possible life loss or economic damage which might occur. On a sudden loss basis earthquakes, hurricanes and tornadoes are of major concern in the U.S. It has been estimated that a major earthquake in the Los Angeles or San Francisco area could result in direct economic damages exceeding 13 Billion dollars (in terms of 1970 dollars). An event of this type, however, occurs only infrequently. In order to gain sor insight regarding the potential losses from natural hazards, a special stud carried out by the John H. Wiggins Company, under NSF support, with the obj of providing an estimate of the annual and sudden (extreme event) losses wh could occur to the U.S. building stock over the years 1970 to 2000. One ob tive of this study was to estimate the effect of various mitigations which be developed through research to provice perspective regarding the size, ki and scheduling of research budgets aimed at developing and applying the ass mitigations. This aspect will not be reviewed here and interested persons referred to the Wiggins report which should be widely available around January 1978.

What will be examined are the lists of annual 1970 losses in terms of 1970 dollars which were compiled as this provides some insight regarding the relative importance (on an annual loss basis) of various natural hazards in the U.S.A. It should also be kept in mind that these estimates were for losses to buildings only and do not include indirect consequences such as lost production or other socio-economic impacts. If damage to other facilities, roads, power systems, etc., were included the figures to be quoted would be much higher, perhaps double the estimates for only buildings.

Figure 2 shows the estimated annual loss, deaths and injuries for nine hazards under 1970 conditions and in terms of 1970 dollars. If these hazards are grouped into five categories the estimated 1970 losses are as follows:

Flood and Storm Surge		$2,340 Millions
Expansive Soils		1,100
Wind		1,231
Landslides		210
Earthquake and Tsunami		631
	Total	$5,512 Millions

Thus the total estimated annual losses for the baseline year 1970 comes to 5.512 Billion dollars for buildings.

It is also interesting to examine the estimated one time most severe sudden loss potential for these same hazards. Figure 3 shows estimates for single sudden loss scenarios which were developed in the Wiggins report. On this basis earthquakes would be the numer one hazard followed by wind and flood effects. It should be kept in mind that there is a large variation in the frequency of these sudden loss events with earthquakes being relatively infrequent and wind and floods being fairly frequent. Figure 4 shows the distribution of estimated annual losses by State for the Nine Natural Hazards listed in Fig. 2.

The large risk to both investment and human life which occurs due to natural hazards seem to indicate the desirability of carrying on research efforts to understand the physical phenomena involved in Natural Hazards, to develop improved planning and design methods for facilities subjected to such hazards and to understand the socio-economic factors which could lead to the most effective hazard mitigation activities. The level of research effort for each of these hazards has not been consistent over the years. Floods have received a fairly high level of attention for many years, whereas research in some of the other areas has been sporadic. Starting in 1964 the National Science Foundation began to approach Natural Hazards research in a more organized way. The first area of concentration was in the earthquake engineering area and a significant program has developed in that field. Around 1970 efforts were started to stimulate wind engineering research, an area which was not receiving much attention by eit universities or Government agencies. At the present, the problem of expans soils is being examined to determine how research can be effectively conduc to help mitigate damage from this phenomenon.

Wind Engineering Research

Because of its importance, both in terms of potential economic damage life loss and because of its importance in human comfort, environmental efi and energy, the area of wind engineering will be examined in detail.

A first question is exactly what topics are important in the field of wind engineering? In order to classify wind engineering research, an outline with 16 categories was developed at NSF as the ingredients of a comprehensive wind engineering program. These categories are shown in Fig. 5. A brief discussion of these categories will be given, a few NSF supported research programs will be summarized and finally, some efforts at achieving overall coordination of U.S. wind engineering research will be discussed.

1. Structure of Wind

Movement of air near the surface of the earth is three dimensional in nature with a horizontal motion which is usually much greater than the vertical motion. The driving force creating air motion is solar radiation which generates pressure differences in air masses. This solar induced air motion is then modified by Coriolis forces and by retardation of flow in the boundary layer at the ground surface. Vertical air motion can reach great heights and is of great interest to meteorologists but is of less importance near the ground surface. The surface boundary layer involving horizontal motion or "wind" extends upwards to a certain height above which the horizontal air flow is no longer influenced by the ground effect. The windspeed at this height is called the gradient windspeed and generally occurs at an altitute greater than 1000 ft. Generally, meteorological studies have been concerned with the movements of large air masses and boundary layer effects which are of secondary importance in such studies have not been of great interest. It is precisely in this boundary layer, 500 meters or so in thickness, where we conduct our daily lives, construct our dwellings and other facilities, emit the gaseous pollution from our modern society and are subjected to the damaging effects of winds. Thus, wind engineering is concerned with what happens in the earth's boundary layer with respect to spatial and temporal effects.

If it would be possible to "see" the wind as it flows over the earth's surface, it would be observed that the flow has quite a complex and turbulent structure. One way to visualize this flow at a particular point would be to establish a mean velocity with respect to a specified time or length of air flow, post a point and to then examine the fluctuations of speed about this mean velocity. If the windspeed spectrum over an extended frequency range and at a specific point, such as shown in Fig. 6, is examined, it would be found that there are long period energy peaks corresponding to large-scale pressure systems and diurnal solar energy cycles at relatively long periods followed by a spectral gap in the range around 1 hour to 5 minutes. The frequency and aerial extant of these effects do not correspond with those of usual engineered works and, except for large-scale effects such as storm surge, are not a serious engineering problem. The shorter period spectral peaks resulting from surface generated turbulence do fall within the range of engineered facilities and are of great interest with respect to the transport and mixing of gaseous or particulate materials in the earth's boundary layer. Thus, there is a great need to develop a better engineering understanding of the characterization c this boundary layer.

In addition to the spectral variation of the boundary layer at a speci fixed point, there is a variation of windspeed (and frequently turbulence) v height up to the level of the gradient wind. This variation of windspeed wi height is strongly influenced by the roughness of the terrain over which the flow takes place. Figure 7 illustrates the changes in mean windspeed with

height which could take place if it is assumed that the variation follows a power law. (Certainly only one possibility.)

The boundary layer flows are also subjected to thermal phenomona which are of particular importance to environmental effects in the boundary layer.

The objective of research on the structure of the wind is to gain a better theoretical and analytical understanding of wind boundary layer aerodynamics and to carry out measurements in the actual boundary layer to develop an engineering data base for purposes of comparison and development of design recommendations. Typical of NSF supported research projects has been the work of Professor R. L. Peskin of Rutgers University on turbulent diffusion in the earth's boundary layer, of Professor Leadon of the University of Florida on fluctuating wind pressures on buildings of Professors Cermak and Peterka of Colorado State University who have examined the statistical characteristics of wind-structure interaction, and Professor A. Chiu of the University of Hawaii who collected spatial data on natural winds. A great deal more needs to be done to establish an adequate characterization of natural winds in the earth's boundary layer which will improve our capabilities in wind engineering.

2. Wind-Wave Effects

The objectives of this area are to gain a better understanding of the interaction of wind and water resulting in wave generation and to study the resulting effects on open sea structures, on off-shore structures and on coasts, harbors and inland waterways and reservoirs. Progress in this area requires improvement of analytical methods, laboratory simulation of wind-wave generation and full-scale measurements to provide a reliable data base. Typical of NSF supported research projects in this area have been the studies of Hsu, Perry and Street at Stanford University, of Shemdin at the University of Florida, and of Plate and Nath at Colorado State University and at Oregon State University. Three research facilities have been developed with the assistance of NSF support. Wind-wave research channels were constructed at Stanford University and at University of Florida. Both of these facilities are of a fixed bed type. A fixed bed type. A smaller facility was constructed at the Colorado State University in which the bed of the channel can be tilted to develop varying gradients in the channel. This facility was constructed to examine wind effects on inland waterways as well as in open bodies of water.

3. Effects on Urban Areas

The objectives of this area are to study any special characteristics of wind flowing over urban regions including the influence of tall structures, the transport and entrainment of pollutants, heat island and micro-thermal phe the influence of changing surface characteristics through urban developmer the influence of industrial operations. Typical of NSF projects in this a the Metromex project involving measurements and observations on the City c St. Louis, Missouri, and studies by Professor J. Cermak of Colorado State University utilizing models and a special micro-meteorological wind tunnel success has been achieved in this area, however, problems of scaling and similitude raise serious questions concerning the extrapolation of model s to full-scale situations for an entire urban region. There is a real need more data to be collected in urban regions under a variety of wind conditi

4. Wind Loading on Structures

The objective of this area is to develop methods to utilize information on wind characteristics to establish the actual loadings which will occur on structures including turbulence fluctuations about a mean wind, drag, vortex shedding and separation effects which will result in not only shear and overturning effects on a structure, but will also include dynamically fluctuating loads on the gross structure or smaller component parts such as glass and cladding. Dynamic methods of analysis must be developed to predict the response of structures and components to dynamic wind loadings. There are certain similarities in procedures to calculate dynamic response to wind or earthquake loadings even though the loads are introduced differently and that maximum earthquake loadings may be allowed to generate greater distortions for extreme events. Because of the complexity of dynamic calculations for even normal structural systems, the use of computers will generally be essential. This means that if dynamic analysis procedures are to find widespread use in practice, computer software must be developed and made available to practitioners before the use of such procedures could be made mandatory for appropriate classes of structures. It is recognized that most smaller residential and commercial structures are not individually engineered and would be covered by appropriate minimum regulations expressed in codes and standards. Computer software for earthquake analysis has been made available through the National Information Service for Earthquake Engineering and many requests are received for these programs. A similar activity for wind engineering data and software might be appropriate.

Of particular interest recently has been the response of glass and cladding to fluctuating wind loadings. Projects have been supported at Texas Tech University, Georgia Institute of Technology, University of Florida, MIT and UCLA to examine this problem analytically, experimentally and through full-scale observations. An objective is to develop technically sound procedures for the design of glass incorporating the best possible information on material characteristics and failure mechanisms. It is hoped that the output of these efforts would be a design handbook which could be based on technically improved methods. Recent difficulties with certain buildings in the U.S. dramatically indicate a need for improvement.

5. Severe Storms

The objective is to gain a better understanding of the features of severe storms which affect constructed facilities. Of interest are hurricanes, severe thunderstorms, tornadoes, and local phenomena which create damage. Research covers analytical studies, laboratory experiments and simulation and full-scale observations. As the severe winds involved frequently flow away conventiona meteorological instrumentation, there is a lack of quantitative data regardi such storms. A great deal of information has been gathered by reconnaissanc teams sent into damaged areas by NSF, NBS and other groups. From this post-disaster information, it is possible to estimate probable maximum wind speed and the chain of events leading to ultimate failure. As a result of studies tornadoes involving field observation, laboratory simulation, and full-scale observations a much better idea has been obtained concerning probable maximu wind speeds and the myth of houses exploding due to pressure changes in tornadoes (they don't). Studies are also underway on missiles generated by extreme storms. Also of great interest are storm-surge effects generated by hurricanes.

6. Design for Hurricanes and Tornadoes

The concern here is with the development of design methods for structures subjected to extreme winds. Critical structures such as nuclear reactors and life-safety facilities can be designed to resist the effects of extreme winds. For residences and other small structures, owners may not be willing to pay cost penalties associated with tornado resistant design. A group at Texas Tech University using observations of actual damage due to tornadoes has developed a concept of in-residence shelters, Fig. 8, in which one room in a house could be reinforced to provide an emergency shelter as shown in Fig. 9. This would be relatively inexpensive if done when the house is constructed and would provide a high degree of protection. Also of concern is the design of building cladding and glass against wind-borne missile damage.

7. Full-Scale Testing

The objective here is to obtain full-scale data for wind pressures on structures and components, on the modification of wind flow by structures and on building motions due to fluctuating wind forces. Data obtained in this way will not only be useful for design, but also is needed to check analytical and model studies. At the present, NSF support has assisted in full-scale studies of the Century City Buildings in Los Angeles, of the Independent Life Tower in Jacksonville, Florida, Figs. 10 and 11, and the John Hancock Building in Boston. The NBS has carried out an excellent study on residential structures in the Philippines under the support of AID. Although a start has been made many more such studies are needed.

8. Model Testing

A desirable objective would be to study models of buildings and regions experimentally because this would allow the study of various configurations and parameters before construction and would make possible the assessment of wind loadings and response. Aeronautical wind tunnels are not directly suitable for such studies because they were designed to minimize turbulence and boundary layer effects. Various approaches to boundary layer simulation are possible. Screens, spires and grids can be used in aeronautical tunnels to generate turbulence and a thickened boundary layer. Special boundary layer wind tunnels have been constructed having a long test section in which a thickened turbulent boundary layer can be generated by introducing appropriate roughness elements in the upstream flow. Another approach is to use a counter-jet technique to generate turbulence structure. Each method has its proponents and has achieved success for certain types of studies. In every case there is always a question whether the natural wind turbulence structure has been appropriately modeled. In almost all cases gust simulation is not included. For even the largest facilities the degree of scaling required is extreme. For tall structures scaling may be the order of 1 to 200 or even 1 to 500. Scaling would be even more extrem urban or terrain studies.

The largest collection of boundary layer wind tunnel facilities are at Colorado State University. Three tunnels are in use, two of which are in Figs. 12, 13 and 14.

9. Environmental Factors

The concern here is the effects of structures on the wind climate surrounding structures. Items of interest are wind concentrations which might endanger or inconvenience pedestrians or vehicles, which might entrap pollutants or have adverse effects on the environmental control systems in buildings.

10. Psycho-Physical Factors

Of concern are the perception levels for motion in structures, human motion tolerance levels in different types of structures and other psychological responses to building drift and motion.

11. Legal Factors

There are many unresolved legal problems associated with wind. Examples might be the buffeting of one building by the wake of another, damage to one building resulting from wind-borne missiles originating on another, etc.

12. Special Problems

Included here might be problems such as wind-driven moisture penetration of buildings and possibilities of wind zoning for cities. A special study carried out by Hart and Lew of UCLA developed a wind microzonation procedure for extreme winds in the Los Angeles basin. It would be interesting to determine whether such procedures would be useful in other parts of the country.

The remaining categories will not be discussed in detail as some aspects will be covered under implementation to be discusses later. Clearly, wind is an international problem and international cooperative research on wind problems would be desirable. It is hoped that such programs might be developed in the future.

Coordination and Implementation of Research Results

Wind engineering has many facets and requires inputs from several different disciplines which may not ordinarily interact. To encourage and coordinate research on winds and wind effects, and to disseminate information, a Wind Engineering Research Council was formed. The purpose, activities, advisory council and other details of WERC are shown in Figs. 15, 16, 17, 18 and 19. Activities of the Council are grouped into eight categories which are largely a combined form of the comprehensive list given in this paper.

Several activities conducted under the auspices of WERC are of general interest. A Wind Engineering Research Digest, Fig. 20, has been compiled by Professor A. Chiu of the University of Hawaii, and has had two editions publ: WERC publishes on an irregular basis a newsletter and has organized two nati conferences on Wind Engineering Research. A third Conference, Fig. 21, is scheduled for early 1978 at the University of Florida. The Council also organized a special meeting on Wind Load Requirements for Buildings, Fig. 22 with an objective of determining future input and improvements for the U.S. ANSI - A58 Lateral Load standard.

Other implementation activities which may be of interest is the NSF sponsored program on tall buildings, Fig. 23, which has a special committee on Wind Loading and Wind Effects, Fig. 24, and the sponsorship of a special meeting on tornadoes in conjunction with the U.S. Nuclear Regulatory Commission. This meeting which was organized and held at Texas Tech University has produced a proceedings which will be significant reference work for years to come.

Summary

The elements of a comprehensive wind engineering program have been presented and a few examples of research activity mentioned. Space would not permit a complete listing of NSF sponsored wind engineering research, which is only one activity in this area. It is clear that there are many opportunities to improve our knowledge of and capability for dealing with wind problems.

FIGURE 1

NATURAL HAZARDS

FLOOD

- Riverine Flood
- Storm Surge

EXPANSIVE SOILS

WIND

- Hurricane
- Tornado
- Severe Wind

EARTHQUAKE

LANDSLIDE

TSUNAMI

FIGURE 2

HAZARD	ANNUAL LOSS $ MILLIONS	DEATHS PER $ MILLIONS (1970)	INJURIES PER DEATH	1970 DEATHS	1970 INJURIES	TOTAL 1970 CASUALTIES
Earthquake	620	0.4	40	248	9,920	10,168
Landslide	210	0.1	100	21	2,100	2,121
Expansive Soils	1100	0.0	0	0	0	0
Hurricane	680	0.1	100	68	6,800	6,868
Tornado	540	0.5	40	270	10,800	11,070
Severe Wind	11	0.1	100	1	100	101
Riverine Flood	1900	0.2 or 0.1*	100	285	28,500	28,785
Storm Surge	440	0.1	100	44	4,400	4,444
Tsunami	11	2.0**	20	22	440	462
				959	63,060	64,019

*0.2 includes flash flooding, 0.1 does not include flash flooding
**no warning

FIGURE 3

NATURAL HAZARD SUDDEN LOSS ESTIMATES FOR BUILDINGS FROM SINGLE MAJOR IMPACT SCENARIOS

EARTHQUAKE	$12,190 MILLIONS
WIND	2,320
FLOOD AND STORM SURGE	1,090

FIGURE 4 ANNUAL LOSSES BY STATE FOR THE NINE NATURAL HAZARDS CONSIDERED FOR 1970 CONDITIONS

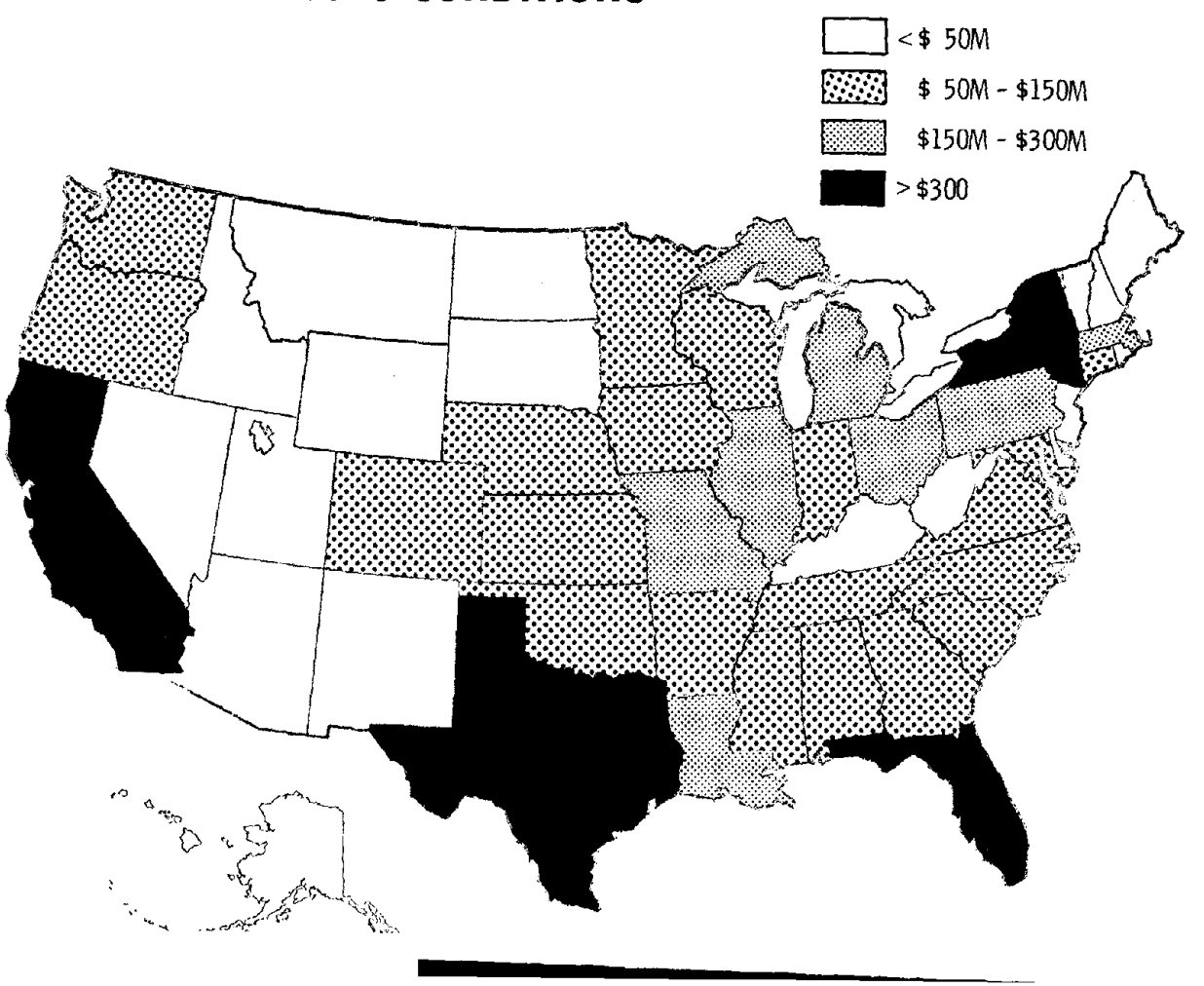

FIGURE 5

WIND ENGINEERING

1) Structure of Wind
   a) Boundary-layer-vertical (50 to 100 meter region) profiles, turbulence intensities
   b) Extremes and durations
   c) Effects of Moisture content - rain, snow, hail

2) Wind-Wave Effects
   a) Wave generation
   b) Open sea structures - floating platforms, ships
   c) Off-shore structures
   d) Coastal structures
   e) Harbors, estuaries, inlets
   f) Inland waterways and reservoirs

3) Effects on Urban Areas
   a) Characteristics of wind build-up areas
   b) Influence of tall structures
   c) Transport and entrainment of pollutants
   d) V/STOL airports and heliports
   e) Micro-thermal phenomena

4) Wind Loading on Structures
   a) Drag, vortex shedding and separation
   b) Dynamic response and stochastic analysis
   c) Numerical algorithms and computer software
   d) Loads on cladding and glass
   e) Static vs. statistical approach
   f) Permeability effects

FIGURE 5

5) Severe Storms
   a) Thunderstorms
   b) Hurricanes - wind velocities, wind-water interactions
   c) Tornadoes - wind and pressure distributions
   d) Local phenomena
   e) Prediction capabilities

6) Design for Hurricanes and Tornadoes
   a) Critical structures - nuclear reactor, etc.
   b) Standard structures - controlled-sequence failure to protect life
   c) Missile damage
   d) Economic considerations

7) Full-Scale Testing
   a) Instrumentation development
   b) Urban and rural profiles for engineering applications
   c) Structure testing - fixed and portable structures, bridges, cooling towers, tall stacks, tall buildings

8) Model Testing
   a) Special wind tunnel facilities
   b) Model scaling and dynamic similitude
   c) Structure testing - fixed and portable structures, bridges, cooling towers and tall stacks
   d) Effects of clustering and wake interaction

FIGURE 5

9) Environmental Factors
   a) Effects of structure on surroundings - entrappment of pollutants, stability of vehicles and pedestrians
   b) Effects on environmental control systems

10) Psycho-Physical Factors
   a) Perception levels for motion in various structures
   b) Motion tolerance
   c) Psychological response to drift

11) Legal Factors
   a) Pollution problems
   b) Buffeting of downstream structures, etc.
   c) Missile damage caused by other structures
   d) Structural damage
   e) Occupancy discomfort
   f) Insurance

12) Special Problems
   a) Moisture penetration of buildings
   b) Wind zoning for cities
   c) Building code requirements

13) Wind Considerations in Urban Planning

14) Building Codes and Regulations

15) Soci-Economic Effects

16) International Cooperation

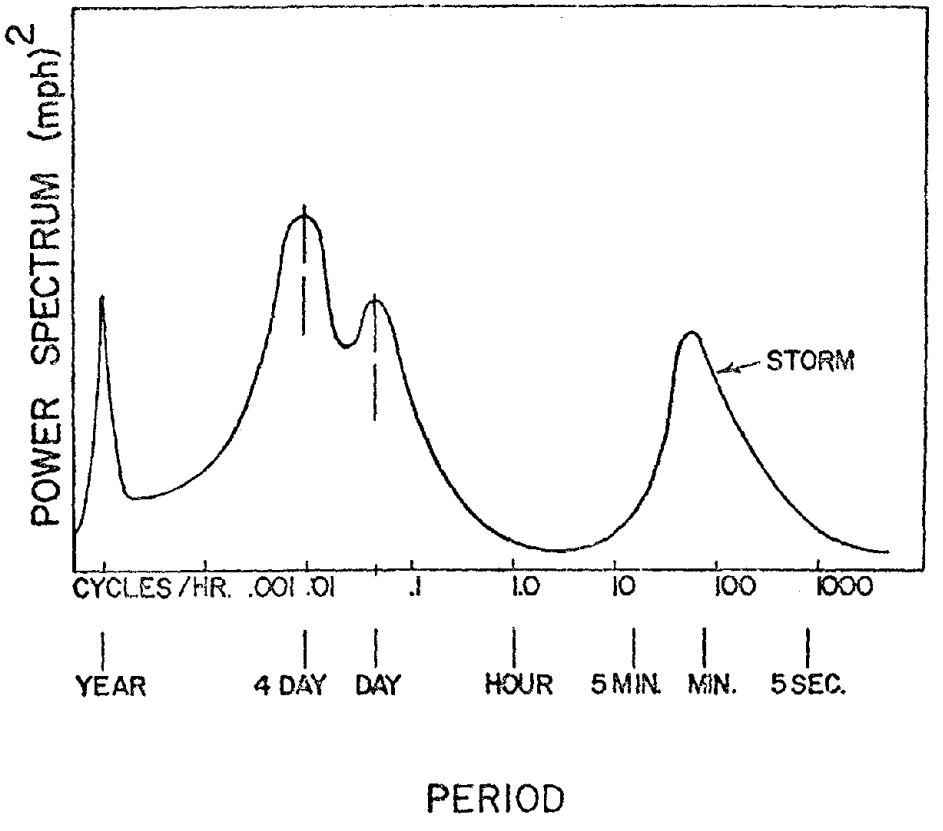

FIGURE 6 Windspeed Spectrum Over and Extended Frequency Range.

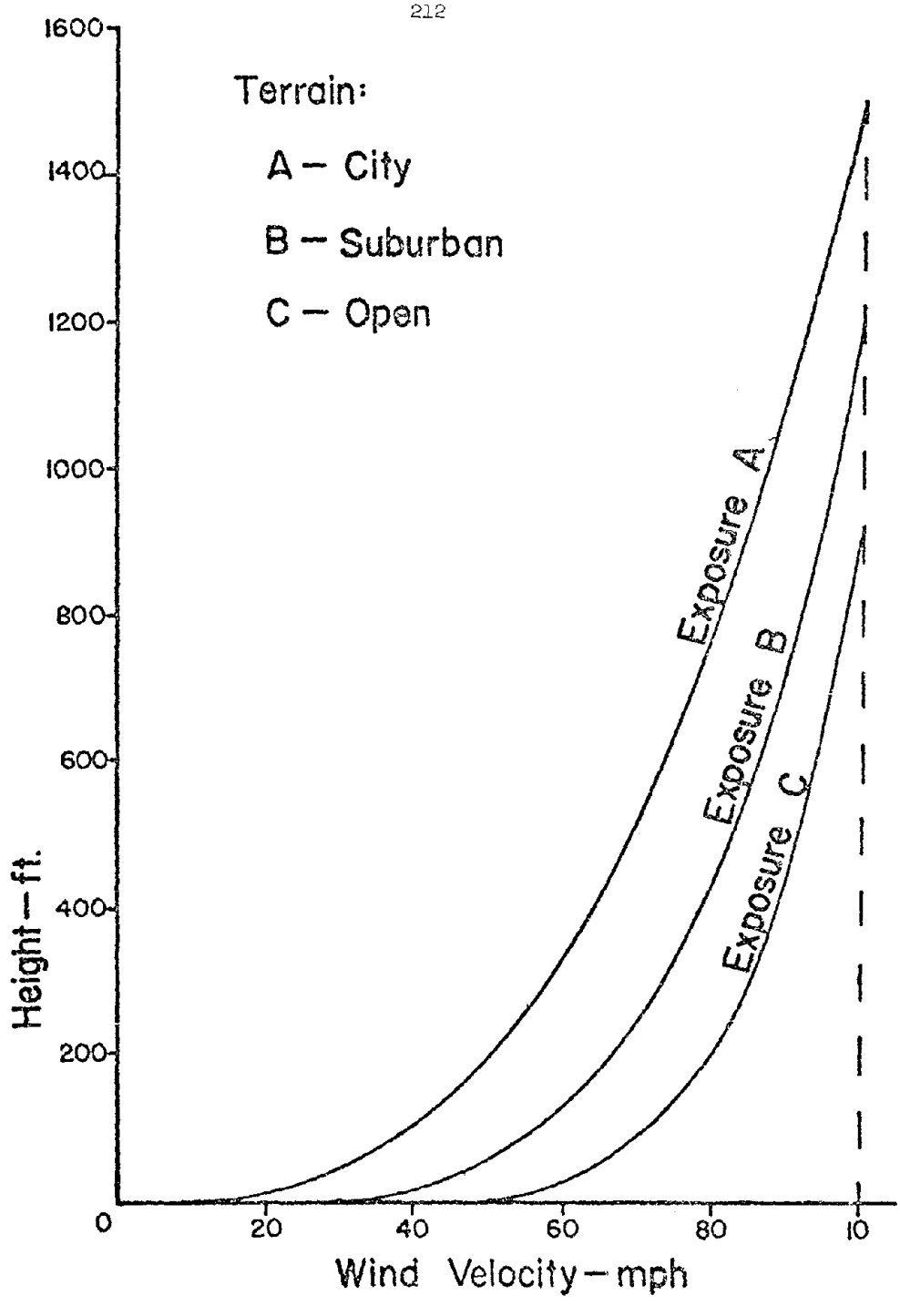

FIGURE 7 Wind Velocity Profiles for City, Suburban, and Open Terrain.

In-residence Shelters from Extreme Winds

TEXAS TECH UNIVERSITY
DEPARTMENT OF CIVIL ENGINEERING
and the
INSTITUTE FOR DISASTER RESEARCH

FIG. 8

WHAT IS AN INRESIDENCE SHELTER?

A small interior room, such as a closet or bathroom, readily accessible from all parts of the house, is designed to provide occupant protection. Such a shelter, inside the residence, becomes the "Inresidence Shelter". The concept is applicable to both existing residences and newly constructed ones.

The cost of constructing the entire house to provide highly reliable occupant protection is prohibitive for most homeowners.

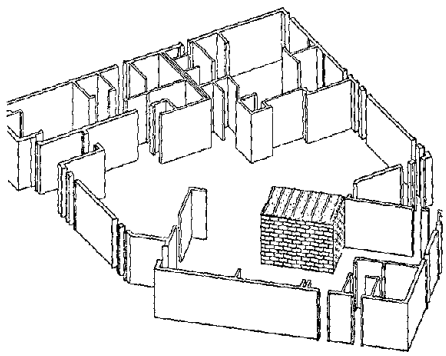

FIG. 9

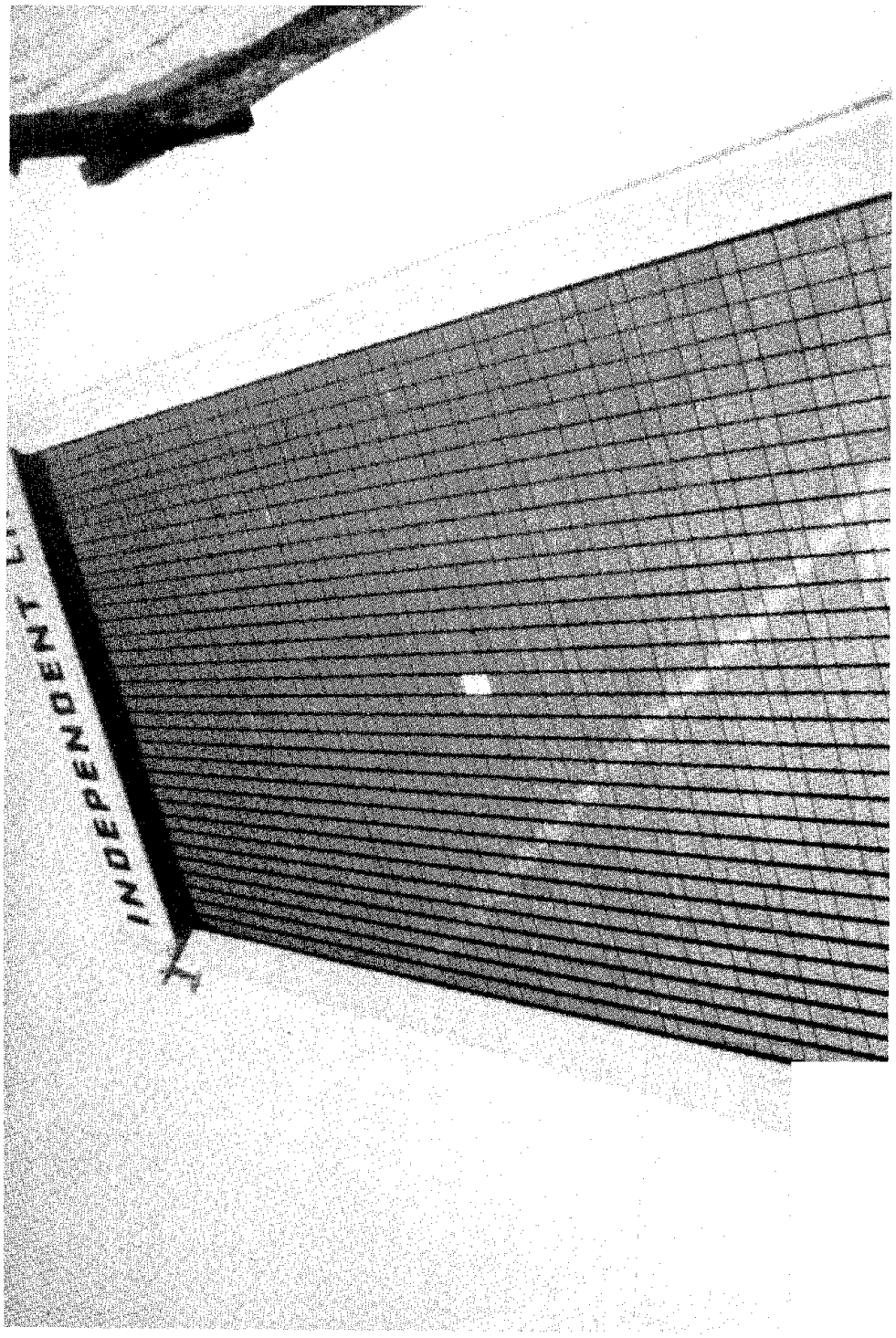

FIG. 10

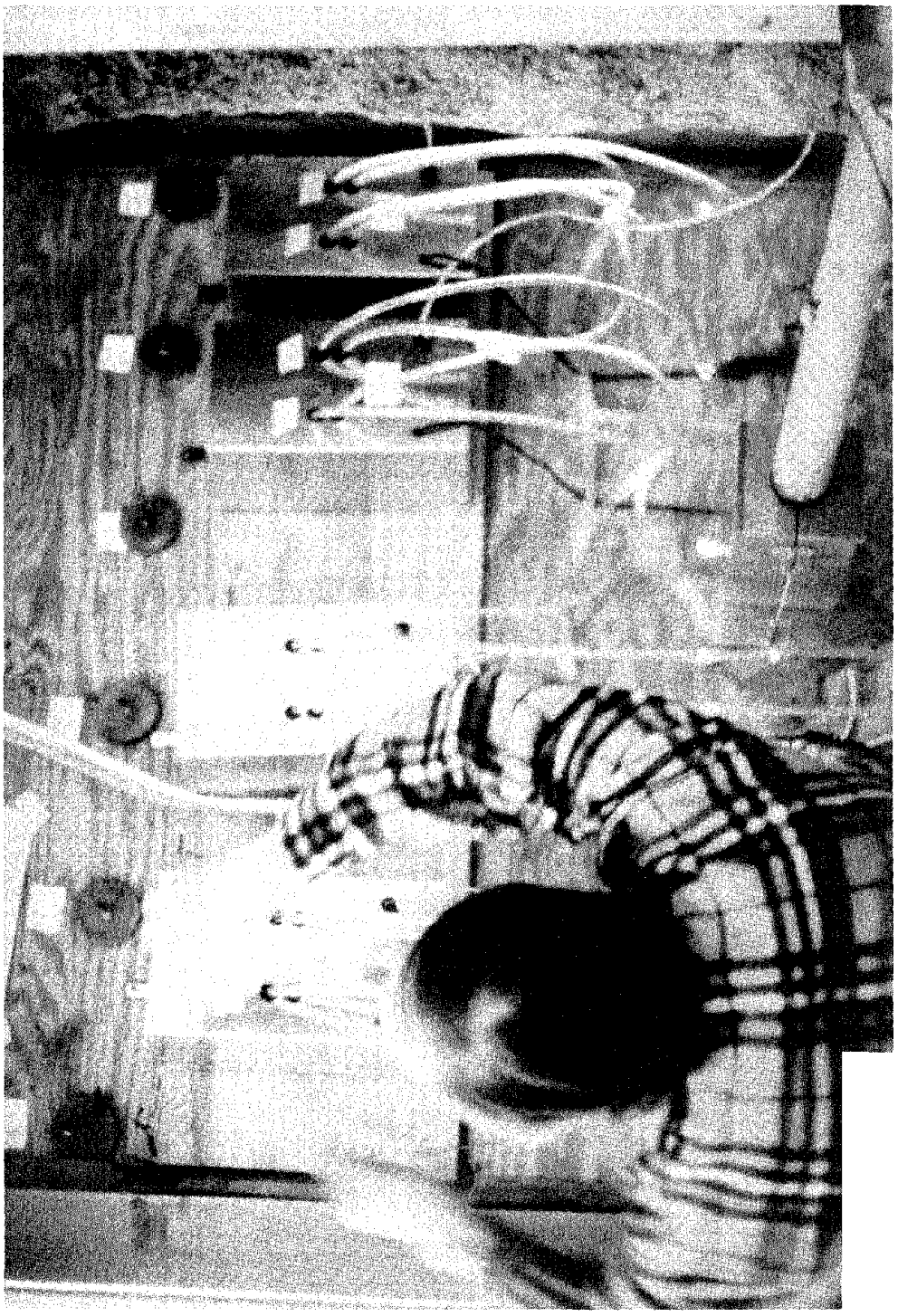

FIG. 11

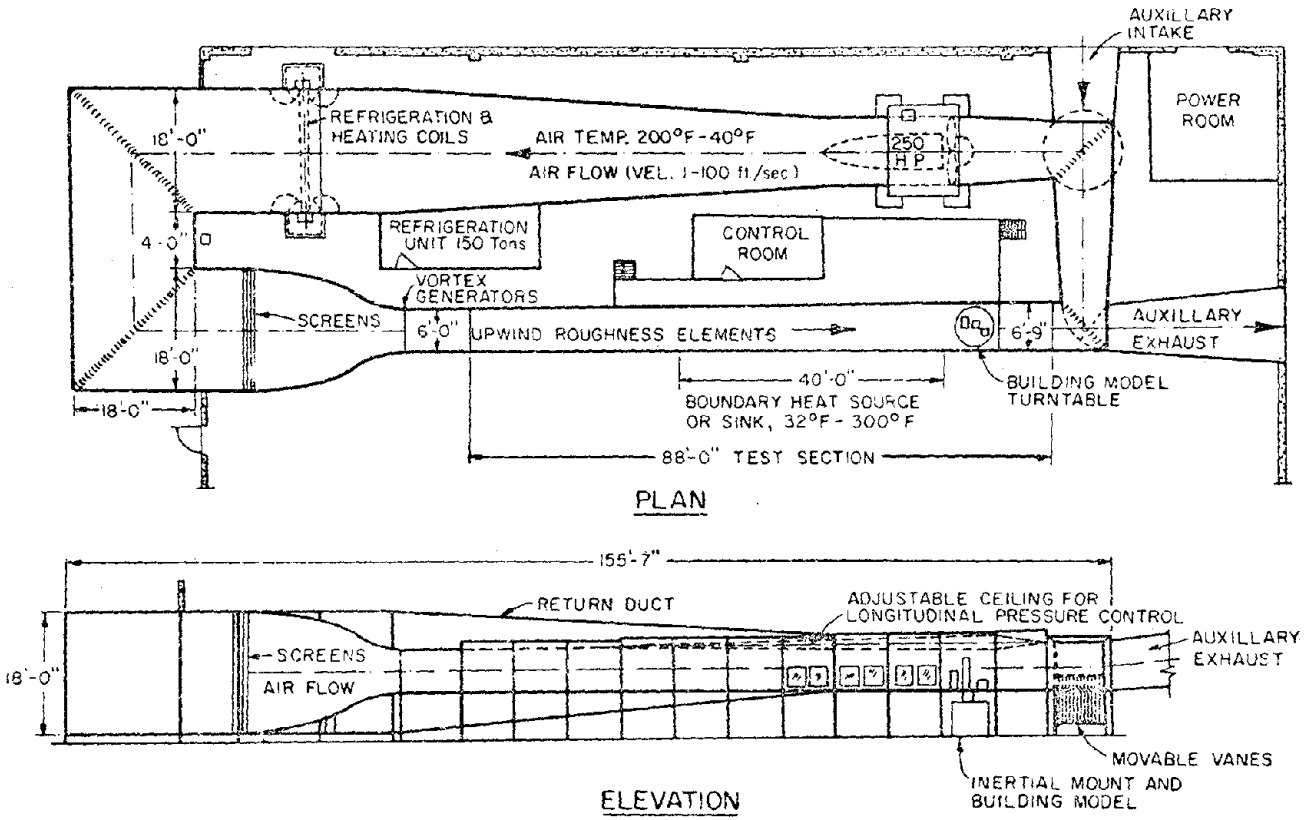

Figure 12 METEOROLOGICAL WIND TUNNEL (Completed in 1963)
FLUID DYNAMICS & DIFFUSION LABORATORY
COLORADO STATE UNIVERSITY

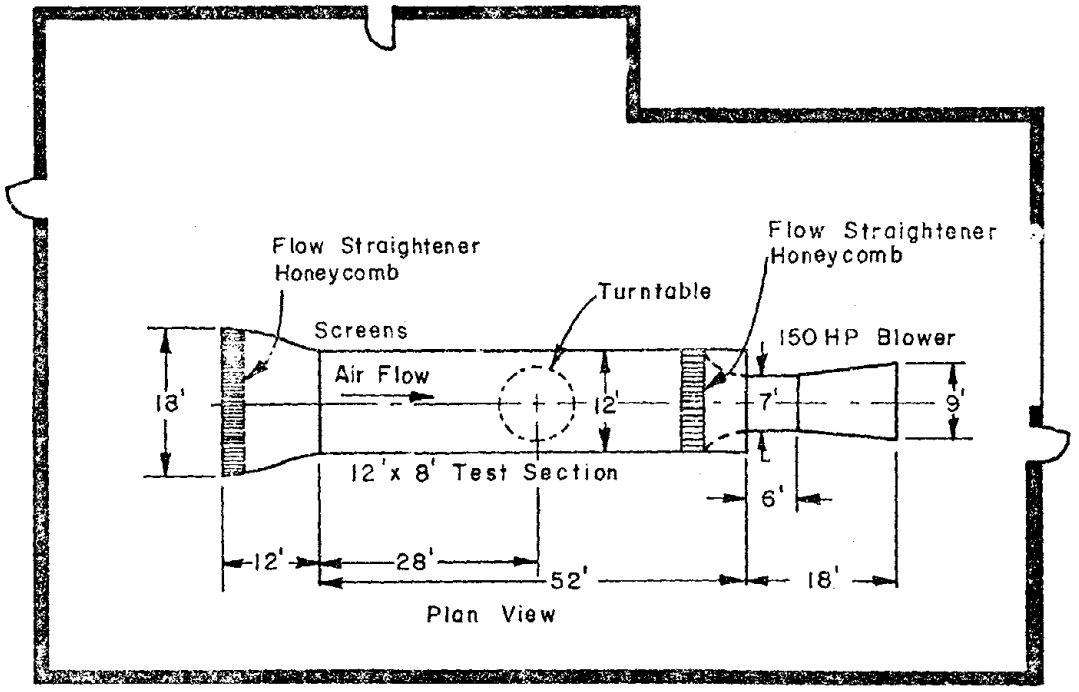

Figure 13 Environmental Wind Tunnel -- Fluid Dynamics and Diffusion Laboratory, Colorado State University

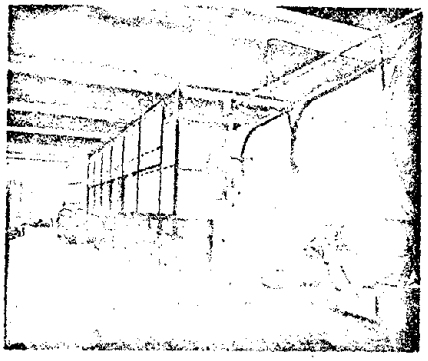

Figure 14 Exterior of Environmental Wind Tunnel

Wind

Engineering

Research

Council

An organization for coordinating
research activity and disseminating information
on Wind Engineering problems

FIG. 15

PURPOSE

The Wind Engineering Research Council was formed to provide a mechanism for the free exchange of information on research plans, priorities, and programs; and to assist in the coordination of research efforts in wind engineering.

The primary objectives of the Wind Engineering Research Council are:

- To stimulate the initiation of, and provide the coordination, of research efforts in wind engineering.
- Implement the dissemination and exchange of information between research workers in the various disciplines of wind engineering.
- Delineate problems that most urgently need research.
- Establish a National Wind Engineering Information Center consisting of a library of publications and research reports.
- Provide advice to government agencies and other interested parties on wind research efforts and problems.

FIG. 16

ACTIVITIES

The Council organizes periodic national meetings of research investigators in Wind Engineering. These meetings consist of reports on current research and discussions in or by working sub-groups on directions for future research. The proceedings of these national meetings are published and sent to those individuals and organizations on the WERC mailing list. In addition, a quarterly newsletter reporting on activities and forthcoming events in Wind Engineering is mailed to all interested parties.

The activities of WERC are supported by a grant from the National Science Foundation.

MEMBERSHIP

Because of the nature of the organization there is no formal membership classification for participants in WERC activities. The "membership" of the Council consists of all persons and organizations, on the WERC mailing list, having an active interest in one of the areas of Wind Engineering. Interested parties may be included on the WERC mailing list by submitting their name, organization, and address to:

Dr. Richard A. Parmelee, Executive Secretary
Wind Engineering Research Council
Department of Civil Engineering
Northwestern University
Evanston, Illinois 60201

Phone: (312) 492-3172

FIG. 17

WIND ENGINEERING

Recognizing that the effects of wind on the works of man result in extensive damage and unacceptable loss of life, the Wind Engineering Research Council was formed to encourage and coordinate research on winds and wind effects, and to disseminate information. WERC is especially concerned with the following aspects of the wind engineering problem.

BOUNDARY-LAYER WINDS

- Distribution of mean air speeds
- Distribution of mean temperature
- Turbulence characteristics
- Orographic effects
- Urban effects
- Joint probability of air velocity, temperature and humidity

SEVERE STORMS

- Thunderstorms
- Hurricanes
- Tornadoes
- Extratropical cyclones
- Downslope winds
- Post-disaster inspections
- Extreme wind statistics

WIND LOADING ON STRUCTURES

- Mean and dynamic responses
- Vortex-shedding excitation and galloping
- Loading on cladding and glass
- Effects of architectural details
- Stochastic analysis
- Impact of wind-driven missiles
- Building code requirements

PSYCHO-PHYSICAL FACTORS

- Preception thresholds of motion
- Tolerance for vibratory motion
- Wind criteria for pedestrian safety and comfort

EFFECTS ON URBAN AREAS

- Transport, entrainment and entrapment of pollutant
- Stability of vehicles and pedestrians
- Location of V/STOL airports and heliports
- Location of industrial and power plants
- Wind zoning for cities
- Micro-thermal characteristics

FULL-SCALE MEASUREMENTS

- Instrumentation development
- Meteorological variables
- Pollutant concentrations
- Wind pressures on building surfaces
- Structural responses

MODEL TESTS

- Wind-tunnel facilities
- Model-prototype similitude
- Blockage effects
- Wind characteristics for complex geometry
- Structural responses
- Building surface pressures
- Diffusion of stack and automobile exhausts

SPECIAL PROBLEMS

- Agricultural aerodynamics
- Air-sea interactions
- Wind-induced noise
- Wind power generation

FIG. 18

WERC ADVISORY COUNCIL

The affairs of the Council are handled by an Advisory Committee which consists of the following members:

EXECUTIVE BOARD

Chairman
Jack E. Cermak
Colorado State University

1st Vice-Chairman
Leslie E. Robertson
Skilling, Helle, Christiansen, Robertson

2nd Vice-Chairman
Anatol Roshko
California Institute of Technology

Executive Secretary
Richard A. Parmelee
Northwestern University

ADVISORY COMMITTEE

Arthur N. L. Chiu
University of Hawaii

Alan G. Davenport
University of Western Ontario

Joseph H. Golden
National Severe Storms Laboratory

Robert J. Hansen
Massachusetts Institute of Technology

George W. Housner
California Institute of Technology

Kishor C. Mehta
Texas Tech University

Nathan M. Newmark
University of Illinois

Hans A. Panofsky
Pennsylvania State University

George W. Reynolds
Woodward-ENVICON Inc.

Robert H. Scanlan
Princeton University

Anshel J. Schiff
Purdue University

H. C. S. Thom
Consulting Meteorologist

FIG. 19

Wind Engineering Research Digest

Volume I - 1974

Sponsored through Grant GK-38047
National Science Foundation

Conducted in Cooperation with the
Wind Engineering Research Council

University of Hawaii
Honolulu, Hawaii

FIG. 20

Sponsored by Wind Engineering Research Council and National Science Foundation

A Call for Papers

on

Conference Scheduled for
February 26 - March 1, 1978
University of Florida
Gainesville

Wind Engineering Research

Presented by College of Engineering and the Division of Continuing Education
University of Florida, Gainesville, Florida

FIG. 21

WIND LOAD REQUIREMENTS FOR BUILDINGS

Proceedings of a Workshop

held at

Northwestern University

Evanston, Illinois

June 3 & 4, 1976

Edited by

Richard A. Parmelee

Sponsored by

National Science Foundation

National Bureau of Standards

Wind Engineering Research Council

FIG. 22

FIG. 23

CRITERIA AND LOADING (CL)

Group Coordinators

T. Naka	University of Tokyo	Tokyo	J
L. E. Robertson	Skilling, Helle, Christiansen, Robertson	New York	USA

Group Editors

E. H. Gaylord	University of Illinois	Urbana	USA
R. J. Mainstone	Dept. of Environment	Watford	GB

GRAVITY LOADS AND TEMPERATURE EFFECTS (5)

R. C. Reese	Consulting Engineer	Toledo	USA
G. B. Godfrey	CONSTRADO	Croydon	GB
G. R. Fuller	U.S. Dept. HUD	Washington, D.C.	USA

Dead load, live load, vibration and impact loads, combined loading, construction loads, load surveys, load reduction factors, temperature effects.

EARTHQUAKE LOADING AND RESPONSE (6)

K. Muto	Muto Inst. Struct. Mechs.	Tokyo	J
R. W. Clough	University of California	Berkeley	USA
G. C. Hart	University of California	Los Angeles	USA

Ground motions, soil and foundation effects, dynamic response, damage evaluation, economic and social aspects, loading and response criteria, field observations, seismic, code requirements.

WIND LOADING AND WIND EFFECTS (7)

A. G. Davenport	University of Western Ontario	London	CDN
S. Mackey	University of Hong Kong	Hong Kong	HK
W. H. Melbourne	Monash University	Victoria	AUS

Wind environment, prediction of performance, wind tunnel studies, field studies, gust factors, design wind speeds, shape factors, damage evaluation, factors influencing design.

FIRE AND BLAST (8)

D. Sfintesco	C. T. I. C. M.	Paris	F
J. F. Fitzgerald	Chicago Dept. of Buildings	Chicago	USA
M. Law (8A)	Ove Arup & Partners	London	GB
R. J. Mainstone (8B)	Dept. of Environment	Watford	GB

Fire, fire codes, fire equipment, fire rating methods, fire protection methods. Blast (internal and external), impact loading, sonic boom.

QUALITY CRITERIA (9)

W. Quasebarth	Atlas Machine and Iron Works Inc.	Gainesville	USA
I. V. Gramolin	GOSSTROY	Moscow	USSR
E. J. White Jr.	Skilling, Helle, Christiansen, Robertson	New York	USA

Mechanical properties and their variation, variation of geometrical properties, fabrication effects and controls, tolerances, environmental conditions, inspection, quality control guidelines.

STRUCTURAL SAFETY AND PROBABILISTIC METHODS (10)

C. A. Cornell	Mass. Inst. Tech.	Cambridge	USA
L. Esteva	Ciudad Universitaria	Mexico City	MEX
R. Meli	Ciudad Universitaria	Mexico City	MEX

Failure criteria, reliability of structures, methodology for consistent safety, methods for evaluating uncertainty, methods for establishing safety levels.

FIG. 24

TURBULENCE AND WIND FORCE EFFECTS ON STRUCTURES

by

Robert H. Scanlan

Department of Civil Engineering
Princeton University
Princeton, New Jersey, USA 08540

Synopsis

The paper first briefly considers the wind profile of the planetary boundary layer. State-of-the-art formulas for spectra and co-spectra of wind gustiness are cited. After reference to turbulence intensity and scales, methods for the experimental simulation of turbulent winds are discussed. The need for correct experimental similitude is emphasized. Types of turbulent flow induction in wind tunnels are reviewed, and some important experimental effects are noted. Methods for calculating wind effects and structural response to wind (where such calculation is presently possible) are cited. Examples of analytical formulations pertinent to the response of tall buildings and bridges, are presented. References are cited for more extensive treatment of the topics discussed.

I The Planetary Boundary Layer

A. The Wind Profile -- Boundary layer theory, and certain simplifications thereof which are beyond the scope of the present paper, result in a definition of the mean horizontal wind velocity U as a function of altitude z according to the following formula:

$$U(z) = \frac{1}{\kappa} u_* \ell n \frac{z-z_d}{z_o} \qquad (1)$$

where $\kappa \cong 0.4$ is Karman's constant, z_d is the average height of surrounding buildings (as defined subsequently), z_o is a roughness length characteristic of the terrain fetch over which the wind arrives at the point in question, and u_* is a "friction" velocity characteristic of the flow. These quantities are defined below; z_o must be selected from information such as that abridged here in Table 1

Table 1

Type of Surface	z_o (cm)
Sea	0.0003 (calm) to 0.5 (windy)
Grass	0.1 (mowed) to 1.0 (high)
Brush	10 to 30
Pine forest (15m high)	90 to 100
Suburbs	20 to 40
Centers of towns	35 to 45
Centers of large cities	60 to 80

Zero-plane displacement is

$$z_d = \bar{H} - z_o/0.4 \tag{2}$$

where $\bar{H}$ is average height of surrounding buildings (if any). Friction velocity is obtainable from reference information, i.e.

$$u_* = \frac{0.4U(z_{ref})}{\ell n \frac{z_{ref}-z_d}{z_o}} \tag{3}$$

where $U(z_{ref})$ is wind velocity specified at some reference height z_{ref}. (Typically z_{ref} = 10 meters for weather data.) Outdoor mean-wind velocity measurements generally conform well to Eq.(1), except for cases involving strong local effects.

B. Autospectra of the Turbulence -- The total horizontal wind velocity may be expressed as U + u, where U is the mean wind velocity defined by the boundary layer profile given above, and u = u(t) is the time-dependent or gust velocity, that is, the horizontal component of the turbulence. The lateral and vertical velocity components of the turbulence are designated v(t) and w(t), respectively.

The principal cause of that turbulence which interests the civil engineer in the atmospheric boundary layer is the mechanical stirring of the wind as it passes over and around objects on the earth's surface. Formulas developed from both theory and outdoor measurements for the distribution of wind turbulent energy have been developed.

The power spectral density S_u (autospectrum) of horizontal gust velocities in strong winds has been given [1], [2] in the form

$$\frac{n\, S_u(z,n)}{u_*^2} = \frac{200f}{(1 + 50f)^{5/3}} \tag{4}$$

where n is frequency in Hertz, and

$$f = \frac{nz}{U(z)} \tag{5}$$

The spectrum of vertical velocity fluctuations up to about 50m may be estimated by the analogous formula [3]

$$\frac{n\, S_w(z,n)}{u_*^2} = \frac{3.36f}{1 + 10f^{5/3}} \tag{6}$$

For lateral velocity fluctuations a corresponding formula [1] is

$$\frac{n\, S_v(z,n)}{u_*^2} = \frac{15f}{(1 + 9.5f)^{5/3}} \tag{7}$$

(Note that the dimension of S_u, S_v, or S_w is m^2/sec)

C. Cross-Spectra of the Turbulence -- Horizontal velocity will be considered first. The cross-spectrum of two wind records $u_1(t)$, $u_2(t)$, taken at two points 1 and 2 a distance r apart is designated

$$S^{Cr}_{u_1 u_2}(r,n) = S^{C}_{u_1 u_2}(r,n) + i\, S^{Q}_{u_1 u_2}(r,n) \tag{8}$$

where $i = \sqrt{-1}$ and S^C, S^Q are the co- and quad-spectra, respectively. The coherence function Coh(r,n) is defined by

$$[Coh(r,n)]^2 = \{[S^{C}_{u_1u_2}(r,n)]^2 + [S^{Q}_{u_1u_2}(r,n)]^2\}/S_{u_1} S_{u_2} \tag{9}$$

where S_{u_1}, S_{u_2} are the autospectra at points 1 and 2, respectively. In homogeneous turbulence, and approximately, in atmospheric turbulence, S^Q vanishes.

Let (y_i,z_i) be the respective horizontal and vertical coordinates of a point i in a vertical plane; the following empirical expression for coherence of horizontal wind velocities has been offered [4], [5]:

$$Coh(r,n) = e^{-\hat{f}} \tag{10}$$

where

$$\hat{f} = \frac{n[C_{1z}^2 (z_1-z_2)^2 + C_{1y}^2 (y_1-y_2)^2]^{1/2}}{\frac{1}{2}[U(z_1) + U(z_2)]} \tag{11}$$

and $C_z \cong 10$, $C_y \cong 16$ are approximations representing present knowledge. Actually, these coefficients are probably dependent upon fetch conditions as well as height above ground. An alternative form of the result (10) for engineering calculations is

$$S^{C}_{u_1u_2}(r,n) = S_{u_1}^{1/2}(z_1,n)\, S_{u_2}^{1/2}(z_2,n) e^{-\hat{f}} \tag{12}$$

The cross-spectrum between vertical velocity fluctuations at two points may be expressed [6], [7] by:

$$S_{w_1w_2}(\Delta y,n) = S_w(z,n) e^{\frac{-8n\Delta y}{U(z)}} \tag{1}$$

where Δy is the horizontal separation of the points 1 and 2.

Cross spectra of lateral velocity fluctuations may tentatively be assumed [8] to be given by an expression like (12) with $C_y = 7$, $C_z \cong 10$.

The present summary of velocity profile and spectral information is taken from Ref. [9].

D. Turbulence Intensities and Scales -- Perceived of as a time-varying function, the wind velocity may be considered to be made up of a steady part, of value U, plus Fourier components of sinusoidal nature associated with various frequencies n ranging from a low of 2 or 3 cycles per hour to high frequencies of 10 or 15 cycles per second. If the concept of "wavelength" λ is introduced in the form $\lambda = U/n$, some measure of "gust size" is obtained thereby. A representative, or average, alongwind wavelength of atmospheric gusts (normally calculated from the autocorrelation function) is termed the scale and varies in the atmosphere from about 65m to 200m, depending upon altitude, the longer wavelengths occurring at higher altitude.

Turbulence intensity I is defined as the ratio of the square root of the mean square value of the gust component in question to the mean velocity; for example the longitudinal intensity is

$$I_u = \frac{\sqrt{\overline{u^2}}}{U} \tag{14}$$

where $\overline{u^2}$ is the mean of $u^2(t)$ over same suitable averaging period. Longitudinal turbulence intensity is dependent upon fetch upstream roughness conditions and may vary from 3 or 4 percent to as high as 20 percent. Typical values may be 8 to 12 percent in high winds.

II Flow Simulations for Test Purposes

Although a few effects of the turbulent wind upon structures can be estimated by direct calculation (as will be discussed in Section IV) the flow over bluff civil engineering structures is in general so complex as to require simulation by modeling. This requires, first, that an acceptable simulation of the natural wind be provided, usually by means of wind tunnels.

A. Similitude Considerations -- Most wind tunnel testing is carried out in air and at wind velocities which are of necessity much reduced with respect to full scale. Also limited test space inevitably implies that the geometric scale of models is greatly reduced compared to prototypes. Under these conditions Reynolds and Rossby numbers* are habitually not properly simulated. Reynolds number affects the development of wake flows, drag on bodies, and turbulence. Rossby number affects the depth of the boundary layer. Space does not permit discussion of the full implications of failure to duplicate these two nondimensional numbers, but it may be stated, in brief, that present state-of-the-art testing remains provisionally acceptable with these shortcomings.

Fixed geometric scale of models is conventionally respected in all thr mutually perpendicular directions. Since this scale is in turn dependent up

---

*Reynolds number $Re = \frac{\rho UB}{\mu}$, where ρ, μ are air density and viscosity, respectively; U is mean wind velocity, and B is a typical structural dimension. Ro number $Ro = \frac{U(z)}{z\, f_c}$, where U(z) is the mean wind velocity at height z; f_c is t Coriolis parameter $f_c = 2\,\omega \sin\phi$, where ω is the angular rate of rotation of th Earth and ϕ is the angle of latitude.

the length scales of turbulence which can be achieved, the basic geometric scale usually employed ranges from 1/500 to 1/100. Larger scales have, to date, not been achieved.

An important consideration which must be respected, both for frequencies of turbulent eddies and for structural frequencies, is the reduced frequency relation requiring that

$$\left(\frac{U}{NB}\right)_{\text{model}} = \left(\frac{U}{NB}\right)_{\text{prototype}} \qquad (15)$$

where U is relocity, N is any frequency, and B any representative structural dimension.

Roughness elements, simulating the earth's surface, tripping the turbulent boundary layer and establishing the spectra of turbulence, are normally duplicated to geometric scale, except for certain special devices to be discussed in relation to short tunnels, below.

B. Long Boundary-Layer Tunnels -- [10] [11] A relatively stable, well-established turbulent boundary layer with duplicated mean velocity profile can be achieved with a 20 to 30-meter long tunnel having a floor covered with appropriately-spaced "roughness elements" often consisting of cubic blocks. At the end of a long fetch of such blocks a test model (often a building immersed in geometrically duplicated building models of the surrounding city) is installed. Pressure taps in a fixed model or accelerometers in an aeroelastic model pick up desired information.

C. Short-Tunnel Devices -- [12] [13] [14] [15] Various schemes have been introduced to create the desired turbulence and/or boundary layer conditions within short distances inside either an aeronautical-type tunnel or a special, short tunnel created for the purpose. The main devices used to set up the desired turbulent boundary layer are 1) air jets parallel to the general flow: 2) air jets counter to the general flow; and 3) spires or other "trip" devices. Each of the devices has its particular attributes.

The longitudinal jets permit, in principal, fine control of the velocity profile, though with considerable adjustment required because of fairly unpredictable jet interaction. The spires set up a boundary layer about equal in depth to the spire height. They are followed by a surface covered with blocks of sizes and locations dictated by test explorations of the boundary layer. Finally the counter-jet technique is a device which in essence replaces the spires as a turbulent boundary layer trip device, through forcing air jets from the floor of the tunnel diagonally upward with a slight upst component. All short-tunnel devices may be conceived of as setting up a turbulent boundary layer by trial and error to achieve assumed "target" profiles and turbulence spectra. In the absence of known target criteria short tunnel methods could not be effective. All turbulence scales are relatively short, the largest (achieved in a 30-foot-diameter aeronautical tunnel) being of the order of 1/100 of full scale.

A final device that should be mentioned is the simple grid of bars p across the wind tunnel [16] [17]. Grid-induced turbulence is usually chara ized by small-scale spectra which reasonably approximate homogeneous turbulence but without a boundary-layer velocity profile.

III Effects of Winds in the Earth's Boundary Layer upon Structures

Most civil engineering structures present bluff contours to the wind. Even without the effects of incident turbulence such structures initiate turbulence of their own making, called "signature" turbulence. Incident and signature turbulence effects together typify the flows over buildings and other structures, and the resulting pressure distributions reflect both these effects. Thus mean as well as time-varying pressure distributions over a given structure are affected by its geometric shape and the fact that, within the planetary boundary layer, it is under the influence of particular fetch conditions.

It is usual to describe local pressures in terms of nondimensional pressure coefficients C_p defined by

$$C_p = \frac{p-p_o}{\frac{1}{2}\rho U_\infty^2} \tag{16}$$

where $p-p_o$ is the local pressure difference with respect to a reference value of and $1/2\ \rho U_\infty^2$ is the velocity pressure based on U_∞ which is some velocity far upstream (or above the bluff body in question, ρ being air density.

A classic experiment by Jensen and Franck [18] early revealed the importance of both boundary layer velocity profile and turbulence as a function of fetch on the steady pressures developed over a small house. When attempting to duplicate, by wind tunnel simulation, the full-scale average, or steady, pressure coefficients developed over the house in question, the investigators found it indispensable to duplicate the upstream fetch properly in the wind tunnel.

In another series of expertments Baines [19] displayed the strong differences that existed between averaged pressure coefficients over building models tested alternately under uniform laminar and simulated boundary layer profile conditions. The condition of turbulence generally has a strong effect upon the pressures developed over structures. Also, the particular geometry of a structure may be such that the signature turbulence shed from it strongly affects local pressure distributions [20]. This is particularly marked, for example, when architectural treatments of windows, corners, or mullions affect the local flows over a building. A few results of full-scale measurement are available. Ref. [21] is one of the few comparing wind tunnel and full-scale results on a large commerical building. Ref. [22] offers a number of papers on full-scale measurements. Ref. [37] gives important information on the effects of turbulence on houses.

IV The Calculation of Turbulent Wind Effects on Structures

Although, as stated earlier, most effects of wind on structures depend strongly on wind-tunnel testing for their confirmation, a few theoretical, o quasi-theoretical, approaches to the definition of wind effects have been ma Notable among these have been methodologies for the prediction of the along-wind response of tall buildings and towers and the prediction of the perfor-ance of long, suspended-span bridges and other line-like structures under wi

Broadly speaking, the approaches to these problems are all based on the theory of random, space- and time-dependent loadings of elastic structures. Both problems assume the wind to have stationary random properties about its mean steady velocity, and both make use of empirical observations, either about the wind alone, or the particular manner in which the wind affects the structure in question.

A. Along-Wind Response of Tall Buildings -- The problem of the along-wind response of tall buildings of simple prismatic form has been the subject of quasi-theoretical calculations [5], [23], [24], [25], [26]. The along-wind response, calculated as though the wind were directed normally to a face of the building, has experimentally been found to be the greatest of the possible responses to wind, and so it has certain design usefulness. Space does not permit development of the entire theory here, but allusion will be made to the conceptual form of the problem and to the variables entering into the final results obtained.

The wind, of velocity U+u(t), is assumed to impinge normally on the building face; the mean wind U is a function of height z: $U = U(z)$. The pressure p against the face is assumed to vary as u(t), since wind dynamic pressure is proportional to $1/2\ \rho U^2 + \rho U u(t)$, when $u^2(t)$ is legitimately neglected. Pressure coefficients C_w on the windward face and suction coefficients C_ℓ on the leeward face of the building are assumed known, or estimated. Building dimensions are taken as width B and height H, with y and z being corresponding local coordinates. The variable wind forces being proportional to u(t), the direct and co-spectra of u between points (y_1,z_1) and (y_2,z_2) play key roles in the response definition. The direct spectrum of u is designated by $S_u(z,n)$ for any height z. Lateral coherence effects of wind are accounted for by the introduction of a coherence function Coh(y,z,n). These parameters account for the main effects of the wind. Most depend to a greater or lesser extent upon empirical observations. Full details will not be given.

In addition, building response to wind depends upon the mechanical characteristics of the structure: notably, for buildings, the first two vibration modes $x_i(z)$ $(i = 1,2)$, the corresponding generalized masses M_i and associated frequencies n_i, and damping ratios ζ_i. One may visualize the building response then as that of a linear, multi-degree oscillator to inputs which are random in space and time.

The net formula for the power spectral density of the along-wind displacement x at a point z along the building height can be given as [9]:

$$S_x(z,n) \cong \frac{\rho^2}{16\pi^4} \sum_i \frac{x_i^2(z)[C_w^2 + 2C_w C_\ell N(n) + C_\ell^2]}{n_i^4 M_i^2 \left\{[1-(\frac{n}{n_i})^2]^2 + 4\zeta_i^2 (\frac{n}{n_i})^2\right\}} \tag{1}$$

$$\times \int_0^B \int_0^B \int_0^H \int_0^H x_i(z_1) x_i(z_2)\, U(z_1)\, U(z_2) S_u^{1/2}(z_1,n) S_u^{1/2}(z_2,n)$$

$$\times \mathrm{Coh}(y_1,y_2,z_1,z_2,n)\ dy_1, dy_2, dz_1, dz_2$$

From this the mean square of the fluctuation x is calculated by

$$\sigma_x^2(z) = \int_0^\infty S_x(z,n)\,dn \tag{18}$$

and the corresponding mean square acceleration by

$$\sigma_{\ddot{x}}^2(z) = 16\pi^4 \int_0^\infty n^4 S_x(z,n)\,dn \tag{19}$$

The maximum variable excursion $x_{max}(z)$ is estimated by

$$x_{max}(z) = K_x(z)\ \sigma_x(z) \tag{20}$$

where K_x is in the neighborhood of 3.5. For gaussian processes this is a good estimate, but it can be improved by existing theory [27] [28] for more general cases. To this deflection must be added the steady deflection $\bar{x}(z)$ calculated under the steady mean wind U(z).

The concept of a gust factor G is conveniently introduced and explained in this context by defining

$$G = 1 + \frac{x_{max}}{\bar{x}} \tag{21}$$

so that G may be thought of as a design factor by which the standard static wind deflection is multiplied to yield the maximum result.

For a complete discussion of the along-wind buffeting problem of tall buildings and extensive aids to making the necessary calculations in practical cases, the reader is referred to the literature cited, particularly Ref. [26].

B. Buffeting Response of Suspended-Span Bridges -- [29]-[34] The problem of building response, treated briefly above, has several parallels. Space does not permit a full treatment of such cases, but one-- that of bridges-- will be discussed briefly. It is worthwhile to suggest here the form which solutions to this problem take.

The power spectral density of response in torsional modes $\alpha_i(x)$ of a long suspended-span bridge is given in the form

$$S_\alpha(x,n) \cong \sum_i \frac{\alpha_i^2(x)\int_0^L\int_0^L \alpha_i(x_1)\ \alpha_i(x_2)\, S^C_{M_1M_2}(x_1,x_2,n)\,dx_1\,dx_2}{16\pi^4 \tilde{n}_{\alpha_i}^4\ I_i^2\left\{\left[1-\left(\frac{n}{\tilde{n}_{\alpha_i}}\right)^2\right]^2 + 4\tilde{\zeta}^2_{\alpha_i}\left(\frac{n}{\tilde{n}_{\alpha_i}}\right)^2\right\}} \tag{22}$$

in which L is span length, I_i is the generalized mass moment of inertia of mode relative to the effective rotation axis, $S^C_{m_1m_2}(x_1,x_2,n)$ is the co-spectral density of the buffeting moment on the bridge relative to section x_1, $\tilde{n}_{\alpha_i}$ is the natural frequency of mode $\alpha_i(x)$ as modified by aerodynamic force

and $\tilde{\zeta}_{\alpha_i}$ is the damping of this mode as influenced by self-exciting aerodynamic effects. The self-excitation effect is a key influence here which the given references treat in a detailed manner. Many details are necessarily omitted in the present review.

C. Buffeting of Towers and Stacks -- [35], [36] These problems are treated in a manner very analogous to that sketched in sections IV A and IV B above.

V Comment and Conclusion

A number of state-of-the-art facts concerning the nature of the turbulent wind and its effects have been rapidly reviewed. References to recent literature are given. This overview may be of value to those interested in how the effects discussed may be dealt with in the process of structural design.

References

1. Kaimal, J. C., et al: "Spectral Characteristics of Surface-Layer Turbulence" Quart. Jnl. Royal Met. Soc. Vol.98, 1972, pp.563-589.

2. Simiu, E.: "Wind Spectra and Dynamic Alongwind Response" Jnl. Struct. Div., ASCE Vol.100, ST.9, Sept. 1974, pp.1897-1910.

3. Lumley, J. L. and Panofsky, H. A.: The Structure of Atmospheric Turbulence Wiley, 1964.

4. Davenport, A. G.: "The Dependence of Wind Loads upon Meteorological Parameters" Proc. Int'l. Seminar on Wind Effects on Buildings and Structures, Univ. of Toronto Press, 1968.

5. Vickery, B. J.: "On the Reliability of Gust Loading Factors" Proc. Technical Conf. on Wind Loads on Buildings and Structures, Nat'l. Bur. Standards, Building Science Series 30, Washington, D.C. 1970.

6. Shiotani, M.: "Structure of Gusts in High Winds" Interim Report, Parts 1-4, The Physical Sciences Laboratory, Nihon University, Furabashi, Chiba, Japan 1967-1971.

7. Shiotani, M. and Iwatani, Y.: "Correlations of Wind Velocities in Relation to the Gust Loading" Proc. Third Int'l. Conf. on Wind Effects on Buildings and Structures, Tokyo, 1971.

8. Blackadar, A. K., Panofsky, H. A., and Fiedler, F.: "Investigation of the Turbulent Wind Field Below 500 Feet Altitude at the Eastern Test Range, Florida" NASA CR-2438, National Aeronautics and Space Administration, Washington, D.C. June 1974.

9. Simiu, E. and Scanlan, R. H.: Wind Effects on Structures Wiley, N. Y. (in Press 1977).

10. Cermak, J. E.: "Laboratory Simulation of the Atmospheric Boundary Layer" AIAA Journal, Vol.9, No.9, Sept. 1971, pp.1746-1754.

11. Davenport, A. G., and Isyumov, N.: "The Application of the Boundary Layer Wind Tunnel to the Prediction of Wind Loading" Proc. Int'l Research Seminar, Wind Effects on Bldgs. and Struct., Ottawa, Univ. of Toronto Press, Canada, 1968.

12. Hunt, J. C. R., and Fernholz, H.: "Wind Tunnel Simulation of the Atmospheric Boundary Layer: A Report on Euromach 50" Jnl. Fluid Mech Vol.70, part3, Aug. 1975, pp.543-559.

13. Cook, N. J.: "A Boundary Layer Wind Tunnel for Building Aerodynamics Jnl. Indust. Aerodynamics, Vol.1, 1975, pp.3-12.

14. Standen, N. M.: "A Spire Array for Generating Thick Turbulent Shear Layers for Natural Wind Simulation in Wind Tunnels" Report LTR-LA-94, NAE National Research Council, Ottawa, Canada, May 1972.

15. Nagib, H. M., Morkovin, M. V., Yung, J. T., and Tan-atichat, J.: "On Modeling of Atmospheric Surface Layers by the Counter-Jet Technique" AIAA Jnl. Vol.14, No.2, Feb. 1976, pp.185-190.

16. Bearman, P. W.: "An Investigation of the Forces on Flat Plates in Turbulent Flow" NPL Aero Report 1296, Teddington, U.K. 1969.

17. Vickery, B. J.: "On the Flow Behind a Course Grid and Its Use as a Model of Atmospheric Turbulence in Studies Related to Wind Loads on Buildings" NPL Aero Report 1143, Teddington, U.K. 1965.

18. Jensen, M. and Franck, N.: "Model-Scale Tests in Turbulent Wind" The Danish Technical Press, Copenhagen, 1965.

19. Baines, W. D.: "Effects of Velocity Distribution on Wind Loads and Flow Patterns on Buildings" Proc. Sympos. on Wind Effects, Vol.I, Nat'l. Phys. Lab., Teddington, U.K. 1963, pp.197-223.

20. Peterka, J. A. and Cermak, J. E.: "Wind Pressures on Buildings—Probability Densities" Jnl. Struct. Div. ASCE Vol.101 No.ST6, June 1975, pp.1255-1267.

21. Dalgliesh, W. A.: "Comparison of Model/ Full Scale Wind Pressures on a High-Rise Building" Jnl. Indust. Aerodyn. 1, 1975, pp.55-66.

22. Davenport, A. G., Editor: Proc. Symposium on Full-Scale Measurements of Wind Effects on Tall Buildings and Other Structures, Univ. Western Ontario, London, Canada, June 1974.

23. Davenport, A. G.: "Gust Loading Factors" Jnl. Struct. Div., ASCE Vol.93, No.ST3, June 1967, pp.11-34.

24. Vellozzi, J. and Cohen, E.: "Gust Response Factors" Jnl. Struct. Div. ASCE Vol.94, No.ST6, June 1968, pp.1295-1313.

25. Simiu, E.: "Gust Factors and Along-Wind Pressure Correlations" Jnl. Struct. Div., ASCE Vol.99, No.ST4, April 1973, pp.773-783.

26. Simiu, E. and Lozier, D. W.: The Buffeting of Tall Structures by Strong Winds Building Science Series 74, National Bureau of Standards, Wash., D.C. Oct. 1975.

27. Davenport, A. G.: "Note on the Distribution of the Largest VAlue of a Random Function with Application to Gust Loading" Proc. Instn. of Civil Engrs Vol.28, 1964, pp.187-196.

28. Rice, S. O.: "Mathematical Analysis of Random Noise" Bell System Tech Jnl. Vol.18, 1944, p.282, Vol.19, 1945, p.46.

29. Davenport, A. G.: "The Response of Slender, Line-Like Structures to a Wind" Proc. Instn. of Civil Engrs. London, 1962, pp.389-407.

30. Davenport, A. G.: "The Buffeting of a Suspension Bridge by Storm Winds" Jnl. Struct. Div., ASCE June 1962, pp.233-264.

31. Davenport, A. G.: "The Action of Wind on Suspension Bridges" Proc. Int'l. Sympos. on Susp. Bridges, Lisbon, 1966, pp.79-100.

32. Scanlan, R. H. and Gade, R. H.: "Motion of Susponded Bridge Spans under Gusty Wind" (in press) Jnl. Struct. Div. ASCE 1977.

33. Scanlan, R. H. and Tomko, J. J.: "Airfoil and Bridge Deck Flutter Derivatives" Jnl. Eng. Mech. Div., ASCE Vol.97, EM6, Dec. 1971, pp. 1717-1737.

34. Scanlan, R. H. and Lin, W. H.: "Response of a Bridge-Like Structure to Turbulence" (in review) Jnl. Eng. Mech. Div. ASCE, 1977.

35. Ruscheweyh, H.: "Wind Loadings on the Television Tower, Hamburg, Germany" Jnl. Indust. Aerodyn., Vol.1, No.4, Aug. 1976, pp.315-333.

36. Vickery, B. J., and Clark, A. W.: "Lift or Across-Wind Response of Tapered Stacks" Jnl. Struct. Div., ASCE, Jan. 1972, pp.1-20.

37. Marshall, R. D. Building to Resist the Effect of Wind National Bureau of Standards Building Science Series, No.100 May 1977 Vols.1 and 2.

AERODYNAMIC RESPONSES OF BRIDGE STRUCTURES SUBJECTED TO STRONG WINDS

Naruhito Shiraishi & Masaru Matsumoto

Department of Civil Engineering
Faculty of Engineering
Kyoto University
Kyoto, Japan

Synopsis: This paper presents the method of analysis of buffeting oscillations of bridge structures subjected to vertical gust. Particular attention is placed on evaluation of unsteady aerodynamic characteristics of bridge structures and also on estimation of unsteady response by using the aerodynamic impulsive lift function.

1. Introduction

During last decade aerodynamic characteristics of long span bridges and high rise buildings have been studied by a number of investigators,placing stress on aerodynamic instability problem. As for bridge structures, one can note a remarkable progress to examine flutter phenomenon of bridge sections in order to have the critical wind velocity sufficiently higher than the specified design wind velocity. The high critical wind velocity of bridge structure, however, may not assure aerodynamic safety since atmospheric strong winds are so turbulent as to induce buffeting. After Davenport(1961)[1] various efforts have been made to present feasible method of wind resistant design for buffeting problem for different type of structures. Through the research project of aerodynamic characteristics of long span suspension bridge at Kyoto University, the method of analysis is searched for on random deflectional responses of bridge structures subjected to turbulent air flows [5].

This paper is concerned with crucial aerodynamic parameters in analysis of buffeting oscillations, namely lift transfer function, aerodynamic damping ratio and spatial coherency function. Numerically the calculated responses by the method presented are compared with the corresponding measured responses obtained by the "Large Scale Test Bridge Model Operation" undertaken jointly by the Honshu Shikoku Bridge Authority and the Technical Committee on Wind Resistant Design of the Japan Society of Civil Engineers (1977) [3].

2. Unsteady Aerodynamic Lift

In this paragraph an unsteady lift and aerodynamic damping associate with typical bridge sections are studied based on wind tunnel tests for bridge models in sinusoidally varying and turbulent air flows.

2.1 Lift Transfer Function

Unsteady lift L(t) per unit length in spanwise direction due to vertical gust w(t) can be written as

$$L(t) = 2\pi \rho b \bar{U} w(t) A_d(k') \tag{1}$$

in which $A_d(k')$ is termed here as the lift transfer function of reduced frequency and characterizes magnitude of timely varying lift and phase difference between lift and vertical gust.

Experimentally the lift transfer function can be determined directly by use of eq. (1) once lift is measured in sinusoidally varying vertical gust. Alternatively it can be determined by

$$\{A_d(k')\}^2 = \left(\frac{1}{2\pi \rho b \bar{U}}\right)^2 \frac{S_L(\omega)}{S_w(\omega)} \tag{2}$$

for randomly varying vertical gust.

Lift transfer functions experimentally obtained for typical cross sections are illustrated in Fig. 1 for both cases of sinusoidal and random vertical gusts, in which solid lines indicate the absolute values of the Sears function and dashed lines indicate corrected values multiplied by the ratio of slope of lift coefficient and 2π . Note the difference between the lift transfer functions for plate-like sections (as NACA 0012 and trapezoidal section) and the lift transfer function for the H-section to which stall flutter is generally incidental.

2.2 Aerodynamic Damping

It is already known that the aerodynamic derivative corresponding to aerodynamic damping takes an important role for analysis of buffeting of bridge structures. The equation of motion for deflectional oscillations of bridge is frequently written as

$$\ddot{\eta} + 2\zeta_0 \omega_0 \dot{\eta} + \omega_0^2 \eta = H_1 \dot{\eta} \tag{3}$$

in which H_1 indicates the aerodynamic damping capacity dependent on reduced frequency [8]. In smooth flow the derivative H_1 is well-defined quantity, while in turbulent flow it is dependent on not only reduced frequency but turbulence characteristics for rectangular cross section [6]. In order to estimate aerodynamic damping in turbulent flow the method proposed by Jeary and Winney (1972) [2] is employed in this investigation; namely the aerodynamic derivative H_1 is experimentally determined from envelope of autocorrelation of random responses in turbulent flows in wind tunnel tests.

3. Analysis of Unsteady Buffeting Responses

The longer the span length of bridge, the more flexible the bridge structure, so that it tends to vibrate with less structural damping and to respond to various types of timely dependent external forces. It should be mentioned that

vibrations due to impulsive action of wind forces for flexible bridge structures will continue for several and sometimes ten times longer duration than natural period and responses are, therefore, remarkably influenced by transient characteristics. Though there are a number of previous reports based on the assumption of buffeting responses as the steady stochastic process, which is considered feasible theoretically, one needs to take transient response characteristics into an account for evaluation of buffeting responses of certain limited length of time.

3.1 Spectral Analysis of Unsteady Buffeting Responses

In this paragraph an effect of aerodynamic damping is sought for on buffeting responses of structures subjected to vertical gust with aid of the evolutionary power spectrum [7,9] for which the damping ratio of vibrational system of narrow band-width filter is taken as 0.05 [4].

Assuming the Sears function for lift transfer function, the deflectional response of plate-like structure is written as

$$\eta(t)=\frac{2\pi\rho b\bar{U}}{m\omega_0^2\sqrt{1-\zeta^2}}\int_0^t h_1(t-\tau)\int_0^\tau h_2(\tau-\tau_1)w(\tau_1)\,d\tau_1\,d\tau \tag{4}$$

where

$$h_1(t)=\mathcal{F}^{-1}\{H(\omega)\}=e^{-\zeta\omega_0 t}\sin\omega_0\sqrt{1-\zeta^2}\,t$$

$$h_2(t)=\mathcal{F}^{-1}\{S(k')\}$$

$$H(\omega)=\left\{1-\frac{\omega^2}{\omega_0^2}+2i\zeta\frac{\omega}{\omega_0}\right\}^{-1}$$

The evolutionary power spectrum $G_\eta(t,\omega)$ for deflectional response is directly obtained by use of eq. (4) and alternatively it can be estimated by the following expression

$$G_\eta^*(t,\omega)=\frac{2\pi\rho b\bar{U}}{m^2\omega_0^4(1-\zeta^2)}|H(\omega)|^2\cdot|S(\omega)|^2\cdot G_w(t,\omega) \tag{5}$$

where $G_w(t,\omega)$ is the evolutionary power spectrum for vertical gust. Thus two unstationary variances for deflectional responses are defined by use of $G_\eta(t,\omega)$ and $G_\eta^*(t,\omega)$, respectively, as

$$\sigma_\eta^2(t)=\int_0^\infty G_\eta(t,\omega)\,d\omega \tag{6}$$

$$\sigma_\eta^{*2}(t)=\int_0^\infty G_\eta^*(t,\omega)\,d\omega$$

An example of numerical results is illustrated in Fig. 2 for the structure which vibrational characteristics are given in Table 1. This shows that the smaller the damping ratio ζ the more remarkable the difference between unstationary variances by eq.(6) and eq.(7). In other words buffeting responses are not only responsible for instantaneous action

of external force but prior history of responses to the action of external force, namely the transient response characteristics, for small damping system. Note that one tends to have the larger peak value by eq.(7) than the peak value by eq.(6).

3.2 Direct Analysis of Unsteady Buffeting Responses

The method of analysis will be introduced in connection with analysis of deflectional responses of test bridge (section model) used in the "Large Scale Bridge Model Operation" [5]. Since the measurement of wind velocities is performed at both right and left hand sides of model, resultant unsteady lifts can be written as

$$L_w(t) = \frac{1}{4}\rho B \ell \frac{dC_F}{d\alpha} \cdot X_{w_1}(f) \cdot X_{w_2}(f) \cdot \left\{ \bar{U}_L w_L(t) + \bar{U}_R w_R(t) \right\} \tag{8}$$

$$L_u(t) = \frac{1}{2}\rho B \ell \left\{ C_F + \frac{dC_F}{d\alpha} \bar{\alpha} \right\} \cdot X_{u_1}(f) \cdot X_{u_2}(f) \cdot \left\{ \bar{U}_L u_L(t) + \bar{U}_R u_R(t) \right\} \tag{9}$$

where L_w denotes the lift induced by vertical gust and L_u is the lift induced by longitudinal gust.

And the effective gust functions are introduced in eq's (8) and (9) as

$$\begin{aligned}
X_{w_1}(f) &= \left\{ \frac{2}{\gamma_{xw}^2} \left(\gamma_{xw} - 1 + e^{-\gamma_{xw}} \right) \right\}^{1/2} & \gamma_{xw} &= k_{xw} \frac{Bf}{\bar{U}} \\
X_{u_1}(f) &= \left\{ \frac{2}{\gamma_{xu}^2} \left(\gamma_{xu} - 1 + e^{-\gamma_{xu}} \right) \right\}^{1/2} & \gamma_{xu} &= k_{xu} \frac{Bf}{\bar{U}} \\
X_{w_2}(f) &= \left\{ \frac{2}{\gamma_{yw}} \left(\gamma_{yw} - 1 + e^{-\gamma_{yw}} \right) \right\}^{1/2} & \gamma_{yw} &= k_{yw} \frac{\ell f}{\bar{U}} \\
X_{u_2}(f) &= \left\{ \frac{2}{\gamma_{yu}} \left(\gamma_{yu} - 1 + e^{-\gamma_{yu}} \right) \right\}^{1/2} & \gamma_{yu} &= k_{yu} \frac{\ell f}{\bar{U}}
\end{aligned} \tag{10}$$

which indicate chordwise or spanwise spatial correlations of lift due to longitudinal or vertical gusts.

Denoting ζ as apparent damping ratio, the sum of structural and aerodynamic dampings, we have

$$\eta(t) = \eta_i(t) + \eta_w(t) + \eta_u(t) \tag{...}$$

where

$$\eta_i(t) = e^{-\zeta\omega_0 t} \left\{ \left(\frac{\dot{\eta}(0)}{\eta(0)\omega_0} + \zeta \right) \eta(0) \sin\omega_0 t + \eta(0) \cos\omega_0 t \right\} \tag{...}$$

$$\eta_w(t) = \frac{\rho B (dC_F/d\alpha)}{4m\omega_0^2\sqrt{1-\zeta^2}} \int_0^t h(t-\tau) \left\{ \bar{U}_L \int_0^\tau H_w(\tau-\tau_1) w_L(\tau_1) d\tau_1 + \bar{U}_R \int_0^\tau H_w(\tau-\tau_1) w_R(\tau_1) d\tau_1 \right\} d\tau \tag{...}$$

$$\eta_u(t) = \frac{\rho B}{2m\omega_0^2\sqrt{1-\zeta^2}}\left\{C_F + \frac{dC_F}{d\alpha}\bar{\alpha}\right\}\int_0^t h(t-\tau)\left\{\bar{U}_L\int_0^\tau H_u(\tau-\tau_1)u_L(\tau_1)d\tau_1 + \bar{U}_R\int_0^\tau H_u(\tau-\tau_1)u_R(\tau_1)d\tau_1\right\}d\tau \qquad (14)$$

$$h(t) = e^{-\zeta\omega_0 t}\sin\omega_0\sqrt{1-\zeta^2}\,t$$

$$H_w(t) = \mathcal{F}^{-1}\{X_{w_1}(f)\cdot X_{w_2}(f)\}$$

$$H_u(t) = \mathcal{F}^{-1}\{X_{u_1}(f)\cdot X_{u_2}(f)\}$$

4. Numerical Illustrations and Concluding Remarks

The vibrational characteristics of Large Scale Bridge Model are given in Table 2. Two components of fluctuating wind velocities at left and right positions of anemometers in above operation are shown in Fig. 3 and deflectional response of the model is evaluated by eq's (11) through (14) using wind velocities in Fig. 3 to compare with the measued response, as in Fig. 4. In this calculation the decay factor (k) in eq.(10) is assumed as 20 and the aerodynamic damping is also assumed by

$$\zeta_a = \frac{\rho\bar{U}B}{4m\omega_0}\frac{dC_F}{d\alpha} \qquad (15)$$

based on the quasi-steady theory.

The power spectral density of buffeting response is obtained from the numerical result of deflectional response, as shown in Fig. 5 - (i). According to the method of Davenport [1], the power spectral density of response is obtained as

$$S_\eta(f) = \left\{\rho\bar{U}B\left(C_F + \frac{dC_F}{d\alpha}\bar{\alpha}\right)\right\}^2\frac{1}{m^2\omega_0^4}|X_{u_1}(f)|^2\cdot|X_{u_2}(f)|^2\cdot|H(f)|^2\cdot S_u(f) + \left\{\frac{1}{2}\rho\bar{U}B\frac{dC_F}{d\alpha}\right\}^2\frac{1}{m^2\omega_0^4}|X_{w_1}(f)|^2\cdot|X_{w_2}(f)|^2\cdot|H(f)|^2\cdot S_w(f) \qquad (16)$$

which are illustrated in Fig. 5 - (ii) and (iii).

One of the causes that the latter method provides comparatively large power spectral density is considered due to the fact that the assumption of stationary stochastic process yields to larger peak value for so small damping structural system as the example shown here (ζ = 0.09).

Through the investigation for "Large Scale Bridge Model Operation", it is noted that power spectral densities of buffeing responses are sensitively dependent on aerodynamic damping as well as the decay factor of spatial correlation functions. An example is exemplified in Fig. 6 to show the effect of decay factor on power spectral density of response. Satisfactory accordance between measured and calculated responses is obtained for k = 1.25 instead of k = 7 which value is generally used for longitudinal wind velocity and k = 20 which value is frequently used for vertical wind velocity.

In our case the decay factor is not definite value but dependent on the mean velocity and satisfactory accordance between power spectral densities of measured deflection and calculated deflection with knowledge of wind velocities is obtained by assuming the proper relation between the decay factor and the mean wind velocity. As for buffeting problem of long span bridge structures it can be said that the effect of atmospheric turbulence is possibly taken into an account by determination of crucial parameters such as aerodynamic damping ratio and decay factor of spatial correlation functions.

References

1. Davenport,A.G.;"A statistical approach to the treatment of wind loading of tall masts and suspension bridges", Ph D Dissertation, University of Bristol, 1961

2. Jeary,A.P. & Winney,P.E.;"Determination of structural damping of large multi-flue chimney from the response to wind excitation", I.C.E., Part 2, Vol.53, 1972, pp 569 - 577

3. Japan Society of Civil Engineers;"Technical report on Large Scale Bridge Model Operation" May, 1977 (in Japanese)

4. Kameda,H.;"On a method of computing evolutionary power spectra of strong motion seismograms", Proc. JSCE, No.235, March, 1975, pp 55 - 62 (in Japanese)

5. Konishi,I.,Shiraishi,N. & Matsumoto,M.;"Aerodynamic response characteristics of bridge structures", 4th Int'l Conf. on Wind Effects on Buildings and Structures, 1975

6. Laneville,A. & Parkinson,G.V.;"Effects of turbulence on galloping of bluff cylinders", 3rd Int'l Conf. on Wind Effects on Buildings and Structures, 1971

7. Priestley,M.B.;"Evolutionary spectra and non-stationary process", Jour. of Royal Statistical Society, B 27, 1965

8. Scanlan,R.H. & Tomko,J.J.;"Airfoil and bridge deck flutter derivatives", Proc. ASCE, EM 6, Dec., 1971

9. Trifunac,M.D.;"Response envelope spectrum and interpretat: of strong earthquake ground motion", Bull. Seim. Soc. Am. Vol. 61, April, 1971

Notations

$A_d(k)$: lift transfer function

$\bar{\alpha}$: mean angle of attack

B : full chord length

b : half chord length

C_F : lift coefficient

$dC_F/d\alpha$: derivative of lift coefficient with respect to pitching angle

$\mathcal{F}^{-1}$: Fourier Inverse Transform

f : frequency

f_0 : natural frequency

$G_\eta(t,\omega)$: evolutionary power spectrum of heaving response

$G_w(t,\omega)$: evolutionary power spectrum of vertical gust

$H(\omega)$: frequency response function

H_1 : aerodynamic derivative (unsteady lift coefficient)

h (t) : unit impulsive response function

$k=b\omega/U$: reduced frequency

k : decay factor

k_{xu} (k_{xw}) : decay factor of chordwise coherency of longitudinal gust (vertical gust)

k_{yu} (k_{yw}) : decay factor of spanwise coherency of longitudinal gust (vertical gust)

L_u (L_w) : unsteady lift due to longitudinal (vertical) gust

ℓ : span length

m : mass per unit spanwise length

ρ : air density

$R_{\eta\eta}$: autocorrelation function of heaving response

$S(K)$: Sears function

S_f : power spectral density of external force

$S_L(\omega)$: power spectral density of fluctuating lift

$S_u(\omega)$: power spectral density of longitudinal gust

$S_w(\omega)$: power spectral density of vertical gust

$\sigma_\eta^2(t)$: non-stationary variance of response

τ : lag time

t : time

U : wind velocity

$\overline{U}$: mean wind velocity

$\overline{U}_L$: mean velocity measured by the left hand side anemometer

$\overline{U}_R$: mean velocity measured by the right hand side anemometer

u : longitudinal component of fluctuating velocity

u_L (u_R) : longitudinal gust measured by the left (right) hand side anemometer

w : vertical component of fluctuating velocity

w_L (w_R) : vertical gust measured by the left (right) hand side anemometer

ω : circular frequency

ω_0 : natural circular frequency

X_{u_1} : chordwise correlation due to longitudinal gust

X_{u_2} : spanwise correlation due to longitudinal gust

X_{w_1} : chordwise correlation due to vertical gust

X_{w_2} : spanwise correlation due to vertical gust

x : coordinates parameter

y : coordinates parameter

η : heaving (vertical) displacement

$\eta_i(t)$: transient response by initial conditions

$\eta_u(t)$: unsteady response due to longitudinal gust

$\eta_w(t)$: unsteady response due to vertical gust

ζ : total damping ratio

ζ_a : aerodynamic damping ratio

ζ_0 : structural damping ratio

Table 1 Vibrational Characteristics of Airfoil NACA 0012

NOTATION	VALUE	DIMENSION	SYMBOL
sampling time	25.0	sec	T
sampling interval	0.05	sec	T
air density	0.125	Kg sec^2 m^{-4}	ρ
mass per unit span length	0.4616	Kg sec^2 m^{-2}	m
half chord length	0.15	m	b
natural circular frequency	11.624	sec^{-1}	ω_o
total damping ratio	0.03,0.07 0.2 ,0.6		ζ
slope of lift coefficient	4.8		$dC_{F/d}$
mean wind velocity	4.0	m/sec	$\overline{U}$
span length	0.93	m	l

Table 2 Vibrational Characteristics of Model Used for "Large Scale Bridge Model Operation"

NOTATION	VALUE	DIMENSION	SYMBOL
span length	8.03	m	l
chord length	3.00	m	B
weight	3238	Kg	W
mass inertia	589	Kg m sec^2	I
height of stiffening girder	1.44	m	h
natural frequency (bending)	0.304	sec^{-1}	n_η
natural frequency (torsion)	0.672	sec^{-1}	n_φ
logarithmic damping decrement(bending)	0.055		δ_η
logarithmic damping decrement(torsion)	0.030		δ_φ
slope of lift coefficient	4.420		$dC_L/d\alpha$
drag coefficient	2.080		C_D
slope of force coefficient	5.00		$dC_F/d\alpha$

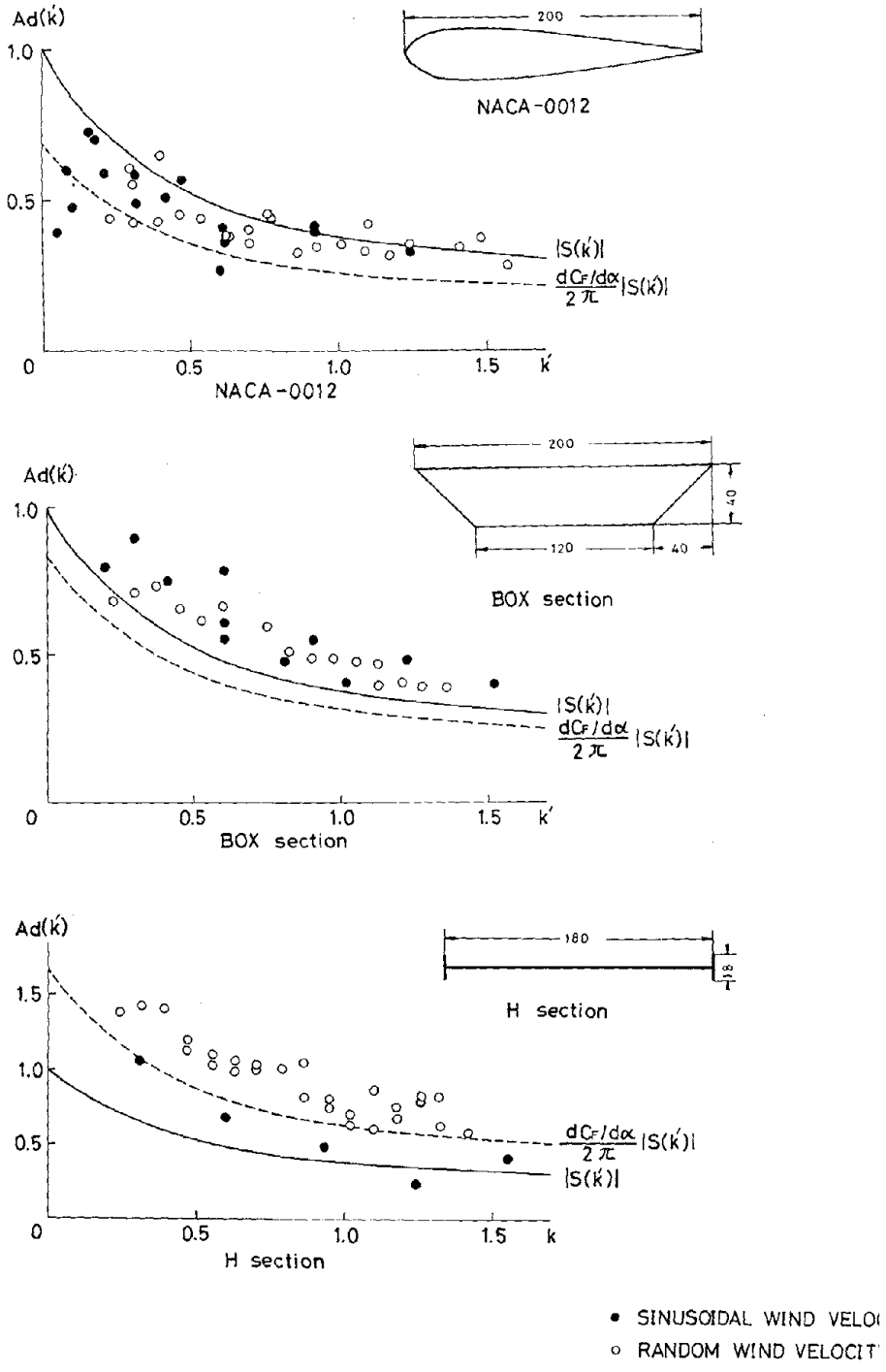

Fig.1 Lift Transfer Functions

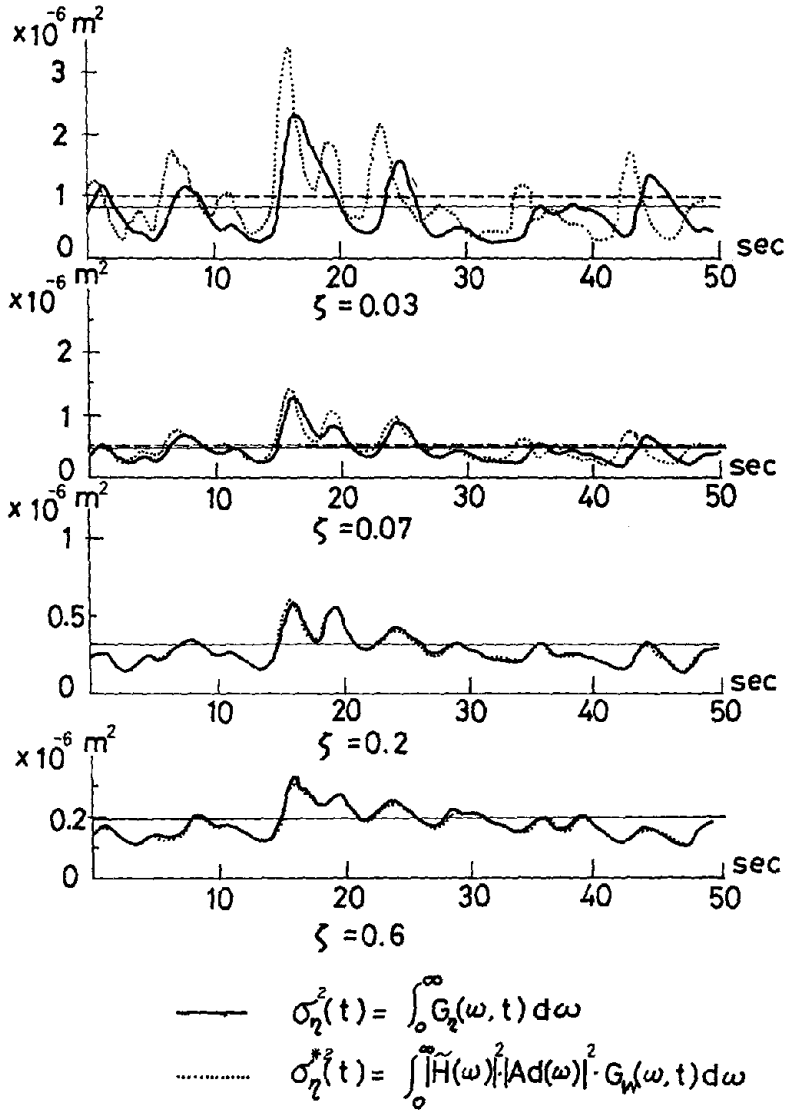

Fig.2 Evolutionary Power Spectrum of Responses

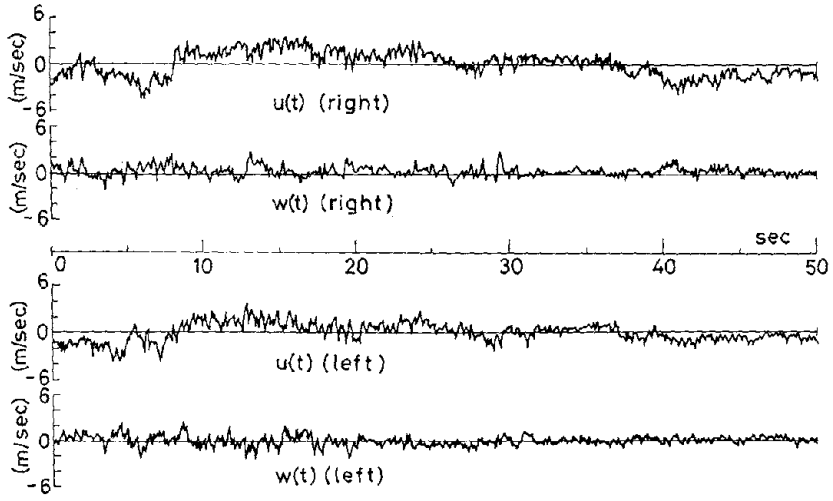

Fig.3 Measured Wind Velocities

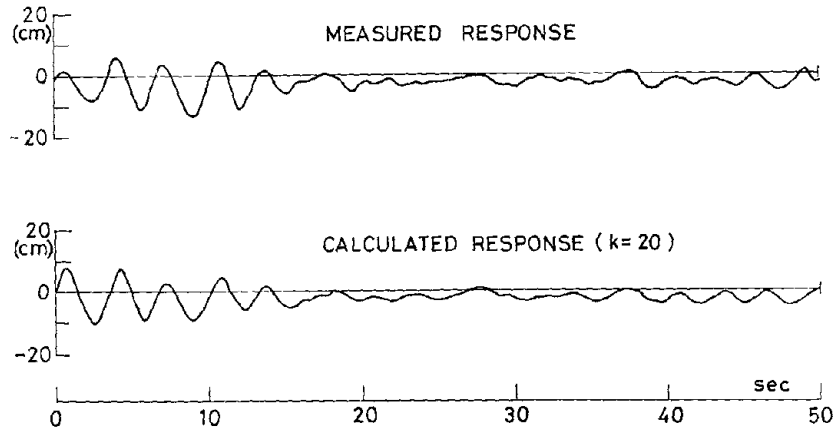

Fig.4 Comparison of Measured and Calculated Responses

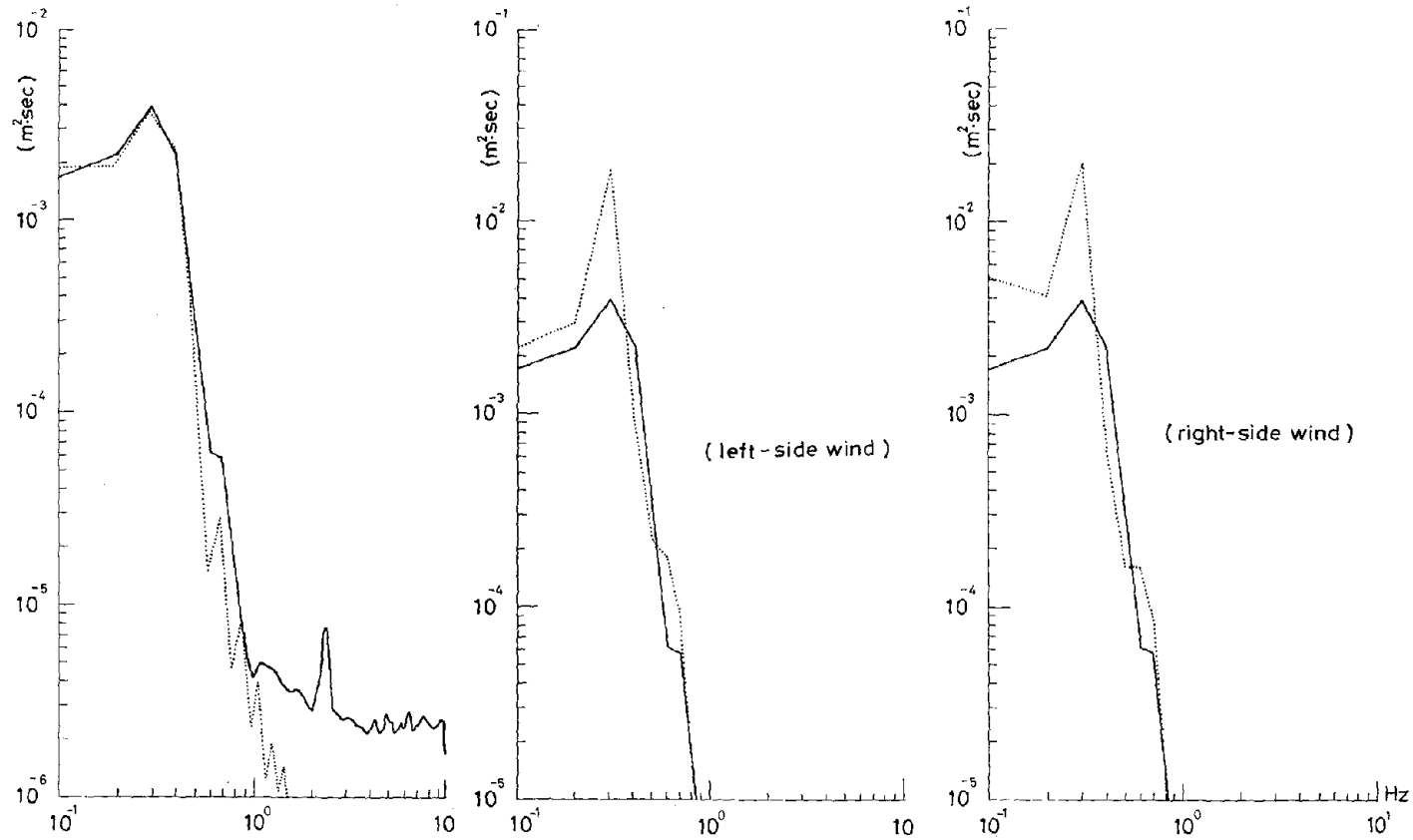

(i) PSD by the method presented (ii) PSD by Ref. [1] (iii) PSD by Ref. [1]

Fig.5 Power Spectral Densities of Responses

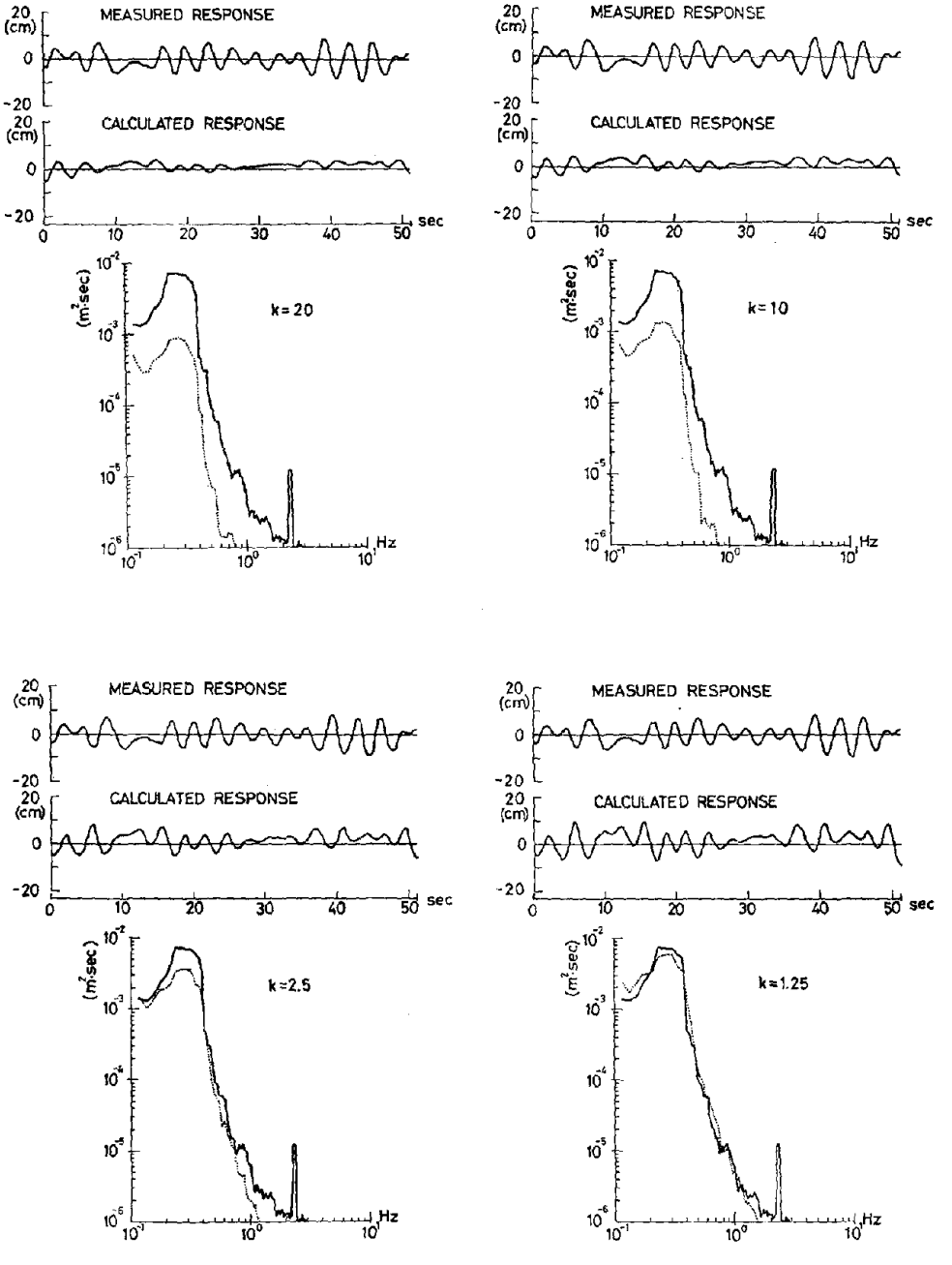

Fig.6 Effect of Decay Factor on PSD of Responses

RECENT DEVELOPMENTS IN THE FORMULATION OF DESIGN WIND LOADS

R. D. Marshall

Structures Section
Center for Building Technology
Institute for Applied Technology
National Bureau of Standards
Washington, D. C. 20234

This paper describes the conventional approach to the determination of wind loads for the design of low-rise buildings as specified by current codes and standards. Shortcomings of this approach are pointed out and a procedure involving the use of a peak factor based upon the distribution of largest departures from the mean is outlined. The sensitivity of the peak factor to length of record and lowpass filtering is discussed. Certain full-scale measurements are presented which indicate the effectiveness of spatial averaging in reducing localized pressure fluctuations. Finally, some comparisons are made between full-scale and model test results.

INTRODUCTION

Considerable progress has been made over the past fifteen years in understanding the physical processes involved in the wind loading of buildings and the response of buildings to these loads. This is due in large part to comprehensive experimental studies in the form of wind tunnel tests and direct measurements in full scale which have been of great value in the development and validation of mathematical theories to predict loads and structural response. The prediction of along-wind response of tall buildings is perhaps the best example of analytical methods that have become highly developed in recent years [4, 17, 18, 14][1/]. Static loads based on these procedures and whose effect is equivalent to that of turbulent wind underlie the provisions of a number of codes and standards dealing with tall-building response.

In contrast, the prediction of cross-wind response has not been so amenable to analytical treatment. In a paper describing the variables and mechanisms associated with cross-wind response of tall structures, Melbourne [12] concludes that considerable fundamental research into bluff-body aerodynamics and the effects of turbulence remains to be done before workable analytical methods of prediction can be developed. In the meantime, reliance must continue to be placed on wind tunnel tests which closely simulate the atmospheric surface layer and the geometric and dynamic characteristics of full-scale structures.

It is, however, in the general area of low-rise buildings where the gre need exists for improved design load criteria. In comparison to tall buildi the initial cost of low-rise buildings has not provided sufficient economic incentive for seeking design refinements. Yet it is low-rise buildings, hou in particular, that invariably constitute the major portion of economic loss caused by hurricanes, typhoons and other strong winds. As used in this pape the term "low-rise" implies a building whose height is less than 10 meters a

[1/] Figures in brackets indicate literature reference.

whose natural frequencies are well above the energy-containing frequencies of the load and pressure fluctuations. Thus it is the maximum instantaneous loads rather than the time histories of loading that are of primary interest.

The determination of wind forces on low-rise buildings is complicated by the fact that, near ground level, the local terrain and adjacent buildings can have a pronounced effect on the mean wind speeds and intensity of turbulence. In addition, the relatively high ratio of wind load to dead load and the small physical size of dwellings and similar structures tend to make them more sensitive to wind effects than is the case for buildings of larger dimensions where spatial averaging can substantially reduce the effectiveness of gusts in producing load fluctuations.

This paper discusses some of the shortcomings of what will be called the "conventional method" for determining design wind loads on low-rise buildings, presents certain findings from recent studies in both model and full scale, and suggests a procedure for formulating design wind loads which utilizes experimentally-determined characteristics of surface pressures.

CONVENTIONAL METHOD

The procedures specified by a number of modern codes and standards for the calculation of design wind loads for low-rise buildings involve four fundamental steps: (1) selection of a basic wind speed appropriate to the anticipated life and intended use of the building; (2) calculation of the corresponding dynamic pressure and adjustment of this pressure to account for local terrain roughness and height of building; (3) calculation of a gust factor to account for wind turbulence or gustiness; and (4) multiplication of the adjusted dynamic pressure and gust factor by appropriate coefficients to obtain overall lift and drag loads as well as pressures acting over tributary areas of the building. Refinements to this general approach include the recognition of several categories of terrain roughness and wind exposure, the influence of size and location of building openings on the internal pressure, and gust factors which discriminate between the primary structural frame of the building, secondary framing, and cladding elements.

While this general approach has in many cases resulted in safe and economical buildings there are several reasons to question the assumptions upon which the general procedure outlined above is based.

Firstly, and perhaps most important, it is assumed that pressure coefficients obtained from model studies carried out in uniform flows of low turbulence can be used in conjunction with gust speeds averaged over two or three seconds. With the exception of building surfaces oriented approximately normal to the oncoming wind, the correlation between pressure fluctuations and streamwise velocity fluctuations is usually weak. In fact, maximum and minimum pressures have often been ol to occur at points in a record which are far removed from the occurrence o peak wind speed. This suggests that changes in wind direction and the sur features of the building, combined with the incident turbulence, play an i role in the generation of pressure fluctuations.

Secondly, the gust factor is based on the assumption that velocity fl tions are normally distributed and that fluctuations in the reference dyna pressure are linearly related to fluctuations in the reference velocity. in itself, is a proper assumption considering the small error involved. H when applied directly to mean pressure coefficients measured in uniform fl

is implied that surface pressure fluctuations are also normally distributed. This is definitely not the case when flow separation and reattachment occurs or when fluid strain appreciably distorts the incident turbulence.

Finally, the gust factor does not account for the shedding of vortices by the building and the resulting pressure fluctuations on surfaces in contact with these vortices.

The complexity of pressure fluctuations associated with turbulent flows precludes the development of purely analytical means of assessment for all but the simplest of geometries and reliance must be placed on measurements obtained in full scale or from properly scaled models. The following sections describe the use of such measurements in formulating design loads.

THE TREATMENT OF LOCALIZED PRESSURES

In analyzing experimental pressure data and in establishing design loads, it is convenient to work in terms of a mean pressure with fluctuations superimposed. As indicated previously, the instantaneous maximum (or minimum) values are of interest when dealing with secondary framing and cladding elements and it is usual to characterize records of wind speed and pressure by their mean, standard deviation and maximum departure from the mean. For a random variable X(t), the maximum (or minimum) value in a record of length T can be expressed as

$$\hat{X} = \overline{X} + g\sigma_X \tag{1}$$

where $$\overline{X} = \frac{1}{T}\int_0^T X(t)dt \tag{2}$$

and $$\sigma_X^2 = \frac{1}{T}\int_0^T [X(t) - \overline{X}]^2 dt \tag{3}$$

Definitions of these quantities are shown graphically in Figure 1. For a given set of conditions, the peak factor, g, will vary from record to record and its distribution function is required in establishing design loads with a specified probability of being exceeded.

Davenport [3] has shown that the probability density function for the largest value X' of a stationary normally distributed process is given by

$$p(x) = x\,\nu T \exp\left[-\frac{x^2}{2} - \nu T \exp\left(-\frac{x^2}{2}\right)\right] \tag{4}$$

in which x is the reduced or standardized variate defined as

$$x = \frac{X' - \overline{X}}{\sigma_X} \tag{5}$$

ν is an average fluctuation rate associated with the occurrence of peak val
T is the length of record. Davenport has also shown that the mean of the d
bution of the largest value is given by

$$\overline{x} = \sqrt{2\ell n\,\nu T} + \frac{0.5772}{\sqrt{2\ell n\,\nu T}}$$

Statistical distributions of maximum peaks for records of localized pr
measured in full scale by Dalgliesh [2] and by Peterka and Cermak [13] on s
models are in satisfactory agreement with Eq. 4 for those surface areas exh

positive mean pressures and where the conversion of velocity fluctuations into pressure fluctuations is reasonably direct. The agreement is less satisfactory for surface areas subjected to large negative pressures such as occur in regions of separated flow. This is not surprising in view of the fact that freestream velocity fluctuations tend to be Gaussian while pressure fluctuations associated with flow separation are often highly intermittent, thus giving rise to extremely large peak factors.

From an experimental point of view, it is desired that the greatest amount of information possible be extracted from recorded data, particularly for full-scale measurements which are usually difficult and expensive to obtain. With this in mind, it is convenient to work with peak factors associated with probability distributions of upcrossings or equivalently, a specified number of occurrences in a given interval of time.

In Ref. 11, Melbourne shows that for a stationary, narrow-band, Gaussian process with a mean value of zero and with most of the energy centered at a frequency n_o, the probability of an upcrossing exceeding some level a following a zero crossing (upcrossing of the mean) is

$$P(x > a) = \frac{n_a}{n_o} = e^{-a^2/2\sigma_x^2} \tag{7}$$

where n_a is the average number of upcrossings of the value $x = a$ per unit time. Defining the peak factor, g, as that level associated with only one upcrossing in period T,

$$\frac{n_a}{n_o} = \frac{1}{n_o T} = e^{-a^2/2\sigma_x^2}$$

or
$$g = \sqrt{2 \ell n n_o T} \tag{8}$$

which is the first term in Davenport's expression for the mean of the distribution of the largest value (Eq. 6). Since the Rayleigh distribution function of Eq. 7 is a special case of the Weibull distribution function

$$P(x > a) = e^{-(a/c)^k} \tag{9}$$

the coefficients c and k can be evaluated as the intercept and slope, respectively, of the distribution function plotted on $\ell n(-\ell n)$ vs ℓn axes or on conventional Weibull probability paper. The degree to which Eq. 7 approximates the mean of the distribution of the largest value given by Eq. 6 depends upon the value of νT. For $\nu T \approx 1000$, the difference is less than 5 percent. Since the distribution of largest value is shown by Davenport to be quite narrow, particularly for large values of νT, the use of Eq. 9 as a basis for the selection of peak factors is justified.

Melbourne has applied the approach outlined above to response data obtained from several aeroelastic models tested in a turbulent boundary layer. As expected, peak factors approach the lower limit of $\sqrt{2}$ as the response becomes sinusoidal with small variation in amplitudes of oscillation. For highly intermittent phenomena, such as pressure fluctuations near regions of separated flow, peak factors in excess of 8 are regularly observed.

APPLICATION TO FULL-SCALE DATA

In an effort to provide a firm basis for the development of improved wind load design criteria, the National Bureau of Standards has conducted a number of field studies in recent years to document wind pressures on low-rise buildings [8, 9, 10]. While much work remains to be done, a number of conclusions can be stated that should be of help in conducting future measurements and in formulating design loads. The length of this paper does not allow a description of instrumentation and experimental techniques used in these studies (see references for a complete discussion) and emphasis will therefore be placed on the analysis of full-scale data and the development of recommended design loads.

It is usual in experimental studies such as these to express pressures in terms of some dynamic reference pressure and a dimensionless pressure coefficient defined as

$$C_p = \frac{p - p_o}{1/2\rho u_h^2}$$

where p is the localized pressure acting on the exterior surface of the building, p_o is the freestream ambient pressure, ρ is the mass density of air and u_h is a reference wind speed recorded at some height h (usually the height of the building) in the undisturbed wind field. As indicated previously, it is convenient to work in terms of a mean value with fluctuations superimposed, or in terms of pressure coefficients

$$C_{\bar{p}} = \frac{\bar{p}}{1/2\rho \bar{u}_h^2} \tag{10}$$

and

$$C_{p_\sigma} = \frac{\sigma_p}{1/2\rho \bar{u}_n^2} \tag{11}$$

where $\bar{p}$ will be understood to indicate the mean pressure over the record length relative to freestream ambient pressure, $(\overline{p - p_o})$, and σ_p is the standard deviation of the pressure fluctuations.

The length of record or time interval for which the mean and standard deviation are determined is somewhat arbitrary. The record should be long enough to reflect the effects of low-frequency components of mechanical turbulence generated by the terrain roughness and adjacent structures, but short enough so that a reasonably stationary time history, free of significant trends, will be obtained. Experience has shown that a record length of from 15 to 30 minutes is generally satisfactory and 1000 seconds has been adopted as a standard record length f the studies referenced above.

Although a stationary, narrow-band, Gaussian process has been assumed i establishing Eq. 7, the analysis has been applied to various full-scale recc many of which are wide-band random and highly intermittent. The procedure u the analysis of pressure fluctuations is to determine the maximum (or minimu value p' of the pressure signal following each upcrossing of the mean and tc x as a reduced variate

$$x = \frac{p' - \bar{p}}{\sigma_p}$$

In addition to the average rate of upcrossings of the mean, n_o, the rate of occurrence of peaks in a record, n_p, is also determined. The probability distribution of x is then determined, usually with a resolution or class interval of 0.25σ. A typical probability distribution of negative-going fluctuations is shown in Figure 2. These fluctuations were measured at tap R4 on the roof of the mobile home shown in Figure 3 (see Ref. 10) with a wind azimuth of 354 degrees, measured clockwise from the front end of the mobile home. While extreme values associated with a normally distributed process imply peak factors of 3.5 to 4, the peak departures plotted in Figure 2 fall well beyond this range.

Selection of Peak Factors

In specifying design pressures, it is necessary to estimate the maximum (or minimum) pressure

$$\hat{p} = q_h \left(C_{\bar{p}} + g C_{p_\sigma}\right) \tag{13}$$

which is likely to occur for a specified set of conditions. These pressures can then be modified to account for spatial averaging and to allow the use of working stress design relationships that many building codes currently prescribe. The selection of the peak factor, g, is based on the average maximum departure or fluctuation associated with a record length of 1000 seconds. The values of the mean pressure coefficient, $C_{\bar{p}}$, and the rms pressure coefficient, C_{p_σ}, are assumed to be invariant with wind speed and averaging time. The mean dynamic reference pressure, $\bar{q}_h$, must reflect the 1000-second averaging time.

In the United States, it is customary to use the "fastest mile of wind" (denoted by u_{FM}) at 30 ft (9.15 m) above ground in open terrain as the basic wind speed to describe the geographic distribution of extreme winds. To obtain corresponding 1000-second averages, reference can be made to data obtained by Durst [5] which, for certain terrain roughnesses, gives the ratio of the average maximum wind speed for various averaging times to the mean hourly speed. For the wind load studies conducted on the full-scale mobile home shown in Figure 3 and described in Ref. 10, a reference height of 3.3 m was used to define the pressure coefficients and a power law index of 0.17 was found to best describe the measured mean velocity profiles. Based on similarity arguments, it can be shown for the conditions stated above that the probability of the peak factor exceeding some value x once in an interval of 1000 seconds is

$$P\ (>x) = \frac{\bar{u}_{3.3}}{660\ n_o\ u_{FM}} \tag{14}$$

where $\bar{u}_{3.3}$ is the measured mean reference speed averaged over 1000 seconds the measured average rate of upcrossing of the mean, and u_{FM} is the specif fastest mile design speed. It is assumed in Eq. 14 that the upcrossing ra directly with the wind speed, i.e.,

$$\left(\frac{n_o}{u_h}\right)_1 = \left(\frac{n_o}{u_h}\right)_2$$

This only requires that the characteristic scales for the two wind speeds

and that the flow process be independent of Reynolds number. Experimental results obtained from studies on bluff bodies in both model and full scale support these assumptions.

Effect of Length of Record

To illustrate the effect of length of record or averaging time on the average maximum fluctuating component of pressure or load for the study described in Ref. 10, peak factors have been calculated for two values of the ratio $\bar{u}_{3.3}/n_o$ and for record lengths ranging from 3 seconds to 1 hr. A basic wind speed (fastest mile at 30 ft in open terrain) of 90 mph (40 m/s) was assumed and the Weibull coefficients c = 0.7 and k = 0.8 were used to obtain the values of g. The results are plotted in Figure 4 as a ratio of $g_{(t)}\,\bar{u}^2_{(t)}$ to $g_{(1000)}\,\bar{u}^2_{(1000)}$ which represents the change in the peak value of the fluctuating component with length of record. The values of the ratio u/n and the Weibull coefficients are typical of the measured values. It is seen from Figure 4 that the maximum change is less than 10 percent for record lengths ranging from 100 to 1000 seconds. The rapid increase in the peak value of the fluctuating component for record lengths in excess of 30 minutes is due to the invariance of the mean dynamic pressure.

Effect of Lowpass Filtering

In the recording and analysis of pressure data, practical considerations usually limit the range of frequencies that can be accommodated. This may be due to limitations in the frequency response of the pressure transducers or the rate at which samples can be acquired if a digital data acquisition system is being used. In some cases the signals are intentionally subjected to lowpass filtering to improve the signal-to-noise ratio or to reduce aliasing errors in spectral analysis. As pointed out in Ref. 7, the peak factor is affected by measurement and analysis techniques, the effects in some cases being far more significant than the actual aerodynamic differences between experimental setups.

The plots presented in Figure 5 indicate the change in the rms, the maximum departure from the mean, and upcrossings of the mean as the signal is subjected to lowpass filtering by averaging adjacent points in the digital record. The signal was obtained by summing and averaging the signals from transducers installed at taps R1, R2 and R5 in Figure 3 with a wind azimuth of 264 degrees, measured clockwise from the front end. The initial sampling rate was 24 per second and a maximum of 64 adjacent points are averaged. Based on the reference wind speed of 9.0 m/s at the height of the roof, the ratio of the mean speed to the sampling rate, $\bar{u}/n$, ranges from 0.38 to 24 m per sample. The plots presented in Figure 5 are typical of measurements made in regions of separated flow. It is observed the rms level is only slightly affected by lowpass filtering, but the maximum departure from the mean is attenuated by approximately 10 percent at $\bar{u}/n$ = 2 sample. Initially, the rate of upcrossing of the mean changes rapidly as th frequency, low-amplitude fluctuations are removed from the signal by averagi adjacent samples. The effect of this is to increase the intercept, c, of th Weibull plot, but the change in the average maximum value of the peak factor typically less than 10 percent.

REDUCTIONS DUE TO SPATIAL AVERAGING

While the measurement of wind pressures acting on the surfaces of a building can most conveniently be accomplished by the installation of pressure taps and transducers, the instantaneous loads acting on cladding elements and structural subsystems, rather than the point pressures, are of interest. Since the pressure fluctuations are never completely coherent, load estimates based on the average of the maximum peak values obtained from an array of pressure taps will always exceed the true maximum load. To improve these estimates, the signals from an array of N pressure taps are multiplied by weighting factors, w_n, such that

$$\sum_{n=1}^{N} w_n = 1 \tag{15}$$

and the signals are then summed and analyzed as previously described. This spatial averaging was accomplished by digital methods in the studies described in Refs. 8, 9 and 10. However, a far simpler technique has been perfected by Stathopoulos [15] in which the pressures are averaged pneumatically and only one transducer is thus required, regardless of the number of pressure taps in the array.

Although a considerable amount of work remains to be done in this area of load definition, results obtained from the mobile home shown in Figure 3 provide a measure of the reductions associated with spatial averaging. In Table I are listed the pressure tap combinations, approximate surface area represented by the pressure tap array, percent reduction in C_{p_σ}, and percent reduction in gC_{p_σ} for various records obtained with the wind blowing face-on to the left wall of the mobile home. The percentages are based on the averages of C_{p_σ} and C_{p_σ} obtained from individual pressure taps.

It is seen from Table I that, for the windward wall, significant reductions are realized only for the line-like array extending over the length of the mobile home. For arrays whose spatial extent is small compared to the lateral scale of the incident turbulence, the reductions are substantially less. The reductions observed on the end wall and on the roof suggest that local flow regimes strongly affect the coherence of pressure fluctuations. For example, the combination of taps R8 to R11 in the spanwise direction involves flow separation and reattachment, as does the combination of taps R1 to R5. The combination R1, R2 and R5, on the other hand, does not extend into the reattachment region and the reductions due to spatial averaging are approximately half those for arrays extending in the spanwise direction. Because the windward edge of the roof experiences large negative mean pressures and large negative-going fluctuations which can be hig coherent, special care must be taken in detailing the roof membrane and it fasteners. Local failures at the windward edge often lead to total failur roof system.

Full-scale measurements obtained to date suggest a range of 4.5 to 10 peak factors associated with tributary areas. Larger values are obtained pressures, values exceeding 18 having been observed by Eaton and Mayne [6] surfaces. The importance to be placed on large pressure fluctuations ulti depends on the properties of the construction materials. Studies by Beck Morgan [1] clearly demonstrate the susceptibility of corrugated high-stren sheet to low-cycle fatigue. On the other hand, glass exhibits significant strength under loads of short duration.

COMPARISON OF PRESSURES IN MODEL AND FULL SCALE

Although full-scale measurements are of great value in establishing the validity of both analytical and wind tunnel modeling techniques, they are not a practical means for the systematic study of wind effects. This can best be accomplished in a wind tunnel capable of simulating the characteristics of the atmospheric surface layer. For the case of low-rise buildings, it is usually necessary to accept some distortion in the flow simulation so that the physical size of the building model does not preclude the installation of pressure taps and transducers.

Certain full-scale results obtained in the study described in Ref. 9 have been compared with results of wind tunnel model tests described in Ref. 16. Models were constructed at a scale of 1:70 and the flow was believed to be scaled at approximately 1:120, based upon the integral scale of the longitudinal component of turbulence. Pressure spectra are compared in Figure 6 for pressure tap No. 5 shown on the full-scale building in Figure 7. The ratio of the wave numbers of the pressure spectra, whose low-frequency ranges have been matched, suggests a scale ratio of 1:60. This, as well as other test results, suggests that the size of the building model rather than the scale of turbulence determines the scale ratio.

Some typical values of model and full-scale pressure coefficients for the building shown in Figure 7 are listed in Table II. Mean wind speeds at the 10-meter level were typically 10 m/s for the full-scale records and turbulence intensities ranged from 19 to 26 percent. Because long-term instrument drift at field test sites cannot be entirely compensated for, more confidence can be placed in the full-scale pressure fluctuations than in the mean pressures. Periodic calibrations of the transducers at field installations suggest that the maximum probable error in the rms pressure coefficients is of the order of $\pm$ 10 percent. The agreement between full-scale rms coefficients for nearly identical wind directions (Rec. Nos. 1-4 and 1-2) is significantly better than is suggested by the mean pressure coefficients. The same can be said for the agreement between model and full-scale results. Based on test results obtained to date, it appears that the intensity of turbulence is an extremely important factor in obtaining realistic surface-pressure fluctuations from wind tunnel model studies.

CONCLUSIONS

Based on results presented in this paper, the following conclusions can be stated:

1. The use of pressure coefficients based on mean wind speeds in turbulent flows represents a significant improvement over the "conventional method" of specifying design wind loads in terms of gust speeds.

2. A Weibull distribution satisfactorily describes the probability dis tion of peak pressure and load fluctuations.

3. The average maximum values of pressure and force coefficients can c veniently be expressed in terms of a mean coefficient and the produ a peak factor and a rms coefficient.

4. Much more attention should be given to the behavior of building mat under fluctuating loads when specifying design values.

REFERENCES

1. BECK, V.R. and MORGAN, J.W., "Appraisal of Metal Roofing Under Repeated Wind Loading - Cyclone Tracy, Darwin, 1974," Technical Report No. 1, Australian Department of Housing and Construction, Housing Research Branch, February 1975.

2. DALGLIESH, W.A., "Statistical Treatment of Peak Gusts on Cladding," Journal of the Structural Division, ASCE, Vol. 97, No. ST9, Proc. Paper 8356, September 1971, pp. 2173-2187.

3. DAVENPORT, A.G., "Note on the Distribution of the Largest Value of a Random Function with Application to Gust Loading," Proceedings, Institution of Civil Engineers, Vol. 28, Paper No. 6739, June 1964, pp. 187-196.

4. DAVENPORT, A.G., "Gust Loading Factors," Journal of the Structural Division, ASCE, Vol. 93, No. ST3, Proc. Paper 5255, June 1967, pp. 11-34.

5. DURST, C.S., "Wind Speeds over Short Periods of Time," The Meteorological Magazine, Vol. 89, July 1960, pp. 181-186.

6. EATON, K.J. and MAYNE, J.R., "The Measurement of Wind Pressures on Two-Storey Houses at Aylesbury," BRE Current Paper CP 70/74, July 1974.

7. EATON, K.J., MAYNE, J.R. and COOK, N.J., "Wind Loads on Low-Rise Buildings --Effects of Roof Geometry," Proceedings, Fourth International Conference on Wind Effects on Buildings and Structures, Cambridge University Press, 1975, pp. 95-110.

8. MARSHALL, R.D., "A Study of Wind Pressures on a Single-Family Dwelling in Model and Full Scale," Journal of Industrial Aerodynamics, Vol. 1, No. 2, June 1975, pp. 67-109.

9. MARSHALL, R.D., and RAUFASTE, N.J., "Building to Resist Wind," Vol. 1: Overview, NBS Building Science Series, No. 100-1, National Bureau of Standards, Washington, D.C., May 1977.

10. MARSHALL, R.D., "The Measurement of Wind Loads on a Full-Scale Mobile Home," NBS Interagency Report, (to be published), 1977.

11. MELBOURNE, W.H., "Peak Factors for Structures Oscillating Under Wind Action," Proceedings, Conference on Probability Theory of Structural Design, The Institution of Engineers, Australia, November 1974, pp. 35-44.

12. MELBOURNE, W.H., "Cross-Wind Response of Structures to Wind Action," Proceedings, Fourth International Conference on Wind Effects on Buildings and Struct Cambridge University Press, 1975, pp. 343-358.

13. PETERKA, J.A. and CERMAK, J.E., "Wind Pressures on Buildings -- Probabi Densities," Journal of the Structural Division, ASCE, Vol. 101, No. ST6 Paper 11373, June 1975, pp. 1255-1267.

14. SIMIU, E., "Equivalent Static Wind Loads for Tall Building Design," Jou of the Structural Division, ASCE, Vol. 102, No. ST4, Proc. Paper 12057, April 1976, pp. 719-737.

15. STATHOPOULOS, T., "Technique of Pneumatically Averaging Pressures," Engineering Science Research Report, No. BLWT-2-1975, University of Western Ontario, December 1975.

16. TIELEMAN, H.W. and REINHOLD, T.A., "Wind Tunnel Model Investigation for Basic Dwelling Geometries," Report No. VPI-E-76-8, Dept. of Engineering Science & Mechanics, Virginia Polytechnic Institute & State Univ., May 1976.

17. VELLOZZI, J. and COHEN, E., "Gust Response Factors," Journal of the Structural Division, ASCE, Vol. 94, No. ST6, Proc. Paper 5980, June 1968, pp. 1295-1313.

18. VICKERY, B.J., "On the Reliability of Gust Loading Factors," Proceedings, Technical Meeting Concerning Wind Loads on Buildings and Structures, NBS Building Science Series, No. 30, National Bureau of Standards, Washington, D.C., Nov. 1970, pp. 93-104.

TABLE I

Reductions Due To Spatial Averaging

Tap Combination	Area (m^2)	C_{p_σ} (percent)	gC_{p_σ} (percent)
29 to 32	0.9	6	16
4, 15, 30, 50, 52, 54	11.2	32	44
26 to 44	4.7	8	9
57, 61, 63, 64, 69, 70	1.5	12	32
R8 to R11	1.5	26	34
R1, R2, R5	2.8	13	14
R1 to R5	4.7	18	24

TABLE II

Mean and RMS Pressure Coefficients

Pressure Transducer No.		1	2	3	4	5	6
Run No.	β	Mean pressure coefficients $\bar{C}_p$					
26*	208°	-0.70	-0.14	-0.05	-0.70	-0.76	-0.02
3-2A	212°	-0.20	-0.11	0.01	-0.33	-0.59	-0.42
3-6A	216°	-0.72	-0.46	-0.31	-0.69	-0.95	-0.20
27*	228°	-0.66	-0.26	-0.12	-0.82	-0.62	-0.02
1-4	243°	-0.34	-0.24	-0.03	-0.53	-0.64	-0.19
1-2	244°	-0.57	-0.37	-0.23	-0.82	-----	0.02
28*	253°	-0.64	-0.21	-0.26	-0.68	-0.12	-0.11
		RMS pressure coefficients C_{p_σ}					
26	"	0.37	0.22	0.10	0.39	0.37	0.10
3-2A		0.22	0.12	0.11	0.36	0.27	0.10
3-6A		0.32	0.17	0.16	0.43	0.46	0.14
27		0.29	0.15	0.10	0.39	0.47	0.09
1-4		0.23	0.13	0.09	0.27	0.34	0.07
1-2		0.27	0.17	0.15	0.51	0.50	0.11
28		0.25	0.11	0.11	0.38	0.31	0.15

* Wind tunnel data

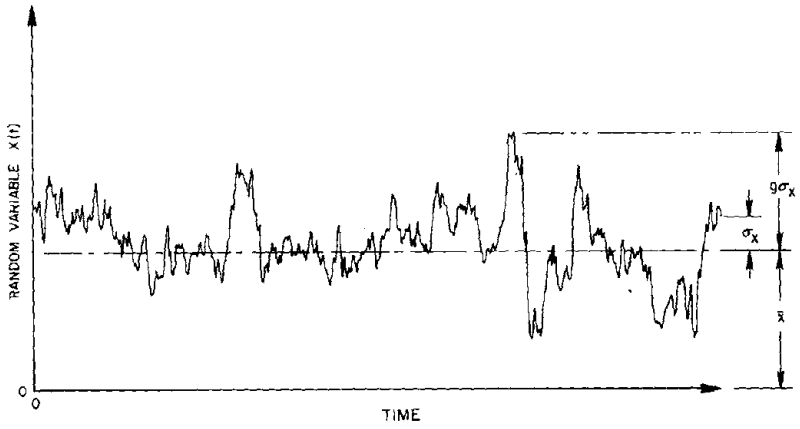

Fig. 1 - Definition Sketch of Mean, Standard Deviation and Peak Factor

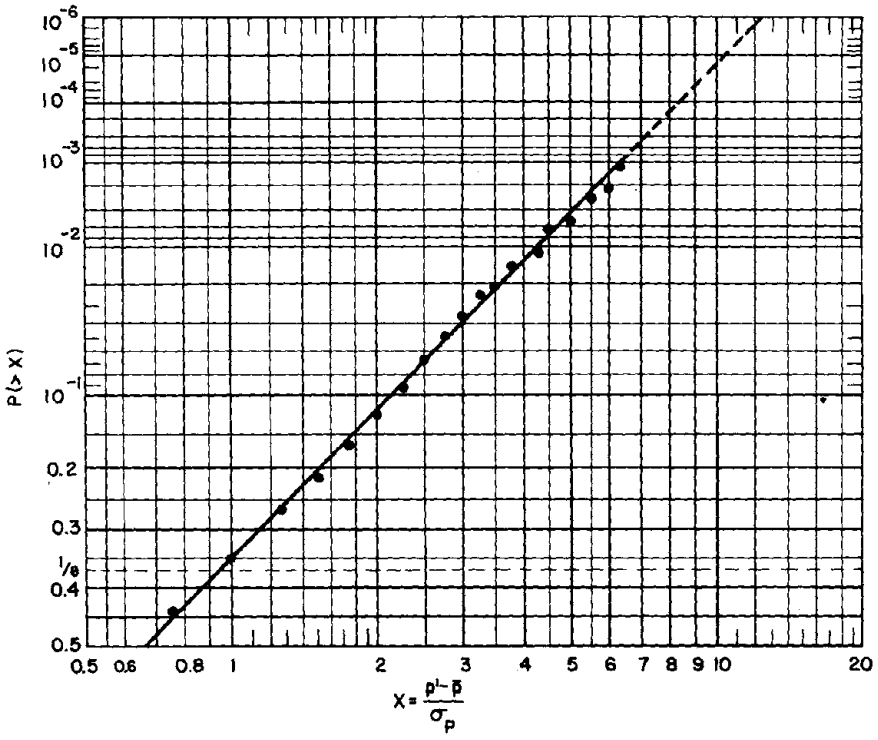

Fig. 2 - Typical Distribution of Negative Pressure Fluctuations on Mobile Home Roof

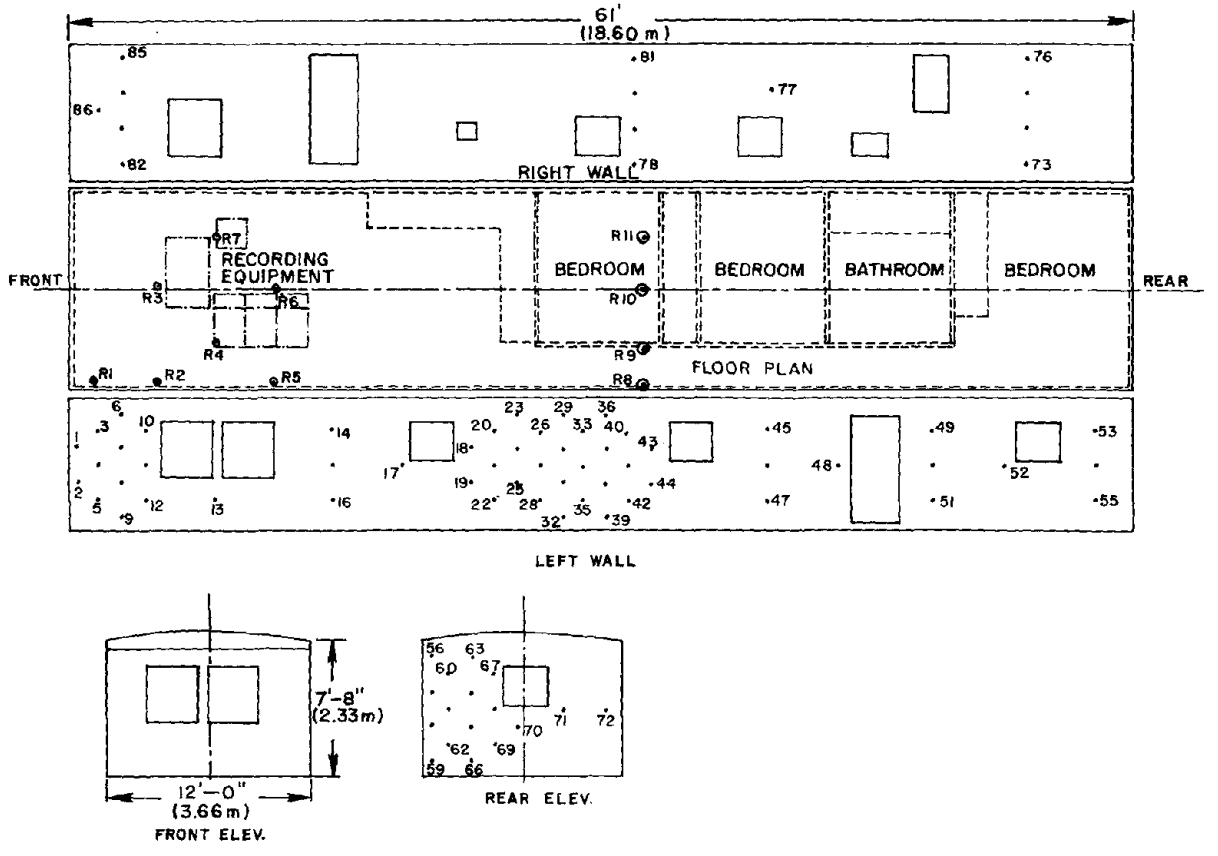

Fig. 3 - Mobile Home Layout and Pressure Tap Designations

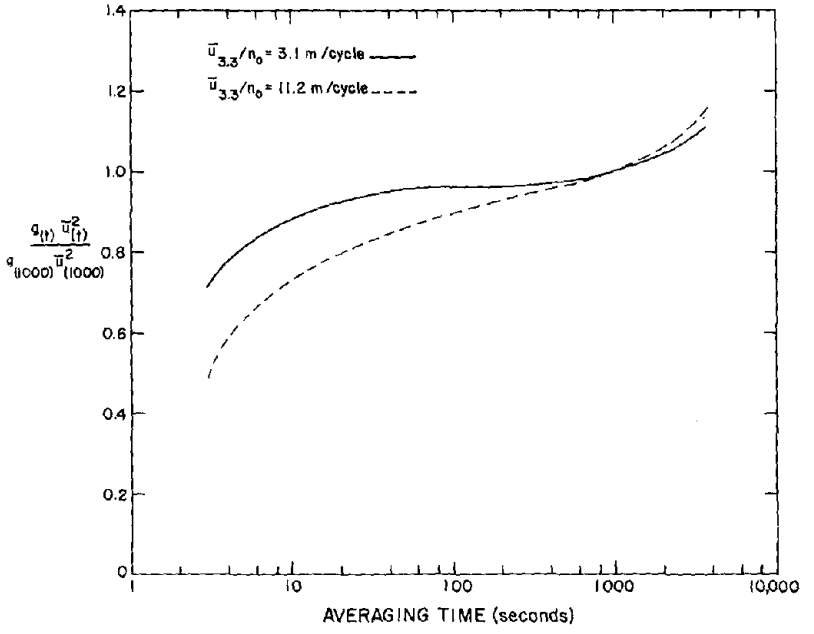

Fig. 4 - Variation of Peak Factor With Length of Record

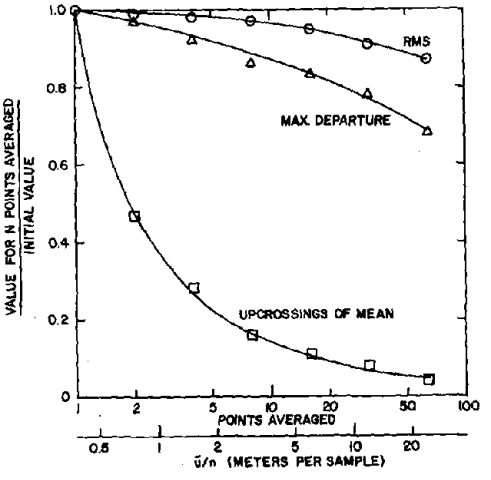

Fig. 5 - Effect of Lowpass Filtering

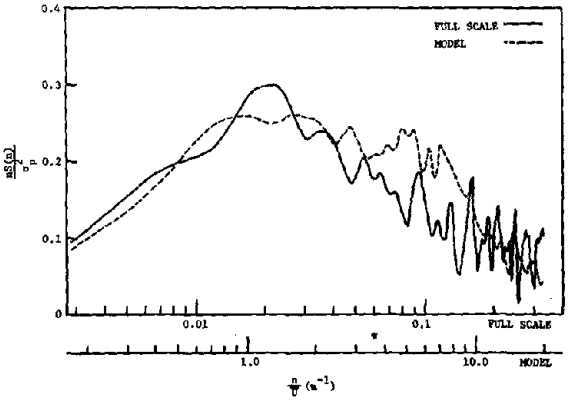

Fig. 6 - Pressure Spectra for Transducer No. 5, Run Nos. 28 (model) and 1-4 (full scale)

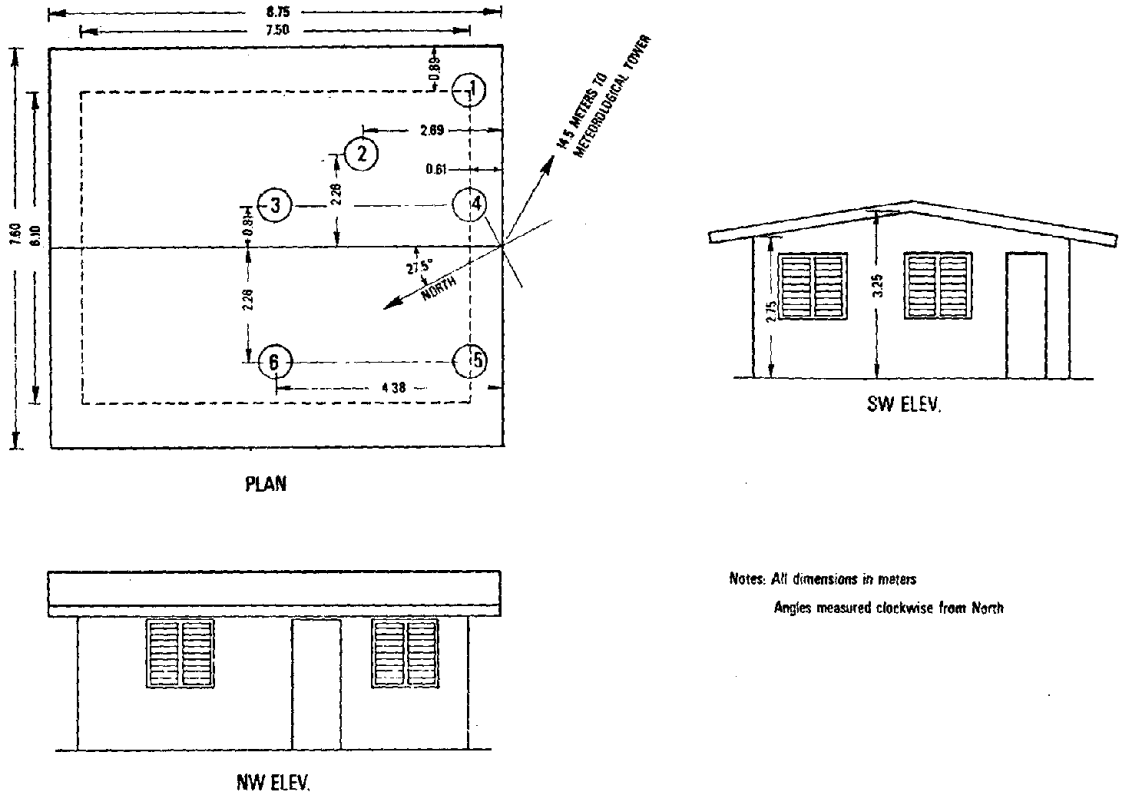

Fig. 7 - Experimental Building, Quezon City, Philippines

SOME PROBABILISTIC CONSIDERATIONS ON WIND RESISTANT DESIGN

Manabu Ito and Yozo Fujino

University of Tokyo

SYNOPSIS

Some considerations are presented on wind resistant design from a probabilistic viewpoint. First, the yearly maximum wind speed records in several locations in Japan are statistically analyzed and fitness of the theoretical distributions of extremes to the records is discussed. A combined distribution is found suitable, in some area, to characterize the yearly maximum wind speed. It is shown that occurrence of strong winds is approximately a Poisson type. Secondly, determination of the design load of a structure subject to multiple loads including a wind load, namely load combination, is considered. Time-varying loads are modeled using stochastic processes and load combination problem is studied in conjunction with load factor design. A numerical example shows how to obtain appropriate load factors in the presence of multiple time-varying loads.

INTRODUCTION

For many structures, particularly, for tall buildings and long spanned suspension bridges, wind loading is a significant factor with respect to safety. Consequence of their failures results in a considerable amount of human, social and economical losses. Required is to establish a safe and yet economical, i.e. rational wind resistant design for such structures. Toward this, a number of promising investigations have been offered in the past decades.

To ensure the safety of a structure against a wind action, rational wind resistnat design should be controlled by many provisions in a structural code. One of the most important provisions is to give a basic design wind speed. The first part of this paper deals with the determination of the basic design wind speed which forms the basis of the dynamic analysis.

Wind speed data observed at a station over years reveal certain random natures of the wind speed in various aspects. Then speed predictions based on data are generally made by using the statistical theory of extremes. Type I and II distributions of extremes are usually considered to be fitted to the data. In this paper, records of the yearly maximum wind speed, which is averaged over ten minutes, at several meteorological stations in Japan are statistically analysed. Then, fitness of one of the two distributions to the records is discussed. It will be indicated that the use of only one set of distribution parameters ma inappropriate to characterize the wind speed probabilistically at some locati In other words, a combined distribution is suggested to adopt. Design wind speeds associated with return periods are also presented. Next, occurrence strong winds is studied from the stochastic viewpoint and found to be appro mately a Poisson type.

Structures exposed to natural environment are usually subject to vario time-varying loadings due to wind, traffic, earthquake and others during the lifetime. Possible simultaneous occurrence of such loadings may affect the structural safety. Then designing structures under this condition should be

made in a consistent manner with respect to safety, which raises, so-called, problem of load combination. Current specifications in the structural codes on this matter are mostly based on engineering judgment and may not be risk consistent. It is of great importance to establish a rule regarding load combination in design.

Another part of the paper is concerned with load combination problem from the viewpoint of the structural safety. Bridges subject to wind and traffic loadings are considered, where both loadings are modeled using the stochastic processes. Safety of structures is evaluated probabilistically in terms of the safety index which has certain shortcomings but is useful nevertheless in analysis because of its simplicity. Load combination problem is studied in conjunction with load factor design which is now widely accepted as suitable for the next generation of structural codes since it contains some probabilistic rationale to account for uncertainty. The objective of this study is, by a numerical example, to show how to obtain appropriate load factors in the presence of multiple time-varying loads. However, it should be mentioned that emphasis is placed on a formulation of establishing a rule in load combination and providing a guide to code decision making rather than obtaining numerical values of load factors for actual use in design.

STATISTICAL ASPECTS OF WIND SPEED

Distribution of Yearly Maximum Wind Speed and Design Wind Speed

Wind speed varies in a nearly random fashion and can be approximately described as a stationary random process to the exclusion of the seasonal change. This makes it possible to predict a wind speed on the statistical basis . Wind speeds are continuously recorded at meteorological stations, but the data of the wind speeds are usually available in the form of daily, monthly and yearly instantaneous (or ten-minute average) maximum speeds.

Strong winds which are of interest usually occur only a few times for a year, and the anticipated lifetime of structures are generally more than 30 years. The yearly maximum wind records are therefore a convenient information form in determining a basic design wind speed. These records can be considered as mutually independent samples from the parent distribution.

Using the yearly maximum wind speed records, the underlying cumulative distribution function can be, at least in theory, estimated to characterize the probabilistic behavior of the yearly maximum wind speed. The basic design wind speed is then defined as the speed v_D which has a specified non-exceedance probability p in the estimated yearly maximum wind speed distribution. Instead of the probability p, an equivalent expression "R year return period" has favoured to use, which is defined by

$$R = 1 / (1 - p) \tag{1}$$

A wind speed corresponding to a R-year return period is commonly referred t the R-year wind speed.

Selection of the return period to be used in design must be made as a function of usage, lifetime of the structure, sensitivity to wind, and pos losses including loss of life in case of failure. But, at the present sta art, it relies fairly upon past experience and professional judgment. In

structural codes, the 50 year design wind speed appears to be specified to use for ordinary structures (1). However, for example, the wind resistant design standard for bridges being constructed and planned by the Honshu-Shikoku Bridge Authority aims at the 150 year wind speed (2).

Concerning the distribution of the yearly maximum wind speed, probabilistic considerations, as well as available empirical evidence suggest that the asymptotic probability distributions of the maximum values with unlimited upper tail are appropriate to employ. There are two such distributions: one is the type I distribution, so-called Gumbel distribution, the other the type II, Frechet distribution, of which cumulative distribution functions take, respectively, the form of

$$F_I(x) = exp\{-exp[-\alpha(x-u)]\}, \qquad -\infty < x < \infty \tag{2}$$

where α is the scale parameter, while u location parameter, and

$$F_{II}(x) = exp[-(w/x)^k], \qquad 0 < x < \infty \tag{3}$$

in which w and k are scale and tail length parameters, respectively (3).

The choice of the underlying distribution, usually among the two, to represent the yearly maximum wind speed can be made after the investigation of fitting closeness to the data. The extensive analysis of fitting the distributions based on the data in USA was carried out by Thom (4). From the results as well as with the theoretical support that the type II has the lower limit zero of a random variable which actually exists in any wind records, he concluded the type II is an appropriate model to employ. In contrast, in Japan and many other countries, it was found that in most cases the type I is appropriate to represent the probabilistic behavior of the yearly maximum wind speed (5), and accordingly it has been commonly used to determine the design wind speed.

Station Data Analysis

Station data are herein statistically analyzed. Four stations, Sapporo, Tokyo, Osaka and Murotomisaki in Japan, are selected and their locations are shown in Fig.1. The yearly maximum wind speeds observed over a number of years in these stations are plotted in the type I distribution papers as presented in Figs.2, 3, 4 and 5, respectively. Necessary adjustments due to the changes of recording instruments and of their elevations have already been carried out and included in the data used, while effects from environmental changes,for example, from appearance of buildings close to meteorological stations are not taken into account. In plotting the station data Hazen's method is used, i.e., the cumulative probability P_i of the ith largest record among n years records is given by

$$P_i = 1 - (2i - 1) / 2n \tag{4}$$

For comparative purpose, the two types of distributions, Type I and II are f by the least square method to the data, and the results are shown by solid dashed lines, respectively in Figs.2～5. The estimated statistical paramet $\hat{\alpha}$, $\hat{u}$, $\hat{w}$ and $\hat{k}$ of the two distributions by the method are presented in Table well. As shown in Figs.2～5, probabilistic characteristics of the yearly m wind speed vary location to location. It is found that, on the basis of statistical evidence, neither type of distributions can be given preference

Next, with the estimated statistical parameters of the types I and II the 50, 75, 100 and 150 year wind speeds are calculated, respectively, as presented in Table 2. For the same return period, the type I distribution gives the smaller wind speeds than the type II does, but the differences are not significant in Sapporo, Tokyo and Osaka. Then, selecting the type I or type II distribution in such stations does not matter much form the design point of view. On the other hand, in Murotomisaki there are some differences between the two as seen in Table 2. In such a location, the selection of one distribution is left to deepened statistical fitting analysis, or is made necessarily by engineering decision.

Fitting of one type of distribution to the data has been considered so far. However, the case that a combined distribution is more satisfactorily fitted to the data may sometimes occur (4). Here Osaka will be found to be the case indeed. It should be mentioned that there are some meteorological distinctions among the selected four locations. In August and September, several typhoons following strong winds visit some region of Japan, and their ordinary path is indicated in Fig.1. Then, the yearly maximum wind speed records in Murotomisaki lying in the path are considered from typhoons, while some of those in Osaka are from typhoons since typhoons are weakened in inlands. In contrast, those in Sapporo and Tokyo are considered to be rarely influenced by typhoons due to their geographical conditions, and are from other sources. In Fig.4, it is interesting to observe that the distribution, either type I or II is not so closely fitted to the data in Osaka as to the data in the other three stations. It appears that the top three wind speed records, of which tangent is as high as that in Murotomisaki, could be attributed to typhoons, and others are almost to seasonal winds. Accepting the type I distributions to the records due to typhoons and seasonal winds, a refined distribution can be drawn as indicated in Fig.4. It appears fitted much closely to the data. By this combined distribution, 50, 75, 100 and 150 year wind speeds are found to be 37.6, 42.0, 45.0 and 49.4 m/s, respectively. These values of wind speeds are significantly larger than the values in Table 2 for longer return periods, which can be seen also in Fig.4. It should be noticed that such a consideration produces a considerable change in the design wind speed.

Occurrence of Strong Winds

The distribution of the yearly maximum wind speed and the return period suffice the determination of a design wind speed. However, more knowledge of the wind speed statistics would be necessary in some situations, for example, in order to construct a stochastic model of a wind speed in time domain. Attention is here paid to the stochastic cahracteristics of occurrence of strong winds which are of concern from the viewpoint of structural safety. A Poisson model, which offers considerable advantage of simplicity regarding analysis, has been accepted as suitable to represent occurrences of earthquakes, tornadoes, flood and so on. Applicability of a Poisson model to occurrence of strong winds is briefly examined.

In the analysis, the station records in Hirato (Fig.1), which are ava in the form of monthly maximum, ten minutes averaged wind speeds from 1940 1975 are used. Since the records fail to include the second and less maxi wind speed at a month, they do not provide complete information for the an but are considered as practically sufficient.

As well known, in a Poisson process, complementary cumulative distrib of waiting time of occurrence is the exponential type, i.e., $e^{-\nu t}$ where ν

mean occurrence rate and t is waiting time (6). The strong wind can be defined in such a way that its speed exceeds a certain value. Selecting speeds 18 and 20 m/s for the lower limit of strong winds, respectively, the calculated complementary cumulative distributions of waiting time from the records in Hirato are presented in Fig.6, where the distributions due to the sample mean occurrence rates for the two cases are shown by solid straight lines. The Poisson model can be accepted if the records fit the straight line. From Fig.6 showing that fairly good fitting of the records to the straight lines, it may be concluded that the occurrence of strong winds in Hirato can be approximated by a Poisson model. However, it should be noted that, in order to induce a more general statement on this matter, obviously, extensive analysis of records in many stations is necessary.

LOAD COMBINATION AND LOAD FACTOR DESIGN

Load Factor Design and Code Calibration

For a limit state, the load factor design format prescribed by structural codes generally takes the form of

$$\phi R^* \geq \sum_{i=1}^{m} \alpha_i S_i^* , \qquad (5)$$

where R^* and S_i^* are nominal resistance and nominal load, while ϕ and α_i are resistance and load factors, respectively, and m is the number of loads considered. The nomial resistance is the value predicted by theoretical or empirical formulas used in conjunction with the design standard, while the nominal value of a load is the value specified by the code authorities. Transition to an load factor design from an old code which is usually allowable stress design raises problem of assigning values of factors ϕ and α_i, called "code calibration" (7, 8).

Various approaches to code calibration would be possible. For example, when American Association of State Highway and Transportation Officials (AASHTO) criteria for load factor design of steel highway bridges were first developed, load factors were chosen to provide the same cross section for all spans as in allowable stress design for a standard case of a 40-ft span (7). With the acceptance of probabilistic rationale in design, such a deterministic approach to code calibration is no longer adequate. A reliability-based approach to code calibration may consist of the following procedures:

i) to determine the target safety level that structures designed according to the concerned format should have. A practical method to determine the target safety level corresponding to various limit states is to investigate a selection of currently acceptable designs. A set of criteria based on experience and judgment may be used to obtain one or a consistent set of acceptable safety levels,
ii) to collect the statistical data, relevant for the reliability analysis of structures, such as ratios of mean to nominal values, coefficents of variation of design random variables, and
iii) to select resistance and load factors in such a manner that values of these factors in conjunction with the design format are judged to provide the structural safety adequately close to the target safety level over frequently occurring design situations.

In the procedures above, the safety of structures can be measured, in the sense of the second-moment first-order reliability, by the safety index which has certain shortcomings, but is nevertheless useful in analysis due to its simplicity. Let $\bar{\theta}(\equiv \bar{R}/\bar{S})$ be the central safety factor, and let V_R and V_S be the coefficients of variation of the resistance, R, and the total load, S, associated with a design. The safety index is then expressed as

$$\beta = \frac{ln\ \bar{\theta}}{\sqrt{V_R^2 + V_S^2}} \equiv \frac{ln(\bar{R}/\bar{S})}{\sqrt{V_R^2 + V_S^2}} \quad . \tag{6}$$

This β used in the following analysis is favored in modern reliability studies for a number of practical reasons although many other definitions of safety indices are available. Probability of failure could be adopted as a measure of safety. Yet it generally necessitates tedious computation and then is discouraging from the practical point of view.

Determination of Factors

In the preceding section, the code calibration procedures to the load factor design are presented. As an application, the load factor design of bridges are herein considered. Among various loads which should be considered in design of a bridge, dead, wind and traffic loads are chosen in this application. A dead load is practically invariant in time, while the other two loads are obviously time-varying. Then, analysis required to the code calibration is simple when dead and only one of the two time-varying loads are considered. On the other hand, the determination of the load factors in the presense of the two time-varying loads requires rather complicated analysis of load comibnation. First, the simple case that dead and wind (or traffic) loads are considered is dealt with (Part I). Next, the determination of the load factors involving load combination analysis follows (Part II).

Part I

The values of resistance, dead load, wind load and traffic load factors in Eq.5 are herein determined according to the calibration procedures. Necessary information to the code calibration is presented in Table 3. The target safety index is chosen to be 4.0, which would be acceptable from the past studies (7, 8, 9). Frequently occurring design situations are expressed in terms of wind-to-dead and traffic-to-dead load ratios. Most of the statistical data in Table 3 have been used in the past calibration studies (7, 8, 9), while some are assumed by the writers as realistic values suitalbe for illustrating the principles and procedures involved. The statistical data of the wind load in Table 3 are based on the yearly maximum wind speed records in Tokyo. Accepting the type I distribution for the records in Tokyo, the statistical parameters α and u estimated to be 0.359 and 14.90, respectively (Table 1). The maximum dist over r years also yeilds to the type I, of which the mean $\bar{v}_r$ and standard d σ_r are, respectively, given by

$$\bar{v}_r = u + (\gamma + ln\ r) / \alpha \ , \tag{7}$$

and

$$\sigma_r = \pi / \sqrt{6}\ \alpha \ = \sigma_1 \ , \tag{8}$$

where the value of γ is 0.577 (Euler's constant) and σ_1 is the standard deviation of the yearly maximum. On the other hand, from Eqs.1 and 2, the R year wind speed $V_{R,D}$ for design yields to

$$V_{R,D} = u - \{ ln [-ln(1 - 1/R)] \} / \alpha \qquad (9)$$

The anticipated lifetime N year of bridges can be assumed to be 50 years. For such structures having a relatively long lifetime, 100 year return period of the design wind speed specified in the code would be reasonable. Then, equating γ to 50 and R to 100, Eqs.7 and 9 yield, respectively, to

$$\bar{v}_{50} = u + 4.49 / \alpha \ , \qquad (10)$$

$$\bar{v}_{D,100} = u + 4.60 / \alpha \ . \qquad (11)$$

Substitution of the values of α and u into Eqs.10 and 11 respectively, finds $\bar{v}_{50}$ = 27.41 and $\bar{v}_{D,100}$ = 27.71 m/s which are considered practically equal, i.e., $\bar{v}_{50} = \bar{v}_{D,100}$. The coefficient of variation v_{50} of the maximum value over 50 years is found 0.13 from Eqs.7 and 8. The pseudostatic force on an object subject to the wind is proportional to the square of the wind speed. Then, the wind load w is expressed as

$$w = c\, v^2 \ , \qquad (12)$$

in which the parameter c is a constant depending on sensitivity of a structure or a structural element to the wind speed. Applying the first-order analysis of uncertainty to Eq.12, the following are found:

$$W^* = \bar{W} \ , \qquad (13)$$

and

$$V_W = 0.26 \ . \qquad (14)$$

The code calibration in the load factor design in the presence of dead and wind loads is now carried out. Given values of resistance, dead load and wind load factors in Eq.5 and the data in Table 3 enable one to calculate the safety index value from Eq.6. The variables associated with these factors are discretized at interval of 0.05. After successive trial of various combinations of ϕ, α_D and α_W values, appropriate values of ϕ, α_D and α_W are found to be 0.90, 1.45 and 2.10, respectively, over the wind-to-dead load ratios from 0.2 to 0.8. Then. Eq.5 yields to

$$0.9R^* \geq 1.45D^* + 2.1W^* \qquad (15)$$

The safety index values β achieved by these values of factors are shown in I It is observed that a constant safety index indicating approximately the equ reliability level, can be fairly attained by the load factor design in this Next, consider the load factor design for the traffic load L in lieu of the load. The values of ϕ and α_D are fixed to be 0.9 and 1.45, respectively. (the traffic-to-dead load ratios of 0.2~0.8, the value of 2.15 for the traf load factor α_L is found suitalbe. Then, Eq.5 yields to

$$0.9R^* \geq 1.45D^* + 2.15L^* \ . \qquad (16)$$

The safety index values β achieved by Eq.16 are also found fairly constant as shown in Fig.7.

Part II

When both wind and traffic loads are considered, the load factor design format takes the form of

$$\phi R^* \geq \alpha_D D^* + \alpha_L L^* + \alpha_W^c W^* \ , \qquad (17)$$

or

$$\phi R^* \geq \alpha_D D^* + \alpha_W W^* + \alpha_L^c L^* \ . \qquad (17')$$

in which the values of ϕ, α_D, α_L and α_W are already found to be 0.9, 1.45, 2.15 and 2.1, respectively, in Part I. In structural codes, the total factored design load would be prescribed to choose larger one of the values corresponding to the right-hand sides of Eqs.17 and 17'. Then,

$$\phi R^* \geq Max[\alpha_D D^* + \alpha_L L^* + \alpha_W^c W^* \ , \ \alpha_D D^* + \alpha_W W^* + \alpha_L^c L^*] \ . \qquad (18)$$

The objective of this part II is to determine appropriate values of α_W^c and α_L^c. For this, basic analysis of the load combination due to the two time-varying loads is to be performed in order to evaluate the safety rationally.

The time behavior of the wind load is modeled as a simple Poisson process having infrequent occurrence and independent random intensities with a short duration. Poisson assumption of occurrence of strong winds has been found acceptable in the preceding section. Strictly speaking, wind loading varies continuously in time; however, the major contribution of the wind loading to structural failure can be attributed to strong winds occurring infrequently. Employing the type I distribution for the yearly maximum wind speed then, the intensity distribution $F_{V,I}(v)$ of the strong wind can be derived from Eq.2:

$$F_{V,I}(v) = 1 - exp[-\alpha(v - u)] \ / \ \nu_W \ , \quad v > u - ln \ \nu_W \ / \ \alpha \qquad (19)$$

in which ν_W/year is the mean occurrence rate of the strong wind (10). From Eqs. 12 and 19, the intensity distribution $F_{W,I}(w)$ of the load due to the strong wind is given by

$$F_{W,I}(w) = F_{V,I}(\sqrt{w/c}) \ . \qquad (20)$$

For the time period t, the maximum wind load distribution is given by

$$F_W(w, \nu_W, t) = exp\{-\nu_W t[1 - F_{W,I}(w)]\} \ . \qquad (21)$$

Concerning the traffic load on bridges, it can be separated into two independent loads due to jammed and smooth traffic flows (Fig.8). One day history of the traffic load generally consists of such two loads. Assume the intensity distributions $F_{L,J}(x)$ and $F_{L,S}(x)$ of the two loads due to jam smooth traffic flows, respectively, have lognormal distributions. Indepen

assumption of the every day traffic load leads to unreasonable statistics of the lifetime maximum load in comparison with the traffic load survey (11). Then it is herein assumed that both of the traffic loads stay constant over one year, but vary independently year to year. Moreover, it is assumed that the jammed flow occurs periodically once in a day with a constant duration, and that the smooth flow is on bridges for the rest of the day.

The yearly maximum distribution $F_{max}(x,\ 1\ year)$ of the combined load can be then given from Eq.21 by

$$F_{max}(x,\ 1\ year) = \int_0^x F_W(x-y, \nu_W p,\ 1)\, dF_{L,J}(y) \times \int_0^x F_W(x-y, \nu_W q,\ 1)\, dF_{L,S}(y) \ . \qquad (22)$$

in which p (or $q = 1 - p$) is the probability of simultaneous occurrence of the strong wind and jammed traffic flow (or smooth traffic flow), and is a function of the duration time of the loads:

$$p = (d_W + d_J) \ / \ (d_J + d_S) \ , \qquad (23)$$

in which d_J, d_S, d_W are the durations of the jammed flow, smooth flow and the strong wind, respectively. Since the yearly maximum of the combined load is mutually independent under the assumptions made, the maximum distribution of the combined load for the lifetime N year is then given from Eq.22 by

$$F_{max}(x,\ N\ year) = [F_{max}(x,\ 1\ year)]^N \qquad (24)$$

from which the mean and the coefficient of variation of the maximum of the combined load are computed. The set of parameters for this computation are used herein: N = 50 year, α = 0.359, u = 14.90, ν_W = 2/year, d_W = 2 hrs, the means of the loads due to jammed flow and smooth flow = 0.65 L^* and 0.25 L^* (including impact effects), the coefficients of variation for the two loads = 0.3 and 0.4, respectively, d_J = 2 hrs and d_S = 22 hrs. Note that these parameters assumed regarding the traffic loads correspond consistently to the statistics in Table 3.

The safety index values calculated for various sets of α_W^c and α_L^c values which are discretized at intervals of 0.05 are examined with respect to the closeness fit to the target safety. The value of 0.65 for both α_W^c and α_L^c are found appropriate after calibration. Then, Eq.18 yields to

$$0.9R^* \geq Max[1.45D^* + 2.15L^* + 0.65W^*,\ 1.45D^* + 2.1W^* + 0.65L^*] \ ,$$

The safety index values associated with the foregoing load factors are given Table 4, which shows that a fairly constant reliability level is maintained c wide ranges of W^*/D^* and L^*/D^*. Eq.25 shows that the factored design load c minor one among wind and traffic loads is allowed to reduce significantly by nearly 70%. From a practical point of view, code formating is desired to be simpler if the loss due to its simplification is negligible. For example, ·ithout much loss, Eq.25 could be simplified into the following practical fo1

$$0.9R^* \geq 1.45D^* + 2.1(S_1^* + 0.3S_2^*) \ , \qquad (26)$$

in which $S_1^* = W^*$ and $S_2^* = L^*$ if $W^* > L^*$

$S_1^* = L^*$ and $S_2^* = W^*$ otherwise

It is emphasized that all numerical values used in Parts I and II are for illustration purpose. The values such as load factors must be establised from elaborate collection of data in actual application.

SUMMARY AND CONCLUSIONS

Some probabilistic considerations have been presented on the wind resistant design. The yearly maximum wind speed records in Japan are fitted to the type I and II extreme distributions (Figs.2~5). It has been found that neither type of distributions can be given preference on the basis of closeness fit, and also that distribution assumption of either type does not significantly change the design wind speed for commonly used return periods (Table 2). Good fit of the combined distribution to the records in Osaka is shown (Fig.4). The meteorological reasons of this good fit are discussed. Using the records in Hirato, occurrence of the strong wind is analyzed and found to be approximated by a Poisson process on the basis of the waiting time fit (Fig.6).

The wind resistant design has been studied in conjunction with the load factor design. The reliability-based code calibration procedures are presented to determine appropriate wind load factors as well as other factors. The load factor design of a bridge or its elements subject to wind and traffic loads is considered as an application. Using the simple stochastic models for such two time-varying loads, the load combination analysis is carried out. Based on the analysis, finally, the values of the load and resistance factors have been calibrated. It has been shown, as expected, that the calibrated factors maintain a fairly constant reliability level over the concerned ranges of the wind-to-dead and traffic-to-dead ratios (Table 4). However, they should not be considered factual; appropriate values for actual use in design must be established from careful study by the responsible code authority.

REFERENCES

1. "American National Standard Building Requirements for Minimum Design Load in Buildings and Other Structures A58.1, "American National Standard Institute, New York, N.Y., 1972.
2. "Design Standard for Honshu-Shikoku Bridges, " Japan Society of Civil Engineers, Tokyo, Japan, 1967 (in Japanese).
3. Gumbel, E.J., *Statistics of Extremes*, Columbia Univ. Press, New York, N.Y., 1958.
4. Thom, H.C.S., "Distribution of Extreme Winds in the United States, "P ASCE, Vol.86, No.ST4, Apr., 1960.
5. Saito, R., "Extreme Winds in Japan," Res. Report, Vol.9, No.7, the Meteorological Agency, 1957 (in Japanese).
6. Parzen, E., *Stochastic Processes*, Holden-Day, San Fransisco, Calif.,
7. Ravindra, M.K. et al., "Illustrations of Reliability-Based Design," P ASCE, Vol.100, No.ST9, Sept., 1974.
8. Galambos, T.V., and Ravindra, M.K., "Tentative Load and Resistance Fa Design Criteria for Steel Buildings," Res. Report No.18, Washington U Sept., 1973.
9. Siu, W.W.C. et al., "Practical Approach to Code Calibration, "Proc. c Vol.101, No.ST7, July, 1975.

10. Wen, Y-K, "Statistical Combination of Extreme Loads, "Proc. of ASCE, Vol.103, No.ST5, May, 1977.
11. Kunihiro, T., and Asakura, H., "Design Load on Bridges and Survey of Traffic Flows, "Report of the Public Works Res. Inst. Ministry of Construction, Japan Vol.15, No.4, Apr., 1973 (in Japanese).

STATION	TYPE I		TYPE II	
	$\hat{\alpha}$	$\hat{u}$	$\hat{k}$	$\hat{w}$
SAPPORO	0.698	14.16	10.62	14.10
TOKYO	0.359	14.90	6.60	14.84
OSAKA	0.224	13.81	4.88	14.00
MUROTOMISAKI	0.139	28.34	4.97	27.99

Table 1 Estimated Statistical Parameters of Type I and II Distributions

LOCATION	TYPE I				TYPE II			
	Return Period (year)							
	50	75	100	150	50	75	100	150
SAPPORO	19.7	20.3	20.7	21.3	20.3	21.1	21.8	22.6
TOKYO	25.8	26.8	27.6	28.8	26.8	28.6	29.8	[illegible]
OSAKA	30.4	32.2	33.4	35.2	31.2	34.0	36.0	[illegible]
MUROTOMISAKI	56.5	59.4	61.5	64.5	61.3	66.6	70.6	[illegible]

Table 2 Design Wind Speeds (m/s) for Return Periods (year)

Target Safety Index β	4.0	Wind Load W	
Resistance R (Yielding in Flexure)		$\overline{W}$ / W^*	1.00
$\overline{R}$ / R^* (= Mean / Nominal)	1.12	V_W	0.26
V_R	0.15	W^* / D^*	0.2~0.8
Dead Load D		Traffic Load L	
$\overline{D}$ / D^*	1.00	$\overline{L}$ / L^*	1.22
V_D	0.07	V_L	0.14
		L^* / D^*	0.2~0.8

Table 3 Data for Code Calibration

Wind-to-dead Load Ratio W^*/D^*	Traffic-to-dead Load Ratio L^*/D^*							
	0.0	0.2	0.3	0.4	0.5	0.6	0.7	0.8
0.0	2.88	3.88	3.96	4.01	4.05	4.06	4.07	4.08
0.2	3.98	3.91	4.09	4.17	4.21	4.22	4.21	4.23
0.3	4.04	4.05	3.96	4.13	4.21	4.25	4.27	4.27
0.4	4.06	4.12	4.06	3.99	4.14	4.22	4.27	4.29
0.5	4.06	4.13	4.11	4.05	3.99	4.13	4.22	4.27
0.6	4.03	4.12	4.12	4.09	4.03	3.98	4.11	4.20
0.7	4.01	4.10	4.11	4.10	4.07	4.01	3.97	4.09
0.8	3.97	4.05	4.08	4.09	4.07	4.04	3.98	

Table 4 Safety Index Values after Calibration (ϕ = 0.9; α_D = 1.45; α_W = 2.1; α_L = 2.15; α_W^c = 0.65; α_L^c = 0.65)

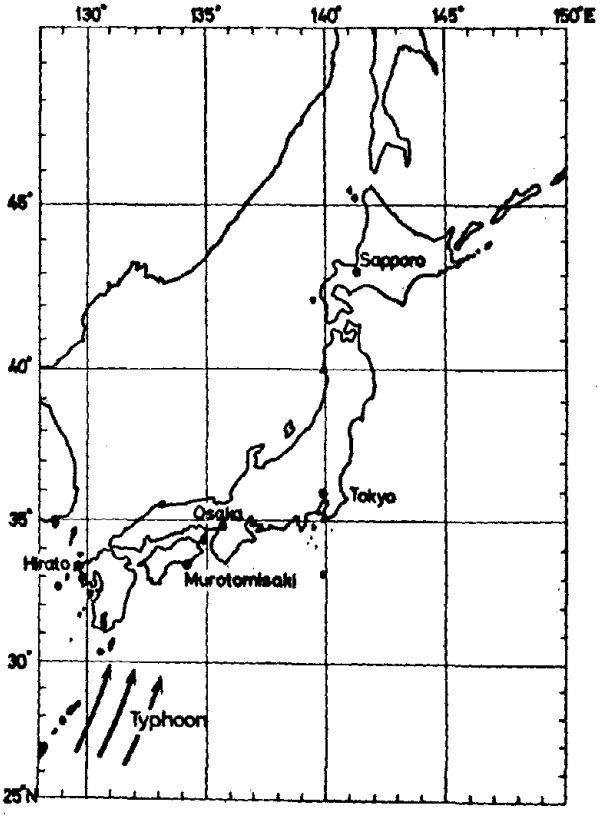

Fig. 1. Selected Meteorological Stations in Japan

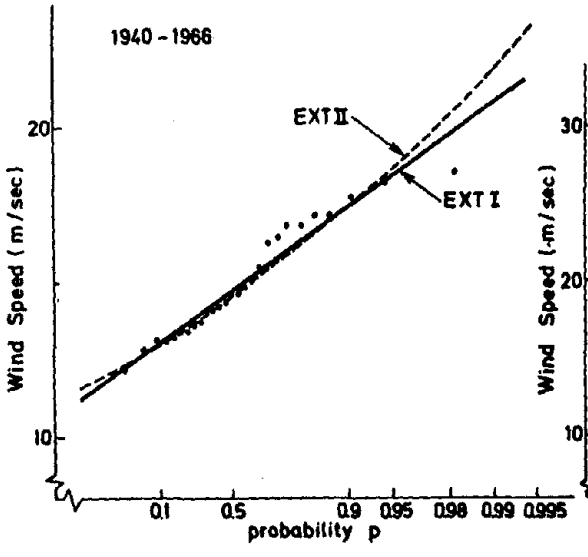

Fig. 2. Yearly Maximum Wind Speeds in Sapporo

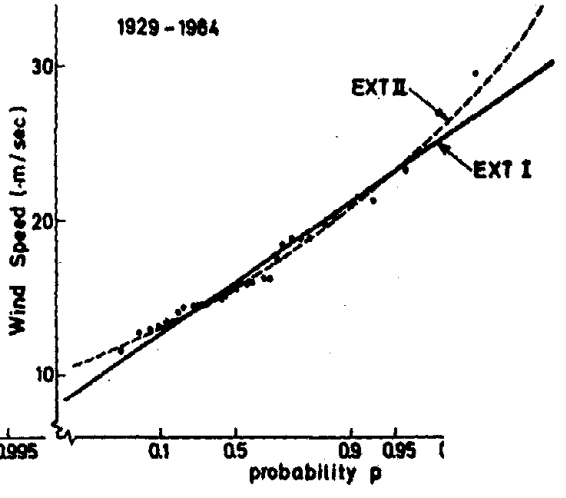

Fig. 3. Yearly Maximum Wind Speed

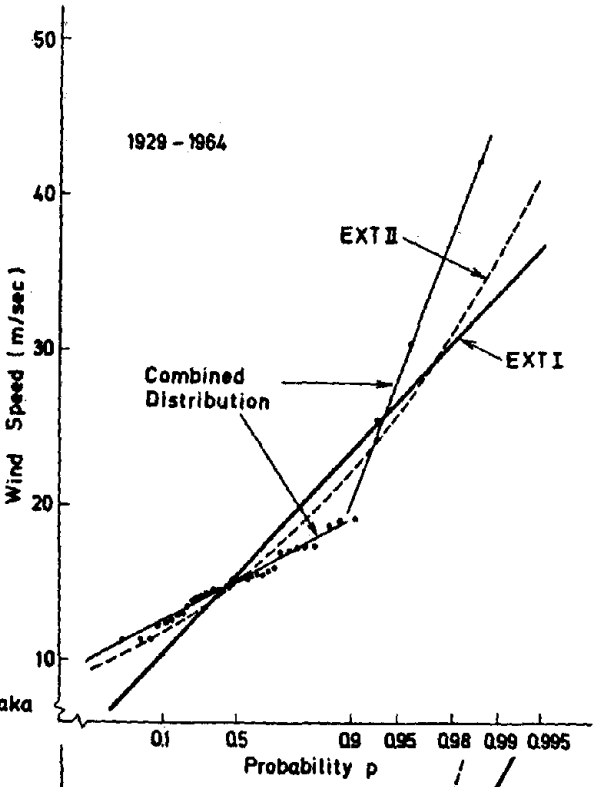

Fig. 4. Yearly Maximum Wind Speeds in Osaka

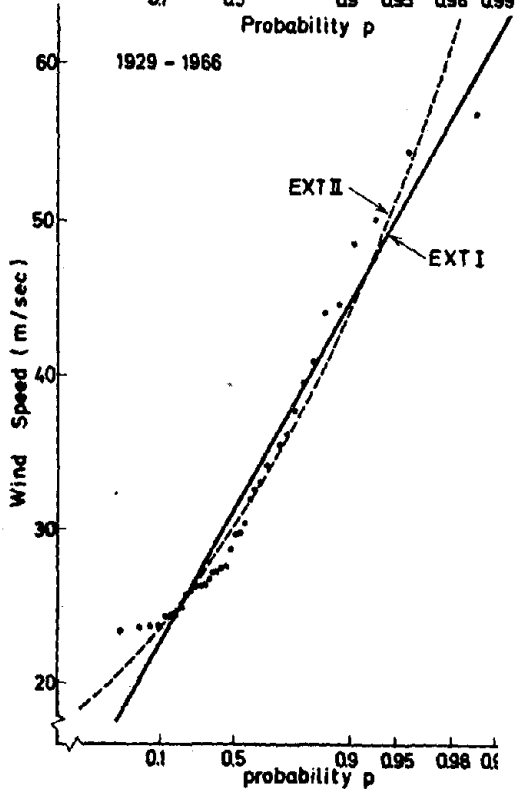

Fig. 5. Yealy Maximum Wind Speeds in Murotomisaki

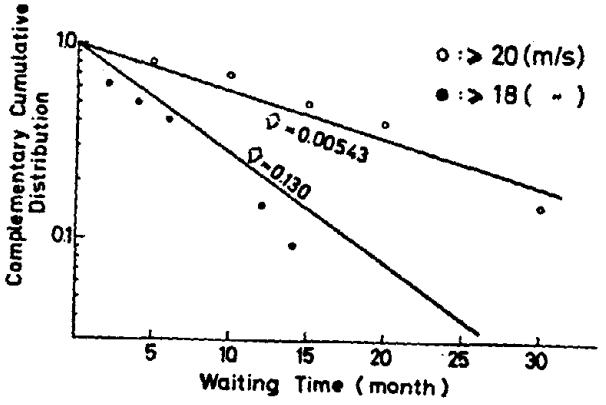

Fig. 6. Poisson Distribution of Waiting Time of Strong Winds (≥ 20 or 18 m/sec) in Hirato Station, 1940 - 1975

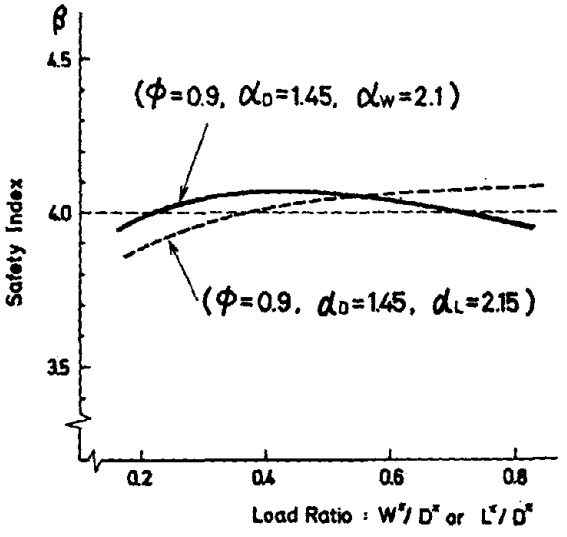

Fig. 7. Safety Indices β due to Factors φ, α_D and α_W (or α_L)

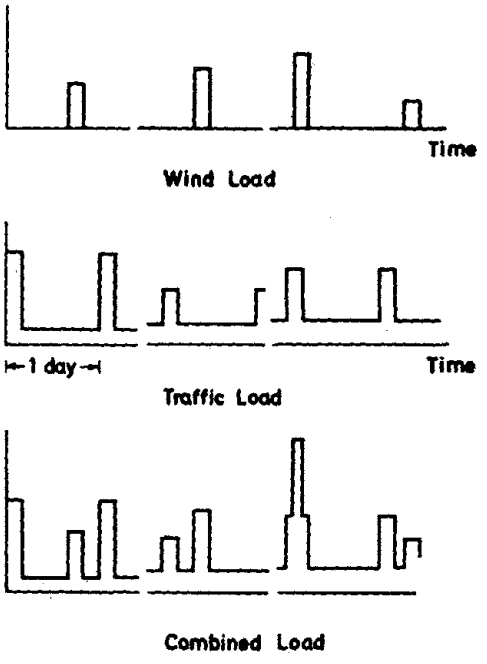

Fig. 8. Temporal Variability of Loads

WIND-RESISTANT DESIGN PRACTICES OF CABLE-SUSPENDED BRIDGES IN JAPAN

Manabu Ito and Naruhito Shiraishi

University of Tokyo Kyoto University

SYNOPSIS

Many suspension bridges and cable-stayed bridges have been recently constructed and are being planned in Japan. They have usually long span length and are in general wind-sensitive. The authors have been involved in the preparation of their design codes. This report presents main features of the wind-resistant design practices of the above-mentioned structures, such as design wind speed, aerodynamic force, countermoves against wind-induced vibrations and cross-sectional shape of bridge deck.

INTRODUCTION

Owing to their material saving and aesthetical advantages, the cable-suspended structures such as suspension and cable-stayed bridges have been constructed for spanning long distances. However, their history is rather new in Japan, as seen in Table 1. Since these structures are sensitive to wind, the environment of which is particularly severe in this country, the special cares must be taken so that they resist to winds.

The intense research activities in this field in Japan were conspicuously motivated by the bridge projects to cross the Seto Inland Sea, that is, to connect the main island with the Shikoku Island. The technical committee concerned was established at the Japan Society of Civil Engineers in 1963 and it published the Specifications for Wind Resistant Design for the proposed bridges, which have also affected on the wind-resistant design of other long-span bridges in Japan afterward.

The behaviors of a flexible structure subjected to wind may be classified as follows, according to the cause or the nature of phenomenon:

(1) static behaviors (due to steady wind forces)

a) deformation and stress
b) static instability

i. divergence
ii. lateral buckling

(2) dynamic behaviors (due to unsteady aerodynamic forces)

a) buffeting

i. due to turbulence of natural wind
ii. due to turbulence in the wakes of windward structures

b) vortex excitation* (aeolian oscillation)

c) self-excited vibrations (due to negative damping effect of aerodynamic force)

i. one-degree bending or torsional instability
ii. coupled flutter

As seen here, a distinctive feature of wind-induced phenomena of the flexible structure is their variety; there is the possibility of multiple failure or unserviceability modes for a specific structure, and some of the behaviors cited above may occur concurrently.

The specifications like the aforementioned provide the basic items which are necessary for structural design, but the principal design information in the area of bridge stability is provided through the wind tunnel test with a scaled model, because the section of bridge decks are complex and different each other. The present report will outline the state-of-the-art of the wind-resistant design practices of suspension bridges and cable-stayed bridges having long span lengths beyond the scope of the standard specifications for Japanese bridges.

DESIGN WIND SPEED

When a wind-sensitive structure is designed, it is important to estimate firstly the wind environment expected at the site. Site studies consist of the gathering of strong wind data over a period of years and knowledge of the local characteristics of wind direction and turbulence, the information of which may be obtained by field measurement at the site or wind tunnel experiment with a geographical model including the surrounding area.

Since the wind data at the bridge site are usually not available, the estimation is to be made from the data recorded at the nearby meteorological stations. This is possible, for example, through the regressive analysis taking into account the topographical factors at the site, but the wind data may be not always enough to obtain a reliable estimation. From such data plots of annual maximum wind speeds at the site using the statistical theory of extreme values,** estimates of the reference wind speed*** for a mean return period given can be made. The return period has been conventionally taken a

---

* Vortex excitation has a nature of self-controled vibration once it deve

** A Type I distribution is used in Japan.

*** e.g. the ten-minute mean wind speed at ten meters above ground or wate level.

twice as the anticipated service life of bridges, while it depends on the acceptable probability of exceedance in conjunction with the factor of safety.

The design wind speed is then obtained from the reference wind speed adjusted for the height above the ground or water level considering the terrain category and for the gust effect on the structure. The concept of gust response factors has been adopted in some building codes, but not yet in bridge specifications. Exception in our country is the suspension bridges of the Honshu-Shikoku Bridge Projects, in which the gust response factors were taken into account to calculate wind loads. In other long span bridges, however, only the effect of spatial and temporal fluctuations of wind on the along-wind bending of bridge deck is considered, and the component of dynamic magnification in the structure due to turbulence is omitted, because along-wind buffeting of bridges in general has not yet been fully studied nor observed except for suspension bridges. Instead the factor of safety is adjusted according as the dynamic magnification is considered or not.

DESIGN PROCEDURES

The design process of the cable-suspended bridges against wind is as shown in Fig. 1. The design wind speed has just been commented and the choice of cross-sectional shape of bridge decks will be discussed later. Here other two items of importance will be examined in a little more detail.

Drag Coefficient

From the results of wind tunnel tests so far reported, the following empirical formulae for drag coefficient C_D are recommended.

For truss girders:

$$C_D = 1.1\sqrt{\frac{3}{2\phi}} \qquad \text{for a single deck}$$

$$C_D = 1.2\sqrt{\frac{3}{2\phi}} \qquad \text{for a double deck}$$

where the solidity factor of windward truss, ϕ , is between 0.2 and 0.45.

For solid web girders:

$$C_D = 2.1 - 0.1\,\frac{B}{D} \qquad \text{for} \quad 8 \geqq \frac{B}{D} \geqq 1$$

$$C_D = 1.3 \qquad \text{for} \quad \frac{B}{D} > 8$$

in which B is the width of bridge deck, D is the depth of solid part of br deck.

The aerodynamic coefficients of such a complex section as the bridge are, however, affected by the relative position and size of component elem and hence the above formulae give only a reference value. After the preli analysis, the wind tunnel test is required to measure the aerodynamic coefficients of the proposed section if the wind load governs the proporti of the structure. When the value of measured drag coefficient under horiz wind differs 5% or more than that used in the preliminary analysis, the

structure shall be proportioned again considering the measured value.

The wind force in the direction of the bridge axis plays a role in proportioning bearings, expansion joints and center-tie of a truss-stiffened suspension bridge. The effects of lift and twisting moment may not be neglected in case of solid web girders. Moreover these nondimensional lift and moment curves, measured for varying steady angles of attack of the wind, are usable to judge the possibility of one-degree vertical and torsional instability, respectively.

Aerodynamic Stability

Usually, the normal procedures of structural design result in bridge deck to be safe against static instability such as lateral buckling and torsional divergence. On the other hand, the wind-induced vibrations often govern the safety and serviceability of cable-suspended structures. The most catastrophic one is flutter, or self-excited oscillations due to the negative aerodynamic damping effect. Once unsteady aerodynamic force is known, the critical wind speed at which flutter onsets in a smooth flow can be calculated, but it is usually assessed through the study of elastically mounted bridge deck section models in a wind tunnel. In order to keep the critical wind speed well above the design wind speed, it is recommended to provide such large torsional rigidity that the torsional natural frequency of the structure exceeds twice as high as the heaving frequency, and to choose aerodynamically stable cross section as discussed in the following section. The hexagonally bundled cable may be, according to circumstances, suffered from galloping, or single-degree lateral instability.

Any bluff and slender bridge component such as solid deck, cable or tower will be prone to vortex-excitation. Its amplitudes are restricted, and then may be the cause of fatigue damage and unserviceability. The increase of stiffness can augment the resonant wind speed and the increase of mass and/or structural damping can suppress the response. But these countermoves are often uneconomical or unfeasible. It is rather judicious to improve the cross section to cut down coherent vortex action or to make a flow smooth.

The presence of turbulence can evidently affect the dynamic instability of the structure; it tends to weaken the vortex-excitation, while its effect on self-excited oscillations has not to date been thoroughly understood.

Wind tunnel investigations are the only realistic approach to the prediction of the bridge's aerodynamic behavior. Their conventional technique at present is the so-called section model test from economical and technical reasons. Three-dimensional effects can be handled by integrating section effects throughout the bridge span. However, a three-dimensional full model test will be significant in such cases that the wind environment along the bridge axis is varying due to geographical or structural situations, or that the behavior of the bridge deck at erection stage must be explored.

CROSS-SECTIONAL SHAPE OF BRIDGE DECK

The cross-sectional shape having smaller drag coefficient such as that composed of circular tube members may sometimes be used for cable-suspended

structures. At the present stage, however, it can be said that small drag sections have been adopted as the result of their aerodynamic stableness rather than aiming at reducing the wind load.

The selection of the bridge deck configuration for cable-suspended structures is made from the following considerations:

(1) to satisfy the requirements of stresses, function of bridges, and aesthetics

(2) to prevent the occurrence of dynamic instability within the specified design wind speed

(3) to refrain from harmful oscillations of restricted amplitudes due to vortex-excitation and buffeting, and

(4) to find the optimal design mainly from economical viewpoint.

As mentioned earlier, use of aerodynamically stable cross-section with appropriate torsional stiffness shall be the most economical and practical solution, while the increase of structural damping and rigidities will serve to improve aerodynamic stability of the structure. Usually use of a very bluff section is avoided except for a cable-stayed girder bridge (Fig. 2) having a short span length or being located at the site where wind environment is not unfavorable, and instead a flow-smoothing or flow-dividing sectional shape to cut down coherent vortex action in the wake and associated strong pressure difference across the deck is adopted. Examples are (1) a stream-lined box girder, (2) a shallow box girder with combination of flaps, fairings or other attachments to control air flow (Fig. 3), and (3) a latticed truss with open grating decks where possible (Fig. 4). It must be borne in mind that the existence of solid handrails, curb stones and other small features in these structures may affect considerably on their aerodynamic characteristics, so that the confirmation of their aerodynamic stability by wind tunnel model test is necessitated.

The streamlined box types have been used in some of European suspension bridges. A rare example in other areas of the world is the Namhae Bridge (center span 400m) in the Republic of Korea, for the design and construction of which Japanese engineers cooperated. The classical flutter theory is applicable to the shallow streamlined sections under horizontal wind, and its flutter speed is rather high. On the other hand, all long span suspension bridges in Japan are truss-stiffened. Even a truss-stiffened deck often exhibits dynamic instability, the type of which is usually coupling of vertical bending and torsion or one-degree torsional flutter. When the phenomenon is in appearance the coupled flutter, the torsional motion seems predominant in nature. Therefore, it intended that these deck-type stiffening trusses have openings between roa deck and upper chords, open gratings provided along the border parts of r lanes, and both upper and lower lateral bracings to constitute closed box structurally. In Japan any full lane is not an open grating structure be of unpleasant driving on it. Since some small obstacles to air flow may, mentioned previously, cause unfavorable effects on overall stability of t stiffening truss, the stringers and handrails are recommended to be an op structure. However, a solid fense of appropriate height at the central r of roadway seems to improve the aerodynamic characteristics of stiffening

In case of cable-stayed bridges, solid web girders are preferred from structural, economical and aesthetical viewpoints. Fig. 2 shows the basic cross-sectional shapes of these structures so far constructed, among which the type (c) is most prevailing. Although cable-stayed bridges are generally stiffer than suspension bridges, they are apt to cause vortex-shedding instability, or eventually self-excited vibrations of vertical or torsional mode, and accordingly are needed to modify the original section as already shown in Fig. 3. The girder of a cable-stayed bridge may be a truss, upon rare occasions, for design reasons such as double deck construction. These trusses will have relatively large solidity factor, and then there is the possibility of aeolian vibration.

CONCLUSIONS

The cable-suspended structures such as suspension and cable-stayed bridges are so wind-sensitive that special design considerations must be exerted. Of particular importance are the assessment of wind environment at the site, the increase of structural stiffness, and the choice of aerodynamically stable cross-section. In order to attain reliable design the wind tunnel model tests are inevitable.

It should be also borne in mind that many problems to be solved remain in this area; some of them are the effects of turbulence of natural wind on various phenomena of the structure, the techniques of reliable wind tunnel experiment, and the establishment of the safety and serviceability rationale for wind resistant design. Since the behaviors of long-spanned bridges are complex and diverse, it is necessary to gather data on various designs both from full scale measurements with prototype structures and from wind tunnel tests with scaled models.

Table 1 Major Cable-Suspended Bridges in Japan (1977)

suspension bridges			cable-stayed bridges		
name	main span (m)	completed	name	main span (m)	completed
Oh-Naruto	876	under construction	Yamato-gawa	355	under construction
In-noshima	770	under construction	Suehiro	250	1975
Kanmon	712	1973	Kamome	240	1975
Hirato	465	1977	Rokko Island	220	1976
Wakato	367	1962	Toyosato	216	1970

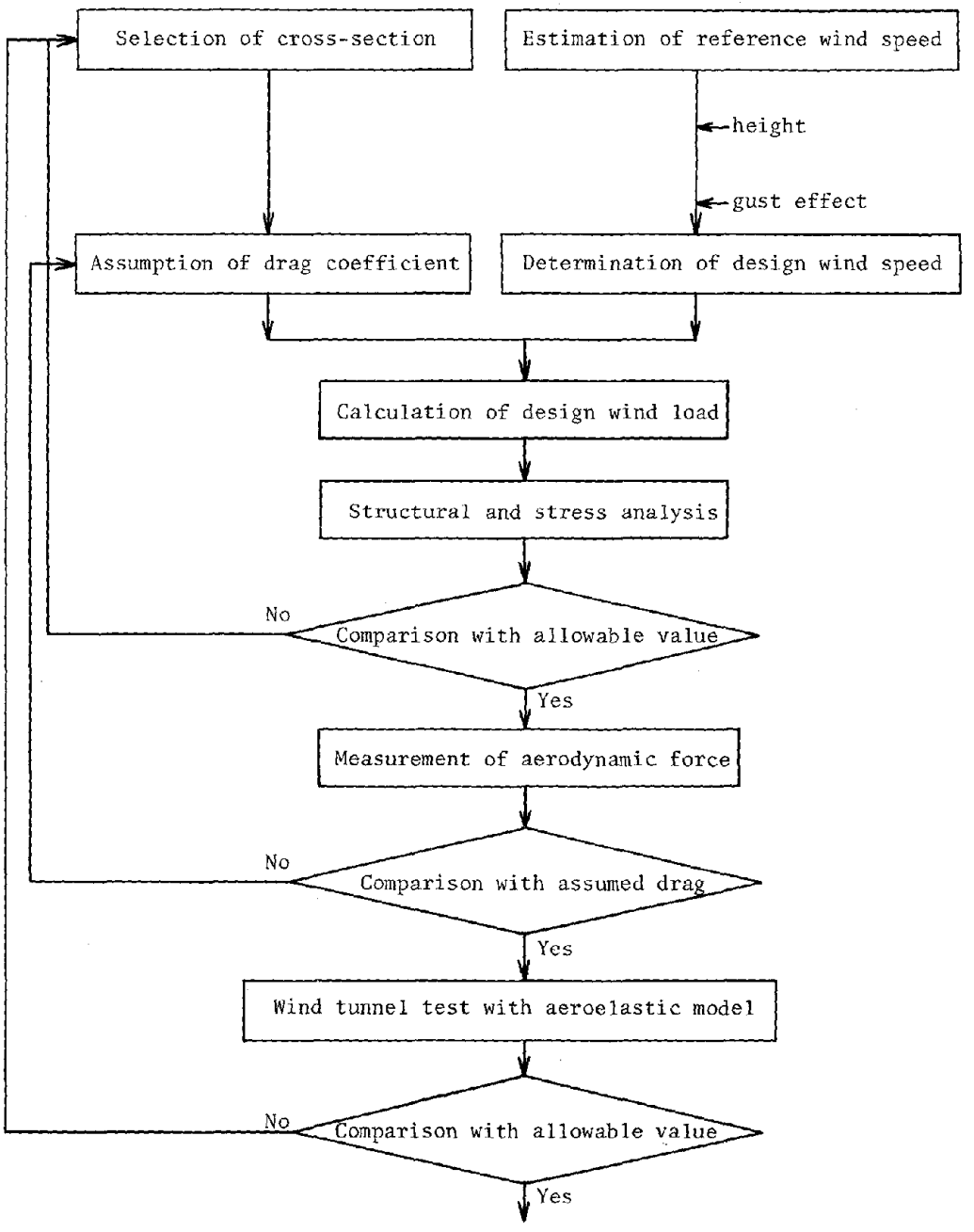

Fig. 1 Flow of Wind-Resistant Design

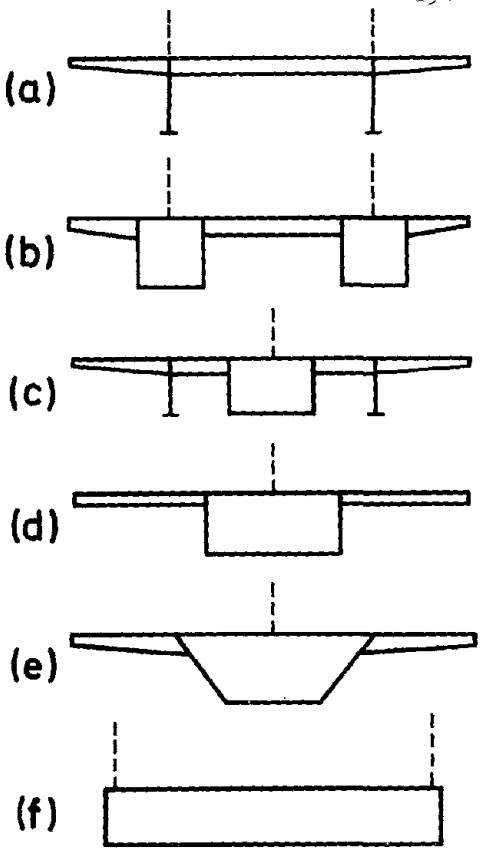

Fig. 2 Basic Cross-Section of Cable-Stayed Girder Bridges

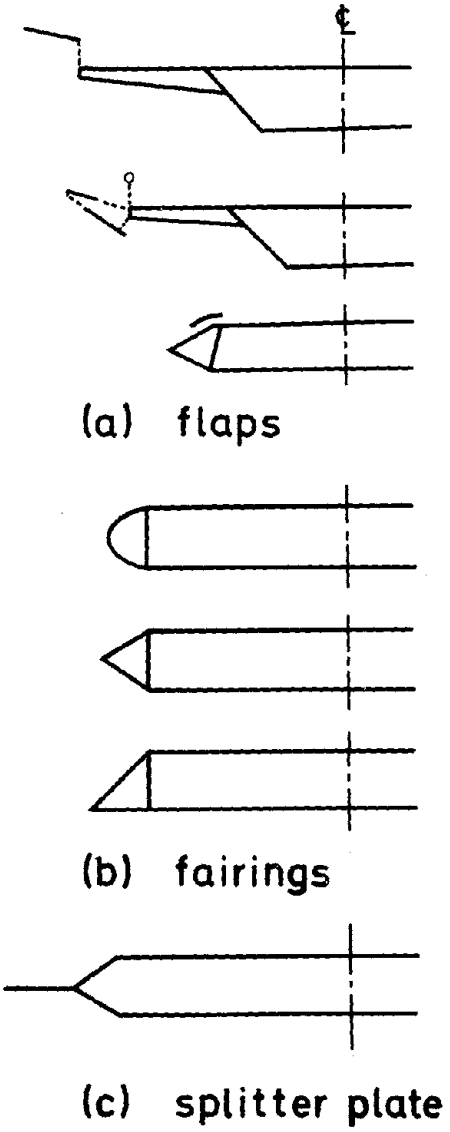

Fig. 3 Various Stabilizers

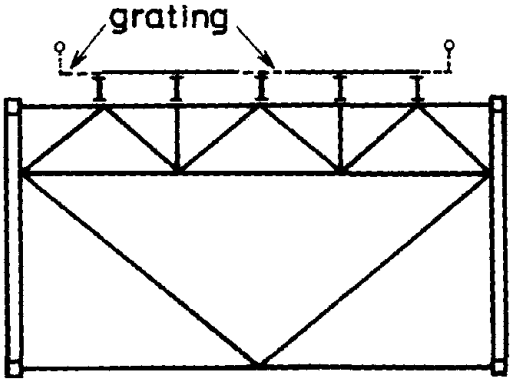

Fig. 4 Example of Stiffening Tru of Suspension Bridge

THE DEVELOPMENT OF DESIGN CRITERIA FOR EXTREME EVENTS ARISING FROM NATURAL HAZARDS

George R. Walker & Kevin P. Stark

Department of Civil and Systems Engineering
James Cook University of North Queensland, Townsville, Australia

*

SYNOPSIS

Natural hazards which produce severe events at very infrequent intervals pose difficult problems for engineers faced with the task of designing structures and planning strategies to mitigate their effects in areas where they are likely to occur. The primary object is to reduce the potential scale of disaster from such an event to a level acceptable to the community. In this paper the various factors which contribute to the potential for disaster are discussed and some basic principles that can be incorporated in the development of design and planning criteria are derived. The problems of predicting the magnitude and frequency of occurrence, public apathy in the absence of a recent extreme event, and the establishment of acceptable levels of disasters are also discussed in relation to the development of criteria. The authors write from first hand experience in observing the effects of tropical cyclones and developing design criteria to mitigate the effect of the associated winds and tidal surges. Examples of this experience are used to illustrate the argument and discussion.

INTRODUCTION

The biggest disaster arising from natural hazards in Australia was that caused by tropical cyclone 'Tracy' to Darwin in December 1974 (Walker, 19[illegible] The economic cost has been put variously between 500 and 1 000 million Aus dollars while the social cost resulting from the evacuation of nearly 35 (the 45 000 inhabitants to centres up to 2 000 miles away, and from the di: living conditions experienced by those who remained, will never be fully

Although it made the biggest impact, cyclone 'Tracy' was by no means only natural hazard to have affected Australia.

Indeed, Australia appears to be particularly susceptible to a wide r natural hazards, so much so that it has probably helped to shape the nati character. Tropical cyclones, tornadoes, floods, bushfires, drought, thu and hail seem to occur surprisingly often, reports of earthquakes are not

and only snowstorms and volcanic activity seem to be missing from a world list of hazards (Australian Academy of Science, 1976). In the last decade Australia has suffered from disastrous bushfires in Tasmania in 1967 causing property damage of the order of 35 million dollars, a major earthquake at Meckering, Western Australia in 1968 with a maximum intensity of MMIX, a severe drought in Queensland from 1967-69, cyclone 'Althea' in 1971 which caused an estimated 20 million dollars of damage to Townsville, tornadoes in Brisbane in 1973 and 1977, major floods in Queensland in 1974 causing an estimated loss of the order of 100 million dollars in addition to major social distress, cyclone 'Tracy' also in 1974, cyclone 'Joan' in Northwest Australia in 1975 with an estimated central pressure of 915 mb but fortunately crossing the coast in a relatively uninhabited area, and a serious hailstorm in Toowoomba, Queensland in 1976, as well as others of less note.

As a result the Australian community has had to look seriously at the problems caused by natural hazards, and the ways in which their effects might be mitigated. The engineering profession has been deeply involved in these studies, especially in respect of tropical cyclones, floods, tornadoes and earthquakes where their activities can significantly influence the community impact of the hazards.

THE OBJECTIVE

Before any meaningful discussion of criteria can take place it is necessary to have a clear idea of the primary objective of planning and designing for natural hazards protection.

A natural hazard is generally only of concern in as much as it causes distress to a community. The greater the distress the greater the concern. If the distress is such as to make a significant impact on the community we call it a disaster and depending on the extent of the affected community it may be described as a local, state, national or even international disaster.

For instance, the Toowoomba hailstorm was a local disaster, since although it seriously disrupted the local community of Toowoomba its impact on the state of Queensland was probably negligible. Cyclone 'Althea', and the Queensland floods of 1974, could be described as state disasters since they not only caused distress to the communities involved but required significant aid on a statewide scale to restore the damage and provide for the welfare of those afflicted. Cyclone 'Tracy' could be classified as a national disaster in that virtually the whole of Australia was affected by it and involved in aid, relief and restoration activities. Australia has probably not suffered a disaster on an international scale such as the Bay of Bengal cyclone or the earthquakes in Managua whose impacts were so great that social, technical and financial aid had to be sou internationally.

The primary objective of engineers in design or planning for a natural hazard is the mitigation of the potential disaster which it may cause to a level which is acceptable to both the affected community and the overall community. Communities generally accept that if a severe natural hazard strikes, some damage may occur, and that in relation to extreme events of infrequent occurrence some balance between the economic cost of protection a he social and economic cost of failure is reasonable. Determining the righ alance is the problem.

Two major implications follow from this statement of objective:

(i) the primary concern is the protection of the community and not individuals;
(ii) the aim is to provide a degree of protection, which may vary as a function of the anticipated frequency and level of the event, and not to provide guaranteed protection.

CHARACTERISTICS OF NATURAL HAZARDS

Common features of the severe natural hazards which are of importance in design and planning are:

(i) they are discrete events;
(ii) they are generally infrequent in their occurrence in any one location;
(iii) they may be associated with events of large magnitude;
(iv) they affect an area, and one event may affect an entire community should it be situated within the area affected.

For structural engineers in particular, these characteristics taken together are quite different from those of the normal loadings for which they are accustomed to design.

Using tropical cyclones as an example, in the cyclone prone areas of North East Queensland any particular locality can expect a direct hit by a tropical cyclone only once in every 20 or 30 years on average. If we consider the winds which may be experienced in these localities arising from tropical cyclones then the hazard can be classified as shown in Table I. During the last 3 years events at each of these levels have been experienced in different localities around Australia. This highlights why tropical cyclones tend to be regarded as Australia's major natural hazard.

The area affected by tropical cyclones varies from one cyclone to another. Cyclone 'Tracy' was small in diameter by average standards, but with a maximum diameter of destructive winds of the order of 20-30 km was still large enough to engulf a small city such as Darwin.

Cyclone 'Joan' was an example of a large tropical cyclone producing in respect of wind an extremely severe event at the centre and a moderate event 50 km from the centre at Port Hedland, and thus large enough to have engulfed a very large city.

Similar examples could be given for ground motion from earthquakes, from tornadoes, floods from heavy rains, tidal surges from tropical cyclo: tsunamis from earthquakes. In most of these cases the difference between and severe events is greater and the frequency of severe events less than for tropical cyclones thus increasing the problem, and areas affected are generally smaller from tornadoes and larger from earthquakes.

FACTORS AFFECTING SCALE OF DISASTER

The scale of disaster arising from a natural hazard is the result of the interaction of a number of factors, the most significant of which are:

(i) the severity of the hazard;
(ii) the size of community affected;
(iii) the vulnerability of the community to the hazard;
(iv) the ability of the wider community at local, state and national levels to cope with the socio-economic consequences.

Disasters arise as a result of the interaction of natural hazards with communities. Where natural hazards occur without impinging on communities they may go entirely unnoticed except by those with a special scientific interest in them. A moderate hazard hitting a large unprepared community can cause a much greater disaster than a severe hazard striking a smaller well prepared community.

Tropical cyclone 'Althea' which hit Townsville in December 1971 had a central pressure between 950 and 960 mb and produced wind gusts of the order of 50-60 m/s and a tidal surge of 3-4 m above predicted tide levels (Trollope, 1972). Just 13 months earlier a tropical cyclone of almost identical characteristics moved up the Bay of Bengal and crossed the Bangladesh coast line. Cyclone 'Althea' caused 3 deaths and 20 million dollars worth of damage to approximately 3 000 houses. The Bay of Bengal cyclone left 300 000 people dead, and damaged or destroyed 400 000 homes, $63 million worth of crops, 100 000 boats and 300 000 cattle. The difference was due to a difference in actual severity of the event from the tidal surge as a result of cyclone 'Althea' crossing at low tide and the Bay of Bengal cyclone crossing at high tide, an order of magnitude difference in the population of the communities affected, and the much greater vulnerability of the Bangladesh community. The inability of the Bangladesh (then East Pakistan) community at large to cope with relief and restoration further aggravated the total magnitude of this disaster.

The interaction between a natural hazard and a community which determines the scale of any resulting disaster may be represented as a Disaster System such as portrayed in Figure 1 (Stark and Walker, 1976).

MITIGATION OF DISASTERS

The scale of disaster arising from a natural hazard may be mitigated by:

(i) reducing the severity of the hazard;
(ii) limiting the size of communities likely to be affected;
(iii) decreasing the vulnerability of communities to the hazard;
(iv) improving the ability of communities to recover from the effects of the hazard.

By the construction of dams and effective management of watercourses and run-off areas flood hazards can be significantly reduced, but otherwise there seems little that can be done at this stage to reduce the severity of the many severe natural hazards. Seeding of tropical cyclones and lubrication of active faults perhaps offers some hope, in this respect, for the future.

In hazard-prone areas, scattered smallish communities would be more appropriate than large centralised communities but the economic and social forces in society make it unlikely that planning in this respect would be feasible. However, it is possible to limit the number of people living in areas likely to be subjected to floods, tidal surges and tsunamis by appropriate long term planning of land usage.

Decreasing the vulnerability and improving relief and restoration services are the main means of mitigating the effects of most natural hazards. Reduction of vulnerability is primarily an engineering role and if successfully undertaken can greatly reduce the civil defence task of relief and restoration, a factor recognised in respect of tropical cyclones in the introduction to a recent report to the Texas Legislature on minimum building standards (Texas Coastal Marine Council, 1976) where the following comment is made: 'The best way - from a technical, political and economic standpoint - to significantly reduce hurricane damage on a wide scale is through the use of hurricane-resistant building practices.'

DEVELOPMENT OF CRITERIA

The potential scale of a disaster from a natural hazard of a given level of intensity can be expressed in terms of a Disaster Index - D.I. - (Stark and Walker, 1976) which is a function of:

(i) the scale of the hazard - H_s
(ii) the population affected - P^s
(iii) the estimated return period of the hazard - N_r

i.e. DI = Function (H_s, P, N_r)

Where the magnitude of the hazard depends on the simultaneous combination of a number of events such as flood levels resulting from tidal surges during cyclones, the scale and the return period would have to take this into account.

The actual scale of disaster will depend on the vulnerability.

Criteria developed to ensure that the impact of a natural hazard is kept within reasonable limits should reflect the potential scale of the disaster, the economic cost of mitigating it by design and planning, the cost of not mitigating it, and the ability of the community to meet these costs, for various levels of event arising from the hazard.

Figure 2 illustrates the interaction in respect of the development c satisfactory structural design criteria for wind, wave and earthquake haz

In respect of structural engineering a rational approach to establis satisfactory design methods would incorporate the following procedure (Wa 1976):

(i) establishment of basic criteria regarding acceptable degrees of damage at various levels of likely event;
(ii) establishmentof the relationship between damage criteria and structural engineering criteria;
(iii) translation of the engineering criteria into design rules.

This provides a framework within which structural engineering research aimed at natural hazard protection can proceed.

A similar framework can be constructed for the establishment of criteria for flooding, where questions of to build or not to build, and to evacuate or not to evacuate must be answered, and practical policy guidelines are required.

In establishing the basic criteria the economic cost of repair and reconstruction and the social cost of loss of life, injuries and community dislocation must both be considered. The former may tend to dominate for moderate to severe events but the latter tends to become the most important factor for the severe to very severe events when the primary objective may reduce to just saving lives by evacuation if warning of the event is available - as may be the case with tropical cyclones - or by designing buildings to hold together even if damaged beyond repair as is the philosophy in design against earthquakes.

Although at present there is insufficient knowledge to develop a fully consistent approach to design and planning along these lines some basic principles can be established and incorporated into current design procedures. These will now be discussed.

COMMUNITY SIZE AND CRITERIA

The effect of community size on the potential scale of disaster from a natural hazard has been discussed, and it has been argued that design and planning criteria should reflect the potential scale of disaster. It therefore follows that large communities require a higher level of protection than smaller communities for similar scale events of similar probability of occurrence.

A small township of a few hundred people suffering serious damage to 50 percent of its buildings resulting in 10 deaths in a severe event is far more acceptable than a city of half a million inhabitants suffering the same level of damage and 10 000 deaths from a similar event. If the probabilities of the severe event occurring are little different in the two communities clearly the buildings in the large community should have greater relative strength.

Although seemingly obvious when stated in this manner there is generally little recognition of this in practice. It is of course at odds with our normal design codes which tend to be based on the premise that individual buildings should have approximately the same risk of failure irrespective of location. The latter is satisfactory for normal loads since these are generally statis ally independent between different buildings in a community, but it is total unsatisfactory where loadings are likely to be highly correlated throughout community as in the case of loads arising from extreme natural hazards.

The situation has arisen no doubt because engineers are commissioned tc design individual buildings for indivual clients to a guaranteed degree of safety, and the fundamental community aspect of design for natural hazards h not been appreciated.

As a consequence most design criteria for natural hazards are expresse solely in terms of the risk of occurrence without any thought of the popula affected.

In Australia, in designing for wind in tropical cyclone regions the basic reference velocity is the 50 year return period velocity for all communities big and small. A tropical cyclone region is defined wherein additional strength is required to account for the greater likelihood of extreme events, the boundary of which passes just north of Brisbane with 10 times the population of any community within the designated cyclone area. Predictions indicate that the risk of severe winds from tropical cyclones in Brisbane is not markedly less than in the more Northern regions, and may indeed be greater than for Darwin (Walker, 1977b). This makes Brisbane one of Australia's major disaster risks, since current criteria tends to make it more vulnerable rather than less vulnerable to such severe events.

The same approach is evident in the proposed Australian earthquake code (Standards Association of Australia, 1976) where again design criteria is based entirely on the risk of occurrence. This had led to the rather ridiculous situation of an area of the almost uninhabited Simpson Desert being zoned with the highest seismic coefficients, and some major capital cities being zoned just outside zones which require higher seismic coefficients though containing no communities of comparable size.

In following this approach Australia has done no more than follow international practice in this respect, which may have been satisfactory in the past when cities were small, but which is inappropriate in this age of huge urban concentrations of population.

CONCERN FOR WHOLE COMMUNITY

Society by and large has only expected engineers to be concerned with large facilities. In designing and planning for natural hazards engineers have consequently tended to direct their attention only to the performance of these facilities and have not concerned themselves with other smaller but sometimes more numerous facilities which contribute to the total community.

In the structural engineering field, industrial, commercial and government buildings have been generally required to be structurally engineered while houses have not. When disasters occur, teams of engineers spend much time examining the small proportion of larger engineered buildings which have failed, making recommendations of changes in criteria, and undertaking extensive follow-up research work, all the while dismissing the much larger proportion of houses which have failed on the grounds that they were substandard and non-engineered and therefore not their concern. Yet it is often the failure of the housing which has been the major contributing factor to the scale of the disaster

Housing generally accounts for approximately half the total value of buildings in a community and hence economically is of similar value to th buildings. Socially houses are probably of much greater value since they the basic shelter and facilities required for living - a fact often overl by engineers in ranking buildings according to order of importance. If i Darwin the damage to houses had been as light as that to larger buildings the larger buildings had suffered the high level of damage which housing suffered, the scale of the disaster would have been much less and no evac would probably have been necessary. It is true that working conditions have been difficult in the recovery period but the social cost of difficu working conditions is far less than the social cost of difficult, or in case, impossible living conditions. The economic cost of course would ha much the same.

The argument has been that an individual house has small value economically and accommodates few people compared with the larger buildings, hence the greater importance of the latter. This again reflects the engineer's tendency to be only concerned with buildings as individual units. It is an argument that cannot be sustained in relation to the protection of communities against natural hazards.

In considering the importance of housing in respect of natural hazards it should also be borne in mind that even where hazards strike without appreciable warning such as earthquakes and tornadoes the population is more likely to be in their homes than in other buildings, and in the case of tropical cyclones where warnings are given the probability is quite high since experience shows that most places of work and schools close down when such a hazard threatens.

Since cyclone 'Tracy' the importance of having structurally engineered houses in tropical cyclone prone areas has been recognised in Australia. The principle has been vigorously applied in the design and construction of the new and reconstructed houses in Drawin, (Darwin Reconstruction Commission, 1976, Australian Department of Construction, 1976), is being incorporated in State building regulations (Queensland State Government, 1975) and is providing the basis for a manual on construction of houses in high wind areas currently in preparation (Standards Association of Australia, 1977) and recommendations on product testing and evaluation for tropical cyclone regions (Experimental Building Station, 1977).

The adoption of this principle represents a radical change to the approach to housing construction and its implementation is not taking place without some considerable pains. The materials and methods of construction most commonly employed in housing are not those with which the structural engineering profession has been generally concerned. Consequently there is little engineering experience, information and design guidelines available. Normal design codes, hand books and methods of structural analysis are often of little value. This has led to the development of major structural research and testing programmes on the behaviour of common housing systems under wind loads (Vickery, 1976; Holmes and Best, 1977, Melbourne, 1977; Leicester and Reardon, 1976a; Morgan and Beck, 1976; Parsons,1976; Byrne, 1976; Beck and Stevens, 1976; Armstrong and Schuster, 1977; Walker and Hughes, 1977; Lawrence, 1977; Best, 1976; Walker, 1977a; Johnson, 1977).

MULTI-LEVEL EVENT ANALYSIS

Natural hazards can produce events at different levels of magnitude with mild to moderate levels occurring more frequently than the more extreme levels. The more infrequent an event the more distress the community will normally accept. If criteria is to reflect this characteristic then different perfo levels need to be specified for different levels of event. Depending on th severity of the event the critical factors and conditions may change.

For instance, in designing buildings for wind from tropical cyclones, mild to moderate conditions because of the frequency with which they occur important that the buildings remain completely serviceable. Thus, deflecti and cracking criteria are of greatest significance at this level. Under se to very severe conditions some local damage, particularly to cladding, wind etc. is acceptable, and the primary concern is strength, for which criteria required to ensure that the number of failures is within acceptable limits.

The normal approach to design provides for this in some ways by requiring serviceability under working loads, and strength to resist ultimate loads which are calculated by factoring the working load. But with tropical cyclones we are dealing primarily with events not loads and the loading distribution on the structure under the severe events when windows may be broken by debris and protection from vegetation lost can be quite different from the loading distribution under mild to moderate events when it is reasonable to assume that debris damage will be small, windows remain intact and vegetation will not be defoliated. In recognition of this it is now being accepted in Australia that design loads for strength and design loads for serviceability may not be directly related to each other, being independently derived from different assumed conditions (Baker and Walker, 1976; Walker, 1977b; Experimental Building Station, 1977).

The need for multi-level anlaysis is also apparent when one considers the varying vulnerability of different populations with different inherent variations in vulnerability between individual units in the populations. Again consider the structural example of two different groups of buildings, one group having an inherently large coefficient of variation of vulnerability and the other an inherently small coefficient of variation of vulnerability. The variations in vulnerability may arise from variations in strength as constructed, variations in exposure due to topography and terrain if considering wind effects, or variations in ground conditions and foundations if considering earthquake effects. The comparative performance of the two groups at different levels of event will be quite different as shown in Figure 3 with the group having a large variation of vulnerability being relatively less sensitive to the extreme events and more sensitive to the mild events. Design based on a moderate to severe event and the characteristic strength of the group can result in a group with a small inherent variation of strength still being an unacceptable disaster risk in an extremely severe event. Conversely in designing for the extreme events the normal strength criteria can sometimes be relaxed when dealing with structural systems or components with large inherent variations in strength (Walker, 1975b, 1977b).

Consideration of these factors highlights the need for statistical studies of performance when natural hazards occur (Leicester and Reardon, 1976b).

PROBLEMS OF EXTREME EVENTS

Disasters can only be mitigated if the the hazards giving rise to them can be foreseen. One of the most difficult parts of planning for extreme events is the prediction of their likely magnitude and frequency, especially in areas where the recorded history is short as is the case in Australia where records go little more than a 100 years in most cases - and the interpretation of the often highly conjectural! Extreme to very extreme events are often associ with average return periods of the order of a 1000 years or more making ext polation of recorded information very uncertain.

Increasing knowledge of the basic characteristics of tropical cyclone the associated winds and tidal surges allowing the construction of sophist computer simulation models are proving of considerable value in Australia this respect (Gomes and Vickery, 1976; Martin and Bubb, 1976; Stark, 1977; Harper and Stark, 1977). However, many uncertainties still remain in rega the extreme events.

Because of economic pressures there is also a tendency for society to be reluctant to accept the need to consider events which may only recur at long intervals of time. Events with return periods of several hundred years of more very often have to occur before they are taken seriously, generally with disastrous results, which can then lead to an over-reaction and demands for criteria and action which assumes there is a strong likelihood of a recurrence within a short time.

The reaction after cyclone 'Tracy' in Darwin has typified this. There are many other Australian communities where the risk of getting a 'Tracy' magnitude event appears significantly greater including Brisbane, but the standards and criteria being imposed on Darwin by the overall community are far more demanding than the same community sees as reasonable in these other centres.

Poor communications, poor records, scattered population centres and the ability of a community to forget very quickly a 'near-miss' all add to the difficulties of recognition of the dangers of rare severe events. Three major storm surge disasters in the Pakistan area in the last century did not provide any lessons to reduce the magnitude of the 1971 Bay of Bengal disaster. In Australia cyclone 'Althea' with a storm surge of 3-4 m was a 'near-miss' because the tide was near low water. Had it come in five hours later the surge would have produced disastrous consequences with probably several hundred lives lost by drowning. Yet property values in the threatened areas have not been affected and plans for further residential development in the most vulnerable area have been approved.

In conjunction with the prediction problem is the determination of acceptable levels of community distress. It is clear that the more infrequent an event the greater the level of distress which is acceptable, and that for events of similar return period the acceptable relative level of distress, (i.e. percentage affected) is greater in a small community than in a large community, although the acceptable absolute level of distress (i.e. number of persons or buildings affected) will be greater in the larger community. The effect on the level of distress due to failure of different engineering systems will also vary - houses appear to be more important than office buildings; power stations and hospitals more important than either of these. These are primarily socio-economic problems and hence ones which engineers should be looking towards the social scientists for the answers.

CONCLUDING REMARKS

The development of criteria for designers and planners to provide protection against natural hazards is not an easy task. The exercise requires a much closer study of the interacting factors of the complex disaster system than has generally been undertaken to date.

In this paper a number of basic principles associated with the natural hazard disaster system have been discussed. They may be summarised as follow

(1) The primary objective of designers and planners in relation to natural hazards is mitigation of their impact on the community.

2) Large communities require a greater degree of protection than small communities for events of similar magnitude and frequency of occurrence.

(3) Housing is as important as other engineering facilities in protecting communities against natural hazards.

(4) Assessment of performance at different anticipated levels of event requires appropriate criteria for each level.

The establishment of rational engineering criteria requires information on:

(i) magnitude and frequency of severe events from natural hazards;

(ii) acceptable levels of community distress from natural hazards;

(iii) the relationship between community distress and engineering performance;

(iv) the relationship between engineering performance and engineering criteria.

Engineers, by and large, concentrate on (i) and (iv) since (ii) and (iii) are of a socio-economic nature. Ignoring these socio-economic factors has often led to the development of quite inappropriate criteria for natural hazards in the past. If the basic objective is to be achieved they must be taken into account.

This may mean an increasing amount of interdisciplinary research in conjunction with social scientists of disaster systems and increasing research by engineers into the performance of systems which have been traditionally regarded as outside their concern. Combined with the problems of improving the reliability of predictions of magnitude and frequency of extreme events the development of relevant criteria for protection against natural hazards will continue to provide considerable scope for research studies in the foreseeable future.

REFERENCES

Armstrong, L.D. and Schuster, K.B. "Plywood Sheathed Wood-Frames to Resist Wind Forces - a Technique of Assessment". Proc. 6th Australasian Conf. on Mech. of Struct. and Materials. Univ. of Canterbury, Christchurch, pp.321-326, 1977.

Australian Academy of Science. "Symposium on Natural Hazards in Australia". Canberra, May, 1976.

Australian Department of Construction. "Structural Design of Cyclone Res: Dwellings: Part A - Design; Part B - Construction". 2 Vol., Melbourne, 1

Baker, K.N. and Walker, G.R. "The Behaviour of Steel Structures in Cyclo and the Implications for Design". Metal Struct. Conf., I.E.Aust., Adelai pp.29-34, 1976.

Beck, V.R. and Stevens, L.K. "Constant Repeated Loading of Corrugated Sh Metal Struct. Conf., I.E.Aust., Adelaide, pp.40-45, 1976.

Best, N.H. "Steel Framing in Domestic Construction". Metal Struct. Conf I.E.Aust., Adelaide, 1976.

Byrne, S.M. "Dynamic Load Testing of Sheet Metal Roofing". Metal Struct. Conf., I.E.Aust., Adelaide, 1976.

Darwin Reconstruction Commission. "Darwin Area Building Manual". Darwin, 1976.

Experimental Building Station. "Guidelines for Cyclone Product Testing and Evaluation". Sydney, 1977.

Gomes, L. and Vickery, B.J. "Tropical Cyclone Gust Speeds along the Northern Australian Coast". Civil Engin. Trans., I.E.Aust., Vol.CE18, No.2, pp.40-48, 1976.

Holmes, J.D. and Best, R.J. "Wind Tunnel Measurements of Mean Pressures on House Models and Comparison with Full Scale Data". Wind Engin. Rep. 3/77, Dept. of Civil and Systems Engin., James Cook Univ., Townsville, July, 1977.

Johnson, P.I. "Impact Testing of Building Products for Cyclone Prone Areas". Workshop on Guidelines for Cyclone Product Testing and Evaluation, Experimental Building Station, Sydney, 1977.

Lawrence, S.J. "Lateral Loading Tests of Brick Walls at Experimental Building Station". Private Communication, 1977.

Leicester, R.H. and Reardon, G.F. "Wind Damage in Australia; a Pictorial View with Particular Reference to Domestic and other Low Rise Structures". Special Report, Division of Building Research, CSIRO, Melbourne, 1976.

Leicester, R.H. and Reardon, G.F. "A Statistical Analysis of the Structural Damage by Cyclone Tracy". Civil Engin. Trans., I.E.Aust., Vol.CE18, No.2, pp.50-54, 1976.

Martin, G.S. and Bubb, C.T.J. "Discussion on Tropical Cyclone Gust Speeds along the Northern Australian Coast". Civil Engin. Trans., I.E.Aust., Vol.CE18, No.2, pp.48-49, 1976.

Melbourne, W.H. "Loading Cycles for Simulation of Wind Loading". Workshop on Guidelines for Cyclone Product Testing and Evaluation, Experimental Building Station, Sydney, 1977.

Morgan, J. and Beck, V.R. "Failure of Sheet Metal Roofing under Repeated Wind Loading". Annual Engineering Conf., I.E.Aust., Townsville, pp.290-294, 1976.

Parsons, A.A. "Practical Development from Static and Cyclic Load Testing of Steel Claddings". Metal Struct. Conf., I.E.Aust., Adelaide, pp.51-56, 1976.

Queensland State Government. "Building Act 1975". Brisbane, 1975.

Sobey, R.J., Harper, B.A. and Stark, K.P. "Numerical Simulation of Tropical Storm Surge on the Queensland Coast". Dept. of Civil and Systems Engin., James Cook Univ., Townsville, 1977.

Standards Association of Australia. "The Design of Earthquake Resistant Buildings". Draft Standard, DR 76100, Sydney, 1976.

Standards Association of Australia. "Structural Details for Houses in High Areas". Draft Manual, DR 77019, Sydney, 1977.

Stark, K.P. "Cyclonic Surges and Their Effects". Queensland Harbour Boards' Conference, Townsville, August, 1977.

Stark, K.P. and Walker, G.R. "Engineering for Natural Hazards with particular reference to Tropical Cyclones". Symp. on Natural Hazards in Australia, Aust. Acad. of Sci., Canberra, 1976.

Texas Coastal Marine Council. "Model Minimum Hurricane-Resistant Building Standards for the Texas Gulf Coast". Austin, 1976.

Trollope, D.H. (Ed.) "Cyclone Althea: Part 1 - Buildings; Part 2 - Storm Surges". 2 Vol., James Cook Univ., Townsville, 1972.

Vickery, B.J. "Wind Loads on Low Rise Buildings". Darwin Reconstruction Commission Seminar, Darwin, 1976.

Walker, G.R. "Report on Cyclone 'Tracy' - Effect on Buildings - December, 1974". Aust. Dept. of Housing and Construction, Melbourne, 1975.

Walker, G.R. "Investigation of Wind Design Criteria Using a Statistical Simulation Model". Proc. 4th Int. Conf. on Wind Effects on Building and Struct., London, pp.745-754, 1975.

Walker, G.R. "The Rational Design of Low Rise Housing in Tropical Cyclone Prone Areas". Annual Engineering Conf., I.E.Aust., Townsville, pp.248-253, 1976.

Walker, G.R. "Testing for Structural Resistance to Tropical Cyclones at the James Cook Universtiy of North Queensland". Dept. of Civil and Systems Engin., James Cook Univ., Townsville, 1977.

Walker, G.R. "The Design of Buildings and Their Components for Cyclonic Conditions". Queensland Division Technical Paper, I.E. Aust., 1977.

Walker, G.R. and Hughes, G.C. "An Investigation of the Racking Strength of Asbestos Cement Clad Timber Framed Walls". Dept. of Civil and Systems Engin., James Cook Univ., Townsville, March, 1977.

TABLE 1

CLASSIFICATION OF WIND HAZARDS FROM TROPICAL CYCLONES
TOWNSVILLE AREA

Classification	Wind Speed m/s	Approx.Return Period (Yrs)	Example
Mild	30 - 45	10	Yeppoon, 'David' 197(
Moderate	50 - 60	40	Port Hedland, 'Joan'
Severe	65 - 75	300	Darwin, 'Tracy' 1974
Extremely Severe	80 - 90	2000	N.W. Aust., 'Joan' 19

N.B. Wind speeds represent 3 sec. gusts at 10 m height in open country.

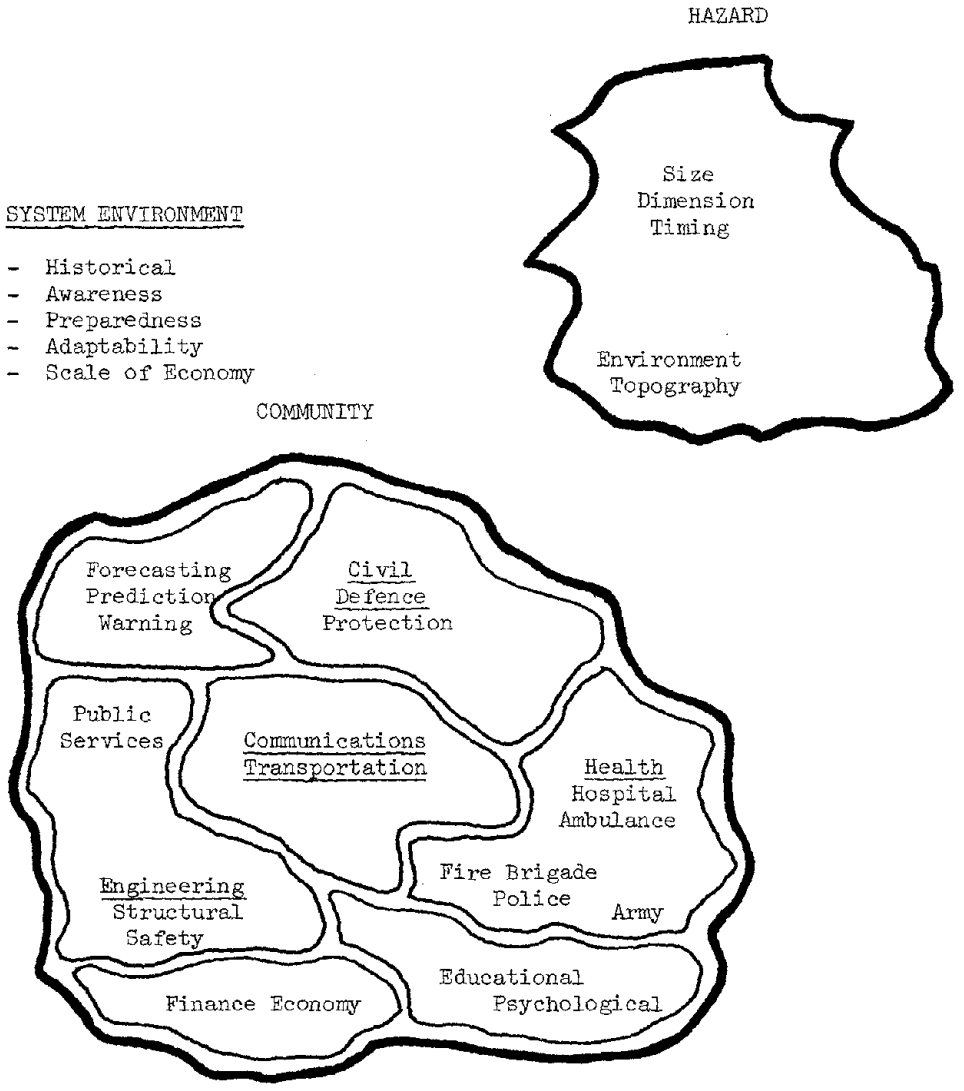

FIGURE 1 : A REPRESENTATION OF A DISASTER SYSTEM

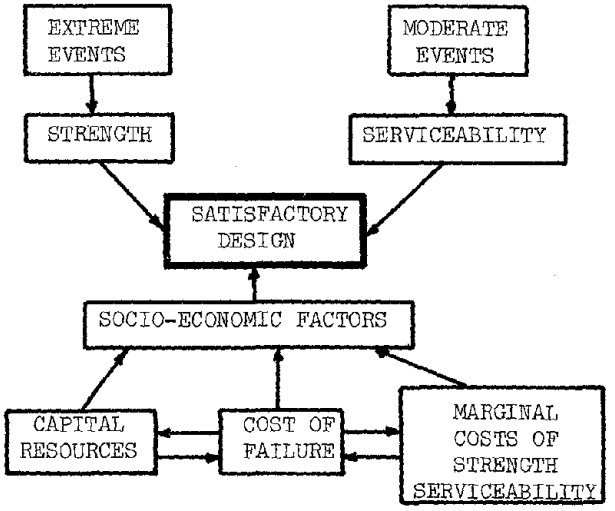

FIGURE 2 : STRUCTURAL DESIGN CRITERIA INTERACTION DIAGRAM FOR NATURAL HAZARDS

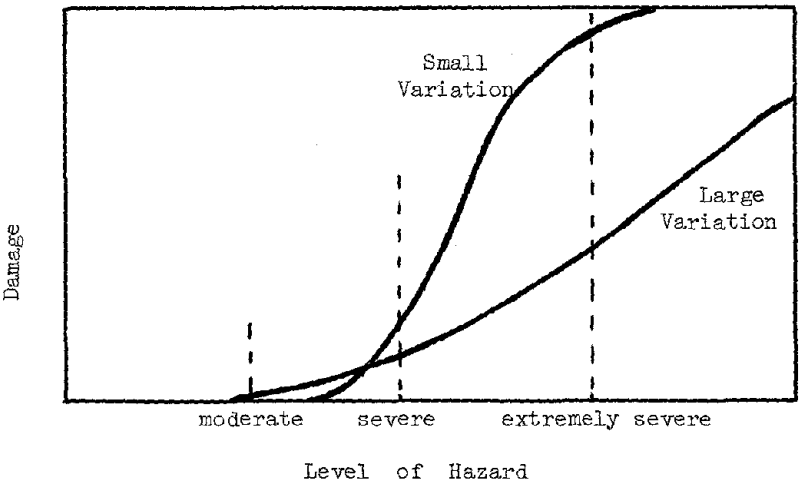

FIGURE 3 : EFFECT OF VARIATION OF VULNERABILITY ON HAZARD DISTRESS

DESIGN CONSIDERATIONS FOR RESISTANCE TO WIND

by

Arthur N.L. Chiu
Professor of Civil Engineering
University of Hawaii at Manoa
Honolulu, Hawaii, U.S.A. 96822

ABSTRACT

Some of the major considerations in designing for wind resistance are briefly described. Findings from experimental studies or field observations are mentioned in connection with design aspects. Details on analytical procedures are not included but referenced for further study as appropriate. Effects on human occupants of buildings can be crucial because modern buildings are taller, more slender and can be sensitive to wind action. The traditional approach of designing for an equivalent static pressure may not be adequate for the flexible structures; dynamic analysis should be included for special structures. Wind tunnel testing of models can provide some of the answers in designing for wind effects.

INTRODUCTION

The past four decades have witnessed a phenomenal increase in the number of taller and more slender structures as well as bridges with longer spans and shallower structural depths. This increase is largely due to such factors as (1) the availability of a variety of more efficient building materials and construction methods; (2) the development of more sophisticated analytical procedures; (3) the capabilities of electronic computers to analyze expeditiously and economically complex structures with large degrees of statical indeterminancy; (4) the acceptance by the design profession of improved methodologies for designing structures to resist wind and earthquake forces; (5) the advances in support systems for environmental control as well as mobility of people within the tall buildings; and (6) the economics of land use in densely populated areas.

The advent of high-strength materials and advances in construction methods have resulted in modern tall structures that are more flexible and have smaller ratios of dead loads to live loads than their predecessors. Although these slender structures are aesthetically more pleasing to the eye, some of them may be sensitive to wind forces with resulting ambient vibrations of such perceptible magnitudes and frequencies so as to become annoying to the building occupants. Cladding for these tall buildings requires special considerations because of the high gust loads that can be expected to act on the large exposed surfaces. The growth of urban areas and the accompanying decline in available land for buildings have contributed immensely to the need for building upwards rather than sideways. Resea the behavior of structural components, joints, and systems subjected to impul repetitive loads has resulted in modifications to the design and analytical cedures. With these updated procedures available to the structural engineer buildings have begun to emerge in many areas that traditionally have maintai restrictive height limitations. In Manila, the skylines of Roxas Boulevard Makati have been pierced by numerous taller and bigger structures that are d to withstand prescribed forces resulting from earthquakes and typhoons.

Presented at U.S.-S.E. Asia Joint Symposium on Engineering for Natural Haza Protection, Manila, Republic of Philippines, September 26-30, 1977.

The purpose of this paper is to point out some of the factors to be considered in designing for wind effects on structures. It will be impossible to cover all the details in such a paper; details and procedures are referenced, where appropriate, for further study. The traditional approach of designing structures to resist an equivalent static wind pressure acting normal to the projected area has been satisfactory in many instances. However, data gathered from various research investigations and from field inspections of structural damages caused by severe storms have shown that there may be certain design inadequacies and problem areas that have been overlooked in the past. There is still much information to be gathered on wind effects and many researchers are actively involved in this subject. A compilation of much of the research in wind engineering can be found in the previous two volumes of the Wind Engineering Research Digest (Ref. 18).

In designing structures to withstand wind forces, especially tall buildings, the following are important factors that must be considered:

(a) Strength and stability requirements for the structural system to resist the expected wind forces;

(b) Possibility of fatigue in the structural members and connections caused by fluctuating wind loads from various directions;

(c) Excessive lateral deflections causing cracking of partitions and external claddings, misalignment of mechanical systems, doors, and possible permanent deformations;

(d) Amplitude and frequency of sway that may cause discomfort to the building occupants; and

(e) Possible environmental conditions that may increase the magnitude of the wind velocities.

Although not included in the factors for strength and stability of the structure, the following should also be considered:

(a) Effects on pedestrians around the base of tall buildings, and

(b) Annoying acoustical disturbances.

Fortunately, there have been no catastrophic structural failures of completed tall buildings to wind effects although tornadoes and hurricanes have caused dramatic destruction of individual houses or multiple-unit low rise structures and industrial buildings. There have been reports of various failures of buildings caused by strong winds, but many of these were primarily due to inadequat bracings, or lack of them, during construction. However, totally unexpec storms can also cause severe damages such as the waterspout that develope the coast of Kailua-Kona, Hawaii (Jan. 1971) and moved towards land and d a seven-story structure under construction, tore off numerous roofs, flat small shopping center under construction, destroyed many units in an apar complex, and obliterated an old office building.

Two high-rise buildings that did suffer extensive damages in storms Meyer-Kaiser Building during the 1936 Miami, Florida hurricane (Ref. 14) Great Plains Life Building during the 1970 Lubbock, Texas storm (Ref. 12) Estimated wind speeds impinging on the Great Plains Life Building varied 95 mph at the 30-ft level to 220 mph at the top of the building (270 ft a

ground). In both cases, torsional-lateral displacements of the structures were very extensive and resulted in permanent yield of the structural frames.

Various free-standing and guyed latticed towers have been damaged in severe wind storms. Typhoon Thelma and typhoon Vera (August 1977) both caused extensive structural damage to the harbor facilities in Taiwan. Typhoon Vera packing winds at more than 130 mph toppled the huge waterfront cranes into the Keelung Harbor. Typhoon Karen (1962) and supertyphoon Pamela (1976) caused widespread damages in Guam (Ref. 16). Based on the findings from inspection of the damages left behind by typhoon Karen, design specifications for U.S. Navy installations were modified and design velocities were increased to 165 mph (Ref. 11). Structures designed in accordance with the updated specifications performed adequately during the onslaught of supertyphoon Pamela.

Various building codes and guidelines specify minimum wind pressures or velocities for designing structures. In the U.S.A., some of the codes and guidelines used are: Uniform Building Codes, the ANSI A58.1-1972 Code, the Electronics Industry Association Code, Design Manuals of the Department of Defense (Army, Navy, and Air Force), and individual city and county building codes (Chicago, Los Angeles, New York, Boston, etc.).

WIND VELOCITIES

Design Wind Speeds

The few examples mentioned above indicate that a realistic design wind speed is of utmost importance. Obviously, it is not economically justifiable to design all structures to withstand tornadoes or supertyphoons, and basic design wind speeds must be selected judiciously with respect to life expectancy and importance of the structure, performance requirements, type of occupancy, and risk to human lives and property in case of failure. These design speeds may be obtained from maps such as those for the U.S.A. in Figs. 1 through 3 (Ref. 1) which show extreme fastest-mile wind speeds for 25-, 50- and 100-year mean recurrence intervals. Data for compiling the maps are obtained by recording the time required for a mile of air to pass a fixed point and are obtained from anemometers located at 30 ft aboveground. The ANSI A58.1-1972 Code also recommends the values shown in Table 1 as design wind speeds for Hawaii and Puerto Rico. In some areas, local topography and environment can cause channeling and may necessitate increases to the design wind speeds selected from maps or tables; these conditions should receive special consideration where appropriate. R.D. Marshall has been working with Philippine researchers to gather wind data and to analyze them for determining extreme winds; these results will enable mean recurrence velocity maps to be drawn up for the Philippines.

Velocity Profile

Most of the available wind velocity records have been measured at airpo using wind sensors located at 30 ft above ground. These records do not give formation needed for determining velocities at higher elevations or at proje sites that may be quite remote and quite different, topographically and envi mentally, from the airport locations. Much research has been conducted in d mining the relationship of horizontal wind velocities at various elevations, the power-law relationship has been found to be adequate for most purposes,

$$\overline{U}_z = \overline{U}_{30}(z/30)^p$$

where $\bar{U}_z$, $\bar{U}_{30}$ are the mean horizontal velocities at elevations z and 30 ft above ground and p is the power-law parameter. An ongoing project (Ref. 19) to measure horizontal wind velocities on a guyed tower, 800 ft tall, has shown fairly good relationship of the mean velocities using the power-law equation. Some preliminary results are shown in Fig. 4.

Davenport (Ref. 6) has analyzed numerous records obtained at various locations and has summarized the values for the power-law exponent in Table 2. For uniformity in deriving design wind velocities, Davenport suggests that the gradient velocity ($\bar{U}_g$) be determined for the type of exposure to which the structure will be subjected. Equation (1) is then used to obtain $\bar{U}_{30}$ as the "design wind speed" and thereafter, the mean velocities at other elevations can be computed from the power law relationship.

Gradient heights suggested for three types of exposures are:

(a) Type A, centers of large cities and very rough, hilly terrain, z_g = 1500 ft.

(b) Type B, suburban areas, towns, city outskirts, wooded areas and rolling terrain, z_g = 1200 ft.

(c) Type C, flat, open country, open flat coastal belts, and grasslands, z_g = 900 ft.

Figure 5 shows the relative velocity profiles for the three types of exposures with the same magnitude of $\bar{U}_g$. Figure 6 shows the relationship of the mean velocities at various elevations relative to the mean velocity at 30 ft for different values of p. Design codes tend to provide for the effect of increasing velocities with elevations by specifying greater pressures at higher elevations; Figure 7 shows comparative wind pressures specified by some U.S. codes.

The value of the power-law exponent should be selected carefully keeping in mind the terrain effects and the accompanying directions for the strong winds. A "microzonation" map for the Los Angeles area is being developed by G. Hart (UCLA); this will include various power-law exponents. Such detailed microzonation maps can be prepared as deemed necessary for the city of Manila and its surroundings.

The power-law relationship is for mean wind velocities. Fluctuations in the wind velocity cause time-varying pressures on the structures and turbulence intensities are used to indicate the degree of fluctuations about the mean values. The turbulence intensities are calculated from

$$\tau = \sigma_U / \bar{U} \qquad (2)$$

where τ is the turbulence intensity, σ_U is the rms of wind velocity fluctu and $\bar{U}$ is the mean velocity. Available wind data results show that the tur intensities tend to decrease with increasing elevations (Fig. 8).

RESPONSES TO WIND

Pressure Distribution Studies on Models and Prototypes

The wind pressure distribution over the surface of a structure is not Pressure measurements have been taken on scaled models in wind tunnels as on prototypes to determine the distribution. Of particular note are the w tunnel studies at Colorado State University directed by Dr. Jack Cermak, a

University of Western Ontario directed by Dr. Alan Davenport, and at California Institute of Technology directed by Dr. Anatol Roshko. Full-scale measurements of wind pressures on buildings have been conducted by Dr. Richard Marshall at the National Bureau of Standards as well as by Mr. Alan Dalgliesh of the National Research Council (Canada). Dr. Robert Scanlan has been actively studying wind pressures on bridge section models. Dr. Sean Mackey's study on the pressure distribution over a ten-story research building at Cape D'Aguilar, Hong Kong (Ref. 22) is well known as well as Dr. Hatsuo Ishizaki's investigation of ambient pressures on prototype single family wooden buildings at Shionomisaki, Japan. Details of various other projects are reported in Ref. 17.

Some Conclusions from Wind Tunnel Studies

Certain features of the steady flow wind pressure distributions observed from wind tunnel studies on bluff bodies are:

(a) Windward faces are subjected to positive pressures that decrease rapidly towards the edges (sides and tops);

(b) Leeward surfaces experience turbulent negative pressures;

(c) Sides and roofs are subjected to negative pressures in the separation zones but where reattachment zones occur, the pressure again changes to positive in those zones;

(d) Corners are extremely turbulent areas and are areas of large negative pressures; and

(e) Positive as well as negative pressures decrease in magnitude downwards to the base of the structure.

These findings show that parts of a structure can experience very large local fluctuating pressure and this situation can result in overstressing of the cladding and window panes if the design is based on average pressures acting over the whole structure. Internal pressures pushing outward coupled with negative pressures on the outside may impose forces on windows that were not designed for this level of combined loads.

Forces on Structures

Wind forces acting on structures or structural elements are determined from:

$$F_D = C_D A_p \rho U^2/2 \qquad (3)$$

where F_D is the drag force, C_D is the drag coefficient, A_p is the projected a normal to the wind direction, ρ is the mass density of air, and U is the wind velocity.

Drag coefficients for structural elements and shape factors for latticed towers can be found in Refs. 20 and 5. These are used for determining the wi forces acting on the structure and it is generally assumed that the coefficie and factors are applicable for all velocities.

tructural Response

In the natural wind field, because of the fluctuating velocities as well he shift in wind directions, wind forces on structures are varying constantl

Strain measurements taken on columns of high-rise buildings (Ref. 7) show continuously fluctuating stresses. These are accentuated during wind storms and reversals of stresses can be expected under extreme conditions. Design of the structural system, therefore, should consider fatigue effects. Besides the dynamic response in the longitudinal direction of the wind, dominant crosswind motions of certain structures may result from fluctuating wind forces due to vortex shedding. Dramatic failures such as the Tacoma Narrows Bridge and the cooling towers in England have provided the impetus for studying such phenomena and finding solutions to avoid such situations.

The wind velocity is not constant but varies with time and is also dependent on elevation. The separation of the wind velocity into its mean and fluctuating components permits the calculation of the structural response as compromising a static (mean) deflection and a dynamic (fluctuating) deflection. The traditional approach of computing only the static deflection without concern for the dynamic deflection is inadequate if the forcing function should be in resonance with the structural system resulting in responses of such large magnitudes that cannot be tolerated by the structural system and result in failure of the system. Hence, in the final analysis, it is necessary to consider the dynamic response of the structure to wind forces.

Davenport has advocated the use of a gust factor approach for predicting peak displacements (Ref. 8) using probability concepts and the Canadian Code reflects Davenport's method. Cohen and Vellozzi have also suggested the gust factor approach (Ref. 21) and this is included in the ANSI Code. Simiu and Lozier (Ref. 15) have presented a procedure for estimating along-wind deflection of a structure to strong winds; the procedure incorporates recent advances in the state-of-the-art.

Latticed Towers

Latticed tower structures experience tremendously high stresses from the turbulent wind forces acting over the whole system, and designs tend to be conservative to minimize possibilities of structural failure that will result in interruption to the operations of the system. Design specifications for line-of-sight communication towers have stringent performance requirements regarding twist or lateral displacements. Guyed towers have soared almost 1500 ft into the sky and in some cases their designs have to provide for the possible loss of a guy without structural failure of the system. With these factors in mind, it is disconcerting to read of various failures that have occurred in the past. Conceivably, dynamic stresses may have been much higher than anticipated and intensive research needs to be conducted to improve the design guidelines.

Wooden Frame Structures

The recurring reports of localized roof failures during wind storms a indicative of a common problem area that does not receive its adequate sha attention in the design and construction for resistance against wind force Many of the failures of single-family wooden frame dwellings are attributa poor connections. The three most common modes of failure are:

(a) wall-to-foundation connection failures when the superstruct been pulled or sheared off the foundations because of insuf anchor bolts, inadequate anchorage for the bolts, and somet there are no provisions at all for uplift resistance or nut missing in some cases.

(b) roof-to-wall connection failures when toe-nailing of the roof truss is insufficient and whole roofs are torn away including the bottom chords.

(c) roof failures when the bottom chords are left in place but the remainder of the roof is torn off (roofing, decking, or half the roof folding over at the ridge line).

A study (Ref. 2) on wind pressures on the roof of a model house (1:50 scale, 10.5° roof slope) in a wind tunnel showed that the wind-induced pressures over the entire roof were negative except for the areas immediately upwind of the chimney. The report also indicated that the upward pressures underneath the overhang can contribute up to 50% of the total wind force on the overhang, and depending on the wind direction, large fluctuating surface pressures can be found along the roof edges. Eagleman, et al. (Ref. 9) conducted an intensive wind tunnel study on models of single wooden frame buildings to determine modes of failures.

Analysis of the reported failures and findings from model studies points out the need for adequate design of the connections, the sheathing and the structural joints. Connections should be equivalent in strength to the truss and general structural design. In regions where wide eaves are commonly used, the need for extra strength to resist the large fluctuating forces acting on the overhangs becomes more crucial.

OTHER EFFECTS OF WIND

Response of Humans to Wind Vibration

Aside from strength and stability factors in the design of tall buildings to resist wind forces, the structural response characteristic as it affects the well being of building occupants must be considered. The taller, more slender and lighter modern high-rise buildings may be sensitive to the fluctuations of wind velocity and direction, and the resulting combination of amplitude and frequency of sway may be of such magnitudes to cause physio-psychological effects on the building occupants. Arbitrarily stiffening the structural system will not be effective. Mechanical dampers have been incorporated into the design of various high-rise buildings to reduce the amount of sway.

Chen and Robertson (Ref. 4) and Chang (Ref. 3) have reported on some studies conducted for determining levels of perception and tolerance to sway by humans. Feld (Ref. 10) reported that data collected in connection with the design of the World Trade Center towers in New York indicated the threshold of human awareness to horizontal acceleration is within the range of 0.006g to 0.015g. Design specification for the World Trade Center towers was set at "0.010g at the top occupied floor, not to exceed an occurrence rate of 12 times a year."

Chang (Ref. 3) extrapolated data from earlier tests and has suggested th comfort limits for human responses shown in Table 3. He presented the zones comfort limits as varying with amplitude versus frequency as shown in Fig. 9. the Empire State Building, N.Y., the behavior in an 80 mph is represented on chart as "just on the threshold of persceptibility" and is in conformance wit experience of the building occupants.

'edestrian Protection

High-rise buildings clustered together can create "canyon" effects and t ay result in wind conditions at ground level that cause discomfort to pedest

Melbourne and Joubert (Ref. 13) report of situations where pedestrians have been knocked down by the resulting wind forces. Even single tall buildings with a broad frontal exposure normal to the wind stream will create problem situations because of the downwash. Covered walkways, reorientation of the building plan during early design stages, trees planted around the plazas, and decorative perforated tile walls are some ways to ameliorate the situation.

Acoustical Vibrations

Wailing or screeching sounds from passage of winds through openings in various parts of a building can be very annoying to the building occupants. A series of papers dealing with this topic was presented at the Symposium on Full-Scale Measurements of Wind Effects on Tall Buildings and Other Structures held at the University of Western Ontario in 1974.

CONCLUSION

Selection of basic design wind speeds is obviously critical and should be selected with respect to life expectancy and importance of the structure, performance requirements, types of occupancy, and risk to human lives and property in case of failure.

The traditional approach to designing for wind resistance for an equivalent static wind load may not be adequate for modern tall slender buildings that can be sensitive to wind effects. Although much knowledge has been gained from research studies (theoretical, experimental and full-scale), more investigations are needed to bridge the many missing gaps in information that still exist about wind effects on structures. In this regard, wind tunnel tests on models have yielded many of the answers. However, reports on structural damage caused by strong wind indicate that there are still deficiencies. Many of the failures of single wooden frame buildings and their roofs could have been mitigated by proper design and construction of the connections and anchorages. Various researchers are working on refinements of the analytical tools for predicting response of buildings to wind forces. Full-scale testing is needed for corroboration of laboratory and theoretical results.

Apart from strength and stability considerations, designers must consider the physio-psychological effects on human occupants of tall buildings because of the frequencies and amplitudes of sway.

REFERENCES

1. Building Code Requirements for Minimum Design Loads in Buildings and Other Structures, ANSI 58.1-1972, American National Standards Institute, Inc., New York, N.Y. 10018, 1972.

2. Cermak, J.E., J. Peterka and K.J. Dreher, "Wind Pressures on a House Roof," pp. 125-140, Proceedings of the Second USA-Japan Research Seminar on Wind Effects on Structures, simultaneously published by University of Tokyo Press, Tokyo, Japan and University Press of Hawaii, Honolulu, Hawaii, 1976.

3. Chang, F.K., "Human Response to Motions in Tall Buildings," Journal, Structural Division, ASCE, Vol. 99, No. ST6, Proc. Paper 9811, pp. 1159-1272, June 1973.

4. Chen, P.W. and L.E. Robertson, "Human Perception Thresholds of Horizontal Motion," Journal, Structural Division, ASCE, Vol. 98, No. ST8, Proc. Paper 9142, pp. 1681-1695, August 1972.

5. Cohen, E. and H. Perrin, "Design of Multi-Level Guyed Towers: Wind Loading," Journal, Structural Division, ASCE, Vol. 83, No. ST5, Proc. Paper 1355, September 1957.

6. Davenport, A.G., "Rationale for Determining Design Wind Velocities," Journal, Structural Division, ASCE, Vol. 86, No. ST5, Proc. Paper 2476, May 1960.

7. Davenport, A.G., "Theme Report, Technical Committee No. 7, Wind Loading and Wind Effect," Proceedings of the International Conference on Planning and Design of Tall Buildings, Lehigh University, Bethlehem, Pennsylvania, Vol. Ib, August 21-26, 1972.

8. Davenport, A.G., "Gust Loading Factors," Journal, Structural Division, ASCE, Vol. 93, No. ST3, pp. 11-34, March 1967.

9. Eagleman, J.R., V.U. Muirhead and N. Willems, Thunderstorms, Tornadoes and Damage to Buildings, Environmental Publications, Lawrence, Kansas 66044, 1972.

10. Feld, L. "Superstructure for 1350-ft World Trade Center," Civil Engineering, ASCE, Vol. 41, No. 6, pp. 66-70, June 1971.

11. "Lessons Learned from Inspection-Evaluation of Damage to Facilities Caused by Typhoon Pamela," Unpublished Report, Pacific Division, Naval Facilities Engineering Command, Makalapa, Hawaii, July 15, 1976.

12. Mehta, K.C., J.R. McDonald, J.E. Minor and A.J. Sanger, Response of Str Systems to the Lubbock Storm, TTU SSR 03, Department of Civil Engineeri Texas Tech University, Lubbock, Texas 79409, October 1971.

13. Melbourne, W.H. and P.N. Joubert, "Problems of Wind Flow at the Base of Buildings," pp. 105-114, Proceedings of the Third International Confere on Wind Effects on Buildings and Structures, Tokyo, 1971; Saikon Shuppa Ltd., Tokyo, Japan, 1971.

14. Schmitt, F.E., "The Florida Hurricane and Some of Its Effects," Enginee News Record, 97, pp. 586-591 and 624-627, 1926.

15. Simiu, E. and D. Lozier, The Buffeting of Tall Structures by Strong Winds, NBS Building Science Series 74, National Bureau of Standards, U.S. Department of Commerce, Washington, D.C. 20234, October 1975.

16. "Studies and Analysis of Damage by Typhoon Karen on Guam," Technical Note 497, U.S. Naval Civil Engineering Laboratory, Port Hueneme, California, March 29, 1963.

17. Wind Effects on Buildings and Structures, Proceedings of the Third International Conference on Wind Effects on Buildings and Structures, Tokyo, 1971; Saikon Shuppan Co., Ltd., Tokyo, Japan, 1971.

18. Wind Engineering Research Digest, Ed. by A.N.L. Chiu; obtainable from National Technical Information Services, Springfield, Virginia 22161; Vol. 1, 1974 (Accession No. PB-241-010) and Vol. 2, 1975 (Accession No. PB-252-83.8/AS).

19. "Wind Forces on Guyed Towers," Technical Memorandum M-51-76-20, Civil Engineering Laboratory, Naval Construction Battalion Center, Port Hueneme, California 93043, November 1976.

20. Woodruff, G.B. and J.J. Kozak, "Wind Forces on Structures: Fundamental Considerations," Journal, Structural Division, ASCE, Vol. 84, No. ST4, Proc. Paper 1709, July 1958.

21. Vellozzi, J. and E. Cohen, "Gust Response Factors," Journal, Structural Division, ASCE, Vol. 94, No. ST6, Proc. Paper 5980, pp. 1295-1313, June 1968.

22. Mackey, S., R.P. Lam and L.C.H. Lam, "A Full-Scale and Wind-Tunnel Study of Wind Loading on a Building," Proceedings of the Regional Conference on Tall Buildings, Bangkok, Thailand, Ed. by S.L. Lee and P. Karasudhi, pp. 515-551, January 1974.

Table 1
Basic Wind Speeds, Hawaii and Puerto Rico (U_{30} mph)

Exposure	Mean Recurrence Interval (years) 25	50	100
Hawaii			
Easterly	70	80	90
Westerly	60	65	70
Puerto Rico	80	95	110

Table 2
Types of Terrain Grouped According to Their Aerodynamic Roughness*

Category	Description	p
1	Very smooth surfaces: e.g. large expanses of open water; low sheltered islands; tidal flats; lowlands verging on the sea	$\frac{1}{8.5}$
2	Level surfaces with only low, surface obstructions; e.g. prairie grassland; desert; arctic tundra	$\frac{1}{7.5}$
3	Level, or slightly rolling surfaces, with slightly larger surface obstructions: e.g. farmland with very scattered trees and buildings, without hedgerows or other barriers; wasteland with low brush or surface vegetation; moorland	$\frac{1}{6.5}$
4	Gently rolling, or level country with low obstructions and barriers; e.g. open fields with walls and hedges, scattered trees and buildings	$\frac{1}{5.5}$
5	Rolling or level surface broken by more numerous obstructions of various sizes: e.g. farmland, with small fields and dense hedges or barriers; scattered windbreaks of trees, scattered two-story buildings	$\frac{1}{4.5}$
6	Rolling or level surface, uniformly covered with numerous large obstructions: e.g. forest, scrub trees, parkland	$\frac{1}{3.5}$
7	Very broken surface with large obstructions: e.g. towns; suburbs; outskirts of large cities; farmland with numerous woods and copses and large windbreaks of tall trees	$\frac{1}{3}$
8	Surface broken by extremely large obstructions: e.g. center of large city	$\frac{1}{2.5} - \frac{1}{1.5}$

*(Source: Davenport, 1960)

Table 3
Comfort Limits*

Comfort Limit	Acceleration
Not perceptible	<0.005g
Perceptible	0.005g - 0.015g
Annoying	0.015g - 0.050g
Very Annoying	0.050g - 0.150g
Intolerable	>0.150g

*(Source: Chang, 1973)

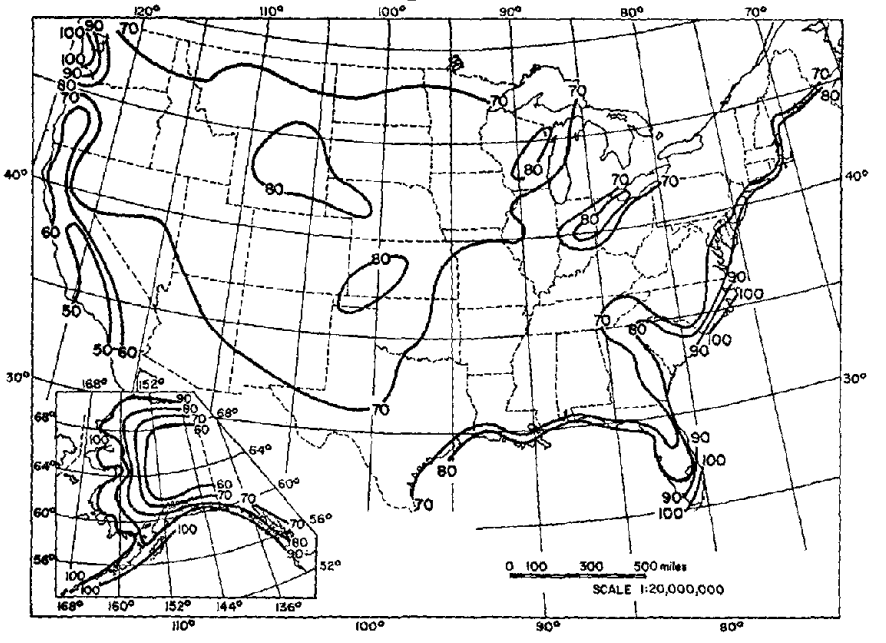

Fig. 1 Annual Extreme Fastest-Mile Speeds (mph) 25-year Mean Recurrence Interval (z=30 ft)

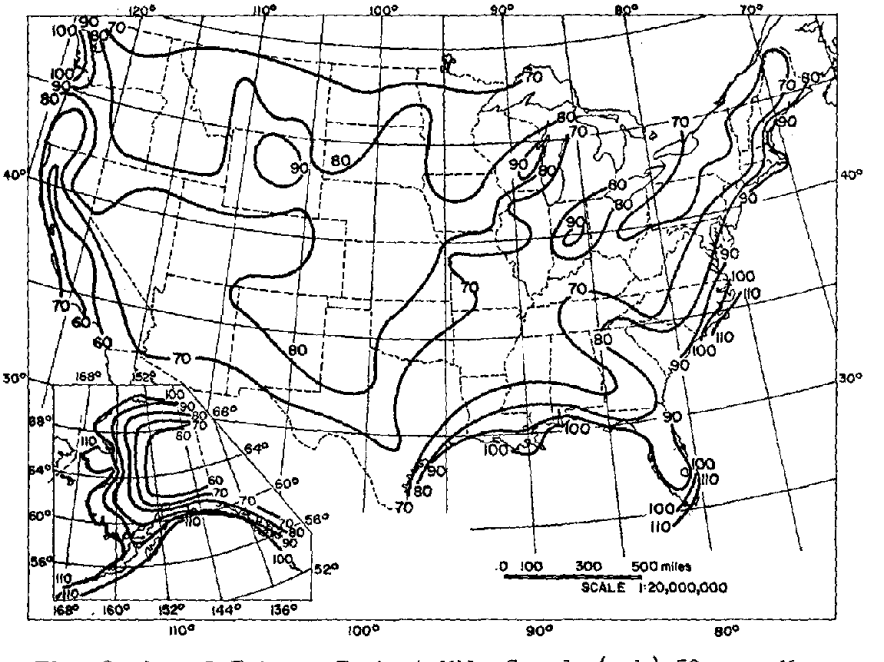

Fig. 2 Annual Extreme Fastest-Mile Speeds (mph) 50-year Mean Recurrence Interval (z=30 ft)

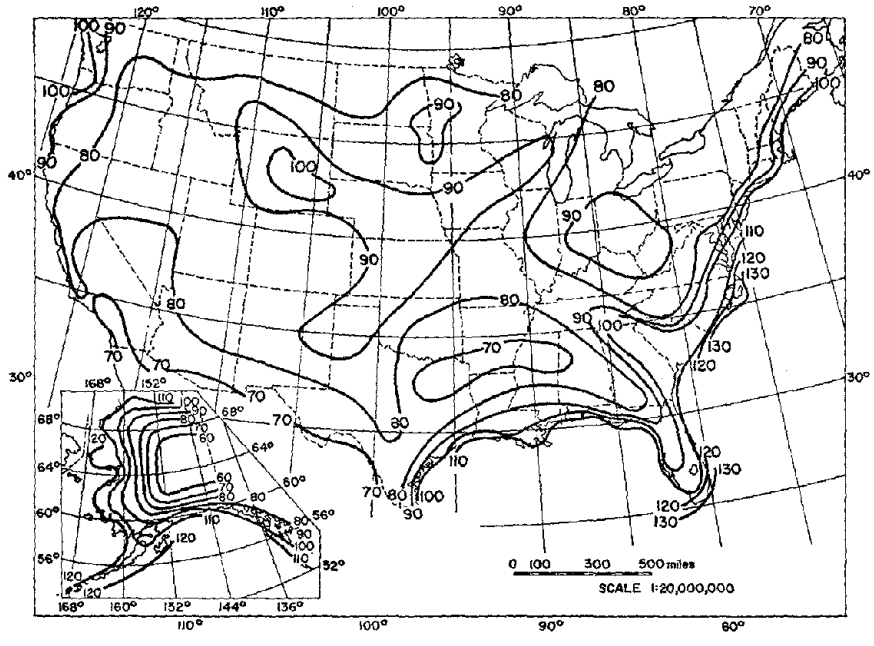

Fig. 3 Annual Extreme Fastest-Mile Speeds (mph) 100-year Mean Recurrence Interval (z=30 ft)

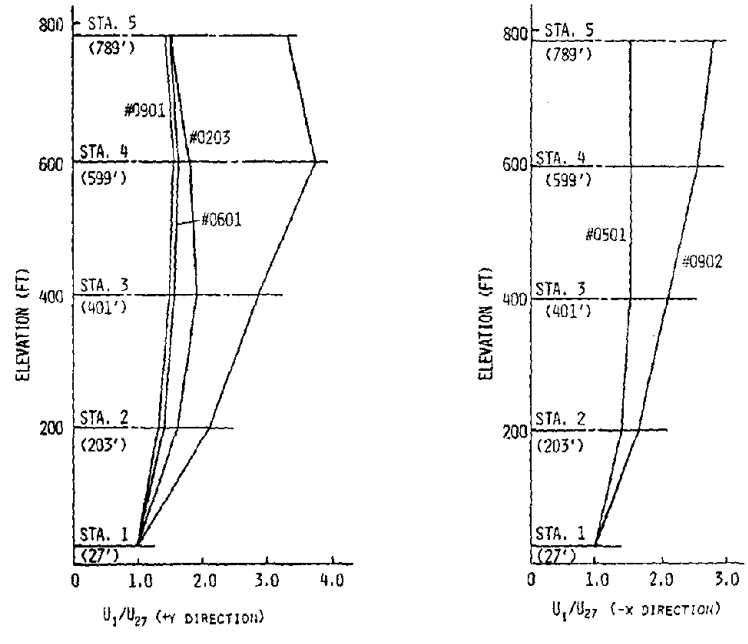

Fig. 4 Velocity Ratios

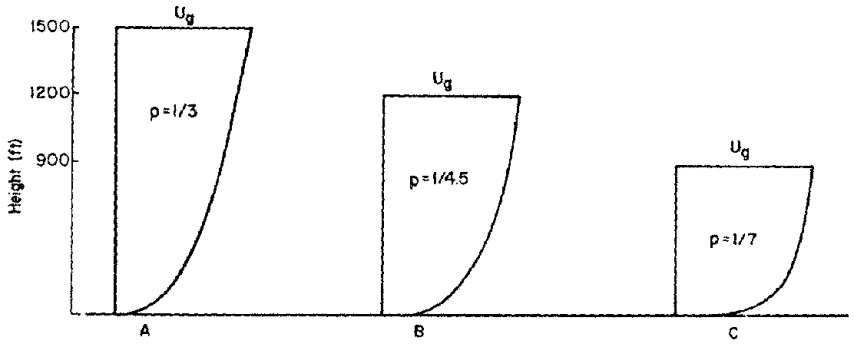

Fig. 5 Profiles of Wind Speed

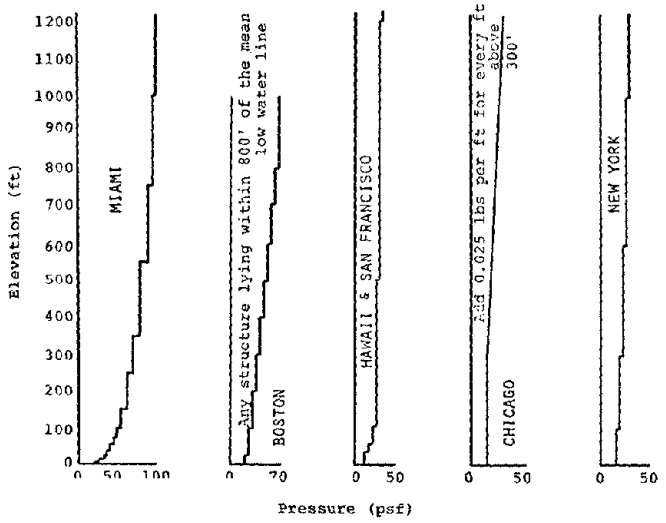

Code Pressures vs Height

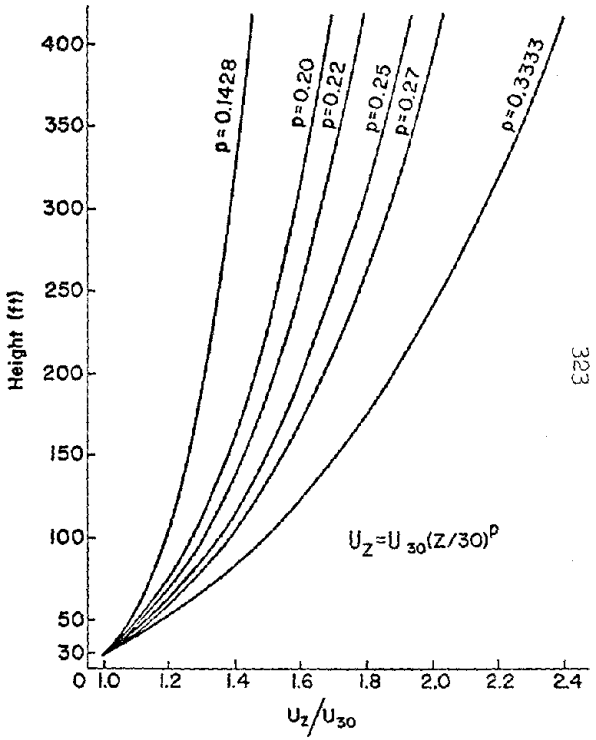

Fig. 6 Power-Law Relationship

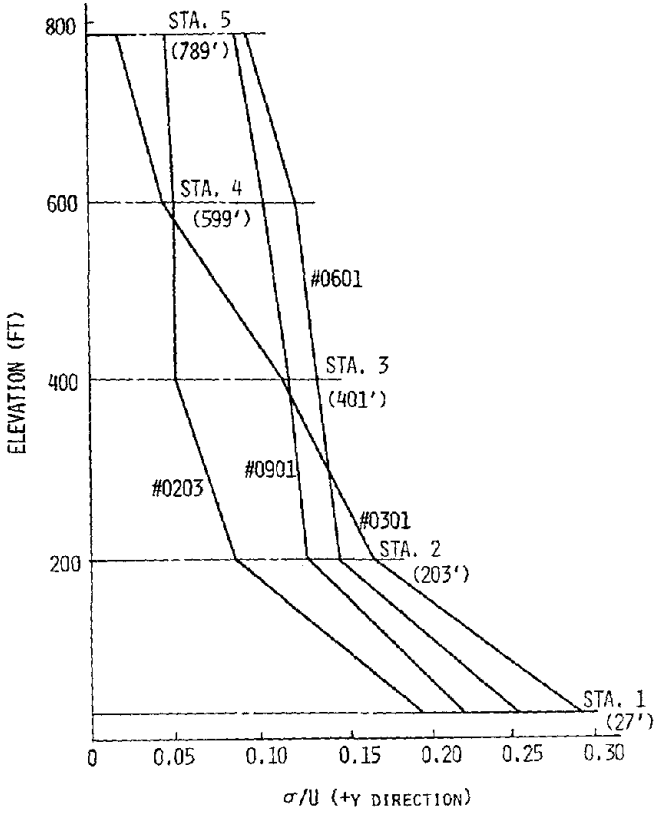

Fig. 8 Turbulence Intensities

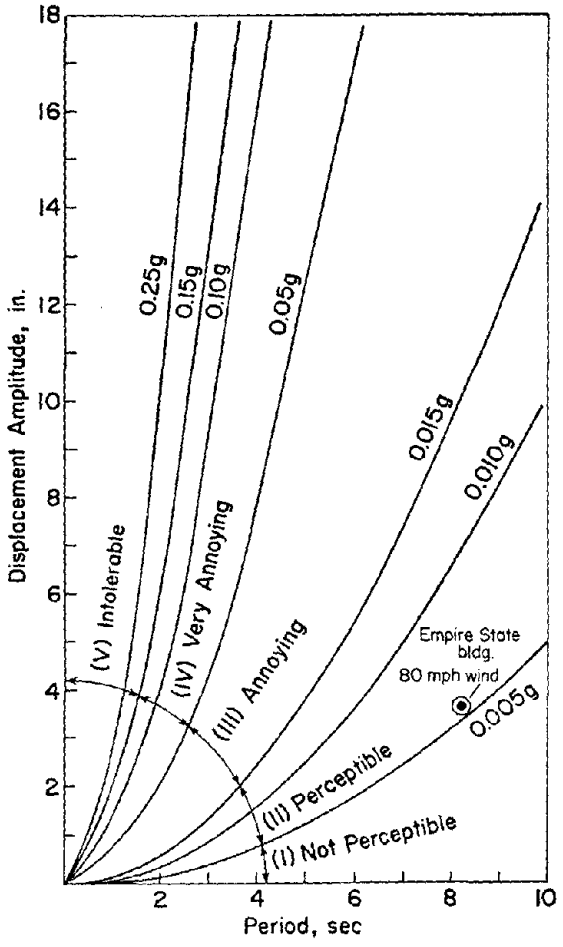

Fig. 9 Human Comfort Curves
(Source: Chang)

THE PREVENTION AND CONTROL OF LANDSLIDES

by

Severino L. Koh
Professor of Mechanical Engineering

and

Wai-Fah Chen
Professor of Civil Engineering

Purdue University
West Lafayette, Indiana 47907, U.S.A.

Synopsis

Landslides and slope failures are triggered by a variety of causes, including severe rainstorms and earthquakes, as well as such disturbances as those caused by construction works and explosions. However, the basic concept underlying the instability of a mass of soil in its simplest form is applicable to these different situations. This concept, the mechanics of landslides, is briefly discussed. Measures to minimize the occurrence of these hazards are considered. Finally, a review is presented of the remedial measures now in use to correct the effects of a landslide or to arrest impending slope failure.

Introduction

Landslides are hazards that are experienced in many countries. They may be induced by natural causes such as severe rainstorms that accompany monsoons or hurricanes, earthquakes and volcanic eruptions. They may also be caused by explosions and construction works. Landslides are observed on the slopes of dams, embankments and other man-made cuts, along the coasts as well as on mountain slopes, in urban areas and in rural regions, on the banks of rivers, lakes and on other natural slopes.

Isolated cases of slope failure attract widespread attention. In recent years a small town in Wales experienced the tragedy of its elementary school and some school children being buried under the slide of a sludge hill piled by the local coal mines. The 1972 and 1976 landslips in Hongkong were particularly disastrous. Yet landslides are common occurrences in many parts of the Southeast Asia. These occur during steady monsoon rains and during the typhoon season. But the most spectacular and devastating effects of landslides are associated with earthquakes. In fact, the major source of damage during several catastrophic earthquakes had been ground failure.

In a recent study of the historic 1906 San Francisco earthquake (M8.2 and Hoose [1976] identified three types of groundfailures caused by the ti ation of the granular material (the soil) from a solid state to a liquefie lateral-spreading landslides, flow landslides and bearing-capacity failure

In the San Francisco earthquake lateral-spreading failures were the n mon and most damaging. They occurred on very gently sloping terrain under by a section or layer of loose saturated granular sediments. Flow landsli loose saturated granular soils lying on moderately to steeply sloping terr occurred on several wet sandy slopes. However, since these occurred in ge undeveloped areas, this type of landslides did little damage. On the othe one can speculate that were these landslides to occur today, they could pc

serious hazard to some areas.

A more recent example of widespread landslides induced by earthquakes is the February 4, 1976 Guatemala earthquake (M7.5). It is estimated that over 10,000 landslides were triggered by this seismic disturbance.

This introductory exposition is simply to establish the importance of landslides in natural hazards consideration. The questions are then posed: How can we establish design criteria for protection against the hazard? How do we assess the stability of slopes? Can we control landslides? Can we prevent their occurrence? The discussions here are addressed to some of these questions.

In the next section, we briefly review the basic concept that underlies the mechanism of slope failure. While it is recognized that landslides may be induced by different causes, we focus in these discussions landslides that are induced by heavy rains and earthquakes. We then consider the preventive measures that one may apply to avoid the failure of man-made slopes. Finally, we discuss the various methods now in use to control landslides, to correct the effects of landslides or to arrest further ground motion.

The Mechanics of Landslides

Basic Mechanism for Slope Failure

The stability of slopes has been the subject of analysis for sometime now dating back to Fellenius, who in 1936 developed the so-called limit-equilibrium approach where a circular arc is taken as the failure surface. Used in conjunction with the method of slices, a statically indeterminate situation arises. Forces along the lateral surfaces must be assumed. Taylor in 1937 developed the so-called logarithmic-spiral method to overcome this difficulty. In this approach, the failure surface is taken to be a logarithmic spiral.

In his recent book, Chen [1975] gives the details in calculating the critical height for two mechanisms of failure. Figure 1 shows the failure mechanism with the failure surface passing through the toe of the slope, while Figure 2 shows the case of the failure surface passing below the toe.

Another group of workers have used the probabilistic theory to analyze the stability of earth slopes. Among these one might mention Wu and Kradt [1970], Cornell [1971], Yuceman, Tang and Ang [1973], and more recently Alonso [1976], and Morla Catalan and Cornell [1976].

Without getting involved in the complexities of analytical calculations for critical heights of slopes, and to concentrate simply on the mechanical causes of slope movements, we consider the mechanism shown in Figure 3. Along the tential surface of sliding, we have shear stress τ and normal stress σ. Sl movement takes place as soon as the average internal shear stress $\bar{\tau}$ exceeds average shear strength or the shearing resistance $\bar{s}$ of the soil.

The shear stress τ is due mainly to external factors such as gravity we W of the soil-rock material, the inertia force I and the surcharge q. In ge the steeper or higher the slopes the greater would the shear stress be ir ground. Inertia forces may be due to earthquake accelerations; these cause sitory increases in the shear stress in the slope material. Deposition of r

rial or structures along the upper edge of the slope contributes to the surcharge, increasing the shear stress along the potential slip surface.

On the other hand, the shear strength s is a basic mechanical property of the slope material, the soil or the rock, against slipping. The strength is a function of the degree of cementation or cohesion c, the friction angle ϕ between component grains which depends on the magnitude of the effective normal pressure p at a given potential surface of sliding. The simplest relation that is widely used as a basis for calculating slope failure is Coulomb's criterion:

$$s = c + p \tan \phi. \tag{1}$$

While factors affecting the shear stress are external, the factors which affect the shear strength are internal. The shear strength along the potential slip surface decreases with an increase of the pore-water pressure u, which in itself results in a reduction of the effective normal stress from p to (p - u) according to the Principle of Effective Stress of soil mechanics. Thus, we have the modified Coulomb's criterion:

$$s = c + (p - u) \tan \phi. \tag{2}$$

The pore-water pressure u may be increased by the vibratory character of seismic motion or the rise of the piezometric surface behind the slope associated with a displacement of air during heavy rainstorm. The degree of cementation may decrease progressively due to cyclic climatic changes of water content or the possible destructive effect of seismic loads on slightly cemented grain aggregates.

Rain-induced Landslides

Excessive saturation of the slope material with water, such as that which accompanies heavy rainstorms, can induce landslides. As the soil is "soaked", there is an increase in the unit weight of the soil: W increases. The shear strength s of the soil also decreases. This reduction in shear resistance may result from different mechanisms. For some soils, e.g. typical loess, as water enters the voids, the soil loses its cohesion, c, due to the solubility of its binder. In fine-grained, cohesionless soils bound largely by apparent cohesion, the water seeping into the ground, displacing the air-filled voids, eliminates the surface tension that holds the soil together.

Moreover, as the soil becomes saturated with infiltrating water, the pore-water pressure increases. This causes a decrease in the effective normal pressure, p. Thus, according to the Coulomb failure criterion equation (2), the shear strength s would decrease.

As soon as the increasing average shear stress $\bar{\tau}$ on the potential fa surface becomes equal to the decreasing average shear strength $\bar{s}$, a state instability is reached. With the continuing tendency in the changes of $\bar{\tau}$ landslide results. The slope continues to move until the pore-water pres are decreased either by evaporation or by drainage.

For man-made slopes, if the slope fails several weeks after construc must be assumed that the shear strength of the slope material has decreas to changes in water content. Most of these delayed slides occur during h

rainstorms.

Earthquake-Induced Landslides

A typical characteristic of many soils, e.g. water-saturated sand, that is quite different from engineering materials is the effect of cyclic loads on the properties of the soil mass. In these cases, a seismic load can significantly decrease the shearing strength, s, of the soil. As a result of the cyclic loading due to a seismic disturbance, the pore-water pressure in the mass of undrained cohesionless soil increases to the point where it equals the externally applied normal pressure. Thus, as easily shown in equation (2), the shear strength decreases. When the soil loses its shear strength completely, it is said to liquefy.

In the case of a slope where the soil mass is in a near-critical stress condition, the earthquake will trigger a landslide. If liquefaction occurs along a large portion of the potential sliding surface, the landslide movements will be very extensive. Such motion is termed flow slide. In other cases, the liquefied zone may not be so extensive so that sliding occurs partly through the liquefied soil and partly through the non-liquefied soil along the slip surface. In such cases the strength of the non-liquefied soil may be sufficient to arrest ground motions. The movements involved are relatively small compared to the size of the slide mass (Seed [1968]).

For some materials, such as medium-dense cohesionless soils, liquefaction may occur over a small deformation range. However, the material stiffens rapidly as a result of the dilation at large deformations. This causes a reduction in the pore-water pressure and results in a self-stabilizing effect against large movements. Similarly, if drainage in the soil is effective, extensive liquefaction cannot develop; thus, the earthquake is not able to induce large landslide displacements. Case studies of this type of landslides and flow slides are discussed by many authors. A notable review is given by Seed [1968].

General Remarks

In the analysis of the stability of slopes as well as in the design of earth slopes, the factor of safety is an important criterion. This is usually taken to be the ratio of the average shear strength $\bar{s}$ to the average shear stress $\bar{\tau}$. This ratio is sufficiently larger than unity in design. In the presence of a disturbance, this ratio decreases. However, landslide does not occur until this ratio reduces to unity. Should this reduction in the ratio occur gradually, a progressive type of deformation results for the earth material above the potential surface of sliding accompanied by some downward motion of points of this mass on the failure surface. In some instances, the differential downward m of the slope preceding the slide may be detected only by careful measurement On the other hand, the associated phenomenon of tension cracks appearing alo the upper boundary of the slide area may be conspicuous enough to attract th attention of animals (Terzaghi [1950]).

While it might take a heavy rainfall some time to cause slope instabili it is not uncommon for earthquakes to induce liquefaction with an instantane reduction of shear strength coupled with an instantaneous increase in shear tress. Nevertheless, earthquakes alone without extensive liquefaction can uce only a cumulative finite displacement as the magnitude of each cycle of

acceleration increases, decreases and reverses. Since the inertia forces are developed in such short periods of time, the factor of safety of the slope may drop below unity several times during an earthquake. A cumulative finite displacement may result but no "failure" will be experienced as taken in the conventional sense of a major collapse or change in configuration.

Catastrophic failure occurs when the earthquake causes liquefaction of the soil along the potential surface of sliding with the liquefied zone extending to a free surface. Under this condition, extensive lateral movements and a change of the shape of the slope, characteristic of flow slides, will be inevitable.

Further aspects of the mechanics of landslides and slope failure are discussed by Chen and Koh (1978). In that paper, a review of the state of the art is also presented for the assessment of the seismic stability of slopes.

The Prevention of Landslides

The loss in life and property caused by landslides is chronicled in many publications and records, in many countries. The questions that naturally follow are these: Could these landslides have been avoided? Could the designer of the slope that had failed have altered the design to prevent the disaster? Failure may sometimes be attributed to the designer, the construction engineer or both, but the paramount question is posed: Barring human mistakes, could one prevent the occurrence of a landslide with a perfect design, one that excludes all risk of slope failure regardless of cost?

The simple answer to this last question is "No". For one, while studies in fundamental geotechnical engineering have been extensive in recent years, there is still much to be learned in the understanding of soil/rock behavior under extreme loading conditions. There is a need for quantifying the constitutive characteristics of soils and rocks to reflect more realistically the unique cause-effect behavior of these materials. Even the testing of material samples to determine the properties of the material has not been totally dependable. There is always the question of relating laboratory test results of small samples of a material that is so susceptible to the environment, to specimen preparation (compaction, e.g.) and other influences -- relating these laboratory results to the actual situation in the field. A recent NSF-sponsored workshop deliberated on these and many other points to determine research needs in geotechnical earthquake engineering (Lee, et al. [1977]).

Should all these open questions be answered completely, one may be able to develop a "perfect design". However, such can only happen if all possible types of causes are taken into account, if the properties of the entire soil mass are known collectively as well as individually for each of its critical mass stituent (simple averages will not be adequate for the "perfect design") if the allowable effects are fully determined in terms of pertinent param and variables.

Under these required specifications, the development of a "perfect d is presently still not possible. More realistically, designs may be made minimize the risk of the occurrence of the disaster but not to eliminate event entirely. Landslides may not be prevented completely, but the risk having disastrous slope failures may be reduced. General preventive meas may be followed to achieve this.

Site Selection

The selection of site for the construction of an embankment for a highway or the slopes of dams is a critical procedure. Accurate geological exploration of the proposed site must be made to determine the types of soils and rocks underlying the site, the strength and other characteristics of these materials, and the overall geological configuration of the site, e.g. the layering of the rocks and soils and the discontinuities in the materials. Orientation of the slope relative to the geological characteristics of the area is also a point of consideration.

The proper selection of a dam site can minimize the occurrence of landslides. Unstable rocks located above sheer slopes are undesirable sites. Slopes of the foundation pit must be stable. In the course of excavation for the foundation, the slope has to be stabilized. If this is not possible, it may even be necessary to abandon the site.

The discharge channels must be located properly to retain the stability of the slopes. In some instances, these canals may have to be located in flood plains even if two dikes have to be constructed. The stability of the shores of the reservoir has to be taken into account also. In particular, one must consider the fact that the stability of the soil and rock masses are affected by submersion. Buffeting waves erode the shorelines. Remedial measures must therefore be taken to take these effects into account.

Design and Construction of Earthslopes

While in general a reduction in the slope angle of an earthwork would minimize the occurrence of landslides, slope failure may still result due to a poorly designed slope bottom. The toe of the slope should be weighted so as to retain the shear strength of the rocks and soils where the overburden has been removed, as well as to correct for the loosening of the slopes after excavation resulting in a decrease of the horizontal stress. In addition, seepage of ground water at the toe of the slope contributes to the deterioration of the slope.

Zaruba and Mencl [1969] discuss three methods by which the slope bottom may be treated to prevent failure of slopes originating from the toe:

Stooped slope -- is constructed with two sections separated by a bench. The upper section which is usually the larger of the two has an angle designed with seepage of rain water taken into account. The height of the lower section is usually small to provide a large slope angle. Drainage of the mass underneath the bench is important. A common method is the use horizontal boreholes. R water collected from the upper section of the slope is drained by means of i permeable ditches.

Retaining walls -- are used at the slope bottom to reduce the removal o material at the slope bottom. In addition, this arrangement protects the to of the slope from the development of slumps caused by freezing ground water.

Gravel bench -- at the bottom of the slope protects the toe of the slop from frost as well as drains the water from the slope. The longitudianl wat collectors at the bottom of the slope can also be protected by the gravel fi

Other Considerations

There are several other considerations that one must take into account in construction operations to ensure the stability of slopes of cuttings. In dangerous soils, it is particularly advisable to excavate in layers. By this method, the ground water level is lowered progressively increasing the stability of the slope. Furthermore, this avoids the formation of high vertical faces, a particularly hazardous situation since the upper layers of soils and rocks adjacent to the excavation are subjected to tensile loads.

Another important consideration to ensure the stability of a cutting is the drainage of the adjacent areas as well as that of the actual cutting. Effective layouts for drainage trenches take into account the actual situation in the site with a view to assuring the drainage of waters in the neighborhood of the slope. Drainage of the bottom of the excavation must not be neglected. Sumps are used wherever necessary.

Finally, explosives can disintegrate rock masses and induce sliding movements. Water seeping through the loosened mass modifies the strength characteristics of the slope material and may also induce slope failure. Therefore, precautionary measures must be taken in the construction of cuttings.

The Control of Landslides

While the careful selection of sites, the conservative design and proper construction of earth slopes and embankments would minimize the occurrence of landslides, while precautionary measures taken in excavations would increase the stability of the cuttings, landslides and slope failures still occur for a variety of reasons under different circumstances. They may be induced by heavy rainfall, by earthquake distrubances or simply by disturbances that are man-made, e.g. explosions. They may also occur while the slope is being constructed. To correct the effects of a landslide or to forestall impending slope failure and ground motion, several control measures may be used. A comprehensive discussion of these measures is presented by Zaruba and Mencl [1969]. We consider below some of the more effective measures now in use and provide some case studies.

Drainage of Landslides

As mentioned above the pore-water pressure plays a significant role in the stability of a slope. It is also cited repeatedly that drainage should be provided for in the construction of a slope as well as in maintaining its stability. In the aftermath of a landslide, slope failure or earth movement, the very first remedial measure to be executed is again the removal of water both from t face and the subsurface.

Surface drainage -- should be accomplished as soon as possible. Whi itself surface drainage is not sufficient to stabilize the slope, it cont to the drying of the affected area and the controlling of the landslide. this operation, water entering the threatened area is diverted. After a stabilization of the landslide, open ditches of proper size and gradient excavated to discharge rain water. Surface cracks are filled to ensure c uous run-off of surface water.

Subsurface drainage -- can effectively enhance the stability of the slope. Three types of drainage have been used: drainage galleries, borings and trenches.

Drainage galleries permit the drainage of large amounts of water and may be effectively used in conjunction with drainage borings in the walls, floor or roof of the gallery. Cost is a big disadvantage for the use of drainage galleries.

Drainage borings are much cheaper than the galleries, but are usually restricted to much shorter distances of drainage. For short drainage borings in low slopes, perforated pipes are driven into the slope. Long horizontal drainage borings may be done either using helical augers to drill the holes with the perforated pipes driven into the holes drilled or using cutter and roller bits for rotary drilling with the perforated drill pipes serving also as permanent casings.

Drainage trenches are still used to drain slopes. They are often excavated by means of bulldozers. At the toe of the slide the water-saturated soil has to be removed and replaced by gravel. The design of drainage trenches is critical in that the drainage trench may puncture an impermeable clay bed, thus emptying the water into the lower level and possible inducing another slide.

D'Appolonia, et al. [1967] report on a recent case where a drainage system, coupled with other measures, was used to stabilize a slope. The problem considered pertained to a slope in the West Virginia panhandle, in Weirton. A large excavation was made for a steel plant expansion at the toe of a colluvial slope. Subsurface investigation was conducted since the slope was formed by slides in the geologic past. The slope was potentially dangerous with a factor of safety of 1.0 against drained failure using residual strength parameters. Stabilization of the slope was achieved with a drainage system for long-term stability and a sheet pile wall anchored with tensioned earth ties that precompressed the toe of the slope for short-term stability.

Retaining Walls and Buttresses

Retaining walls and buttresses are used largely to consolidate existing landslides, particularly in areas which are restricted in space or those close to other structures such as in cities and railroad tracks and highways. Retaining walls are used to support slopes in clayey soils to prevent loosening of the toe and to protect it from frost. Low walls are used to fasten the toe of existing landslides, and large retaining walls, subjected to full earth pressures, are used if no other design of a cutting is possible.

During the 1964 Alaska Earthquake, a retrogressive translatory slide of the Fourth Avenue in Anchorage was induced. The 900-ft by 1800-ft slide are threatened the very heart of the Anchorage business area. Long and George [discuss the construction of a gravel buttress to resist forces caused by san clay liquefaction, horizontal and circular sliding, or slumping, static or d ic forces.

Hardening of Soils

While stabilization of a slope by means of a drainage system is effecti any applications, this method fails where the slope soil is impermeable. A

method known simply as hardening of soils may then be considered. There are three ways most commonly used to achieve this: electro-osmosis, thermic treatment, and by grouting. Zaruba and Mencl [1969] describe these procedures in some detail.

Electro-osmosis -- has the same effect as subsurface drainage; however, in the present case, water is drained not by gravity but by means of the flow of water from an anode to a cathode, with the two electrodes embedded in the soil. The cathode is a perforated pipe from which the water that had penetrated into the pipe may be pumped out. Electro-osmosis is most suitable for silty soils with particles between 0.05 and 0.005 mm. in size.

This method of drainage was conceived by Reuss [1809] and was used effectively through the years. As an example, Casagrande [1941] used this method to stabilize the slopes of railway cuttings. More recently, the electro-osmosis treatment of the soil was used to stabilize the Turnagain Slide in Alaska, which was the result of the earthquake of March 27, 1964 (Long and George [1967b].

Another interesting application was in the construction of the dam on the West Branch of the Mahoning River about 20 miles west of Warren, Ohio. During the construction of the closure section of the 80-ft high dam, rapid spreading and settlement of the embankment and outlet works conduit occurred when the embankment was just within 5 ft of the crest. Slope movement was arrested by first removing 12 ft of the material from the top of the embankment over a length of 700 ft. The electro-osmosis process was employed to reduce the pore-water pressure, the slope was stabilized, and the embankment was finally completed. Fetzer [1967] gives the details of the circumstances surrounding this construction.

Thermic treatment -- has also been used to stabilize landslides. This method was discovered by Litvinov in 1955 (Zaruba and Mencl [1969]). While it has been used in several cases in Europe, its application has not been as widespread as the electro-osmosis method.

Briefly, the thermic treatment of the soil involves the driving of air into a mixing burner where oil conveyed from a pump is burned. The exhaust gas of about 1000° C temperature is forced into the borehole and penetrates into the pores of the soil (loess in the application used by Litvinov) baking the soil into a hard material. In a modified manner, Beles and Stanculescu [1957] used the thermic treatment to stabilize landslides in clay. In this application two holes were bored to produce a draft since unlike loess clay has no large pores. At the exit a heated chimney tube was set up, improving the effectiveness of the circulation, thus making the use of a compressor unnecessary.

Grouting -- with portland cement has been used effectively for the f
of soils in railway subgrades and mud pockets underneath the roadbed as v
for stabilizing landslides on railways. In principle, grouting is a mecl
stabilization that simply displaces water from the fissures with cement r
As a short term measure, this is effective. However, long-term stabili:
of the slope will still depend on the drainage of ground water.

Other Control Measures

Several other measures have been used to control earth movements and to stabilize slopes. Several of these, namely: the use of piles and bolts to stabilize slopes, and the breaking of slip surfaces by explosion, have been used with mixed success. Two methods: stabilization by vegetation and the treatment of the slope shape, however, are important considerations.

Treatment of the shape of the slope -- contributes to the stability of the slope if properly applied. Essentially, this involves a reduction of the surcharge or the load of soil at the head or by stabilizing the toe of the landslide with an enlargement. While this new configuration increases the stability of the slope, other problems (e.g. poor drainage) should also be remedied.

Stabilization of landslides by vegetation -- is effective particularly for shallow sheet slides where a reforestation of the slope is undertaken. Landslides with deep slide surfaces cannot be completely stabilized by vegetation. However, even in these cases reforestation will minimize the infiltration of surface water, thus contribute indirectly to the stabilization of the slope.

Conclusions

Landslides and slope failures pose as serious hazards to life and properties whether they are induced by natural causes or triggered by man-made disturbances. Through hard experience, preventive measures have been developed for the construction of slopes to minimize the chances for the occurrence of landslides. In the presence of a landslide that is active, to arrest further earth movements, also where impending soil failure exists, control measures may be applied.

However, in spite of these preventive and control measures, landslides and slope failures will still occur. A "perfect design", whereby the risk of failure is totally eliminated, does not exist in reality. This is largely due to the fact that the design will still be based on idealized cases. There is still a need for improving our analytical methods that would use more realistic mathematical characterization of the soil-rock masses. Surely, as knowledge of the mechanics of this instability phenomenon is advanced better design criteria may be developed. This is an area where geotechnical engineering can gainfully set its thrust.

References

Alonso, E. E. , "Risk Analysis of Slopes and Its Application to Slopes in Canadian Sensitive Clays," Geotechnique, v26, n3, pp. 453-472, 1976.

Beles, A. A., "Le traitment thermique du sol," Proceedings, Fourth International Conference in Soil Mechanics and Foundations Engineering, v3, pp. 2 1957.

Casagrande, L., "Die elektrische Entwässerung feinkörniger Böden," Die Strasse, pp. 324-326, 1941.

Chen, W. F., Limit Analysis and Soil Plasticity, Elsevier, Amsterdam, 1

Chen, W. F. and Koh, S. L., "Earthquake-Induced Landslide Problems," Proceedings, Central American Conference on Earthquake Engineering, January 9-1978, San Salvador, v1, pp. 665-685, 1978.

Cornell, C. A., "First Order Uncertainty Analysis of Soils Deformation and Stability," Proceedings of the First International Conference on Applications of Statistics and Probability to Soil and Structural Engineering, University of HongKong, pp. 130-144, 1971.

D'Appolonia, E., Alpertstein, R. and D'Appolonia, "Behavior of a Colluvial Slope," Journal of the Soil Mechanics and Foundations Division, ASCE, v93, nSM4, pp. 447-473, 1967.

Fetzer, C. A., "Electro-osmotic Stabilization of West Branch Dam," ibid., ASCE, v93, nSM4, pp. 85-106, 1967.

Lee, K. L., et al. "Reasearch Needs and Priorities for Geotechnical Earthquake Engineering Applications," Report of Workshop, The University of Texas at Austin, June 2-3, 1977, NSF Grant No. AEN77-09861.

Long, E. and George, W., "Buttress Design Earthquake-Induced Slides," Journal of the Soil Mechanics and Foundations Division, ASCE, v93, nSM4, pp. 595-609, 1967a.

Long, E. and George, W., "Turnagain Slide Stabilization, Anchorage, Alaska," ibid., v93, nSM4, pp. 611-627, 1967b.

Morla Catalan, J. A., and Cornell, C. A., "Earth Slope Reliability by a Level-Crossing Method," Journal of the Geotechnical Engineering Division, ASCE, v102, nGT6, pp. 591-604, 1976.

Seed, H. B., "Landslides during Earthquakes due to Soil Liquefaction," Journal of the Soil Mechanics and Foundations Division, ASCE, v94, nSM5, pp. 1055-1122, 1968.

Terzaghi, K., "Mechanisms of Landslides," Engineering Geology (Berkey) Volume, The Geological Society of America, pp. 83-123, 1950.

Wu, T. and Kraft, L. M., "Safety Analysis of Slopes," Journal of the Soil Mechanics and Foundation Division, ASCE, v96, nSM2, pp. 609-627, 1970.

Youd, T. L. and Hoose, S. N., "Liquefaction during 1906 San Francisco Earthquake," Journal of the Geotechnical Engineering Division, ASCE, v102, nGT5, pp. 425-439, 1976.

Yucemen, M. S., Tang, W. H. and Ang, A. H-S., "A Probabilistic Study of Safety and Design of Earth Slopes," Department of Civil Engineering Technical Report No. 402, University of Illinois, Urbana, Ill., 1973.

Zaruba, Q. and Mencl, V., Landslides and Their Control, Elsevier, Am 1969.

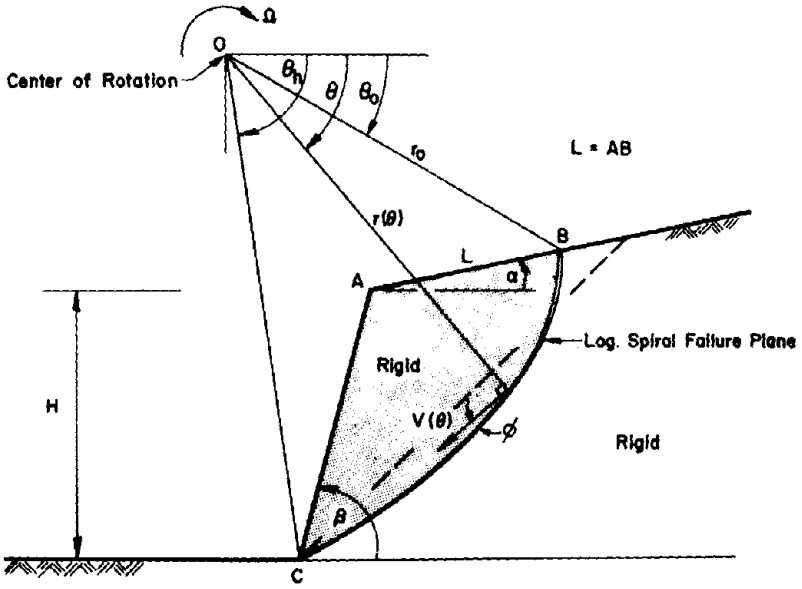

Figure 1. Failure mechanism for slope stability with failure surface passing through toe. (Chen [1975])

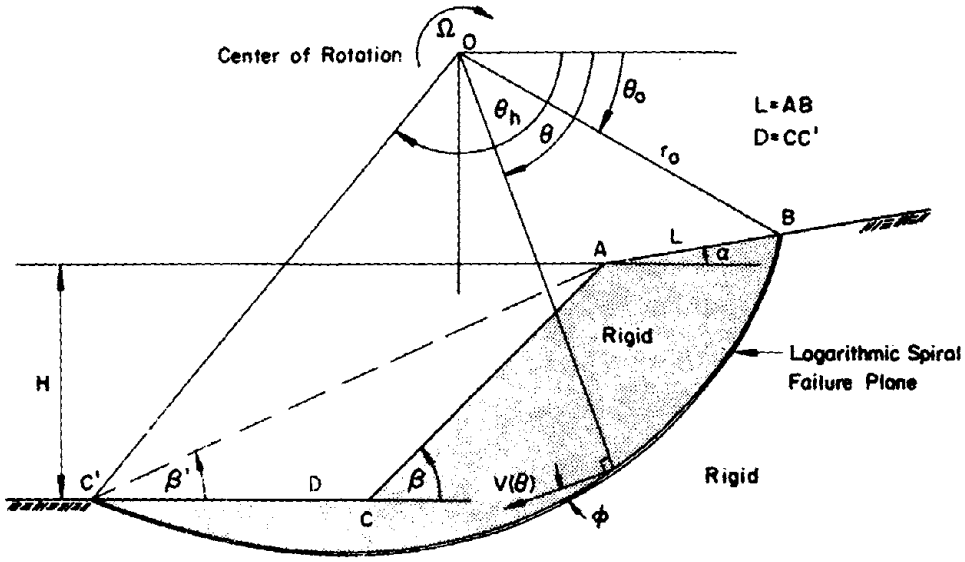

Figure 2. Failure mechanism for slope stability with failure surface pas: below toe. (Chen [1975])

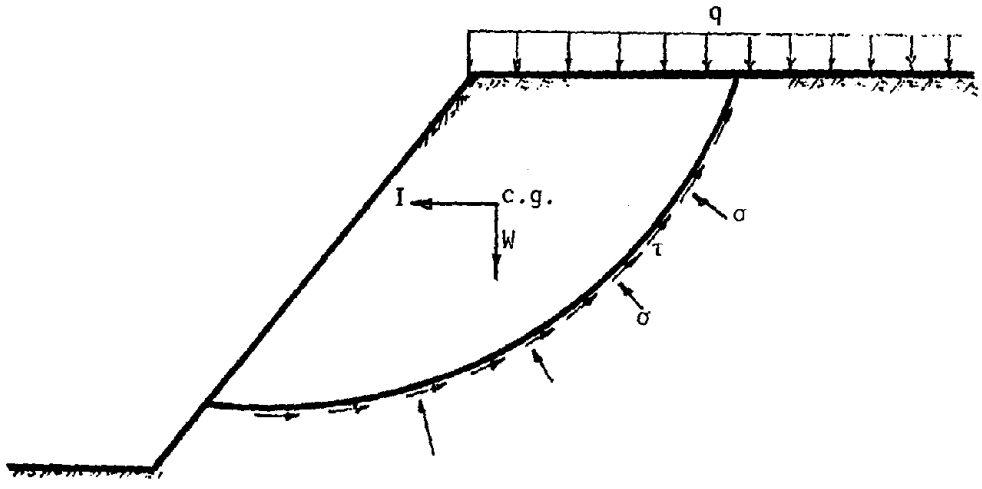

Figure 3. Simple mechanism for slope failure.

HURRICANE WAVES, STORM SURGE AND CURRENTS: AN ASSESSMENT OF THE STATE OF THE ART

Omar H. Shemdin and David B. King
Oceanography Group, Jet Propulsion Laboratory
California Institute of Technology, Pasadena

ABSTRACT

This paper reviews the state of the art for measuring and predicting the three most destructive elements associated with hurricanes; waves, currents and storm surge. The use of numerical modeling is found to be promising for predicting the hurricane generated wave spectra and the storm surge elevation along straight, open coastlines. Prediction of the storm surge along indented or broken coastlines and the associated nearshore currents appears to be most feasible with physical models. Recent advances have been made in instrumentation that now allows reliable data collection to be made. These include both surface sensors and more importantly, airborne remote sensors. The need and the ability now exists for the development of more reliable hurricane wave generation models and for the development of a carefully designed laboratory facility to study coastal currents and storm surge under high wind conditions.

INTRODUCTION

Much progress has been made in recent years in understanding and predicting hurricane behavior. Due to improved satellite and aircraft surveilence techniques, the loss in human lives can now be kept to a minimum when a hurricane hits a coastal area. However, the meteorology of this cyclonic heat engine is not yet fully understood. The present predictive capabilities deal with the gross aspects of the storm and are accurate only in short term forecasts. The predictions are usually subject to large uncertainties introduced by the meteorological conditions surrounding the hurricane.

Furthermore, while the loss of human lives can now be kept to a minimum in a community that responds intelligently to hurricane warnings, the loss of property can be astronomical. The damage to coastal areas is caused by a combination of forces. The most important of these is a rising sea level with its associated currents and high waves. Other destructive but usually less important forces are the direct affects of wind, changes in atmospheric pressure and increased flooding due to rainfall. Structures usually fail because they do not withstand the forces of debris laden waves combined with the erosion of their foundations by rapid currents.

Offshore structural damage is primarily attributed to excessive forces on piles caused by the combined action of waves and currents. Uplift forces can effectively destroy any platform which has a deck level lower than the height of the elevated wave crests. Wave induced soil motion can also play a major destructive role if unaccounted for in the design stage.

The mechanisms that generate hurricane waves and storm surge are partially understood and are marginally predictable under conditions which are normally encountered. Currents are poorly understood and cannot be simulated

accurately with existing numerical techniques. These three aspects of hurricanes; waves, storm surge and currents; will be discussed from the standpoint of developing predictive models. The associated methods for obtaining environmental measurements will also be reviewed in order to assess present capabilities for use and verification.

STATE OF THE ART IN PREDICTIVE CAPABILITY

Wave Generation

The simplest approach to the problem of predicting the damage to offshore and coastal structures due to hurricane waves is to use the significant wave height approach. The main advantage of this technique is that it is relatively easy to use. The major disadvantages are that the approach is only moderately accurate, yields only partial information and, since it is an emperical technique, gives no insight into the wave generation mechanisms.

A more complete approach is to use the wave spectrum concept. For a simplified windfield a one-dimensional wave spectra can be sufficient. However, a hurricane has a translating circular wind which produces a very complicated wavefield with propagation in all directions. In this case, a two dimensional wave spectrum, where the wave energy is described as a function of both frequency and propagation direction, is needed, and it must be founded upon both theory and accurate measurements if reliable results are to be produced.

The development of a hurricane wave prediction model can be considered a special case of the general wave prediction problem. This general model, even under ideal conditions, has not yet been fully resolved. The main stumbling block to a general wave prediction model is a lack of understanding of the exact energy transfer mechanisms from wind to waves, from waves to other frequency waves and from waves to turbulence. It is know that the wind transfers energy to the waves in the mid-frequency range. The waves then shift the energy in a non-linear manner to both higher and lower frequencies. The higher frequencies become saturated so that breaking occurs, with the energy being lost to turbulence. The spectrum continues to grow at the low frequency end. This mechanism accounts for the documented phenomena of spectral equilibrium overshoot during wave growth. However, the entire process is not yet fully understood.

The first attempts at any wave prediction models grow out of efforts during World War II. Sverdrup and Munk (1947) and Bretschneider (1952) developed what became known as the SMB method, a model that predicted significant wave height. Pierson, Neumann and James (1955) developed the first wave spectrum prediction method. These were simple models, needing only hand calculati and requiring subjective decisions on the part of the user.

Since that time there have been many models and model refinements proposed for both the significant wave height concept and the wave spectr concept. These are discussed at length in Barnett and Kenyon (1975). Of special importance are the fully developed spectrum by Pierson and Moskow (1964) and the model by Pierson, Tick and Baer (1966) which is currently being used by Fleet Numerical Weather Central to operationally predict th deep water wave climate in the North Atlantic and North Pacific. The mos recent major work is a parametric wave prediction model by Hasselmann, et (1976).

A major problem in the development of these wave models has been the absence of comprehensive and accurate data collected under the appropriate generation conditions. Recently, steps have been taken to aleviate this problem. A number of large scale collaborative experiments have been conducted including the JONSWAP experiment (Hasselmann, et. al., 1973), the Marineland Experiment during December, 1975 (Shemdin, Blue and Dunne, 1975) and the West Coast Experiment in spring, 1977 (Shemdin, Inman and Blue, 1977). Analyses of the data from these major experiments are contributing substantially to the understanding of wave generation and dissipation.

In the general context of the development of wave prediction models, a few investigators have turned their attention to the specific problem of hurricane wave generation. Much of the earliest work was done by Bretschneider (1959, 1972). However, his work and the work by Ijima (1968), Patterson (1971) and Bea (1974) all predict only the significant wave height. The predicted typical significant wave heights during hurricane Camille are shown in Figure 1 at different distances from the U.S. Gulf coast.

There are currently only two models that use the two-dimensional spectral analysis approach to predict hurricane waves, and both are very recent. The first is by Cardone, Pierson and Ward (1976) and the other is a simplified model by Ross (1976) based upon the parametric model of Hasselmann, et. al. (1976). Neither of these models has been calibrated with directional hurricane wave data.

Storm Surge

Considerable interest in the measurement and prediction of storm surges has been caused by the continuing increase in coastal development and the resulting increase in potential damage. Early documentation of storm surges was reported by Harris (1963). The time histories of storm surges recorded at tide stations were shown for nearby hurricanes. These records have been used extensively to verify the various numerical models advanced for storm surge predictions. An example of storm surge innundation is given in Figure 2 for Hurricane Camille.

Significant advances have been achieved in numerical storm surge prediction over the past two decades. The simplified one dimensional equations that were initially used, incorporated only the effects of surface and bottom stresses on the water surface displacement. Freeman, Baer and Jung (1957) introduced a quasi two-dimensional model by including the set-up contribution of the along shore motion. This model, known as the Bathstrophic Storm Surge model, neglects the non-linear terms in the equation of motion. The model is sometimes useful, but it is not sufficiently accurate in the nearshore areas where some of the neglected terms become important.

Since then, a number of more advanced numerical models have been propo for the open coast; such as those reported by Welander (1961), Jelesnianski (1965, 1967), Reid and Bodine (1968, 1971), Pearce (1972) and more recently by Pararas-Carayannis (1975), Yeh and Yeh (1976) and Sobey (1976). They al use the vertically integrated equations of motion with different assumption regarding the importance of various terms in the equations. Also, differen forms of the surface and bottom stresses are adopted in these models as wel as a variety of boundary conditions in deep and shallow water. These model can generally predict the storm surge level along an open and unbroken coastline very well. The storm surge predictions are not sensitive to the

form used for bottom stress nor the point of initial computation in deep water as demonstrated by Pearce (1972). At the same time these models only provide information on the average motion in the water column at each grid point and cannot be relied on for providing the three dimensional current profile under storm conditions. These models also show limitations when applied to the more complicated innudation of bays under storm actions. Damsgaard and Dinsmore (1975) applied this type of model to the prediction of storm surge in Biscayne Bay, Florida by making a jetty-weir assumption for the flow across the shoals that separate the bay from the open ocean. The storm surge in the bay was predicted after calibration of the model with tidal records around the bay. The predicted currents in and out of the bay represented the vertically averaged values.

While the usefulness of Damsgaard and Dinsmore's model is evident, its limitations can not be overlooked. The assumptions made in specifying losses across the island barriers and shoals are tailored to produce expected surge levels in the bay. Alternate modeling techniques for predicting such behavior are needed. Physical models can be used to predict storm surges in bays when certain scaling requirements are enforced as demonstrated by Shemdin (1972).

Hurricane Currents

Hurricane currents are primarily driven by the wind induced stress at the water surface. Substantial current magnitudes are generated in deep water under hurricane conditions as demonstrated by Forristall (1974) who also introduced a numerical model for computing the current profile throughout the water column. Forristall used the equation of motion with a suitable assumption for the eddy viscosity to arrive at the velocity profile which was substantiated by comparison with measurements obtained from offshore towers in the Gulf of Mexico.

In nearshore areas the hurricane induced current is affected by the bottom boundary and a three dimensional approach is necessary to predict such currents. Pearce (1972) made an unsuccessfull attempt to predict the current measurements obtained by Murray (1970) in the nearshore zone of the Gulf of Mexico under hurricane conditions. Pearce found the currents prediced by his vertically averaged model to be sensitive to bottom stress assumptions. The predicted average remained considerably different from the magnitudes measured by Murray for a range of bottom stress coefficients.

Alternate modeling techniques are desirable for predicting the three dimensional current structure induced by high winds. Shemdin (1972) demonstrated the feasibility of using physical models to simulate wind induced currents. This concept requires further development through basic investigations and construction of suitable facilities with provisions for air and water

MEASUREMENT TECHNIQUES

Until recently there have been very few reliable measurements of wav surge and currents in hurricanes. One reason is that the probability of encountering any given properly instrumented site is small. Also, the te to provide instrumentation that will withstand the hurricane environment recent and has been triggered by offshore oil and gas industry. In spite these difficulties in the past few years some valuable data have become a

Offshore Platforms

The first comprehensive attempt to collect oceanographic data under hurricane conditions was the Ocean Data Gathering Program. The effort was formulated by a consortium of oil companies. The effort employed the use of six offshore oil platforms in the Gulf of Mexico from which the instruments were deployed. The instrumentation on each platform included two wave staffs, an anemometer, a barometer, a clock and a self recording automatic system capable of providing data over one month of continuous operation. The systems were operated from October, 1968 to November, 1971; during which time data were collected on four hurricanes, including Camille, and a number of other less severe storms. Reports on the program and its results were made by Ward (1974) and Hamilton and Ward (1974). The data were used to calibrate the wave prediction models proposed by Patterson (1971), Bea (1974) and Cardone, Pierson and Ward (1976).

Oil platforms in the Gulf of Mexico have also been used to measure the offshore currents produced by hurricanes. An Ocean Current Measurement Program was begun in 1971. Currently, there are three stations, each equiped with an Aerovane, a wave staff, a barometer and three or four current meters as described by Hall (1972).

Data from one tropical storm, Delia, in September 1973, have been reported in the literature. This storm passed almost directly over one of the instrumented platforms which was located 20km off the coast of Galveston, Texas. These have been used in the hurricane current model of Forristall, Hamilton and Cardone (1977).

In 1972, the NOAA Data Buoy Office (NDBO) began deploying deep ocean data buoys. These have been located around the coast of the U.S. in the Atlantic, the Gulf of Mexico and the Pacific, including the Gulf of Alaska. These buoys measure a wide variety of environmental parameters; including one dimensional wave spectra, significant wave height, wave period, wind speed and direction, atmospheric pressure, air and water temperatures and current speeds and directions at different depths. They can be remotely commanded to perform various sampling schemes and to self record the data or to transmit it in real time to shore based stations. These buoys are described in a report by the NOAA Data Buoy Office (1973).

On September 22, and 23, 1975, Hurricane Eloise passed near two NDBO buoys in the Gulf of Mexico. These data are presented in a report by Withee and Johnson (1975). The reported wind speed and directions are shown in Figure 3. The corresponding significant wave height and dominant period are shown in Figure 4. These data were used in the development of the parametric hurricane wave model by Ross (1976). Also, the Ross (1976) model and the Cardone, Pierson, and Ward (1976) model were used to make a real time forecast of Hurricane Be in 1976 and Hurricane Anita in 1977. The two models were compared with data obtained from NDBO buoys off the New Jersey coast and in the Gulf of Mexico. The results are reported in Cardone, Ross and Ahrens (1977).

Florida Prepared Sites Program

Deepwater buoys and offshore oil platforms have been of great value in providing data under extreme conditions. However, these systems m be permanently stationed, and this considerably reduces their probability o encountering hurricanes. Mobile instruments have an advantage in this rega and a program incorporating such a concept has been formulated.

The concept of prepared sites was introduced in Florida by Shemdin and O'Brien (1975) whereby several prepared but uninstrumented sites would be maintained during the hurricane season. A site would be instrumented only when threatened by an approaching hurricane. Preparedness and mobility became essential for the success of such a program. The sites selected are shown in Figure 5. This concept was later modified to incorporate the collection of year-round wave data as part of a wave climate program. As such, the prepared sites on the east coast have now been permanently equipped with wave and storm surge recording instruments. These systems are shown in Figure 6. Future plans include other data recording equipment and also the permanent instrumentation of the sites on the Gulf Coast of Florida as well.

Remote Sensing Technique Using Aircraft

The advent of remote sensing has created exciting new possibilities for obtaining wave information in hurricanes. The airborne Synthetic Aperture Radar (SAR) can be used to collect information to generate a photograph-like image of the sea surface. This radar has the ability to penetrate cloud cover, and, since it is airborne, it can collect data throughout the entire region of the hurricane. The image is used to derive information on wave lengths and directions.

The SAR has been flown into hurricanes during 1976 and 1977; as reported in Thompson, McMillan and King (1976). Some of the results of the analysis of this data have been reported in Elachi, Thompson and King (1977) and King and Shemdin (1977). Figure 7a shows a wave image obtained with the SAR in Hurricane Gloria in 1976.

The directional alignment of waves can be seen more easily in the Fourier transform of the image shown in Figure 7b. The data obtained from different sectors of this hurricane are shown in Figure 8.

The results in Figure 8 represent the first directional wave information ever collected in a hurricane. This figure shows that the waves are not symmetrically distributed around the hurricane eye. Dominant waves propagate ahead of the hurricane along lines normal to the local wind direction. (The windfield blows in a counter-clockwise spiral around the eye.) Confused and unexplained directional distributions can be seen in the lower right sector of the hurricane. While much of the information in Figure 8 is yet to be fully explained some major observations can be stated. The axial asymmetry of the wavefield is attributed to the forward motion of the hurricane. The residence time for wave generation is significantly greater in the region to the right of the eye if the hurricane has a moderate forward velocity. The dominant growth appears to be associated with waves that have group velocities equal to or somewhat greater than the speed of the hurricane. The dominant waves s out in an arc ahead of the hurricane eye and have wave lengths of the ord of 250 m with a corresponding group velocity of 10 m/sec. The hurricane forward speed is 8 m/sec. These waves appear to have optimum hurricane residence time with respect to wave generation.

Two important advantages of an airborne remote sensor system are tha a hurricane can be intercepted at an arbitraty location and then informat on waves can be gathered throughout the region of the hurricane influence. In contrast a surface platform only yields a time history of a hurricane s it passes a fixed point. Clearly, both types of data are valuable for a complete understanding of associated processes.

RESEARCH NEEDS AND OPPORTUNITIES

Improved Numerical Models for Hurricane Wave Predictions

The recent advances in wave generation theories and the recently acquired hurricane wave measurements create an opportunity for developing an advanced wave prediction model for hurricanes. The advanced wave generation models for fetch limited constant wind situations are not directly applicable to the complex translating circular wind patterns associated with hurricanes. The existing hurricane wave models are empirical and do not incorporate the energy transfer mechanisms associated with wave generation. An advanced generation model is being developed by the authors.

Physical Modeling of Storm Surge and Currents in Bays

The existing numerical models for storm surge use vertically averaged equations which do not provide details of the current variation in a water column. In nearshore areas and in bays insight into the latter is essential for determining the longshore and onshore-offshore directions and magnitudes of sediment movements. The currents also determine the magnitude of lossess encountered in storm surge propagation across barrier islands and in bays. A schematic of such a process is shown in Figure 9. Given the limitation of numerical models and the need for insight into the ocean environment under hurricane conditions, it is clear that adequate use of physical models for simulating wind induced phenomena has not been fully explored. Shemdin (1972) successfully simulated wind induced current in San Nicolas Lagoon in Aruba by utilizing a laboratory basin in which the bottom hydrography was simulated. The wind was generated by a blower and duct system which was placed over the model (see figure 10). While the above model was small and limited in scope it is clear that a more carefully planned storm surge facility equipped to generate waves, wind and current can be used effectively to simulate nearshore phenomena induced by high wind. Development of the design concepts for such a facility is presently in progress.

SUMMARY AND CONCLUSIONS

The catastrophic damage imposed by hurricanes at landfall necessitates continued research and developmental effort to gain insight into the ocean environment under high wind conditions. Existing techniques for predicting storm surge, waves and currents have not been extremely reliable. Improvements in methodology are now seen to be possible in two areas: (a)numerical modeling of wave generation becuase of newly acquired remote sensing data, and (b)physical modeling of the three dimensional structure of hurricane-induced currents and storm surge.

1. Barnett, T. P. and Kenyon, K. E., "Recent Advances in the Study of Wind Waves", Rep. Prog. Phys. 38, p. 667-729, 1975

2. Bea, R. G., "Gulf of Mexico Hurricane Wave Heights", Paper OTC 2110 Sixth Annual Offshore Technology Conference, Houston, May 6-8, 1974.

3. Bodine, B. R., "Storm Surge on the Open Coast: Fundamentals and Simplified Prediction", TM-35, U.S. Army Corps of Engineers, Coastal Engineering Research Center, May 1971.

4. Bretschneider, C. L., "The Generation and Decay of Wind Waves in Deep Water", Trans. Am. Geophysical Union, Vol. 33, 381-389, 1952.

5. Bretschneider, C. L., "Hurricane Design - Wave Practices", Trans, ASCE, Vol. 124, 39-62, 1959.

6. Bretschneider, C. L., "A Non-Dimensional Stationary Hurricane Wave Model", Paper OTC 1517, Fourth Offshore Technology Conf., Houston, May 1-3, 1972.

7. Pierson, W. J. and Ward, E. G., "Hindcasting the Directional Spectra of Hurricane Generated Waves", J. Pet. Tech., p. 385-394, April, 1976

8. Cardone, Vincent J., Ross, Duncan B. and Ahrens, Merlin R., "An Experiment in Forecasting Hurricane Generated Sea States", Proceedings of the 11th Technical Conference on Hurricanes and Tropical Meteorology, Miami, Florida, December 13-16, 1977.

9. Damsgaard, A. and Dinsmore, A. F., "Numerical Simulation of Storm Surge in Bays", Symposium on Modeling Techniques, ASCE, San Francisco, California, September 3-5, 1975.

10. Elachi, C., Thompson, T. W. and King, D. B., "Observations of the Ocean Wave Pattern under Hurricane Gloria with a Synthetic Aperture Radar", Science, Vol. 198, November 11, 1977.

11. Forristall, G. Z., "Three Dimensional Structure of Storm Generated Currents", J. Geophys. Res., 79, 2721-2729, 1974.

12. Forristall, G. Z., Hamilton, R. C., and Cardone, V. J., "Continental Shelf Currents in Tropical Storm Delia: Observations and Theory", J. Phys. Ocean. Vol 7, #4, 532-546, July, 1977.

13. Freeman, J. C., Jr., Baer, L., and Jung, G. H., "The Bathystrophic Storm Tide", Journal of Mar. Res., Vol. 16, No. 1, 1957.

14. Hall, J. M., "Hurricane Generated Ocean Currents", Paper OTC 1518, Fourth Offshore Techn. Conf., Houston, May 1-3, 1972.

15. Hamilton, R. C. and Ward, E. G., "Ocean Data Gathering Program - Quality and Reduction of Data", Paper OTC 2108-A, Sixth Offshore Techn. Conf., Houston May 6-8, 1974.

16. Harris, D. L. "Characteristics of the Hurricane Storm Surge", Technical Paper No. 48, U.S. Dept. of Commerce, Washington, D.C., 1963.

17. Hasselmann, K., Barnett, T. P., Bouws, E., Carlson, H., Cartwright, D. E., Enke, K., Ewing, J. A., Gienapp, H., Hasselmann, D. E., Krusemann, P., Meerburg, A., Muller, P., Olbers, D. J., Richter, K., Sell, W. and Walden, H., "Measurement of Wind-Wave Growth and Swell Decay During the Joint North Sea Wave Project (JONSWAP)", Deut. Hydrogr. Z., Suppl. A, 8, No. 12, 1973.

18. Hasselmann, K., Ross, D. B., Muller, P., and Sell, W., "A Parametric Wave Prediction Model", J. Phys. Oceanogr. Vol. 6, No. 2., 220-228, March

19. Ijima, T., Soejima, T., and Matsuo, T., "Ocean Wave Distribution in T Area", Proc. Coastal Engineering in Japan, Vol II, 29-42, 1968.

20. Jelesnianski, C. P., "A Numerical Computation of Storm Tides Induced I a Tropical Storm Impinging on a Continental Shelf", Monthly Weather Revie Vol. 93, No. 6, 1965.

21. Jelesnianski, C. P., "Numerical Computation of Storm Surges with Bottom Stress", Monthly Weather Review, Vol. 95, No. 11, 1967.

22. King, David B., and Shemdin, Omar H., "Remote Sensing of Hurricane Waves," Conference Proceedings of NASA Office of Applications FY 77 Weather and Climate Review, Goddard Space Flight Center, Greenbelt, Maryland, 1977.

23. Murray S. P., "Bottom Currents Near the Coast During Hurricane Camille", J. of Geo. Res., Fol. 75, No. 24, 1970.

24. NOAA Data Buoy Office, "Practical Experience with Buoys developed by the NOAA Data Buoy Office", U.S. Department of Commerce, November, 1973.

25. Pararas-Carayannis, George, "Verification Study of a Bathstrophic Storm Surge Model", Tech. Mem. No. 50, U.S. Army Corps of Engineers, Coastal Engineering Research Center, May, 1975.

26. Patterson, M. M., "Hindcasting Hurricane Waves in the Gulf of Mexico", Soc. Pet. Eng. J., 321-328, August, 1972.

27. Pearce, Bryan R., "Numerical Calculation of the Response of Coastal Waters to Storm Systems - With Application to Hurricane Camille of August 17-22, 1969," Technical Report No. 12., Coastal and Oceanographic Engineering Laboratory, University of Florida, August, 1972.

28. Pierson, W. J. and Moskowitz, L., "A Proposed Spectral Form for Fully Developed Wind Seas Based upon the Similarity Theory of S. A. Kitaigorodske", J. Geophy. Res. 69, 5181-5190, 1964.

29. Pierson, W. J., Neumann, G. and James, R. W., "Practical Methods for Observing and Forecasting Ocean Waves by Means of Wave Spectra and Statistics", H. O. Pub. No. 603, U.S. Navy Dept. p. 284, 1955.

30. Pierson, W. J., Tick, L. J., and Baer, L., "Computer Based Proceedure for Preparing Global Wave Forecasts and Wind Field Analysis Capable of Using Data Obtained from a Spacecraft", Proc. Sixth Symposium on Naval Hydrodynamics, Washington D.C., p. 499, 1966

31. Reid, R. O. and Bodine, B. R., "Numerical Models for Storm Surges in Galveston Bay", J. of the Waterways and Harbors Division, ASCE, Vol, 94, no. WW1, 1968

32. Ross, D. B., "A Simplified Model for Forecasting Hurricane Generated Waves", (Abstract), Bull. A.M.S. January, p. 113, 1976. Presented at Am. Meteorol. Soc. Conf. on Atmospheric and Oceanic Waves, Seattle, Washingt March 29-April 2.

33. Shemdin, Omar H., "Modeling of Wind Over Water", Paper OTC 1515, Fourth Annual Offshore Technology Conference, Houston, May 1-3, 1972.

34. Shemdin, O. H. and O'Brien, M. P., "Hydrodynamics and Meteoroligical of High Wind Over Shallow Water Along the East Coast of Florida", Proposal submitted to the U.S. Nuclear Regulatory Commission, ERDA, 1975.

35. Shemdin, O. H., Blue, J. E., and Dunne, J. A., "Seasat-A: Surface Truth Program Marineland Test Plan", Jet Propulsion Lab 622-5, 1975.

36. Shemdin, O. H., Inman, D. L.,and Blue, J. E., "West Coast Experiment Test Plan", Jet Propulsion Lab, 900-765, 1977.

37. Sobey, R. J., "The Generation and Propagation of Cyclonic Storm Surges", Proc. 1976 Annual Engineering Conf., I. E. Aust., Townsville, May, 1976.

38. Sonu, C. J., "Beach Changes by Extraordinary Waves Caused by Hurricane Camille", Coastal Studies Institute, Louisiana State University, Technical Report 77, February, 1970.

39. Sverdrup, H. U. and Munk, W. H., "Wind, Sea, and Swell: Theory of Relationships for Forecasting", H. O. Pub. No. 601, U.S. Navy Dept., March, p. 44, 1947.

40. Thompson, T. W., McMillan, E. S., and King, D. B., "JPL Radar Operations Summer '76 Hurricane Expedition 17 August - 3 October 1976", Jet Propulsion Lab 622-18, December, 1976.

41. U.S. Army Corps of Engineers, Mobile District, Hurricane Camille 14-22 August 1969, May, 1970.

42. Ward, E. G., "Ocean Data Gathering Program - An Overview", Paper OTC 2108-B Six Offshore Techn. Conf. Houston, May 6-8, 1974.

43. Welander, P., "Numerical Prediction of Storm Surges", Advances in Geophysics, Vol. 8, p. 316-379, 1961.

44. Withee, G. W. and Johnson, A., "Data Report: Buoy Observations During Hurricane Eloise (September 19 to October 11, 1975)", Environmental Science Div., Data Buoy Office, NOAA, U.S. Dept. of Commerce, November 1975.

45. Yeh, Gour-Tsyh, and Yeh, Fei-Fan, "Generalized Model for Storm Surges" Fifteenth Coastal Engineering Conference, ASCE, Honolulu, July 12-13, 1976.

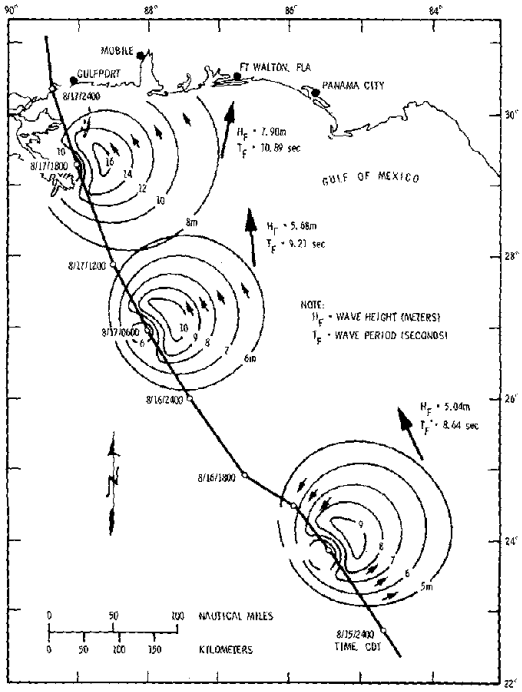

Figure 1 - Hurricane Camille hindcast wave fields at different times prior to landfall (after Sonu, 1970).

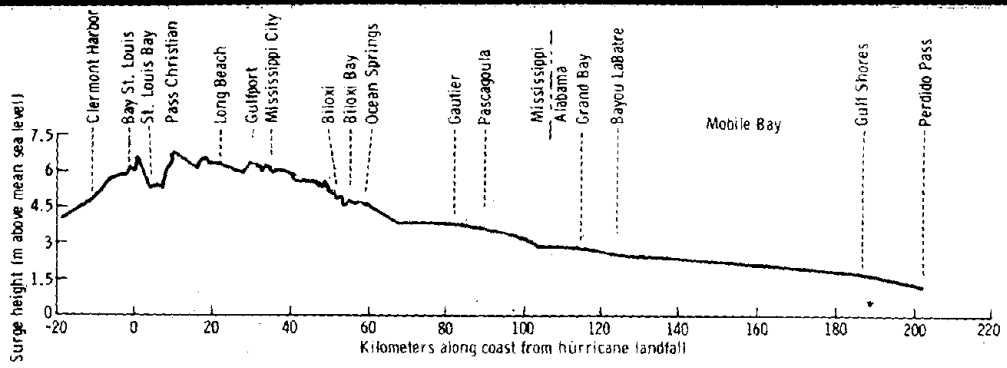

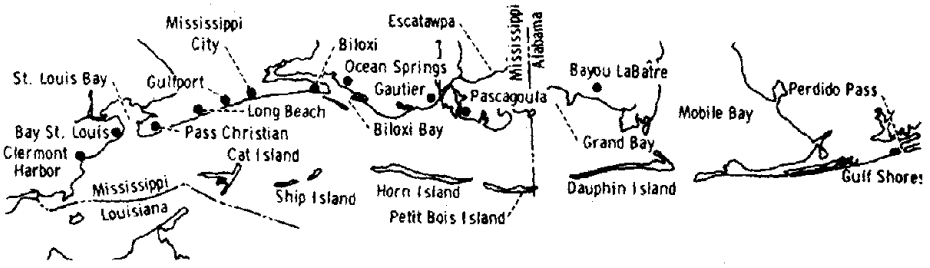

Figure 2 - Maximum surge envelope of hurricane Camille along the U.S. Gulf (after U.S. Army Corps of Engineers, 1970).

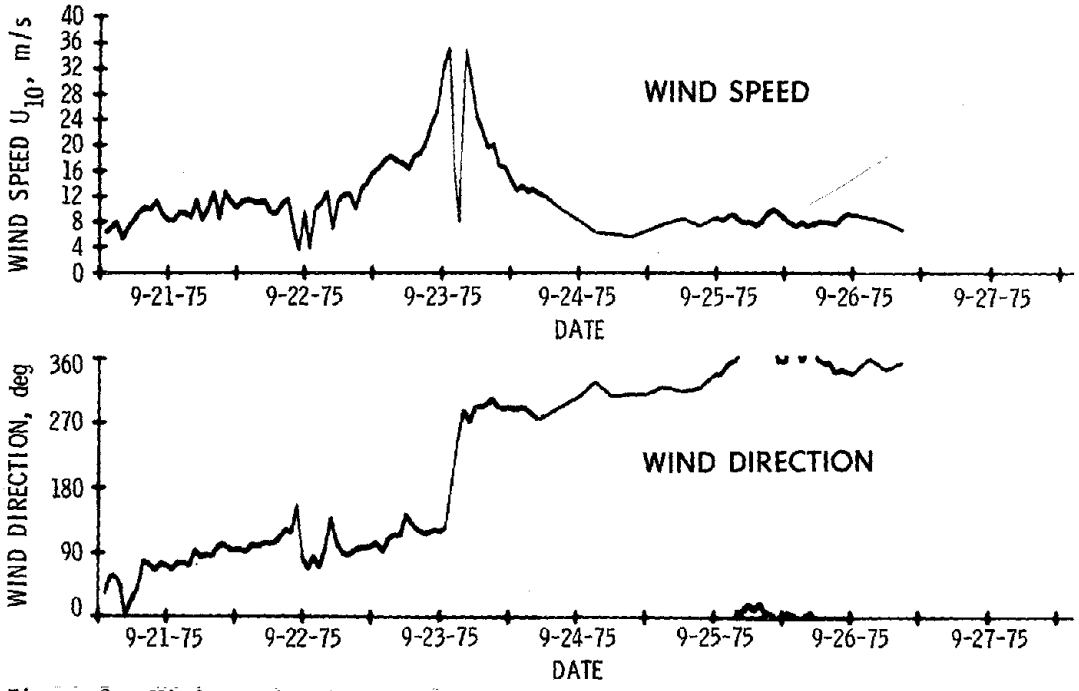

Figure 3 - Wind speed and direction records measured by NDBO EB-10 for hurricane Eloise in 1976 (after Withee and Johnson, 1975).

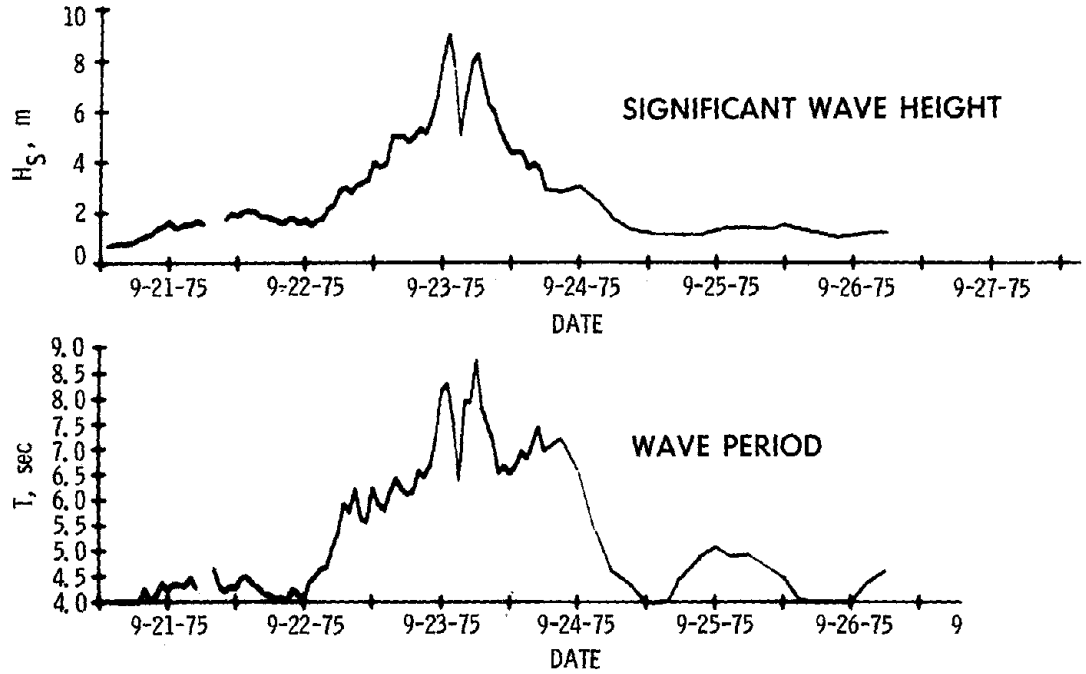

Figure 4 - Significant wave height and period records of hurricane Elois measured by NDBO EB-10 (after Withee and Johnson, 1975).

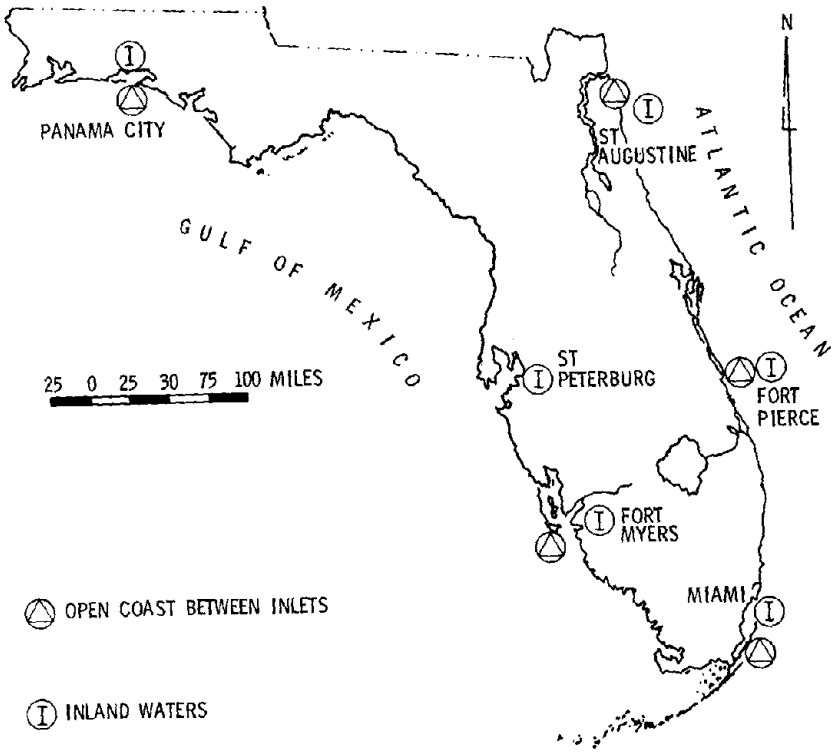

Figure 5 - Proposed locations of instrumented sites along the Florida Atlantic and Gulf Coasts.

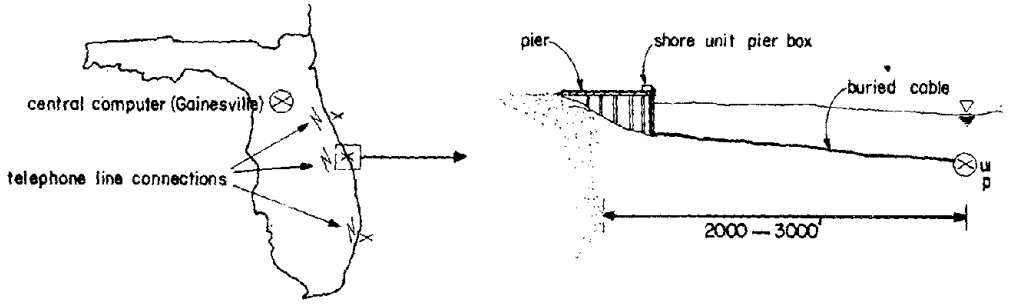

Figure 6 - Coastal stations presently operated by the University of Florida. (after Howell, 1975; personal communication).

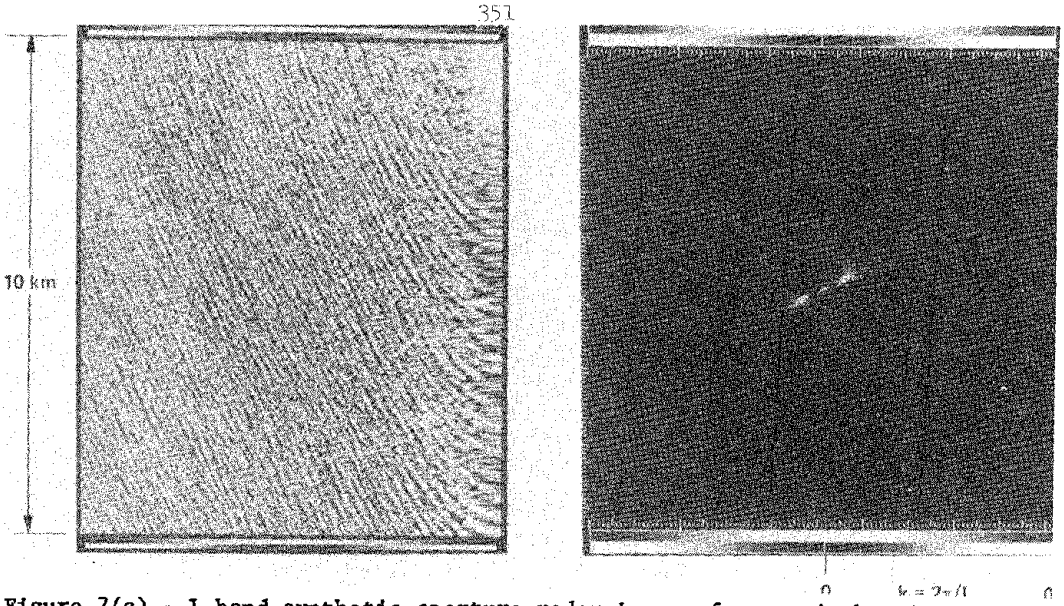

Figure 7(a) - L-band synthetic aperture radar image of waves in hurricane Gloria 1976.
Figure 7(b) - Corresponding Fourier transform of wave image.

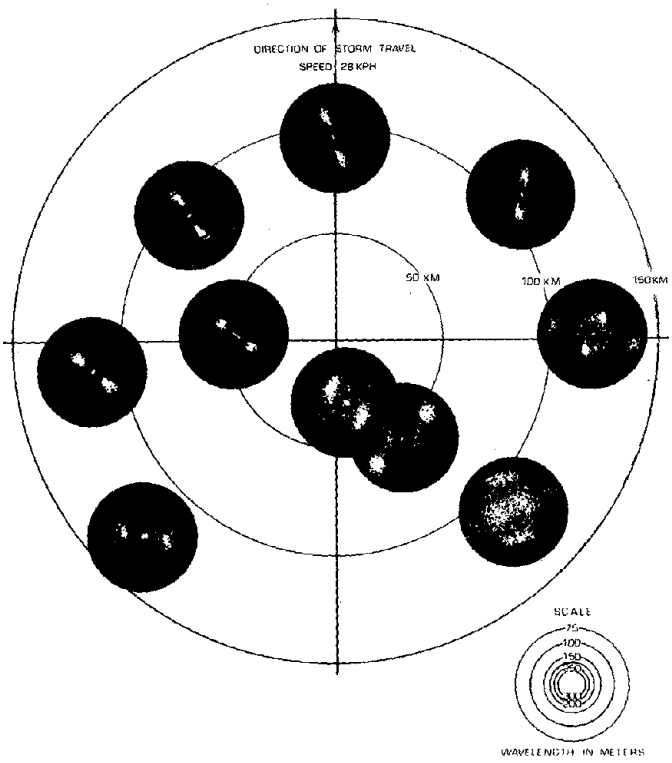

Figure 8 - Directional wave patterns in different sectors of hurricane Glo measured by an L-band airborne synthetic aperture radar.

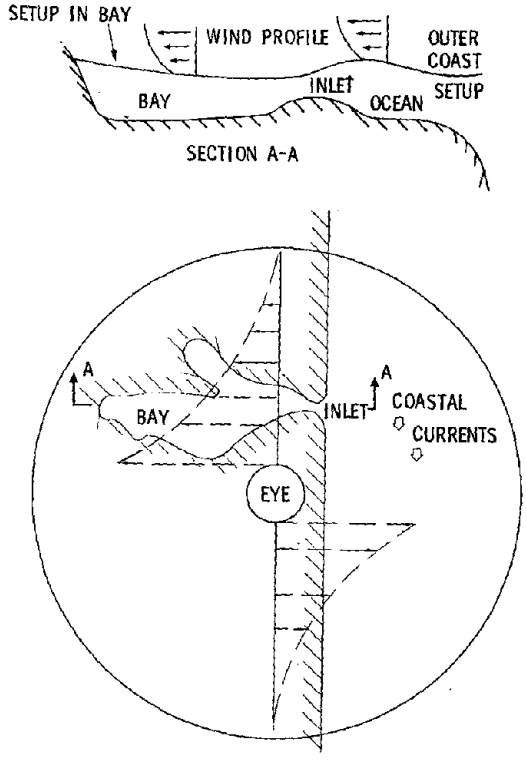

Figure 9 - Schematic of a storm surge flooding pattern in a bay by a hurricane at land fall.

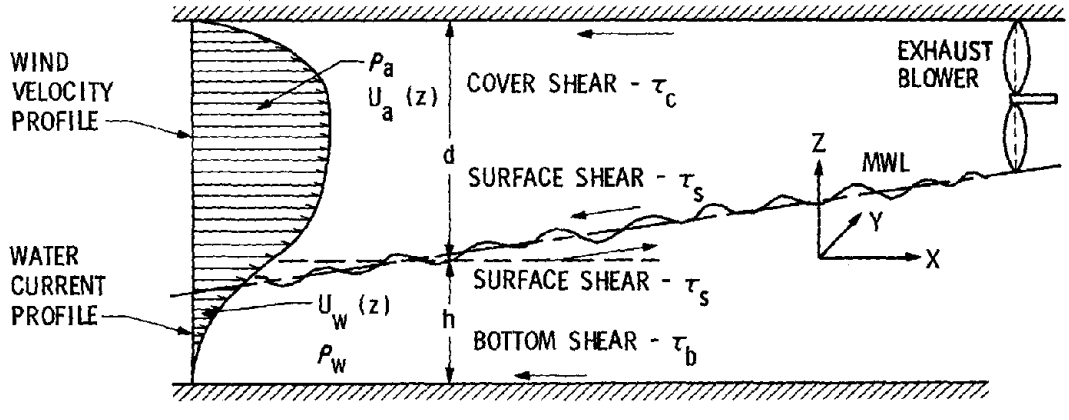

Figure 10 - Definition sketch for a storm surge and current simulation facility.

MANAGEMENT OF STORM SURGES AND FLOODS IN MANILA BAY

Fei-Fan Yeh*
TETRA TECH Inc., USA

Synopsis: Storm surge and high tide in Manila Bay, together with torrential rain, have long been considered the common "natural hazards" throughout the Metro Manila Area. Therefore, this paper begins with a description of the flat, low-lying terrains, tide, storm surge and rain, which are believed to account for the ineffectual systems in stormwater management. Suitable analytical methods are given in the current context of state-of-art techniques which are essential to quantify the performance objectives and to develop and evaluate alternatives. Finally, viable nonstructural as well as structural solutions on current planning concepts are briefly discussed.

---

* Presently in Manila as the hydraulic consultant to the Philippine National Housint Authority under a contract with James M. Montgomery Consulting Engineers, Inc., USA.

I. Physical Characteristics of Manila Bay and Metro Manila

Manila Bay has a coastline of about 190 kilometers and an area of approximately 1,800 square kilometers. Its mouth, which is only about 15 kilometers from the 200 meter contour of the continental shelf, is about 22 kilometers wide. The island of Corregidor divides the entrance into a North Channel with a maximum depth of 90 meters and a South Channel of about 50 meters deep. The bottom of the Bay has a rise of about one meter per kilometer of horizontal distance from the mouth to the northeast. The total drainage area contributing to Manila Bay is approximately 17,000 square kilometers which does not include the 900 square kilometer Laguna de Bay. The northern part of the Bay is characterized by extensive tidal flats which are completely submerged during the flood months.

The Metro Manila which includes 4 cities and 16 municipalities has an area of 58.4 square kilometers. Situated at the east of Manila Bay, Metro Manila is characterized by three belts of terrain running north-south parallel to the bayshore. These belts are identified as the coastal plain, the Guadalupe hills, and the Marikina-Laguna Valley. The parallel configuration is broken by the Pasig River which breaks through the hills at Guadalupe pass and dissipates in the coastal plain. The coastal plain was at one time a series of low sandy islands which, in modern times, have been filled and extended until only a network of esteroes still exist. Most of the coast plain is less than two meters above the mean sea level (MSL). The Marikina-Valley is also flat, it is narrow at the north and widens toward the south and Laguna de Bay, and has an average elevation of about 2.3 meters above the mean sea level (MSL). The Pasig River, which connects the Marikina-Laguna Valley and the coastal plain through the Central Manila, is less than 17 kilometers in length and has an extremely flat grade with the bottom elevation change in its entire length of only about three meters. The action of the tides in the Manila Bay determines the flow of water in all the watercourses of the coast plain. So tide responsive is the Pasig-Marikina river system that high intensity storms or occasional torrential typhoon rains have frequently caused widespread floodings covering most of the low-lying coastal plain and the Marikina-Laguna Valley.

II. Astronomical Tide and Storm Surge in Manila Bay

Astronomical tides in Manila Bay vary between diurnal and semi-diurnal with the latter occuring about 55 percent of the time. The tide becomes diurnal around the times of the moon's maximum declination. The mean tidal range is just over a meter but a couple of times a year the diurnal range may be about 2 meters. For a 19-year average of actual observations between January 1, 1951 to December 31, 1969, the following tidal levels in reference to the mean sea level (MSL) in

Manila Bay were determined by the Philippine Coast and Geodetic Survey.

1. Mean higher high water (MHHW) = 0.54 meter above MSL
2. Mean high water (MHW) = 0.39 meter above MSL
3. Mean low water (MLW) = 0.38 meter below MSL
4. Mean lower low water (MLLW) = 0.48 meter below MSL

However, for the engineering interest, the duration of various tidal levels would be more consequential in selecting design performance criteria. Based on the averages of the 1967 tidal series, the following durations in terms of percentage of time, that the tide stage would be greater than certain specified level, were determined as:

Specified Level	Yearly Average	August Average
One Meter Above MSL	2 %	9 %
MHHW	20 %	30 %
MHW	28 %	40 %
MSL	62 %	83 %
MLW	90 %	98 %
MLLW	93 %	100 %

August averages in 1967 are of particular interest because the August month in general has not only the highest tides in a year, also the highest rainfall. Therefore, there is greater probability that a prolonged flooding in Metro Manila may occur in August when high tides in Manila Bay are concurrent with the torrential rains.

The term "storm surge" is used to indicate departure from normal astronomical tidal level due to the action of storms. Determination of storm surge is a complex problem involving interaction among the bathymetry and geometry of water body, the forces of the wind field and atmospheric depression, the resistance of the bottom, the momentum generated in the water body, and the effects by other mechanisms unrelated to the storms, such as astronomical tide, earth rotation, stream flows, etc. The highest storm surge observed since 1946 by the Philippine Coast and Geodetic Survey was about 1.50 meters above the mean sea level (MSL), of which the level was occurred twice during the typhoon passages to the north of Central Luzon; one in 1972 and another in 1974. The highest storm surge recorded does not necessarily reflect the highest storm surge in Manila Bay because the peak storm surge may have occurred some distance away from the tide gage station in the bay. Besides, extreme storm surges are rarely recorded by water level gages because the gages tend to become inoperative with extremely high waves.

A numerical simulation on typhoon surge in Manila Bay was performed recently in accordance with a mathematical model (Chen et al 1977) adopted by the U.S. Department of Housing and Urban Development. Since the surge-producing parameters in the historical typhoons passing over

the Philippines were not yet available, the analysis was done based on a so-called "standard typhoon" defined by the PAGASA (formerly Philippine Weather Bureau) as follows:

1. Pressure drop between the ambient and the typhoon center = 56 milibars
2. Average forward speed of the typhoon = 24 km per hour
3. Maximum wind radius = 24 and 48 kilometers
4. Track being oriented from east to west at a distance of maximum wind radius north from the Philippine North port and parallel with the lattitude.

The results indicated that storm surges for a "standard typhoon" so defined would be about 1.4 meters and 1.6 meters near to the Philippine North Port, for maximum wind radius of 24 km and 48 km respectively. It is, of course, impossible to specify a precise recurrence interval of the "standard typhoon" without consideration of a far greater number of typhoons and without frequency analyses of each surge-producing parameter of the historical typhoons. Nevertheless, considering the rarity of typhoon tracks passing over in the vicinity of the Manila Bay and the moderate 155 kilometer-per-hour center wind of the "standard typhoon", it appears that a storm surge component of the order of 1.5 meters would be an infrequent event at most, but definitely not a rare event as the strongest typhoon wind ever hit the Philippines was more than 270 kilometers per hour during the passage of Typhoon Sening (Joan) in 1970.

The analysis also indicated that the storm surge in Manila Bay was primarily generated in the bay itself. The effect of the wind over the bay is almost independent of that over the open sea. The storm surge near to the Corregidor Island was less than 0.6 meter due to the relatively narrow width of the continental shelf in front of the Manila Bay mouth. The penetration of surge water through the Corregidor Channels in a manner similar to the astronomical tide would be insignificant in contributing to the surge level in the bay because of the divergent nature of the bay and the restricted conveyance in the Corregidor Channels.

As typhoon storms in the Philippine area are frequently occuring during July, August, and September which are the months normally associated with the higher astronomical tides in Manila Bay, the potential hazards due to the high tide in addition to the storm surge directly or indirectly generated as a result of the presence of tropical cyclones including typhoons may be briefly described as follows:

1. In the Coastal Area of Manila Bay -- Rises in water levels (storm surge on top of high tide) in nearshore regions will not only flood low-lying terrain, but provide a base on which the attendant high waves generated by the strong wind can penetrate farther inland. Flooding of this type combined with the action of higher surface waves can cause severe damage to low-lying land and backshore improvements. Wind induced surge, accompanied by wave action, also accounts

for most of the damage to coastal engineering works and beach areas. Displacement of stone armor units of jetties, groins and breakwaters, scouring around structures, accretion and erosion of beach materials, shoaling of navigational channels, impeding vessel traffics, and hampering harbor operations.

2. In the coastal plain and the Marikina-Laguna Valley of the Metro Manila -- Typhoons may dump as much as 300 milimeters of rainfall in 24 hours over large areas and evenmore over areas of less than 25 square kilometers. The fluvial flood resulting from this rainfall can increase the water level near the head of many tidal estuaries. The existence of storm surge together with high astronomical tide at the mouth of the estuarine river may eliminate or reverse the normal hydraulic gradient in river level so that the rainwater accumulates in the river to form a tidal wedge of much greater depth than would be the case with normal tides at the coast. For example, during the passage of Typhoon Gertrude on September 1, 1948, which caused a maximum storm surge of only 1.2 meters above MSL in Manila Bay and a maximum 24-hour rainfall of 503 mm observed at Luna Mt. Province, the flooded area including most of the Metro Manila totalled about 78 square kilometers.

III. Analytical Techniques in Tidal Hydraulics

The role of tidal hydraulic is that of forecasting the coastal water levels and currents, temporally and spatially throughout the estuarine bay and river systems for use in establishing performance objectives and developing and evaluating alternatives in various engineering designs. Tidal hydraulic refers to the technical analysis that is applied in order to develop the needed hydraulic information in an estuarine system. With the assistance of high speed computers, modern engineers practicing in the field of tidal hydraulic tend to use more extensively the mathematical models rather than the physical laboratory models. These mathematical models applied to the study of long-wave propagation in various coastal water bodies, are generally in a complete forms of the continuity equation and the equation of motion. Reliable solutions may be achieved by verification and parametric sensitivity analysis, which require the comparison of the theoretical system response and computed values with those actually observed. A brief description of these mathematical models applies to Manila Bay and Metro Manila, and references to them follows:

1. Two-dimensional model for estuarine bays -- The development of mathematical models for predicting storm surges and tidal propagation in coastal area has been advanced rapidly during the past decade (Reid and Bodine 1968; Jelesnianski, 1966, 1967 and 1970; Leendertse, 1967; Pearce and Pagenkopf, 1975; Damsgaard and Dinsmore, 1975). Most of models are found to be useful only for specific localities to where one must approximate its underlying assumptions. As

Manila Bay is a semi-enclosed basin, of which the irregular geometry is complicated by the presence of Corregidor Island, navigational channels, Bacoor Bay and harbors, the model must be able to provide a high degree of resolution on the non-linear effects of the advection terms. Moreover, extensive low-lying areas at the north of the bay may be subject to extensive flooding during high surge conditions and a time-dependent moving boundary mechanism must be specified. The water present at any time in the bay is also dependent upon the state in South China Sea, so a satisfactory estimate of water motions can only be achieved by modeling both of these two bodies of water at the same time. In view of these requirements, only a more generalized model (Yeh and Yeh 1976) is described here for the purpose of discussion.

The fundamental assumption in the theory of storm surge and tidal propagation is that vertical accelerations are negligible, leading to a hydrostatic pressure variation in the vertical direction. The vertically integrated forms of the conservation equations in a Cartesian coordinate system with x and y on the horizontal plan can be written as

$$\frac{\partial H}{\partial t} + \frac{\partial U}{\partial x} + \frac{\partial V}{\partial y} = qH \tag{1}$$

$$\frac{\partial U}{\partial t} + \frac{\partial}{\partial x}\left(\frac{U^2}{H}\right) + \frac{\partial}{\partial y}\left(\frac{UV}{H}\right) - 2qU - fV$$

$$= -\frac{g}{2}\frac{\partial H^2}{\partial x} + gH\left(\frac{\partial h}{\partial x} - \frac{1}{\rho g}\frac{\partial P_s}{\partial x}\right) + \frac{\tau_x^w - \tau_x^b}{\rho} \tag{2}$$

$$\frac{\partial V}{\partial t} + \frac{\partial}{\partial x}\left(\frac{UV}{H}\right) + \frac{\partial}{\partial y}\left(\frac{V^2}{H}\right) - 2qV + fU$$

$$= -\frac{g}{2}\frac{\partial H^2}{\partial y} + gH\left(\frac{\partial h}{\partial y} - \frac{1}{\rho g}\frac{\partial P_s}{\partial y}\right) + \frac{\tau_y^w - \tau_y^b}{\rho} \tag{3}$$

The symbols used in Equations (1), (2), and (3) are defined as follows:

H	=	total water depth
h	=	undisturbed water depth
U, V	=	flux density in x- and y-directions, respectively
g	=	gravitational acceleration
f	=	coriolis coefficient
τ_x^w , τ_y^w	=	wind stress components in x- and y-directions, respectively.

τ_x^b, τ_y^b	=	bottom stress components in x- and y-directions, respectively
P_s	=	atmospheric pressure
x,y	=	horizontal orthogonal coordinates
t	=	time
ρ	=	water density
q	=	stream flows

The terms included in the momentum equations are from the left to the right representing inertia term; nonlinear longitudinal and lateral advection momentum terms; the momentum attributed to the artificial discharges or river inflows and outflows; coriolis acceleration; nonlinear gravity terms; forces due to bottom slope and atmospheric pressure gradient; and wind and bottom stresses. It is interesting to note that the atmospheric depression column and the water depth column are equivalent. Therefore, the accurate reading of the undisturbed water depth is more important than the consideration of atmospheric pressure depression.

Variables in Equations (1), (2) and (3) are H, U, V, h, q, p_s, τ_y^w, τ_y^w, τ_x^b, and τ_x^b. Among these variables, p_s, τ_y^w, and τ_y^w are the forcing functions depending on the atmospheric pressure and wind field distributions of the storms, h and q are given functions of x and y. Thus, if bottom stress components, τ_x^b and τ_y^b, are related to H, U and V, Equations (1), (2) and (3) will constitute three simultaneous partial differential equations for three unknowns, H, U, and V.

In this particulat model, a modified alternate direction implicit (ADI) method, together with the difference scheme of filtering or smoothing technique (Vasilier and et al, 1965) has been utilized to improve the resolution of non-linear advection terms. The time-dependent moving boundaries for the low lying areas are accomplished by progressively advancing (retreating) the land-water interface as surge increase (decrease). Both continuity and momentum equations are actually utilized in tallying these moving inundation boundary grids. This model is also useful in predicting the interaction of tidal current and river inflows in Manila Bay under normal weather conditions since the river inflows are included in the momentum equations as well as the continuity equation.

2. One-dimensional model for esturine rivers -- Many one-dimensiona unsteady-flow models to predict the propagation of long waves (Liggett and Woolhiser, 1967; Amein, 1974; Price, 1974; U.S. Army Corps of Engineers, 1976) has successively applied to the time-dependent problems in tidal channels, flood routings, operation of river control works, and even dam failures. The development of the model is again based on the assumption that the pressure variation with the vertical coordinate

is hydrostatic. As long as the variation of momentum transport with vertical coordinate dominates those with the longitudinal coordinate, almost all the unsteady-flow analyses in a river are based on the simultaneous solution of the following equations of continuity and momentum.

$$\frac{\partial A}{\partial t} + \frac{\partial Q}{\partial x} = q \qquad (4)$$

$$\frac{\partial Q}{\partial t} + \frac{\partial}{\partial x}(VQ) + qA\left(\frac{\partial h}{\partial x} + S\right) = 0 \qquad (5)$$

where

A = cross-sectional area of flow
Q = discharge across a section
V = average velocity of flow (Q/A)
h = water surface elevation above reference datum
t = time
x = distance along channel
q = lateral inflow per unit distance and time
g = gravitational acceleration
S = friction slope.

The friction slope is emprically determined from

$$S = \frac{n^2 V|V|}{a^2 R^{4/3}} = \frac{Q|Q|}{K^2} \qquad (6)$$

where

R = hydraulic radius
n = Manning's coefficient
a = constant (1.49 and 1.0 for English and Metric units, respectively)
K = conveyance ($aAR^{2/3}/n$)

Exact solutions to the preceeding equations are not known except for the simplest of cases. Numerical methods of integration with characteristic, explicit, or implicit schemes are generally used to facilitate the solutions. The irregular geometry of the natural rivers may also be programmed to calculate the flow area, hydraulic radius, top width and conveyance for a given cross-sectional data. In the case of Metro Manila, many rivers and esteroes are interconnected, the flows and stage at each confluence point interfere one and another in both upstream and downstream directions. An appropriate junction

analysis must be incorporated in the adopted numerical scheme. For a simple three-branch confluence, the continuity equation requires

$$Q_1^{n+1} + Q_2^{n+1} = Q_3^{n+1} \tag{7}$$

and stage relationship also requires

$$h_1^{n+1} = h_2^{n+1} = h_3^{n+1} \tag{8}$$

which may be linearized in terms of dependent variable A, such as

$$h_1^n + \frac{1}{B_1^n}\left(A_1^{n+1} - A_1^n\right) = h_2^n + \frac{1}{B_2^n}\left(A_2^{n+1} - A_2^n\right)$$

$$= h_3^n + \frac{1}{B_3^n}\left(A_3^{n+1} - A_3^n\right) \tag{9}$$

As the flow of rivers in Metro Manila is a function of the differentials between the water elevations in the rivers and the tide elevation in Manila Bay. This model becomes essential in determining the operation rules of maximum efficiency in the case of any structural measures being built to regulate the stormwater in preventing downstream flooding.

IV. Management of Storm Surge and Floods

There are basically two approaches possible in stormwater management; controlling water or controlling people. The first category fits within the usual notion of structural measures in which the basic objective is to prevent the water from contacting damageable property by physically controlling the stormwater. The second category is referred to as non-structural measures which control people and reduce the incidence of flood damage by implementing land use controls and defining flood plains.

1. Structural measures -- In highly developed urban settings with an existing problem, structural measures are virtually the only feasibly means of accomplishing a reasonable degree of performance. For a small local system, the need for open space within the urban settings such as reclamation of foreshore areas in Manila Bay, reclamation of flood detention basins in coastal lagoons and fishponds, and filling of the inefficient esteroes, requires conversion of natural drainage systems to more efficient man-made systems. Even the most expensive mode of underground conveyance may become viable because of the joint use of space and the requirements of environmental quality. For a large regional system, surface detention storage and open channel conveyance works have proven especially valuable during major storm events. Most

of these alternatives are viable only for upstream areas that are not yet developed. The scheme is simply to store the peak stormwater during high tide and to release the excessive stormwater during low tide through a controlled structure. This system may be designed to affect local flooding to the extent that the water level at the outfall point of the river would be minimized and more local stormwater could be conducted away by gravity at the lower river stage.

2. Nonstructural Measures -- The techniques most frequently used are zoning ordinances, building codes, and flood insurance which encourage compatible land use. Flood forecasting is an alternative that, particularly in Metro Manila, is considered a useful service that should always be provided. Consider for instance a flood-plain occupied by uses reasonably compatible with the risk, such as warehouse storage, parking facilities, or regional parks. With proper design, these facilities would sustain very little damage provided adequate forecasts of storm surge and runoff events would permit evacuations of items that would be subject to damage from the stormwater. Flood forecasting as a management technique, however, is not inexpensive and is not necessarily technologically easily accomplished. In Metro Manila, a storm surge and flood forecasting system could well be a useful component of an urban major drainage system which requires a timingly operation of the flood control structure involving large storage basins. An adequate forecast lead times may be achieved provided that (a) verified mathematical models are established for predicting hydrographs for storm surge and runoff at the point of interest; (b) remote data acquisition from Joint Typhoon Warning Center in Guam is available, and (c) a high speed computer with large storage capacity is accessible.

REFERENCES:

Amein, M., "Stream Flow Routing on Computer by Characteristics", Water Resources Research, Vol. 2, No. 1, 123-130, 1966.

Chen, M., A. Ashley, D. Divorky, and L. S. Hwang, "Draft Report - Coastal Flooding Handbook, Part 1 - Methodology", prepared for U.S. Department of Housing and Urban Development, Washington D.C., May 1977.

Damsguard, A. and A. F. Dinsmore, Numerical Simulation of Storm Surges in Bays, Symposium of Modeling Techniques, Vol. II, 1535-1551, Second Annual Symposium of the Waterways, Harbors, and Coastal Engineering, San Francisco, California, September 3-5, 1975.

Leendertse, J. J., Aspects of a Computational Model for Long Period Water Wave Propagation, RM 5294-PR, The Rand Corporation, 1967.

Ligget, J.A., and D. A. Woolhiser, "Difference Solution of Sallow-Water Equation, "J. of Engineering Mechanics Div., ASCE, Vol. 93, No. EM2, 39-71, April 1967.

Jelesnianski, C.P., "Numerical Computations of Storm Surges Without Bottom Stress," Monthly Weather Review, Vol. 94, No. 6, 1966, pp. 379-394.,

Jelesnianski, C.P., "Numerical Computations of Storm Surges With Bottom Stress," Monthly Weather Review, Vol. 95, No. 11, 1967, pp. 740-756.

Jelesnianski, C.P., "Bottom Stress Time-History in Linearized Equations of Motion of Storm Surges," Monthly Weather Review, Vol. 98, No. 6, 1970, pp. 462-478.

Pearce, B. R. and J.R. Pagenkopf, "Numerical Calculation of Storm Surges", An evaluation of Techniques, Paper Presented at Seventh Annual Offshore Technology Conference, Houston, Texas, May 5-8, 1975.

Price, R. K., "Comparison of Four Numerical Methods for Flood Routing," J. of Hydraulic Div., ASCE, Vol. 100, No. HY 7, 879-899, July, 1974.

Reid, R. O. and B. R. Bodine, "Numerical Model for Storm Surges in Galveston Bay," J. Waterways and Harbor Division, ASCE, Vol. 94, No. WW1, 33-57, 1968.

U.S. Army Corps of Engineers, "Gradually Varied Unsteady Flow Profiles," Computer program 723-G2-L2450, The Hydrologic Engineering Center, Davis, California, 1976.

Vasilier, O. F., M. T. Gladysher, and V. G. Sudobicher, "Numerical Methods for the Calculation of Shock Wave propagation in Open Channels", Proc. of the Inter. Assoc. for Hydraulic Research, 11th International Congress, Leningrad, No. 3, 44, 1965.

Yeh, G. T. and F.F. Yeh, "A Generalized Model for Storm Surge", proceedings of the 15th International Conference on Coastal Engineering, Chapter 54, 921-933, Honolulu, Hawaii, July 1976.

STORM SURGE POTENTIALS OF SELECTED PHILIPPINE COASTAL BASINS

Catalino P. Arafiles[1] and Catalino P. Alcances, Jr.[2]

ABSTRACT

A historical review of storm surges in the Philippines for the period 1897-1975 reveals certain areas inundated by storm surges. To identify storm surge potentials of Philippine basins, peak storm surges were estimated with the use of a simple empirical relation requiring only the knowledge of three meteorological parameters and the basin shoaling factor. The shoaling factor for each basin was computed by the use of a set of regression equations. Comparisons of actual observed storm tide and computed storm surge shows that the effect of coastal configuration and astronomical tide significantly affect the magnitude of the total storm tide.

I. INTRODUCTION

The storm surge phenomenon has almost always been observed in coastal areas frequently traversed by tropical cyclones. Thousands of people had been reported to have perished due to this calamity producing natural phenomenon. In the Bay of Bengal area, the so called "Backergunge" cyclone of November 1876 moved inland through the Grangetic estuary between Calcutta and Chittagung generating a storm surge reaching as high as 40 ft. which resulted in the drowning of about 100,000 people and subsequently the loss of another 100,000 lives due to the outbreak of diseases. In almost the same area in 1970, the storm surge generated by a tropical cyclone resulted in the loss of 200,000 lives. In Japan, the storm surge generated by the Ise Bay Typhoon in September 1959 killed almost 5000 people. In the north American continent, the September 1900 storm surge in Galveston, Texas killed about 6000 people, while the Lake Okeechobee storm surge of 1928 claimed the lives of close to 2000 people.

The Philippines, with many landfalling tropical cyclones, maybe considered a naturally surge-prone area. Historical records show that certain areas in the Philippines such as northwestern and portions of southeastern Luzon, eastern Visayas and northeastern Mindanao had experienced the disastrous effects of storm surges. The earliest record of storm surge occurence in the Philippines was the report of Father Algue about the typhoon of Samar and Leyte in October 1897 which resulted in the death of 1300 persons directly attributed to storm surge. In 1908 a typhoon passed through Aparri, Cagayan and completely destroyed a barrio called "Tarol" situated along the coastal area. Thirty foot high storm surges

[1]Director, National Institute of Atmospheric, Geophysical and Astronomica Sciences (NIAGAS), PAGASA

[2]Deputy Weather Services Chief, NIAGAS, PAGASA

were observed in southern Leyte during a typhoon passage in October 1912 and in Barrio Sulvec, Narvacan, Ilocos Sur during the passage of typhoon "Didang" in 1968. Recently, in January 1975, Typhoon "Auring" passed through eastern Mindanao, generating a storm surge which destroyed 108 houses along the coast of Tandag, Surigao del Sur.

With such studies as identifying coastal areas susceptible to storm surge inundation, maps of storm surge potential maybe prepared not only to assist people involved in community preparedness activities but most especially to guide planners and policymakers in determining priorities and alternatives in planning the development of coastal areas and the protection of surge prone areas.

II. SOME NOTABLE PHILIPPINE STORM SURGES

A historical survey of storm surges in the Philippines shows many instances when storm surges have inundated certain portions of the country. The following cases that are cited here are just some of the more notable storm surges which caused considerable damage to life and property.

A. Typhoon of Samar and Leyte, October 12, 1897 - - Father Depperman refers to the storm surge generated by this typhoon as a classical example of a large typhoon wave. The typhoon was described in detail by Fr. Algue in his article "El Baguio de Samar y Leyte" published in 1898. There were 1300 deaths attributed to the total observed storm tide. The observed surge was 7.3 meters (24 ft.)above mean sea level at Hernani and Tanglad, Samar and the water level remained at this height for about two hours. This unusual height of the observed surge was to some extent magnified by the coastal configuration. In comparison, Pambuyan, which is better protected had a rise of only 1.5 meters (4.9 ft.) while Guiuan, only 0.7 meters (2.3 ft.). Again to illustrate the effects of coastal topography, Basey had an observed surge of 4.9 meters (16 ft.) while Tacloban only 0.4 meters (1.3 ft.). It will be noted that there were many instances when coastal configuration played a vital role in further magnifying the total storm tide.

B. Typhoon of October 13, 1908 - - The storm surge accompanying this typhoon was described by Father Algue "as extraordinary and exceptional". Manuel Delgado, Weather Bureau Observer at Aparri wrote the following: "It was about 4 A.M. of the 13th, when we observed that the water was rising and beginning to flood the lowland of the town, but no one gave this fact any importance as it is usual, when a typhoon passes, that the water of the river rises about a meter. But at about 6 A.M. almost suddenly the waves of the sea like mountains of water precipitated themselves upon the barrio of Tarol destroying houses and whatever they met in their way. The level of the sea rose so rapidly that only some of the inhabitants had time to escape and save their lives. The whole district of nipa houses from the banks of the river to the barrio of Minanga where I live, a d[illegible]-tance of one kilometer from the sea, was almost wiped out by the hurricane wa At 7 A.M. when I went to the window I thought I was aboard a ship in the midd the sea, nearly all the houses in the neighborhood had disappeared. Up to th present time 22 corpses of men, women, and children have been found and about persons are missing from the barrio of Tarol alone . . . . The old people in town say that they have passed through more severe typhoons but they had neve seen any hurricane wave at all". The surge was estimated to be from two to f

meters (6.6 to 13.1 ft.) in height, while barometric minimum was placed at 720.00 mm. (959.92 mb.).

C. The Typhoon of Leyte and Cebu, October 12-15, 1912 - - During the passage of this typhoon, there had been a question as to whether a cyclonic wave was really present. A certain M. B. Cogan of the house of "Viuda y hijos de F. Escano" wrote "There was no cyclonic wave, the wave which destroyed Sogad Norte and Consolacion being a storm wave increased greatly in size by being forced into a pocket. Sogod Sur was washed by a combination of the 'avenida' and the heavy waves sweeping along the beach. We estimated the greatest height of the waves at Malitbog at 15 ft. (4.6 meters) while Sogod Norte and Consdlacion report the waves there at 30 feet (9.1 meters)". What is referred to as a storm wave is a wave produced by the wind. The cyclonic wave, a huge mountain or mass of water, which accompanies the vortex in its movement, is produced by the same difference of pressure between the interior and exterior parts of a typhoon. The height of the water remains permanent as long as the cause remains. The direction of the wave in invading the coast depends on the position of the vortex with respect to the coast and independent of the wind direction.

D. Typhoon Sening of October 11-15, 1970 - = This typhoon passed through the Bicol provinces and has registered a mean sea level pressure of 870 mb at Virac, Catanduanes on 13 October - the lowest sea level pressure recorded so far in the Philippines. In Sorsogon, the water was reported to have risen to four feet (1.2 meters) along the coastal areas. Over the western sections of Luzon waves as high as twelve feet (3.6 meters) were reported.

E. Typhoon "Auring" of January 25-31, 1975 - - This is the first time that first hand information, including photographs of damages, became available to the present investigators on the occurenceof a storm surge. The height of the total storm tide based on water marks left on a house in the area is about 2.4 meters (7.8 ft.). Damage to property in Surigao del Sur was reported to have reached ₱0.98M, including 108 houses "washed out", 15 units of school building and a public market either partially or totally destroyed; and more than six hundred persons rendered homeless.

Our study of historical records, shows that storm surges are not rare occurrences in the Philippines. Figure 1 shows places in the Philippines where storm surge inundation was reported for the period 1897 to 1975.

Considering that we are presently developing our coastal areas at a faster pace, it is imperative therefore that storm surge studies be initiated in our country, and the results even if only preliminary, be communicated to planners and decision makers, for their consideration as additional input in evolving development plans for coastal areas.

III. ESTIMATING PEAK STORM SURGES

Developing countries desiring to initiate studies on storm surges f difficulty in developing numerical models for storm surge studies primari to lack of technical know-how and expert guidance from more experienced r on the subject. However, there are available dynamical models like that by Jelesnianski (1972), which with the use of locally derived input paran and handy nomograms generated by the dynamical model could prove very use

mating peak surges along straight coasts.

A simple empirical relation may then be used for estimating peak storm surges, i.e. :

$$SS = S_P \cdot F_B \cdot F_M \qquad (1)$$

where: SS = peak surge (feet)

S_P = preliminary surge magnitude from the nomograms for arguments ΔP and R

F_M = correction factor for vector storm motion, to be obtained from the nomogram for arguments direction of motion and speed of storm.

F_B = correction factors for bathymetry of the basin, to be determined for each basin.

The simple relation makes use of two nomograms derived using the numerical hurricane surge model and a correction factor for local basin bathymetry. Hence, only the knowledge of three input parameters is required to estimate peak storm surge magnitude. These input parameters are : a) the pressure difference between the lowest sea level pressure of the storm and the ambient pressure, b) the vector motion of the storm, and c) the shoaling factor, which is based on the bathymetry of the basin.

Inasmuch as there is a nomogram which can be used to estimate the preliminary peak surge based on pressure drop of the storm and another nomogram to correct the preliminary number for vector motion, only the correction factor for bathymetry has to be determined for each basin. This is one of the objectives of this study.

At present, due to various limitations, it is not possible to use a dynamical surge model in the country. However, a possible approach is to generate regression equations using the dynamical model for estimating shoaling factors. Then use equation (1) to estimate peak surge at each coastal basin.

Following this approach regression equations were developed to obtain shoaling factors for tropical cyclones of radius of maximum winds of 15 and 30 statute miles. Predictors for the regression equations are the bathymetry for 12 grid points spaced three and one-half nautical miles seaward perpendicular to the coast line, up to a miximum grid point depth value of 300 ft. The latitude of th is the 13th predictor used. Shoaling factors for basins along straight coa the country may then be estimated using the regression equations. Comparis ween the shoaling factors obtained using the dynamical model and the regres equations shows multiple correlation coefficient of 0.9989 and 0.9985 for R and R=30 miles respectively.

The regression equations for estimating the basin shoaling factor, ar given below for the following cases:

A. Case 1. Radius of Maximum Winds of Storm is 15 statute miles:

$$Y = 1.53162 - 0.00154X_1 + 0.000130X_2 - 0.001050X_3 - 0.000940X_4 + 0.002390X_5 - 0.000700X_6 - 0.002910X_7 - 0.004320X_8 - 0.011270X_9 + 0.015550X_{10} - 0.002130X_{11} - 0.007460X_{12} - 0.002390X_{13} \quad (2)$$

B. Case 2. Radius of Maximum Winds of Storm is 30 statute miles

$$Y = 1.125480 - 0.0014040X_1 + 0.000110X_2 - 0.000950X_3 - 0.0005804X_4 + 0.001810X_5 + 0.001010X_6 - 0.002460X_7 + 0.005660X_8 - 0.009730X_9 + 0.010390X_{10} - 0.003860X_{11} - 0.001920X_{12} - 0.002430X_{13} \quad (3)$$

where : Y is the shoaling factor

$X_1, X_2 \ldots\ldots X_{12}$ are basin point depths in feet along a line perpendicular to the coast seawards and distance interval of 3 1/2 nautical miles for basin depths not exceeding 300 ft.

X_{13} is the latitude of the basin

IV. SURGE PRONE COASTAL BASINS IN THE PHILIPPINES

An examination of the bathymetry of Philippine coastal basins including the distance from the coast of the 50 fathom isobath enabled us to determine some 35 coastal basins which maybe potential storm surge areas. Of the 35 basins, eleven are on the west coast, twenty on the east coast, one on the northern tip of Luzon and three in Palawan. With the use of the regression equations formulated for Philippine basins, shoaling factors for basins for given storms with radius of maximum winds of 15 statute miles and 30 statute miles respectively were determined. The basin shoaling factor was then used as a correction factor to the preliminary surge value derived from the nomogram having arguments ΔP and R assuming a landfalling standard storm which follows standard vector motion.

Table I shows the basin data for the 35 basins identified as surge prone basins and the shoaling factors for each basin for two cases, R=15 st. mi and R= 30 st. mi. These basins are identified in Figure 2, the basin locator chart. Figure 3 shows the surge potentials for Philippine basins using regression equation for a standard storm. The storm was assumed to have crossed the basi right angle with a speed of 15 miles per hour. The pressure drop of the s assumed to be 56 milibars.

In order to be of practical use in the Philippines a 20 year climatc storm data (1951-1970) was used. A map (Figure 4) was prepared showing is of ΔP based on lowest recorded pressure at synoptic stations. Potential I surge was then computed for each basin, using modal storm track, climatol ΔP and basin shoaling factor as input parameters. The result of this cor

is shown in Figure 5.

A comparison of some basins with high values of peak storm surge magnitude for both cases when a theoretical storm with pressure drop of 56 millibars follows standard vector motion and when climatological data is used, is given below.

	BASIN	PEAK SURGE (FEET) FOR R=30	
		AA	BB
1.	EC3 (Tagdon)	4.8	3.5
2.	K (Longos Point)	6.2	4.6
3.	L. (Canton Island)	5.9	4.9
4.	M (Port Tambang)	5.5	6.7
5.	EC5 (Abuyog)	5.0	2.6
6.	N (Tagon Bay)	7.7	13.3
7.	WC 3 (La Paz)	6.3	1.7
8.	W5 (Farola Point)	8.5	4.7
9.	NL (Buguey)	5.5	3.6
10.	W4 (Guecet Point)	5.4	1.2

Where : AA refers to a standard storm following standard vector motion.

BB refers to a climatological storm with modal vector motion.

It may be noted that basins M and N registered an increased magnitude of peak surge for BB. This maybe explained by looking at the climatological ΔP which shows the values of at least eighty millibars. The other basins exhibit a decrease from case AA to case BB, owing to a climatological ΔP value of less than 56 millibars. For basins in the western side of Luzon the general decrease in peak surge values is due to a smaller vector correction factor since case BB now refers to exiting storms rather than landfalling storms as assumed in case AA. It is also noted that the value of climatological ΔP for the western basins is very much less than 56 millibars, further influencing the decrease in peak surge value.

We have identified surge-prone coastal basins in the country. The value given in case AA assumes a theoretical storm landfalling normal to a coastal basin, while case BB assumes a climatological storm characterized by the lowest recorded pressure drop of the basin and following the model storm motion.

As a first approximation, our estimate based on climatological data show that the Camarines provinces are highly susceptible to storm surge inundations with potential storm surge magnitude of from three and one-half feet to as high as thirteen feet. The eastern coast of central and southern Luzon has poten surge of about three and one-half feet. Northwestern Luzon embracing the I provinces and La Union have a surge potential of about two and one-half feet Eastern Samar and Eastern Leyte have surge potential of from two and one-hal to three and one-half feet.

Care must however be taken in using the figures in this report at its value. It should be noted that the storm generated surge is sensitive to th

magnifying effects of astronomical tide and shoreline configuration. The total storm tide is therefore an aggregate of the different contributions of the storm surge, the astronomical tide and the local basin shoreline effects.

The storm surge in Tandag, Surigao del Sur associated with "Typhoon Auring" of January 1975 illustrates the important effect of astronomical tide and perhaps shoreline configuration to the total storm tide.

With the use of an empirical relation (equation 1), the peak surge was estimated with meteorological data and basin shoaling factor as input parameters. The computed surge gave only a value of 3.64 feet but the actual observed storm tide based on the finding of the survey team dispatched to the area was 7.8 feet.

A closer look at the astronomical tide at Tandag shows that at the time of the occurrence of the storm surge, the astronomical tide was rising. In fact assuming linear interaction between the storm surge and the astronomical tide, the estimated surge height of 3.64 feet when added to the predicted astronomical tide of 3.65 feet for the same time, gave a surge height of 7.29 feet (2.22 meter) which is definitely nearer to the observed storm tide height of 7.8 feet.

An attempt was made to compare observed storm tide with computed storm surge using the regression equations to estimate shoaling factors and the other meteorological data of individual storms as input parameters. There were only nine cases out of the possible 52 where meteorological data needed are complete.

Table 2 shows that only several of the cases considered closely approximate the observed surge. Unfortunately astronomical tide tables for the early 1900's are not available for making at least a rough estimate of the total storm tide.

As in the case of "Typhoon Auring" of 1975, wherein the astronomical tide contributed actually to doubling the initial value given by the computation, it is entirely possible that the effect of the astronomical tide when taken together with the computed storm surge would perhaps show the significant contribution of astronomical tide to the total storm tide.

Of course, the magnifying effect of coastal configuration should also be properly taken into consideration.

V. COMMENTS AND CONCLUSIONS

Sufficient data have been gathered to show that storm surges are not rare occurrences in the Philippines and should therefore be properly considered in planning the development of coastal areas.

With certain limitations, shoaling factors maybe estimated using a regression equations with basin bathymetric data and latitude as input pa The peak surge may then be estimated knowing the shoaling factor, pressur of the storm and incorporating appropriate corrections for the storm's ve motion.

However the model applies only to theoretical standard basins along straight coasts; some important factors such as shoreline configuration and astronomical tide which have been noted to significantly affect the observed storm surge should be considered in estimating the magnitude of the actual peak surge.

A study of the observed and computed values of storm surge showed that the two envir nmental factors that may significantly affect the observed storm surge are coastal configuration and astronomical tide. If an operational storm surge prediction technique is to be developed such important parameters should be given due consideration.

This present work is but the beginning of a more intensive research on storm surges here in the Philippines. The results are preliminary in nature which will have to be improved as more knowledge is gained on the characteristics of storm surges.

However, at this present time, even if we can only focus the attention of planners and decision makers to the potential danger posed by storm surges, and a positive step is taken to consider storm surge hazards in the long-range planning of the development of coastal areas, then we shall consider this research to have attained one of its objectives.

ACKNOWLEDGEMENT

This study is part of the NSDB-PAGASA Project No. 7206En-Typhoon Research Project (TRP). The help of the TRP Central Technical Staff in gathering and processing the data used in this study is gratefully acknowledged.

Regression equations for the computation of shoaling factors were developed by the Project Leader- Mr. C. P. Arafiles, in the Techniques Development Laboratory, NOAA, U.S.A, while he was a WMO fellow. The assistance of the Marine Techniques, TDL especially that of Dr. C.P. Jelesnianski is gratefully acknowledged.

REFERENCES

1. Depperman, C. E. -- "Some Characteristics of Philippine Typhoons" Manila, 1939

2. Jelesnianski, Chester P. -- "Numerical Computation of Storm Surges Without Bottom Stree", Monthly Weather Review, Vol. 94, No. 6 pp. 379-394, 1966

3. Jelesnianski, Chester P. -- "Numerical Computation of Storm Surge Bottom Stress", Monthly Weather Review, Vol. 95, No. 11, No pp. 740-756

4. Jelesnianski, Chester P. --"SPLASH" (Special Program to List Ampl of Surges from Hurricane), NOAA Technical Memorandum NWS, T

5. Kajura, K. -- "A Theoretical and Empirical Study of Storm induces Level Anomalies", Texas A & M University, Dept. of Oceanogr and Meteorology A & M Project 202, December, 1959.

6. Platzman, G. W. -- "Dynamical Prediction of Wind Tides on Lake Eric" Meteorological Mimeographs, Vol. 4, No. 26, Sept. 1963.

7. Suman, F. -- "Numerical Experiment with the Primitive Equation", The Proceedings of the International Symposium on Numerical Weather Predictions, Tokyo, Nov. 7-13, 1960.

8. Ueno, T. -- "Non-Linear Numerical Studies on Tide and Surges in the Central Part of Seto Inland Sea", Oceanographical Magazine, Vol. 16, Nos. 1-2, Dec. 1964, pp. 53-124.

9. Welander, P. -- "Numerical Prediction of Storm Surges", Advances in. Geophysics Vol. 8, Academic Press, New York, 1961.

10. Collected Papers -- Volume 3 and 4 (Typhoon Research Laboratory), Meteorological Research Institute, Tokyo, Japan, 1970, 1971.

11. Weather Bureau Monthly Bulletins, Manila, 1907-1931.

12. Manila Bulletin, Manila, 1960-1972

13. The Manila Times, Manila, 1969-1972.

14. The Manila Chronicle, Manila, 1970-1972.

15. The Philippine Daily Express, Manila, 1972-1975

TABLE 1 : BASIN DATA

Basin Designation	Coordinates of Intersection of Basin Center with Coast North	East	Local Identification of Points	Bearing of Basin Centerline from Intersection Point	Shoaling factor R=15	R=30
EXTREME NORTHERN LUZON						
NL	18°17.8	121°496	Buguey, Cagayan	N30E	.4047	.4372
EASTERN LUZON and EASTERN VISAYAS						
EC1	17° 27.3	122° 13.25		N64.5E	.2032	.2733
EC2	16° 30.5	122° 14.7	21/2 mi. of Dinapiquit pt.	S65W	.2574	.3140
A	16° 15	122° 08	Casiguran Bay	S42W	.3374	.3844
B	16° 49.6	121° 49.6	3 1/4 NM NE Nebutunan pt.	S30E	.2420	.3044
C	15° 53.3	121° 33	Baler Bay	S80E	.2679	.3244
D	15° 33.6	121° 31.8	3 1/2 NM N of Dicapanisan Pt.	S50E	.2506	.3120
E	15° 14.8	121° 21.2	2 NM NNW Umiray R.	N62E	.2481	.3104
F	14° 57.3	121° 34	1 1/2 NM WSW Prueba RK	N65E	.2508	.3113
G	14° 37.5	121° 36.5	3 1/2 NM NNW Binangonan Pt.	N80E	.2618	.3217
H	14° 18.8	121° 43.8	11/8 NM NNW Caluba Pt.	N71E	.2460	.3086
I	14° 10.8	122° 11	11/8 NM NE Lagichic Pt.	N37W	.3340	.3891
J	14° 20.8	122° 29	11/8 NM NW Capalonga RK	N09W	.2838	.3394
K	14° 17	122° 49	3/4 NM Longos Pt.	N29E	.4589	.4943
L	14° 05	123° 05.8	West Coast Canton Is.	N19E	.4088	.4708
M	13° 59	123° 25	W side Port Tambang	N19E	.3605	.4374
N	13°53	123° 44	Tagon Bay Caramoan Pt.	N19E	.6450	.6112
EC3	12°50.5	124° 09	Tagdon	E	.5202	.3840
O	12° 31	124° 39.5	Cawayan, Nrn. Samar	N	.3413	.3893
EC4	11° 56.7	125° 25.8	San Luis, Samar	S76E	.2342	.2987
EC5	10° 44.9	125° 08	Abuyog, Leyte	N68E	.3476	.3996

W E S T E R N L U Z O N						
W1	18° 20.6	120° 35.8	Payupuan, B. Pasuquin	N82W	.2574	.3141
W2	17° 59.8	120° 29.7	Gan. Currimao I.N.	N61W	.2689	.3225
W3	17° 46.5	120° 25.5	Salomague, Ilocos Sur	N83W	.2758	.3301
WC1	17°00	120° 26.9		N85W	.2608	.3159
W4	16° 04.4	120° 19.9	Lingayen, Guecet Pt.	N29W	.3772	.4246
WC2	15°19.5	119° 58	Iba Pt. Landing	S51W	.2345	.2952
WC3	15°09	120° 04.7	La Paz San Narciso	N84W	.4596	.4979
W5	14° 35.9	120° 57.5	Manila (Farola Pt.)	S53W	.6608	.6740
WC4	14° 42	120° 37.3	Nasugbu	W	.3015	.3591
WC5	13° 25	120° 27.5	Lipa	S49W	.2344	.2967
WC6	12° 54.5	120° 47	Mouth of Pandan R.	S82W	.2621	.3195
P A L A W A N						
PM	10° 17	119° 15.5	Malcampo, Palawan	S51E	.5545	.5466
PR	09° 59	118° 53.5	Barbacan R. Pal.	S10E	.4795	.4986
PI	10° 38.5	119° 19.5	Imuran Bay	N77W	.5022	.5155

TABLE 2: COMPARISON BETWEEN COMPUTED AND OBSERVED VALUES OF STORM SURGES

NAME OF CYCLONE-MONTH	LANDFALL	AP	PRELIMINARY SURGE R=30	PRELIMINARY SURGE VMC	SHOALING FACTOR R=30	FINAL SURGE R=30	OBSERVED SURGE (Ft)
1. TYPHOON OF SEPTEMBER 17-24 1908	11.5,125.5	78.0	18	0.76	.2843	3.9	6.6
2. TYPHOON OF OCTOBER 12-15 1908	17.8,122.2	51.2	11.4	0.75	.3964	3.4	6.6
3. TYPHOON OF LEYTE & CEBU OCTOBER 14-16 1912	10.2,125.6	32.1	7.0	0.83	.3456	2.0	15.1
4. TYPHOON OF SAMAR LEYTE & PANAY,NOV. 24-25 1912	11.3,125.7	86.5	20.0	0.90	.3562	6.4	6.6
5. TYPHOON OF SAMAR & LUZON, JUNE 15-24 1914	12.0,125.6	77.5	17.9	0.82	.4053	5.9	6.6
6. TYPHOON OF CAGAYAN & BATANES, SEPTEMBER 27-29 1912	18.2,122.3	34.2	7.4	0.78	.3928	2.3	10.0
7. TYPHOON OF BILIRAN & NORTHERN LEYTE, JAN. 10-16 1916	11.7,125.4	16.3	3.5	0.83	.2892	0.8	6.6
8. TYPHOON OF SENING OCTOBER 11-15 1970	13.5,124.3	139.8	33.3	0.94	.5079	15.9	4.0 in Sorsogon, 12.0 in Bataan & Ilocos Sur
9. TYPHOON AURING JANUARY 23-31 1975	(9.4,126.2)	37.0	8.0	0.84	.5416	3.6	7.8 (Tandag)

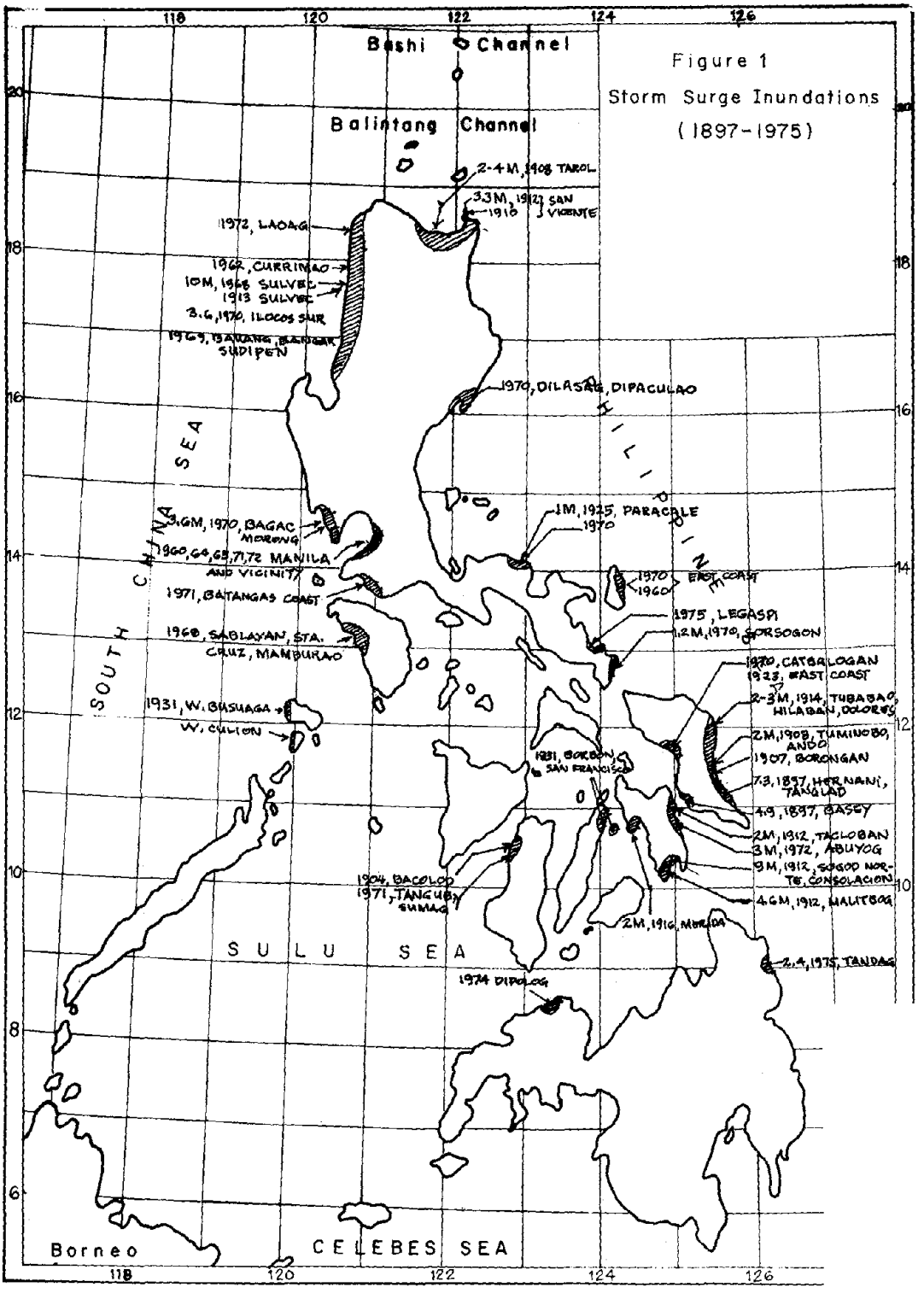
Figure 1
Storm Surge Inundations
(1897-1975)
Bashi Channel
Balintang Channel
SOUTH CHINA SEA
PHILIPPINE
SULU SEA
CELEBES SEA
Borneo
2-4 M, 1908 TAROL
3.3 M, 1927 SAN VICENTE
1918
1972, LAOAG
1968, CURRIMAO
10M, 1968 SULVEC
1913 SULVEC
3.6, 1970, ILOCOS SUR
1969, BAUANG, BANGAR SUDIPEN
1970, DILASAG, DIPACULAO
3.6M, 1970, BAGAC MORONG
1960, 64, 65, 71, 72 MANILA AND VICINITY
1971, BATANGAS COAST
1968, SABLAYAN, STA. CRUZ, MAMBURAO
1931, W. BASUAGA
W. CULION
1M, 1925, PARACALE
1970
1970 1960 EAST COAST
1975, LEGASPI
1.2M, 1970, SORSOGON
1970, CATBALOGAN
1923, EAST COAST
2-3M, 1914, TUBABAO, HILABAN, DOLORES
2M, 1908, TUMINOBO, ANDO
1907, BORONGAN
7.3, 1897, HERNANI, TANGLAD
4.9, 1897, CASEY
2M, 1912, TACLOBAN
3M, 1972, ABUYOG
3M, 1912, SOGOD NORTE, CONSOLACION
4.6M, 1912, MALITBOG
1931, BORBON SAN FRANCISCO
1904, BACOLOD
1971, TANGUB, SUMAG
2M, 1916, MORIDA
2.4, 1975, TANDAG
1974 DIPOLOG
118
120
122
124
126
20
18
16
14
12
10
8
6

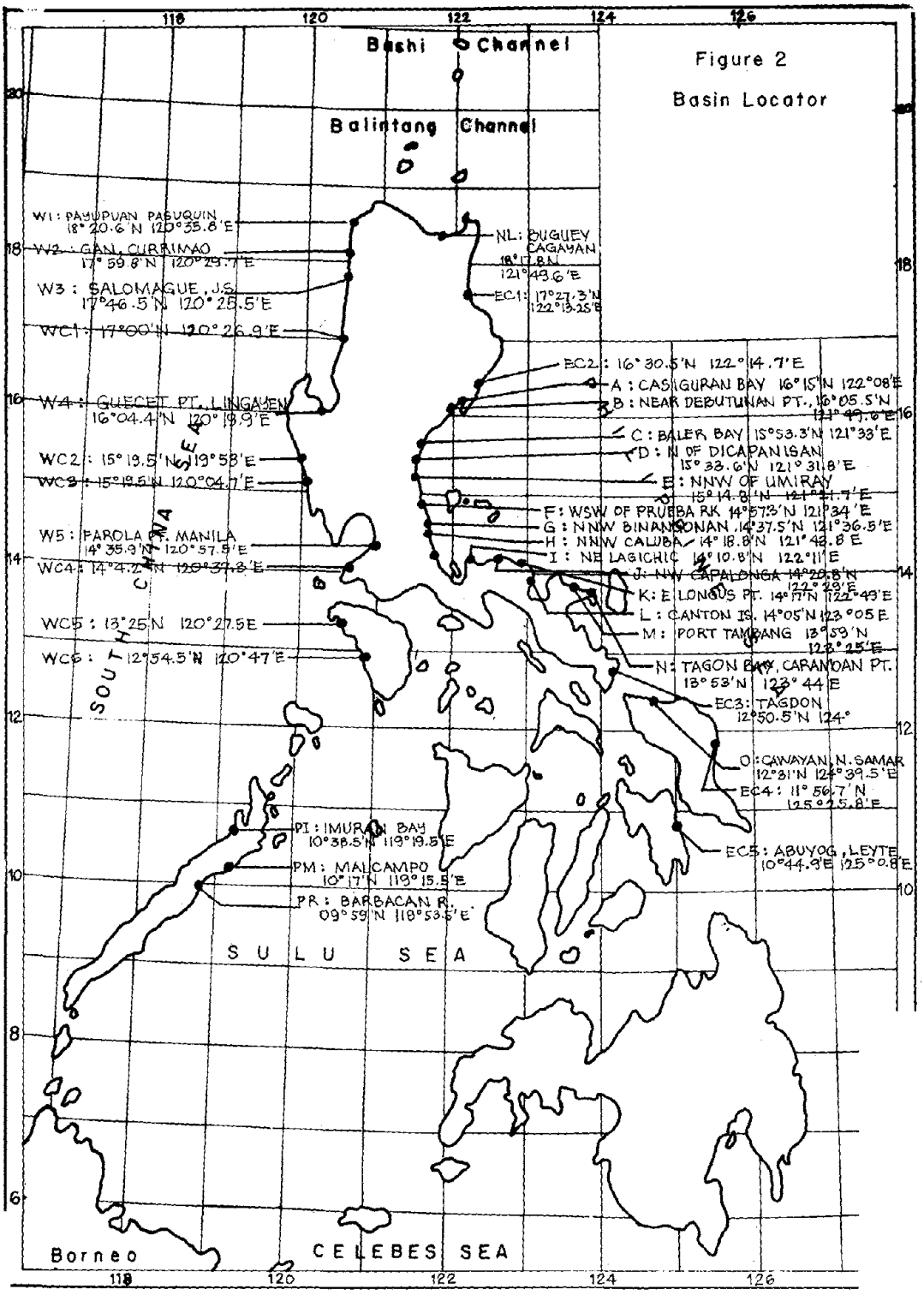
Figure 2
Basin Locator
Bashi Channel
Balintang Channel
W1: PAGUPUAN PABUQUIN 18°20.6'N 120°35.8'E
W2: GAN, CURRIMAO 17°59.8'N 120°29.7'E
W3: SALOMAGUE, J.S. 17°46.5'N 120°28.5'E
WC1: 17°00'N 120°26.9'E
W4: GUECET PT., LINGAYEN 16°04.4'N 120°19.9'E
WC2: 15°18.5'N 119°58'E
WC3: 15°12.5'N 120°04.7'E
W5: PAROLA PT. MANILA 14°35.9'N 120°57.5'E
WC4: 14°4.2'N 120°37.8'E
WC5: 13°25'N 120°27.5E
WC6: 12°54.5'N 120°47'E
NL: DUGUEY CAGAYAN 18°17.8'N 121°43.6'E
EC1: 17°27.3'N 122°13.25'E
EC2: 16°30.5'N 122°14.7'E
A: CASIGURAN BAY 16°15'N 122°08'E
B: NEAR DEBUTUNAN PT., 16°05.5'N 121°49.6'E
C: BALER BAY 15°53.3'N 121°33'E
D: N OF DICAPANIGAN 15°33.6'N 121°31.8'E
E: NNW OF UMIRAY 15°14.8'N 121°21.7'E
F: WSW OF PRUEBA RK 14°57.3'N 121°34'E
G: NNW BINANGONAN 14°37.5'N 121°36.5'E
H: NNW CALUBA 14°18.8'N 121°42.8'E
I: NE LAGICHIC 14°10.8'N 122°11'E
J: NW CAPALONGA 14°20.8'N 122°20'E
K: E LONGOS PT. 14°17'N 122°49'E
L: CANTON IS. 14°05'N 123°05'E
M: PORT TAMBANG 13°59'N 123°25'E
N: TAGON BAY, CARAMOAN PT. 13°53'N 123°44'E
EC3: TAGDON 12°50.5'N 124°
O: CAWAYAN, N. SAMAR 12°31'N 124°39.5'E
EC4: 11°56.7'N 125°25.8'E
EC5: ABUYOG, LEYTE 10°44.9'E 125°0.8'E
PI: IMURAN BAY 10°38.5'N 119°19.5'E
PM: MALCAMPO 10°17'N 119°15.5'E
PR: BARBACAN R. 09°59'N 118°53.5'E
SOUTH CHINA SEA
SULU SEA
Borneo
CELEBES SEA
118
120
122
124
126
20
18
16
14
12
10
8
6

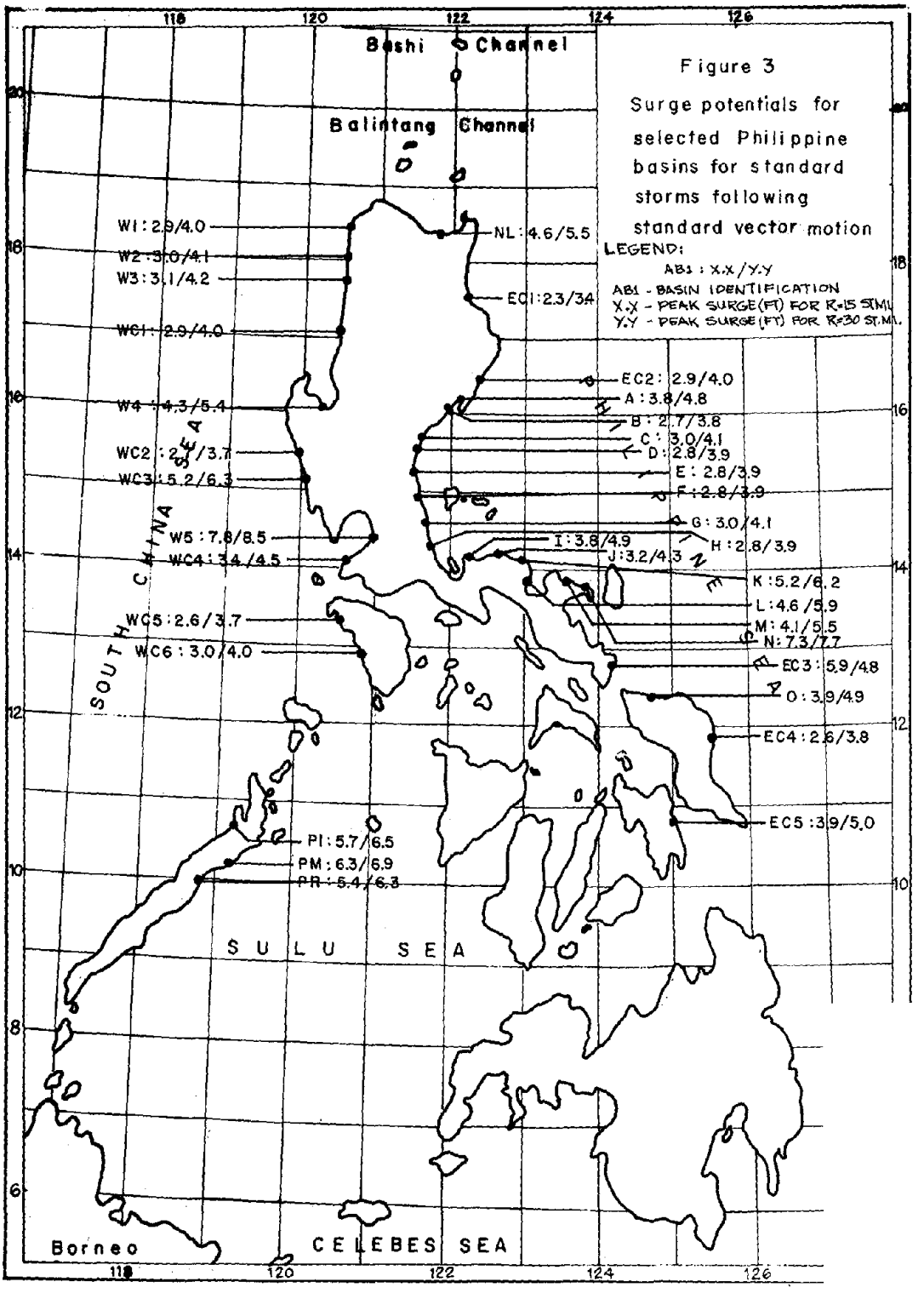

Figure 3

Surge potentials for selected Philippine basins for standard storms following standard vector motion

LEGEND:

AB1 : X.X / Y.Y

AB1 - BASIN IDENTIFICATION
X.X - PEAK SURGE (FT) FOR R=15 STM.
Y.Y - PEAK SURGE (FT) FOR R=30 ST.M.

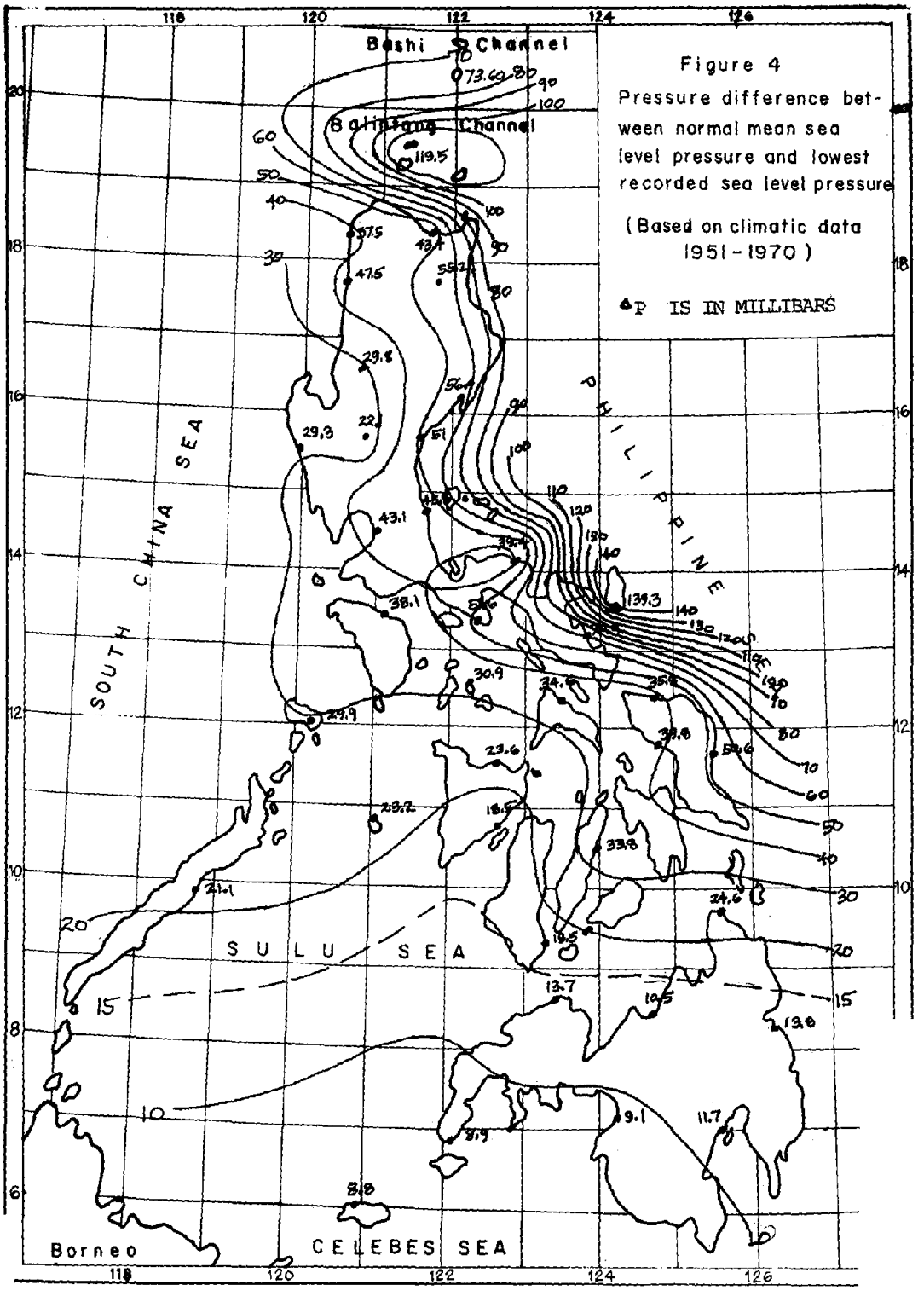

Figure 4

Pressure difference between normal mean sea level pressure and lowest recorded sea level pressure

(Based on climatic data 1951 - 1970)

ΔP IS IN MILLIBARS

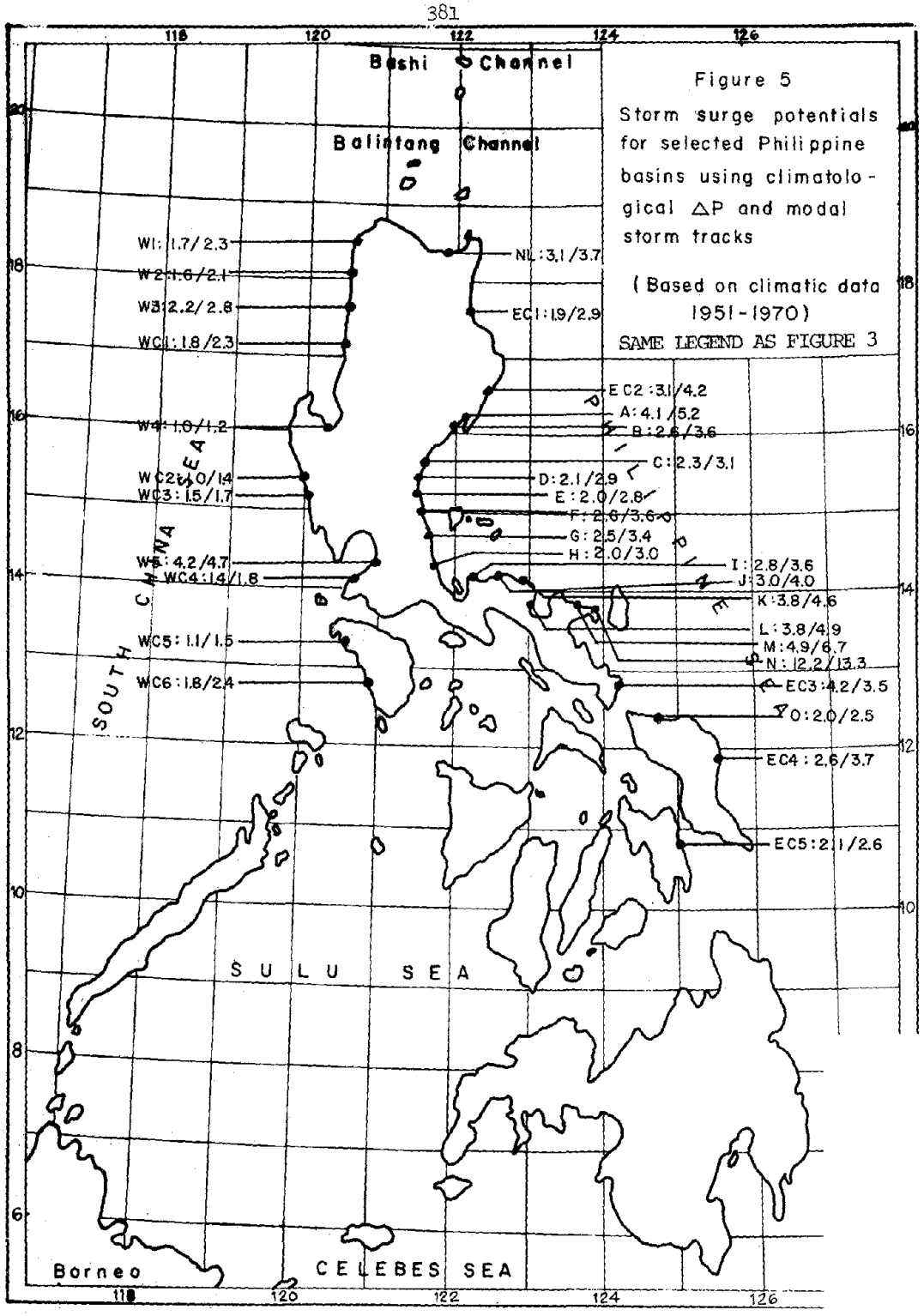

Figure 5

Storm surge potentials for selected Philippine basins using climatological ΔP and modal storm tracks

(Based on climatic data 1951-1970)

SAME LEGEND AS FIGURE 3

SOME OBSERVATIONS ON THE DAMAGES RESULTING FROM THE MINDANAO EARTHQUAKE OF AUGUST 17, 1976

by

Andres O. Hizon*

SYNOPSIS

Some major damages resulting from the Mindanao Earthquake of August 17, 1976 in Southern Philippines are pictured and described. The paper presents some engineering lessons learned from the damages and makes some recommendations for seismic code revisions under Philippine conditions.

I. THE EARTHQUAKE AND TSUNAMI

On August 17, 1976 at about 12:11 past midnight, an earthquake occurred in the Moro Gulf of Southern Mindanao, Philippines.

The World Data Center A (NOAA) at Boulder, Colorado, U.S.A. gave the following final determination of this earthquake as follows:

August 16, 1976 16:11:07.2 UTC in latitude 6.3° N, longitude 123.7° E, magnitude 8.0.

The earthquake produced ground accelerations of intensity VII in Cotabato City and intensity VI in Zamboanga City and Pagadian City on the Philippine Rossi-Forel Scale of IX. Tsunami waves of varying heights were reported at about 15 feet to 25 feet high at the shores around the Moro Gulf of Mindanao.

The earthquake magnitude is expressed in the Gutenberg-Richter formula as follows:

$\text{Log}_{10}\ E=11.8+1.5M$, where E is the energy released in ergs and M is the Richter magnitude.

Some idea of the energy released by an earthquake of magnitude 8.0 would be as follows:

At scale 6.3 the energy released would be roughly equal to the energy released by the Hiroshima Bomb. At magnitude 7.3, the energy released would be roughly equal to 30 Hiroshima Bombs. At about magnitude 8.3 the energy released would be roughly equivalent to 900 Hiroshima Bombs. At 8.0 the energy released would be roughly equivalent to 350 Hiroshima Bombs.

---

*Andres O. Hizon is the past President of the National Society for Seismol and Earthquake Engineering of the Philippines.

A relationship between earthquake magnitude M and tsunami magnitude m is given by Professor R. L. Wiegel as shown on the 2 figures below.

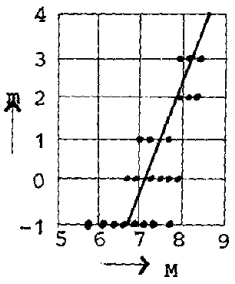

Relationship between earthquake magnitude M and tsunami magnitude m. (From Iida, 1963a.)

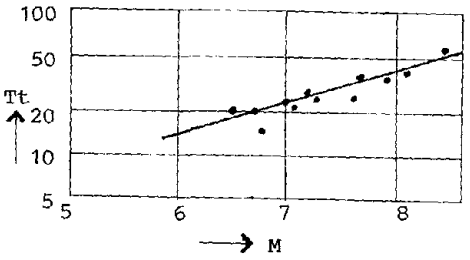

Relationship between the maximum period of a tsunami and earthquake magnitude. (From Iida, 1963b.)

The tsunamis designated by the magnitude m of 2 and 3 which are major ones, generated by submarine earthquakes of focal depth from 20 to 50 kilometers, have water running up on land to an elevation of 20 feet or more above the normal sea level at the time of the tsunami.

II. RELATED EARTHQUAKE ENGINEERING IN THE PHILIPPINES

Previous to 1959, Earthquake Engineering in the Philippines was left entirely to the competence and discretion of the practicing engineers and architects. On May 5, 1959, Ordinance No. 4131 of the City of Manila established regulations for the design and construction of buildings up to forty-five (45) meters in height with requirements for resistance to seismic lateral forces. These regulations had no binding effect outside Manila City limits and in fact were not even well known throughout the Philippines, although these regulations had some persuasive effect on the building officials of the suburbian cities adjacent to Manila.

In 1966, the Association of Structural Engineers of the Philippines (ASEP) adopted and recommended a set of Earthquake Regulations, patterned after the contemporary seismic regulations recommended by the Structural Engineers Association of California (SEAOC) but with local modifications applicable to Philippine conditions.

Sometime before September 21, 1972 the ASEP Earthquake Engineering Regulations, with some modifications adopted from the new SEAOC Code, were incorporated into the Philippine National Building Code which passed into law about this date.

A new Building Code has recently been reported as promulgated but official copies have not yet been widely circulated to the general public

III. TOPOGRAPHY OF THE MINDANAO AREA AFFECTED

The Mindanao region affected by the earthquake of August 17, 1976 comprises approximately an arc of a circle concave towards the South with

the seacoast generally planted to coconut trees and inhabited by people living mostly on fishing and coconut growing. Some of the coastline areas are swampy deltas of rivers or creeks. The Cotabato City area which is located inland on the Mindanao River is generally flat, in contrast to the City of Pagadian which is located on a gradually sloping ground. Zamboanga City is also somewhat high. Bongo Island Near the mouth of the Mindanao River is fairly high unlike Saco Island on the east coast of Zamboanga City which is fairly flat.

The geology of the area indicates that Zamboanga City and Pagadian City are located on fairly stable ground while Cotabato City on Mindanao River is somewhat on soft alluvial soil.

IV. SOME OF THE MAJOR DAMAGES OBSERVED

The earthquake caused considerable damages to buildings and structures in Cotabato City and in many cities and municipalities around the Moro Gulf. Many nipa houses and wooden structures around the coastline affected were completely damaged or swept out to sea. Piers, wharves and sea walls along the coastline for hundreds of kilometers were damaged or destroyed. It is estimated that about 1,000 persons were killed by the earthquake and more than 7,000 persons lost their lives as a result of drowning or being swept out to sea by the tsunami.

In Cotabato City alone about 8 buildings collapsed with about 12 more buildings severely damaged. Many buildings suffered partial or minor damage. One span of the Quirino Bridge just outside Cotabato City fell down into the river. Some of the major damages are described briefly below. All the buildings which totally or partially collapsed were designed and constructed before the effectivity of the earthquake regulations adopted in the National Building Code. In all probability, therefore, these buildings were not subjected to design seismic analysis. It is to the credit of the civil engineering and architectural professions that buildings and structures in Cotabato City performed very well during this earthquake even without seismic design requirements.

The following is a partial list of the major damages to buildings and structures in Cotabato City:

1. Notre Dame Auditorium and Science Building. Burned and collapsed. Probable cause of failure: Insufficient lateral strength, weak spans which probably caused progressive failure.

2. Sultan Hotel. First floor and theater collapsed. Probable cause of failure: Vertical stiffness inbalance with insufficient stiffness on the ground floor. Progressive failure in the theater portion.

3. Chinese Gymnasium. Collapsed totally. Probable cause of failure: Insufficient lateral strength, weak joints.

4. Tamontaca Church. Partially collapsed. Probable cause of failure: Insufficient lateral strength combined with torsion.

5. Cotabato Auto Supply. Ground floor collapsed. Probable cause of failure: Vertical stiffness inbalance with insufficient stiffness on ground floor.

6. New Society Hotel. Ground floor on street corner collapsed. Probable cause of failure: Vertical stiffness inbalance with insufficient stiffness on ground floor combined with torsion.

7. Harvardian College. Ground floor columns collapsed and building tilted. Probable cause of failure: Vertical stiffness inbalance with insufficient stiffness on ground floor, weak joints.

8. Francel Theater. Front protion of theater collapsed. Probable cause of failure: Insufficient lateral strength and vertical stiffness inbalance.

9. South Sea Trading. All floors collapsed. Probable cause of failure: Torsion combined with insufficient lateral strength.

10. LCT Hardware and Auto Supply. First floor collapsed. Probable cause of failure: Vertical stiffness inbalance with insufficient stiffness on ground floor combined with torsion.

11. Sagittarius Hotel. Completely destroyed. Probable cause of failure: Insufficient lateral strength.

12. D'Max Restaurant. Completely destroyed. Probable cause of failure: Reported destroyed by the falling down and collapse of the adjoining Sagittarius Hotel.

13. First Gift Shop. Completely destroyed. Probable cause of failure: Burning and insufficient lateral strength.

14. Quirino Bridge. One span fell down. Probable cause of failure: No anchorage or limitation of displacement between the pier and end of span, insufficient provision for horizontal displacement.

There were also numerous minor damages to many buildings and houses i Cotabato City. These were generally shear cracks at the ends of concrete columns and in the shear walls. Heaves and cracks in the concrete pavemen tend to indicate appreciable vertical component of the earthquake motion i this city.

In Zamboanga City and vicinity and around Pagadian City, minor damage and cracks in some buildings were observed but a great loss of lives was reported from the outlying low islands whose coastlines were swept by the tsunami.

According to reliable information, in Tabina Municipality, about 130 kilometers from the epicenter, all buildings except one, were completely destroyed by the earthquake and not by the tsunami.

In the vicinity of Linek, visited by the writer about 100 kilometers from the epicenter, all the nipa shacks and houses within 200 meters of the coastline numbering into hundreds were completely demolished by the tsunami. According to surviving eyewitnesses, the earthquake woke them up, then they heard sounds of cascading rain but there was no rain and then the tsunami waves came within about 5 to 10 minutes.

V. SOME LESSONS LEARNED FROM THE DAMAGES

It is apparent from the damages observed that there is a great need for earthquake engineering education among the majority of practicing civil engineers and architects in the Philippines as well as for a wider dissemination of the present seismic code.

Practically all high rise buildings in Cotabato City, which appeared to have small or no vertical stiffness inbalance and small horizontal torsional eccentricity particularly on the ground floor, survived the earthquake with little or no damage.

Damages and cracks at the ends of concrete columns indicate that the columns had insufficient ties or hoops at these ends and the columns could not act as beams with reinforcement in diagonal tension, which the earthquake motion required.

The common practice of designing high rise buildings with stiff upper floors and insufficient stiffness on the ground floor together with appreciable horizontal torsional eccentricity should be restricted by the building code.

For people living on low areas along the coastline, if they experience earthquake motion and they hear sounds of cascading rain but can see no rain, they should be taught to run inland at once since conventional warning systems like radio messages and the like would come too late. The sound of cascading rain without rain should be their warning system.

VI. RECOMMENDATIONS FOR SEISMIC CODE REVISION

In line with the observations of damages resulting from this Mindanao Earthquake, the present provisions of the Philippine Seismic Code should be revised to include the following:

1. Restrictions on eccentricities for horizontal torsional moments. Not more than a maximum eccentricity of about 12% for horizontal torsional moments along each axis of

the building should be required. For fully symmetric and balanced buildings, a minimum eccentricity of 5% shall be considered in design. Computed horizontal torsional moments should be increased by 50% to allow for erratic building response during earthquakes.

2. Restrictions on vertical stiffness changes.

   a. When the eccentricity on any floor for horizontal torsional moment is 5% or less along both axes of the building, the maximum change in stiffness per unit weight from any floor to the next upper or lower floor should not exceed 20%.

   b. When the eccentricity on any floor for horizontal torsional moment along any axis of the building is more than 5% but does not exceed 12%, the maximum change in stiffness per unit weight from any floor to the next upper or lower floor should not exceed 15%.

3. Restrictions or anchorages for bridge spans.

The above restrictions should be in addition to previously recommended updating of the seismicity map, micro-regionalization or micro-zoning of cities, and the introduction of an importance factor, I, in the base shear equation.

ASSESSMENT OF SEISMIC DAMAGE IN EXISTING STRUCTURES

by

James T. P. Yao
Professor of Civil Engineering
Purdue University
W. Lafayette, INDIANA USA

Synopsis

It is desirable to assess the extent of damage in existing buildings following each major earthquake. As a result of such damage assessment, appropriate decisions can be made as to whether a structure can and should be repaired. In addition, it is desirable to rate building structures according to their respective damageabilities to be expected during future earthquakes. In this paper, several methods of damage assessment and damageability evaluation are reviewed. Moreover, possible applications of various techniques in system identification to damage assessment are discussed.

Introduction

Whenever the need exists and necessary funds become available, a structure can be designed and built accordingly. Traditionally, structural engineers are responsible for the design and analysis of the structure, which are then constructed under the management of general contractors. Following the completion of the construction process, the use and maintenance of most civil engineering structures do not require the service of structural engineers until the occurrence of some disastrous events such as strong-motion earthquakes.

In Figure 1, a schematic diagram is given to illustrate the beginning portion of the lifetime of a structure. At time t_0, the construction of the structure is completed. Suppose that a strong-motion earthquake occurrs at time t_1 and causes some damage. Structural engineers are requested to inspect the structure and may perform non-destructive tests at time t_2. The resulting data can be analyzed for damage assessment. Alternatively, the structure can be inspected and tested without having experienced any disastrous events as a routine and periodic maintenance procedure or as a safety precaution. In any event, a decision can be made on the basis of such damageability evaluation or damage assessment as to the type and extent of repair or strengthening required. This cycle can be repeated until the structure is no longer needed or totally destroyed beyond repair.

The objective of this paper is to (a) review and summarize several exi methods of damage assessment and damageability evaluation, and (b) discuss possibility of developing a new methodology incorporating available techniq system identification as well as the concept of structural reliability.

Damage Assessment and Damageability Evaluation

Whenever there are signs of distress or failure in a structure, an inv tion can be initiated by one or more interested parties. Alternatively, ex structures can be examined as a routine and periodic procedure. Typically, investigations consist of both experimental and analytical studies [Bresler

Hanson (1977)]. Recommendations for specific repairs can also be included if they are so requested. The experimental studies can be either field surveys or laboratory tests or both. Field surveys include the determination of exact locations of failed components and other evidence of distress, the application of various non-destructive testing techniques to the remaining structure, the discovery of poor workmanship and construction details, and proof-load and other load testing of a portion of a very large structure. On the other hand, samples can be collected from the field and tested in the laboratory for strength and other mechanical and structural properties. Analytical studies frequently consist of the examination of the original design calculations and drawings, the review of project specifications, the performance of additional structural analyses incorporating field observations and test data, and the possible explanation and description of the event under consideration.

In studying the building damage resulting from the Caracas Earthquake of 29 July 1967, Seed et al. (1970) used several quantities representing building damage for the purpose of comparison. For a given region, the structural damage intensity denotes the ratio of the number of damaged buildings to the total number of buildings in this region. For individual buildings, the ratio of maximum induced dynamic lateral force to static design lateral force is used for brittle structures, and the ratio of spectral velocity to lateral force coefficient is used for ductile structures. More generally, Bresler, Okada, and Zisling (1977) proposed the use of capacity ratio, c, which is defined as follows:

$$c = \frac{r_c}{r_d} \tag{1}$$

where r_c and r_d respectively denote calculated (available) and design (required) earthquake resistance of the structure. The quantity $\ell = 1 - c$ is called the leniency ratio . Either of these two ratios can be specified along with permissible time for hazard abatement of three categories of buildings structures according to their relative importance [Bresler, Okada, and Zisling (1977)].

Bertero and Bresler (1977) stated that (a) the lateral displacement ductility factors generally provide a good indication of structural damage, and (b) the interstory drift is a more important factor in causing nonstructural damage. Bresler (1973) discussed the relative merits of using plasticity ratio (residual deformation to yield deformation) and the ductility. For structures which are subjected to cyclic plastic deformations with degrading resistance, the following ratio was also suggested:

$$\lambda_j = \frac{r_j}{r_o} \tag{2}$$

where r_o and r_j respectively denote the initial and j^{th}-cycle resistance . same cyclic peak deformation.

Wiggins and Moran (1971) proposed an empirical procedure for grading building structures in Long Beach, California. A total of up to 180 poin assigned to each structure according to the evaluation of the following f items:

1. Framing system and/or walls (0, 20, 40 points). A well-designed concrete or steel building less than 3-stories in height is assi

zero-value. On the other hand, an unreinforced masonry filler and bearing walls with poor quality mortar is assigned a value of 40 points.

2. Diaphram and/or Bracing System (0, 10, 20 points). As an example, zero value corresponds to well anchored reinforced slabs and fills. On the other hand, incomplete or inadequate bracing systems correspond to the high 20 points on the scale.

3. Partitions (0, 10, 20 points). Those partitions with many wood or metal stud bearings rate zero points. On the other hand, unreinforced masonry partitions with poor mortar will draw 20 points.

4. Special Hazards (0, 5, 10, 15, 20, 35, 50 points). The high hazards include the presence of non-bearing, unreinforced masonry walls, parapet walls, or appendages.

5. Physical Condition (0, 5, 10, 15, 20, 35, 50 points). The high hazards include serious bowing or leaning, signs of incipient structural failure, serious deterioration of structural materials, and other serious unrepaired earthquake damage.

All of these assigned points are summed for each building thus inspected. Rehabilitation is not required if the sum is less than 50 points (low hazard). Some strengthening is required if the sum is between 51 and 100 points (intermediate hazard). Demolition or major strengthening is necessary when the sum exceeds 100 points (high hazard).

Culver et al. (1975) proposed the field evaluation method (FEM), in which a rating of 1 to 4 is assigned for geographic location, structural system, and nonstructural systems. The composite rating, CR, is given as follows:

$$CR = (e + 2s)/3I \tag{3}$$

where e = general rating, e = 1 for steel and ductile moment-resisting frames, and e = 4 for unreinforced masonry or unsheathed wood frames

s = structural system rating, and

$$s = \max\{[\tfrac{1}{6}(q + m) + \tfrac{2}{3} p], a, h, f\} \tag{4}$$

where q = quantity rating (a function of the number of vertical resisting elements)

m = symmetry rating

p = present condition rating

a = connection and anchorage rating

h = chord adequacy rating

f = roof and floor rigidities rating

and

$$I = \begin{cases} 1, & \text{MMI} \geq \text{VIII} \\ 2, & \text{MMI} = \text{VII} \\ 3, & \text{MMI} = \text{VI} \\ 4, & \text{MMI} \leq \text{V} \end{cases} \tag{5}$$

where MMI denotes the modified Mercalli intensity scale. The building is said to be in good condition, if CR < 1.0; in fair condition, if 1.0 < CR < 1.4; in poor condition, if 1.4 < CR < 2.0; and in very poor condition, if $\overline{CR} > \overline{2}.0$. Bresler, Okada, and Zisling (1977) commented that the algebraic formulation as given in Equations 3 through 5 is arbitrary, and that too much weight is given for present condition and too little weight is assigned to quantity rating.

Bertero and Bresler (1977) presented damageability criteria according to local, global, and cumulative damage in the following manner. For i^{th} structural element, an index of local damageability is given as

$$d_i = \frac{s_i}{r_i} \tag{6}$$

where s_i = response (or demand) in the i^{th} element due to loads

r_i = resistance (or capacity) in the i^{th} element

Damage is said to result in this i^{th} element whenever $d_i > 1$. The global damage index for a structure consisting of n elements can be computed by using the following relationship:

$$d_g = \sum_{i=1}^{n} w_i d_i \tag{7}$$

where w_i is the importance factor of the i^{th} element depending upon such factors as life hazard and cost. This quantity can also be normalized as follows for the purpose of comparison among different buildings.

$$\delta_g = \frac{d_g}{\Sigma w_i} \tag{8}$$

Similarly, a cumulative damageability index for structures subjected to cyclic loading conditions can be defined as follows:

$$d_c = \sum_{i=1}^{n} \frac{w_i n_i s_i}{\chi_i r_i}$$

where n_i and χ_i denote the service history influence coefficients for dema for capacity, respectively. The normalized cumulative damageability index fined as

$$\delta_c = \frac{d_c}{\Sigma w_i}$$

Recently, Hsu (1977) used the ratio of the number of plastic hinges resulting from expected earthquakes to the total number of plastic hinges for a collapse mechanism as a measure of structural damage.

Okada and Bresler (1977) discussed the screening method, in which the reinforced concrete buildings are classified according to three types of failure mechanisms (bending, shear, and shear-bending) by considering nonlinear response of the structure to two levels of earthquake motion (0.3 g and 0.45 g). The "first screening" deals with approximate evaluation of the load-deflection characteristic of the first story or of the weakest story. The "second screening" consists of a time-history nonlinear response analysis of each story. The "third screening" makes use of a dynamic response analysis including the nonlinearity of each member.

Recently, a safety evaluation program has been developed [Kudder (1977)]. Subjective evaluations are obtained for exposure, vulnerability, and combined safety index. A digital scale of 0 through 9 is used with 0 denoting non-impact and 9 denoting severe impact. Weighting factors are applied to obtain a combined index for safety evaluation.

Structural Identification

During this past decade, techniques of system identification [e.g., Eykhoff (1974)] have been successfully applied to solve structural engineering problems [e.g., see Chen (1976) , Hart and Yao (1976), Ibanez (1973), Marmarelis and Udwadia (1976), Matzen and McNiven (1976), Rodeman (1974), and Shinozuka et al. (1976)]. In most of these structural identification studies, a mathematical model (such as the lumped-mass model) with unknown parameters is assumed to represent the structural system. Responses (output) of the real structure to known forcing functions (input) are recorded then analyzed to estimate the unknown parameters in the assumed mathematical model. Although the resulting representation for the structure is still an idealized model with estimated parameters, it is a more realistic one than any apriori representation. The structural response to expected loading conditions can then be computed using such a mathematical model for damageability evaluation or damage assessment.

In addition to using system identification techniques in obtaining the mathematical equation of motion for the structure, attempts can be made to directly assess the present damage level in existing structures. As an example, full-size structural members and connections have been tested under reversed plastic deformations [e.g., Popov and Bertero (1973)]. If the behavior of these full-scale specimens at various damage levels can be identified with the use of available techniques of system identification, a methodology may be established for the direct estimation of damage level of structural elements and thus of existing structures.

As shown in Figure 2, a virgin structure immediately after completion of construction can be assumed to have an initial damage level, $d(t_0)$, on some

which may be caused by poor workmanship, inferior quality of materials used, accidental loading conditions during construction. On the other hand, the t collapse of a structure can be assumed to correspond to a damage level of u which serves as the reference value on this damage scale. The damage of a s ture can be indicated by (a) visually observable physical changes such as ca ndicated by initiation and propagation of cracks or progressive failure of structural components, (b) directly measurable physical changes such as perm r plastic deformations, (c) changes in abstract structural characteristics s the damping coefficients, (d) change in mathematical modeling required to

describe the behavior of the structure (e.g., the necessity of using nonlinear models for adequate representation indicates an advanced damage level). Lacking a precise understanding and thus definition of structural damage at present, it is necessary to make use of as many of these damage indicators as is practical and economically feasible.

For our purposes, the structure can be divided into major components (structural elements such as connections and members), each of which can be subdivided into localized points (macroscopic behavior of materials). At each level, there can be separate damage scales as shown in Figure 3. In this regard, the normalized local and global damage indices as suggested by Bertero and Bresler (1977) correspond to the last two columns in Figure 3. More generally, the methods of Wiggins and Moran (1971) and Culver et al. (1975) can also be summarized and illustrated in a similar manner as shown in Figures 4 and 5, respectively. As another example of damage measure in elements, Shinozuka (1977) referred to the use of "break (or leakage) damage index" as given in an unpublished Japanese report by K. Kubo and T. Katayama. This break damage index is defined by the number of pipe breaks in the area element per unit length (in km.) of pipeline in each area (1 km x 1 km). Some statistics of this index were collected at the time of the 1923 Kanto Earthquake in Japan.

Various kinds of nondestructive tests can be conducted on the structure. Such test data can be used to estimate the appropriate damage level(s). For example, results of ultrasonic and/or X-ray tests are effective in detecting cracks and thus can be used in estimating the damage of localized points. The damage at this level thus estimated can be used for correlation with the damage level of structural elements and that of the whole structure, which can also be estimated directly or indirectly using results of other types of tests and/or observations.

Alternatively, various tests can be conducted to estimate the current (residual) values of strength, ductility, damping (energy absorption capacity), stiffness, and continuity. On the basis of these data, the overall structural damage may be estimated as illustrated in Figure 6. Each of these quantities can be evaluated at several levels. For example, it is of interest to assess the continuity between (a) structure and foundation, (b) member to member, and (c) point to point.

Discussion

Since Freudenthal (1947) published his first treatise on this subject, much progress has been made in the theory and application of structural reliability [Freudenthal et al. (1975)]. At one end of the spectrum, various approaches have been proposed to formulate the so-called Level I reliability-based design codes [e.g., see Ang and Cornell (1974)], which resemble current codes with relatively simple design formulas. At the other end of the spectrum, the state-the-art approach includes the application of random processes [e.g., see Trapp (1974)], and optimum design of structures [e.g., see Lin et al. (19 Rosenblueth (1976)]. These advanced studies add a new dimension to the p of structural engineering in treating natural phenomena involving various of uncertainty. Once again, most of the investigations conducted to date the use of idealized mathematical models. Recently, Galambos and Yao (197 pointed out the need for more experimental work in developing new design

The ultimate objective of making damage assessment and damageability tion is to decide on necessary measures for hazard abatement [e.g., see B

Okada, and Zisling (1977)]. Recently, a suggestion was made to attempt the assessment of structural reliability as well [Yao (1976)]. The possible application of such a methodology to nuclear structures was discussed recently [Yao and Anderson (1977)].

An important step in establishing such a methodology is to obtain a practical and unified definition of damage for various types of structures as well as for different scales of structural elements as shown in Figure 3. Moreover, it is desirable to study the inter-relationships among damage from one scale to another. As an example, it is possible to evaluate the damage in the form of a crack at a certain location of the wall by performing one or more non-destructive tests. It is then desirable to find the influence of this particular damage in this wall element to the damage level of the whole structure.

The possibility of applying the techniques of system identification and the incorporation of the concept of structural reliability in damage assessment is now being explored in an NSF-supported collaborative research project between the School of Civil Engineering at Purdue University (J. T. P. Yao, P.I.) and the Earthquake Engineering Research Center at the University of California at Berkeley (H. D. McNiven, P.I.). The writer wishes to acknowledge the encouragement of Dr. S. C. Liu in this regard.

References

Ang, A. H-S. and Cornell, C. A., "Reliability Bases of Structural Safety and Design", Journal of the Structural Division, ASCE, v. 100, n. ST9, pp. 1755-1769, September 1974.

Bertero, V. V. and Bresler, B., "Design and Engineering Decisions: Failure Criteria (Limit States)", Developing Methodologies for Evaluating the Earthquake Safety of Existing Buildings, Earthquake Engineering Research Center, University of California at Berkeley, Report No. UCB-EERC-77/06, pp. 114-142, February 1977.

Bresler, B., "Behavior of Structural Elements--A Review", Building Practices for Disaster Mitigation, Edited by R. Wright, S. Kramer, and C. Culver, National Bureau of Standards, Building Science Series No. 46, pp. 286, 351, February 1973.

Bresler, B., "Evaluation of Earthquake Safety of Existing Buildings", Developing Methodologies for Evaluating the Earthquake Safety of Existing Buildings, Earthquake Engineering Research Center, University of California at Berkeley, Report No. UCB/EERC-77/06, pp. 1-15, February 1977.

Bresler, B., Okada, T., and Zisling, D., "Assessment of Earthquake Safety and of Hazard Abatement", Developing Methodologies for Evaluating the Earthquake Safety of Existing Buildings, Earthquake Engineering Research Center, Univer of California at Berkeley, Report No. UCB/EERC-77/06, pp. 17-49, February 19

Chen, S. J. Hong, Methods of System Identification in Structural Engineering Thesis, School of Civil Engineering, Purdue University, West Lafayette, Indi August 1976.

Culver, C. G., Lew, H. S., Hart, G. C., and Pirkham, C. W., Natural Hazards ation of Existing Buildings, National Bureau of Standards, Building Science lo. 61, January 1975.

Eykhoff, P., System Identification-Parameter and State Estimation, John Wiley & Sons, 1974.

Freudenthal, A. M., "Safety of Structures", Transactions, ASCE, v. 112, pp. 125-180, 1947.

Freudenthal, A. M., Shinozuka, M., Konishi, I., and Kanazawa, T., Editors, Reliability Approaches in Structural Engineering, Maruzen Company, Tokyo, Japan, 1975.

Galambos, T. V. and Yao, J.T. P., "Additional Comments on Code Formats", DIALOG 2-76, Edited by O. Ditlevsen and G. Mohr, Denmarks Ingeniorakademi, Denmark, pp. 24-26, 1976.

Hanson, J. M., Private communication, 11 June 1977.

Hart, G. C. and Yao, J. T. P., "System Identification in Structural Dynamics", Invited paper, Proceedings, ASCE EMD Specialty Conference on Dynamic Response of Structures, UCLA, California, pp. 61-85, March 1976.

Hsu, D. S., Risk Analysis of Structures in Earthquake Engineering, Ph.D. Thesis, School of Civil Engineering, Purdue University, West Lafayette, Indiana, August 1977.

Ibanez, P., "Identification of Dynamic Parameters of Linear and Non-linear Structural Models from Experimental Data", Journal of Nuclear Engineering and Design, v. 25, pp. 30-41, 1973.

Kudder, R., Private communication, 20 April 1977.

Liu, S. C., Dougherty, M. D., and Neghabat, F., "Optimal Aseismic Design of Buildings and Equipment", Journal of the Engineering Mechanics Division, ASCE, v. 102, n. EM3, pp. 395-414, June 1976.

Marmarelis, P. Z. and Udwadia, F. E., "The Identification of Building Structural Systems-II. The Nonlinear Case", Bulletin of the Seismological Society of America, v. 66, n. 1, pp. 153-171, February 1976.

Matzen, V. C. and McNiven, H.D., Investigation of the Inelastic Characteristics of a Single Story Steel Structure Using System Identification and Shaking Table Experiments, Earthquake Engineering Research Center, University of California at Berkeley, Report No. EERC 76-20, August 1976.

Okada, T. and Bresler, B., "Seismic Safety of Existing Low-Rise Reinforced Concrete Building", Developing Methodologies for Evaluating the Earthquake Safety o[illegible] ing Buildings, Earthquake Engineering Research Center, University of Calif at Berkeley, Report No. UCB/EERC-77/06, pp. 51-113, February 1977.

Popov, E. P. and Bertero, V. V., "Cyclic Loading of Steel Beams and Connec Journal of the Structural Division, ASCE, v. 99, n. ST6, pp. 1189-1204, Ju

Rodeman, R., Estimation of Structural Dynamic Model Parameters, Ph. D. The School of Civil Engineering, Purdue University, West Lafayette, Indiana, A 1974.

Rosenblueth, E., "Towards Optimum Design Through Building Codes", Journal Structural Division, ASCE, v. 102, n. ST3, pp. 591-607, March 1976.

Seed, H. B., Idriss, I. M. and Dezfulian, H., Relationships Between Soil Conditions and Building Damage in the Caracas Earthquake of July 29, 1967, Earthquake Engineering Research Center, University of California at Berkeley, Report No. EERC 70-2, February 1970.

Shinozuka, M., Imai, H., Enami, Y., and Takemura, K., "Identification of Aerodynamic Characteristics of a Suspension Bridge Based on Field Data", IUTAM Symposium on Stochastic Problems in Dynamics, Southampton, England, July 19-23, 1976.

Shinozuka, M., and Kawakami, H., Underground Pipe Damages and Ground Characteristics, Technical Report No. CU-1, Department of Civil Engineering and Engineering Mechanics, Columbia University, June 1977.

Wiggins, J. H., Jr., and Moran, D. F., Earthquake Safety in the City of Long Beach Based on the Concept of Balanced Risk, J. H. Wiggins Company, Redondo Beach, California, September 1971.

Yang, J. N. and Trapp, W. J., "Reliability Analysis of Aircraft Structures Under Random Loading and Periodic Inspection", AIAA Journal, v. 12, n. 12, pp. 1623-1630, December 1974.

Yao, J. T. P., Summary report presented at the Fourth National Meeting of the Universities Council for Earthquake Engineering Research, University of British Columbia, Vancouver, Canada, June 28-29, 1976.

Yao, J. T. P. and Anderson, C. A., "Reliability Analysis and Assessment of Existing Structural Systems", to be presented at the Fourth International Conference on Structural Mechanics in Reactor Technology, San Francisco, California, August 15-19, 1977.

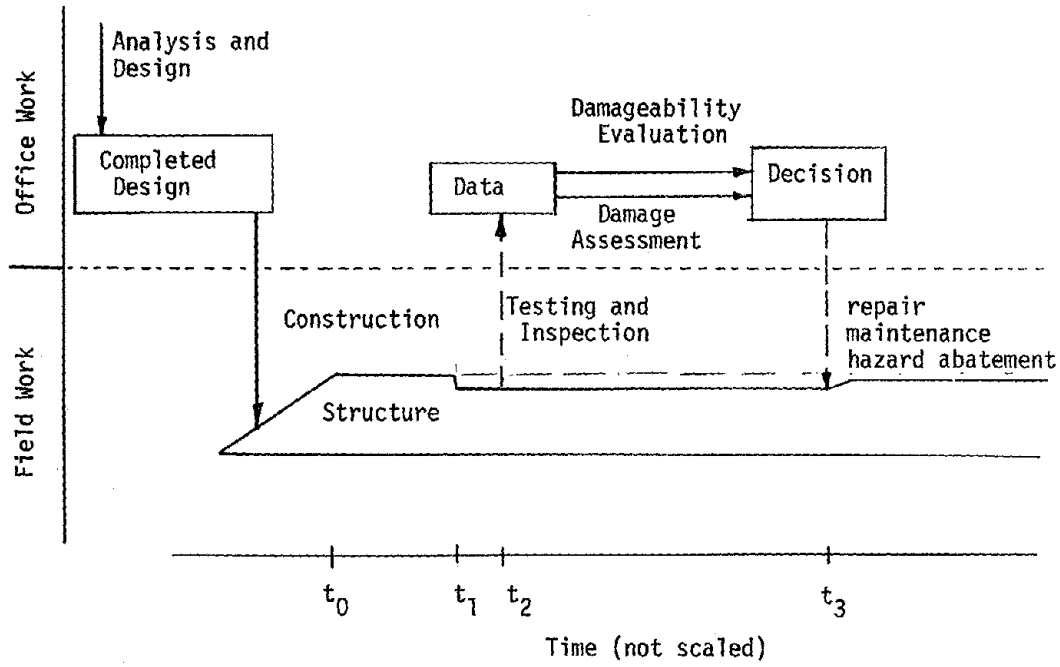

Figure 1. Roles of Damage Assessment and Damageability Evaluation During the Lifetime of a Structure.

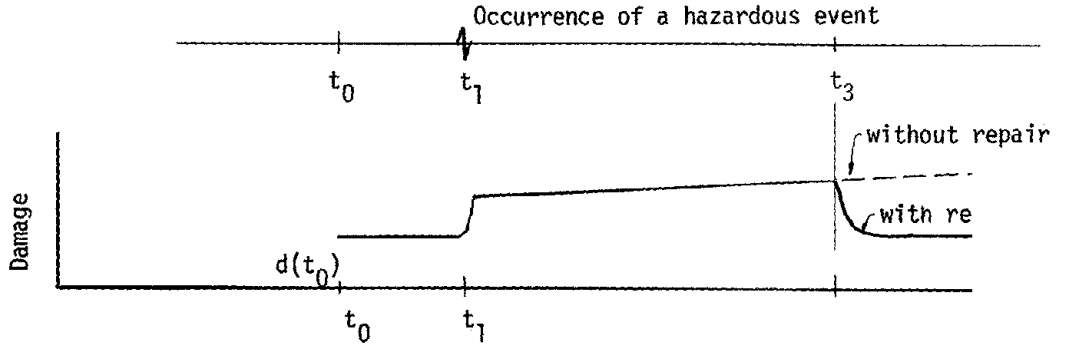

Figure 2. Damage Function

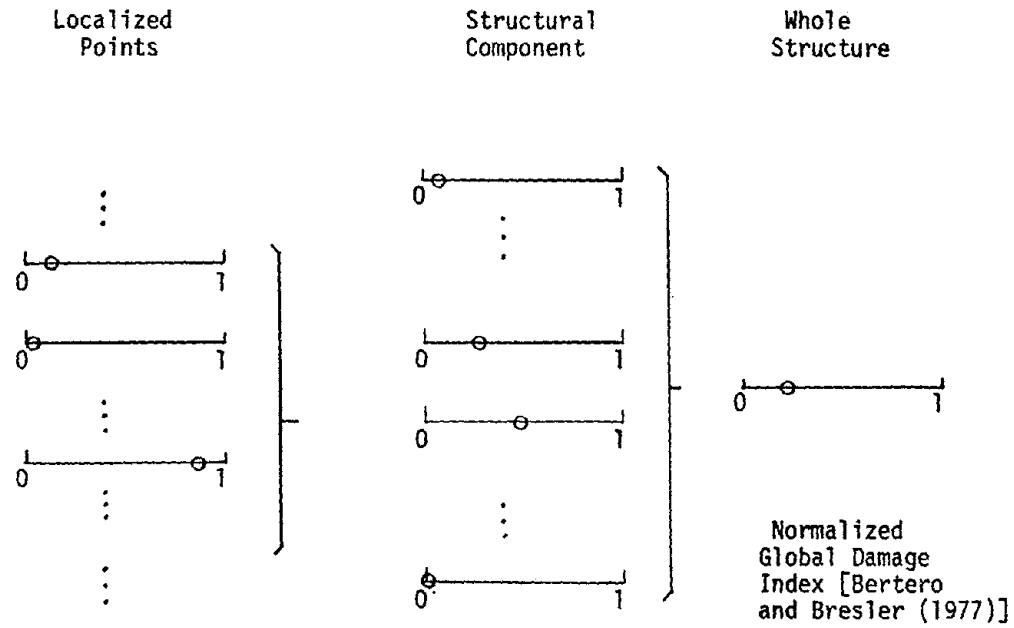

Figure 3. Hierarchy of Damage Levels

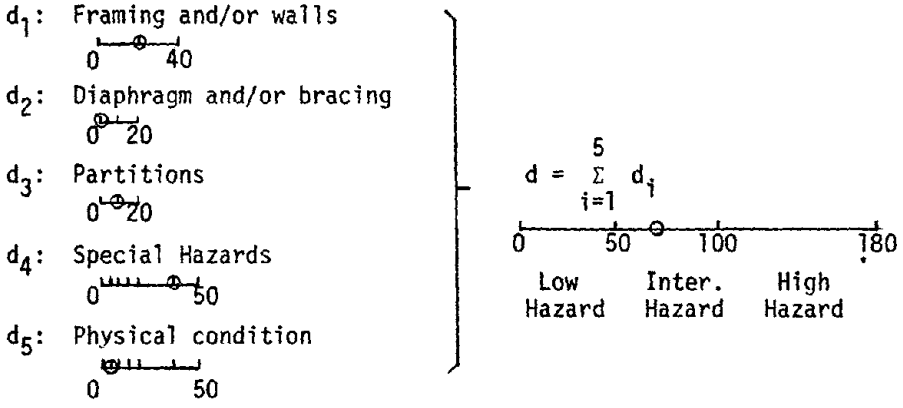

Figure 4. Method of Wiggins and Moran (1971).

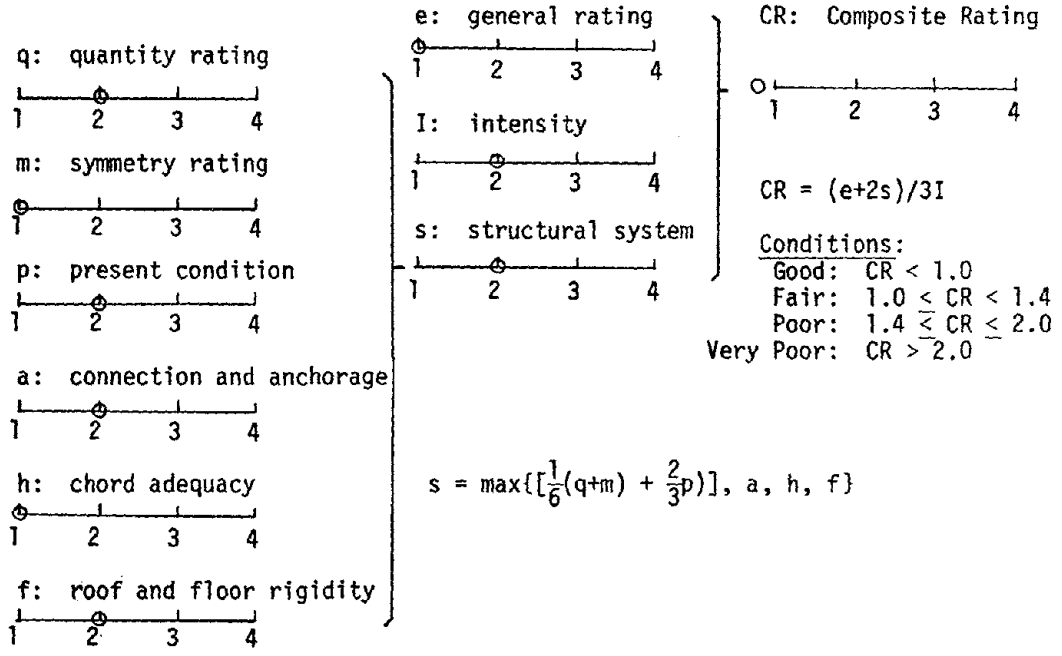

Figure 5. Methods of Culver, et al (1975).

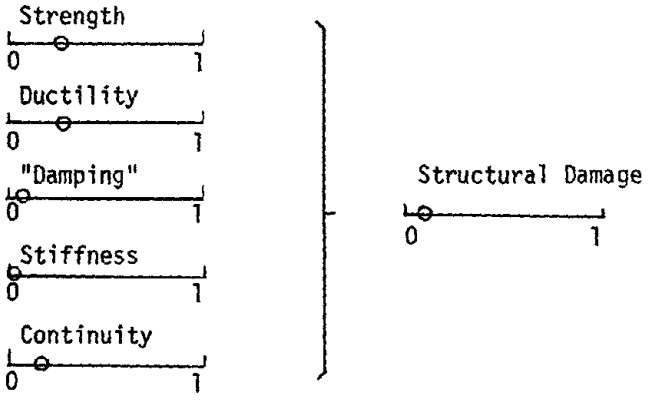

Figure 6. An Alternative Approach.

WIND DAMAGE EXPERIENCES: FAILURE ASSESSMENT, PRACTICES, SOLUTIONS

Joseph E. Minor, P.E.
Institute for Disaster Research
Texas Tech University
Lubbock, Texas, U.S.A.

Synopsis

Societies throughout the world must contend with five basic types of wind related hazards--the tropical cyclone, the tornado, down-slope winds, thunderstorm outflows and extra-tropical cyclones and cold fronts. Basic characteristics of these windstorm events are presented in engineering terms (windspeeds, gustiness, atmospheric pressure change, duration) for use in disaster planning and building design. The effects of these hazardous windstorm events are measured in terms of degrees of damage to buildings, classified according to the degree of engineering attention given to them. Fully-engineered buildings resist extreme winds well, while marginally-engineered and non-engineered buildings are the source of major problems. Engineering practice is tied to building codes; wind design practices are seen to be different in the United States when compared with certain other countries. Finally, solutions are presented which relate principally to the gaining of professional and public awareness of wind problems and the fact that technology is available to solve them.

Introduction

Intensive research in the field and in the laboratory has placed the wind hazard and building response mechanisms into relatively sharp focus. Scientists and engineers are able to define the general character of the several types of wind hazards, and engineers understand the fundamental modes of building response to wind-induced forces. Engineering practice has been slow to assimilate this new technology, especially in the United States. This situation seems to stem from two factors: (1) a lack of awareness of the magnitude of the problem on the part of the public as well as on the part of the professional, and (2) a lack of awareness of the availability of new wind engineering technology on the part of the design professional.

This paper is advanced as an overview of wind engineering experiences and knowledge. The first of four major sections summarizes the general character of five important types of hazardous windstorms. This section is followed by a summary of windstorm caused failures and attributes varyir degrees of damage to the level of engineering attention given to the desigr of the buildings. A summary of engineering practice as reflected in buildi codes throughout the world constitutes the third section. Possible solutic to problems identified in the previous three sections are addressed in the final section.

The Character of Extreme Winds

A. Extreme Winds

Wind engineers must be conversant with the nature of extreme winds which may affect their structures and facilities. Characteristics of extreme wind events, their frequency and location of occurrence, and certain special features must be understood if the engineer is to act responsibly in responding to the conditions which these events present. Because some confusion exists within the professional community with some meteorological terms, selected definitions are included below. The definitions are followed by summary discussions of the five types of windstorms against which the wind engineer must contend: tropical cyclones, tornadoes, downslope winds, thunderstorm outflows and extra-tropical cyclones and cold fronts.

B. Definitions

Several meteorological terms arise repeatedly in discussions of severe wind events. The working definitions given below will serve as a framework for more detailed descriptions given in the following sections. (The Glossary of Meteorology, 1959, is the standard reference, although many newly coined terms are not included.):

(1) Synoptic scale - the scale of the migratory high and low pressure systems (weather map features) with wave lengths of 500-1500 mi.

(2) Meso-scale - a scale of atmospheric motions with horizontal dimensions and durations of 100 yds and 1 min to 100 mi and 1 day, including features such as tornadoes, thunderstorms, mountain-valley circulations and sea breezes.

(3) Cyclone - an atmospheric circulation with horizontal winds flowing counterclockwise in the Northern Hemisphere (clockwise in the Southern Hemisphere) around an area of low pressure. The "lows" on the weather map are extratropical cyclones. Hurricanes are the most intense form of tropical cyclones. (In the Indian Ocean "cyclone" is used instead of "hurricane.")

(4) Anticyclone - an atmospheric circulation with horizontal winds flowing clockwise in the Northern Hemisphere around an area of high pressure.

(5) Tropical cyclone - a cyclone which originates over the tropical oceans. Gradations of intensity range from tropical disturbance, tropical depression, tropical storm to hurricane. Local terms replacing "hurricane" include typhoon, boguio, and simply cyclone.

(6) Front - a transition zone between two air masses having different properties.

(7) Convective cloud - a cloud which owes its vertical development to convection--either free (due to density differences caused by heat) or forced (due to mechanical lifting forces). The most intense form of convective cloud is a cumulonimbus (Cb).

(8) Thunderstorm - a local storm usually produced by a cumulonibus cloud and accompanied by lightning and thunder, strong wind gusts, heavy rain, and sometimes hail and tornadoes.

(9) Tornado - a violently rotating column of air extending from the base of a cumulonimbus cloud, often visible as a funnel cloud. Colloquially termed a "twister" or "cyclone" (although this usage has been opposed by meteorologists since the 1890's).

(10) Dust devil - a rapidly rotating column of air which develops over strongly heated land, usually with no connection to clouds above.

(11) Waterspout - a rotating column of air extending from the base of a convective cloud over a water body, bearing similarities to tornadoes over land (though usually less intense). Sometimes a fair weather whirlwind develops over water, similar to a dust devil over land.

(12) Downslope winds - warm or cold descending winds, characterized by localized high velocities and gustiness.

(13) Vorticity - the local rotation of the air due to curving motion and wind shears.

C. Tropical Cyclones

Fully mature tropical cyclones may range in size from 60 to over 1000 mi in diameter; thus, tropical cyclones are at lower end of the synoptic scale. For much of the average lifetime of 9-10 days the storms may be monitored by satellite, radar, and reconnaissance aircraft. Nevertheless, there are major unresolved questions regarding tropical cyclones; some recent events underscore their highly variable and erratic nature.

Maximum windspeeds generally occur to the right or left of the eye (depending on its location north or south of the equator) of the tropical cyclone (looking along the direction of its path), because of the vector addition of the translational and rotational wind components. The direction of the wind is typically inclined 20°-30° toward the center of the storm except near the edge of the wall cloud (towering clouds surrounding eye) where there is no longer any inflow. The windfield is a function of the radius of maximum winds, the central pressure difference, the forward speed, and the geographic location of the storm. The strongest winds occur along the edge of the eye near the wall cloud. Winds frequently reach speeds (averaged over one minute and referenced to 30 ft height) of 100 to 135 mph. In more severe storms windspeeds may reach 200 mph, although this value has never been confirmed for hurrican Reliable measurements of windspeeds in tropical cyclones are difficult to ob tain because many anemometers are not accurate in the high ranges, because many instruments blow away, because standard instruments are often not locat directly in the storm path, or because instrumentation and windspeed measuri techniques employed aboard aircraft are difficult to calibrate. Caution is advised, therefore, in viewing maximum windspeed data. Wind gust speeds wit a tropical cyclone may exceed sustained winds by 30 to 50 percent (depending

upon frames of reference). Streaks of wind damage have been observed in tropical cyclones (e.g., Hurricane Celia, 1970); these damage streaks are indicative of windspeeds which are higher than the average rotational windspeeds.

While tropical cyclones have been monitored and studied for years, some important information needed by wind engineers is not available. Of particular concern are data on (1) the windspeed vs height relationship, (2) maximum values for windspeed, (3) the windfield (velocity vs r and θ), (4) gustiness (gust factors and gustiness vs height), and (5) wind effects over water. Until new research produces needed data, the standard of practice will be to continue to apply our general understandings of the nature of wind to tropical cyclone situations.

D. Tornadoes

Tornadoes are mesoscale events, usually spawned by severe thunderstorms but appearing occasionally in tropical cyclones. The tornado itself is an atmospheric vortex which extends from cloud base to the ground. The vortex is sometimes narrow (a few yards in diameter) and smooth in appearance, but more often is wide and turbulent in appearance. A cloud of condensed moisture is often visible within the vortex (the characteristic funnel cloud), but the vortex (and, hence, the tornado) is much larger in dimension and may extend well beyond the area of the visible funnel.

The major flow of air at ground level is circular and translational at the same time. The translational speed of a tornado is considered to be a well known quantity, since the measurement is not too difficult to make. The range of translational speed varies from 5 to 70 mph with an average of 45 mph.

A value of perhaps 500 mph was once believed to be an upper bound on maximum wind velocity. Maximum velocities are seldom recorded, because anemometers in a position to make the measurement are not likely to survive. Recent studies of tornado damage and motion picture records have led tornado experts to reduce their estimation of maximum velocity to values less than 300 mph.

One common feature of all tornadoes is the relatively low pressure at the center of the storm. As in the case of wind velocity, maximum values for the magnitude of the atmospheric pressure change are not known precisely. The probability of a tornado passing directly over a barograph is small. Even if the instrument were not destroyed, recorded values would be subject to question because most barographs are not designed to respond to the rapid pressure variations produced by a moving tornado. The maximum pressure change is probably about 2 1/2 in. of mercury (1.2 psi).

E. Downslope Winds

Strong, gusty localized windstorms are observed in and near mountain regions in many parts of the world. Over the centuries, local terms have used to designate these winds: zonda in Argentina, foehn in the Alps, Santa Ana in Southern California, chinook in the Rocky Mountains, bora in South Europe, etc. In many cases there is a characteristic temperature fall or

To a degree, warm descending winds have been termed foehns and cold descending winds are boras. In the United States the most destructive and best-documented example occurs in the Boulder, Colorado vicinity. While this phenomenon does not display all of the features observed worldwide, the Boulder downslope winds have shown a diversity which may be typical.

In Boulder, a windstorm period is one during which maximum speeds exceed 50 mph with at least one recording station recording at least 73 mph at an elevation of 11 ft. Severe windstorms occur about once per year in Boulder, Colorado; however, a total of 20 storms were observed in 3 years with large interannual variability. January is the prime month; however, other winter months have a fair share. Some occur as early as September and as late as March.

The extreme gustiness is an outstanding feature; from 20 mph to 80-90 mph. The peak gust duration is usually 3-5 sec. Compared to other wind observations, the gust factor is generally higher for Boulder's wind. Peak gusts of 100-120 mph have been recorded in populated areas of Boulder. In some cases the wind blows strongly during an entire storm; in other cases there are marked periods of relatively low velocities, lasting for several hours.

The storm may last on the order of a day or more. The most frequent strong winds and high gusts occur between midnight and 10 AM. Relative humidity decreases of 10-20 percent are common as well. Some cases are accompanied by cooling but some show temperature increases.

F. Thunderstorm Outflows

Wind gusts in excess of 60 mph sometimes accompany thunderstorms. Quite often these winds may strike well before the onset of precipitation, although usually their advance may be foreshadowed by an ominous horizontal roll cloud or a wall of dust. These winds are an integral part of the thunderstorm circulation termed the outflow, and the leading edge of the strong winds is called the gust front.

Severe thunderstorms are characterized by a vigorous column of high speed rising air which provides the moisture for subsequent formation of precipitation. The release of latent heat which occurs with condensation lends to the continued growth of the storm. As the precipitation falls, often into a drier region of the storm, evaporation takes place; the heat for the evaporation is supplied by the air, leading to a cooling of the descending rain-filled air. This cold air production contributes to an acceleration downward. In addition, cold, fast-moving air entering the storm at upper levels may mix with the sinking air, enhancing its descent. When this downdraft impinges the groun it spreads in all directions, undercutting the warmer air at low levels. Th outward thrust of air produces noticeable events at the surface. Warm mois air is lifted rapidly to produce a turbulent, rolling, cigar-shaped cloud a the leading edge of the cold air. As the cold air passes, the windspeed exhibits large fluctuations and there is a shift in direction. This wind shift line is often coincident with a sharp pressure rise. Shortly thereaf an intense gust surge occurs, followed by a break in the temperature and dr air. The density difference is also detectable on radar, appearing as a "f

line." The cold air may expand many tens of miles beyond the storm; satellite pictures often reveal the arc of clouds at the leading edge, far from the area of intense rain production.

The low-level outflow is usually strongest just behind the gust front, where surface gusts often exceed 60 mph. Vertical shears of the horizontal wind are most dramatic in the lowest 100-150 ft, where shears of the component normal to the front have been measured at over 10 mph/100 ft in moderate gust fronts. Shears of the component parallel to the front may also be substantial. Multiple surges may occur due to thunderstorm pulsations.

G. Cyclones and Cold Fronts

Windspread strong winds may be experienced with the passage of intense cyclones (lows) and cold fronts, especially during colder months. The strength of the winds are roughly proportional to the pressure gradient which exists across the front at a distance from the center of the low. The gustiness, however, may be enhanced by the sinking of colder air from aloft as a part of the three-dimensional structure. The duration of strong winds with frontal passages may be relatively short compared to those associated with passage of a low. Preferred regions of low formation (cyclogenesis) and intensification exist for the United States in the lee of the Rockies and along the Gulf and Atlantic Coasts. These areas may experience prolonged windiness with gradual intensification before the low accelerates away to the east and north. At inland locations these periods may be accompanied by heavy snow, producing hazard conditions, or blowing dust reducing visibility to a fraction of a mile. Along coastal sectors, such periods are accompanied by heavy precipitation. Preferred cyclone tracks lead the storms commonly into the Great Lakes-Ohio Valley area, or along the Eastern Seaboard.

Failure Assessments

A. Damage Investigations

Windstorm damage investigations conducted by the authors and other engineers (Almuti, 1974; McDonald, 1971; Mehta et al., 1971; Mehta et al., 1975; and Walker 1972, 1975) are similar in that they all describe windstorm damage to structures in like terms. Each investigator has come to the conclusion that most buildings are damaged when a connection or an anchorage detail fails, thus leading to collapse of the structure through a progression of component failures. The work of these investigators may be summarized as follows:

(1) structures fail, principally, because of wind-induced forces (rather than from atmospheric pressure change);

(2) non-engineered and "marginally" engineered structures are susce to wind-induced failure at relatively low windspeeds because of limited attention to details of design and construction; and

(3) small increases in degrees of engineering attention (using new wind engineering technology) can produce very large dividends i increased wind resistance.

Hence, the understanding of building failures in windstorms is relatively well advanced. This knowledge and boundary-layer wind tunnel investigations have combined to produce significant advances in the technology of wind effects on buildings.

B. Performance of Buildings in Windstorms

Attention to studies of damage has produced a classification of buildings according to the character of response which they exhibit. Advanced originally in the comprehensive report on the Lubbock Storm (Mehta et al., 1971) and in an article in the Structural Journal of ASCE (Minor et al., 1972), this classification scheme recognizes differences in relative resistance of buildings in relation to the amount of engineering attention given to them. Other authors have advanced the same or similar schemes in reporting damage (Walker, 1972; Walker, 1975; Sanders et al., 1975). In this method, buildings are classified as fully-engineered buildings, pre-engineered buildings, marginally-engineered buildings, and non-engineered buildings. Discussions of the response exhibited by these structures will assist the reviewer of windstorm damage in assessing building failures and in placing the damage into a proper perspective with respect to attendant, damage-causing windspeeds.

1. Fully-Engineered Buildings--Buildings which receive specific, individualized design attention in a professional architectural-engineering sense are called "fully-engineered." If the building has received the degree of detailed engineering attention that is representative of the standard of practice for major buildings, its performance in the face of extreme winds is likely to be very good. A hospital in Omaha, Nebraska which was impacted directly by the Omaha Tornado of May 7, 1975, typifies this performance (Figure 1). This building was comprised of a reinforced concrete frame with reinforced concrete floor slabs of "pan" type construction ("waffle" appearance when viewed from underneath). The reinforced concrete roof of the structure was also of pan type construction. Damage to the part of the hospital which was built in this manner was limited to broken windows, a limited number of "fill-in wall" failures, and some interior partition failures. The Great Plains Life building in Lubbock experienced winds peripheral to the Lubbock Tornado of May 11, 1970 which were sufficient to severely wrack the structure leaving a permanent deformation in the structural steel frame (McDonald, 1970). While the frame was permanently deformed, the exterior masonry was cracked, and interior partitions were broken, the building was not at any time near collapse. The building has been repaired and restored to useful service. The First National Bank - Pioneer Natural Gas Company building in Lubbock experienced similar winds during the same storm. Windows were broken on both windward and leeward faces of the building, and considerable damage was done to interior furnishings. The reinforced concrete building frame was not damaged and the building was restored to service.

2. Pre-engineered Buildings--A unique classification of buildings described as "pre-engineered" metal buildings has been exposed to extreme wind effects. These buildings receive engineered attention in advance; the buildings are subsequently marketed in many units. Many manufacturers of these units do an excellent job of "balancing" the engineered design so that all components are equally strong; hence, an optimum economy of construction is achieved. However, windstorm events have revealed certain weaknesses in these building systems. Several failure modes are characteristic of this building classification. Detailed treatments of failure modes in metal building systems are outlined in a report by A. J. Sanger and R. R. Minor (1971). Often failures in overhead doors allow winds to enter the building, producing internal pressures and the large pressures across wall and roof components. Many metal building manufacturers design the overhead doors in conjunction with the balance of the building and avoid this weakness. Other manufacturers "subcontract" the overhead door design and installation, and, by yielding this responsibility, often obtain a door which is not as strong as the balance of the building. The door, then, represents a weak point insofar as wind resistance is concerned. Buildings in this classification often appear to have "exploded" because of the wind-induced pressure increase inside the building. Another common failure mode for metal buildings is loss of cladding along corners, eaves, and ridges, the location of localized outward acting pressures (Figure 2). Both of these failure modes commonly occur at relatively low windspeeds, e.g. less than 125 mph (55.9 m/s).

3. Marginally-Engineered Buildings--Commercial buildings, light industrial buildings, schools, and certain types of motels and apartments which are built with some combination of masonry, light steel framing, open-web steel joists, wood framing, wood rafters, and concrete comprise this group of structures. The term "marginally" engineered comes about because while a degree of engineered attention is given to designs, this attention is limited in extent, relative to the amount of attention given to a fully-engineered building. The engineering process tends to become conventional, i.e., once a structure of a given type has been built in a certain area, similar structures of the same type are erected without repeating the detailed calculations and inspections attendant to good design and construction practices.

Buildings of this type which contain masonry are most often major contributors to damage. Three types of buildings containing masonry are common: (1) buildings in which the roof system is supported by the walls, making the walls "loadbearing," (2) buildings with light steel framing (often steel pipe columns and light "I" beams) with masonry walls between columns called "fill-in walls," and (3) buildings with non-loadbearing walls outside of the framing system. Wind induced forces commonly push the masonry walls inward or outward, depending upon wind approach direction and the character of windward wall openings. In the case of loadbearing masonry, the roof system falls downward the walls collapse. In the case of non-loadbearing masonry, wall collapse does not produce frame collapse, but the contents of the affected building destroyed, thus compounding the value of damage. Windspeeds as low as 10((44.7 m/s) can cause failures of this type. Figure 3 illustrates a typica failure of a loadbearing masonry wall. While such failures are illustrati severe damage and give outward appearances of extreme forces and windspeec most often they are induced by relatively nominal winds, e.g. 125 mph (55. or less.

Motel and apartment units which are framed principally with wood usually receive some engineered attention. Again, however, this attention is marginal and tends to leave the buildings vulnerable to wind-induced forces. Common are roofs removed because of inadequate connection to walls, and roof failures brought about by "overhangs" over walkways (e.g. along the pathway in front of rooms) being lifted when wind-induced pressures build underneath. In these failures, damage appears to be severe and is usually described as "total destruction", yet the windspeeds causing the damage are nominal, e.g. 125 mph (55.9 m/s) or less.

Commercial, school and motel type structures may also be built with other combinations of steel, masonry, wood, and concrete. Construction using unique combinations of these building materials are common. While combinations of these materials can be used effectively in engineered designs, often these hybrids are carelessly assembled and provide only minimal resistance to wind-induced forces.

4. Non-Engineered Buildings--A large class of buildings receives no engineering attention at all. These buildings are single and multifamily residences, certain apartment units, and many small commercial type buildings. Consisting largely of wood frame construction, these buildings are, generally, poorly designed and constructed to resist lateral and uplift forces generated by the wind. Roof to wall connections, wall to foundation connections, resistance to lateral or "wracking" loads, and inadequate overall structural integrity typify these buildings (Figure 4). Windspeeds of hurricane velocity (73 mph; 33 m/s) represent the threshold of damage for these buildings, and total destruction may occur when winds reach 125 mph (55.9 m/s).

Professional Practice

A. Codes and Standards

While the understanding of the effects of wind on buildings has advanced significantly in recent years, the new technology is only slowly finding its way into professional practice. In the United States, new methods for developing wind loads on buildings have been particularly slow in gaining acceptance.

Professional practice is reflected in building codes and standards. It is sometimes thought that building codes serve to establish standards of practice; actually, the characters of code provisions are good indicators of the accepted practice in countries or regions of countries where they app

There is an important difference between a building code and a standard Building codes can become legal documents by action of some political body. Standards, on the other hand, are developed by "consensus" groups, professio societies, or governmental agencies for use by building code bodies or other independent organizations.

Activities of building code organizations are not the same in the Unite tates as in other countries. Canada, England, and Australia, for example,

have national codes which are influenced by governmental bodies at the federal level. While practicing professionals, industry, and trade associations are represented on code committees, the direct involvement of government in research and code writing activities provides these governmental bodies with considerable influence over the final character of the codes. In the wind area this governmental influence has produced more rapid incorporation of recent research and technological advancement into the codes of these three countries.

B. States of Development

The English, the Canadians, and the Australians have moved the new wind technology more rapidly into their national codes and standards (BRI, 1972; NRCC, 1975; SAA, 1973) than have the Americans. Further, they have written excellent commentary on the new approach to defining wind loads and on the details of code use (Newberry and Eaton, 1974; NRCC 1975a). The new technology has moved into codes and standards of practice more slowly in the United States. ANSI A58.1-1972 (ANSI, 1972) represents this country's first attempt to assimilate this new technology into a national standard. This standard is an excellent beginning as it embodies most of the relevant phenomena that wind engineering research has produced. The standard falls short, however, in that its provisions are not as refined nor are its provisions as clearly presented as the codes and standards of other countries. Furthermore, an allied commentary on the basis for the standard, including amplification of the details of its utilization, is not available.

Major code administrations in the United States are beginning incorporate ANSI A58.1-1972 into their respective codes of practice. The Southern Building Code Congress adopted ANSI A58.1-1972 in their 1974 revision (SBCC, 1974) to the 1973 Southern Standard Building Code (SBCC, 1973) as an "alternate," but rejected it in favor of NAVFAC DM-2 (NAVFAC, 1970) in their 1975 revision (SBCC, 1975). The 1976 revision (now called the Standard Building Code) reflects ANSI A58.1-1972 as an alternate again (SBCC, 1976) along with NAVFAC DM-2. The International Conference of Building Officials is considering the use of the ANSI A58.1-1972 approach for the Uniform Building Code (UBC, 1976). The current Uniform Building Code is based on American Standards Association (now ANSI) A58.1-1955 (ANSI, 1955). The Building Officials and Code Administrators International Incorporated (Basic Building Code) do not reference the 1972 ANSI Standard in their Basic Building Code. The American Insurance Association (National Building Code) has adopted ANSI A58.1-1972 in the 1976 edition of their code (AIA, 1976). Table I summarizes the major U.S. and other codes and contains addresses for their sponsoring organizations.

C. Comparisons of Approaches

Wind-structure interaction concepts gained from failure assessments tunnels represent the state of knowledge as it is currently understood by engineers. This knowledge is utilized in the several codes and standards ferent ways. While the person studying wind load provisions may wonder, casion, if each authority is using the same information base, it can be s that the fundamental concepts are the same, but that approaches differ. following paragraphs outline approaches employed in several major codes a standards.

1. National Building Code of Canada*--The National Building Code of Canada (NBC) is a model building by-law published by the National Research Council as a service to provincial and municipal governments. Over 90 percent of the 162 cities in Canada have adopted this code (in while or part) and approximately 80% of all Canadians live in areas where the NBC is used. Through recent provincial legislation it is being adopted more widely.

The NBC is revised every five years. In the 1970 revision embracing the "Canadian Structural Design Manual" several major changes were made in the subsection dealing with wind effects for building design. These changes introduced several new concepts to improve the formulation and understanding of some of the complex effects of wind, particularly the interaction of turbulence with dynamically responsive structures. They have been slightly extended in the 1975 edition (NRCC, 1975).

Previously, in the third edition issued in 1960, the NBC contained only brief instructions on how to determine design pressures from the referenced gust velocity pressure and pressure coefficients (detailed values of which were provided in supplements) and a factor accounting for the increase in the velocity pressure with height above ground. In addition, a warning was given of the danger to tall slender structures of dynamic overloading and vibrations at critical frequencies.

In the 1970 edition of the NBC the design pressure, p, is defined by the equation

$$p = qC_gC_eC_p$$

where q is a reference hourly mean velocity pressure at 30 ft height in open country and having a specified probability of occurrence, C_g is a gust effect factor, C_p is a mean pressure coefficient and C_e an exposure factor.

Substitution of the mean velocity pressure instead of the previously used gust velocity pressure allows the meteorological measurements to be used directly and the complex fluctuating response due to gusts to be considered separately through the factor C_g. The exposure factor C_e allows for the modifying effects of both height and a new consideration, the terrain roughness. The pressure coefficient C_p is used conventionally and allows for the influence of structural shape.

To allow for the spatial nonuniformity of gusts it is required that the structure be analysed for a removal of 25 percent of the wind load over any portion. This may be significant in the torsion of taller buildings and in the loading of roofs.

The NBC permits two design procedures; a simple procedure and a detail procedure. In the simple procedure C_g = 2.0; for most places in Canada the quantity C_gq is then close to the "gust velocity pressures" used in previou climate supplements; C_e is based on a 1/10 power law profile for wind speec providing continuity with previous code editions. Simplified pressure coef cients C_p are tabulated. The simple procedure is intended to be short, eas apply, conservative and safe.

* Discussion taken from Davenport and Dalgliesh (1975).

The detailed procedure is intended mainly for use with somewhat taller structures and, for a broad class of structures, offers economy over the simple procedure. For structures over 400 ft height the detailed procedure is obligatory since the simple procedure may then be inadequate. Wind tunnel testing using dynamic models in appropriate turbulent flow is permitted under the detailed procedure. There is also a recommended theoretical procedure.

2. The English 'Code of Basic Data'"--The English Code (BSI, 1972) and its commentary (Newberry and Eaton, 1974) comprise an advanced approach to the definition of wind loads that is based on the latest information that research and technology have provided. The code contains several refinements that U.S. codes and standards do not treat (e.g. local terrain and terrain changes); hence, these documents can serve as excellent references for the U.S. wind engineer who has requirements or situations that are not addressed in his code.

Basically, the English Code follows a three step procedure. First, the design wind speed is calculated from

$$V_s = V \times S_1 \times S_2 \times S_3$$

where: V is the basic wind speed for the locality of interest. This value is the 3-second gust speed at 10m height in open level country likely to be exceeded on average once in 50 years.

S_1 is a factor for local topographical influences.

S_2 is a factor for surface roughness of the environment, gust duration appropriate to the size of the building, and height of the structure or component above the ground.

S_3 is a factor which considers the design life of the building.

Second, the design wind speed is converted to a dynamic pressure q using the relationship

$$p = C_p q$$
$$F = (C_{pe} - C_{pi}) q A_e$$
$$F = C_f q A$$

where: C_p is a pressure coefficient

C_{pe} is a pressure coefficient for external surfaces

C_{pi} is a pressure coefficient for internal surfaces

F is resultant wind load on an element of surface

A is the area of the surface

A_e is the effective frontal area of a building as a whole.

3. The Australian Code--Perhaps even more refined and sophisticated the English Code is the Australian Code (SAA," 1973). This Code specifies wind forces can be obtained by one of four methods:

(1) rules of the code

(2) reliable references used with rules of the code

(3) wind-tunnel or similar tests used with rules of the code

(4) wind-tunnel or similar tests alone.

Accordingly, a considerable amount of material and discussions in the code pertain to approaches beyond method (1), which is the method used almost exclusively by other codes.

The method which relies on "applicable rules" of the code employs the same basic three steps advanced by the English:

(1) calculation of a design wind velocity V_z

(2) conversion to a free-stream dynamic pressure q_z

$$q_z = 0.6\ V_z^2 \times 10^{-3}\ \text{kPa}$$

(3) calculation of surface pressures and forces

$$P_z = C_p q_z \qquad F_D = C_D A_z q_z$$

$$F_p = \Sigma p_z A_z \qquad F_L = C_L A_z q_z$$

Calculations in Step (1) recognize geographical location, including special treatment of cyclone areas, four terrain categories, direction of wind in terrain categories, changes in terrain categories, local topographical effects, and height of structure. Some of these considerations reflect refined assessments of the state of knowledge.

Calculations in Step (2) recognize that the conversion constant (0.6) is "most suitable for Australia." Calculations in Step (3) apply to pressures on a surface, forces on complete buildings, forces on buildings which enclose a space, and resultant forces on isolated solid bodies.

3. United States Codes--The major "model" building codes in the U.S., and several regional codes, each use different approaches to the development of wind loads. Summarized briefly are these approaches.

(1) The Standard Building Code--The Standard Code uses a table to spe "basic wind load pressures" in psf as a function of wind speed and height a ground. The tabular values are "velocity pressures" for 100 year recurren fastest mile wind and terrain category "B" from ANSI A58.1-1972. Basic wi speeds for a geographical region are taken from a map. The basic wind loa sures are multiplied by "shape factors" to obtain pressures on building cor nents: vertical surfaces, horizontal surfaces, inclined surfaces, and com which transfer wind loads to the structural frame.

(2) The Uniform Building Code--This code currently uses a tabular approach as well. An "allowable resultant wind pressure" obtained from a map is used to enter a table which provides "wind pressures for various heights above ground." These values are applied directly to surfaces of the building as "horizontal pressures" or "uplift pressures". As noted previously, the Wind Loads Committee of the the UBC is currently considering changes in wind load provisions to incorporate an approach similar to that advanced by ANSI A58.1-1972.

(3) The National Building Code--The National Building Code has adopted ANSI A58.1-1972 in its entirety.

(4) The Basic Building Code--The Basic Building Code takes, perhaps, the most simple and direct approach of the model building codes to the specification of wind loads. The code specifies 15 psf of wind pressure on exposed vertical surfaces less than 50 ft in height, and 20 psf on exposed vertical surfaces 50 to 100 ft above the ground. Above 100 ft the wind pressure increases 0.025 psf for each foot above 100 ft. For external wall design, these values are distributed 2/3 (inward on windward wall) and 1/3 (outward on leeward wall). Internal pressures are treated by imposing 10 psf if there are 1/3 or more wall openings. Local pressures are recognized through a 1.5 factor applied to external wall design pressures in application to "secondary wall framing, wall panels, and sheathing." A special wind pressure table specifies design pressures for glass.

(5) The South Florida Code--The South Florida Building Code has gained some recognition in the U.S. as the most stringent of the U.S. Codes. While the minimum velocity pressures are, generally, larger than those specified by other codes for south Florida locations, the approach and application of this code is much the same as presented in the Standard Building Code. Velocity pressures are multiplied by shape factors to obtain design pressures for buildings and building components. The Code states that design wind velocity shall be taken as not less than 120 mph at a height of 30 ft above the ground. Velocity pressure is 37 psf at 30 ft.

(6) ANSI A58.1-1972--The "ANSI Standard" comprises the first attempt by U,S. standard writers to place into tractable form procedures for calculating wind loads that have been recognized by foreign codes for years. As noted in the discussion of states of development, the ANSI Standard of 1972 has not been through a cycle of public comment, nor has a commentary on its use been written. The ANSI Standard A58.1-1972 approach is outlined below.

(1) A basic wind speed is selected from maps for several mean recurrence intervals.

(2) Effective velocity pressures are computed for buildings and struc (q_F), for parts and portions (q_p), and for internal pressures (q_M considering type of exposure and height above ground (K_z), gust f (G_F and G_p), and the classic $.00256V_{30}^2$ term:

$$q_F = K_z G_F \ (.00256V_{30}^2)$$

$$q_p = K_z G_p \ (.00256V^2_{30})$$

$$q_M = K_z \ (.00256V^2_{30})$$

(3) Resultant design pressures acting on an element of an enclosed structure are computed from

$$q = (q_f \text{ or } _p) \ C_p - q_M \ C_{pi}$$

where C_p and C_{pi} are pressure coefficients, internal and external.

Solutions

Problems in wind engineering are principally ones of technology application. While much remains to be learned about the nature of extreme winds, it is clear that much can be done with the technology at hand. We understand building failure modes, and we can place windspeed maxima and probabilities of windspeed occurrences into perspective for any geographical region. This means that engineering for extreme winds can be reduced to the same logical, systematic, and thorough process that characterizes current professional practice.

The greatest opportunities for achieving significant impact are presented by the classes of building which receive the least engineering attention--non-engineered buildings and marginally-engineered buildings. The modern research engineer continues to be attracted by the appealing and mathematically tractable analysis of major multistory structures. However, the challenge which reflects the greatest potential lies with the complex and difficult tasks identified with applications of engineering principles to the vast numbers of low-rise buildings which can use additional wind resistance.

If the increasing exposure of our cities to wind caused disaster is to be reversed, we must act in two areas. First, we have a responsibility to speak out regarding the hazards and vulnerability to disaster presented by careless construction practices in wind-prone areas. Public awareness of the problem is critical to the engineers' being able to act in this new area. Secondly, we must move to assure that our colleagues in the practice of engineering are made aware of the available technology. We can no longer expect that publication, alone, can effect the necessary information exchange. We must become more active in code groups, in standard writing, in continuing education, and in extension. Specifically, we must examine methodologies for bringing increasing degrees of engineering expertise into the construction of housing and low-rise commercial and industrial buildings. Small adjustments building practices can produce tremendous improvements in wind resistance. placement of these principles into the building trades will not be an easy ta but it is a task which carries promise of solution to wind damage exposures throughout the world.

Acknowledgments

The author wishes to acknowledge close associations with Drs, Kishor C. Mehta, James R. McDonald, and Richard E. Peterson of the Institute staff who made this presentation possible. Support of Institute activites provided by the National Science Foundation, the National Severe Storms Laboratory, and the Nuclear Regulatory Commission are also gratefully acknowledged.

References

AIA, 1976: "The National Building Code," American Insurance Association, New York.

ANSI, 1955: "American Standard Building Code Requirements for Minimum Design Loads in Buildings and Other Structures," A58.1-1955, American Standards Association, New York (now American National Standards Institute).

ANSI, 1972: "American National Standard Building Code Requirements for Minimum Design Loads in Buildings and Other Structures," A58.1-1972, American National Standards Institute, New York.

Brinkmann, W. A. R., 1974: "Strong Downslope Winds at Boulder, Colorado," Monthly Weather Review, Vol. 102, No. 8, August.

BSI, 1972: "British Standard Code of Basic Data for the Design of Buildings, CP3 (Chap. V: Part 2: 1972, Wind Loads), "British Standards Institution, London.

Davenport, A. G. and W. A. Dalgliesh, 1975: "Treatment of Wind Loads in the National Building Code of Canada," paper presented at the National Meeting of ASCE, Denver, November 3-7.

Davies-Jones, R. P. and E. Kessler, "Tornadoes," Weather and Climate Modification, W. N. Hess, ed., John Wiley & Sons, Inc., New York, New York.

Dunn, G. E. and B. I. Miller, 1960: Atlantic Hurricanes, Louisiana State University Press, Louisiana.

Eagleman, J. R., V. U. Muirhead, and N. Williams, 1975: Thunderstorms, Tornadoes and Building Damage, Lexington Books, Lexington, Massachusetts.

Flora, S. D., 1954: Tornadoes of the United States, University of Oklaho Press, Norman, Oklahoma.

Frank, Neil, 1974: "The Hard Facts about Hurricanes," NOAA Magazine, Vol pp. 4-9.

Fujita, T. T., 1973: "Tornadoes Around the World," Weatherwise, Vol. 26, April.

Hill, E. L., W. Malkin and W. A. Schulz, Jr., 1966: "Tornadoes Associated with Cyclones of Tropical Origin--Practical Features," Journal of Applied Meteorology, Vol. 5, No. 6.

Huschke, R. E., 1959: Glossary of Meteorology, American Meteorological Society.

Model Minimum Hurricane-Resistant Building Standards for the Texas Gulf Coast, The Texas Coastal and Marine Council, General Land Office of Texas, September 1976.

NAVFAC, 1970: "Design Manual, Structural Engineering," NAVFAC DM-2, Naval Facilities Engineering Command, Department of the Navy, Washington, D.C.

Newberry, C. W. and K. J. Eaton, 1974: "Wind Loading Handbook," Building Research Establishment Report K4f, Her Majesty's Stationery Office, London.

NRCC, 1975: "National Building Code of Canada - 1975," NRCC No. 13982, Associate Committee on the National Building Code, National Research Council of Canada, Ottawa, Canada.

NRCC, 1975a: "Supplement No. 4: Commentaries of Part 4; Commentary B (Wind Load)" NBC Supplement No. 4, Associate Committee on the National Building Code, National Research Council of Canada, Ottawa.

Peterson, R. E. (ed.), 1976: Proceedings of the Symposium on Tornadoes: Assessment of Knowledge and Implications for Man, Texas Tech University, June 22-24.

SAA, 1973: "Rules for Minimum Design Loads on Structures -- SAA Loading Code (Metric Units): Part 2 -- Wind Forces," AS 1170, Part 2-1973, Standards Association of Australia, Standards House, 80 Arthur St., North Sydney.

SBCC, 1973: "Southern Standard Building Code -- 1973 Edition," SBCC, Birmingham, Alabama.

SBCC, 1974: "Amendments to Southern Standard Building Code -- 1974 Revision to 1973 Edition," SBCC, Birmingham, Alabama.

SBCC, 1975: "Amendments to Standard Building Code -- 1975 Revision to 1973 Edition," SBCC, Birmingham, Alabama.

SBCC, 1976: "Amendments to Standard Building Code -- 1976 Revision," SBCC, Birmingham, Alabama.

UBC, 1975: "Uniform Building Code -- 1973 Edition," ICBO, Whittier, Califo

TABLE I MAJOR BUILDING CODES AND STANDARDS

Code or Standard	Recent Edition	Parent Organization	Address
ASA A58.1 - 1955	1955	American National Standards Institute	1430 Broadway New York, New York 10018
ANSI A58.1 - 1972	1972	American National Standards Institute	1430 Broadway New York, New York 10018
NAVFAC DM-2	1970	Naval Facilities Engineering Command	Department of the Navy Washington, D. C. 20390
Standard Building Code	1976	Southern Building Code Congress	3617 8th Avenue South Birmingham, Alabama 35222
Uniform Building Code	1977	International Conference of Building Officials	5360 South Workman Mill Road Whittier, CA 90601
National Building Code	1976	American Insurance Association	85 John Street New York, New York 10038
Basic Building Code	1975	Building Officials Code Administrators International, Inc.	1313 East 60th Street Chicago, Illinois 60637
South Florida Building Code	- - -	Dade County Florida	Building Department Dade County Courthouse Dade Co., Florida
British Code of Basic Data for Design of Buildings (CP3)	1972	British Standards Institution	British Standards Institution 2 Park Street London W1A 2BS England
Wind Loading Handbook (Commentary on CP3)	1974	Building Research Establishment	Building Research Station Garston, Watford WD2 7JR England
National Building Code of Canada (NRCC No. 13982)	1975	National Research Council of Canada	NRCC Ottawa Ontario, K1A 0R6 Canada
Commentaries on Part 4 of the National Building Code of Canada (NRCC No. 13989)	1975	National Research Council of Canada	NRCC Ottawa Ontario, K1A 0R6 Canada
Australian Standard 1170, Part 2-Wind Forces	1973	Standards Association of Australia	Standards House 30 Authur Street North Sydney, N.S.W. Australia

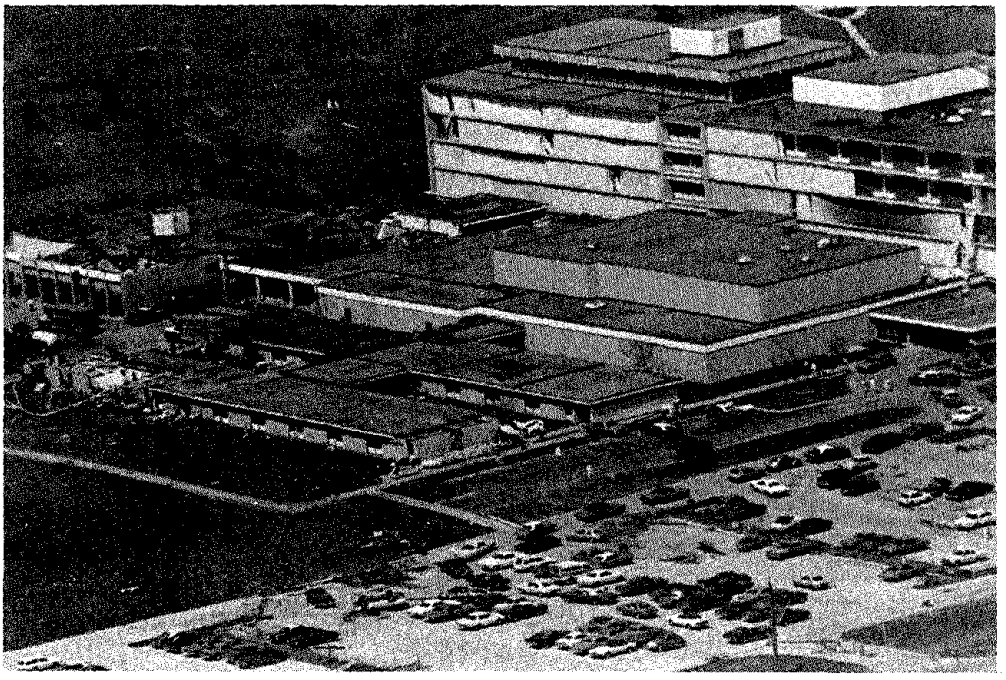

Figure 1 Fully-Engineered Buildings Such as This Hospital in Omaha, Nebraska (USA) Perform Well in the Face of Extreme Winds

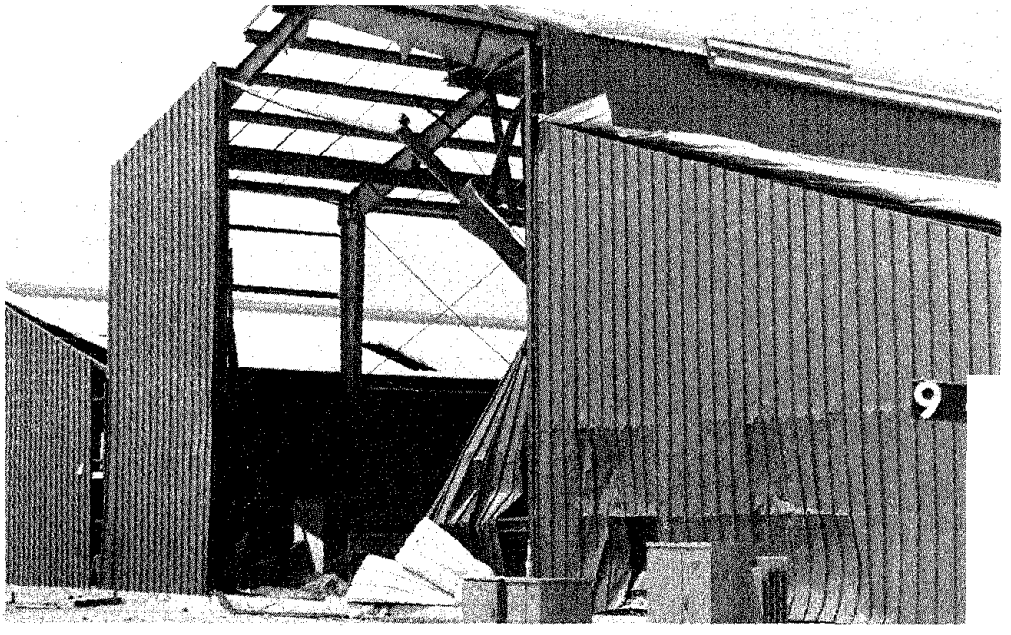

Figure 2 Pre-Engineered Metal Buildings Often Exhibit Failures of Compone (Cladding or Doors) When Affected by Extreme Winds (Lubbock, Texas).

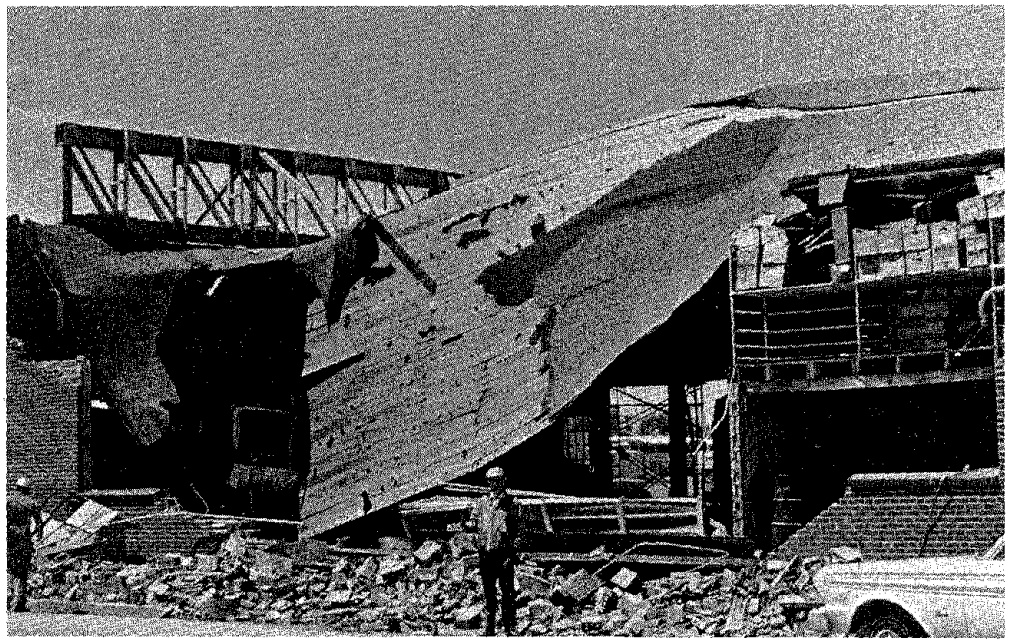

Figure 3 Marginally-Engineered Buildings Such as This Loadbearing Masonry Structure in Lubbock, Texas (USA) Perform Poorly in Extreme Winds.

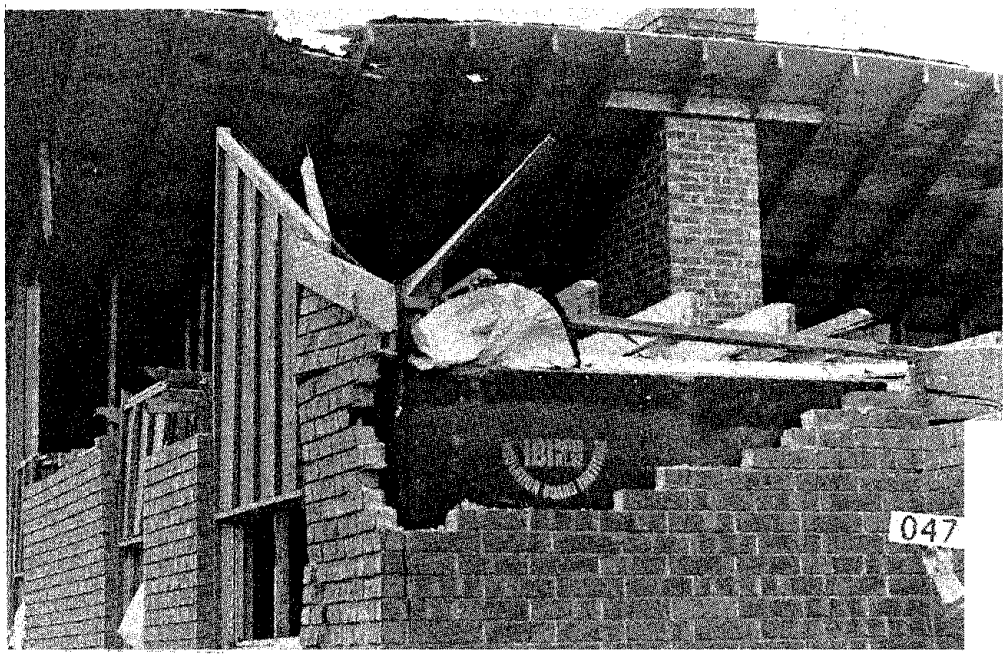

Figure 4 Non-Engineered Buildings Perform Poorly in Extreme Winds; Engine Principles Can Mitigate Wind Effects at Reasonable Cost.

FULL SCALE PRESSURE PROBABILITY DISTRIBUTIONS AND SPECTRAL MEASUREMENTS ON A MULTI STOREY BUILDING

by

R. Feasey and D.H. Freeston

University of Auckland

ABSTRACT

Full scale wind pressure measurements have been taken on a 30 m high building on the Auckland University Campus. Data was collected at a rate of ten samples per second per transducer and analysed to give probability and spectral information through a range of wind directions.

The system and analysis procedures are described. The major conclusions are that the approach flow is significant in determining peak pressures and the probability distributions are non-Gaussian on all faces of a building.

INTRODUCTION

New Zealand is a windy country with strong cyclonic type winds producing a predominately SSW/NNE airflow across the country. In addition, there are about 20 to 30 tornadoes occurring per year, fortunately mostly along the sparsely populated west coast districts during the passage of active cold fronts. The New Zealand Meteorological service anemograph network, of 53 stations throughout North and South Islands, give mean annual wind speeds ranging from 9.4 m/s at 8.1 m/s at the extreme south western and northern tips of the country to 2. at Levin Airport in the South West of the North Island.

The topography of the two islands, with the Alps down the west coast of South Island and the high ground on the east coast of North Island, produce funneling of the wind such that Wellington City, which is situated in the p the prevailing north/south winds experiences high winds for long periods o

The hourly mean wind speed at Wellington Airport is over 10 m/s for 2200 hours per year and over 15 m/s for 450 hours per year. The basic 50 year return period three second gust for Wellington is 52 m/s. In April 1968 during the "Wahine storm" which cost the Earthquake and War Damage Commission 1.75 million dollars from 11,000 claims, gusts of 50 to 72 m/s were recorded at anemograph stations around the City.

However, despite the general strong wind climate across New Zealand it is usual to find, that except for buildings of unusual shape for example a lenticular plan form, the requirements of the N.Z. Earthquake loading code designs the main structure of the building. Of recent years however cases have been reported in New Zealand as elsewhere (Eaton 1975) of glazing and cladding failures due to wind. Design of these components requires a knowledge of peak pressures to be expected during the structures design life. The wind pressure probability distribution is therefore of importance but very few significant full scale distributions have been reported. Fujii, Hibi and Kaneko (1974) obtained data from a 120 m building in Tokyo and showed that the wind pressure distribution was substantially different from Gaussian beyond two or three standard deviations. Dalgliesh (1971) presented probability distributions on a high rise building but was primarily concerned with predicting the peak pressure value rather than the distribution itself. Lam Put (1971) measured a few probability distributions on a building and concluded that a Gaussian description was adequate. However this data was of low resolution and covered an insufficient range of standard deviations to be able to generalise from the results presented. Recent work by Peterka and Cermak (1975) suggests that on the windward face of a building the pressures are Gaussian, while those from locations whose mean pressure coefficients were less than -0.25, showed a greater negative tail than that predicted by the Gaussian distribution.

It is noticeable on reviewing the recent full scale pressure measurements conducted around the world that the range of terrain conditions, data acquisition systems and analysis techniques by which the data has been obtained and analysed are as diverse as the variety of structures on which measurements have been made. A study of the early measurements of Dalgliesh, Wright and Schriever (1967) and Newberry, Eaton, Mayne (1967) on high rise buildings in which analogue recordings of wind were digitised by hand and analysed by computer does cast some doubts on the collection and analysis procedures used at that time. What is evident from their work and others making full scale measurements is that 1) a reliable reference wind speed and direction signal is required 2) if differential transducers are used to determine pressure coefficients, a reliable and adequate reference pressure is essential 3) a data acquisition and analysis system is necessary which allows the collection and analysis of very large quantities of numbers without introducing errors in the data reduction process.

This paper presents some full scale pressure measurements which have l analysed to give pressure probability and spectral information appropriate the cladding/glazing type of problem.

THE EXPERIMENT

The School of Engineering Tower Block is a 12 storey building with nor plan dimensions of 20 x 20 m. It is sited in terrain of variable roughnes sloping upwards from the sea about 3 km to the N.E. With ground to the we the building being higher than the east, the northwest face of the buildin eight stories above street level while the southeast side has eleven above level.

Ten pressure transducers, mounted in small window frames on the 9th and 11th floors in positions shown in Fig.1, were used. The locations were selected with prior knowledge of the prevailing strong-wind directions for the city (NE and SW), with the intention of giving a coverage of the three faces instrumented, of windward, side and leeward situations. Transducers 1,3,4 and 6 are located 1.75m from the corners on the 9th floor while transducers 2,5 and 7 are at the centres of the N.E., S.E. and S.W. faces at the same level. Transducers 8,9 and 10 are located directly above 2,5 and 7 respectively, on the 11th floor.

The transducers which were manufactured to a Building Research Establishment design, described by Mayne (1970), were referenced to a 25mm I.D. rigid P.V.C. tube loop running completely around the ninth floor, the pipe entering a room on the N.W. side of the building at the same level. A standard meteorological office Munro cup anemometer and wind direction vane were mounted on a pivotting mast with the cups 13m above roof level, the output of both devices being recorded on a 24hr chart recorder.

The data acquisition system used is shown as a line diagram in Fig.2. Since hardware available for the experiment was limited, the analysis of the collected data was performed on the University Computer Centre's Burroughs B6700. Amplified signals from the velocity and pressure transducers are low-pass filtered at 4.0 Hz (using a 4-pole Butterworth filter) and the analogue signals passed to an Input unit (I/O unit) containing a 16 channel analogue multiplexer and a very high speed 12 bit analogue to digital converted (A/D converter) with a maximum conversion rate of 250 kHz. The I/O unit is controlled by an Alpha LSI-2 (Computer Automation Inc.) mini-computer with a 16K core memory, which regulates the sampling and output of digitised information to a Facit high speed paper tape punch at a maximum rate of 75 bytes/second. Because of the lack of core or peripheral storage in the computer for the long data runs required (20 to 60 minutes) and the limit imposed by the speed of the tape punch, it was only possible to run 3 channels simultaneously in real time at the design rate of 10 samples per channel per second. The paper tape is read into the B6700 digital computer and the data stored on magnetic tape for later retrieval.

With the above limitations, the usual operational procedure was to output data from up to 3 channels to the punch in real time, the span of operation depending on the length of the roll of paper tape. With 3 channel operation, data sequences of 30 minutes duration could be obtained. Records were tested for stationarity using a run test based on the mean square level of 20 uncorrelated segments. Because data was usually obtained over periods of strong wind generated by mature cyclonic weather disturbances during which the mean wind speed and direction remained constant for many hours, the stationarity check was usually successful. If unsuccessful, the data was filtered with a digital highpass filter to remove low frequency components and trends after which the stationarity criterion was generally satisfied.

RESULTS

Probability Density Distributions

The Mean, Variance, Skewness and Kurtosis were calculated for numerous velocity and wind pressure records using stationary data sequences containi between 10,000 and 16,000 points. Emphasis was placed on the variation of 3rd and 4th moments with wind direction and upstream surface roughness sinc is these quantities that determine the likelihood of extreme pressures bein

produced. The skewness describes the symmetry of the distribution being zero for a Gaussian p.d.f., while the kurtosis describes the "peakiness" of the distribution being equal to 3 for a Gaussian p.d.f.

Since the tower block is at the edge of a group of approximately equally tall campus buildings, the immediate upstream surface roughness varies considerably with the direction of the prevailing wind. Data obtained with a mean wind direction of 220° - 330°, which corresponds to the roughest upstream fetch, generally have high kurtosis values, implying that the p.d.f. is less peaked than Gaussian and the tails of the distribution are of a substantially greater extent. Kurtosis values for wind directions from 0.10° - 180°, which correspond to an upstream fetch largely unobstructed by tall buildings, are generally lower, with values between 3 and 5 predominating.

The variation of skewness and kurtosis with wind direction is somewhat more complicated and is displayed in Fig.3 which shows the skewness and kurtosis of the p.d.f. obtained at transducer 5 (in middle of the S.E. face on the 9th floor) as a function of wind direction. It can be seen that there is a tendency for the skewness to be positive if the mean wind direction is within 60° of normal to the transducer, while for wind directions placing transducer 5 on the side or leeward face the skewness is usually substantially negative (from 0 to -1). The kurtosis figures are relatively constant for mean wind directions $\bar{\theta} = 090^{\circ}$ - 270° with values near 5. For directions between 270° - 090°, through north, substantial variation occurs which must be correlated with the interference effects of the upstream campus buildings in these directions.

From this plot there is some justification in proposing that the skewness of the wind pressure p.d.f. is a function primarily of the relative direction of the wind, while the kurtosis of the p.d.f. is a function largely of the local terrain roughness.

The skewness and kurtosis of the wind velocity p.d.f. obtained from the reference anemometer are shown in Fig.4. It can be seen that the skewness is consistently positive, generally between 0 and 0.5, a slight directional dependency being apparent since the higher values of skewness are clustered around $\bar{\theta} = 270^{\circ}$ which is the direction of the Chemistry/Physics building immediately upstream. The reliability of these anemometer measurements depends on the accuracy with which the instrument can follow the real wind speed fluctuations. The failings of large cup anemometers are detailed by Mazzarella (1972) and Kaganov and Yaglom (1976). the lack of frequency response will modify the p.d.f. such that the hypothesis that the wind speed probability distribution is Gaussian cannot be refuted.

To enable visual comparisons to be made, the cumulative probability density functions (c.p.d.f.) of numerous data files were plotted with that of a Ga process for comparison. Although the overall shape of the p.d.f. given by mean, variance, skewness and kurtosis is of interest, it is the extreme ta the p.d.f. which are of importance in wind loading studies. Thus two c.p. can be presented for each data file indicating the behaviour of the c.p.d. deviations above and below the mean. Figs. 5 and 6 show typical results o from data file SEPT 6/6 with the cumulative probability plotted against th number of standard deviations from the mean. This data file gives results glancing wind onto the Northern face of the building.

In general, analysis of the data obtained over a nine month period fo in excess of 10 m/s recorded by the local anemometer gave results as indic

below

1) Windward face locations showed c.p.d.f's substantially greater than Gaussian beyond +1.5 standard deviations but significantly less than Gaussian for all negative deviations. This result is in variance with the wind tunnel studies of Peterka and Cermak (1975).

2) Transducers on side faces show a mixture of behaviours depending on the exact direction of the wind. With the mean wind direction slightly on to the face, the probability distribution is greater than Gaussian beyond ± 2 standard deviations although the difference is smaller in the case of negative deviations. With the wind blowing off the side face, leading to a separated flow off the leading edge of the building, the probability distribution is less than Gaussian for positive deviations, but significantly greater than Gaussian for deviations beyond -1.5. It is this latter case that is most critical in terms of wind loading of cladding panels.

3) Locations on the leeward face generally show a sub-Gaussian p.d.f. for positive standard deviations, but significantly greater than Gaussian probabilities beyond -2 standard deviations. Although the behaviour in this case is similar to that in (2) above, the importance in terms of wind loading is less important, since the variance of the pressure signal is much lower than for side or windward faces. Since the energy of the pressure fluctuations is a function of the signal variance, the low power in the pressure fluctuation on the leeward face implies negligible probability of serious wind loading effects in spite of the unfavourable probability distribution beyond -2 standard deviations.

Wind Pressure Power Spectral Density Function

Wind pressure spectra are important in any discussion on glazing and cladding loads. Numerous pressure spectra, obtained on full scale buildings and wind tunnel models, have been reported in the literature. However much of the data has been compared with the Davenport strong wind spectrum, which in its non-dimensional form gives a $-2/3$ slope at high frequency.

Estimates of wind pressure power spectral density were obtained for all the data files. Each time history was 16,384 points using a 0.1 second time interval.

Figures 7,8 show typical results. Nearly all measured spectra were found to be at variance with the Davenport spectra, the main difference was in the rate of decrease of spectral density at high frequencies. The typical mean slope for the collected spectra is $-3/2$. The best fit curve for all the data analysed was of the form

$$\frac{nS(n)}{\sigma^2} = \frac{x}{(2 + x^2)^{5/4}} \quad \text{where} \quad x = \frac{nL}{\bar{V}}$$

$\frac{n}{\bar{V}}$ = reduced frequency (cycles/m) L = length scale (m

The wind spectra, when corrected for frequency response, was found to f Davenport. By analysis of the spectral peak, Length Scales can be determine There is a distinct continuous reduction in length scale through the series windward to leeward location from 330m on the windward side to 208m on the l ward face. It is also noticeable that the spectra are more peaked on side a leeward faces than those on the windward side. 95% confidence intervals are presented and it is seen there appears to be little evidence to suggest the occurrence of any large scale vortex shedding.

CONCLUSIONS

The approach flow is significant in determining peak pressures on all faces of a building.

The peak pressures on both windward and lee faces are significantly different than those predicted by a Gaussian probability distribution with those when the wind is blowing off a side face giving significantly greater than Gaussian for standard deviations beyond -1.5.

The pressure spectra obtained show an increased slope at the high frequency end when compared with wind spectra. No evidence of vortex shedding was detected.

ACKNOWLEDGEMENTS

The authors acknowledge the financial aid of the N.Z. University Grants Committee to purchase equipment and the support for Mr Feasey and UNESCO for a travel grant to Mr Freeston to attend the Symposium.

REFERENCES

DALGLIESH, W.A. (1971) "Statistical Treatment of Peak Gusts on Cladding" J. Struct. Div., Proc. A.S.C.E., Vol.97, No.ST6, Sept. 1971, pp. 2173-2187.

DALGLIESH, W.A., WRIGHT, W. and SCHRIEVER, W.R. (1967) "Wind Pressure Measurements on a Full-Scale High-Rise Office Building" Paper 6, International Research Seminar, Wind Effects on Buildings and Structures, Ottawa, Sept. 1967.

EATON, K.J. (1975) "Cladding and the Wind" Building Research Establishment Current Paper, CP 47/75, May 1975, pp.13.

FUJII, K., HIBI, K. and KANEKO, T. (1974) "The Full Scale Measurement of Wind Pressures on a Tall Building - Further Results from the Asaki-Tokai Building" Symposium on Full Scale Measurements of Wind Effects on Tall Buildings and Other Structures. University of Western Ontario, June 1974.

KAGANOV, E.I. and YAGLOM, A.M. (1976) "Errors in Wind-Speed Measurements by Rotation Anemometers" Boundary-Layer Meteorology, 10, pp.15-34.

LAM PUT, R. (1971) "Dynamic Response of a Tall Building to Random Wind Loads" Paper III.4, Proc. Third International Conference on Wind Effects on Buildings and Structures, Tokyo, 1971, pp.429-440.

MAYNE, J.R. (1970) "A wind Pressure Transducer" Building Research Station Current Paper, CP17/70, May 1970, pp.3.

MAZZARELLA, D.A. (1972) "An Inventory of Specifications for Wind Measuring Instruments" Bulletin American Meteorological Society, Vol.53, No.9 Sept. 1972, pp.860-871.

NEWBERRY, C.W., EATON, K.J. and MAYNE, J.R. (1967) "The Nature of Gust L on a Tall Building" Paper 15, International Research Seminar on Win on Buildings and Structures, Ottawa, 1967, pp.399-428.

(also) Building Research Station Current Paper, CP66/68.

PETERKA, J.A. and CERMAK, J.E. (1975) "Wind Pressures on Buildings - Prol Densities" J.Struct.Div., Proc. A.S.C.E., Vol.101, No.ST6, June 197 pp.1255-1267.

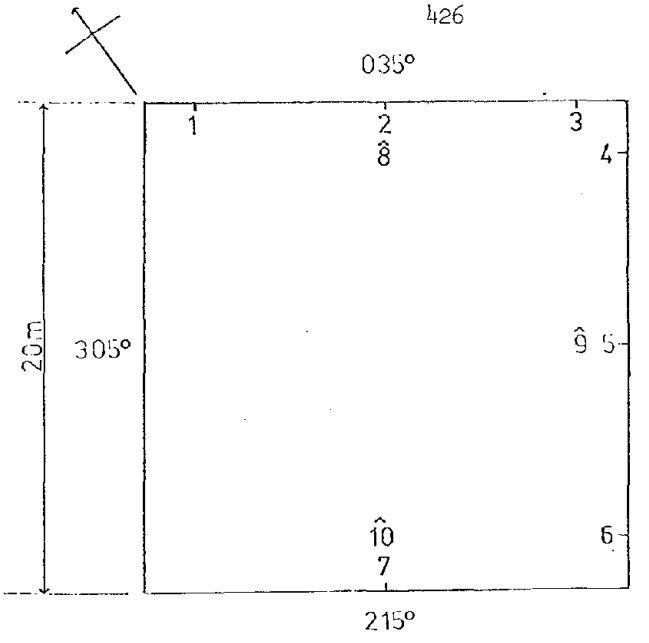

FIGURE 1

Pressure Transducer Location

Transducers indicated (^) are located on 11th floor

True wind directions perpendicular to each face are shown.

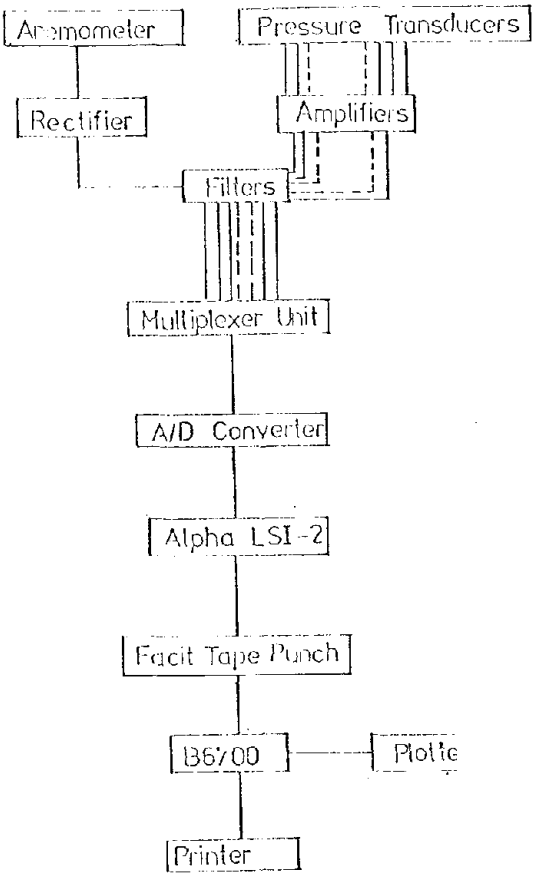

FIGURE 2

Data Acquisition System

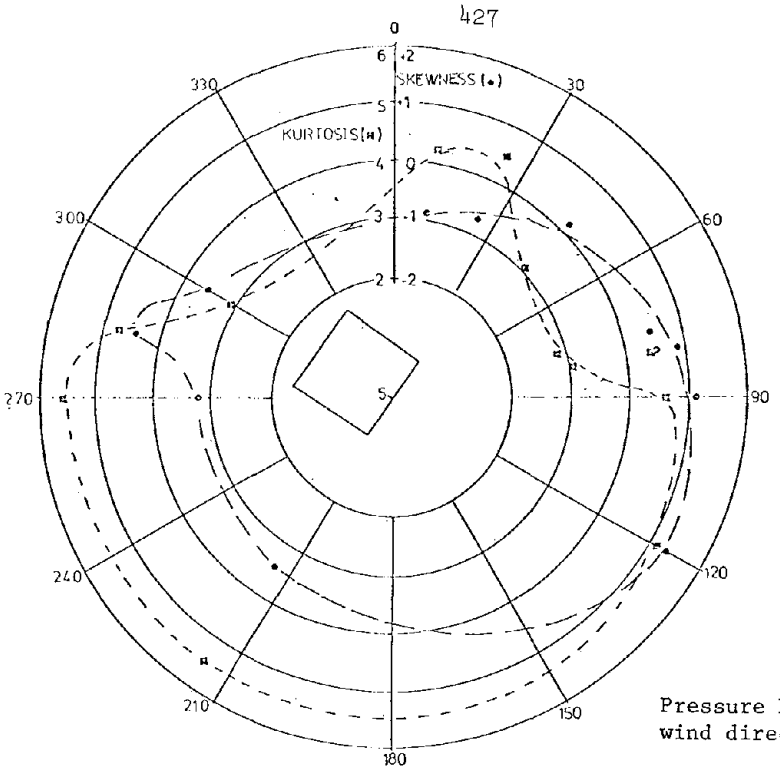

FIGURE 3

Pressure PDF shape and wind direction

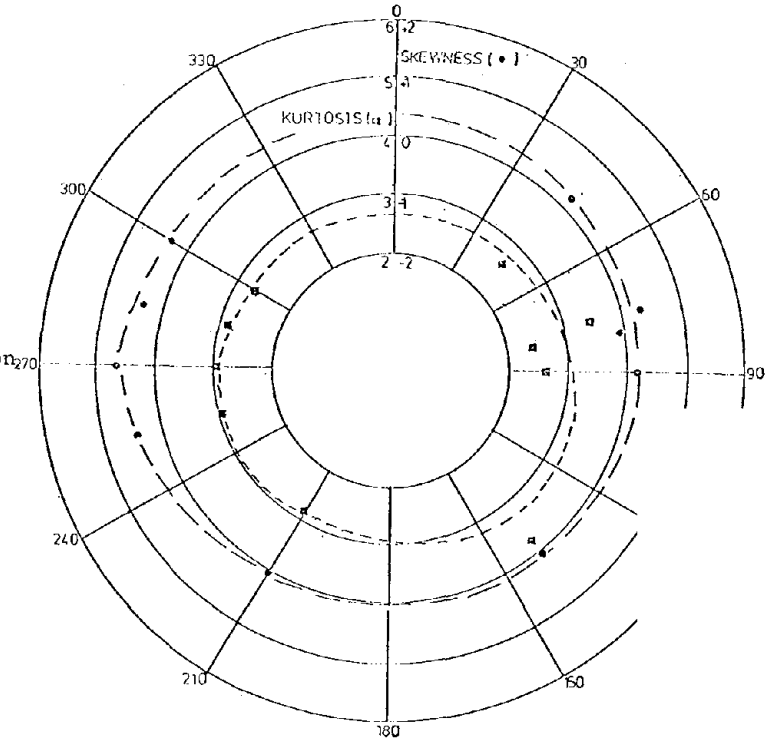

FIGURE 4

Wind Velocity PDF shape and wind direction

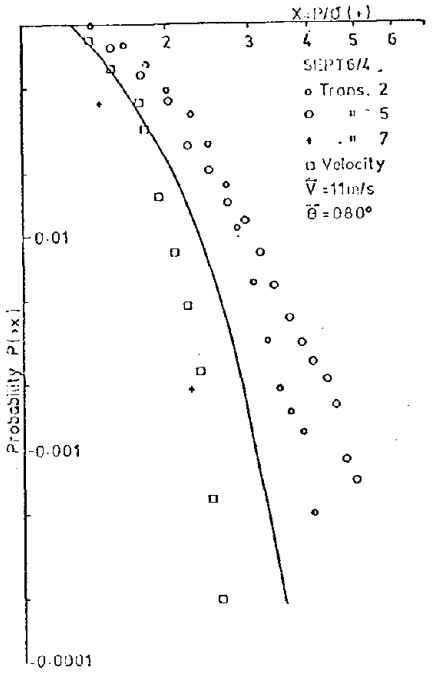

FIGURE 5

Positive cumulative pressure probability density as a function of the number of standard deviations from mean

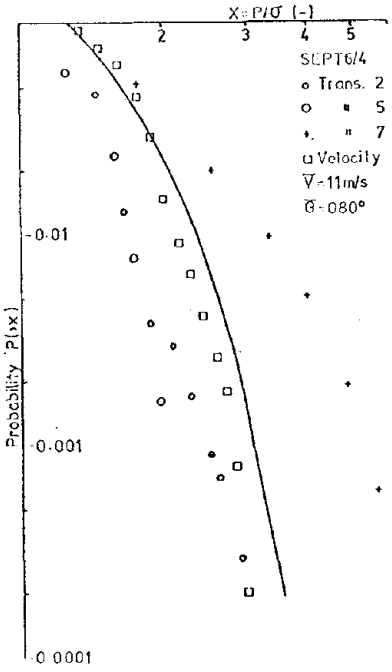

FIGURE 6

Negative cumulative pressure probability density as a function of the number of standard deviations from the mean

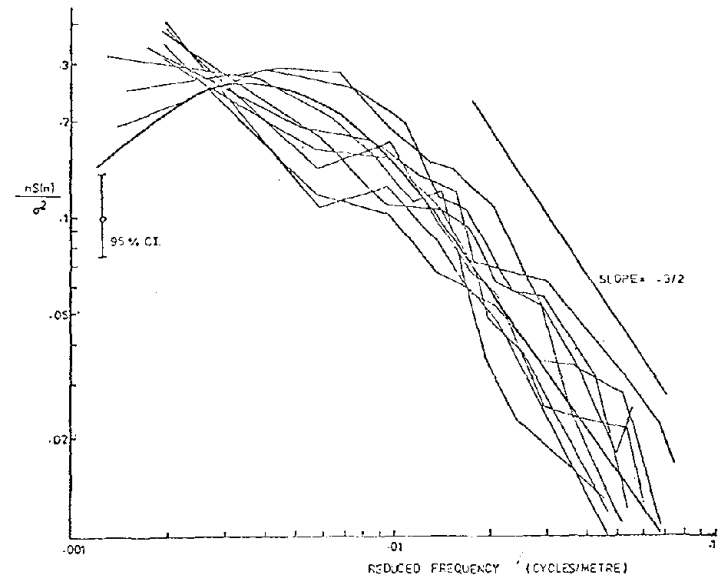

FIGURE 7 Pressure Spectra Windward Transducers ± 20°

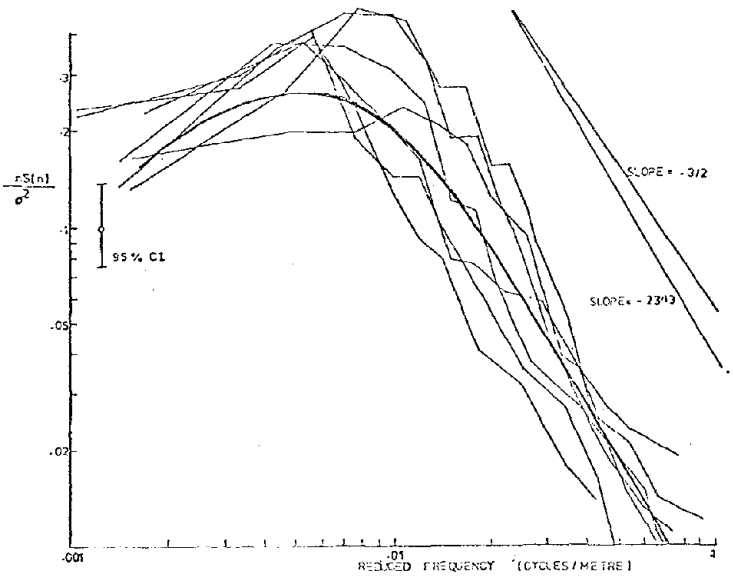

FIGURE 8 · Pressure Spectra Leeward Transducers